

DESIGN AND SYNTHESIS OF FLAVIN-BASED ORGANOCATALYSTS FOR
BIOMIMETIC AEROBIC OXIDATION REACTIONS

SHUAI CHEN

Presented to the Faculty of the Graduate School of
The University of Texas at Arlington in Partial Fulfillment
of the Requirements
for the Degree of

DOCTOR OF PHILOSOPHY

THE UNIVERSITY OF TEXAS AT ARLINGTON

DECEMBER 2013

Acknowledgements

I want to express my sincere gratitude, respect and thank to my mentor, Professor Frank W. Foss Jr., who was brave enough to take a young and naive boy just came to US, barely spoke a whole English sentence or told the differences between NMR and IR, as his first graduate student. I am fortunate that I made my choice to join this group. Professor Foss created a lab that aims to develop the knowledge, skill, creativity and attitude of each student on learning organic chemistry. He is very confident and open minded and because of that he always encourages and gives me freedom to explore my own ideas. Freedom of research is extremely important for a graduate student to grow into an independent researcher because it allows a student to learn from failures, overcome barriers and finally enjoy the beauty of science. What makes Professor Foss a great mentor is that he is very knowledgeable and experienced in chemistry so that he can point out the right direction from numerous distractions for me to pursue my study. Not only is he a great teacher, Professor Foss is close friend of mine out of the lab. I share my happiness and sadness of my life with him. We played softball together before both of us broke a knee from it. He and Ann invited us to their house for delicious homemade food that I can never resist. He wants everyone in his lab to succeed as much as possible by supporting us to go to academic conferences, workshops and training sections. He encourages me to go to internship from where I have experienced the everyday research in a state of art pharmaceutical company. In a word, I cannot be what I am now without him. Professor Foss, you lift me up.

I want to thank my committee members, Professor Carl Lovely, Professor Roshan Perera and Professor Martin Pomerantz, who have been guiding me throughout my whole PhD. I want to give my special gratitude to Professor Lovely. He is a great organic chemist and educator, from whom I have learned and understood organic

chemistry systematically. He gave me numerous invaluable suggestions and advises throughout my entire study in UTA. His high standard in doing research enforces me to push my limits to think scientifically, conduct research carefully and present the result accurately. I feel so lucky to have him as my chemistry professor.

I must thank my awesome coworker, Mr. Mohammad S. Hossain. Most work I have done, I did it with the help of him. He has broad knowledge and excellent skill of organic chemistry and analytical chemistry, which helped the flavin project went to a totally different level. I am sure he will continue his success in conducting flavin chemistry into a more exciting state.

Lastly, I would give my warmest thanks to my family. My dad and mom, without their support and understanding, I might have given up half way. My wife, Chen, with whom I spent every day in the last 5 years, always holds me up when I am weak, shares my up and down, sacrifices her benefits for mine. I am an extremely lucky guy to marry her and I owe her so much in the five years. I love you!

There are so many people that have guided, helped and taken care of me during my study in the last five years in and outside of the lab. I am so fortunate that I have come across all of these great people around me. I owe my thanks to you and when you need me I will be there for you too!

November 7, 2013

Abstract

DESIGN AND SYNTHESIS OF FLAVIN-BASED ORGANOCATALYSTS FOR
BIOMIMETIC AEROBIC OXIDATION REACTIONS

SHUAI CHEN, PhD

The University of Texas at Arlington, 2013

Supervising Professor: FRANK W. FOSS JR.

Oxidation reactions are among the most costly and least selective transformations in synthetic chemistry. Catalytic methods that utilize O₂ as a terminal oxidant strive to reduce the inefficiency in this large area of synthesis. Recent efforts have been aimed primarily at metal-/organometallic- or enzyme-catalyzed transformations. The goal of the research described in this dissertation was to develop organocatalytic systems based on natural biosynthetic catalysts in order to develop selective metal-free aerobic oxidations that function at room temperature. Prior to our work, riboflavin mimics were previously investigated to understand flavoenzyme function and to perform catalytic oxidations of primarily heteroatom systems. We set out to extend this relatively limited area of organocatalysis to the oxidation of more valuable carbon centers in a mild, chemoselective and stereoselective manner.

In Chapter 1, a description of the development and application of biomimetic flavin organocatalysts thus far reported in the literature are summarized.

In Chapter 2, the flavin-catalyzed Dakin oxidation is discussed. A range of riboflavin derivatives is used as catalysts to accelerate the transformation of *o*- or *p*-hydroxyl benzaldehydes into dihydroxybenzenes using H₂O₂ as the terminal oxidant. An

aerobic version of this transformation is developed using the flavin catalysts and NAD(P)H mimics.

In Chapter 3, an aerobic asymmetric Weitz-Scheffer epoxidation of enals using flavin and chiral, non-racemic pyrrolidines in a dual catalysis strategy is discussed. High enantioselectivity and diastereoselectivity are observed in the epoxides obtained using this method. A mechanistic study is conducted to elucidate the characteristics of the reaction pathway.

In Chapter 4, the flavin catalyzed aerobic aromatization of heterocycles is discussed. Riboflavin derivatives are used to convert substituted dihydropyridines and benzothiazolines to pyridines and benzothiazoles with molecular oxygen as terminal oxidant under mild reaction conditions.

Table of Contents

Acknowledgements	ii
Abstract	iv
List of Illustrations	viii
List of Tables	xiii
Chapter 1 Introduction to Biomimetic Flavin Catalysis	1
1.1 Flavoproteins and the mechanisms of their function	1
1.1.1 Flavoprotein monooxygenase	3
1.1.2 Dehydrogenases	5
1.2 Biomimetic Flavin Organocatalysts	6
1.2.1 Flavin Catalyzed Electrophilic Oxidations	7
1.2.1.1 Sulfur Oxidation	7
1.2.1.2 Amine Oxidation	15
1.2.2 Flavin Catalyzed Nucleophilic Oxidation	16
1.2.2.1 Baeyer-Villiger Oxidation	17
1.2.3 Applications of Flavin Other Than as Organocatalyst	19
1.2.3.1 Flavin Biomarker	19
1.2.3.2 Flavin drug carrier	20
1.3 Outline of Dissertation	20
Chapter 2 Flavin Catalyzed Dakin Oxidation	22
2.1 Baeyer-Villiger Oxidation	22
2.2 Dakin Oxidation	29
2.2.1 Current Methods for Dakin Oxidation	29
2.2.2 Flavin Catalyzed Dakin Oxidation Using H ₂ O ₂ as Terminal Oxidant	31

2.2.3 Flavin Catalyzed Dakin Oxidation Using O ₂ as Terminal Oxidant	43
Chapter 3 Flavin Catalyzed Weitz-Scheffer Oxidation.....	52
3.1 Dual Catalysis Strategy for Flavin Catalyzed Asymmetric Oxidations	52
3.2 Aerobic Asymmetric Weitz-Scheffer Epoxidation	54
Chapter 4 Flavin Catalyzed Heterocycle Aromatization	73
4.1 Heterocycle Aromatization Reactions.....	73
4.1.1 Dihydropyridine.....	73
4.1.2 Benzothiazoline	77
4.2 Flavin Catalyzed Dihydropyridine and Benzothiazoline Aromatization Reaction.....	81
Appendix A List of Abbreviations	92
Appendix B General Experimental Procedure	94
Appendix C NMR Spectra of Compounds	127
References.....	275
Biographical Information	282

List of Illustrations

Figure 1.1 Riboflavin cofactors: FMN and FAD	1
Figure 1.2 Overall flavin catalytic mechanism (single electron transfer process not shown)	2
Figure 1.3 Mechanism of flavin containing monooxygenase	4
Figure 1.4 Mechanism of flavin containing dehydrogenase and reductase.....	5
Figure 1.5 Proposed mechanism of flavin containing dehydrogenase	6
Figure 1.6 Artificial flavin organocatalysts: Alloxazine and isoalloxazine	7
Figure 1.7 H ₂ O ₂ sulfur oxidation with isoalloxazine.....	8
Figure 1.8 O ₂ sulfur oxidation with isoalloxazine	9
Figure 1.9 H ₂ O ₂ sulfur oxidation with alloxazine	10
Figure 1.10 Comparison of a range of alloxazine and isoalloxazine catalysts' ability to accelerating amine and sulfur oxidation ¹⁴	11
Figure 1.11 Functionalized flavins to meet special application.....	12
Figure 1.12 Synthesis of bridged flavinium catalysts	12
Figure 1.13 L-valinol derived bridged flavinium catalysts	13
Figure 1.14 Basket-shaped flavinium salt catalyst catalyzed sulfur oxidation	13
Figure 1.15 Planar chiral flavinium salt catalyst catalyzed sulfur oxidation	14
Figure 1.16 Beta-cyclodextrin flavin conjugates catalyzed sulfur oxidation.....	14
Figure 1.17 Riboflavin polymer catalyzed sulfur oxidation.....	15
Figure 1.18 Isoalloxazinium catalyzed <i>N</i> -oxidation of secondary amine	15
Figure 1.19 O ₂ <i>N</i> -oxidation of secondary amine with isoalloxazinium.....	15
Figure 1.20 H ₂ O ₂ <i>N</i> -oxidation of tertiary amines with alloxazine	16
Figure 1.21 H ₂ O ₂ Baeyer-Villiger oxidation of cyclobutanones catalyzed by isoalloxazinium	17

Figure 1.22 Asymmetric Baeyer-Villiger oxidation of cyclobutanones catalyzed by bis-isoalloxazinium	18
Figure 1.23 Aerobic Baeyer-Villiger oxidation of cyclobutanones catalyzed by riboflavin derived isoalloxazinium	18
Figure 1.24 Riboflavin derived biomarker for detecting tumor cell.....	20
Figure 1.25 Blue light induced dissociation of flavin from dodecin	20
Figure 2.1 Aerobic Baeyer-Villiger oxidations	23
Figure 2.2 Stereoelectronic requirement of 1, 2 migration of Criegee intermediate	24
Figure 2.3 Activation mode of Baeyer-Villiger oxidation	24
Figure 2.4 Synthesis of five alloxazine catalysts	26
Figure 2.5 Synthesis of isoalloxazine catalyst	26
Figure 2.6 Lewis acid BF ₃ assisted BV oxidation of acetone	27
Figure 2.7 Mechanism of Dakin oxidation under basic condition	29
Figure 2.8 Methyltrioxorhenium(MTO), mono-peroxo complexes (mpRe) and active intermediate bis-peroxo complexes (dpRe)	30
Figure 2.9 MTO catalyzed Dakin oxidation in ionic liquid	30
Figure 2.10 Dakin oxidation using sodium percarbonate as oxidant	31
Figure 2.11 Dakin oxidation using urea-hydrogen peroxide complex as oxidant	31
Figure 2.12 Dakin oxidation inspired by flavin H ₂ O ₂ shunt process.....	32
Figure 2.13 Possible alloxazine degradation pathway under strong basic condition	33
Figure 2.14 Base effect of flavin catalyzed Dakin oxidation	34
Figure 2.15 Solvent effect of flavin catalyzed Dakin oxidation.....	35
Figure 2.16 Comparison of the catalytic abilities of alloxazines on Dakin oxidation of salicylaldehyde.....	36
Figure 2.17 Rate acceleration effect of alloxazine catalyst.....	37

Figure 2.18 Rational of the rate acceleration by alloxazine catalyst.....	38
Figure 2.19 Alloxazine catalyzed Dakin oxidation of hydroxyl benzaldehyde	39
Figure 2.20 Non-hydroxylated substrates failed to undergo Dakin oxidation	40
Figure 2.21 Benzoic acid formation from electron poor benzaldehyde	40
Figure 2.22 Dakin Oxidation of hydroxylated acetophenones	41
Figure 2.23 Hammett Plot for meta (7-substituent), para (8-substitution), and meta+para inductive effects vs. relative initial rates.....	42
Figure 2.24 Proposed mechanism of alloxazine catalyzed Dakin oxidation.....	43
Figure 2.25 Dakin oxidation inspired by flavin biomimetic cycle using O ₂ as oxidant.....	44
Figure 2.26 Zinc complexes were formed for the various 2-hydroxyl benzaldehydes.....	45
Figure 2.27 Hantzsch ester as a NAD(P)H mimics.....	46
Figure 2.28 Dakin oxidation using dihydropyridine as reducing agent	46
Figure 2.29 Alloxazine screening on aerobic Dakin oxidation	47
Figure 2.30 Base screening on aerobic Dakin oxidation	48
Figure 2.31 The effect of base on flavin catalyst	49
Figure 2.32 The substrate scope of aerobic Dakin oxidation.....	50
Figure 3.1 Asymmetric sulfur and Baeyer-Villiger oxidation flavin catalysts.....	52
Figure 3.2 Dual catalysis strategy of asymmetric oxidation.....	53
Figure 3.3 Proposed mechanism of Weitz-Scheffer oxidation.....	54
Figure 3.4 Recent development of aerobic epoxidation of enones	56
Figure 3.5 Examples of flavin protein catalyzed epoxidation.....	57
Figure 3.6 Aerobic Dakin oxidation condition failed on epoxidation of enal	58
Figure 3.7 L-proline derived organocatalysts.....	58
Figure 3.8 Comparison of pyrrolidine cocatalyst.....	59
Figure 3.9 Comparison of reductant in aerobic epoxidation	60

Figure 3.10 Hydrolysis of benzothiazoline	60
Figure 3.11 5 mol % flavin: Product/Reductant Vs Time	66
Figure 3.12 10 mol % flavin: Product/Reductant Vs Time	67
Figure 3.13 20 mol % flavin: Product/Reductant Vs Time	67
Figure 3.14 Epoxide formation progress for reactions with different flavin loadings	68
Figure 3.15 Benzothiazoline concentration progress for reactions with different flavin loadings	69
Figure 3.16 Initial rate of epoxide formation and reductant consumption as a function of flavin loading	70
Figure 3.17 Proposed mechanism for alloxazine/pyrrolidine catalyzed aerobic epoxidation	71
Figure 3.18 Aerobic H ₂ O ₂ formation by alloxazine catalyzed dehydrogenation of benzothiazoline	71
Figure 4.1 Dihydropyridine containing drugs for hypertension treatment	73
Figure 4.2 Cerivastatin for the treatment of atherosclerosis and other coronary diseases	74
Figure 4.3 Aerobic DHP aromatization catalyzed by RuCl ₃	75
Figure 4.4 DHP oxidation in the presence of of H ₆ PMo ₉ V ₃ O ₄₀	75
Figure 4.5 DHP oxidation with hypervalent iodine	76
Figure 4.6 DHP oxidation catalyzed Pd/C in acetic acid.....	76
Figure 4.7 DHP oxidation catalyzed by KMnO ₄	76
Figure 4.8 Aerobic 1, 4-DHP oxidation induced by irradiation	77
Figure 4.9 Chiral phosphoric acid catalyzed asymmetric ketimine reduction with benzothiazoline	78

Figure 4.10 Chiral phosphoric acid catalyzed asymmetric ketimine reduction with 2-deuterated benzothiazoline	78
Figure 4.11 Biologically active compounds contains benzothiazole	79
Figure 4.12 catalyzed one pot synthesis of benzothiazole from simple starting materials	80
Figure 4.13 Aerobic benzothiazole synthesis catalyzed by I ₂	80
Figure 4.14 Copper catalyzed benzothiazole synthesis in ethanol.....	81
Figure 4.15 Aerobic benzothiazole synthesis in DMSO at high temperature	81
Figure 4.16 Biomimetic flavin catalyzed oxidative dehydrogenation	82
Figure 4.17 Alloxazine catalyzed dihydropyridine aromatization	85
Figure 4.18 Alloxazine catalyzed multi component dihydropyridine synthesis and aromatization process	86
Figure 4.19 Acid mediated isoalloxazinium catalyzed aromatization mechanism	87
Figure 4.20 Isoalloxazine catalyzed C ⁴ -substituted dihydropyridine aromatization	88
Figure 4.21 Alloxazine catalyzed benzothiazoline aromatization	89
Figure 4.22 Alloxazine catalyzed two-component one pot two steps benzothiazoline aromatization.....	90

List of Tables

Table 1.1 The choice of conditions for different oxidations.....	19
Table 2.1 Conditions examined with flavin catalyzed BV oxidation of 5-and 6-membered cycloketones.....	28
Table 3.1 Asymmetric aerobic epoxidation of 4a: condition optimization.....	62
Table 3.2 Flavin/pyrrolidine catalyzed epoxidation substrate study.....	64
Table 3.3 Epoxide concentration Vs Time.....	65
Table 3.4 Benzothiazoline concentration Vs Time.....	66
Table 3.5 Peroxide formation reaction initial rates.....	68
Table 3.6 Reductant consumption reaction initial rates.....	69
Table 4.1 Initial solvent screening of alloxazine catalyzed aerobic aromatization.....	83
Table 4.2 Careful solvent study of alloxazine catalyzed aerobic aromatization.....	84
Table 4.3 Acid screening with isoalloxazine 4.57 as catalyst.....	88

Chapter 1

Introduction to Biomimetic Flavin Catalysis

1.1 Flavoproteins and the mechanisms of their function

The first report of riboflavin isolation dates back to 1879. A. Wynter Blyth, an English chemist, isolated a bright-yellow pigment in his study on the composition of cow's milk. He termed the matter lactochrome at that time which is known now as riboflavin.¹ The same pigment was later isolated from a variety of sources and the structure was determined by Richard Kuhn in Heidelberg and Paul Karrer in Zurich in 1934 and 1935.^{2,3} The compound was recognized as a component of vitamin B complex and the name was finalized to be riboflavin, derived from the *N*¹⁰-ribityl substitution and bright yellow color of the conjugated ring system, 'flavus' meaning yellow in latin and vitamins end in 'in'.

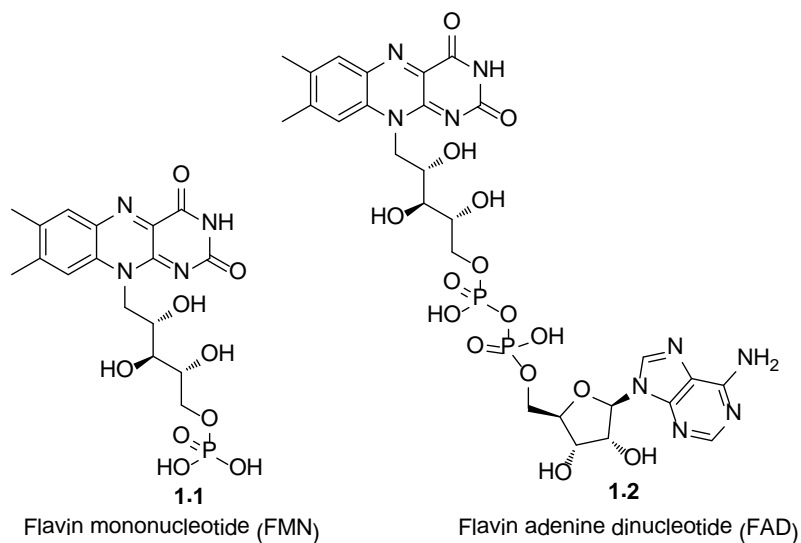


Figure 1.1 Riboflavin cofactors: FMN and FAD

Riboflavin derivatives were determined to be enzyme cofactors based on studies by Hugo Thorell in 1935.⁴ Apoprotein and the flavin-related pigment were separated from a bright-yellow-colored yeast protein which was essential for cellular respiration. Thorell found that neither apoprotein nor the pigment alone could catalyze the oxidation of

NADH, but combination of the two restored the enzyme activity. The catalytic pigment was later identified as flavin mononucleotide 1.1 (FMN), which along with flavin adenine dinucleotide 1.2 (FAD), are the two of the most common flavin cofactors (Figure 1.1).

In flavoproteins, flavins exist either as a covalently-bonded components or non-covalently bonded as coenzymes or prosthetic group. Depending on the nature of the substrate, the type of the chemical reaction they catalyze, the physicochemical properties of the enzyme, flavoproteins are classified into distinctive categories.⁵

1. biological agents which are responsible for oxidation of substrates via activation of triplet molecular oxygen;
2. biological dehydrogenating agents; and
3. flavodoxins which are responsible for electron transfer by alternating between the flavin semiquinone radical and reduced state.

Examples of such enzymes are monooxygenases, hydroxylases; dehydrogenases; and DNA photolyase, respectively. Here, the detailed mechanism and structure of flavin monooxygenase and dehydrogenase will be discussed. The following scheme is the general flavin catalytic mechanism in biologic system (Figure 1.2). It served as a guide for the development of flavin-related chemistry throughout this dissertation.

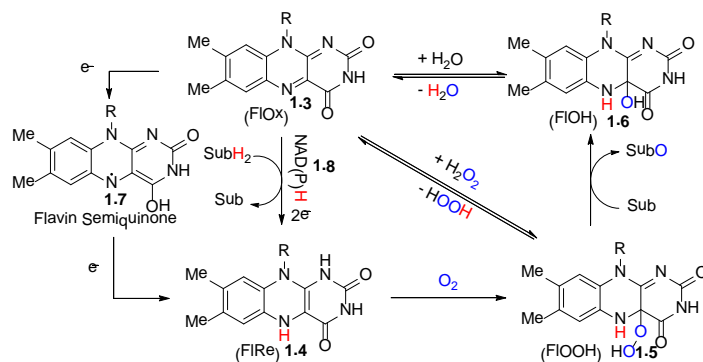


Figure 1.2 Overall flavin catalytic mechanism (single electron transfer process not shown)

As is shown in Figure 1.2, the oxidized flavin (FIOx 1.3) can be reduced to the reduced flavin (FIRe 1.4) by via two single electron transfer or one two electron transfer process. The one electron reduced flavin radical is defined as flavin semiquinone (1.7). The reduced flavin 1.4 reacts with triplet oxygen by donating one electron to oxygen followed by spin inversion to form 4a-hydroperoxyflavin (FIOOH 1.5). The FIOOH can oxidize substrates by transfer one oxygen atom to substrates to form products and the resulting 4a-hydroxyflavin (FIOH 1.6). FIOH regenerate FIOx by eliminating one molecule of water. The direct process of adding H_2O_2 to FIOx to generate 4a-FIOOH is known as the peroxide shunt process. It is worth noting that the peroxide shunt process is reversible, the FIOOH can eliminate H_2O_2 to regenerate the oxidized flavin FIOx.

1.1.1 *Flavoprotein monooxygenase*

Flavoprotein monooxygenases incorporate a single atom of oxygen from molecular oxygen into an organic substrate. The process starts with the generation of reduced flavin 1.4 from the reduction of oxidized flavin 1.3 with external electron donors such as NAD(P)H 1.8.(Figure 1.3) Then, the reduced flavin 1.4, which contains a polarized and electron-rich alkene, reacts with triplet molecular oxygen to form hydroperoxyflavin 1.5. The direct reaction between triplet and singlet molecules to yield a singlet product is a spin-forbidden process because chemical combination reaction rates are much faster than spin inversion rates. However, easily oxidizable singlet organic molecules, such as reduced flavin 1.4, are able to react with triplet oxygen by forming a resonance-stabilized (one-electron oxidized) radical 1.7, which pair with superoxide to form a triplet complex 1.10. The singlet 4a-hydroperoxyflavin 1.5 is generated by spin inversion sequentially.⁶⁻⁷

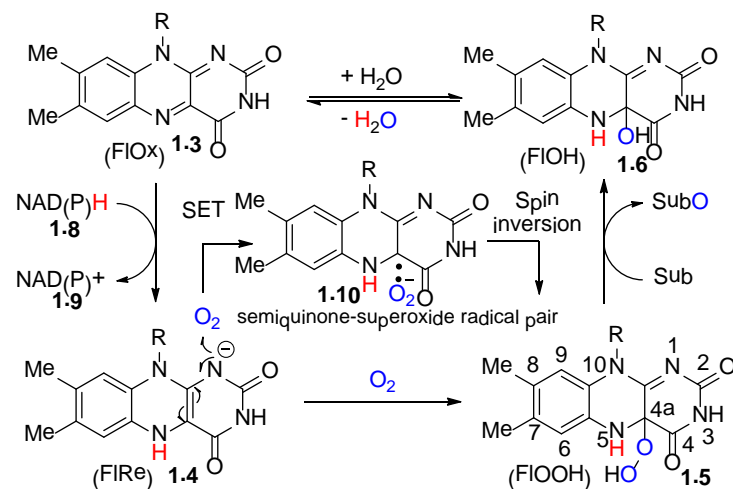


Figure 1.3 Mechanism of flavin containing monooxygenase

The O-O bond of 4a-FIOOH 1.5 is inductively polarized by the electronegativity of the N^1 , N^5 , N^{10} and $C^4=O$ of the ring. The electronegativity of the C^{4a} position is responsible for the low pKa value of the FIOOH terminal proton and the electrophilicity of the peroxide terminal oxygen. 4a-FIOOHs are powerful reagents for the electrophilic *N*-oxidation of tertiary, secondary and hydroxyl amines as well as *S*-oxidation of sulfides. These oxidations are first order in both 4a-FIOOH and substrate to generate *N*-oxide or *S*-oxide and the 4a-FIOH pseudobase 1.6. The second-order rate constant of flavin catalyzed reaction exceeds those obtained with H_2O_2 and *t*-BuOOH by 10^4 to 10^5 times.⁵

In addition to the electrophilic oxidations mentioned above, the nucleophilic Baeyer-Villiger oxidation of ketones to lactone or esters are known to be achieved by flavin containing monooxygenase.⁸ These flavoproteins were found in various bacteria and fungi. The most extensively studied and utilized Baeyer-Villiger monooxygenase (BVMO) is cyclohexanone monooxygenase(CHMO) from *Acinetobacter* sp. NCIB 9871, which has been shown activities of oxidizing a range of acyclic, cyclic, bicyclic, tricyclic and heterocyclic ketones with variety of substituents and substitution patterns, to chiral lactones and esters with high chemo-, regio- and enantioselectivity.⁸ The crystal

structures of several types of BVMO have been obtained.⁹ These structures revealed that the monooxygenase (phenylacetone monooxygenase and cyclohexanone monooxygenase) is constructed with a FAD-binding and a NADPH-binding domain, where the active site can be found in a cleft at the interfaces of the two domains. The enzyme active site contains a strictly conserved arginine (R337 in PAMO) which was suggested to play an important role in the stabilization of the 4a-hydroperoxyflavin and Criegee intermediate. However, recent detailed kinetic study showed that 4a-hydroperoxyflavin is still formed and stabilized upon replacing Arg337 by an alanine in these enzymes, questioning the need for cationic activation and stabilization of this transformation.¹⁰

1.1.2 Dehydrogenases

Dehydrogenase and reductase enzymes transfer electrons from one substrate to another. Dehydrogenases oxidize an organic substrate with the use of a specific acceptor such as NADP⁺ 1.9, while reductases transfer electrons from a specific electron donor such as NADH to their organic substrate.(Figure 1.4)

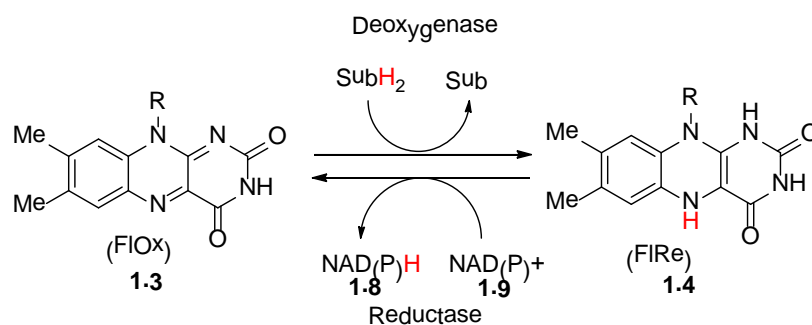


Figure 1.4 Mechanism of flavin containing dehydrogenase and reductase

For example, the introduction of unsaturation α , β to a carboxyl group is performed by an important group of flavoenzymes. Acyl-CoA dehydrogenases involved in the oxidation of fatty acids 1.11 and 1.14. (Figure 1.5) The mechanism has been

proposed that the initial step is the ionization of the proton α to the carboxyl group followed by flavin oxidation of the resultant carbanion 1.12 and 1.15 to form products 1.13 and 1.16. The mechanistic details of how the flavin oxidizes the carbanion (radical process or two-electron transfer) are still unknown.⁵

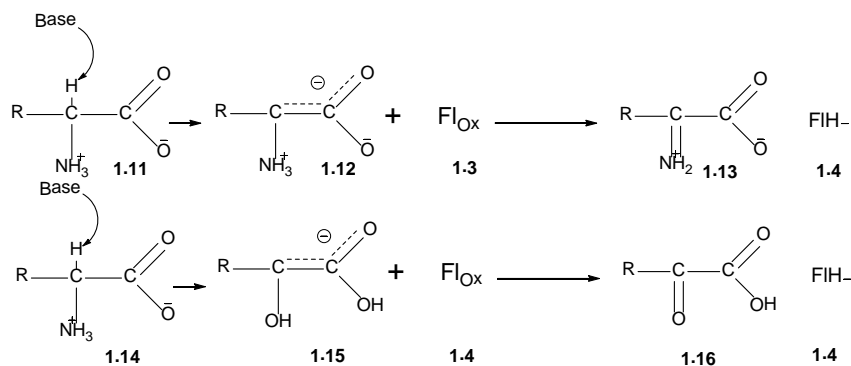


Figure 1.5 Proposed mechanism of flavin containing dehydrogenase

1.2 Biomimetic Flavin Organocatalysts

The catalysis with small organic molecules, where an inorganic element is not part of the active mechanism, has become a highly dynamic area in chemical research. The catalyst utilized is defined as organocatalyst.¹¹ Organocatalysis has superior advantages over biocatalysis and metal catalysis in many aspects. Compared to biocatalysis, which requires sensitive and specific enzymatic system and expensive stoichiometric bio-reagent such as NAD(P)H, organocatalysts have broader substrate scope, more tolerance of large concentration changes in substrates and products, heat, air and moisture, as well as considerable lower cost. Compared to metal catalysis, organocatalysis has the advantages of lower toxicity and cost. Therefore, organocatalysis is very attractive in the development of selective, mild, sustainable, and cost effective reaction processes.¹¹

Flavin organocatalysis thrived over the last two decades because of its high reactivity toward a range of electrophilic and nucleophilic oxidation reactions. In general,

two categories of flavin organocatalysts were designed and synthesized in the literature: alloxazine 1.17 and isoalloxazine 1.18. (Figure 1.6) Depend on the role of flavin organocatalyst in specific reactions, they can be utilized for catalyzing both electrophilic oxidations and nucleophilic oxidations. Besides electrophilic and nucleophilic oxidations, flavin's application on photooxidation, reduction reaction, drug delivery and bio-image will also be discussed.

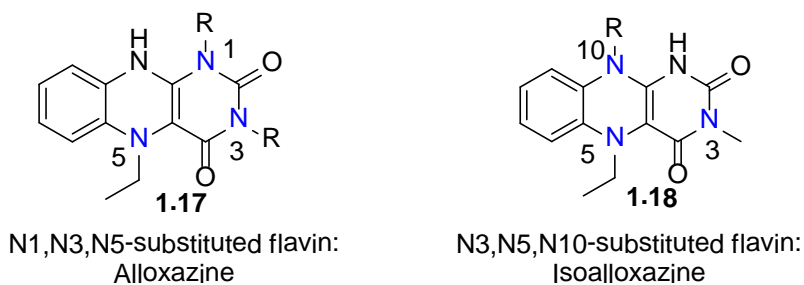


Figure 1.6 Artificial flavin organocatalysts: Alloxazine and isoalloxazine

1.2.1 Flavin Catalyzed Electrophilic Oxidations

1.2.1.1 Sulfur Oxidation

Murahashi and coworkers utilized lumiflavin derived catalyst 1.21a to oxidize aromatic and aliphatic sulfide 1.19 to sulfoxide 1.20. (Figure 1.7) Sulfoxide can be further oxidized to sulfone with one additional equivalent of H_2O_2 . The mechanism can be summarized in the catalytic cycle shown below.¹²

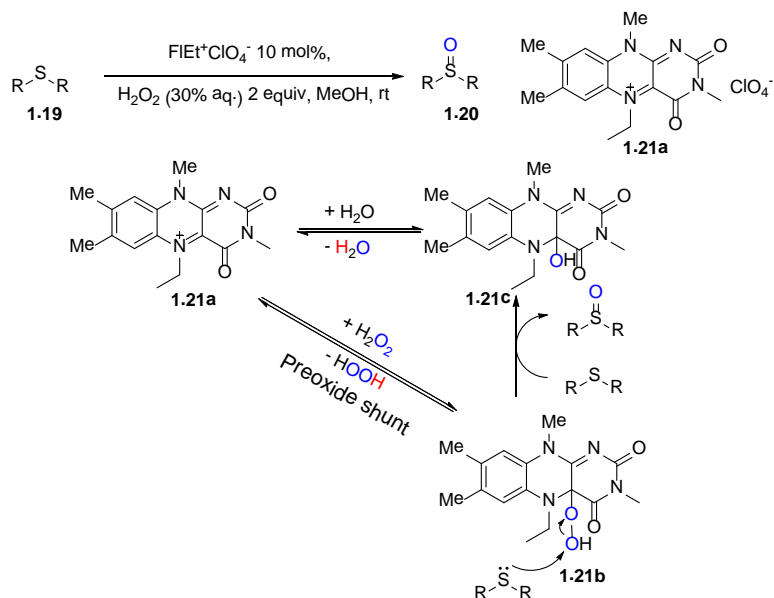


Figure 1.7 H_2O_2 sulfur oxidation with isoalloxazine

The same group published the aerobic version of sulfur oxidation of sulfide to sulfoxide using the same lumiflavinium catalyst 1.21a.¹³ (Figure 1.8) Instead of using H_2O_2 as terminal oxidant, the authors take advantage of oxygen and a reducing agent, hydrazine monohydrate 1.22, to turn over the flavin catalyst. The only byproducts are nitrogen gas and water. These oxidations were carried out in trifluoroethanol ($\text{CF}_3\text{CH}_2\text{OH}$), a solvent known for good oxygen solubility and a relatively pK_a . Great atom economy was achieved with this biomimetic transformation. The mechanism is as shown below.

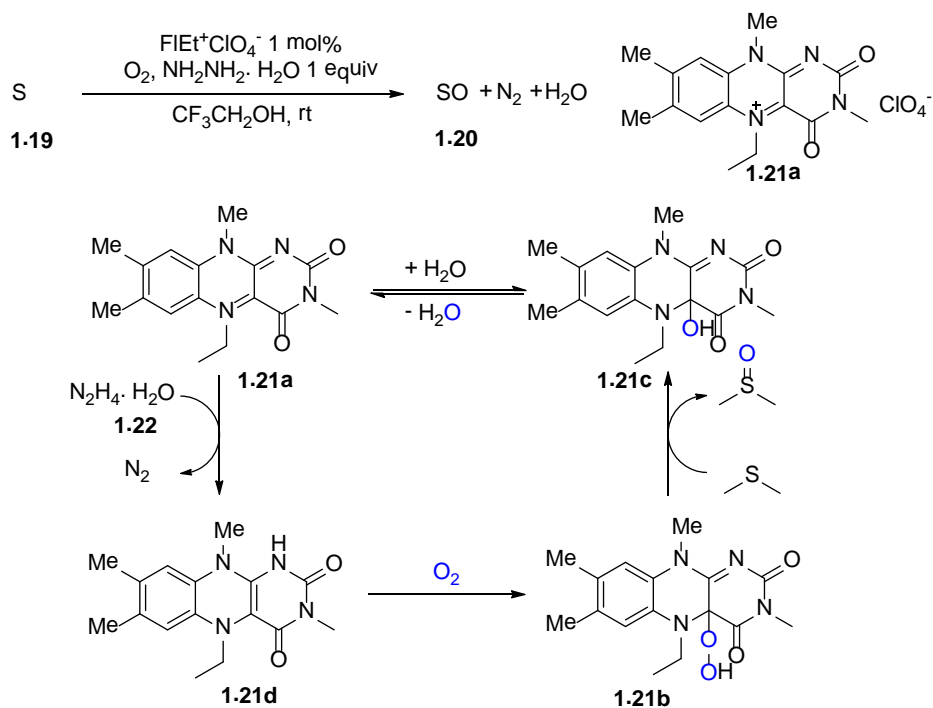


Figure 1.8 O_2 sulfur oxidation with isoalloxazine

Bäckvall and coworkers used *N,N,N*-1,3,5-trialkylated flavin organocatalyst **1.23a** to accelerate the H_2O_2 S-oxidation of a range of vinyl sulfides with great chemoselectivity.¹⁴ (Figure 1.9) No sulfones were isolated in this case. These reactions were performed in methanol. The advantage of using this alloxazine catalyst over isoalloxazine catalysts **1.21a** (Scheme 1.5) which were utilized by the Murahashi group is that the elimination of OH^- from 4a-hydroxyflavin **1.23c** to form oxidized flavin **1.23d** is favored due to aromatization. Since reduced flavin FIET_2 **1.23a** was used as a precatalyst, the activation of the catalyst using oxygen gas was necessary.

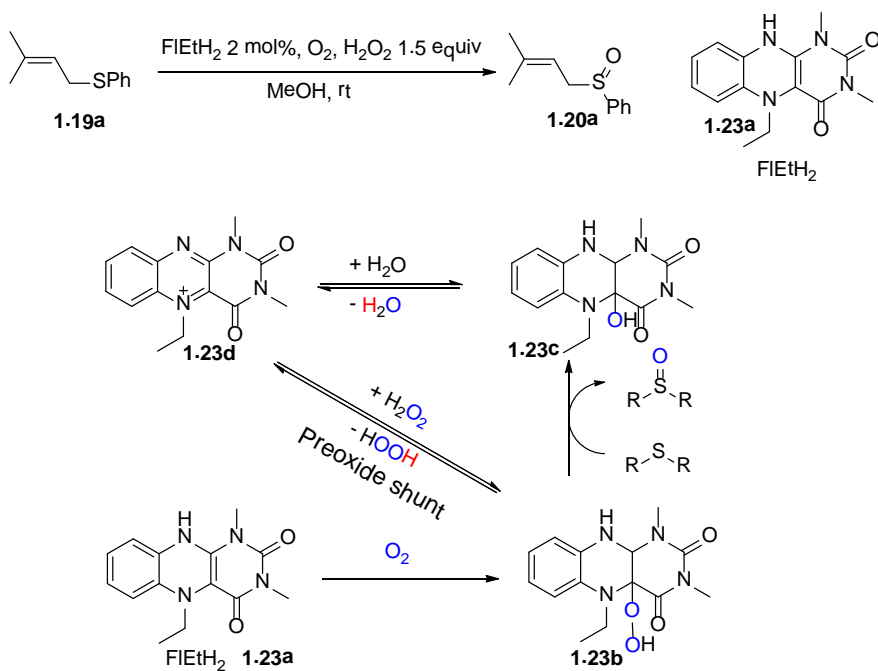


Figure 1.9 H₂O₂ sulfur oxidation with alloxazine

A range of alloxazine flavin catalysts with different substituents on the C⁷, C⁸ positions of the ring was synthesized by Bäckvall and coworkers. (Figure 1.10) The catalytic efficiencies of these alloxazine and isoalloxazine were compared using *N*-oxidation and *S*-oxidation as model reactions. They showed that alloxazine catalysts 1.23a, 1.24 and 1.27 are better catalysts than isoalloxazine on both *S*-oxidation and *N*-oxidation under the conditions given. They believed that electronegative substituents such as fluorines on the alloxazine could increase the electrophilicity of 4a-hydroperoxyflavin through inductive effects. The main reason why isoalloxazines 1.25, 1.26 and 1.21d had poorer catalytic effect is that they likely had difficulty eliminating the hydroxyl group from 4a-hydroxyflavin 1.21c to oxidized flavin 1.21a (Figure 1.8). In fact in the presence of a tertiary amine, the deprotonation of the 4a-hydroxyl group further prevents the elimination process.

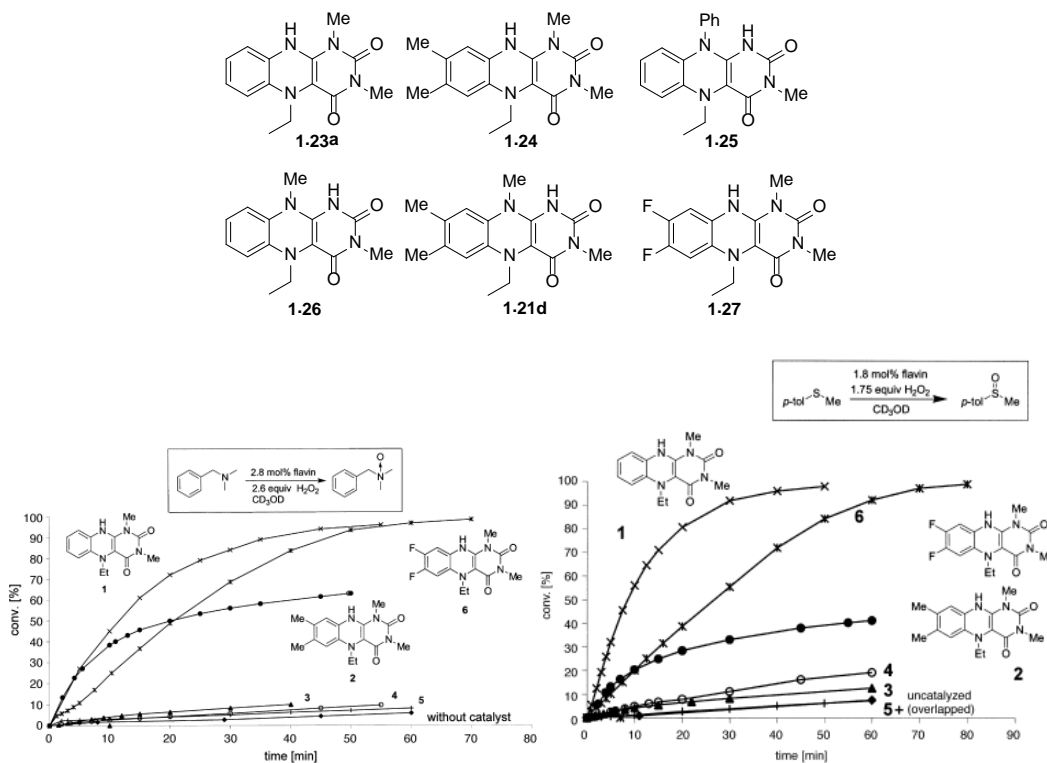


Figure 1.10 Comparison of a range of alloxazine and isoalloxazine catalysts' ability to accelerating amine and sulfur oxidation¹⁴

Based on established catalyst core structure, the flavin could be functionalized further to achieve specific applications. Carboxylated flavin 1.28 immobilized in an ionic liquid ([BMIm]PF₆) was used for the highly selective oxidation of sulfides to sulfoxides by hydrogen peroxide.¹⁵ (Figure 1.11) The sulfoxides were obtained in good to high yields and high selectivity without any detectable overoxidation to sulfone. The catalyst in the ionic liquid was recycled up to seven times without loss of activity or selectivity. A long alkyl chain substituted on *N*¹⁰ of isoalloxazine organocatalyst 1.29 was designed and synthesized by Cibulka and coworkers.¹⁶ This catalyst was solubilized in micelles of sodium dodecylsulfate (SDS), hexadecyltrimethylammonium chloride (CTAC), hexadecyltrimethylammonium nitrate (CTANO₃) or Brij 35. Reaction rates were strongly

dependent on the type of micellar matrix and on the pH value. The highest acceleration rate was found in SDS micelles at pH 4.4 (TOF = $3 \times 10^3 \text{ h}^{-1}$). The reaction rate was higher compared to the reaction in homogeneous solution. The factor of acceleration ranged from approximately 1.5 (non-ionic micelles) to 3 (anionic micelles).

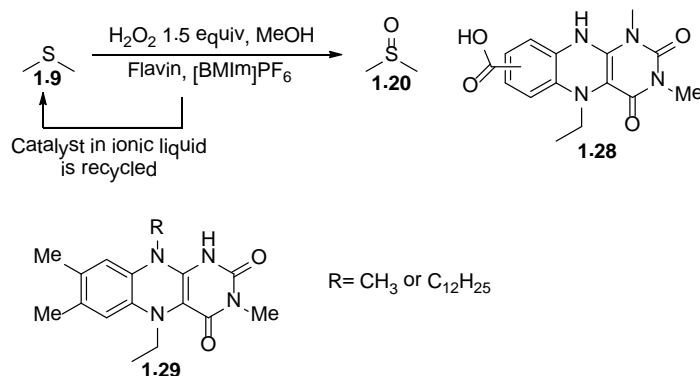


Figure 1.11 Functionalized flavins to meet special application

Carbery's group focused on applying bridged flavinium catalysts on different oxidation reactions.¹⁷ (Figure 1.12) 1.31c showed good catalytic activity on S-oxidation. No over oxidation product was observed in the H_2O_2 based oxidation.

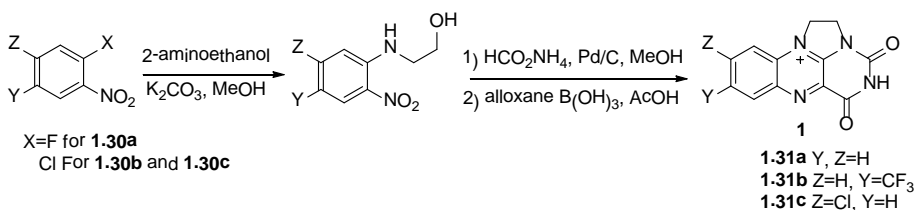


Figure 1.12 Synthesis of bridged flavinium catalysts

Cibulka's group utilized non-racemic N^1, N^{10} -ethylene-bridged flavinium salts with a stereogenic center derived from L-valinol to catalyze oxidation of sulfides to sulfoxides and the oxidation of 3-phenylcyclobutanone to the corresponding lactone at room temperature.¹⁸ The flavinium salts react with hydrogen peroxide to form flavin-10a-hydroperoxides 1.32a and 1.32b, which were the agents responsible for oxidation of the

substrate. (Figure 1.13) Although the flavin-10a-hydroperoxides existed with a diastereomeric ratio of 3:1, the attempts to utilize the flavin for asymmetric S-oxidation failed.

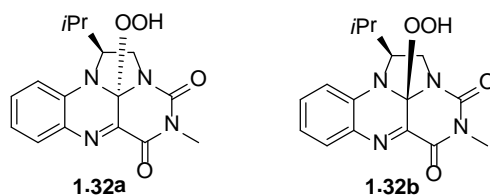


Figure 1.13 L-valinol derived bridged flavinium catalysts

Asymmetric sulfur oxidation to enantioenriched sulfoxide is a targeted research area for flavin chemists for a long time. The oxidation of sulfides with H_2O_2 using basket-shaped, optically active flavin 1.33 affords the corresponding sulfoxides with high enantioselectivity.¹⁹ (Figure 1.14)

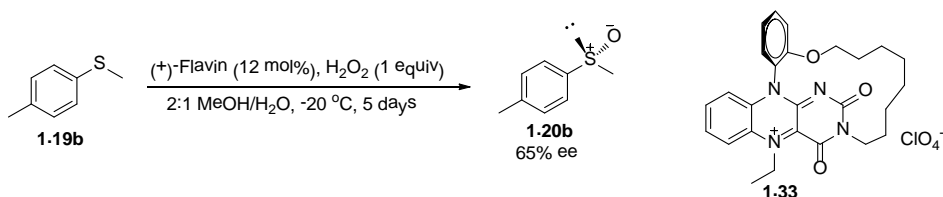


Figure 1.14 Basket-shaped flavinium salt catalyst catalyzed sulfur oxidation

Cibulka's group designed a novel planar chiral flavinium salt, 3-benzyl-5-ethyl-10-(8 phenylnaphthalen-1-yl)isoalloxazinium perchlorate 1.34, which bears a phenyl cap that covers one side of the isoalloxazinium skeleton plane. (Figure 1.15) Chiral HPLC was used to separate the racemic precatalyst followed by N^5 reductive alkylation to activate the catalyst. Sulfoxides with 34-54% e.e. was obtained using enantiopure catalyst at $-20\text{ }^\circ\text{C}$.²⁰

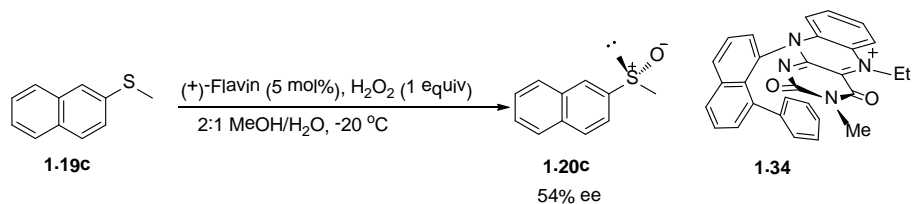


Figure 1.15 Planar chiral flavinium salt catalyst catalyzed sulfur oxidation

A beta-cyclodextrin flavin conjugate 1.35 was demonstrated by Cibulka and coworkers as highly efficient catalyst for the oxidation of electron-rich methyl phenyl sulfides to sulfoxides by hydrogen peroxide.²¹ (Figure 1.16) The catalyst showed fast near quantitative conversions and high enantioselectivities, reaching up to 80% e.e.. It is also remarkable that the reactions can proceed in neat aqueous media with only 0.2 mol% loading of the catalyst.

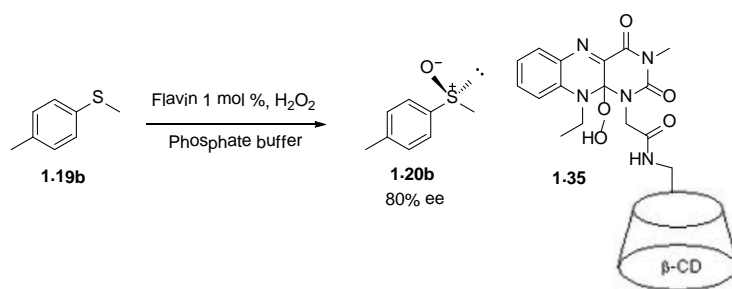


Figure 1.16 Beta-cyclodextrin flavin conjugates catalyzed sulfur oxidation

Main-chain optically active riboflavin polymer 1.36 was synthesized and used for chiral sulfur oxidation.²² Sulfur oxidation was achieved with up to 60% e.e. in THF at -40 °C.(Figure 1.17)

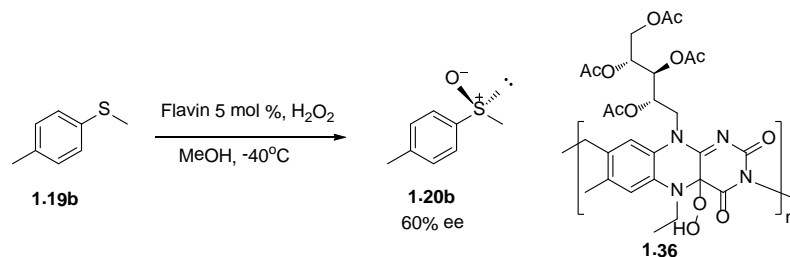


Figure 1.17 Riboflavin polymer catalyzed sulfur oxidation

1.2.1.2 Amine Oxidation

Murahashi and coworkers utilized lumiflavin derived isoalloxanium catalyst 1.21a to oxidize secondary amines 1.37a to nitrones 1.38a, hydroxyl amine 1.37b to nitrone 1.38b with excess H_2O_2 as terminal oxidant in methanol.¹²(Figure 1.18)

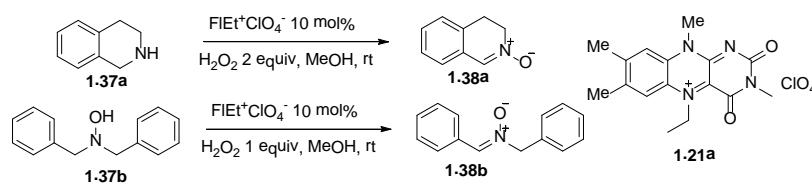


Figure 1.18 Isoalloxanium catalyzed *N*-oxidation of secondary amine

The same group published the aerobic version of *N*-oxidation of a series of secondary amine, hydroxyl amine and tertiary amines using the same lumiflavinium catalyst 1.21a.¹³ (Figure 1.19) The oxidations were carried out in $\text{CF}_3\text{CH}_2\text{OH}$. The mechanism of aerobic *N* oxidation is similar as that of the aerobic sulfur oxidation.

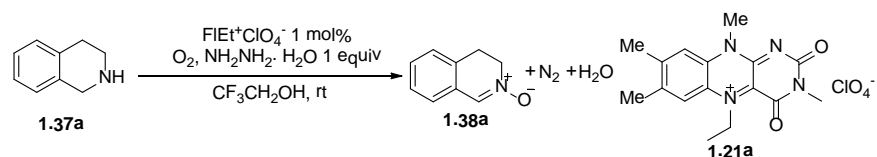


Figure 1.19 O_2 *N*-oxidation of secondary amine with isoalloxanium

Bäckvall and coworkers used their alloxazine catalyst 1.23a to oxidize the tertiary amine to *N*-oxide in methanol efficiently.(Figure 1.20) The reduced alloxazine 1.23a was used, so oxygen activation of the precatalyst was necessary.²³



Figure 1.20 H₂O₂ N-oxidation of tertiary amines with alloxazine

Cibulka's group performed a systematic study of the comparison of the catalytic abilities of various alloxazine and isoalloxazine sources on sulfur oxidation and tertiary amine oxidation.²⁴ They concluded that in the case of sulfur oxidation, for alloxazine catalysts, both alloxazine 4a-methoxy adduct and alloxazinium salt can be used as catalyst. But the latter needs a base as a cocatalyst to generate HOO⁻ because the neutral H₂O₂ is not nucleophilic enough to attack alloxazinium to form 4a-hydroperoxyflavin. In the isoalloxazine series, the C^{4a}-hydroxy adduct FIOH or dihydroform FIH₂ can also be utilized but only in the presence of the catalytic amount of an acid. The acid is needed to help elimination of the hydroxyl group to generate the oxidized isoalloxazinium anion, which is the rate determining step for this series of catalysts. In the case of amine oxidation, only alloxazine derivatives, i.e. dihydroalloxazines FIH₂ and their methoxy adducts FIOCH₃ or alloxazinium salts can be used as catalysts for the oxidation, as the catalytic activity of isoalloxazinium salts and their derivatives is inhibited under basic conditions.

In the flavin catalysis, it is very important to understand the property of different types of catalysts and the pH of system as well as solvent effect, as each factor could dramatically alter the reactivity of the catalysts.

1.2.2 Flavin Catalyzed Nucleophilic Oxidation

In flavin catalyzed nucleophilic oxidations, 4a-hydroperoxyflavin or 4a-hydroperoxyflavin anion attack the electrophilic site of the substrate followed by the dissociation of the hydroxyl flavin anion. Hydroxyl flavin eliminates one molecule of water

to complete the catalytic cycle by regenerating the oxidized flavin. The following examples showed the applications of flavin on Baeyer-Villiger oxidation.

1.2.2.1 Baeyer-Villiger Oxidation

Furstoss and coworkers first demonstrated the use of isoalloxazinium catalyst 1.25 in the Baeyer-Villiger oxidation of cyclobutanones 1.41a into γ -lactone 1.42a in *t*-BuOH with two equivalents of H_2O_2 .²⁵ (Figure 1.21) However, this catalyst only performed the oxidation on cyclobutanones. Five membered and six membered cycloketones were not effective substrates under the published condition.

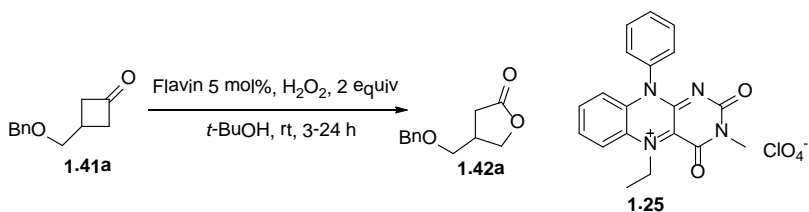


Figure 1.21 H_2O_2 Baeyer-Villiger oxidation of cyclobutanones catalyzed by isoalloxazinium

Murahashi's group synthesized a C_2 -symmetric bis-isoalloxazinium perchlorate salt 1.43 for the asymmetric Baeyer-Villiger oxidation of cyclobutanones.²⁶ (Figure 1.22) Substrates needed to have an aromatic substituent to interact with the catalyst through pi-pi stacking. Good facial selectivity was achieved and up to 74 % e.e. was obtained when the reaction was carried out at $-50\text{ }^\circ\text{C}$ in a solvent mixture of $\text{CF}_3\text{CH}_2\text{OH}/\text{MeOH}/\text{H}_2\text{O}$. Similarly to the previous example, no cyclopentanone or cyclohexanone was reported.

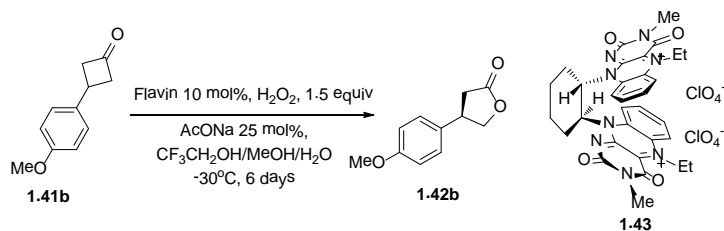


Figure 1.22 Asymmetric Baeyer-Villiger oxidation of cyclobutanones catalyzed by bis-isoalloxazinium

The same group developed an aerobic Baeyer-Villiger oxidation methodology using a riboflavin derived isoalloxazinium 1.44 as catalyst and zinc metal as stoichiometric reducing agent to oxidize cyclobutanone with oxygen as terminal oxidant.²⁷ (Figure 1.23) This catalyst also showed excellent chemoselectivity of nucleophilic BV oxidation over electrophilic sulfur oxidation. Unfortunately, no cyclopentanone or cyclohexanone was reported with this catalyst.

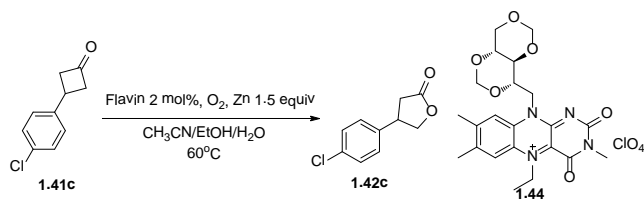
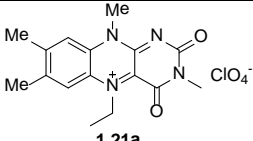
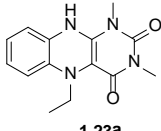


Figure 1.23 Aerobic Baeyer-Villiger oxidation of cyclobutanones catalyzed by riboflavin derived isoalloxazinium

In most case, isoalloxazine 1.21a or alloxazine 1.23a can be used to conduct sulfur, amine or Baeyer-Villiger oxidation. This following Table 1.1 summarizes the types of oxidation reactions versus kinds of catalysts that have been utilized and the conditions (additive, solvent) needed in each case.

Table 1.1 The choice of conditions for different oxidations

Oxidation	Sulfur oxidation		Amine oxidation			BV oxidation	
Oxidation	H ₂ O ₂	Aerobic	Secondary		Tertiary	H ₂ O ₂	Aerobic
Mode			H ₂ O ₂	Aerobic			
Catalyst	1.21a or 1.23a	1.21a or 1.23a	1.21a	1.21a	1.23a	1.21a	1.21a
Solvent	MeOH	CF ₃ CH ₂ O H	MeO H	CF ₃ CH ₂ OH	MeOH	<i>t</i> -BuOH	Mix- solvents
Reductant	N/A	NH ₂ NH ₂	N/A	NH ₂ NH ₂	N/A	N/A	Znic
<div style="display: flex; justify-content: space-around; align-items: center;"> <div style="text-align: center;">  <p>1.21a</p> </div> <div style="text-align: center;">  <p>1.23a</p> </div> </div>							

1.2.3 Applications of Flavin Other Than as Organocatalyst

Not only used as organocatalysts in synthetic organic chemistry, but flavins also find their applications in many other areas such as medical and pharmaceutically devices.

1.2.3.1 Flavin Biomarker

One example is that riboflavin was utilized to target tumor cells. Riboflavin is an essential component for cellular metabolism and is highly upregulated in metabolically active cells. Tumor cells are highly energy-demanding; therefore they require a relative large amount of flavin cofactor to activate the necessary catabolic enzymes. Target-specific and fluorescent flavin mononucleotide (FMN) coated Ultra Small Super Paramagnetic Iron Oxide nanoparticles (USPIO) 1.45 was designed by Fraaije's group to

mark the riboflavin carrier protein. (Figure 1.24) High efficiency of labeling cancer cells (PC-3, DU-145, LnCap) and activated endothelial cells was demonstrated with this novel biomarker.

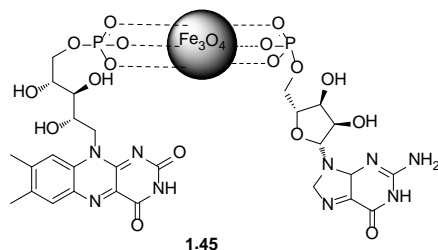


Figure 1.24 Riboflavin derived biomarker for detecting tumor cell

1.2.3.2 Flavin drug carrier

Riboflavin binding protein dodecin from *Halobacterium salinarum* was used by Nöll's groups to deliver riboflavin bonded drugs to the targeted position.²⁹ Dodecin binds oxidized flavin with high affinity 1.46 but releases the flavin when the flavin is reduced 1.47. (Figure 1.25) Upon blue-light triggered reduction of riboflavin, drugs can be transported at desired time and to desired location with high accuracy.

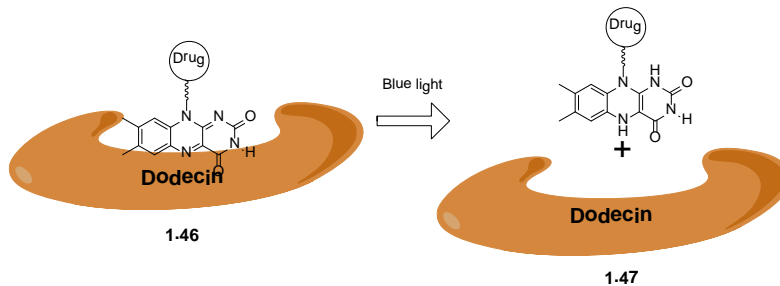


Figure 1.25 Blue light induced dissociation of flavin from dodecin

1.3 Outline of Dissertation

In this dissertation, I will focus on the discussion on the recent development of flavin organocatalysts as nucleophilic oxidizing agents for oxidizing carbon centers, i.e. Dakin oxidation and Weitz-Scheffer oxidation. A dual catalytic system will be described to

conveniently impose stereoselectivity to flavin catalyzed reactions in a cost effective manner Also, the flavin's application on the oxidation of pre-aromatic heterocyclic compounds will also be described.

Chapter 2

Flavin Catalyzed Dakin Oxidation

2.1 Baeyer-Villiger Oxidation

The Baeyer-Villiger oxidation (BVO), reported by Adolf Baeyer and Victor Villiger in 1899, is one of the most well-known and widely applied reactions in organic synthesis.³⁰ A variety of carbonyl compounds such as acyclic or cyclic ketones, benzaldehydes could be oxidized into esters, lactones, phenols or benzoic acids.

One advantage of this reaction is that the chemoselectivity can be precisely predicted with migratory aptitude as following: alkyl > cyclohexyl > secondary alkyl > benzyl > phenyl > primary alkyl > CH₃.³¹ Various oxidants could perform Baeyer-Villiger oxidation, with their reactivity decreasing in the order CF₃CO₃H > monopermaleic acid > monoperphthalic acid > 3,5-dinitroperbenzoic acid > *p*-nitroperbenzoic acid > *m*-CPBA ≈ HCO₃H > C₆H₅CO₃H > CH₃CO₃H » H₂O₂ > *t*-BuOOH.

The most active oxidants are expensive and hazardous peracids, which significantly limit the usage of BVO in industrial setting. BVO conducted by H₂O₂ with the activation of a catalyst in non-halogenated solvents is attractive because it avoids many issues such as high cost of oxidant, environmental, health and safety issues.³²⁻³³

Although H₂O₂ is a preferred green oxidant in chemistry industry for BVO, there are several problems associated with it. Commercially available hydrogen peroxide is in aqueous solution (30% or 60%). Water labile compounds may hydrolyze or decompose under reaction condition using aqueous H₂O₂. Also, H₂O₂ could be decomposed by metal impurities to generate O₂ therefore build up pressure and create a potentially unsafe combination with flammable organic solvents.³¹

Precautions to avoid such problems include: 1) avoid any contamination of reaction vessel. 2) avoid build-up O₂ pressure by purging with N₂. 3) keep the

concentration of peroxy compounds below 20% mol/mol by slow addition of H₂O₂. 4) Destroy excess H₂O₂ before work up. 5) avoid using acetone or any other low boiling ketone as the solvent for cleaning or workup.³¹

Molecular oxygen has been used as a terminal oxidant for BVO. Free radical autoxidation of an aldehyde is facile and affords the corresponding peracid, which oxidizes ketones 2.1 into esters 2.2.³⁵ (Figure 2.1) Ishii group reported the “aerobic” BVO of a cyclohexanol/cyclohexanone mixture to yield lactones.³⁶ However, in this reaction hydrogen peroxide generated by autoxidation of cyclohexanol 2.3 instead of peracid is the true oxidant in the BV reaction. Using O₂ for the in situ formation of hydrogen peroxide as the actual oxidants has been receiving much attention over the past years because it is cheaper than hydrogen peroxide itself.

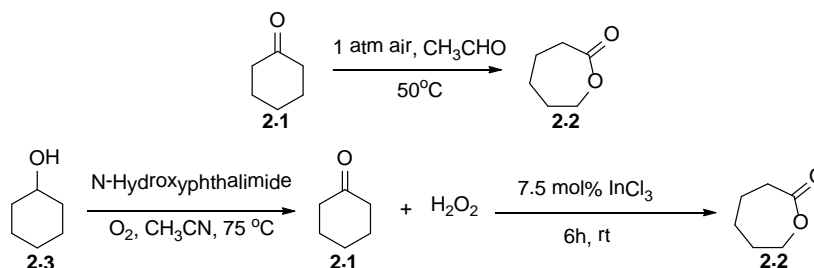


Figure 2.1 Aerobic Baeyer-Villiger oxidations

The mechanism of BV oxidation is a two-step reaction that involves the so-called Criegee intermediate. (Figure 2.2) In the first step, a peroxide 2.5 attacks the polarized C=O bond of 2.4 to form Criegee intermediate 2.6. The second step follows a concerted migration pathway. In the Criegee intermediate 2.6, a proper alignment is required for the rearrangement step: The migrating group R^M needs to be antiperiplanar to the O-O bond of the leaving group (primary stereoelectronic effect) and antiperiplanar to a lone pair of the hydroxyl group (secondary stereoelectronic effect). The elimination of an acid 2.7 affords the product ester 2.8.

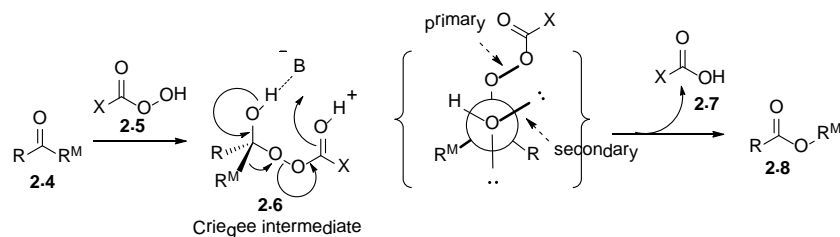


Figure 2.2 Stereoelectronic requirement of 1, 2 migration of Criegee intermediate

There are several activation modes that one can use to achieve catalysis of BVO using hydrogen peroxide as terminal oxidant (Figure 2.3). 1. Electrophilic activation of the substrate, 2. electrophilic activation of the intermediate, 3. nucleophilic activation of the intermediate, 4. nucleophilic activation of hydrogen peroxide, and 5. electrophilic activation of hydrogen peroxide.³¹

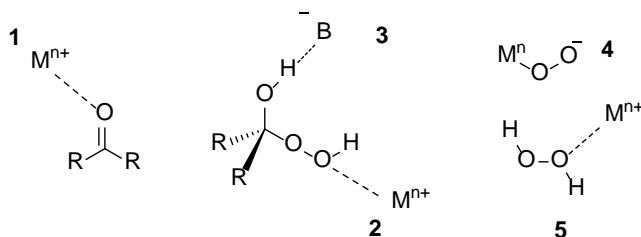


Figure 2.3 Activation mode of Baeyer-Villiger oxidation

The attempts to extend the current flavin catalyzed BVO of cyclobutanones to cycloketones with larger ring size, i.e. cyclopentanones and cyclohexanones, was conducted regarding the importance of this transformation.

Five alloxazine catalysts and one isoalloxazine catalyst were synthesized to be used as the BVO catalysts.

The synthesis of the five alloxazine was adopted from Bäckvall's publication.¹⁴ Condensation of *o*-phenylenediamine 2.9 with alloxan monohydrate 2.14 in acidic condition affords the tricyclic core structure 2.10. (Figure 2.4) Methylation of *N*¹ and *N*³ position happens smoothly with iodomethane in the presence of K_2CO_3 to form 2.11. The

reductive alkylation of N^5 position of 2.11 was conducted under strictly anaerobic condition by Pd/C-catalyzed hydrogenation using excess freshly distilled acetaldehyde in the presence of acid. Instead of keeping the product 2.12 at reduced state by working up the reaction under strictly inert atmosphere, the reaction is exposed to air to generate the active hydroperoxyflavin 2.13. This strategy not only simplifies the work up procedure greatly but also provides stable and useful flavin catalysts that are ready to enter the catalytic cycle without the additional oxygen activation step. Catalysts 2.13a and 2.13e were not previously reported. The reductive amination of dichloroalloxazine 2.11a gave exclusive dechlorinated product 2.13c in EtOH/H₂O under standard condition. To obtain the desired dichlorocatalyst 2.13a, extensive optimization of the reductive amination step was conducted. Changing the types of metal catalysts (Pd/C, Pt or Lindlar catalyst), amount of acid (0-10 equivalents) or H₂ pressure (15 psi or 80 psi) did not affect the dehalogenation process. However, when EtOH/H₂O solvent mixture was replaced with 1:1 EtOH/DCM, 1:1 of dichloro catalyst 2.13a/dehalogenated product 2.13c was isolated. 1.7:1 2.13a:2.13c was observed with in 1:4 EtOH/DCM. By omitting the protic solvent ethanol and using pure dichloromethane, 2.13a can be obtained in 80% isolated yield. Luckily, difluoro alloxazine 2.11b underwent Pd/C catalyzed reductive amination without the formation of dehalogenated products. However, higher H₂ pressure (80 psi) was needed in order to obtain good yield of the 2.13b.

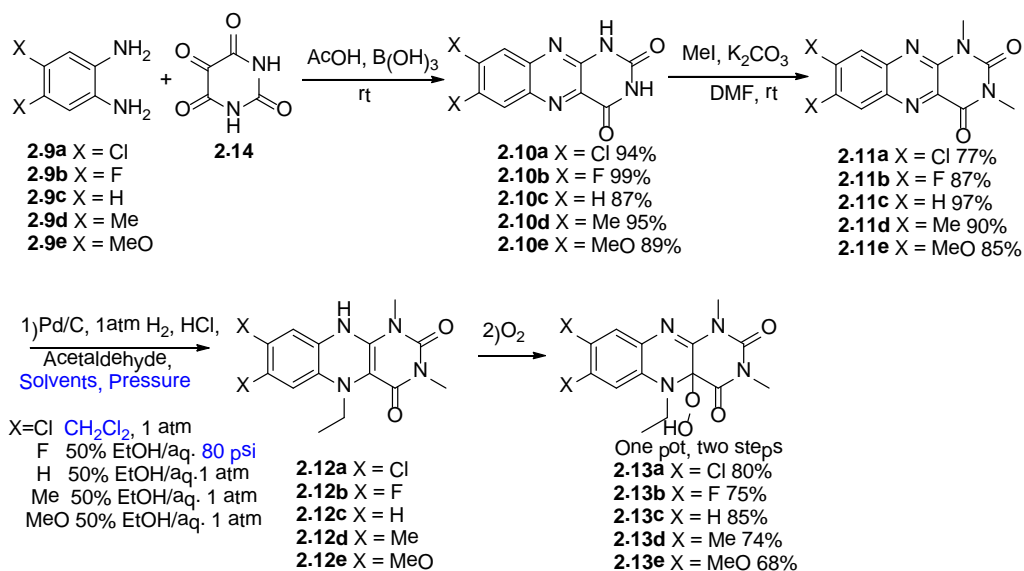


Figure 2.4 Synthesis of five alloxazine catalysts

Synthesis of isoalloxazine catalysts starts with nucleophilic substitution of chloride in 6-chlorouracil 2.16 by aniline 2.15 in neat condition. (Figure 2.5) Cyclization of 2.17 with nitrosobenzene 2.18 gives compound 2.19. A similar reductive amination step affords *N*⁵ ethylated isoalloxazine. The reduced isoalloxazine is then oxidized and converted to stable isoalloxazinium perchlorate catalyst 2.20, which is ready for catalysis.³⁷

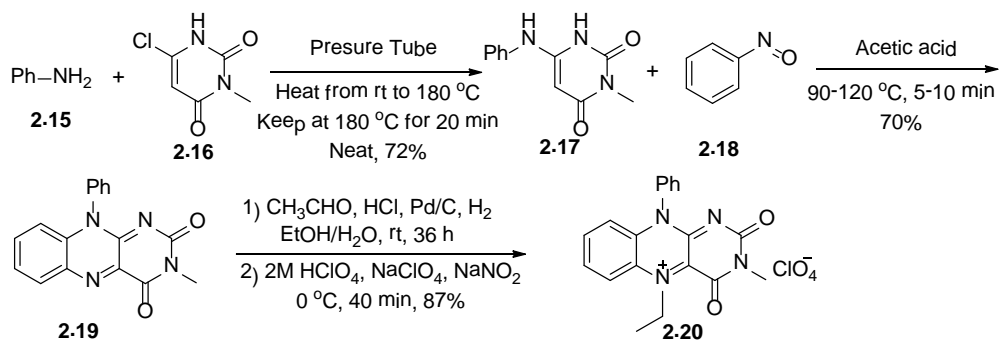


Figure 2.5 Synthesis of isoalloxazine catalyst

Three factors were considered in the condition screening: 1. Lewis acids; 2. solvents; 3. temperatures.

Lewis acid are known to facilitate the BVO in two aspects.³⁶ (Figure 2.6) One, they activate the carbonyl functionality toward nucleophilic attack of peroxide or peracid via increasing the polarization of the C=O double bond. Lewis acid increases H₂O₂'s acidity and therefore increases hydrogen bonding to the carbonyl functionality TS1. Two, the Lewis acid also facilitates the rearrangement step by migrating to the outer peroxygen, creating a BF₂OH leaving group rather than a hydroxide leaving group TS2.

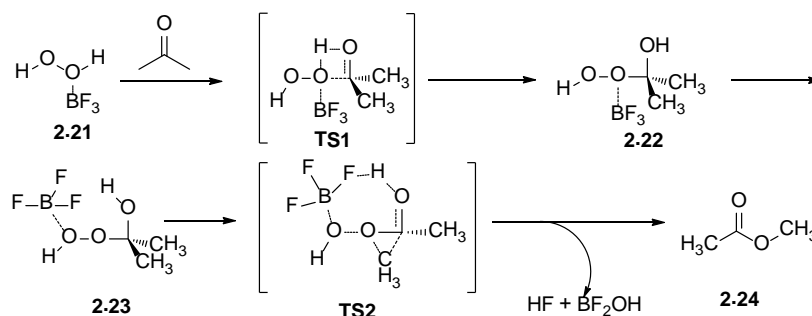


Figure 2.6 Lewis acid BF₃ assisted BV oxidation of acetone

However, with flavin catalysts and H₂O₂, neither cyclopentanones 2.25 and 2.26 nor cyclohexanones 2.27 and 2.28 were converted to desired lactones in the presence of CaCl₂, BF₃.OEt₂, LiCl, Zn(OAc)₂, AlCl₃ or MgCl₂. (Table 2.1) The reactions were conducted at room temperature and 50 °C, only starting materials were recovered in these reactions. This initial failure led us to question the mechanistic barriers to flavin activation of H₂O₂, flavoperoxide BVO, and catalytic cycle turnover.

Table 2.1 Conditions examined with flavin catalyzed BV oxidation of 5-and 6-membered cycloketones

	Cyclopentanone 2.25	2-methylcyclopentanone 2.26	Cyclohexanone 2.27	Cyclohexenone 2.28
Lewis acid	$\text{AlCl}_3, \text{BF}_3 \cdot \text{OEt}_2$	$\text{AlCl}_3, \text{BF}_3 \cdot \text{OEt}_2$	$\text{CaCl}_2, \text{BF}_3 \cdot \text{OEt}_2, \text{LiCl}, \text{AlCl}_3, \text{Zn}(\text{OAc})_2, \text{MgCl}_2$	$\text{AlCl}_3, \text{BF}_3 \cdot \text{OEt}_2$
Catalyst	2.13c, 2.13d, 2.20	2.13c, 2.13d, 2.20	2.13c, 2.13d, 2.20	2.13c, 2.13d, 2.20
Solvent	MeOH	MeOH	MeOH	MeOH
Temperature (°C)	25°C/ 50°C	25°C/ 50°C	25°C/ 50°C	25°C/ 50°C

The difficulty of conducting BVO with acyclic ketones, cyclopentanone as well as cyclohexanone was described in Ding and coworker's study by performing theoretical calculations on phosphoric acid catalyzed BVO using H_2O_2 as oxidant.³⁸

In the phosphoric acid catalyzed BVO, the rate determining step was believed to be the acid mediated 1, 2 -rearrangement of alkyl group starting from the Criegee intermediate. The activation barriers of the migration for cyclobutanone, acetone, cyclopentanone and cyclohexanone were calculated to be 20.2, 31.2, 27.0 and 25.5 kcal/mol respectively. These results are interpreted in terms of the larger ring strain in cyclobutanone weakens the C-C bond and makes the migration of methylene group more

favorable. Similarly, they failed to apply phosphoric acid catalyzed BVO to more challenging larger ring ketones.³⁸

2.2 Dakin Oxidation

2.2.1 Current Methods for Dakin Oxidation

The Dakin oxidation is a variant of Baeyer-Villiger oxidation, bearing a broadly similar mechanism. Instead of an aliphatic ketone substrate, the Dakin oxidations convert *o*- or *p*-hydroxyl substituted benzaldehydes and acetophenones into phenols or hydroquinones and a carboxylate byproducts with H₂O₂ in the presence of sodium hydroxide. Overall, the sp²-sp² aryl bond is oxidized and H₂O₂ is reduced.

The mechanism of Dakin oxidation differs with different reaction conditions. In general, it can be categorized into acid-catalyzed or base-catalyzed mechanisms. Both conditions involve a 1, 2-aryl shift associated with the collapse of tetrahedral Criegee intermediate 2.31. The proposed mechanism for base-catalyzed Dakin oxidation of 2-hydroxybenzaldehyde or acetophenone generates catechol 2.33 via an aryl formate 2.32, followed by hydrolysis. (Figure 2.7)

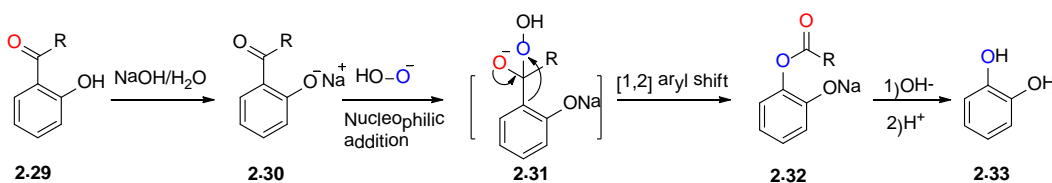


Figure 2.7 Mechanism of Dakin oxidation under basic condition

Many methodologies were developed to facilitate this transformation.

Methyltrioxorhenium (MTO) 2.34 can be used as a catalyst to achieve Dakin oxidation of *meta* or *para* methoxy or hydroxyl substituted benzaldehydes to give

corresponding phenols with H_2O_2 in good yield.³⁹ (Figure 2.8) The reactive intermediate is a bis-peroxo metal $[\text{CH}_3\text{ReO}(\text{O}_2)_2]$ complexes dpRe 2.36. In this system, 2 mol% of MTO was generally applied and excess H_2O_2 was needed. EtOH was proving the best solvent. The reaction typically was stirred at 50 °C for 24 hours. No base or acid is required. 57-86% phenol products were isolated. However, noticeable amount of benzoic acid byproduct and unhydrolyzed ester were isolated in some cases.

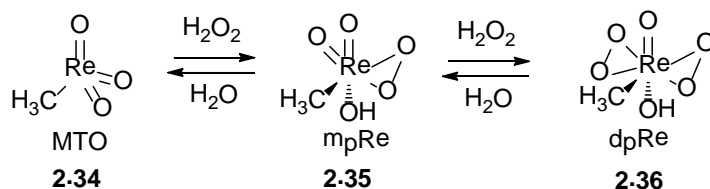


Figure 2.8 Methyltrioxorhenium(MTO), mono-peroxo complexes (mpRe) and active intermediate bis-peroxo complexes (dpRe)

The same catalyst 2.34 has been used with the help of ionic liquid $[\text{bmim}]\text{PF}_6$ 2.37 as a solvent.⁴⁰ (Figure 2.9) Good yield was achieved in 2-24 hours, which was relatively faster than the reactions conducted in traditional organic solvents.

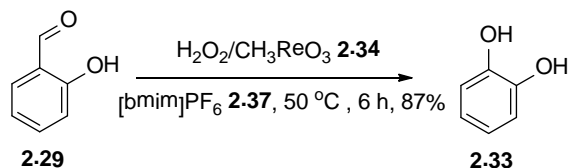


Figure 2.9 MTO catalyzed Dakin oxidation in ionic liquid

Solvent free Dakin oxidation was achieved by mixing starting benzaldehydes and solid *m*CPBA using pestle and mortar.⁴¹ A range of non-hydroxylated benzaldehydes was converted to phenols in the absence of a base.

Sodium percarbonate 2.38 ($\text{Na}_2\text{CO}_3 \cdot 1.5 \text{H}_2\text{O}_2$) was used as a stoichiometric oxidant for Dakin oxidation of a range of hydroxyl benzaldehydes and acetophenones.⁴² (Figure 2.10) The oxidant acts as its own base and a typical reaction was conducted in

2:5 water:THF dual solvent system under ultrasonication in argon atmosphere. A THF-DMF-H₂O solvent system was used for Dakin oxidations for acetophenone.

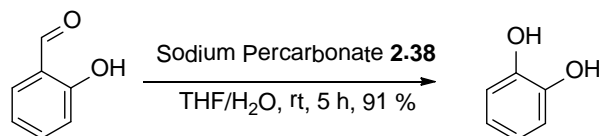


Figure 2.10 Dakin oxidation using sodium percarbonate as oxidant

Strong acid conditions were shown to be suitable for oxidizing benzaldehydes and acetophenones to phenols. Boric acid has been used to conduct Dakin oxidation in the presence of H₂O₂ and concentrated H₂SO₄.⁴³ Typical reactions use 5 equivalents of boric acid, 2 equivalents of H₂O₂ and excess of H₂SO₄. Although phenol was the main product, benzoic acid was detected for most of the substrates.

Urea-hydrogen peroxide 2.39 (UHP) can be used as stoichiometric oxidation for the Dakin oxidation in neat conditions.⁴⁴ (Figure 2.11) Benzaldehydes and acetophenones are active substrates. These reactions were conducted at 85 °C.

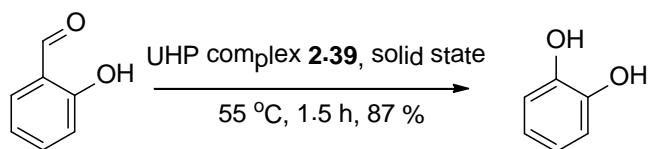


Figure 2.11 Dakin oxidation using urea-hydrogen peroxide complex as oxidant

2.2.2 Flavin Catalyzed Dakin Oxidation Using H₂O₂ as Terminal Oxidant

Although a handful of reagents and conditions are available for Dakin oxidation, many of them require heat, metal catalysts, harsh pH conditions as well as stoichiometric strong oxidants. We thought that flavin analogs could be used as an organocatalyst to accelerate this transformation in ambient temperature and milder pH conditions, which could be attractive for the application of Dakin oxidation on structural complex molecules or large scale reactions. Inspired by the H₂O₂ shunt process in the flavin biomimetic cycle

(Figure 2.12 highlighted in red), we planned to develop a flavin catalyzed Dakin oxidation using H_2O_2 as a terminal oxidant to turn over the reaction catalytic cycle.

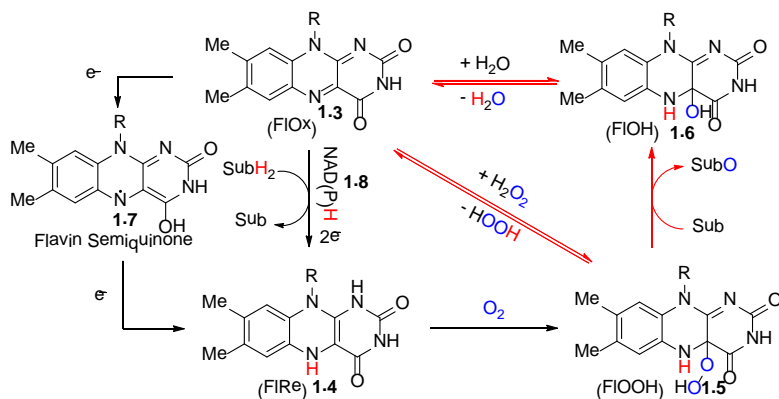


Figure 2.12 Dakin oxidation inspired by flavin H_2O_2 shunt process

Due to the lower pKa and O-O heterolytic bond lability of 4a-hydroperoxy alloxazine in comparison to H_2O_2 and other alkyl peroxides, we envisioned that alloxazine catalyzed reactions should be more effective under mild conditions compared to hydrogen peroxide and other alkyl peroxide reactions.

To understand how electronic effect alters the reactivity of alloxazine catalysts, previously synthesized five alloxazines 2.13a-e were used as Dakin oxidation catalysts.

We initially used 7, 8-diH alloxazine catalyst 2.13c for the catalysis of Dakin oxidation of salicylaldehyde under strong basic condition (with 1 equiv NaOH). In this case, both catalyzed reaction and non-catalyzed reaction were very fast. Within 10 minutes, all of the starting material was converted to catechol. We envisioned that the fast background HOO^- oxidation dominated the reaction pathway. Also, under strong basic condition, we have observed hydrolysis degradation of alloxazine catalyst 2.11c. Byproduct such as 2.40 could be formed, which may cause the loss of catalytic activity of the alloxazine. (Figure 2.13)

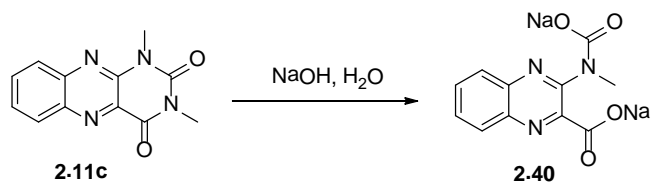


Figure 2.13 Possible alloxazine degradation pathway under strong basic condition

In order to create a condition that does not need a strong base like NaOH, which may cause problems of chemoselectivity when there are base labile functional groups in more complex molecules, we performed a base study to find the mildest base that was needed for the flavin catalyzed Dakin oxidation. The following Figure 2.14 showed relative rate of difluoroalloxazine catalyzed Dakin oxidation of salicylaldehyde compared to non-catalyzed reaction using different types of bases. The data was obtained using HPLC by calculating the concentration of salicylaldehyde after 30 minutes and 60 minutes (Figure 2.14. The first bar of the same color represent the non-catalyzed reaction, the second bar represent the catalyzed reaction).

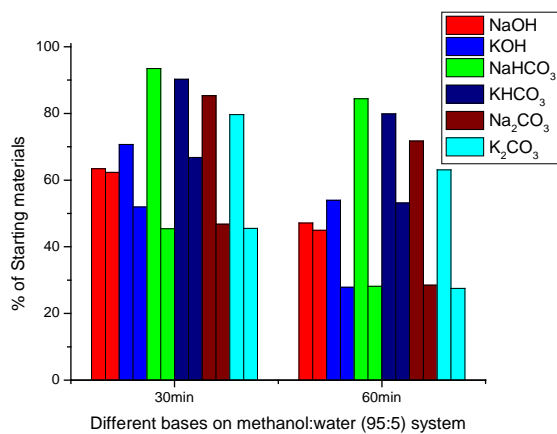
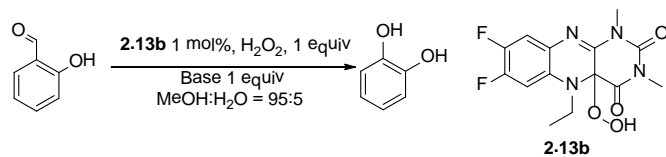


Figure 2.14 Base effect of flavin catalyzed Dakin oxidation

The reactions with hydroxide bases (NaOH and KOH) showed almost no flavin catalytic effects. Both the catalyzed reaction and the control had similar amount of starting material left after 30 minutes and one hour. However, for weaker bases (NaHCO₃, KHCO₃ and Na₂CO₃), the catalyzed reactions were faster in all cases, leaving less starting material after 30 minutes and 60 minutes. Control reactions with weaker bases were a lot slower compared to controls with strong bases, while catalyzed reactions with weaker bases were generally faster or equivalent to catalyzed reactions with strong bases. We were pleased to find out weaker bicarbonate bases perform Dakin oxidation with flavin catalyst very efficiently.

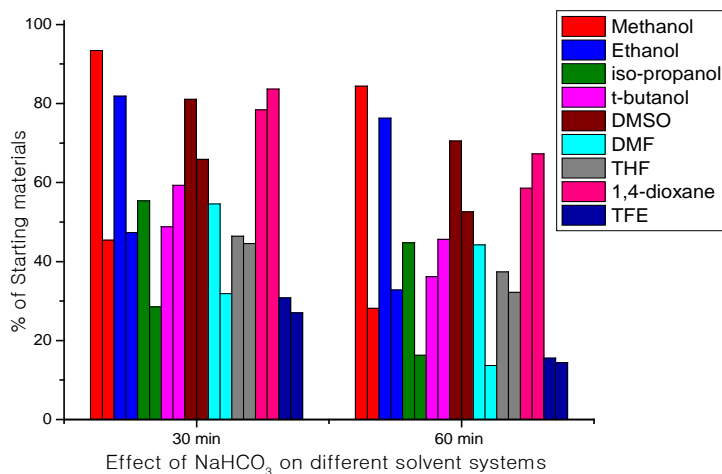
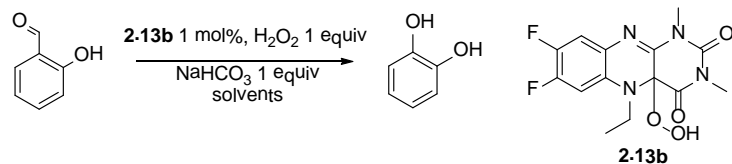


Figure 2.15 Solvent effect of flavin catalyzed Dakin oxidation

Solvent plays an important role in the progress of the flavin catalyzed reaction (Figure 2.15). A similar HPLC study was conducted with different solvents for catalyzed reaction as well as controls. Most alcoholic solvents showed rate acceleration for catalyzed reactions except for *t*-BuOH. DMSO is a poor solvent for Dakin oxidation, even with the help of flavin catalyst. DMF showed good reaction rate, but due to work-up difficulties associated with the solvent, we did not use it for further substrate study. TFE (2, 2, 2-trifluoro ethanol) showed good result for both catalyzed and non-catalyzed reactions. However, due to environmental safety and cost concerns, we did not use it as a solvent in our further study. As a result, we finalized methanol as the solvent for the substrate studies.

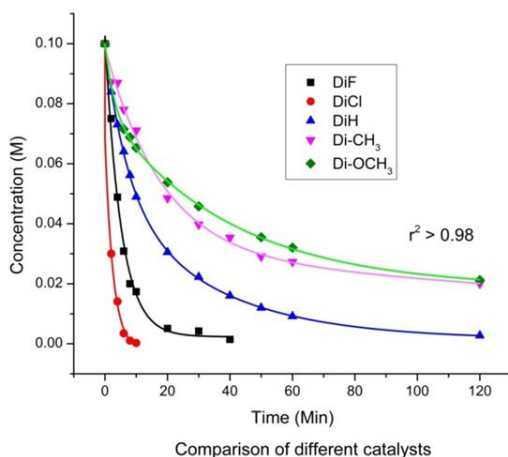


Figure 2.16 Comparison of the catalytic abilities of alloxazines on Dakin oxidation of salicylaldehyde

The catalytic efficiency of Dakin oxidation was evaluated by comparing the rate of Dakin oxidation of salicylaldehydes using five different alloxazine catalysts (Figure 2.16). The reaction progresses were monitored by HPLC and the concentrations of starting material salicylaldehyde were calculated with the reference of anisole as an internal standard. As shown in Figure 2.4, dichloro-alloxazine 2.13a resulted in the fastest consumption of starting material, followed by difluoro 2.13b, dihydrogen 2.13c, dimethyl 2.13d and dimethoxy-alloxazine 2.13e.

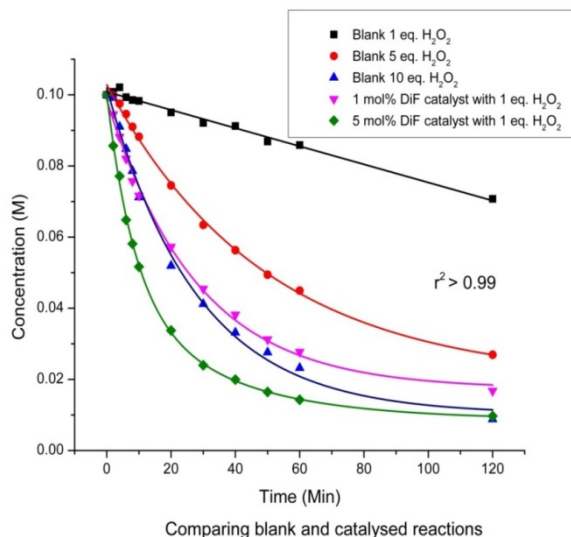


Figure 2.17 Rate acceleration effect of alloxazine catalyst

To illustrate the rate acceleration effect of flavin catalyzed Dakin oxidation, uncatalyzed reactions with different amount of H_2O_2 were set up along with the catalyzed reactions. (Figure 2.17) Similar to last chart, starting material concentrations versus time was shown in Figure 2.17. 1 mol% difluoro-alloxazine 2.13b catalyzed reaction with 1 equivalent of H_2O_2 (magenta) had similar initial reaction rate as that of the un-catalyzed reaction with 10 equivalents of H_2O_2 (Blue), which was faster than uncatalyzed reaction with 5 equivalents H_2O_2 (red). By increasing the catalytic loading to 5 mol% (green), the reaction rate was much faster than the control reaction (black).

These results showed that alloxazine accelerated the Dakin reaction under mild basic condition (NaHCO_3 as base). Presumably, alloxazine could facilitate Dakin oxidation in two aspects. (Figure 2.18) First, because of the electron deficient nature of the alloxazine ring, the terminal proton of the 4a-hydroxy alloxazine 2.13 is more acidic than that of the hydrogen peroxide, so that it can undergo deprotonation very well in the presence of sodium bicarbonate to generate the active nucleophilic oxidative

species, hydroperoxy alloxazine anion. Second, in the 1, 2 aryl migration step of Dakin oxidation mechanism, hydroxyl anion leaving group is generated. Alloxazine 2.41 can stabilize the negative charge by inductive effect of either the electron-withdrawing groups on the aromatic ring or the nearby N^{δ} -nitrogen and C^{δ} -carbonyl group.

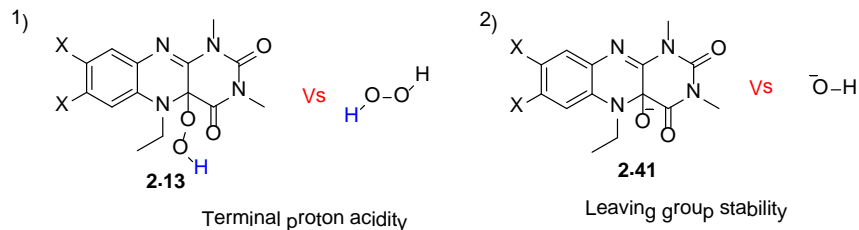


Figure 2.18 Rational of the rate acceleration by alloxazine catalyst

With the optimized condition, we established the standard reaction condition for the substrate scope study: 10 mol% dichloro-alloxazine 2.13a, 5 equivalents H_2O_2 , 1 equivalent $NaHCO_3$ with 95% aqueous methanol as solvent at room temperature. (Figure 2.19) 0.2 mmol scale reactions were set up for different substrates and monitored by TLC. To our delight, most of *ortho* or *para* hydroxyl benzaldehyde we tested underwent Dakin oxidation very efficiently under standard reaction condition. Typically, reactions finished within 30 minutes and more than 75% yields were isolated. Catechols or hydroquinones were the only products observed and isolated for these substrates. No hydride migration products, benzoic acids, were detected in these reactions. For 2.42f, quinone was generated through phenol intermediate, likely due to their electron rich nature.

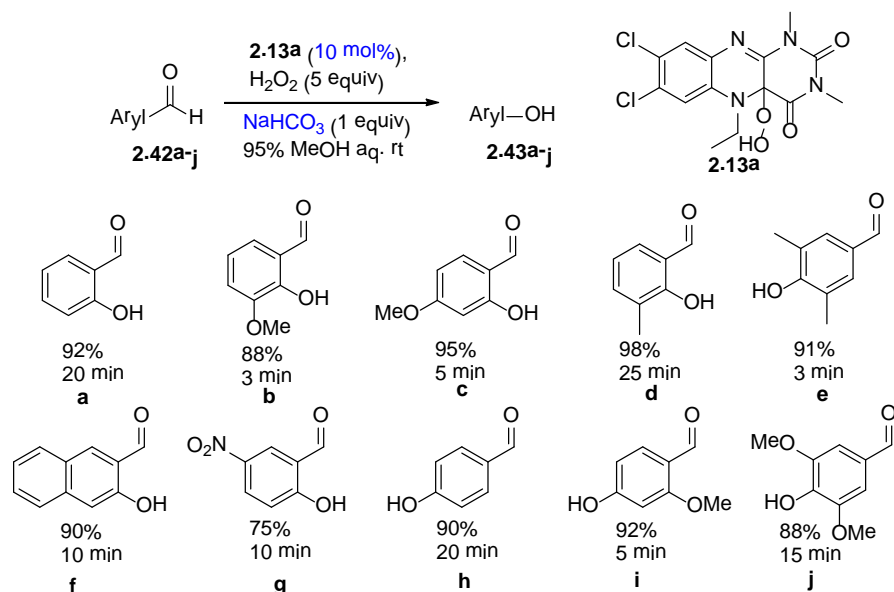


Figure 2.19 Alloxazine catalyzed Dakin oxidation of hydroxyl benzaldehyde

Benzaldehyde substituents and their substitution pattern are important to the results of the flavin catalyzed Dakin oxidation. Benzaldehydes without hydroxyl substitution mostly did not generate phenol product. With one exception, 2.42k was converted to phenol product 2.43k by difluoro-alloxazine 2.13b catalyzed condition with extended reaction time. Presumably, the 1, 2-aryl migration of the Criegee intermediate is facilitated through the resonance electron donating effect of the *ortho* or *para* hydroxyl substitution, which is even better if hydroxyl is deprotonated to form more electron-rich hydroxyl anion. (Figure 2.20)

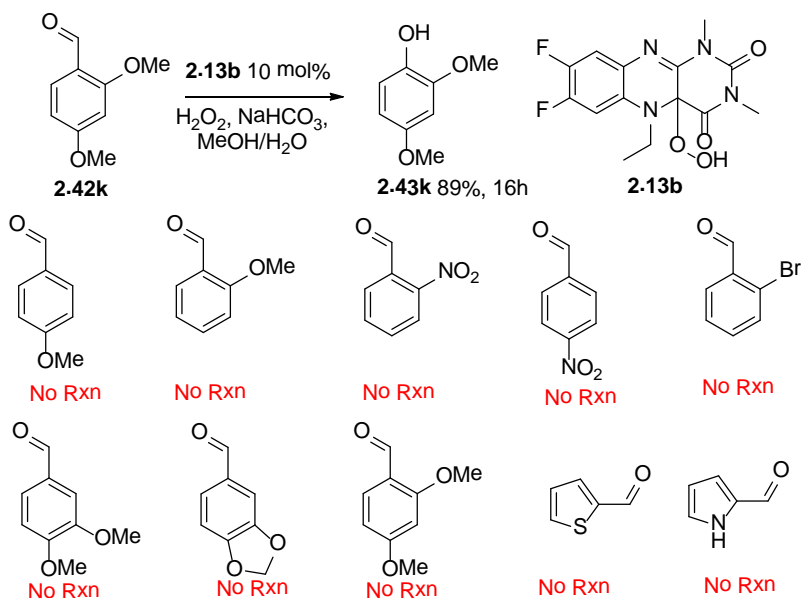


Figure 2.20 Non-hydroxylated substrates failed to undergo Dakin oxidation

In fact, a recent relevant finding by Carbery's group showcased the bridged flavin 2.44 catalyzed Dakin oxidation of electron-withdrawing group substituted benzaldehyde 2.42l. (Figure 2.21) In this case, 1, 2-hydride migration was favored over aryl shift because the aryl group was too electron-poor. So, benzoic acids 2.43l were obtained instead of phenols.⁴⁵

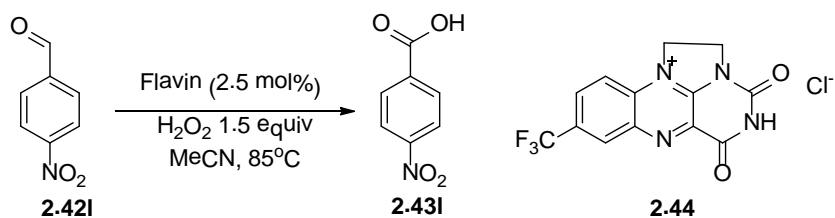


Figure 2.21 Benzoic acid formation from electron poor benzaldehyde

Dakin oxidation of less reactive acetophenones is more challenging because ketone carbonyl is less reactive towards nucleophilic attack. A range of Lewis acids additives was tested but resulted in no product. (Figure 2.22) Serendipitous finding allowed the Dakin oxidation of 2-hydroxyl acetophenone to catechol by using 10% DMSO

as a co-solvent in aqueous MeOH solution. However, 4-hydroxyacetophenone failed the Dakin oxidation even with enhanced solvent system.

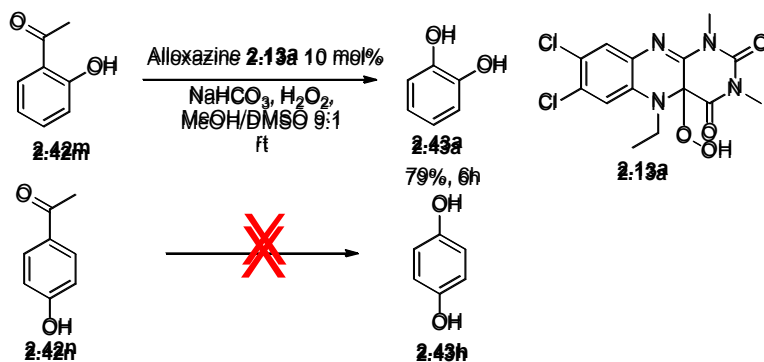


Figure 2.22 Dakin Oxidation of hydroxylated acetophenones

To identify the rate-determining step within the oxidation experimentally, a Hammett linear free-energy relationship was constructed between the initial rates of Dakin oxidations by different catalysts with various inductive effects. Linear agreements occurred between the individual or summed σ_i values and $\log(k_R/k_H)$ yielding a positive slope ($\rho > 0$). (Figure 2.23) This indicates an increase of charge on the catalyst during the rate-determining step. This is consistent with formation of a 4a-alkoxyflavin anion (FIO-2.13-3) during collapse of Criegee intermediate 2.13-2 (Figure 2.24).

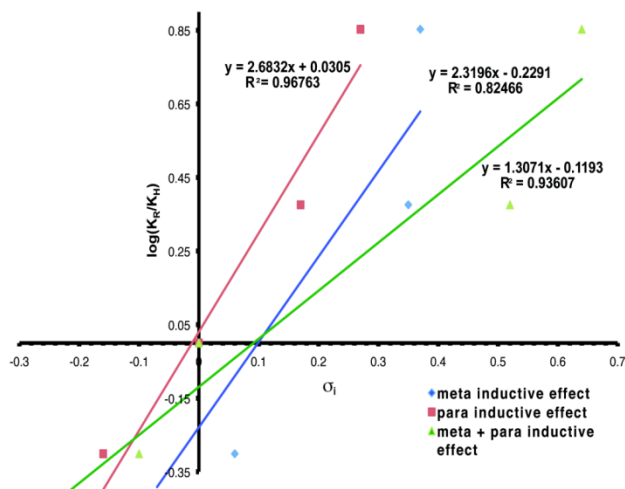


Figure 2.23 Hammett Plot for meta (7-substituent), para (8-substitution), and meta+para inductive effects vs. relative initial rates.

Therefore, we propose the mechanism of alloxazine catalyzed Dakin oxidation as following. (Figure 2.24) FIOOH 2.13 enters the catalytic cycle by base deprotonation to form nucleophilic oxidant FIOO⁻ 2.13-1, which attacks substrates to generate Criegee intermediate 2.13-2. The rate determining collapse of the CI⁻ affords a leaving group FIO⁻ 2.13-3 and the product. FIO⁻ is protonated by solvent to form FIOH 2.13-4. Then it ionized to form an ion pair 2.13-5, which undergoes nucleophilic attack by a H₂O₂ molecule in the presence of a base to regenerate 2.13-1.

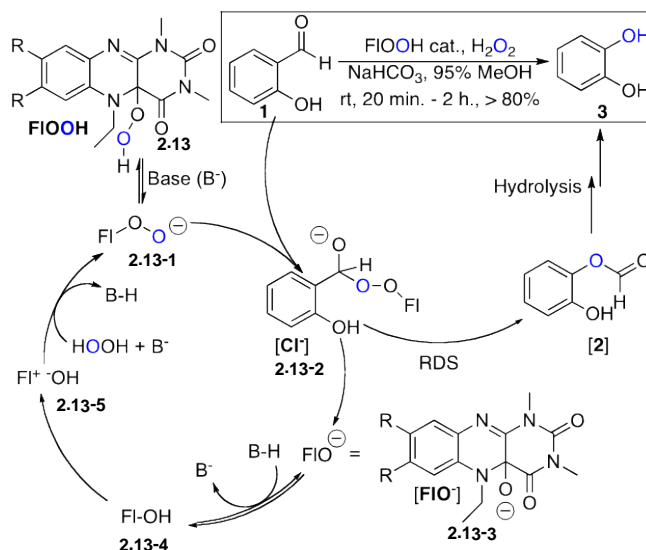


Figure 2.24 Proposed mechanism of alloxazine catalyzed Dakin oxidation

In conclusion for the alloxazine catalyzed Dakin oxidation using H₂O₂ as terminal oxidant, the biomimetic H₂O₂ shunt process was used as a guideline. Electron-withdrawing groups on the C⁷ and C⁸ positions of the alloxazine facilitate catalysis. Mild reaction conditions including a weak base and room temperature were achieved with the help of alloxazine catalyst. Electron rich *o*-hydroxybenzaldehydes generally were good substrates. Additional optimization is needed to extend this methodology to more challenging substrates such as non-hydroxylated benzaldehydes or acetophenones. The mechanistic study indicated that the rate determining step was the collapse of the Criegee intermediate.

2.2.3 Flavin Catalyzed Dakin Oxidation Using O₂ as Terminal Oxidant

Conducting the Dakin oxidation using molecular oxygen as a terminal oxidant is a logical development inspired by the flavin biomimetic cycle. Nature utilizes NAD(P)H to reduce oxidized flavin cofactor via hydride transfer to form the reduced flavin that takes molecular oxygen to generate 4a-hydroperoxy flavin. (Figure 2.25 Highlighted by red

color) Excess H_2O_2 is not needed in this process, which could be dangerous to organisms. With limited concentration of active peroxide, substrates could be converted to products very high efficiency and selectivity.

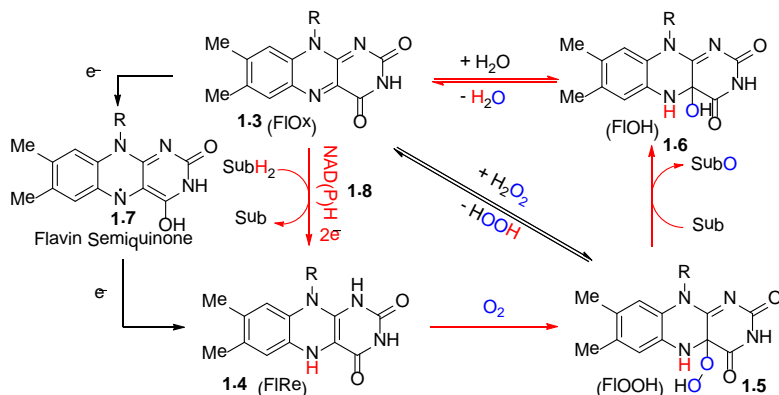


Figure 2.25 Dakin oxidation inspired by flavin biomimetic cycle using O_2 as oxidant

Previously, flavin catalyzed aerobic oxidations were conducted mimicking the cycle showed above. In aerobic amine and sulfur oxidation reactions, hydrazine monohydrate was used to reduce isoalloxazine catalyst to turn over the catalyst.¹³ The same group developed aerobic Baeyer-Villiger oxidation with metallic zinc as a two-electron reductant to reduce oxidized isoalloxazine to complete reaction cycle.²⁷ Although not mentioned, the switch of the reductant from hydrazine to zinc in BVO was presumably due to undesired hydrazone formation between cyclobutanones and hydrazine. Nonetheless, both of the aerobic oxidations were very successful in terms of atom economy and chemoselectivity.

Similarly, in Dakin oxidation system, reducing agent selection was the key to the success. Hydrazine predictably formed hydrazones with benzaldehyde substrates, yielding no desired product. Activated zinc showed good reactivity in the oxidation of salicylaldehyde to produce catechol. However, when applying the Zn/O_2 protocol to substituted salicylaldehydes, products were isolated in very low yields. Either robust

bisphenolate zinc complexes, such as 2.44 or polyphenols are believed to form, sequestering the desired product.⁴⁶ (Figure 2.26) Various methods (acid, base, EDTA treatment and extraction) to liberate product from the possible organometallic structures were unsuccessful.

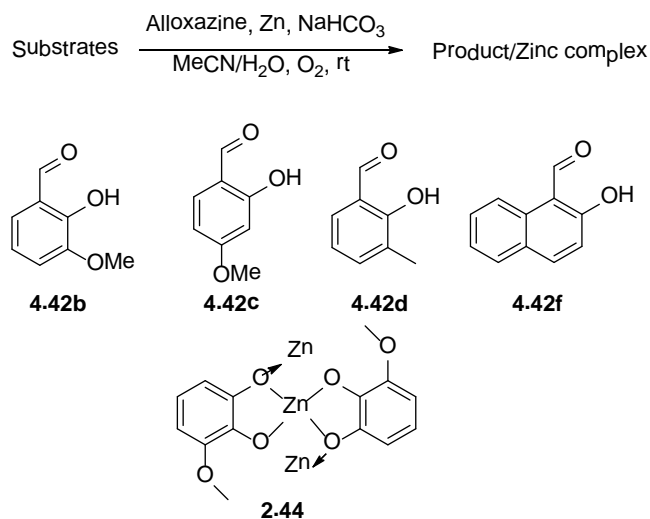


Figure 2.26 Zinc complexes were formed for the various 2-hydroxyl benzaldehydes

Other reducing agents, such as $\text{Na}_2\text{S}_2\text{O}_4$, NaBH_3CN , $\text{NaBH}(\text{OAc})_3$ and trialkylsilanes yielded no desired products. Other d-block species (Mg, Cu, and Fe) were expected to result in decomposition of the reactive hydroperoxyflavins by Fenton or Fenton-like chemistry. No catechol was detected by these metal reducing agents.

Knowing that the mechanism of flavin reduction is actually C=N double bond reductions, mild reducing agents that selectively reduce C=N were investigated to accomplish flavin reduction. Hantzsch ester, the hydrogen transfer reagent closely related to NAD(P)H's 2.45 nicotinamide reactive core,⁴⁷ selectively reduces imines in the presence of aldehydes.⁴⁸⁻⁴⁹ (Figure 2.27) Access to Hantzsch ester is fairly easy. Multi-component condensation between an aldehyde such as formaldehyde 2.46, 2 equivalents of a β -keto ester such as ethyl acetoacetate 2.47 and a nitrogen donor such

as ammonium acetate 2.48 or ammonia in polar protic solvents gives rise to Hantzsch dihydropyridine 2.49.

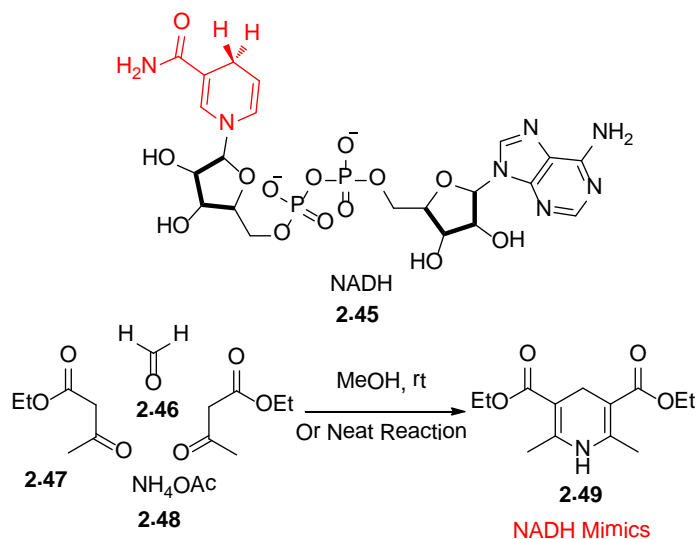


Figure 2.27 Hantzsch ester as a NAD(P)H mimics

When zinc powder was replaced with one equivalent of 2.49, aerobic Dakin oxidations proceeded smoothly to form corresponding phenol products. (Figure 2.28) The production of undesired benzyl alcohols or benzoic acids were not detected. Diethyl 2,6-dimethylpyridine-3,5-dicarboxylate 2.50, could be isolated from reactions as the oxidized byproduct. Control reactions without flavin catalysts ensured that no peroxyacid formation resulted by autooxidation of benzaldehydes occurred.⁵⁰⁻⁵² Reactions were also performed in the dark to eliminate possible photooxidation pathways.

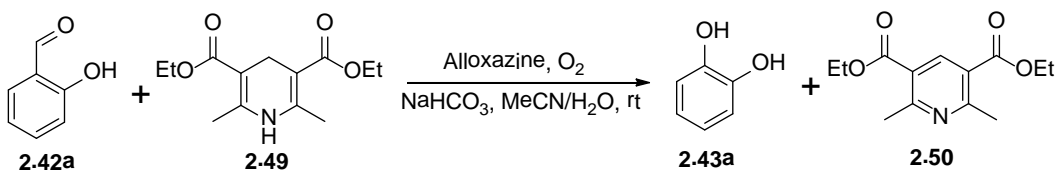


Figure 2.28 Dakin oxidation using dihydropyridine as reducing agent

The aerobic Dakin oxidation condition was then optimized by changing three variables: catalyst substitution, solvent, and base.

Using the five alloxazine catalysts 2.13a-e available from the H₂O₂ based Dakin oxidation study, we set up aerobic Dakin oxidation of salicylaldehyde with 5 mol% of each alloxazine and Hantzsch ester (HEH) as a stoichiometric reducing agent. The conversion of salicylaldehyde to catechol was calculated by NMR, utilizing DMSO as an internal standard. Flavin 2.13c showed the greatest reactivity, followed by 7,8-dimethyl 2.13d and 7,8-dimethoxy 2.13e substituted alloxazines. Electron-poor 7,8-difluoro 2.13b and 7,8-dichloro 2.13a alloxazines, which provided the fastest reaction rates in H₂O₂-fueled Dakin oxidations, performed the aerobic oxidation poorly. (Figure 2.29)

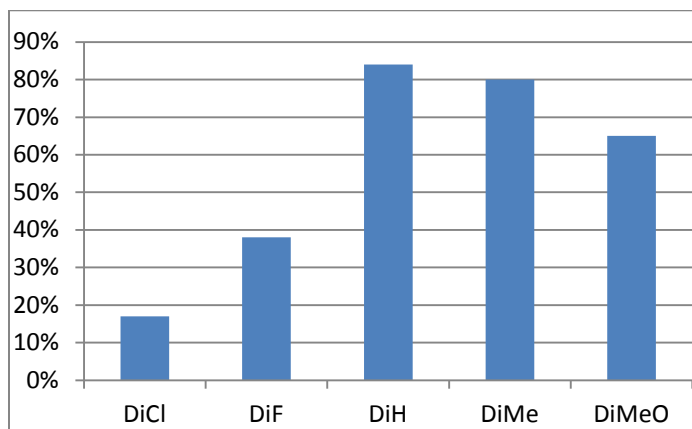


Figure 2.29 Alloxazine screening on aerobic Dakin oxidation

The catalyst reactivity results suggest that competing rate determining steps influence the observable reaction rate: (1) collapse of the Criegee intermediate via 1,2-aryl shift (the putative rate-determining step of the Dakin oxidation indicated from our previous study) and (2) molecular oxygen activation by reduced flavins.^{5,53} While we previously showed that electronwithdrawing groups facilitate the Dakin oxidation by stabilizing the 4a-oxaflavin anion (FIO- 2.13-3 Figure 2.24) leaving group, the same substituents attenuate the single electron transfer process from flavin to triplet oxygen by

altering the oxidation potentials of the reduced flavins.⁵⁴⁻⁵⁵ The hypothesis, in correlation with previous data, is that: electron-poor hydroperoxyflavin 2.13a and 2.13b, in comparison to more electron-rich catalysts, are more efficient Dakin oxidation catalysts, but their respective reduced structures FlH_2 react with O_2 more slowly.

Solvents were investigated. Water miscible solvents were investigated to solvate sodium bicarbonate by 5% water addition, which also promotes hydrolysis of the Dakin oxidation intermediate. Acetonitrile, 95% in water, achieved the fastest reaction rate and highest yields. In general, alcohols suppressed reaction rates. Anhydrous acetonitrile failed as an aerobic Dakin oxidation solvent.

Base is essential in the flavin catalyzed Dakin oxidation system. However, only mild bases (sodium bicarbonate or carbonate) were necessary. Hydroxides were not as effective in this system, presumably due to hydrolysis of the flavin catalyst. (Figure 2.30)

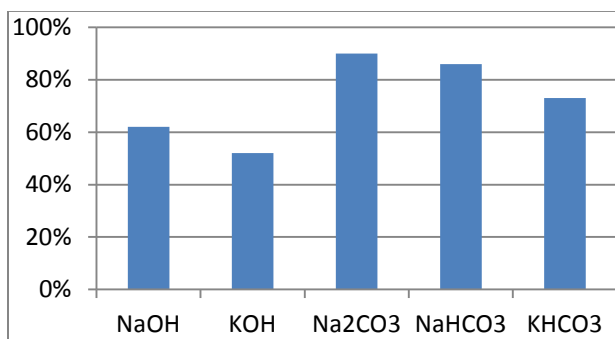


Figure 2.30 Base screening on aerobic Dakin oxidation

In the aerobic Dakin oxidation system, another function of the base is to depress 2.13-6 formation and H_2O_2 shunt elimination from 4a-hydroperoxy alloxazine 2.13 by deprotonating the hydroperoxyl proton to form 4a- hydroperoxyanion 2.13-1. (Figure 2.31) An aerobic reaction was set up without adding salicylaldehyde. No pyridine was detected by flavin catalyzed HEH oxidation. However, when acetonitrile was changed into trifluoroethanol, even without the presence of substrate, HEH was fully converted into

pyridine. Trifluoroethanol facilitates elimination of H_2O_2 and regeneration of oxidized flavin, presumably because of the acidic nature of the solvent.

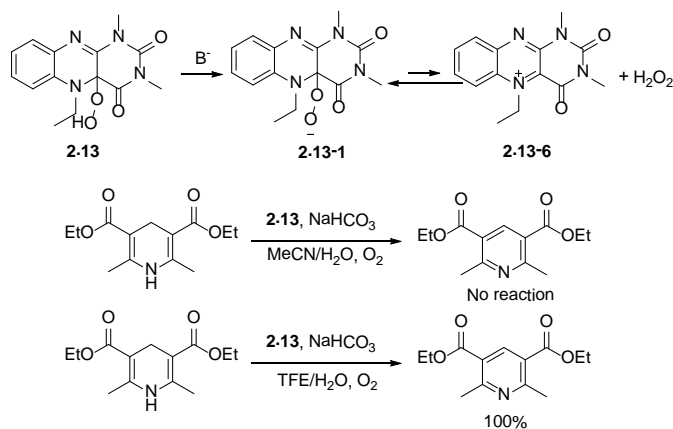


Figure 2.31 The effect of base on flavin catalyst

The substrate scope of the aerobic Dakin oxidation is similar to that of the H_2O_2 based Dakin oxidation. (Figure 2.32) Electron rich benzaldehydes underwent aerobic oxidation efficiently. Nitro-containing substrates were converted to catechols but with longer reaction time. No benzoic acid byproduct was observed in any of the substrates evaluated. However, similarly to the H_2O_2 based Dakin oxidation, non-hydroxylated benzaldehydes or acetophenones were generally not successful, even at elevated temperature.

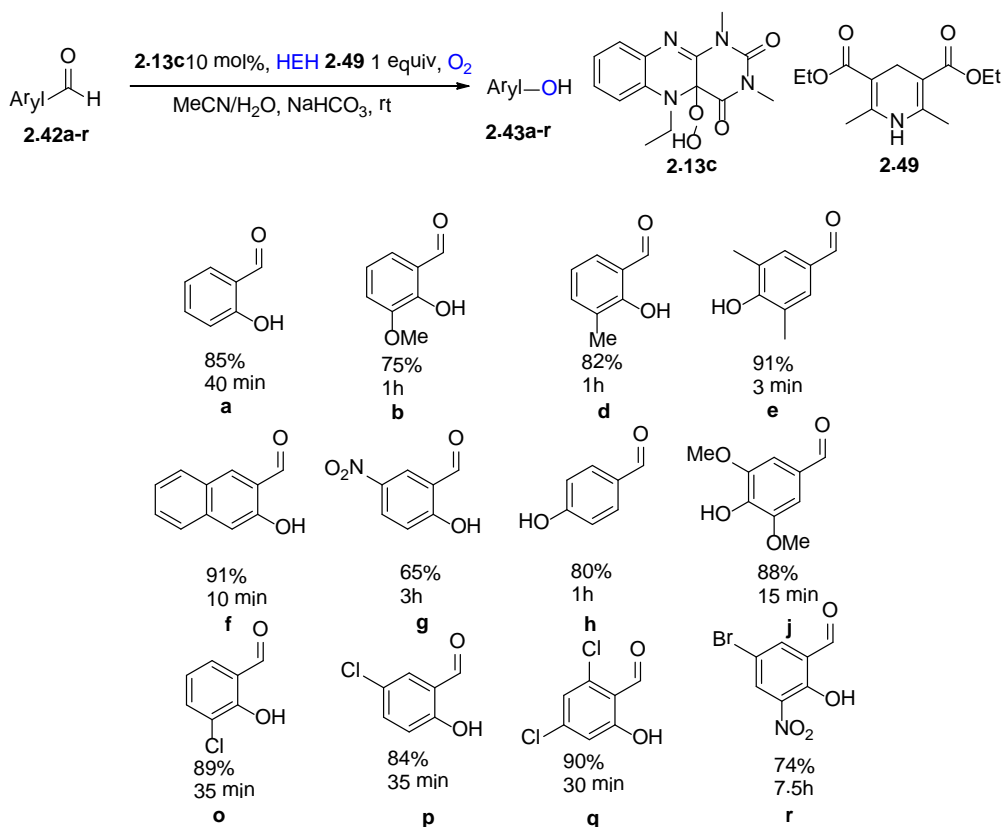


Figure 2.32 The substrate scope of aerobic Dakin oxidation

The aerobic Dakin reaction worked with low catalytic loading and air as the oxygen source. A 10 mmol scale Dakin oxidation of 2.42a, with 0.1 mol % of catalyst 2.13c and air as oxygen source, was performed to challenge our catalytic system; 91% yield of the product was achieved after three days at room temperature.

In conclusion, we have developed an aerobic and mild catalytic system for the Dakin oxidation. A range of electron rich benzaldehydes react in the presence of two biomimetic redox partners: alloxazine catalysts and Hantzsch ester. The selection of Hantzsch ester was crucial to the success of this reaction and provides an alternative reductant for flavin-catalyzed aerobic oxidations, especially those with ketones and

aldehydes. Catalyst loading was effective at 0.1 mol %. Again, extensive condition optimization is needed to broaden substrate scope to more challenging starting materials.

Chapter 3

Flavin Catalyzed Weitz-Scheffer Oxidation

3.1 Dual Catalysis Strategy for Flavin Catalyzed Asymmetric Oxidations

The excellent rate accelerating performance of flavin in various oxidation reaction draws people's attention on developing asymmetric methodologies to generate more valuable enantio rich oxidation product using this biomimetic organocatalyst.

The strategy that was used to conduct asymmetric oxidation with flavin organocatalyst had been designing and synthesizing enantiopure chiral flavin organocatalysts which covalently bonded to chiral substituents. The following examples 3.1-3.6 have been shown in the literature and mentioned earlier in this dissertation.^{19-22,}

²⁶ (Figure 3.1)

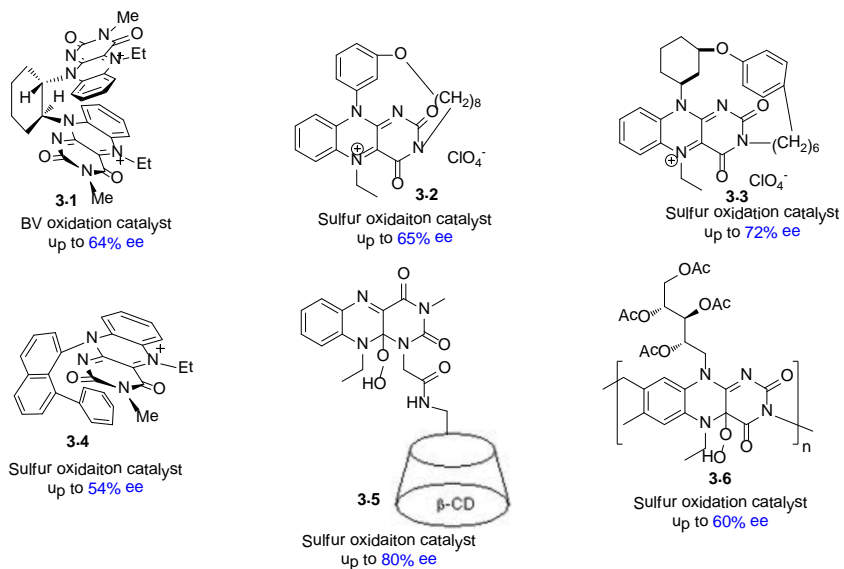


Figure 3.1 Asymmetric sulfur and Baeyer-Villiger oxidation flavin catalysts

However, the non-racemic flavins have many drawbacks. First, chiral flavins are more difficult to prepare compared to simple alloxazines and isoalloxazines. Five to nine steps were generally required to synthesize these compounds^{20, 22, 26} and sometimes

chiral separation was required to obtain the organocatalyst.²⁰ Second, the enantioselectivity of the oxygen transfer of these chiral flavin catalyzed reaction was not optimal. The enantiometric excess of the products obtained from these reactions rarely exceeded 80%. Lastly, the substrate scope was quite limited. Effective substrates usually contained an aromatic substituent, which was believed to interact the aromatic moiety of flavin tricyclic structure via π - π stacking.^{20, 22} These shortcomings of these known chiral flavin derivatives strategy limit the development of flavin catalyzed asymmetric reactions using these catalysts and an alternate way of methodology designing is needed.

We proposed to use a dual catalysis strategy in which one catalyst is a simply prepared flavin 3.7 or 3.8 which is responsible for oxygen transfer; the other is a chiral ligand 3.9-3.13 that controls the facial selectivity of oxygen transfer by interacting with the substrate through a covalent bond or a hydrogen bond. (Figure 3.2) A range of chiral cocatalyst is ready available in the literature that is able to induce an asymmetric environment of substrates efficiently.⁵⁶⁻⁵⁹

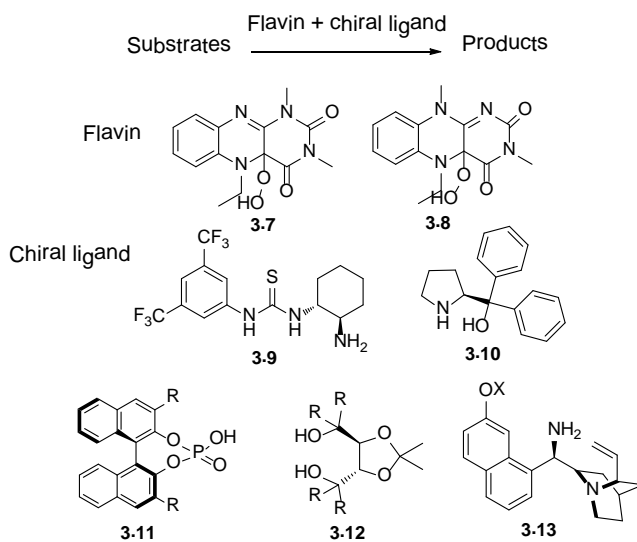


Figure 3.2 Dual catalysis strategy of asymmetric oxidation

3.2 Aerobic Asymmetric Weitz-Scheffer Epoxidation

The Weitz-Scheffer oxidation is a type of nucleophilic epoxidation of electron-deficient double bonds through the attack of alkaline hydroperoxides.⁶⁰ Nucleophilic epoxidation methods represent an alternative to electrophilic methods such as Sharpless epoxidation,⁶¹ Jacobsen epoxidation⁶² and Shi epoxidation,⁶³ which often do not perform epoxidation on electron-deficient double bonds efficiently.

The mechanism of Weitz-Scheffer oxidation is described by Bunton and Minkoff to be a two-step process.⁶⁴ (Figure 3.3) First, conjugate addition of a peroxy anion 3.15 which is generated by H₂O₂ or alkyl peroxide under basic condition at the β position of α , β -unsaturated ketone 3.14 affords β -peroxyenolate 3.16. Then, intramolecular nucleophilic displacement at the proximal oxygen atom breaks the weak O-O single bond generating a leaving group, hydroxide or alkoxide 3.17, to furnish epoxide 3.18.

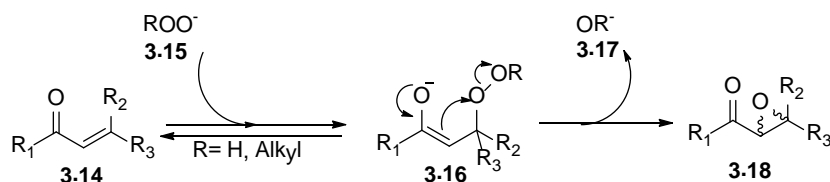


Figure 3.3 Proposed mechanism of Weitz-Scheffer oxidation

The non-stereospecificity of these reactions is a strong indication for the formation of an intermediate 3.16 in the course of the reaction. The epoxidation of both *trans*- and *cis*-configured α , β -unsaturated ketone with alkaline hydrogen resulted in *trans*-epoxide as the main product. The convergent result further implies that hydroperoxide addition is reversible and causes isomerization by rotation about the vinylic bond in the peroxyenolate.

Numerous catalysts were developed to furnish asymmetric epoxidation of enones or enals. Representative work in this area including: 1) Asymmetric epoxidation using

alkylated Cinchona alkaloids as phase transfer catalysts.⁶⁵⁻⁶⁸ 2) Polyamino acid mediated epoxidation (Juliá-Colonna epoxidation).⁶⁹⁻⁷⁰ 3) Epoxidation using chiral ligands and metal peroxides.⁷¹⁻⁷² 4) Epoxidation using LUMO lowering organocatalysts.⁷³⁻⁷⁴ In most of these methods, 35% aqueous H₂O₂ or other strong oxidants were used as stoichiometric oxidant. No example used oxygen as the terminal oxidant to perform epoxidation of enals or enones.

The topic of aerobic alkene epoxidation has attracted significant attention within the last decade. Predominately, aerobic epoxidation of isolated and unactivated alkenes can be achieved via radical-mediated autooxidation pathways or via monooxygenase like oxidation with a coreductant.⁷⁵ Both approaches can be catalyzed by a range of transition metal bearing catalysts, such as Schiff's base complexes, metalloporphyrin complexes and metal cyclam complexes.⁷⁶⁻⁷⁸ In addition, the asymmetric aerobic epoxidation of unfunctionalized alkenes was also achieved by metal salen catalysts.⁷⁹⁻⁸⁷

Aerobic Weitz-Scheffer oxidation is surprisingly rarely reported. Until recently, Shibata's group disclosed a groundbreaking one pot aerobic asymmetric epoxidation of trifluoromethyl substituted β , β -disubstituted enones 3.19 using cinchona derived catalyst 3.20 and H₂O₂, which was generated in situ by methylhydrazine, a base and molecular oxygen. (Figure 3.4) However, only β CF₃ substituted enones participated in this aerobic epoxidation with high enantioselectivity.⁸⁸ Itoh's group published a two-step process where H₂O₂ was first generated in situ using the known anthraquinone 3.23 oxidation (AO) process with excess isopropanol as a sacrificial reductant, followed by adding enone 3.19 and a strong base to achieve epoxidation.⁸⁹ While the initial foundation of aerobic Weitz-Scheffer oxidation is established, diversified methods are urgently demanded to broaden of utility of this interesting transformation.

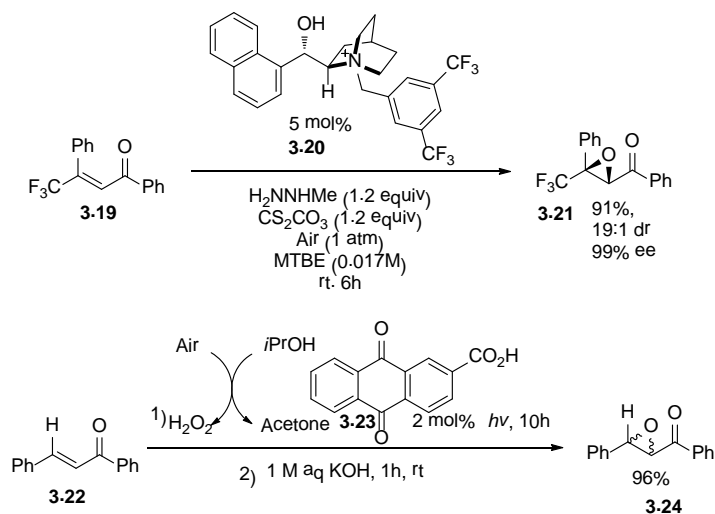


Figure 3.4 Recent development of aerobic epoxidation of enones

Many literature reports showed flavin containing monooxygenases' role in the epoxidation of unactivated alkenes, enones and enals, there is no direct application of this phenomenon as a bio-inspired epoxidation methodology.⁹⁰⁻⁹² (Figure 3.5)

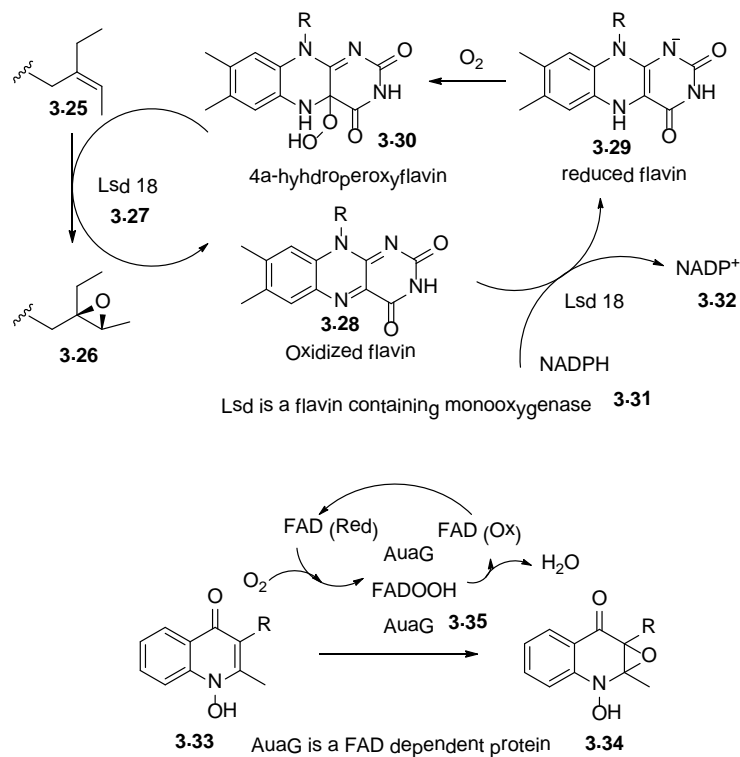


Figure 3.5 Examples of flavin protein catalyzed epoxidation

To our knowledge, there is no method that achieves the asymmetric epoxidation of enals aerobically in an organocatalyst catalyzed system. Herein, we describe the first asymmetric aerobic epoxidation of α,β -unsaturated aldehydes catalyzed by flavin/pyrrolidine dual catalytic systems using benzothiazoline as a stoichiometric coreductant, achieving good yield, excellent diastereoselectivity and enantioselectivity.

We know that flavin catalyzed aerobic Dakin Oxidation of aryl aldehydes can be turned over with Hantzsch esters 3.38 as the stoichiometric reductant. Starting from established method, we initially attempted to transplant the aerobic Dakin oxidation system directly to the epoxidation of enal, using cinnamaldehyde 3.35a as a model compound. (Figure 3.6) Unfortunately, no epoxide was detected from the reaction. We envisioned two possible problems of the system: 1, the active oxidant, either 4a-

hydroperoxy flavin 3.37 or H₂O₂ (eliminated from 4a-hydroperoxy flavin), is not nucleophilic enough to attack the β position of enal. 2, the β-carbon of enal is not electrophilic enough to attract the peroxide lone pair electrons.

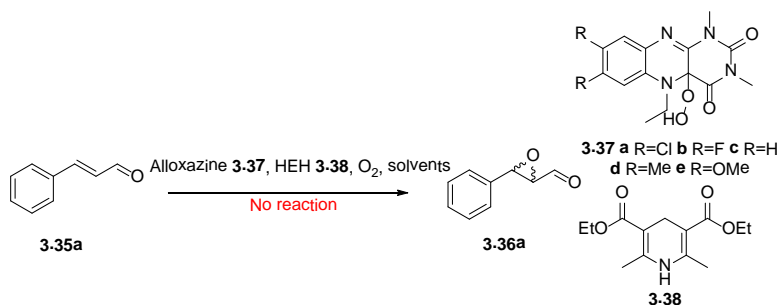


Figure 3.6 Aerobic Dakin oxidation condition failed on epoxidation of enal

Luckily, there is a ready answer to solve the second problem. A range of L-proline derived organocatalysts was available in the literature, first recognized by Jørgensen's group as a LUMO lowering catalyst to achieve asymmetric epoxidation of enal with H₂O₂.⁷³ (3.39a-d Figure 3.7) Inspired by this research, we tried to add different prolinols or prolinol silyl ethers as a LUMO lowering co-catalyst into our aerobic oxidation system.

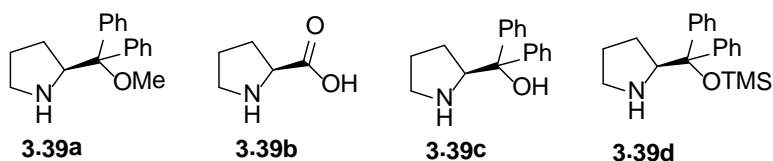


Figure 3.7 L-proline derived organocatalysts

Not surprisingly, with the help of further activation of the iminium, epoxidation of cinnamaldehyde was achieved. (Figure 3.8) Trimethylsilyl protected diphenyl prolinol 3.39d resulted in higher chemical yield and diastereomeric ratio of epoxide than the non-protected prolinol 3.39c and methyl protected prolinol 3.39a, for its excellent steric

blocking effect.⁹³ In our system, 20 mol% of prolinol catalyst 3.39d was needed to obtain good yield of product within a few hours.

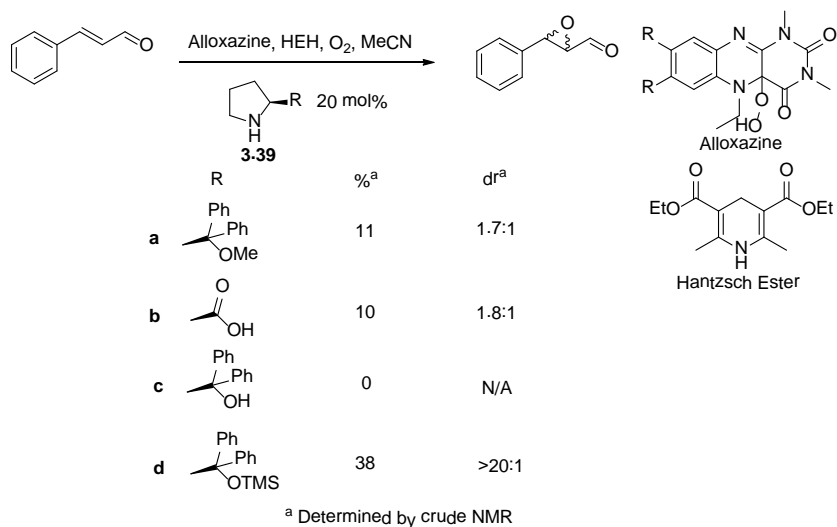


Figure 3.8 Comparison of pyrrolidine cocatalyst

However, before we moved on to the optimization process, an unexpected conjugate reduction product, hydrocinnamaldehyde 3.40, was detected. (Figure 3.9) Indeed, prolinol catalyzed conjugate reduction of enals with Hantzsch esters as hydride transfer reagent was well-known in the literature.⁹⁴ In our epoxidation system, the Hantzsch ester 3.38 not only reduced the flavin but also the activated double bond of the enal. To avoid this chemoselectivity issue, the Hantzsch ester must be substituted by another reductant, which can differentiate the C=N double bond in flavin and the double bond in enal selectively. Therefore, a range of reductants that can potentially reduce flavin were tested. (Table 3.1 Entry 4-8) Metal reductant, such as Zn, led to no epoxide formation. Hydrazine, known to be able to reduce flavin, formed hydrazone with enal immediately and precipitated out of solution, and performed no epoxidation. Thus, attention was turned to benzothiazoline 3.41, a prearomatic heterocycle readily obtained by the condensation of benzaldehyde and 2-aminothiophenol. Benzothiazolines were

known as very mild hydride transfer reagents which selectively reduce C=N double bond under neutral conditions.⁹⁵⁻⁹⁶ Fortunately, with 1.2 equivalent benzothiazoline 3.41b as reductant, aerobic epoxidation of cinnamaldehyde 3.35a proceeded as expected without the formation of hydrocinnamaldehyde.

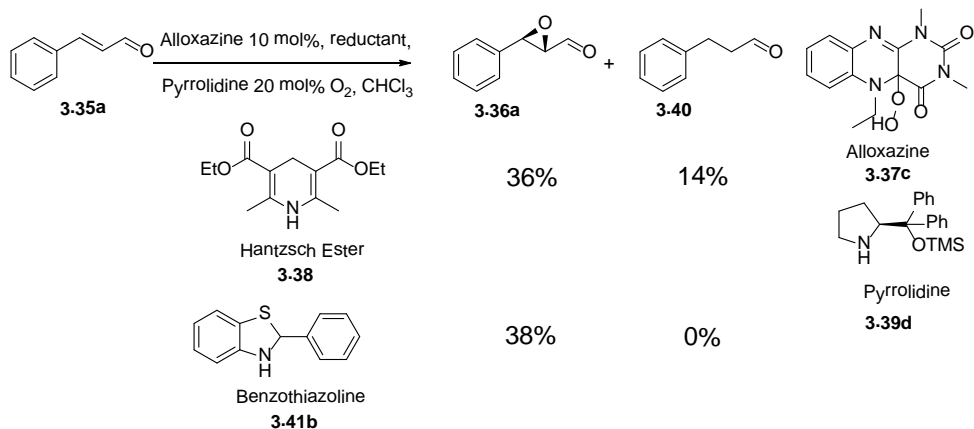


Figure 3.9 Comparison of reductant in aerobic epoxidation

Among benzothiazolines (Table 3.1, entry 4-8), some, such as 3.41b, tended to undergo hydrolysis to form benzaldehyde 3.43 and 2-aminothiophenol 3.42, especially when the substrate or the chloroform was contaminated by acid impurities. (Figure 3.10) To prevent this from happening, the chloroform and substrates used in the reaction were freshly purified. The nitro containing benzothiazoline (3.41a Table 3.1 Entry 2), proved to be less liable to hydrolysis under acid catalysis, was chosen as the stoichiometric reductant in our system.

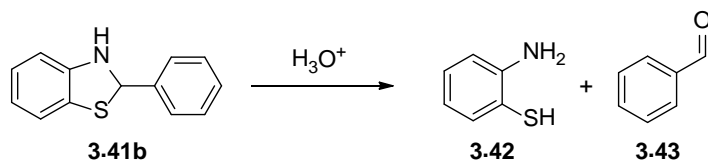


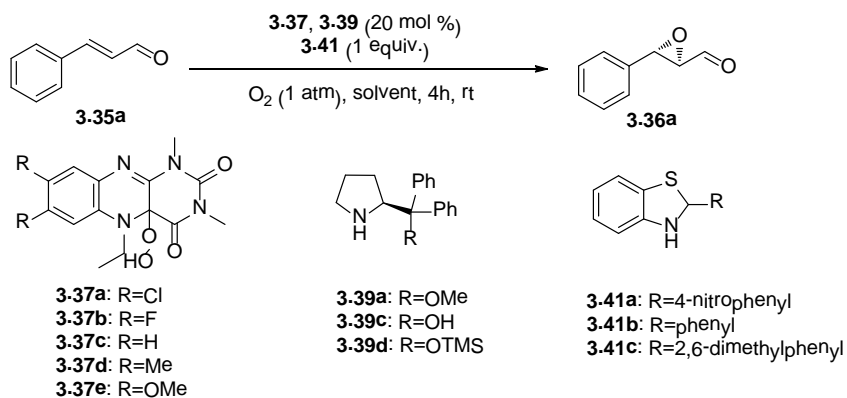
Figure 3.10 Hydrolysis of benzothiazoline

Next, flavin catalyst was optimized. (Table 3.1 Entry 10-14) In aerobic Dakin oxidation system, 7,8-dihydrogen substituted alloxazine (3.37c) was proven to be the best flavin compared to catalysts with other substitutions. In the aerobic epoxidation system, the same trend was observed. Also, the flavin catalytic loading was very important to the success of aerobic epoxidation. Lower catalyst loading (0.1 - 5 mol%) led to longer reaction times, but the chemical yield was not affected. However, when 10-20 mol % flavin catalyst was added, the chemical yield was reduced substantially. This can be explained by flavin catalyzed N-oxidation of prolinol nitrogen. It is known that flavins accelerates the oxidation of secondary amine to nitron with hydrogen peroxide.¹²⁻¹³ Nitron formation was confirmed by taking HRMS of crude reaction mixture. Once oxidized, the prolinol catalyst was poisoned and therefore lost its ability to form an iminium ion with enal. Therefore, we chose to use 5 mol% flavin catalyst 3.37c to perform the aerobic epoxidation. Good rate and maximized chemical yield was obtained.

Chlorinated solvents such as dichloromethane or chloroform were chosen to perform asymmetric epoxidation of enals. We have screened several other solvents and finalized chloroform as the solvent considering yield and enantioselectivity. (Table 3.1 Entry 15-19) Chloroform proved to be a great solvent in our system because it solubilizes everything at the beginning of the reaction. As the reaction proceeds, the benzothiazole byproduct generated in situ precipitates out of chloroform.

The summarized condition screening and results are presented in the following Table 3.1

Table 3.1 Asymmetric aerobic epoxidation of 4a: condition optimization

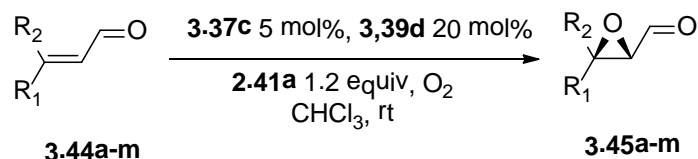


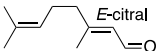
Entry	Polinol	Red	Flavin	Solvent	d.r.	Yield ^e (%)
1	-	HEH ^a	10 mol % 3.37c	CHCl ₃	n.d.	n.d.
2	3.39d	3.41a	10 mol % 3.37c	CHCl ₃	10:1	38
3	3.39a	3.41a	10 mol % 3.37c	CHCl ₃	2:1	44
4	3.39c	3.41a	10 mol % 3.37c	CHCl ₃	n.d.	7
5	3.39d	Zn	10 mol % 3.37c	CHCl ₃	n.d.	n.d.
6	3.39d	HEH	10 mol % 3.37c	CHCl ₃	10:1	36 ^b
7	3.39d	3.41b	10 mol % 3.37c	CHCl ₃	10:1	38 ^c
8	3.39d	3.41c	10 mol % 3.37c	CHCl ₃	10:1	56 ^d
9	3.39d	3.41a	5 mol % 3.37c	CHCl ₃	10:1	74
10	3.39d	3.41a	20 mol % 3.37c	CHCl ₃	10:1	32
11	3.39d	3.41a	10 mol % 3.37b	CHCl ₃	10:1	16
12	3.39d	3.41a	10 mol % 3.37a	CHCl ₃	10:1	14
13	3.39d	3.41a	10 mol % 3.37 d	CHCl ₃	10:1	6
14	3.39d	3.41a	10 mol % 3.37e	CHCl ₃	10:1	7
15	3.39d	3.41a	5 mol % 3.37c	DCM	10:1	54
16	3.39d	3.41a	5 mol % 3.37c	MeCN	10:1	34
17	3.39d	3.41a	5 mol % 3.37c	C ₆ H ₆	10:1	16
18	3.39d	3.41a	5 mol % 3.37c	THF	10:1	n.d
19	3.39d	3.41a	5 mol % 3.37c	Hexane	10:1	n.d.

^a HEH stands for Hantzsch ester. ^b 14% hydrocinnamaldehyde was detected. ^c 30% benzaldehyde from hydrolysis was detected. ^d 13% 2,6-dimethylbenzaldehyde from hydrolysis was detected. ^e NMR yield was determined using DMSO as an internal standard. d.r. was determined by NMR

With the optimized condition, 5 mol% flavin 3.37c and 20 mol% prolinol 3.39d, 1.2 equivalent of benzothiazole 3.41a, 1 atm of oxygen gas in chloroform, we started to exploit the scope of this aerobic epoxidation. First of all, a range of enals with aryl substitutions on beta position was epoxidized under standard condition. (Table 3.2. Entry 1-4) Good yield was achieved with all of them (74-85%) after 4-6 hours. Good diastereoselectivity (7:1 to 17:1) of trans versus cis product was detected. To our delight, the enantioselectivity of epoxide was excellent. The e.e. values ranged from 94% to 96% for the favored 2S,3R-oxirane with the (S)-prolinol as the LUMO lowering catalyst. Beta mono alkyl -substituted enals generally obtain epoxide with higher d.r.(13:1 to >20:1) but slightly lower e.e.(87-92%). For low molecular weight short chain enals, the oxirane 2-carbaldehydes obtained were directly reduced to corresponding alcohols with sodium borohydride before isolation. (Table 3.2. Entry 6-12) Beta disubstituted enals oxidized efficiently under aerobic condition, however, with a reduced ratio in diastereoselectivity and enantioselectivity. (Table 3.2. Entry 6, 13)

Table 3.2 Flavin/pyrrolidine catalyzed epoxidation substrate study



Entry	3.45	R ₁	R ₂	Yield ^a (%)	Time (h)	d.r. ^b	% ee ^c
1	a	Ph-	H	78	4	13:1	94
2	b	<i>o</i> -NO ₂ -Ph-	H	85	5	7:1	95
3	c	<i>p</i> -NO ₂ -Ph-	H	84	6	17:1	96
4	d	<i>p</i> -Cl-Ph-	H	74	6	14:1	96
5	e	Me-	Me	55 ^d	2	N/A	73
6	f	Et-	H	48 ^d	2	13:1	87
7	g	isopropyl-	H	53 ^d	2	>20:1	93
8	h	<i>n</i> -propyl-	H	63 ^d	2	>20:1	92
9	i	<i>n</i> -butyl-	H	69	3	14:1	90
10	j	<i>n</i> -hexyl-	H	71	5	15:1	91
11	k	<i>n</i> -heptyl-	H	74	5	>20:1	92
12	l	-CO ₂ Et	H	61	4	10:1	93
13	m			62	6	2:1	53

^a Isolated yields. ^b d.r. were determined by NMR and GC. ^c % e.e. were determined by chiral GC or HPLC (see SI). ^d Isolated yields refer to the corresponding alcohols after NaBH₄ reduction.

When compared our results with the values (reaction time, yield, d.r. and e.e.) achieved by existing enal epoxidation methods using prolinol catalyst and hydrogen peroxide as oxidant, we found that they were coincidentally very similar.^{73,93} This led us to think about the mechanism of the epoxidation: What is the real oxidant in the reaction,

4a-hydroperoxy flavin or H_2O_2 (eliminated from 4a-hydroperoxy flavin)? What is the role of flavin in changing the course of the reaction? Considering that increased steric effect of alkylperoxide led to a loss of stereoselectivity in their work, we hypothesized that the true oxidant was not the hindered 4a-hydroperoxyflavin but H_2O_2 , a dissociation product in equilibrium with hydroperoxyflavins.

To answer these questions, three reactions were set up with different loadings of flavin catalyst. One of the advantages of choosing benzothiazolines as the reductant was the ease with which its consumption may be tracked by integration of 1H NMR signals of benzothiazoline and its oxidized product, benzothiazole. Therefore, the courses of these reactions were monitored with 1H NMR. The consumption of benzothiazoline (Table 3.4) and the generation of epoxide (Table 3.3) were calculated over 4.5 hours. Each experiment was carried out three times and the results were the average of repeated reactions.

Table 3.3 Epoxide concentration Vs Time

Time(Min)	5mol% average	10mol% average	20mol% average
10	12.2	14.13	14.73
20	18.13	22.16	20.93
30	26	28	25
40	35	34.1	27
60	45.33	39.1	29.56
90	56.66	42.66	32.33
180	67.9	44.66	32.33
270	73.2	46.33	32.83

Table 3.4 Benzothiazoline concentration Vs Time

Time(Min)	5mol% average	10mol% average	20mol% average
10	71.83	51.13	27.4
20	57.96	35.33	13.33
30	46.6	20.7	0
40	37.66	15.83	0
60	23	4.333	0
90	13.33	0	0
180	0	0	0
270	0	0	0

With 5 mol % loading, benzothiazoline was consumed in a moderate rate. After 3 hours, no benzothiazoline was left. While epoxide concentration increased gradually with the consumption of the reducing agent and stopped at 74 % by 4.5 hours. (Figure 3.11)

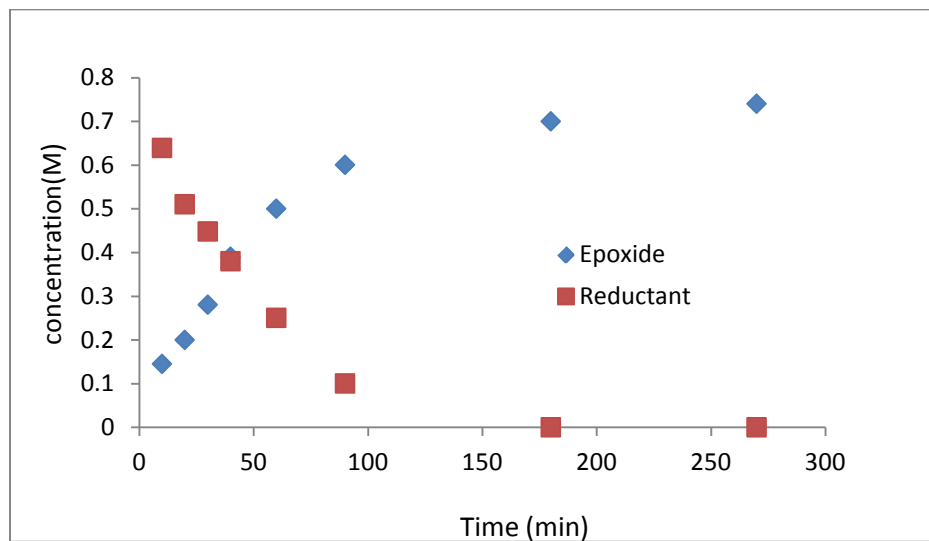


Figure 3.11 5 mol % flavin: Product/Reductant Vs Time

With 10 mole % loading, benzothiazoline consumption was significantly faster. Within 50 minutes, all of reducing agent was oxidized. However, the epoxide formation

was not as fast as 5 mol % reaction and after 4.5 hours, only yielded 39% product.

(Figure 3.12)

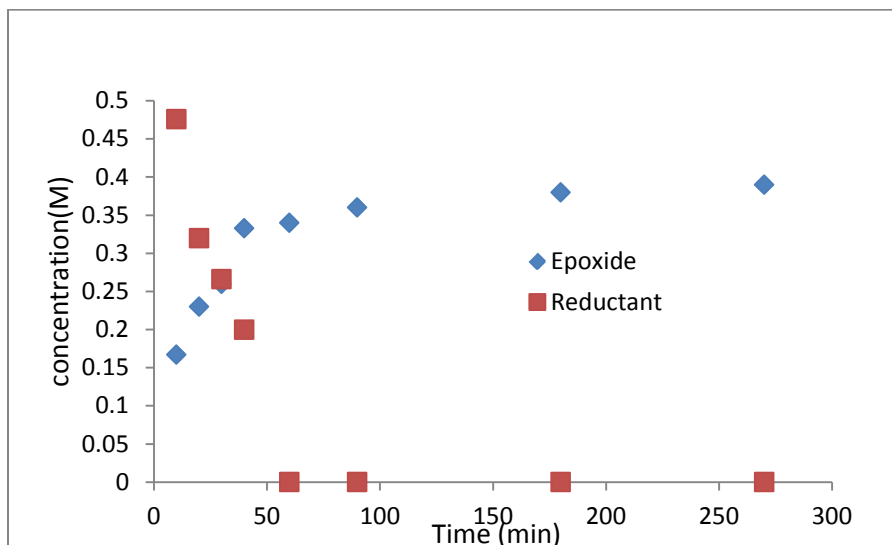


Figure 3.12 10 mol % flavin: Product/Reductant Vs Time

When the flavin loading was increased to 20 mol %, the consumption of reductant required only 30 min. Surprisingly, the product formation was even slower, yielding only 32% epoxide after 4.5 hours. (Figure 3.13)

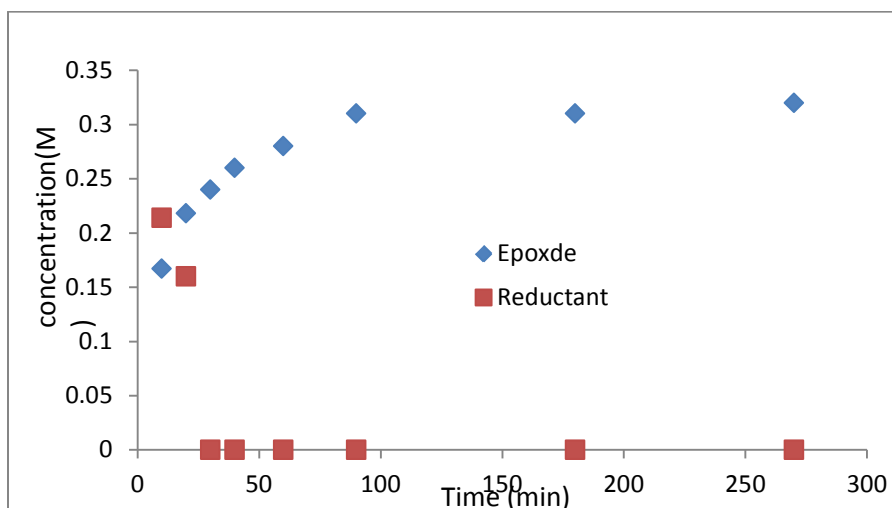


Figure 3.13 20 mol % flavin: Product/Reductant Vs Time

The information of peroxide formation versus time was plotted as following Figure 3.14. And the initial rate of three reactions was calculated and summarized below. (Table 3.5)

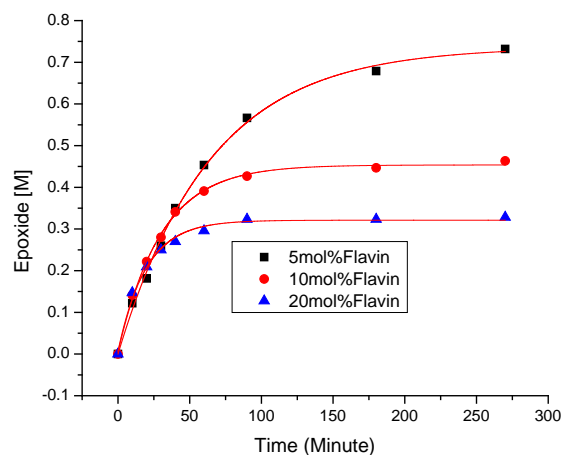


Figure 3.14 Epoxide formation progress for reactions with different flavin loadings

Table 3.5 Peroxide formation reaction initial rates

Flavin loading	Initial rate(M/min)
5mol%	0.011
10mol%	0.0148
20mo%	0.015

The information of benzothiazoline concentration versus time was plotted as following figure. (Figure 3.14) And the initial rate of three reactions was calculated and summarized below. (Table 3.6)

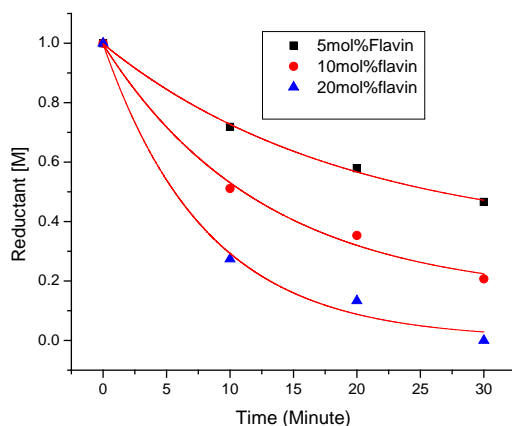


Figure 3.15 Benzothiazoline concentration progress for reactions with different flavin loadings

Table 3.6 Reductant consumption reaction initial rates

Flavin loading	Initial rate(M/min)
5mol%	0.035
10mol%	0.0675
20mo%	0.1225

The initial rates of both peroxide formation and reductant consumption were plotted as a function of flavin catalytic loading to reveal how flavin concentration affected the reaction progress. (Figure 3.16)

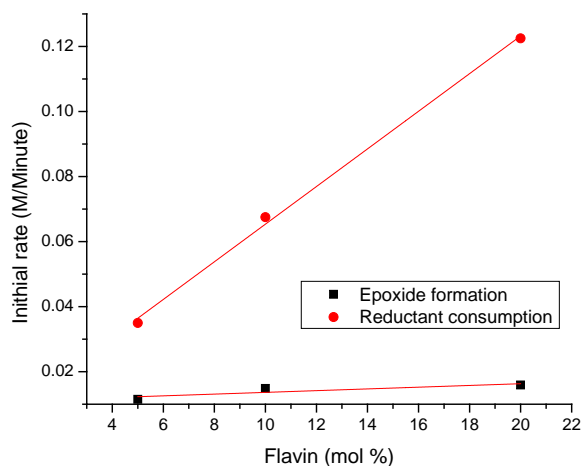


Figure 3.16 Initial rate of epoxide formation and reductant consumption as a function of flavin loading

As is shown in the plot, the initial rate of product formation was almost independent of flavin loading. In contrast, reductant consumption rate was proportional to flavin loading. The dramatically different initial rates for epoxide formation and reductant consumption support an uncoupled redox process.

We believe that oxidized flavinium 3.47b are reduced by benzothiazoline 3.41a to form the reduced dihydroalloxazine FIH_2 3.47c, which reacts with oxygen to form 4a-hydroperoxyflavin FIOOH 3.47a. (Figure 3.17) In polar solvents, 4a-hydroperoxyflavin can dissociate to give the oxidized alloxazinium 3.47b and H_2O_2 , which directly oxidizes enal. The rate of this process is proportional to the concentration of flavin. However, the rate of product 3.36a formation is determined by the concentration of iminium ion 3.48. Therefore flavin concentration does not affect the initial rate of epoxide formation. This hypothesis is reinforced by the oxidative poisoning of pyrrolidine 3.39d to nitron 3.47 in the presence of additional flavin.

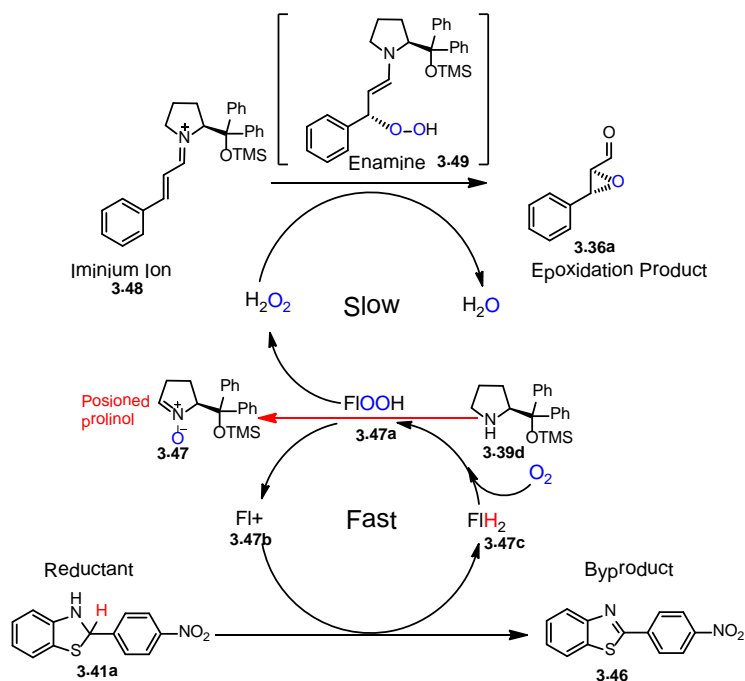


Figure 3.17 Proposed mechanism for alloxazine/pyrrolidine catalyzed aerobic epoxidation

Realizing H_2O_2 was the direct oxidant of the system, one should be able to detect its generation with only flavin catalyst, reducing agent, and oxygen. Indeed, in the reaction of 0.2 mmol of Hantzsch esters or benzothiazoline, 10 mol % flavin catalyst, and O_2 (1 atm) in chloroform yielded 0.11-0.13 mmol (55-65%) hydrogen peroxide, as detected after 30 minutes by titration of Fe^{3+} with UV-Vis detection or oxygen electrode.⁹⁷ (Figure 3.18)

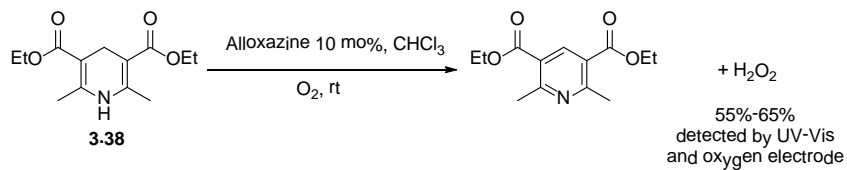


Figure 3.18 Aerobic H_2O_2 formation by alloxazine catalyzed dehydrogenation of benzothiazoline

Some flavoenzymes generate superoxide in the presence of oxygen.⁹⁸ While the direct role of superoxide species in the epoxidation is unlikely and not detected by KO_2 control reactions, the disproportionation of superoxide produces O_2 and H_2O_2 .

In conclusion, we have developed a flavin/pyrrolidine dual catalytic approach to aerobic organocatalytic oxidation and shown its application in the asymmetric epoxidation of enals. This metal-free organocatalytic system uses oxygen as the terminal oxidant to achieve epoxidation of enals. This dual catalysis system, different from previous chiral flavin strategy, utilized easily synthesized flavin catalyst and a commercially available chiral cocatalyst to achieve oxidation of substrates with high yield, diastereoselectivity, and enantioselectivity.

Stoichiometric reductant benzothiazoline chemoselectively reduced flavin in the presence of enals/eniminiums. Benzothiazolines, together with Zn, hydrazine and dihydropyridines, provided another alternative category of reductant for aerobic flavin chemistry.

This method provides also opportunities to introduce isotopically labeled oxygen atoms to substrates with $^{18}\text{O}_2$ as the terminal oxidant in anhydrous systems. While sustainable and cost effective reducing agents and solvents would enhance the system, this dual catalysis synergistic effect may enable transformations that flavin or chiral catalyst alone cannot perform, such as Baeyer-Villiger oxidation of cyclopentanones and cyclohexanones.

Chapter 4

Flavin Catalyzed Heterocycle Aromatization

4.1 Heterocycle Aromatization Reactions

Heterocyclic compounds, such as dihydropyridine, benzothiazole, benzimidazole and benzoxazoles, are important building core in numerous natural products and biologically active reagents which are of great interests to synthetic community and pharmaceutical industry.

4.1.1 Dihydropyridine

The first synthesis of a dihydropyridine is attributed to Arthur Hantzsch for the work done more than a century ago.⁹⁹ The reaction produced 1,4-dihydropyridines (DHPs), or “Hantzsch esters”, as isolable intermediates, he found that these could then be oxidized to pyridines. The synthesis had not drawn much attention until 1970s and 1980s, when it was known to be able to treat hypertension. Amlodipine 4.1, Felodipine 4.2, Isradipine 4.3 and Nifedipine 4.4 are among the best selling drugs.¹⁰⁰ (Figure 4.1)

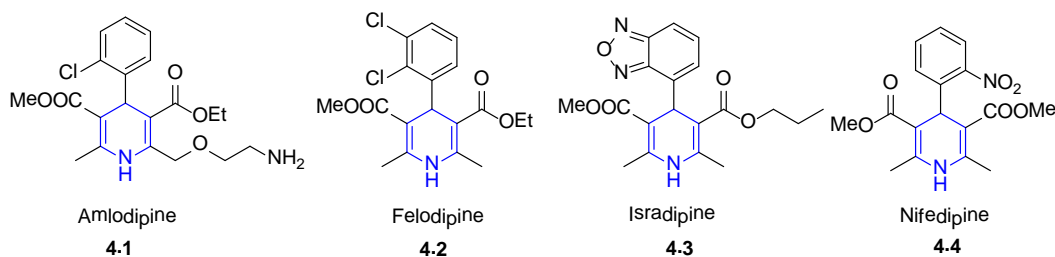


Figure 4.1 Dihydropyridine containing drugs for hypertension treatment

The way these drug effects is to bind to calcium channels and consequently to decrease the passage of the transmembrane calcium current, associated in smooth muscle with a long lasting relaxation and in cardiac muscle with a reduction of contractility throughout the heart.¹⁰¹⁻¹⁰²

Metabolic studies of 1,4-DHP drugs in the human body have shown that these compounds are oxidized to pyridine derivatives by the action of cytochrome P450 in the liver.¹⁰³ The results indicate that the enzyme P-450 IIIA4 is probably the major human catalyst involved in the formal dehydrogenation of most but not all 1,4-dihydropyridine drugs. Although it is well known that these 1, 4-DHP drugs are closely related to NAD(P)H structurally and NAD(P)H can be oxidized by flavin cofactors, there is no direct evidence that the metabolism of these drugs is a function of flavin containing proteins in human body.

The pyridines as the oxidation product of readily available 1, 4- dihydropyridine showed anti-hypoxic and anti-ischemic activities. The main representative of oxidized 1,4-DHPs is cerivastatin 4.5, which has activity in the treatment of atherosclerosis and other coronary diseases.¹⁰⁴ (Figure 4.2) Therefore, oxidative aromatization of 1,4-DHPs has attracted continuing interests of organic and medicinal chemists.

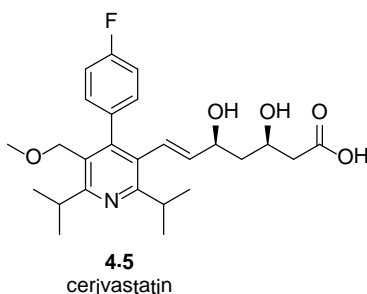


Figure 4.2 Cerivastatin for the treatment of atherosclerosis and other coronary diseases

Numerous methods have been developed to conduct the oxidative aromatization of dihydropyridines to pyridines.

Ru(III)Cl 4.7 /molecular oxygen system was developed as a catalytic system for 1,4-DHP 4.6 oxidation.¹⁰⁵ The proposed mechanism involved single electron oxidation of DHP via Ru(III). The DHP went through radical intermediates 4.9 and 4.10 The resulting

Ru(II) 4.8 was reoxidized to Ru(III) by oxygen to turn over the catalytic cycle to afford pyridines 4.11.(Figure 4.3)

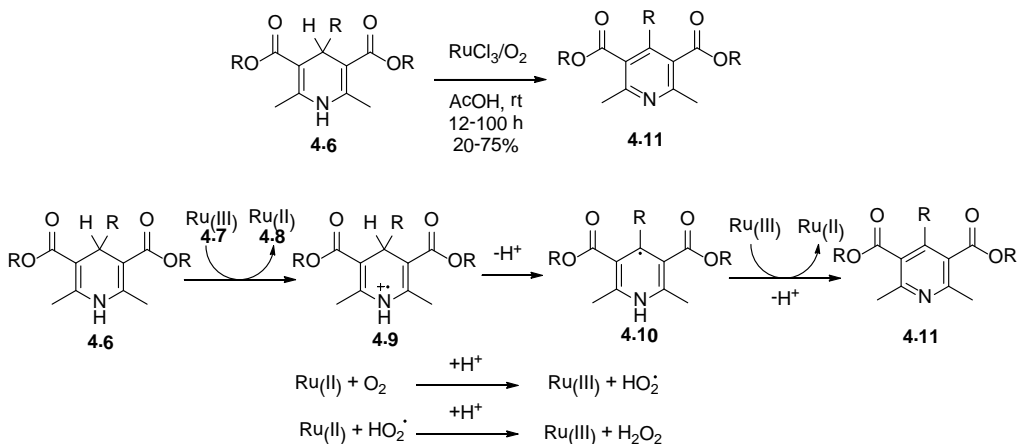


Figure 4.3 Aerobic DHP aromatization catalyzed by RuCl₃

A variety of Hantzsch 1,4-dihydropyridines were oxidized to the corresponding pyridines in high yields in the presence of H6PMo9V3O40 4.12, a Keggin type heteropolyacid, in refluxing acetic acid. In this system, terminal oxidant is believed to be molecular oxygen. The heteropolyacid was found to be reusable.¹⁰⁶(Figure 4.4)

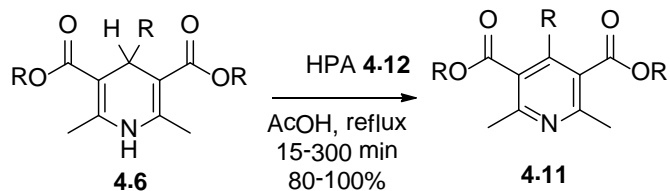


Figure 4.4 DHP oxidation in the presence of of H6PMo9V3O40

Hantzsch 1,4-dihydropyridines 4.6 and 1,3,5-trisubstituted pyrazolines 4.13 were converted to the corresponding pyridines 4.11 and pyrazoles 4.14 efficiently by the treatment of I2O5 in water.¹⁰⁷ The detailed mechanism is uncertain but believed to via radical process with hypervalent iodine as terminal oxidant.(Figure 4.5)

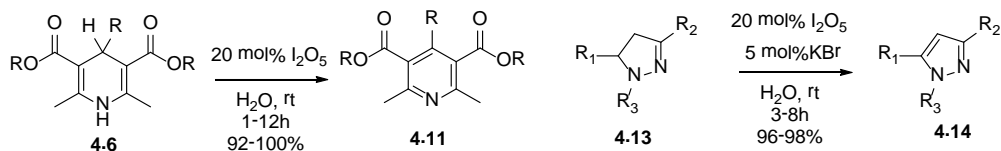


Figure 4.5 DHP oxidation with hypervalent iodine

1,3,5-Trisubstituted pyrazolines 4.13 and Hantzsch 1,4-dihydropyridines 4.6 were converted to the corresponding pyrazoles 4.14 and pyridines 4.11 effectively by the treatment of a catalytic amount of Pd/C in acetic acid at 80°C.¹⁰⁸ (Figure 4.6)

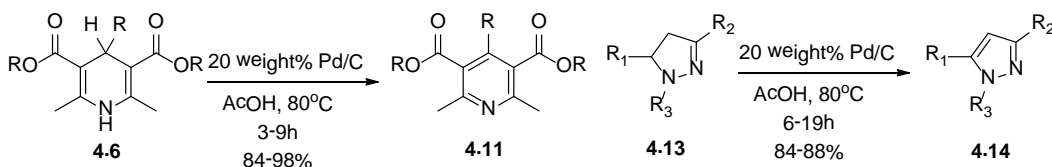


Figure 4.6 DHP oxidation catalyzed Pd/C in acetic acid

A variety of Hantzsch esters have been oxidized with potassium permanganate.¹⁰⁹ The author observed significant amount of dealkylation product 4.15 when the 4-substituent of the DHP is benzyl or secondary alkyl group like CH₃CH₂. Single product 4.11 was isolated when C⁴ substituent is aryl group. (Figure 4.7)

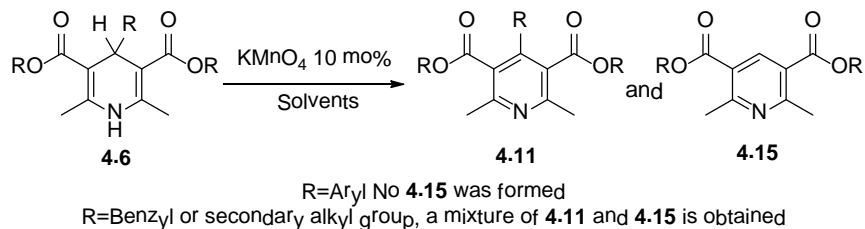


Figure 4.7 DHP oxidation catalyzed by KMnO₄

Photooxidation of Hantzsch 1,4-DHP by direct irradiation ($\lambda > 300$ nm) under an oxygen atmosphere.¹¹⁰ Spectroscopic and electrochemical studies demonstrate that photoinduced singlet electron transfer from 1,4-DHP to molecular oxygen occurs. The

generated superoxide radical anion ($O_2^{\cdot-}$) is proposed to be responsible for photochemical oxidation. (Figure 4.8)

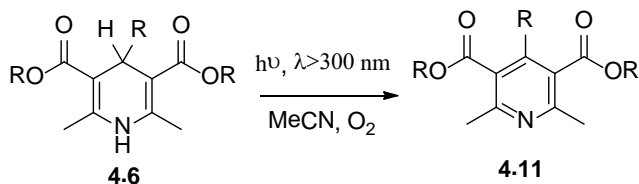


Figure 4.8 Aerobic 1, 4-DHP oxidation induced by irradiation

4.1.2 Benzothiazoline

Benzothiazoles occur naturally,¹¹¹ but numerous synthetic species display broad biological activities and are found in functional materials. Benzothiazole can be seen as the formal dehydrogenation product of benzothiazoline. The gained aromaticity of benzothiazole is the driving force for dehydrogenation to occur. Because of this, benzothiazolines have been utilized as organic reductants in many literature examples.¹¹²

Akiyama and coworkers have described the first example of the use of benzothiazoline 4.17 as the hydrogen source in the asymmetric transfer hydrogenation of ketimines 4.16 with catalytic amount of chiral phosphoric acid 4.20.¹¹³ Chiral amines 4.19 were obtained in high enantioselectivity. Benzothiazole 4.18 was obtained as a byproduct. This is a simple and complementary approach that gives higher enantioselectivity in the imine reduction. (Figure 4.9)

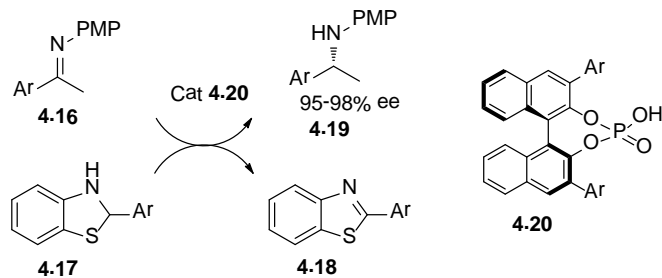


Figure 4.9 Chiral phosphoric acid catalyzed asymmetric ketimine reduction with benzothiazoline

The same group used of 2-deuterated benzothiazoline **4.17a** as a deuterium donor in combination with a chiral phosphoric acid **4.20a**, the transfer deuterium of ketimine and R-iminoester took place smoothly to give R-deuterated amines in high yields with excellent enantioselectivities.¹¹⁴ (Figure 4.10)

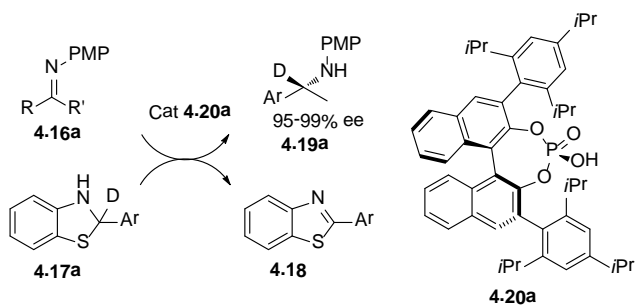


Figure 4.10 Chiral phosphoric acid catalyzed asymmetric ketimine reduction with 2-deuterated benzothiazoline

Benzothiazole derivatives are an important class of heterocyclic compounds that attracted strong interest due to their biological and pharmacological properties. The benzothiazole containing compounds involved in research aimed at evaluating new drugs that possess biological activities, such as antimicrobial, anticancer, antifungal, anthelmintic, anti-diabetic.¹¹⁵ (Figure 4.11)

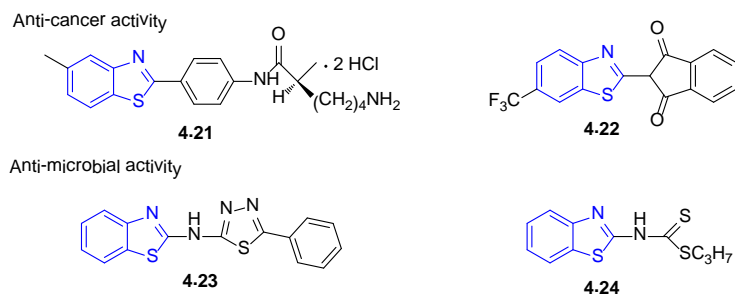


Figure 4.11 Biologically active compounds contains benzothiazole

There many ways to synthesize benzothiazoles in the literature.

Lang and coworkers developed a multi components on pot palladium-catalyzed synthesis of benzothiazoles 4.28 directly from an aryl halide 4.25, tert-butyl isocyanide 4.26 and an aminothiophenol 4.27.¹¹⁶ (Figure 4.12) Experimental observations suggest that the desired process proceeds by an initial formation of imine 4.29, which cyclizes to form 4.30. 4.30 undergoes copper catalyzed C–H activation gives rise to intermediate 4.31. Oxidative addition of the iodobenzene to the palladium catalyst facilitated formation of palladium(II) species 4.32, which can undergo a transmetalation process to give compound 4.33 and regenerate the copper cocatalyst. Subsequent reductive elimination allows for formation of 2-phenyl benzothiazole 4.28.

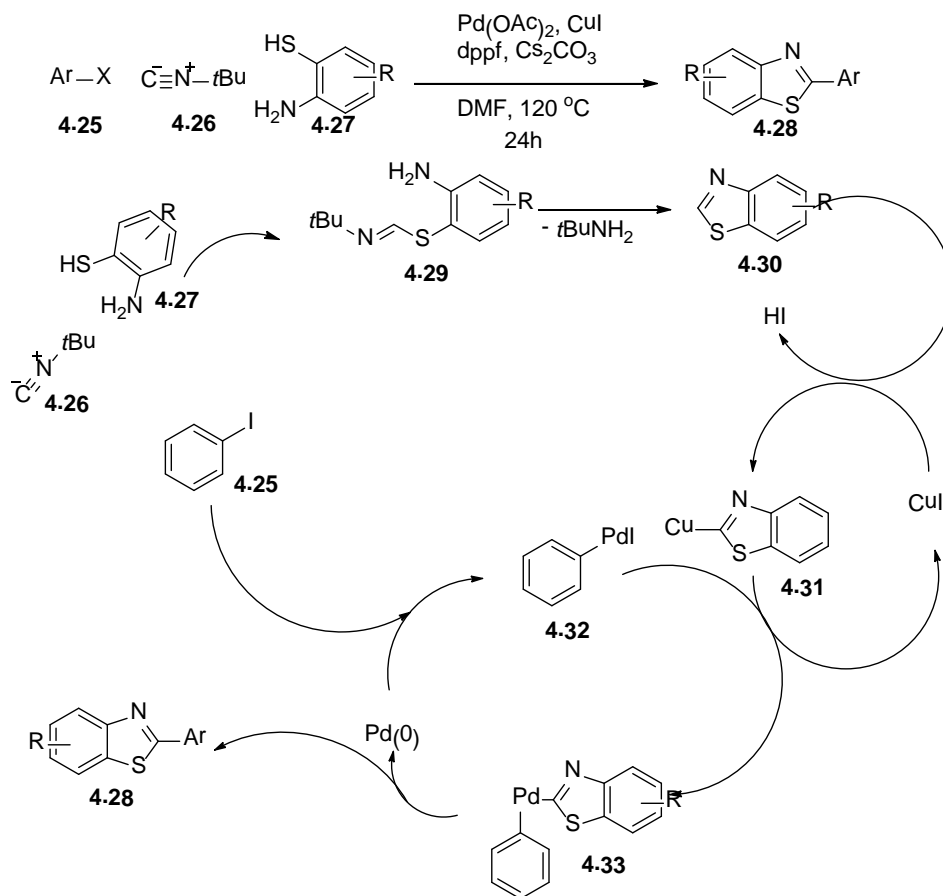


Figure 4.12 catalyzed one pot synthesis of benzothiazole from simple starting materials

A recent metal-free process for the synthesis of 2-aminobenzothiazoles 4.36 from cyclohexanones 4.34 and thioureas 4.35 has been developed using catalytic iodine and molecular oxygen as the oxidant under mild conditions.¹¹⁷ (Figure 4.13)

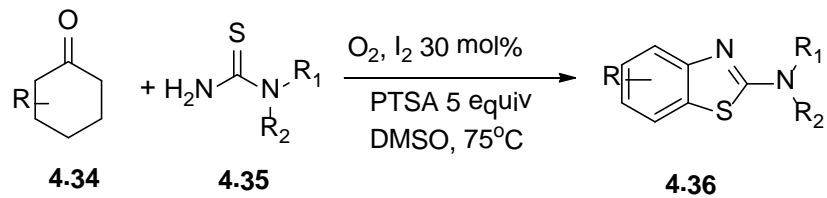


Figure 4.13 Aerobic benzothiazole synthesis catalyzed by I₂

Recently, a method was developed for the formation of 2-substituted benzothiazoles via a copper-catalyzed condensation of 2-aminobenzenethiols with nitriles.¹¹⁸ (Figure 4.14) Ethanol as the environmentally friendly solvent, the inexpensive catalytic system, mild conditions combined with an operationally simple procedure render this method a valuable addition to the traditional benzothiazole synthesis.

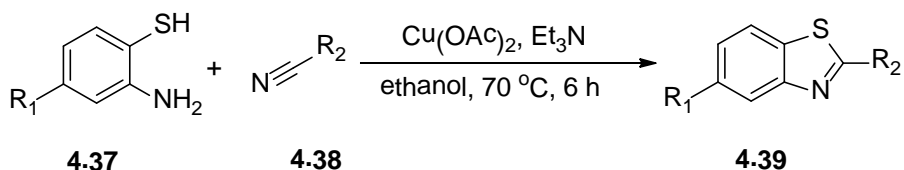


Figure 4.14 Copper catalyzed benzothiazole synthesis in ethanol

2-Aryl benzothiazole formation from aryl ketones 4.40 and 2-aminobenzenethiols 4.27 under metal- and I₂-free conditions was described.¹¹⁹ Various 2-aryl benzothiazoles were selectively obtained in good yields using molecular oxygen as oxidant. DMSO played an important role in this transformation. High temperature was required to obtain good yield. (Figure 4.15)

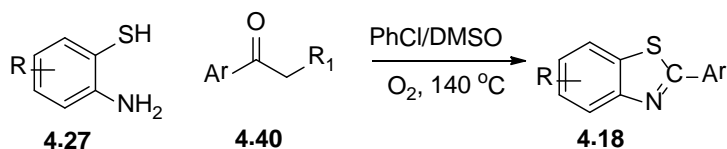


Figure 4.15 Aerobic benzothiazole synthesis in DMSO at high temperature

4.2 Flavin Catalyzed Dihydropyridine and Benzothiazoline Aromatization Reaction

In this work, a flavin catalyzed biomimetic oxidation of dihydropyridines and benzothiazolines using molecular oxygen is conducted. Biomimetic route is highlighted with red color. (Figure 4.16)

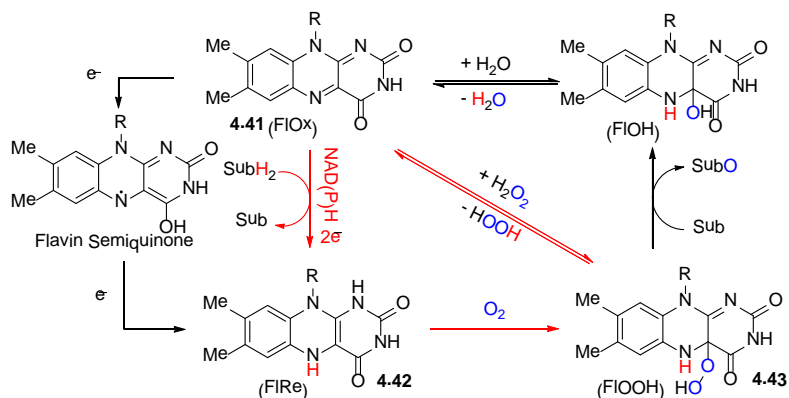


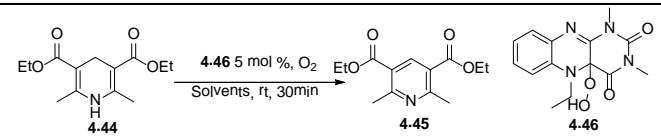
Figure 4.16 Biomimetic flavin catalyzed oxidative dehydrogenation

In organic solvents, hydroperoxyflavin 4.43 is in equilibrium with oxidized flavin 4.41 and hydrogen peroxide. (Figure 4.16) The equilibrium constant is solvent dependent in this case. To facilitate the oxidation of dihydropyridine or benzothiazoline, a solvent in which the hydroperoxyflavin 4.43 is instable will be optimal.

So we started the initial screening of common organic solvents on the aerobic oxidation of Hantzsch ester 4.44 with 5 mol % alloxazine catalyst 4.46 which has been proven to be the most active flavin catalyst in aerobic oxidation condition. (Table 4.1) Among the polar protic solvents, methanol gave the best result after 30 minutes' stirring filled with excess oxygen gas, while water showed low efficiency on pyridine formation. In fact, Bruce and coworkers found that in protic solvent like water or methanol, the 4a-OOH group of 4a-hydroperoxy-3-methylalumiflavine can be easily replaced by OH- or MeO- group, and a molecule of H₂O₂ is released into solution.¹²⁰ The unexpected low yielding in water is probably because of the low solubility of DHP 4.44 in water. Polar chlorinated solvents like dichloromethane and chloroform gave good yield of pyridine, but the non-polar carbon tetrachloride had low yield. Non-polar aprotic solvents like 1,4-dioxane and toluene provided low yield of pyridine, which was in accordance with Bruce's results that in dioxane hydroperoxy-3-methylalumiflavine can be preserved for

days. Most of polar aprotic solvents gave low yields of pyridine with the exception of acetonitrile. Interestingly, in our Dakin oxidation solvent system where we used 95:5 MeCN/H₂O and one equivalent of NaHCO₃, the pyridine formation has not been observed after 24 hours.

Table 4.1 Initial solvent screening of alloxazine catalyzed aerobic aromatization



Entry	Solvent	Conversion(%) ^a
1	water	9
2	methanol	44
3	ethanol	19
4	<i>tert</i> -butanol	2
5	dichlormethane	58
6	chloroform	53
7	carbon tetrachloride	6
8	tetrahydrofuran	6
9	acetonitrile	33
10	ethyl acetate	1
11	acetone	2
12	dimethylformamide	1
13	1,4-dioxane	8
14	toluene	9

^aConversions were detected by NMR using DMSO as internal standard

A more careful solvent study was carried out among the five solvents of the best conversions. (Table 4.2) In these tests, 0.5 equivalent of oxygen was added into degassed reaction mixture and the conversion of 4.44 to 4.45 was measured by NMR. Without out addition of catalyst 4.46, no pyridine was detected. With 5 mol % of flavin catalyst 4.46, 50% conversion was detected in chloroform reaction after 30 minutes. The catalyst loading was therefore lowered to 1 mol%, so that reactions had slower rates to be compared within 30 minutes. Within the five selected solvents, although DCM and

chloroform dissolved the HEH better than others, methanol gave the best yield (26.5%) after 30 minutes with 1 mol% alloxazine catalyst. Based on the concept of green chemistry, methanol was selected as the solvent for the substrate study.

Table 4.2 Careful solvent study of alloxazine catalyzed aerobic aromatization

Entry	Solvent	Catalyst loading(mol%)	Conversion ^a (%)
1	Chloroform	0	0
2	Chloroform	5	50
3	Chloroform	1	22
4	Dichloromethane	1	16
5	Methanol	1	26
6	Ethanol	1	8
7	Acetonitrile	1	9

^a Conversion was determined using NMR

With the optimized condition, we started looking into the oxidation of 1, 4-dihydropyridines catalyzed by alloxazine catalyst 4.46 with oxygen gas as terminal oxidant. (Figure 4.17) We were pleased to see that when the dihydropyridines C⁴ position only has hydrogen as substituent, the aromatization proceeded smoothly and cleanly at room temperature within 90 minutes. Quantitative yield was obtained by simply evaporating off solvent, and the purity of product was greater than 95%.

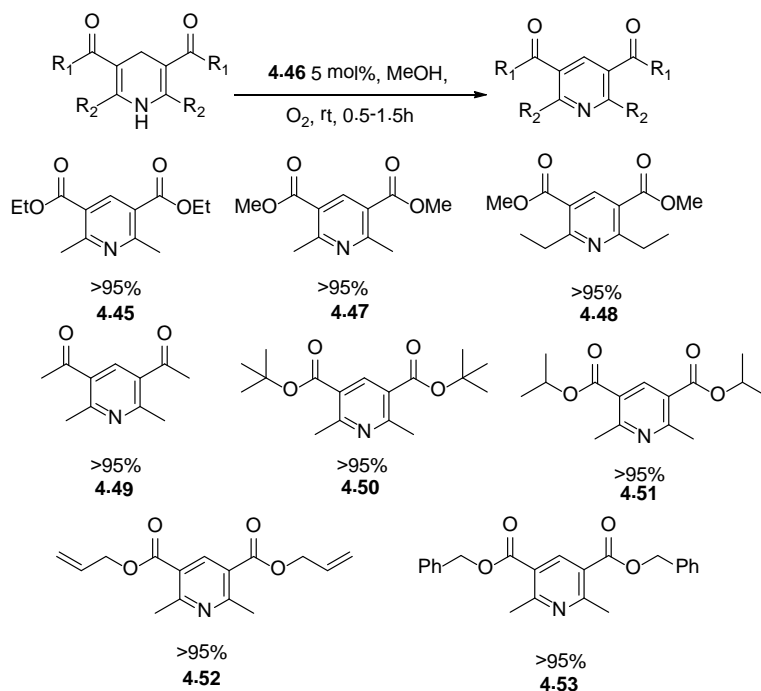


Figure 4.17 Alloxazine catalyzed dihydropyridine aromatization

Encouraged by the positive result, we tried to extend the same protocol to the tandem synthesis of pyridine starting with formaldehyde **4.54** (37 % wt in H₂O), ammonium acetate **4.56** and the corresponding acetonacetates **4.55** using air as the oxygen source. (Figure 4.18) To our delight, 1 mmol scale synthesis of pyridines can be achieved in good to excellent yield with only 2 mol % of flavin catalyst in 2 mL of methanol within 22 hours. The only exception was **4.53** since the intermediate dihydropyridine has bad solubility in methanol.

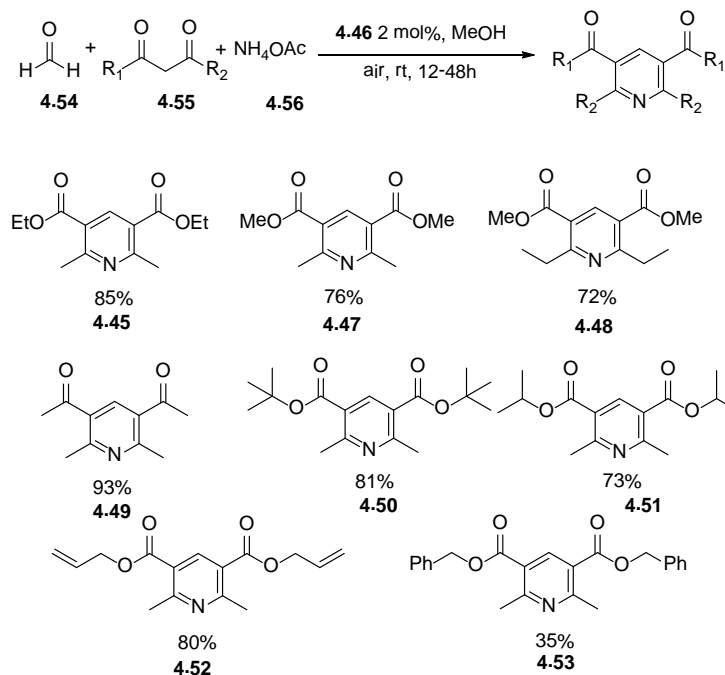


Figure 4.18 Alloxazine catalyzed multi component dihydropyridine synthesis and aromatization process

C^4 -substituted dihydropyridines (Figure 4.19) were not oxidized with alloxazine catalyst 4.46 after long reaction time and at elevated temperatures. Měnová and Cibulka recently described isoalloxazine catalysts 4.57 are $\sim 10^6$ times more electrophilic than similar alloxazine species.²⁴ This information, combined with the redox potentials for 4.57 ($E^0 = 0.388 \text{ V}$, -0.389 V) and 1a ($E^0 = 0.109 \text{ V}$, -0.695 V),¹²¹ suggest that catalyst 4.57 would accept a hydride from unreactive C^4 -substituted dihydropyridines more readily than 4.46. Indeed, with 5 mol % of isoalloxazine catalyst 4.57, 4.58 formation occurred at 50°C. However, the yield was low compared to the alloxazine catalyzed oxidation (48 hours, 20%). It was also pointed out by Cibulka that by adding an acid to isoalloxazine reactions, the elimination of H_2O from flavin pseudobase would be accelerated.²⁴ In our system (Figure 4.19), when pyridine 4.58 is formed, it deprotonates hydroxyflavin

4.57b to form flavin hydroperoxy anion, which will not eliminate H_2O_2 to regenerate the isoalloxazinium ion 4.57. So, we imagined that the elimination of H_2O_2 from hydroperoxyflavin 4.57c to regenerate isoalloxazinium ion 4.57 would also be accelerated by an acid via similar mechanism.

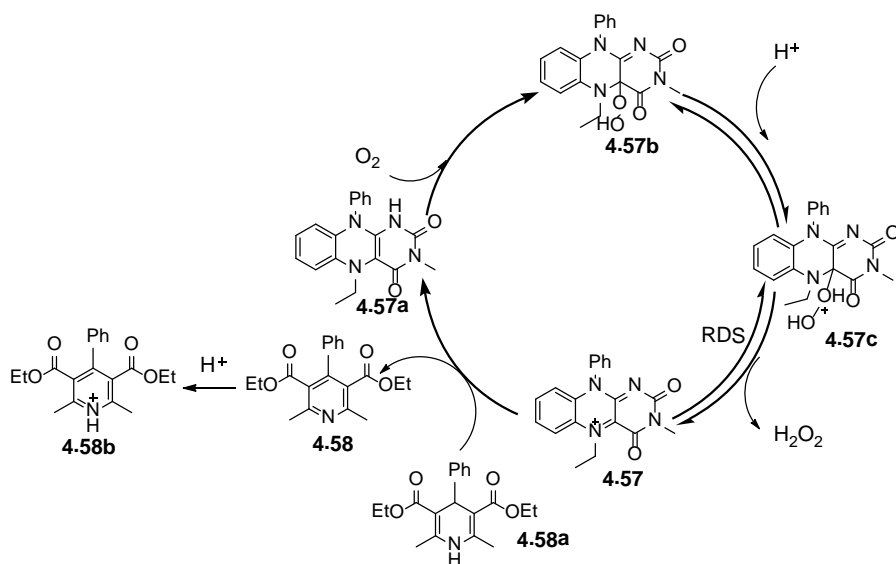


Figure 4.19 Acid mediated isoalloxazinium catalyzed aromatization mechanism

As expected, after adding 1.2 equivalent of HClO_4 , the 4.58 formation was greatly enhanced and much shorter reaction time was required. After the consumption of the starting material, aqueous sodium carbonate was added into reaction mixture to free the protonated pyridine 4.58b. An acid screening was performed and the oxidation rate was increased with acids that have low pK_a . The unexpected result of sulfuric acid is due to the strong oxidative effect of concentrated sulfuric acid itself mediated background aromatization. (Table 4.3)

Table 4.3 Acid screening with isoalloxazine 4.57 as catalyst

Entry	Acid	Conversion(%)	pK _a of the acid
1	HClO ₄	>95	-10.0
2	HCl	31	-8.0
3	H ₂ SO ₄	78	-3.0
4	TFA	11.5	-0.25
5	H ₃ PO ₄	11.5	2.12
6	HCOOH	9	3.77
7	AcOH	8	4.76

Using acidic system, we successfully oxidized a range of C⁴ substituted dihydropyridines with good to excellent yields. (Figure 4.20)

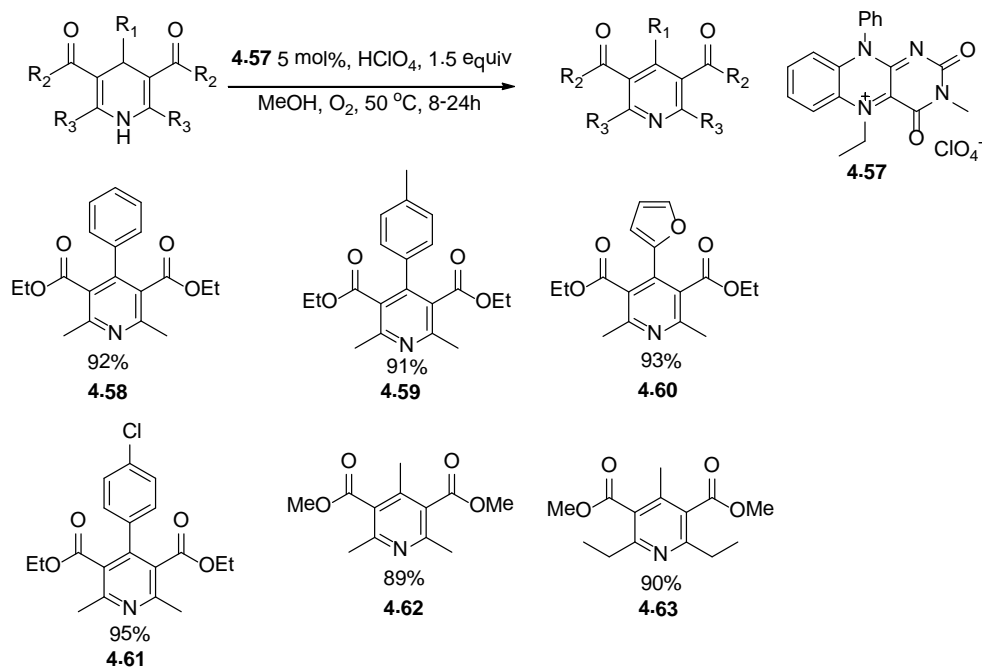


Figure 4.20 Isoalloxazine catalyzed C⁴-substituted dihydropyridine aromatization

The initial alloxazine 4.46 catalyst system was applied to benzothiazolines. Electron rich benzothiazolines were reported to undergo autoxidation in chloroform without additional catalyst.¹²² We found that acid contaminants from solvent or aldehyde oxidation enhanced the rate of benzothiazoline oxidation for electron rich substrates but also led to benzothiazoline fragmentation to amino-thiophenol and aryl aldehydes. Purification of chloroform eliminated benzothiazoline oxidation for nearly all substrates investigated in this work. In our acid free and metal-free catalytic system, control experiments without flavin catalysts were explored for all benzothiazolines that we tried. After 1.5 h, most compounds showed no detectable (<5%) benzothiazole formation, except for electron rich entries 4.69 and 4.72, which generated 20% and 25% benzothiazole conversion as background oxidation product. The alloxazine catalyzed oxidation of benzothiazolines yielded products within 1.5 h in methanol (Figure 4.21). Solvent evaporation gave products with purity greater than 95%.

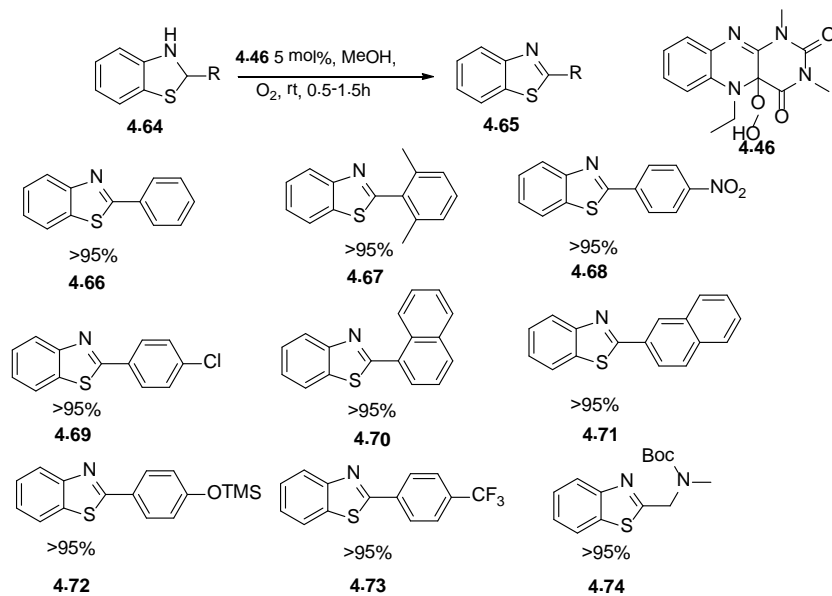


Figure 4.21 Alloxazine catalyzed benzothiazoline aromatization

On the basis of the high yields obtained by this method, a one-pot preparation of 2-substituted benzothiazoles from 2-amino-thiophenol and a range of aldehydes was sought. (Figure 4.22) A simple two-stage, one-pot operation yielded the best results. Following preparations of benzothiazolines from aminothiophenols and aldehydes in MeOH, within 6 h, flavin catalyst was added directly to the reaction without purification of the intermediate or solvent exchange.

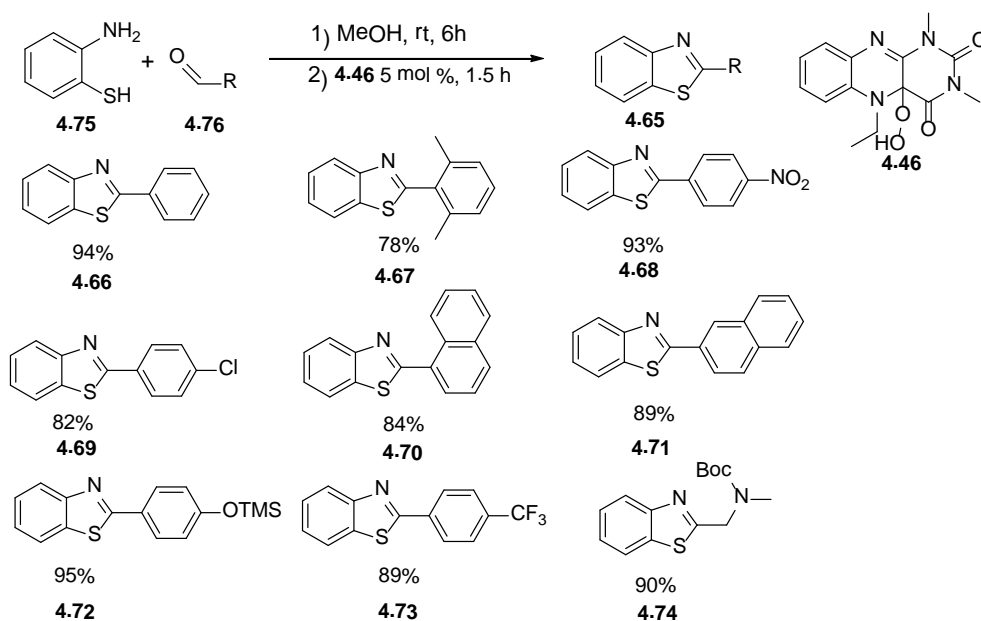


Figure 4.22 Alloxazine catalyzed two-component one pot two steps benzothiazoline aromatization

In conclusion, green and bioinspired oxidative aromatizations were developed by robust flavin organocatalysts. Flavin mimics catalyze the oxidation of dihydropyridines and benzothiazolines using oxygen as a terminal oxidant in methanol. The simple and high-yielding one-pot multicomponent synthesis of pyridines was described using 2 mol% of catalyst. Related two-stage one pot synthesis of benzothiazoles were achieved. This catalytic process is consistent with observations in the literature of flavoenzyme and

flavin mimic reactivity involving the dissociation of 4a-hydroperoxyflavins in polar protic environments, as mentioned above. Though not previously indicated in the metabolism of dihydropyridine-derived drugs, it seems chemically possible that flavoenzymes may perform the direct oxidation of various dihydropyridines drugs. Small molecule flavin mimics continue to unlock new areas of opportunity in synthesis, especially in the realm of aerobic organocatalysis. These advances are emblematic of the dynamic nature of flavin mimic catalysts and their ability to perform selective oxidations based on bioinspired method development, providing an attractive platform for efficient and sustainable oxidation research.

Appendix A
List of Abbreviations

MeCN Acetonitrile
DMF *N,N*-dimethylformamide
DMSO Dimethylsulphoxide
MeOH Methanol
EtOH Ethanol
DCM Dichloromethane
CHCl₃ Chloroform
TFE 2,2,2-Trifluoroethanol
Cat. Catalyst
NEt₃ Triethylamine
PTSA Para toluene sulfonic acid
KOH Potassium hydroxide
NaOH Sodium hydroxide
Na₂CO₃ Sodium carbonate
NaHCO₃ Sodium bicarbonate
AlCl₃ Aluminum chloride
BF₃·OEt₂ Boron trifluoride diethyl etherate
LiCl Lithium chloride
CaCl₂ Calcium chloride
HClO₄ perchloric acid
B(OH)₃ Boric acid
AcOH acetic acid
MeI iodomethane
InCl₃ Indium(III) chloride
HPLC high-performance liquid chromatography
HR-MS High-resolution mass spectrometry
GC Gas chromatography
MS Mass spectroscopy
NMR Nuclear atomic resonance
TLC Thin layer chromatography
rt Room temperature, ambient temperature
equiv Equivalent

Appendix B
General Experimental Procedure

2.10a-e general procedure:

In a 50 mL round bottom flask, *o*-phenylenediamine (3.0 mmol), alloxane monohydrate (426 mg, 3.0 mmol), boric acid (185 mg, 3.0 mmol) and 20 mL acetic acid were added. The mixture was stirred under argon at room temperature for 2 hours. During this time, solid precipitated out in the solution. The solid was collected by filtration then washed with 30 mL of acetic acid and 30 mL of diethyl ether. Product was dried further with high vacuum pump.

7,8-dichloroalloxazine (2.10a)

Yield: 94% ; Yellow solid, Mp: 387-388 °C; ¹H NMR (500 MHz, DMSO-d) δ 12.00 (br. s., 1 H), 11.77 (br. s., 1 H), 8.41 - 8.16 (m, 1 H), 7.95 (dd, J = 8.3, 11.2 Hz, 1 H); ¹³C NMR (125 MHz, CDCl₃) δ 160.50, 150.38, 147.53, 141.03, 140.93, 136.60, 136.51, 132.31, 116.41, 116.28, 113.44, 113.31; IR(Neat) 3055, 2894, 1738, 1706, 1575, 1563, 1456, 1448, 1341, 1188, 1139, 1120, 839, 625, 581, 498, 448, 411 cm⁻¹.

7,8-difluoroalloxazine (2.10b)

Yield: 99% ; Light blue solid, Mp: 310 - 312 °C; ¹H NMR (300 MHz, DMSO-d) δ 12.08 (s, 1 H), 11.82 (s, 1 H), 8.47 (d, J = 3.4 Hz, 1 H), 8.17 (d, J = 3.8 Hz, 1 H); ¹³C NMR (75 MHz, DMSO-d) δ 160.5, 150.5, 148.2, 142.1, 138.5, 136.5, 133.7, 131.3, 131.2, 128.3; ¹⁹F NMR (470 MHz, CDCl₃) δ -133.70 --133.35 (m, 1 F), -126.57 - -126.20 (m, 1 F) IR(Neat) 3190, 3054, 2938, 2896, 1732, 1674, 1634, 1577, 1288, 1263, 1229, 1205, 1147, 875, 588, 495, 444 cm⁻¹.

Alloxazine (2.10c)

Yield: 87%; Yellow solid, Mp: >400°C; ¹H NMR (500MHz, DMSO-d) δ 8.13 (d, J = 8.0 Hz, 1 H), 7.92 - 7.86 (m, 2 H), 7.79 - 7.71 (m, 1 H); ¹³C NMR (75MHz, DMSO-d) δ 161.00, 150.67, 147.40, 143.15, 139.71, 133.87, 132.22, 130.66, 128.94, 127.50; IR(Neat) 3174, 3105, 3084, 1733, 1688, 1572, 1446, 1272, 1035, 1014, 989, 768, 705, 584, 539, 511, 427, 379 cm⁻¹.

7,8-Dimethylalloxazine (2.10d)

Yield: 95% ; Bright yellow solid, Mp: 368 - 370°C; ¹H NMR (500MHz, DMSO-d) δ 11.70 (br. s., 2 H), 7.86 (br. s., 1 H), 7.65 (br. s., 1 H), 2.45 (s., 3H), 2.42 (s., 3H) NMR (125 MHz, DMSO-d) (cannot obtain due to low solubility); IR(Neat) 3084, 3054, 1723, 1683, 1557, 1483, 1455, 1355, 1213, 1004, 803, 574, 525, 475, 449, 414 cm⁻¹.

7,8-dimethoxyalloxazine (2.10e)

Yield:89% ; Bright yellow solid, Mp: 364 - 366°C; ¹H NMR (500 MHz, DMSO-d) δ 11.74 (br. s., 1 H), 11.57 (br. s., 1 H), 7.46 (s, 1 H), 7.19 (s, 1 H), 3.98 (br. s., 3 H), 3.93 (br. s., 3 H); ¹³C NMR (125 MHz, CDCl₃) δ 161.36, 156.30, 152.24, 150.66, 146.35, 141.49, 137.15, 127.80, 107.78, 105.12, 56.96, 56.69; IR(Neat) 3073, 2935, 2846, 1690, 1555, 1502, 1434, 1372, 1344, 1291, 1236, 998, 870, 539, 501, 427 cm⁻¹. HRMS: C₁₂H₁₁N₄O₄ (Calculated = 275.0780 *m/z*) Found = 275.0776 *m/z*

2.11a-e general procedure:

Alloxazine (3.0 mmol) and K₂CO₃ (1.38 G, 10 mmol) were added to 20 mL of dry DMF under argon. Mel (0.6 mL, 10 mmol) was then added to the above solution. The mixture was stirred at room temperature for 4 hours. DMF was removed at 80 °C under vacuum. The resulting solid was dissolved in 20 mL of dichloromethane and 20 mL of H₂O then transferred into a separation funnel. The aqueous layer was washed with dichloromethane (4 x 20 mL). The combined organic phase was washed with 40 mL of brine, then dried with MgSO₄. Solvent was removed under reduced pressure. The crude material was purified by column chromatograph (2:98 CH₃OH/CH₂Cl₂).

7,8-dichloro-1,3-dimethylalloxazine (2.11a)

Yield:77% ; Light yellow solid, Mp: 248 - 250°C; ¹H NMR (500 MHz, CDCl₃) δ 8.37 (s, 1 H), 8.12 (s, 1 H), 3.77 (s, 3 H), 3.57 (s, 3 H); ¹³C NMR (125 MHz, CDCl₃) δ 159.2, 150.4, 146.2, 142.0, 139.1, 138.5, 134.0, 130.9, 130.5, 128.4, 29.8, 29.4; IR(Neat) 3078, 3038, 2948, 1720, 1674, 1597, 1552, 1490, 1355, 1294, 1211, 1189, 1110, 1065, 1017, 1002, 745, 673, 469, 445, 418, 396 cm⁻¹7,8-difluoro-1,3-dimethylalloxazine (2.11b)

Yield: 87% ; Orange solid, Mp: 196-197°C; ^1H NMR (300 MHz, CDCl_3) δ 8.09 (dd, J = 8.4, 9.8 Hz, 1 H), 7.78 (dd, J = 7.9, 10.3 Hz, 1 H), 3.81 (s, 3 H), 3.60 (s, 3 H); ^{13}C NMR (125 MHz, CDCl_3) δ 159.50, 156.49, 156.37, 154.40, 154.27, 153.14, 153.01, 151.08, 150.96, 150.56, 145.73, 141.51, 141.41, 137.19, 137.09, 129.81, 129.78, 116.27, 116.13, 113.65, 113.51, 29.78, 29.38; ^{19}F NMR (470 MHz, CDCl_3) δ -129.42- -129.01 (m, 1 F), -122.46- -121.71 (m, 1 F) IR(Neat) 3044, 2967, 1720, 1676, 1559, 1482, 1375, 1359, 1297, 1220, 1197, 1173, 1101, 911, 857, 744, 457, 441, 418, 398 cm^{-1} .

1,3-dimethylalloxazine (2.11c)

Yield: 97% ; Bright yellow solid, Mp: 234 - 235°C; ^1H NMR (300 MHz, CDCl_3) δ 8.39 - 8.29 (m, 1 H), 8.08 - 8.00 (m, 1 H), 7.90 (dt, J = 1.5, 7.7 Hz, 1 H), 7.80 - 7.72 (m, 1 H), 3.83 (s, 3 H), 3.61 (s, 3 H); ^{13}C NMR (75MHz, CDCl_3) δ 159.88, 150.80, 145.45, 143.44, 140.10, 133.93, 130.90, 129.75, 129.21, 127.92, 29.67, 29.27; IR(Neat) 1717, 1652, 1552, 1455, 1417, 1377, 1201, 1103, 1063, 810, 772, 443, 424, 405 cm^{-1} .

7,8-DiMethyl-1,3-dimethylalloxazine (2.11d)

Yield: 90% ; Bright yellow solid, Mp: 246 - 248°C; ^1H NMR (500 MHz, CDCl_3) δ 8.04 (br. s., 1 H), 7.76 (br. s., 1 H), 3.78 (s, 3 H), 3.57 (s, 3 H), 2.51 (s, 3 H), 2.48 (s, 3 H); ^{13}C NMR (125 MHz, CDCl_3) δ 160.20, 150.90, 145.74, 145.11, 142.46, 140.09, 139.25, 129.54, 128.63, 126.88, 29.55, 29.19, 20.96, 20.39; IR(Neat) 3058, 3046, 2946, 2921, 2846, 1720, 1667, 1557, 1482, 1471, 1361, 1257, 1217, 873, 747, 558, 488, 467, 439, 419 cm^{-1} .

7,8-DiMethoxy-1,3-dimethylalloxazine (2.11e)

Yield:85% ; Bright yellow solid, Mp: 218 - 219°C; ^1H NMR (500 MHz, CDCl_3) δ 7.57 (s, 1 H), 7.26 (s, 1 H), 4.10 (s, 3 H), 4.04 (s, 3 H), 3.79 (s, 3 H), 3.58 (s, 3 H); ^{13}C NMR (125 MHz, CDCl_3) δ 156.68, 152.68, 150.97, 144.79, 141.87, 137.51, 126.49, 115.45, 107.57, 105.05, 56.82, 56.61, 29.47, 29.14; IR(Neat) 3079, 3006, 2942, 1714, 1663, 1549, 1248, 1230, 1202, 1060, 848, 746, 487, 457, 408 cm^{-1} . HRMS: $\text{C}_{14}\text{H}_{15}\text{N}_4\text{O}_4$ (Calculated = 303.1093 m/z) Found = 303.1088 m/z .

2.12a-e general procedure:

2.12c and 2.12d

2 mmol of 1,3-Dimethylalloxazine (2.11c or 2.11d) and 150 mg 10% Pd/C was added in a round bottom flask, the flask was then charged with Argon. 20 ml of degassed solvent (1:1 Ethanol/H₂O) was added under argon. The mixture was degassed 2 times using Freeze-Pump-Thaw technique with acetone and dry ice. 2 ml (36 mmol) of distilled acetaldehyde and 1.66 ml (20 mmol) of concentrated HCl was added via syringe into reaction mixture. The mixture was frozen again under vacuum. H₂ balloon was prepared to refill the reaction flask vacuum with H₂, and then reaction was warmed up to room temperature. Reaction was stirred for 2 days under H₂ atmosphere. The Pd/C was filtered off with Celite and the Celite was washed extensively with ethanol until the color of the wash became clear. During the wash, the filtrate color turned from light yellow to dark brown because of the auto oxidation of flavin by air. NH₃ was added drop-wise with stirring until the pH of the solution was adjusted to 7-8. A dark precipitate started to form while the solution was neutralized. Ethanol was removed under pressure at 30 °C, leaving most of the water in the round bottom flask. The flask was then cooled in an ice-bath for 10 minutes, precipitating most of the product. The brown colored product was collected by filtration, and then washed with an additional 10 mL of cold water and 5 mL of cold ethanol. The product was dried under vacuum and was stable to be stored at room temperature. The NMR experiment was performed by placing 5 mG of product in an Argon-filled NMR tube with 30 mG sodium dithionite then dissolved by 0.25 mL of degassed CDCl₃ and 0.25 mL of degassed D₂O. The NMR tube was shaken until the color of solution turned from dark red-brown to light yellow.

2.12b

For 7,8-difluoro-1,3-dimethyl-5-ethyl-5,10-dihydroalloxazine 2.12b, 80 psi hydrogen was applied to the reaction mixture for 2 days, instead of 1 atm pressure of hydrogen.

2.12e

For 7,8-Dimethoxy-1,3-dimethyl-5-ethyl-5,10-dihydroalloxazine 2.12e, workup is different from the other 4 catalysts. The reaction mixture was filtered through Celite. The PH of the filtrate was adjusted to 7-8 using ammonia hydroxide solution. All of the solvent was evaporated under reduced pressure. The resulting dark brown solid was re-dissolved with DCM, insoluble salt was filtered off. The DCM of the filtrate was reduced under reduced pressure to get product as dark brown powder.

2.12a

For 7,8-Dichloro-1,3-dimethyl-5-ethyl-5,10-dihydroalloxazine 2.12a, standard reaction solvent condition result in de-chloronation of the aromatic ring. So Dichloromethane is used as solvent instead of ethanol and water mixture. In a typical reaction, 160mg (0.5 mmol) of 7,8-Dichloro-1,3-Dimethylalloxazine and 50 mg 10% Pd/C was added in a round bottom flask, 20 ml of DCM was added to dissolve to starting material. The reaction mixture was degassed under reduced pressure while cooling with acetone and dry ice. 0.5 ml (36 mmol) of distilled acetaldehyde and 0.6 ml (5 mmol) of concentrated HCl was added via syringe into reaction mixture. H₂ balloon was prepared to refill the reaction flask vacuum with H₂, and then reaction was warmed up and stirred at room temperature. After 12 hours, the reaction is stopped. 30 ml of ethanol was added into the reaction flask to dissolve the black solid on the wall of the glass. The Pd/C was filtered off with Celite and the Celite was washed using a lot of ethanol (until the color of wash become clear). NH₃ was added drop-wise with stirring until the pH of the solution was adjusted to 7-8. Removed most of ethanol under pressure at 30 °C, left most of water in the round bottom flask. Cool the flask in ice-bath for 10min, most of product should precipitate out. Collected the brown colored product by filtration, and then washed with additional 10 ml of cold water.

7,8-Dichloro-1,3-dimethyl-5-ethyl-5,10-dihydroalloxazine (2.12a)

Yield:80% ; brown solid (corresponding peroxide), Mp:134-140°C decompose; ¹H NMR (500 MHz, CDCl₃) δ 6.86 (s, 1 H), 6.61 (s, 1 H), 3.48 (q, J = 7.3 Hz, 2 H), 3.44 (s, 3 H), 3.33 (s, 3 H),

1.17 (t, J = 7.2 Hz, 3H); ^{13}C NMR (125 MHz, CDCl_3) δ 157.66, 150.21, 145.06, 136.84, 134.38, 127.97, 125.86, 124.91, 122.87, 115.60, 50.22, 28.70, 28.46, 11.88 IR(Neat) 3319, 3063, 3040, 2974, 2943, 2881, 1722, 1683, 1626, 1158, 1446, 1423, 1404, 1164, 1150, 1129, 1099, 1035, 870, 746, 615, 546, 412, 396 cm^{-1} . HRMS: $\text{C}_{14}\text{H}_{13}\text{N}_4\text{O}_2\text{Cl}_2$ (Calculated = 339.0416 m/z)
Found = 339.0411 m/z

7,8-difluoro-1,3-dimethyl-5-ethyl-5,10-dihydroalloxazine (2.12b)

Yield: 75% ; Black solid (corresponding peroxide), Mp: 183 – 184°C decompose; ^1H NMR (500 MHz, CDCl_3) δ 6.70 (dd, J = 7.7, 11.2 Hz, 1 H), 6.42 (dd, J = 7.4, 10.3 Hz, 1 H), 3.44 (s, 3 H), 3.41 (q, J = 6.9 Hz, 2H), 3.33 (s, 3 H), 1.15 (t, J = 6.9 Hz, 3 H); ^{13}C NMR (125 MHz, CDCl_3) δ (not obtained due to high air sensitivity) ^{19}F NMR (283MHz, CDCl_3) δ -141.93,-143.34; IR(Neat) 3055, 3013, 2990, 2946, 1683, 1624, 1473, 1458, 1344, 1264, 1234, 1180, 1135, 1102, 1084, 880, 747, 681, 628, 526, 456, 435, 404 cm^{-1} . HRMS: $\text{C}_{14}\text{H}_{13}\text{N}_4\text{O}_2\text{F}_2$ (Calculated = 307.1007 m/z) Found = 307.1009 m/z .

1,3-dimethyl-5-ethyl-5,10-dihydroalloxazine (2.12c)

Yield 85%: ; Brown solid(corresponding peroxide), Mp: 155-160°C decompose; ^1H NMR (500 MHz, CDCl_3) δ 6.93 - 6.81 (m, 2 H), 6.81 - 6.74 (m, 1 H), 6.59 (d, J = 7.4 Hz, 1 H), 3.46 (s, 3 H), 3.44 (q, J = 6.9 Hz, 2 H) 3.33 (s, 3 H), 1.13 (t, J = 7.2 Hz, 3 H); ^{13}C NMR (125 MHz, CDCl_3) δ 158.14, 150.47, 146.43, 136.33, 135.06, 125.17, 123.59, 122.62, 114.79, 99.71, 50.77, 28.79, 28.42, 11.53; IR(Neat) 3055, 2982, 2946, 2879, 1718, 1674, 1558, 1485, 1472, 1100, 1085, 1056, 1045, 744, 736, 491, 419 cm^{-1} . HRMS: $\text{C}_{14}\text{H}_{15}\text{N}_4\text{O}_2$ (Calculated = 271.1195 m/z)
Found = 271.1190 m/z .

7,8-Dimethyl-1,3-dimethyl-5-ethyl-5,10-dihydroalloxazine (2.12d)

Yield: 74% ; Brown solid(corresponding peroxide), Mp: 155- 160°C decompose; ^1H NMR (500 MHz, CDCl_3) δ 6.69 (s, 1 H), 6.33 (s, 1 H), 3.44 (s, 3 H), 3.43 (q, 2 H), 3.33 (s, 3 H), 2.11 (s, 6 H), 1.10 (t, J = 6.9 Hz, 3 H); ^{13}C NMR (125 MHz, CDCl_3) δ 158.20, 150.52, 146.41, 133.40, 133.16, 132.43, 131.79, 124.03, 116.00, 99.69, 50.83, 28.69, 28.38, 19.33, 19.18, 11.30;

IR(Neat) 2989, 2944, 1677, 1609, 1464, 1386, 1347, 1181, 1157, 1135, 1095, 1073, 1046, 750, 711, 552, 487, 423, 397, 388 cm^{-1} . HRMS: $\text{C}_{16}\text{H}_{19}\text{N}_4\text{O}_2$ (Calculated = 299.1508 m/z) Found = 299.1510 m/z

7,8-Dimethoxy-1,3-dimethyl-5-ethyl-5,10-dihydroalloxazine (2.12e)

Yield:68% ; Black solid(corresponding peroxide), Mp: 85 – 88 °C decompose; ^1H NMR (500 MHz, CDCl_3) δ 6.59 (s, 1 H), 6.20 (s, 1 H), 3.81 (s, 3 H), 3.79 (s, 3 H), 3.46 (s, 3 H), 3.40-3.36 (q, $J = 6.9$ Hz, 2 H), 3.34 (s,3 H), 1.11 (t, $J = 6.9$ Hz, 3 H); ^{13}C NMR (125 MHz, CDCl_3) δ 158.49, 150.54, 146.86, 146.32, 145.56, 128.09, 128.01, 107.90, 100.07, 99.23, 56.39, 56.29, 51.24, 28.80, 28.40, 11.03; IR(Neat) 3367, 3128, 2941, 1714, 1664, 1615, 1489, 1428, 1394, 1259, 1217, 1138, 1105, 985, 844, 536, 518, 485, 456, 415 cm^{-1} . HRMS: $\text{C}_{15}\text{H}_{23}\text{O}_8$ (Calculated = 331.1393 m/z) Found = 331.1393 m/z .

3-methyl-6-(phenylamino)pyrimidine-2,4(1H,3H)-dione 2.17

A mixture of chlorouracil (20 mmol) and aniline (60 mmol) was stirred at 180 °C in a sealed tube without any solvent for 30 minutes. After cooling, the resulting solid was crushed in ester, collected by filtration, washed with water and recrystallized in ethanol to give 72% yield of white powder 2.17.

^1H NMR (500MHz, $[\text{D}_6]$ DMSO, 25°C) δ = 10.48 (br. s., 1 H; NH), 8.24 (s, 1 H; C=CH), 7.38 - 7.31 (m, 2 H; ArH), 7.17 (d, $^3J(\text{H,H}) = 7.4$ Hz, 2 H; ArH), 7.13 (t, $^3J(\text{H,H}) = 7.4$ Hz, 1 H; ArH), 4.81 (d, $^4J(\text{H,H}) = 2.3$ Hz, 1 H; NH), 3.03 (s, 3 H; CH₃); ^{13}C NMR (75MHz, $[\text{D}_6]$ DMSO, 25 °C) δ = 163.9, 151.6, 151.2, 138.5, 130.3, 129.9, 123.0, 76.0, 26.6

3-methyl-10-phenylisoalloxane 2.19

2.17 (10mol) and nitrosobenzene (30 mmol) in a round bottom flask was added 50 mL of acetic acid. The round bottom flask was immediately merged into preheated oil bath (120 °C) to reflux and stir for 5 minutes (prolonged heating will result in formation of complex byproducts). After 5 minutes, the reaction was cooled to room temperature then added into 200 mL of cold ether. The product was precipitated out in ether was a orange-yellow powder, which

was collected by suction filtration and washed with cold ether to give 2.19 in 70% yield as a yellow powder.

^1H NMR (500 MHz, $[\text{D}_1]\text{CHCl}_3$, 25 °C) δ = 8.35 (d, $^3J(\text{H,H})= 7.4$ Hz, 1 H; ArH), 7.71 - 7.54 (m, 5 H; ArH), 7.29 (d, $^3J(\text{H,H})= 7.4$ Hz, 2 H; ArH), 6.89 (d, $^3J(\text{H,H})= 8.6$ Hz, 1 H; ArH), 3.50 (s, 3 H; CH₃); ^{13}C NMR (125 MHz, $[\text{D}_1]\text{CHCl}_3$, 25 °C) δ =159.7, 155.6, 150.0, 137.8, 135.7, 135.4, 135.1, 134.3, 132.8, 130.9, 130.6, 127.6, 126.7, 117.2, 28.9.

3-methyl-5-ethyl-10-phenylisoalloxanium prechlorate 2.20

2.19 (3 mmol) and 10% Pd/C (150 mg) was added to a round bottom flask. The flask was then charged with Argon and 20 mL of degassed Ethanol/H₂O (1:1) under argon. The mixture was degassed two additional times using Freeze-Pump-Thaw technique with an acetone and dry ice bath. Distilled acetaldehyde (3 mL, 54 mmol) and concentrated aqueous HCl (1.66 mL, 36 mmol) was added via syringe to the reaction mixture. The mixture was frozen again under vacuum. An H₂ balloon was prepared to refill the reaction flask vacuum with H₂, and then reaction was warmed up to room temperature. The reaction was stirred for two days under H₂ atmosphere. The Pd/C was filtered off with Celite and the Celite was washed extensively with ethanol until the color of the wash became clear. During the wash, the filtrate color turned from light yellow to dark brown because of the auto oxidation of flavin by air. The solvent of the filtrate was then evaporated under vacuum to yield brown oil which was mixed with 12 mL of 2N HClO₄ and cooled to 0 °C. 5 gram of NaClO₄ was added into the above acidic solution followed by 1.5 gram of NaNO₂. The resulting purple solution was stirred at 0 °C for an additional 2 hours. The product 2.20 precipitated out of the water solution and it can be collected by suction filtration and washed with water to yield 87% as purple powder.

^1H NMR (500 MHz, $[\text{D}_1]\text{CHCl}_3$, 25 °C) δ = 7.68 - 7.56 (m, 3 H; ArH), 7.33 (d, J = 8.0 Hz, 2 H; ArH), 6.96 - 6.92 (m, 1 H; ArH), 6.91 - 6.86 (m, 1 H; ArH), 6.65 (t, $^3J(\text{H,H})= 7.7$ Hz, 1 H; ArH), 5.93 (d, $^3J(\text{H,H})= 8.0$ Hz, 1 H; ArH), 3.54 (q, $^3J(\text{H,H})= 6.9$ Hz, 2 H; CH₂), 3.28 (s, 3 H; NCH₃), 1.27 (t, $^3J(\text{H,H})= 6.9$ Hz, 3 H; CH₂CH₃); ^{13}C NMR (125 MHz, $[\text{D}_1]\text{CHCl}_3$, 25 °C) δ =

159.0, 149.2, 143.9, 138.6, 137.1, 134.2, 131.7, 130.8, 130.4, 125.1, 123.3, 122.9, 114.3, 99.9, 50.7, 27.4, 11.2; HRMS: C₁₉H₁₇N₄O₂+Na, Calculated = 356.1238 *m/z*, Found = 356.1222 *m/z*

General Procedure for H₂O₂ based Dakin oxidation:

In a 1 dram glass vial equipped with stir bar, substrate (0.2 mmol), flavin(0.02 mmol, 0.1 equiv), 1M sodium bicarbonate aqueous solution (200 μ l, 1 equiv), 35% H₂O₂ solution(5equiv, 120 μ l) and 2mL solvent (MeOH/H₂O=95/5) were added. The reaction was stirred at room temperature and monitored by TLC until the disappearance of starting material. The reaction mixture was transferred to a round bottom flask and added 50 mG silica gel. The solvent was evaporated with reduced pressure. The product-silica gel was loaded on a column and purified by flash chromatography using 1:3 ethyl acetate/ hexane as eluent.

General Procedure for O₂ based Dakin oxidation:

A solution of 95:5 organic solvents/H₂O was prepared. Then an one dram glass vial was equipped with stir bar, salicylaldehyde (0.2 mmol), catalysts (5 mol%), Hantzsch Ester (1 equiv), 1 M aqueous base solution (0.2 mL), and the above solvent (2 mL). Then oxygen balloon was equipped. Reactions were stirred at room temperature for 1h. At that time, a 10 μ L aliquot was taken from each reaction and dissolved in 0.5 mL of CDCl₃. Conversion was measured by comparing the integration of starting material signal and product signal.

Catechol 2.43a

White solid, Mp: 103 – 104 °C. ¹H NMR (500 MHz, CDCl₃) δ 6.90 - 6.84 (m, 2 H), 6.84 - 6.74 (m, 2 H), 5.19 - 5.06 (m, 2 H); ¹³C NMR (125 MHz, CDCl₃) δ 143.5, 121.4, 115.6 Flash column chromatography ethyl acetate/ hexanes, 1:3, R_f= 0.23.

3-methoxycatechol 2.43b

Colorless oil. ^1H NMR (500 MHz, CDCl_3) δ 6.75 (dt, $J = 2.3, 8.3$ Hz, 1 H), 6.60 (d, $J = 7.4$ Hz, 1 H), 6.47 (d, $J = 7.4$ Hz, 1 H), 5.44 (br. s., 1 H), 5.37 (br. s., 1 H), 3.87 (s, 3 H); ^{13}C NMR (125 MHz, CDCl_3) δ 147.1, 144.2, 132.6, 119.9, 108.9, 103.2, 56.3 Flash column chromatography ethyl acetate/ hexanes, 1:3, $R_f = 0.32$.

4-methoxycatechol 2.43c

White solid, Mp: 56 – 57 °C. ^1H NMR (500 MHz, CDCl_3) δ 6.76 (d, $J = 8.6$ Hz, 1 H), 6.50 (d, $J = 2.9$ Hz, 1 H), 6.34 (dd, $J = 2.9, 8.6$ Hz, 1 H), 5.52 (br. s., 2 H), 3.72 (s, 3 H); ^{13}C NMR (125 MHz, CDCl_3) δ 154.3, 144.7, 137.4, 116.0, 105.5, 102.6, 55.9 Flash column chromatography ethyl acetate/hexanes, 1:3, $R_f = 0.27$.

3-methylcatechol 2.43d

White solid, Mp: 40-43°C. ^1H NMR (500MHz, CDCl_3) δ 6.71 (s, 3 H), 5.25 (br. s., 1 H), 5.18 (br. s., 1 H), 2.26 (s, 3 H); ^{13}C NMR (125MHz, CDCl_3) δ 143.13, 142.20, 124.61, 123.05, 120.27, 113.07, 15.58 Flash column chromatography ethyl acetate/hexanes, 1:3, $R_f = 0.5$.

2,6-dimethylhydroquinone 2.43e

White solid, Mp 148-149 °C. ^1H NMR (300MHz, DMSO-d_6) δ 8.43 (s, 1 H), 7.38 (s, 1 H), 6.27 (s, 2 H), 2.03 (s, 6 H); ^{13}C NMR (75 MHz, DMSO-d_6) δ 150.26, 145.94, 125.99, 115.09, 115.03, 17.32 Flash column chromatography ethyl acetate/ hexanes, 1:3, $R_f = 0.35$

1,2-naphthoquinone 2.43f

White solid, Mp 145-146 °C. ^1H NMR (500 MHz, CDCl_3) δ 8.12 (d, $J = 7.4$ Hz, 1 H), 7.65 (d, $J = 1.1$ Hz, 1 H), 7.51 (t, $J = 7.7$ Hz, 1 H), 7.44 (d, $J = 10.3$ Hz, 1 H), 7.37 (d, $J = 7.4$ Hz, 1 H), 6.44 (d, $J = 9.7$ Hz, 1 H); ^{13}C NMR (125 MHz, CDCl_3) δ 180.9, 178.9, 145.4, 135.9, 134.9, 131.7, 130.9, 130.4, 129.9, 128.1 Flash column chromatography ethyl acetate/ hexanes, 1:3, $R_f = 0.25$

4-nitrocatechol 2.43g

Yellow solid, Mp 173-177 °C. ^1H NMR (300MHz, DMSO-d_6) δ 10.26 (dd, $J = 4.9, 8.3$ Hz, 2 H), 7.60 (dd, $J = 2.6, 8.9$ Hz, 1 H), 7.56 (d, $J = 2.9$ Hz, 1 H), 6.86 (d, $J = 9.2$ Hz, 1 H); NMR (75 MHz,

DMSO-d₆) δ 153.43, 146.00, 140.00, 117.07, 115.55, 110.93. Flash column chromatography ethyl acetate/hexanes, 1:2, R_f= 0.3.

hydroquinone 2.43h

White solid, Mp 172-174 °C. ¹H NMR (300 MHz, DMSO-d₆) δ 8.62 (s, 2 H), 6.53 (s, 4 H); ¹³C NMR (75 MHz, DMSO-d₆) δ 150.3, 116.2 Flash column chromatography ethyl acetate/hexanes, 1:3, R_f= 0.25

2-methoxyhydroquinone 2.43i

White solid, Mp 89-90°C. ¹H NMR (500 MHz, CDCl₃) δ 6.75 (d, J = 8.6 Hz, 1 H), 6.44 (d, J = 2.9 Hz, 1 H), 6.31 (dd, J = 2.9, 8.6 Hz, 1 H), 5.32 - 5.11 (m, 1H), 5.10 - 4.71 (m, 1 H), 3.84 (s, 3 H); ¹³C NMR (125 MHz, CDCl₃) δ 149.3, 147.2, 139.6, 114.5, 106.9, 99.8, 56.0 Flash column chromatography ethyl acetate/ hexanes, 1:3, R_f= 0.22.

2,6-dimethoxy-1,4-benzenediol 2.43j

White solid, Mp 158-162°C. ¹H NMR (500 MHz, CDCl₃) δ 5.84 (s, 2 H), 3.81 (s, 6 H); ¹³C NMR (125 MHz, CDCl₃) δ 186.95, 176.78, 157.41, 107.51, 56.58 Flash column chromatography ethyl acetate/hexanes, 1:3, R_f= 0.3.

2,4-dimethoxyphenol 2.43k

White solid, Mp 219-220 °C. ¹H NMR (300 MHz, CDCl₃) δ 6.83 (d, J = 8.9 Hz, 1 H), 6.49 (d, J = 2.8 Hz, 1 H), 6.39 (dd, J = 2.8, 8.6 Hz, 1 H), 5.34 (s, 1 H), 3.85(s, 3 H), 3.76 (s, 3 H); ¹³C NMR (125 MHz, CDCl₃) δ 153.6, 147.2, 139.9, 114.2, 104.3, 99.5, 55.96, 55.9 Flash column chromatography ethyl acetate/hexanes, 1:3, R_f= 0.45

3-chlorocatechol 2.43o

White solid, Mp 48-49 °C. ¹H NMR (500MHz, CDCl₃) δ 6.90 - 6.82 (m, 2 H), 6.81 - 6.74 (m, 1 H), 5.46 (br. s., 2 H); ¹³C NMR (125MHz, CDCl₃) δ 144.93, 139.33, 121.34, 120.51, 119.86, 114.38

5-chlorocatechol 2.43p

White solid, Mp 90-91 °C. ¹H NMR (500MHz, CDCl₃) δ 6.88 (s, 1 H), 6.78 (d, J = 1.1 Hz, 2 H), 5.44 (br. s., 1 H), 5.25 (br. s., 1 H); ¹³C NMR (125MHz, CDCl₃) δ 144.28, 142.27, 125.75, 121.05, 116.23, 115.9.

3,5-dichlorocatechol 2.43q

White solid, Mp 80-82 °C. ¹H NMR (500MHz, CDCl₃) δ 6.90 (s, 1 H), 6.86 (s, 1 H), 5.69 - 5.18 (m, 2 H); ¹³C NMR (125MHz, CDCl₃) δ 145.26, 138.24, 125.99, 120.14, 120.05, 115.07.

3-bromo-5-nitrocatechol 2.43r

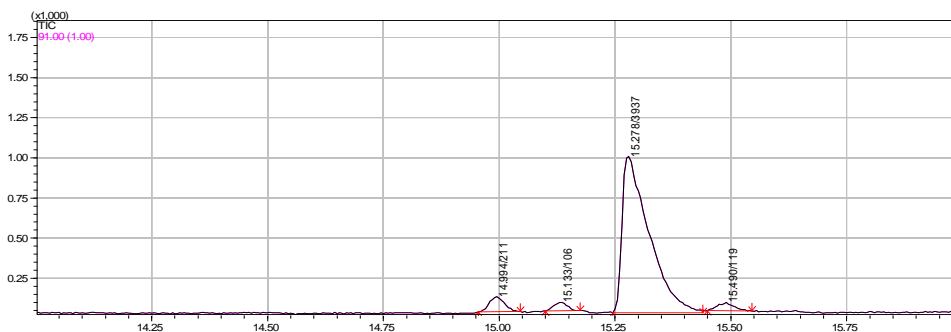
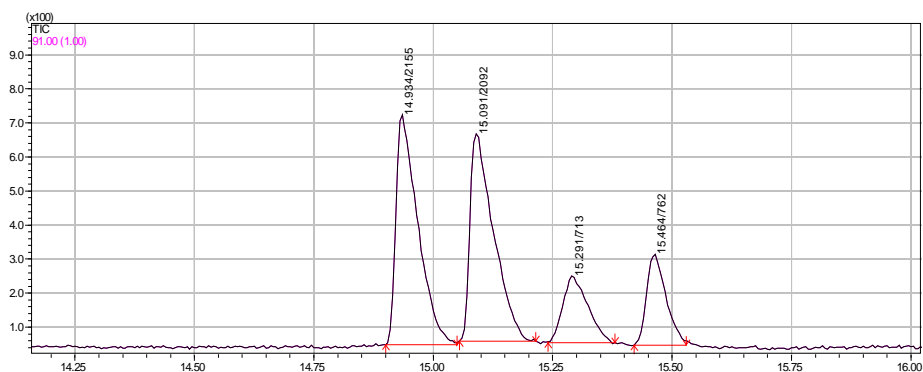
¹H NMR (500MHz, DMSO-d₆) δ 11.21 - 10.55 (m, 2 H), 7.85 (d, J = 2.3 Hz, 1 H), 7.58 (d, J = 2.3 Hz, 1 H); ¹³C NMR (75 MHz, DMSO-d₆) δ 150.75, 146.32, 139.88, 119.80, 109.74, 109.2.

General procedure for aerobic epoxidation:

In a 1 dram vial equipped with a stir bar, enal (0.2 mmol), flavin catalyst (3 mg, 5 mol %), pyrrolidine catalyst (13 mg, 20 mol %) and benzothiazoline (62 mg, 1.2 equivalent) were added. Then, 2 mL of freshly distilled chloroform was added to the vial. The vial was sealed and degassed at -78°C under vacuum for 1 minute. An oxygen filled balloon was connected to the vial via a needle. The reaction was warmed up to room temperature and stirred for the time given in Table 2. During the reaction, 2-(4-nitrophenyl)benzo[d]thiazole was formed and precipitated out of the solution as white powder. When the reaction was complete (monitored by NMR), the reaction was cool at 0°C for 5 minutes to precipitate out most of the 2-(4-nitrophenyl)benzo[d]thiazole. Then the reaction mixture was filtered through a cotton plug twice to remove the solid byproduct. The filtrate was concentrated under vacuum followed by flash column chromatography (ethyl acetate/hexanes) to give oxiranes as oily liquids. For low boiling aldehydes, after filtration, the filtrate was diluted with 2 mL methanol, cooled to 0°C. Sodium borohydride (20 mg, 2.5 equivalent) was added into the filtrate to reduce the aldehydes to corresponding alcohols. After 10 minutes, the reaction was quenched by sat. NH₄Cl solution. The product was extracted with dichloromethane three times, concentrated and columned to give the oxirane-alcohols.

(2S,3R)-3-Phenyl-oxirane-2-carbaldehyde 3.45a

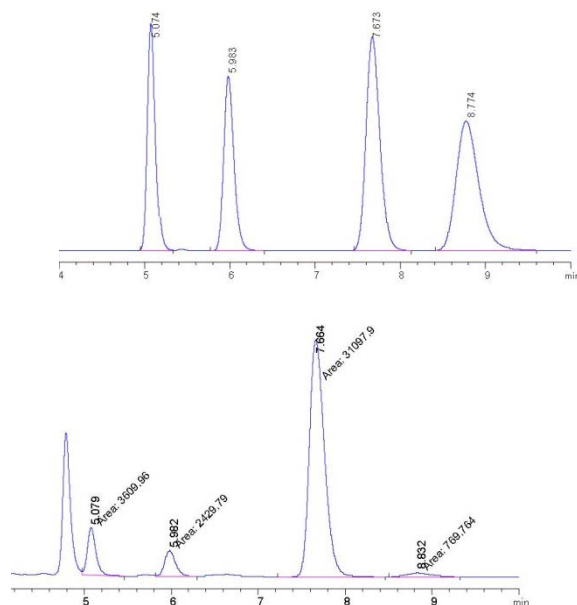
Colorless oil. ^1H NMR (500 MHz, CDCl_3) δ 9.20 (d, $J = 5.7$ Hz, 1 H), 7.42 - 7.27 (m, 5 H), 4.17 (d, $J = 1.7$ Hz, 1 H), 3.44 (dd, $J = 1.7, 5.7$ Hz, 1 H); ^{13}C NMR (125 MHz, CDCl_3) δ 196.9, 134.3, 129.3, 128.9, 125.8, 63.0, 56.7; The enantiomeric excess of the aldehyde was determined by GC-MS on a Chromasil CPChirasil-Dex CB-column. Temperature program: 70-160 $^\circ\text{C}$, rate: 10 $^\circ\text{C min}^{-1}$, hold 10 min, major enantiomer: $t_{\text{R}} = 15.28$ min, minor enantiomer $t_{\text{R}} = 15.49$ min; $[\alpha]_{\text{D}}^{25}$: -20.2 ($c=0.01$, CHCl_3).



(2S,3R)-3-(2-nitrophenyl)oxirane-2-carbaldehyde 3.45b

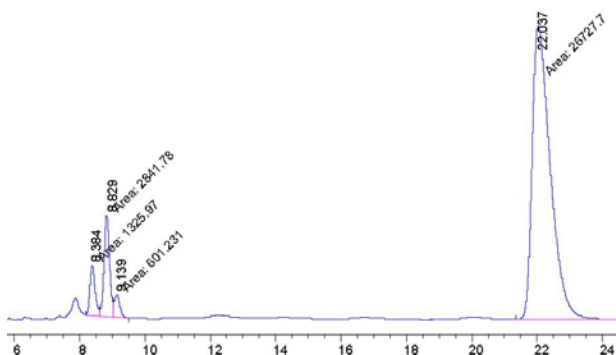
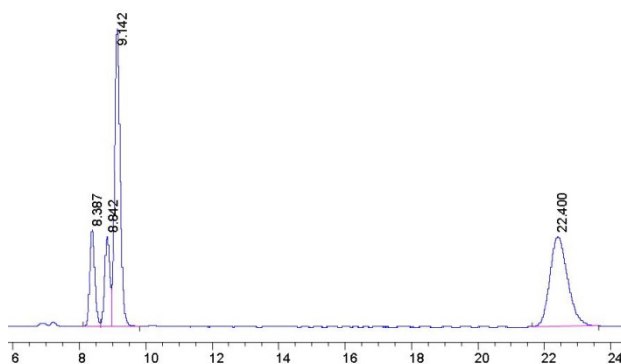
Yellow oil. ^1H NMR (500 MHz, CDCl_3) δ 9.30 (d, $J = 5.7$ Hz, 1 H), 8.98 (d, $J = 5.2$ Hz, 1 H*), 8.23 (d, $J = 8.6$ Hz, 1 H), 8.23 (d, $J = 8.6$ Hz, 1 H*), 7.93 (d, $J = 8.0$ Hz, 1 H*), 7.77 - 7.68 (m, 1 H), 7.77 - 7.68 (m, 1 H*), 7.63 (d, $J = 7.4$ Hz, 1 H), 7.59 - 7.52 (m, 1 H), 7.59 - 7.52 (m, 1 H*), 4.82 (s, 1 H), 4.82 (s, 1 H*), 3.89 (t, $J = 5.2$ Hz, 1 H*), 3.33 (dd, $J = 2.0, 6.0$ Hz, 1 H);) (* for

the (2R, 3R) isomer); ^{13}C NMR (125 MHz, CDCl_3) δ 195.7, 147.5, 134.8, 131.6, 129.7, 127.2, 125.22, 61.6, 55.2; The enantiomeric excess of the corresponding alcohol was determined using HPLC with a CHIRALPAK ID (250x4.6mm i.d.) column and a 40/60 heptane/ethanol mobile phase pumped at 1mL/min, major enantiomer: t_R =7.66 min, minor enantiomer t_R =8.83 min; $[\alpha]_D^{25}$: -28.4 (c=0.01, CHCl_3).



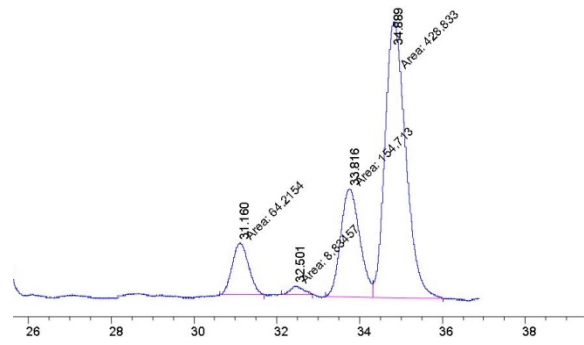
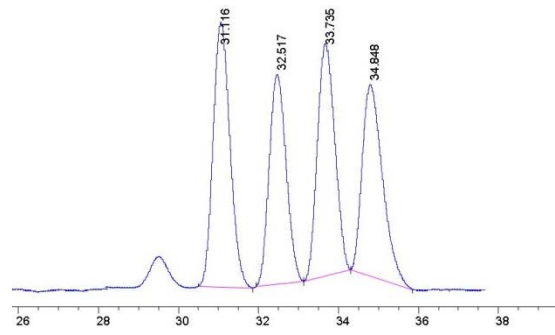
(2S,3R)-3-(4-nitrophenyl)oxirane-2-carbaldehyde 3.45c

Yellow oil. ^1H NMR (500 MHz, CDCl_3) δ 9.22 (d, J = 5.7 Hz, 1 H), 8.25 (d, J = 8.6 Hz, 2 H), 7.49 (d, J = 8.6 Hz, 3 H), 4.28 (d, J = 1.7 Hz, 1 H), 3.44 (dd, J = 1.7, 5.7 Hz, 1 H); ^{13}C NMR (125 MHz, CDCl_3) δ 195.7, 141.5, 126.7, 124.2, 62.9, 55.6. The enantiomeric excess of the corresponding alcohol was determined using HPLC with a CHIRALPAK ID (250x4.6mm i.d.) column and a 80/20 heptane/ethanol mobile phase pumped at 1mL/min. $[\alpha]_D^{25}$: -6.7 (c =0.01, CHCl_3).



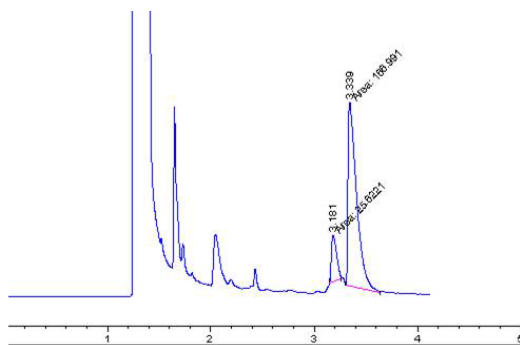
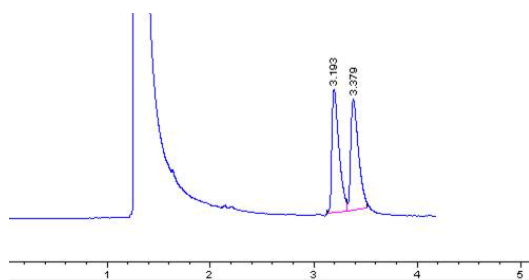
(2S,3R)-3-(4-chlorophenyl)oxirane-2-carbaldehyde 3.45d

Colorless oil. ^1H NMR (500 MHz, CDCl_3) δ 9.19 (d, J = 5.7 Hz, 4 H), 7.36 (d, J = 8.6 Hz, 2 H), 7.23 (d, J = 8.6 Hz, 2 H), 4.15 (s, 1 H), 3.40 (dd, J = 1.4, 6.0 Hz, 1 H); ^{13}C NMR (125 MHz, CDCl_3) δ 196.6, 135.2, 132.8, 129.2, 127.1, 62.9, 56.1; The enantiomeric excess of the corresponding alcohol was determined using HPLC with a CHIRALPAK IC (250x4.6mm i.d.) column coupled to a CHIRALPAK ID (250x4.6mm i.d.) column and a 96/4 heptane/ethanol mobile phase pumped at 1mL/min, major enantiomer: t_R =9.14 min, minor enantiomer: t_R =22.40 min; $[\alpha]_D^{25}$: -34.3 (c =0.01, CHCl_3).



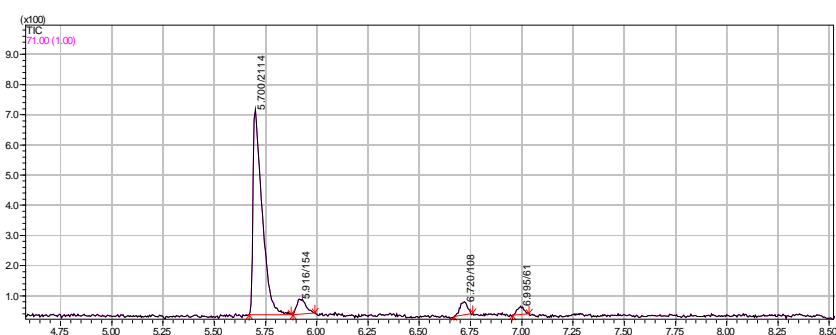
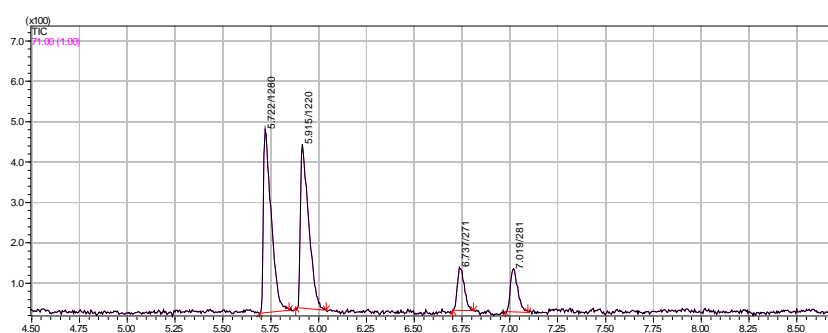
(S)-(3,3-dimethyloxiran-2-yl)methanol 3.45e

Colorless oil. ^1H NMR (500 MHz, CDCl_3) δ 3.83 (dd, $J = 4.0, 12.0$ Hz, 1 H), 3.67 (dd, $J = 6.3, 12.0$ Hz, 1 H), 2.97 (dd, $J = 4.6, 6.3$ Hz, 1 H), 1.88 (br. s., 1 H), 1.33 (d, $J = 17.2$ Hz, 7 H); ^{13}C NMR (125 MHz, CDCl_3) δ 63.8, 61.6, 58.9, 24.9, 18.9; The enantiomeric excess of the corresponding alcohol was determined using GC-MS on a CHIRALDEX B-DM (20m) column. Temperature program: 100°C with a 1mL/min He carrier gas flow rate, major enantiomer: $t_R = 3.37$ min, minor enantiomer $t_R = 3.19$ min. $[\alpha]_D^{25}$: +8.5 ($c = 0.01$, CHCl_3).



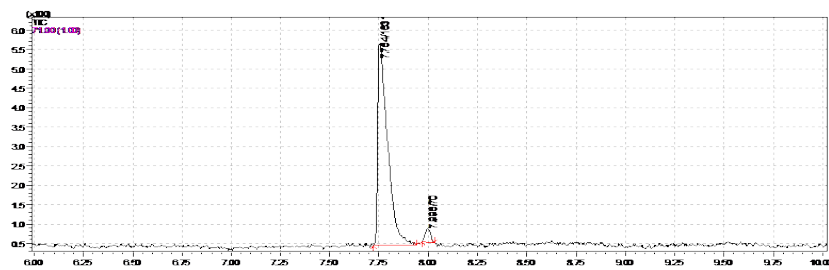
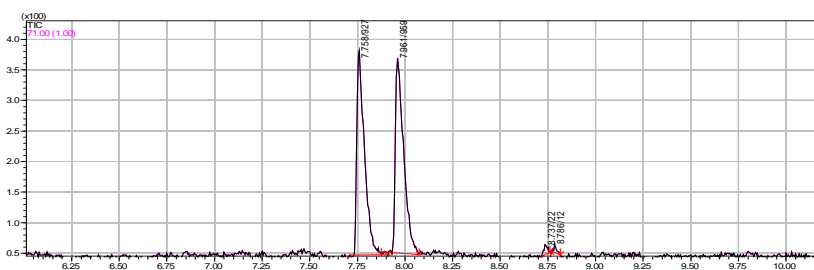
((2S,3S)-3-ethyloxiran-2-yl)methanol 3.45f

Colorless oil. ^1H NMR (500 MHz, CDCl_3) δ 3.91 (d, $J = 12.6$ Hz, 1 H), 3.62 (dd, $J = 2.9$, 12.6 Hz, 1 H), 2.94 (d, $J = 4.0$ Hz, 2 H), 1.82 (br. s., 1 H), 1.66 - 1.55 (m, 2 H), 1.00 (t, $J = 7.4$ Hz, 3 H); ^{13}C NMR (125 MHz, CDCl_3) δ 61.8, 58.2, 57.1, 24.7, 9.9; The enantiomeric excess of the aldehyde was determined by GC-MS on a Chromasil CPChirasil-Dex CB-column. Temperature program: 70-110 $^\circ\text{C}$, rate: 5 $^\circ\text{C min}^{-1}$, hold 10 min, major enantiomer: $t_R = 5.70$ min, minor enantiomer $t_R = 5.92$ min; $[\alpha]_D^{25}$: +24.6 ($c = 0.01$, CHCl_3).



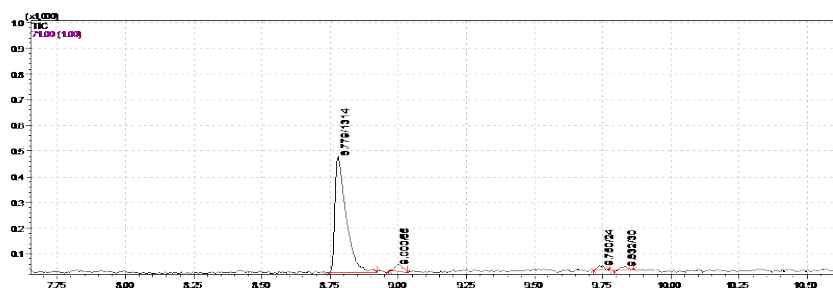
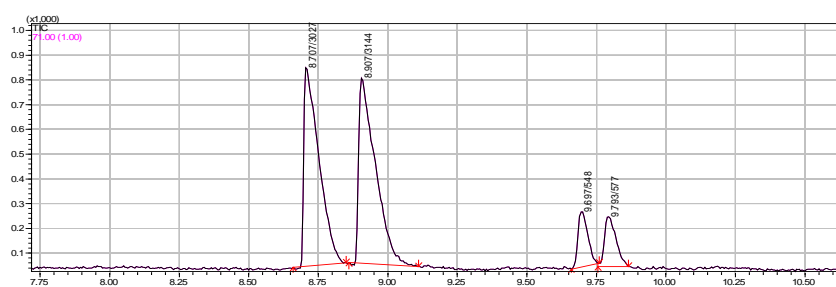
((2R,3R)-3-isopropoxyiran-2-yl)methanol 3.45g

Colorless oil. ^1H NMR (500 MHz, CDCl_3) δ 3.89 (dd, $J = 2.3, 12.6$ Hz, 1 H), 3.58 (dd, $J = 4.6, 12.6$ Hz, 1 H), 2.98 - 2.92 (m, 1 H), 2.73 (dd, $J = 2.0, 6.6$ Hz, 1 H), 2.17 (br. s., 1 H), 1.63 - 1.50 (m, 1 H), 1.00 (d, $J = 6.9$ Hz, 3 H), 0.94 (d, $J = 6.9$ Hz, 3 H); ^{13}C NMR (125 MHz, CDCl_3) δ 62.0, 61.3, 57.7, 30.1, 19.1, 18.4; $[\alpha]_D^{25}$: +26.2 (c = 0.01, CHCl_3).



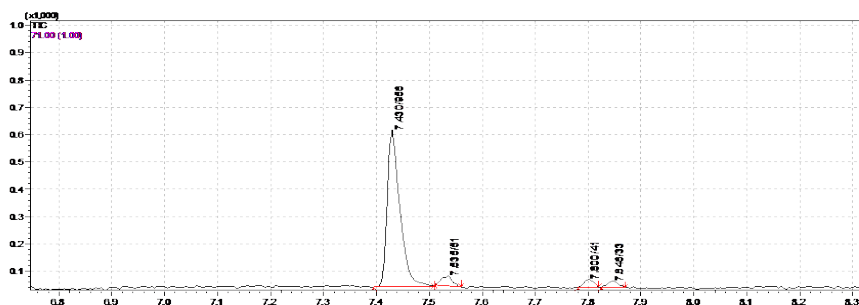
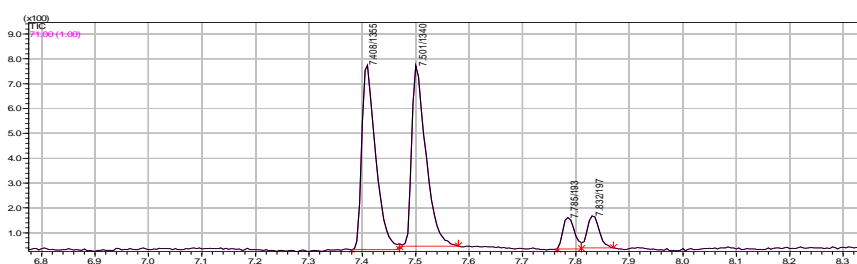
(2S,3R)-3-propyloxirane-2-carbaldehyde 3.45h

Colorless oil. ^1H NMR (500 MHz, CDCl_3) δ 9.00 (d, $J = 6.3$ Hz, 1 H), 3.24 - 3.20 (m, 1 H), 3.12 (dd, $J = 1.7, 6.3$ Hz, 1 H), 1.68 - 1.58 (m, 2 H), 1.56 - 1.45 (m, 2 H), 0.97 (t, $J = 7.4$ Hz, 3 H); ^{13}C NMR (125 MHz, CDCl_3) δ 198.6, 59.3, 56.88, 31.0, 27.9, 22.4, 14.0; Enantiomeric excess of the aldehyde was determined by GC-MS on a Chromasil CPChirasil-Dex CB-column. Temperature program: 50-110 $^\circ\text{C}$, rate: 5 $^\circ\text{C min}^{-1}$, hold 10 min, major enantiomer: $t_{\text{R}} = 8.78$ min, minor enantiomer $t_{\text{R}} = 9.00$ min; $[\alpha]_{\text{D}}^{25}$: -26.5 ($c = 0.01$, CHCl_3).



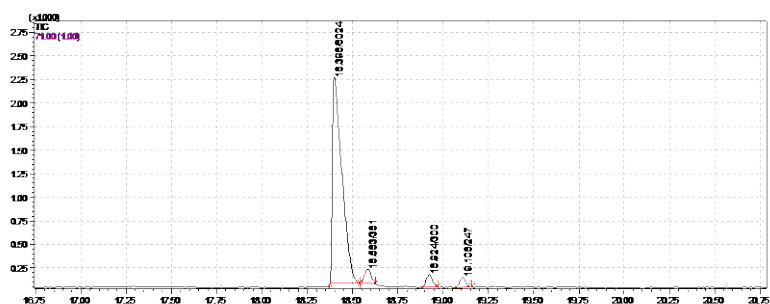
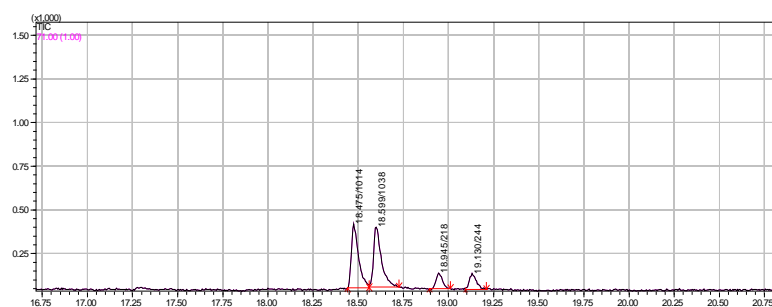
(2S,3R)-3-butyloxirane-2-carbaldehyde 3.45i

Colorless oil. ^1H NMR (500 MHz, CDCl_3) δ 9.01 (d, $J = 6.3$ Hz, 1 H), 3.26 - 3.19 (m, 1 H), 3.13 (dd, $J = 1.7, 6.3$ Hz, 1 H), 1.73 - 1.61 (m, 2 H), 1.45 (td, $J = 6.9, 13.7$ Hz, 2 H), 1.41 - 1.33 (m, 2 H), 0.92 (t, $J = 7.2$ Hz, 3 H); Enantiomeric excess of the aldehyde was determined by GC-MS on a Chromasil CPChirasil-Dex CB-column. Temperature program: 50-150 $^\circ\text{C}$, rate: 10 $^\circ\text{C min}^{-1}$, hold 10 min, major enantiomer: $t_{\text{R}} = 7.43$ min, minor enantiomer $t_{\text{R}} = 7.53$ min; $[\alpha]_{\text{D}}^{25}$: -20.4 ($c = 0.01$, CHCl_3).



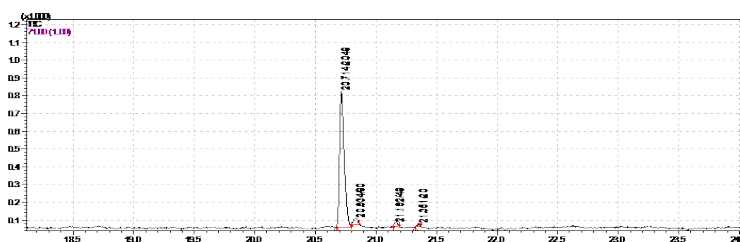
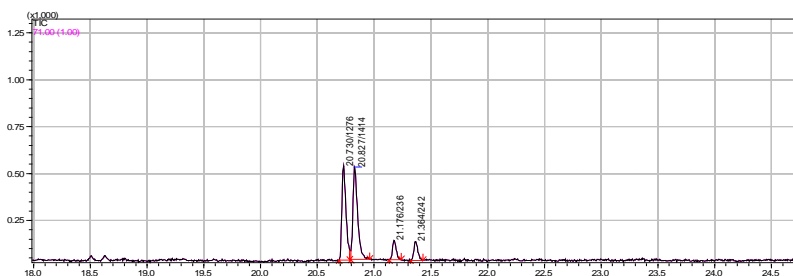
(2S,3R)-3-hexyloxirane-2-carbaldehyde 3.45j

Colorless oil. ^1H NMR (500 MHz, CDCl_3) δ 9.01 (d, $J = 6.3$ Hz, 1 H), 3.25 - 3.20 (m, 1 H), 3.13 (dd, $J = 1.7, 6.3$ Hz, 1 H), 1.69 - 1.62 (m, 2 H), 1.50 - 1.45 (m, 2 H), 1.38 - 1.33 (m, 6 H), 0.91 - 0.85 (m, 3 H); ^{13}C NMR (125 MHz, CDCl_3) δ 198.6, 59.3, 56.9, 31.7, 31.3, 29.0, 25.82, 22.6, 14.1; Enantiomeric excess of the aldehyde was determined by GC-MS on a Chromasil CPChirasil-Dex CB-column. Temperature program: 50-180 $^\circ\text{C}$, rate: 10 $^\circ\text{C min}^{-1}$, hold 10 min, major enantiomer: $t_R = 18.40$ min, minor enantiomer $t_R = 18.58$ min; $[\alpha]_D^{25}$: -76.2 (c = 0.01, CHCl_3).



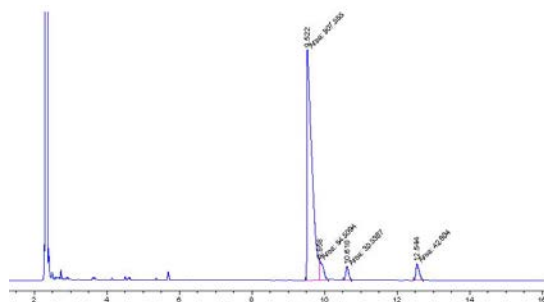
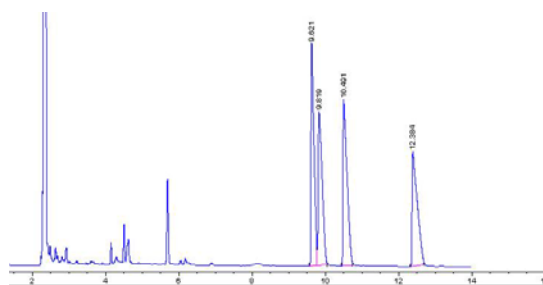
(2S,3R)-3-heptyloxirane-2-carbaldehyde 3.45k

Colorless oil. ^1H NMR (500 MHz, CDCl_3) δ 8.98 (d, $J = 6.3$ Hz, 1 H), 3.24 - 3.16 (m, 1 H), 3.10 (dd, $J = 2.0, 6.0$ Hz, 1 H), 1.67 - 1.56 (m, 2 H), 1.51 - 1.39 (m, 3 H), 1.36 - 1.24 (m, 9 H), 0.85 (t, $J = 6.9$ Hz, 3 H); ^{13}C NMR (125 MHz, CDCl_3) δ 198.6, 59.2, 56.9, 31.8, 31.3, 29.2, 29.1, 25.8, 22.7, 14.1; Enantiomeric excess of the aldehyde was determined by GC-MS on a Chromasil CPChirasil-Dex CB-column. Temperature program: 50-180 $^\circ\text{C}$, rate: 10 $^\circ\text{C min}^{-1}$, hold 10 min, major enantiomer: $t_R = 20.71$ min, minor enantiomer $t_R = 20.83$ min; $[\alpha]_D^{25}$: -76.0 (c = 0.01, CHCl_3).



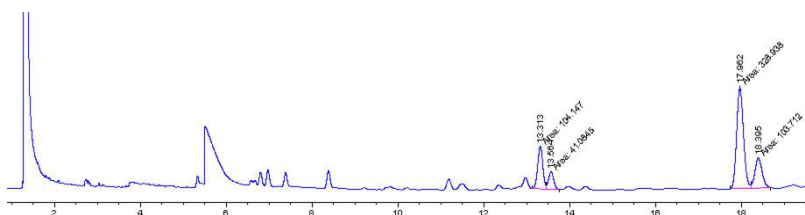
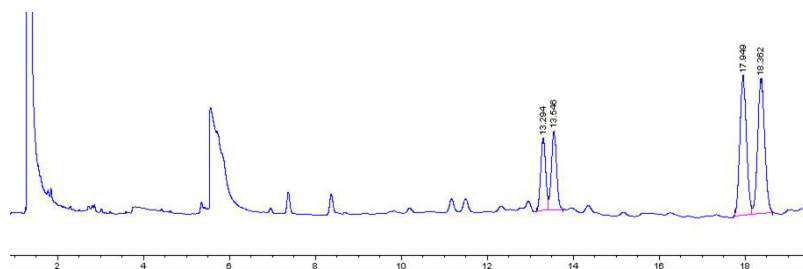
(2S,3S)-ethyl 3-formyloxirane-2-carboxylate 3.45f

Colorless oil. ^1H NMR (500 MHz, CDCl_3) δ 9.04 (d, $J = 6.3$ Hz, 1 H), 4.28 (dd, $J = 5.7, 6.9$ Hz, 2 H), 3.73 (d, $J = 1.7$ Hz, 1 H), 3.61 (dd, $J = 1.1, 6.3$ Hz, 1 H), 1.32 (t, $J = 7.2$ Hz, 3 H); NMR (125 MHz, CDCl_3) δ 195.1, 166.3, 62.6, 57.6, 50.9, 14.1; The enantiomeric excess of the aldehyde was determined using GC-MS on a CHIRALDEX G-TA (30m) column, Temperature program: 120 °C with a 1mL/min He carrier gas flow rate; $[\alpha]_{\text{D}}^{25}$: -15.6 ($c = 0.01, \text{CHCl}_3$).



(2S, 3R)-3-Methyl-3-(4-methylpent-3-enyl)-oxirane-2-carbaldehyde 3.45m

Colorless oil. ^1H NMR (500 MHz, CDCl_3) δ =9.45 (d, $J=5.2$ Hz, 1H), 9.41 (d, $J=5.1$, 1H*), 5.02-5.07 (m, 1H and 1H*), 3.18 (d, $J=4.6$, 1H), 3.13 (d, $J=5.2$, 1H*), 2.04-2.20 (m, 2H and 2H*), 1.65-1.85 (m, 5H and 5H*), 1.59 (s, 3H), 1.58 (s, 3H*), 1.43 (s, 3H) and 1.41(s, 3H*)(* for the (2R, 3R) isomer); The ee was determined using GC with a CHIRALDEX B-DM (20m) column at 90 °C with a 1mL/min He carrier gas flow rate. $[\alpha]_D^{25}$: -63.8 (c=0.01, CHCl_3).



General procedure of flavin catalyzed oxidation of dihydropyridine to pyridine:

0.2 mmol of dihydropyridine , 0.01 mmol of flavin catalyst (3 mg) and 2 mL methanol was added in a 1 dram vial. The vial was filled with oxygen gas by applying an O₂ balloon via a needle. The reaction was stirred at room temperature for the time given. After the completion of reaction (followed by TLC and NMR), the reaction mixture was transferred to a small round bottom flask and the solvent was evaporated under vacuum to give pyridine as products. No column chromatography was needed since the purity of the product was higher than 95% by NMR.

General procedure of flavin catalyzed tandem synthesis of pyridine:

To a 2 dram vial, formaldehyde (37 wt% in H₂O, 1 mmol), 1, 3-dicarbonyl compound (2 mmol), ammonium acetate (1 mmol), catalyst (6 mg, 0.02 mmol, 2 mol %) and 2 mL of methanol was added. The reaction was stirred with the vial open to atmosphere at room temperature for the time given. After the complete of the reaction, the reaction mixture was dried under vacuum. Flash column chromatography (ethyl acetate/hexane) was used to purify the crude product to give pure product.

General procedure of flavin catalyzed oxidation of dihydropyridine to Pyridine

0.2 mmol of dihydropyridine, 0.01 mmol of catalyst (4.3 mg), perchloric acid (28.6mg of 70% wt HClO₄) and 2 mL methanol was added in a 1 dram vial. The vial was filled with oxygen gas by applying an O₂ balloon via a needle. The reaction was stirred at 50°C for the time given. After the disappearance of the starting material, the reaction mixture was neutralized by adding 0.2 mL of saturated Na₂CO₃ solution. The solvent was evaporated under vacuum and the resulting material was directly purified by flash column chromatography (ethyl acetate/hexane) to give as pure product.

General procedure of flavin catalyzed oxidation of benzothiazoline to benzothiazole

0.2 mmol of benzothiazoline, 0.01 mmol of catalyst (3 mg) and 2 mL methanol was added in a 1 dram vial. The vial was filled with oxygen gas by applying an O₂ balloon via a needle. The reaction was stirred at room temperature for the time given. After the completion of reaction (followed by TLC and NMR), the reaction mixture was transferred to a small round bottom flask and the solvent was evaporated under vacuum to give benzothiazoles as products. No column chromatography was needed since the purity of the product was higher than 95% by NMR.

General procedure of flavin catalyzed one-pot two-steps synthesis benzothiazole 12a-i

1 mmol of 2-aminothiophenol (125mg) and 1 mmol of aldehyde was mixed in 3 mL methanol in a 1.5 dram vial. The reaction was stirred at room temperature for 6 hours to ensure complete formation of corresponding benzothiazolines. Then, 0.02 mmol of catalyst (15mg) was added into the reaction. At the same time, an O₂ balloon was also applied on the vial. The reaction was stirred under 1 atm oxygen for an additional 1.5 hour. After completion of the reaction, the solvent was evaporated under reduced vacuum, and the corresponding benzothiazoles were purified by flash column chromatography with silica gel.

4.45 diethyl 2,6-dimethylpyridine-3,5-dicarboxylate

White solid. M.P.: 69 - 71 °C. ¹H NMR (500 MHz, [D₁]CHCl₃, 25 °C) δ=8.46 (s, 1H; CH), 4.20 (q, ³J(H,H) = 6.9 Hz, 4H; CH₂CH₃), 2.63 (s, 6H; CH₃), 1.23 (t, ³J(H,H)= 7.4 Hz, 6H; CH₂CH₃); ¹³C NMR (125MHz, [D₁]CHCl₃, 25 °C) δ=165.6, 162.1, 140.7, 122.8, 61.19, 24.8, 14.2

4.47 dimethyl 2,6-dimethylpyridine-3,5-dicarboxylate

White solid. M.P.: 99 - 100 °C. ¹H NMR (500 MHz, [D₁]CHCl₃, 25 °C) δ= 8.68 (s, 1 H; CH), 3.91 (s, 6 H; OCH₃), 2.83 (s, 6 H; CH₃); ¹³C NMR (125 MHz, [D₁]CHCl₃, 25 °C) δ= 166.3, 162.7, 141.1, 122.7, 52.4, 25.0

4.48 dimethyl 2,6-diethylpyridine-3,5-dicarboxylate

White solid. M.P.: 99 - 100 °C. ^1H NMR (500 MHz, $[\text{D}_1]\text{CHCl}_3$, 25 °C) δ = 8.62 (s, 1 H; CH), 3.91 (s, 6 H; OCH₃), 3.18 (q, $^3J(\text{H,H})$ = 7.5 Hz, 4 H; CH₂CH₃), 1.28 (t, $^3J(\text{H,H})$ = 7.4 Hz, 6 H; CH₂CH₃); ^{13}C NMR (125 MHz, $[\text{D}_1]\text{CHCl}_3$, 25 °C) δ = 167.38, 166.4, 141.4, 122.2, 52.4, 30.4, 13.9

4.49 1,1'-(2,6-dimethylpyridine-3,5-diyl)diethanone

White solid. M.P.: 68 - 70 °C ^1H NMR (500 MHz, $[\text{D}_1]\text{CHCl}_3$, 25 °C) δ = 8.22 (s, 1 H; CH), 2.75 (s, 6 H; CH₃), 2.61 (s, 6 H; CH₃); ^{13}C NMR (125 MHz, $[\text{D}_1]\text{CHCl}_3$, 25 °C) δ =199.4, 160.4, 138.0, 130.3, 29.5, 24.9

4.50 di-tert-butyl 2,6-dimethylpyridine-3,5-dicarboxylate

White solid. M.P.: 108-109 °C ^1H NMR (500 MHz, $[\text{D}_1]\text{CHCl}_3$, 25 °C) δ = 8.49 (s, 1 H; CH), 2.77 (s, 6 H; CH), 1.57 (s, 18 H; CH₃); ^{13}C NMR (125MHz, $[\text{D}_1]\text{CHCl}_3$, 25 °C) δ = 165.5, 161.2, 140.9, 124.8, 82.2, 28.3, 24.9

4.51 diisopropyl 2,6-dimethylpyridine-3,5-dicarboxylate

White solid. M.P.: 63 - 65 °C ^1H NMR (500 MHz, $[\text{D}_1]\text{CHCl}_3$, 25 °C) δ = 8.58 (s, 1 H; CH), 5.22 (sep, $^3J(\text{H,H})$ = 6.2 Hz, 2 H; CH(CH₃)₂), 2.79 (s, 6 H; CH₃), 1.35 (d, $^3J(\text{H,H})$ = 6.3 Hz, 12 H; CH(CH₃)₂); ^{13}C NMR (125MHz, $[\text{D}_1]\text{CHCl}_3$, 25 °C) δ = 165.7, 161.8, 141.0, 123.8, 69.3, 24.8, 21.9

4.52 diallyl 2,6-dimethylpyridine-3,5-dicarboxylate⁷

White solid. M.P.: 64 - 66 °C ^1H NMR (500 MHz, $[\text{D}_1]\text{CHCl}_3$, 25 °C) δ = 8.71 (s, 1 H; CH), 6.06 - 5.95 (m, 2 H;), 5.38 (d, J = 17.2 Hz, 2 H), 5.28 (d, J = 10.3 Hz, 2 H), 4.80 (d, J = 5.7 Hz, 4 H; CH₂), 2.82 (s, 6 H; CH₃); ^{13}C NMR (125MHz, $[\text{D}_1]\text{CHCl}_3$, 25 °C) δ = 165.5, 162.7, 141.3, 131.8, 123.0, 119.0, 66.2, 50.7, 24.7.

4.53 dibenzyl 2,6-dimethylpyridine-3,5-dicarboxylate¹¹

White solid, Mp: 87-88 °C; ^1H NMR (500 MHz, $[\text{D}_1]\text{CHCl}_3$, 25 °C) δ = 8.76 (s, 1 H; CH), 7.51 - 7.27 (m, 10 H; C₆H₅), 5.35 (s, 4 H; CH₂), 2.85 (s, 6 H; CH₃); ^{13}C NMR (125MHz, $[\text{D}_1]\text{CHCl}_3$,

25 °C) δ = 165.7, 162.8, 141.3, 135.6, 128.8, 128.4, 122.9, 67.2, 25.1; IR(Neat): 3038, 2967, 1782, 1717, 1593, 1542, 1498, 1439, 1285, 1252, 1215, 1111, 1026, 1002, 769, 749, 729, 692; HRMS: C₂₃H₂₁NO₄+H, Calculated = 376.1543*m/z*, Found = 376.1525*m/z*.

4.58 diethyl 2,6-dimethyl-4-phenylpyridine-3,5-dicarboxylate

White solid. M.P.: 60 - 61 °C ¹H NMR (500 MHz, [D₁]CHCl₃, 25 °C) δ = 7.42 - 7.31 (m, 3 H; CH), 7.29 - 7.17 (m, 2 H; CH), 3.99 (q, ³J(H,H)= 7.4 Hz, 4 H; CH₂CH₃), 2.59 (s, 6 H), 0.89 (t, ³J(H,H)= 7.2 Hz, 6 H; CH₂CH₃); ¹³C NMR (125MHz, [D₁]CHCl₃, 25 °C) δ = 168.0, 155.5, 146.2, 136.7, 128.5, 128.2, 127.0, 61.4, 23.0, 13.6

4.59 diethyl 2,6-dimethyl-4-(p-tolyl)pyridine-3,5-dicarboxylate

White solid. M.P.: 70 - 73 °C ¹H NMR (500 MHz, [D₁]CHCl₃, 25 °C) δ = 7.15 (d, ³J(H,H)= 8.0 Hz, 2 H; CH), 7.13 (d, ³J(H,H)= 8.6 Hz, 2 H; CH), 4.02 (d, J = 7.4 Hz, 4 H; CH₂CH₃), 2.58 (s, 6 H; CH₃), 2.35 (s, 3 H; CH₃), 0.94 (t, ³J(H,H)= 7.2 Hz, 6 H; CH₂CH₃); ¹³C NMR (125MHz, [D₁]CHCl₃, 25 °C) δ = 168.1, 155.3, 146.3, 138.4, 133.6, 128.9, 128.0, 127.2, 61.4, 23.0, 21.3, 13.7

4.60 diethyl 4-(furan-2-yl)-2,6-dimethylpyridine-3,5-dicarboxylate

Oil. ¹H NMR (500 MHz, [D₁]CHCl₃, 25 °C) δ = 7.47 (s, 1 H; CH), 7.42 (s, 1 H; CH), 6.44 (s, 1 H; CH), 4.18 (q, ³J(H,H)= 7.3 Hz, 4 H; CH₂CH₃), 1.15 (t, ³J(H,H)= 7.2 Hz, 6 H; CH₂CH₃); ¹³C NMR (75 MHz, [D₁]CHCl₃, 25 °C) δ = 168.2, 155.2, 143.1, 141.2, 136.7, 127.2, 120.4, 111.3, 61.7, 22.8, 13.9

4.61 diethyl 4-(4-chlorophenyl)-2,6-dimethylpyridine-3,5-dicarboxylate

White solid. M.P.: 69 - 71 °C ¹H NMR (500 MHz, [D₁]CHCl₃, 25 °C) δ = 7.17 (d, ³J(H,H)= 8.6 Hz, 2 H; CH), 6.87 (d, ³J(H,H)= 8.6 Hz, 2 H; CH), 4.02 (q, ³J(H,H)= 6.9 Hz, 4 H; CH₂CH₃), 3.79 (s, 3 H; CH₃), 2.56 (s, 6 H; CH₃), 0.96 (t, ³J(H,H)= 7.2 Hz, 6 H; CH₂CH₃); ¹³C NMR (75 MHz, [D₁]CHCl₃, 25 °C) δ = 168.2, 159.9, 155.3, 145.8, 129.5, 128.7, 127.3, 113.7, 61.4, 55.4, 22.9, 13.8.

4.62 dimethyl 2,4,6-trimethylpyridine-3,5-dicarboxylate

White solid. M.P.: 78 - 80 °C ^1H NMR (500 MHz, $[\text{D}_1]\text{CHCl}_3$, 25 °C) δ = 3.50 (s, 6 H; CH₃), 2.08 (s, 6 H; CH₃), 1.82 (s, 3 H; CH₃); ^{13}C NMR (75 MHz, $[\text{D}_1]\text{CHCl}_3$, 25 °C) δ = 168.9, 155.3, 142.5, 127.4, 52.5, 23.1, 17.2

4.63 dimethyl 2,6-diethyl-4-methylpyridine-3,5-dicarboxylate

Colorless oil; ^1H NMR (500 MHz, $[\text{D}_1]\text{CHCl}_3$, 25 °C) δ = 3.90 (s, 6 H; CH₃), 2.73 (d, $^3J(\text{H,H})$ = 7.4 Hz, 4 H; CH₂CH₃), 2.20 (s, 3 H; CH₃), 1.24 (t, $^3J(\text{H,H})$ = 7.4 Hz, 6 H; CH₂CH₃); ^{13}C NMR (75 MHz, $[\text{D}_1]\text{CHCl}_3$, 25 °C) δ = 169.2, 160.2, 142.1, 126.9, 52.5, 29.9, 17.1, 14.0; IR(Neat): 2974, 2951, 2878, 1725, 1561, 1435, 1296, 1221, 1108, 1072, 972, 917, 832, 805, 755, 733; HRMS: C₁₄H₁₉NO₄+H, Calculated = 266.1387 *m/z*, Found = 266.1375 *m/z*.

4.66 2-phenylbenzo[d]thiazole

White solid. M.P.: 113 - 114 °C ^1H NMR (500 MHz, $[\text{D}_1]\text{CHCl}_3$, 25 °C) δ = 8.15 - 8.02 (m, 3 H; CH), 7.90 (d, $^3J(\text{H,H})$ = 8.0 Hz, 1 H; CH), 7.54 - 7.44 (m, 4 H; CH), 7.42 - 7.34 (m, 1 H; CH); ^{13}C NMR (125 MHz, $[\text{D}_1]\text{CHCl}_3$, 25 °C) δ = 168.2, 154.2, 135.2, 133.7, 131.1, 129.1, 127.7, 126.4, 125.3, 123.3, 121.7.

4.67 2-(2,6-dimethylphenyl)benzo[d]thiazole

White solid. M.P.: 123 - 124 °C ^1H NMR (500 MHz, $[\text{D}_1]\text{CHCl}_3$, 25 °C) δ = 8.12 (d, $^3J(\text{H,H})$ = 8.0 Hz, 1 H; CH), 7.95 (d, $^3J(\text{H,H})$ = 8.0 Hz, 1 H; CH), 7.53 (t, $^3J(\text{H,H})$ = 7.7 Hz, 1 H; CH), 7.48 - 7.40 (m, 1 H; CH), 7.30 - 7.26 (m, 1 H; CH), 7.14 (d, $^3J(\text{H,H})$ = 7.4 Hz, 2 H; CH), 2.21 (s, 6 H; CH₃); ^{13}C NMR (125 MHz, $[\text{D}_1]\text{CHCl}_3$, 25 °C) δ = 167.6, 153.6, 137.4, 136.4, 133.6, 129.7, 127.7, 126.1, 125.3, 123.6, 121.7, 20.3.

4.68 2-(4-nitrophenyl)benzo[d]thiazole

Yellow solid. M.P.: 225 - 226 °C ^1H NMR (500 MHz, $[\text{D}_1]\text{CHCl}_3$, 25 °C) δ = 8.35 (d, $^3J(\text{H,H})$ = 8.6 Hz, 2 H; CH), 8.27 (d, $^3J(\text{H,H})$ = 8.6 Hz, 2 H; CH), 8.13 (d, $^3J(\text{H,H})$ = 8.0 Hz, 1 H; CH), 7.96 (d, $^3J(\text{H,H})$ = 8.0 Hz, 1 H; CH), 7.55 (t, $^3J(\text{H,H})$ = 7.7 Hz, 1 H; CH), 7.46 (t, $^3J(\text{H,H})$ = 7.5 Hz, 1 H; CH); ^{13}C NMR (125 MHz, $[\text{D}_1]\text{CHCl}_3$, 25 °C) δ = 164.9, 154.2, 149.1, 139.3, 135.6, 128.3, 127.0, 126.3, 124.4, 124.0, 121.9.

4.69 2-(4-chlorophenyl)benzo[d]thiazole

White solid. M.P.: 115 - 117 °C. ¹H NMR (500 MHz, [D₁]CHCl₃, 25 °C) δ= 8.06 (d, ³J(H,H)= 8.0 Hz, 1 H; CH), 8.02 (d, ³J(H,H)= 8.6 Hz, 2 H; CH), 7.89 (d, ³J(H,H)= 8.0 Hz, 1 H; CH), 7.53 - 7.43 (m, 3 H; CH), 7.39 (t, ³J(H,H)= 7.5 Hz, 1 H; CH); ¹³C NMR (125 MHz, [D₁]CHCl₃, 25 °C) δ= 166.72, 154.17, 137.13, 135.15, 132.22, 129.37, 128.81, 126.59, 125.52, 123.40, 121.76.

4.70 2-(naphthalen-1-yl)benzo[d]thiazole

White solid. M.P.: 126 - 127 °C ¹H NMR (500 MHz, [D₁]CHCl₃, 25 °C) δ= 8.57 (br. s., 1 H; CH), 8.21 (d, ³J(H,H)= 8.0 Hz, 1 H; CH), 8.12 (d, ³J(H,H)= 7.4 Hz, 1 H; CH), 8.02 - 7.82 (m, 4 H; CH), 7.61 - 7.47 (m, 3 H; CH), 7.40 (t, ³J(H,H)= 7.2 Hz, 1 H; CH); ¹³C NMR (125 MHz, [D₁]CHCl₃, 25 °C) δ= 168.2, 154.4, 135.2, 134.7, 133.3, 131.1, 128.9, 128.0, 127.7, 127.6, 127.0, 126.5, 125.4, 124.6, 123.4, 121.8.

4.71 2-(naphthalen-2-yl)benzo[d]thiazole

White solid. M.P.: 126 - 128 °C. ¹H NMR (500 MHz, [D₁]CHCl₃, 25 °C) δ= 9.09 (s, 1 H; CH), 8.13 (d, ³J(H,H)= 7.4 Hz, 1 H; CH), 8.01 (d, ³J(H,H)= 8.6 Hz, 1 H; CH), 7.93 (d, ³J(H,H)= 8.0 Hz, 1 H; CH), 7.75 (d, ³J(H,H)= 8.0 Hz, 1 H; CH), 7.67 (t, ³J(H,H)= 7.4 Hz, 1 H; CH), 7.58 (m, 2 H; CH), 7.28 - 7.23 (m, 2 H; CH), 7.22 - 7.13 (m, 2 H); ¹³C NMR (125 MHz, [D₁]CHCl₃, 25 °C) δ= 160.5, 149.6, 134.1, 132.6, 132.3, 131.6, 131.3, 128.8, 128.0, 127.1, 127.1, 126.5, 126.2, 125.3, 125.0, 117.2.

4.72 2-(4-((tert-butyldimethylsilyl)oxy)phenyl)benzo[d]thiazole

Colorless oil; ¹H NMR (500 MHz, [D₁]CHCl₃, 25 °C) δ= 8.03 (d, J = 8.0 Hz, 1 H), 7.98 (d, J = 8.6 Hz, 2 H), 7.86 (d, J = 8.0 Hz, 1 H), 7.46 (t, J = 7.4 Hz, 1 H), 7.38 - 7.32 (t, J = 7.4 Hz, 1 H), 6.94 (d, J = 8.6 Hz, 2 H), 1.01 (s, 9 H), 0.25 (s, 6 H); ¹³C NMR (125 MHz, [D₁]CHCl₃, 25 °C) δ=186.0, 158.6, 154.3, 135.0, 129.2, 129.1, 126.3, 124.9, 122.9, 121.6, 120.7, 25.9, 18.4, -4.2; HRMS: C₁₉H₂₃NOSSi+H, Calculated = 342.1342 *m/z*, Found = 342.1323 *m/z*.

4.73 2-(4-(trifluoromethyl)phenyl)benzo[d]thiazole

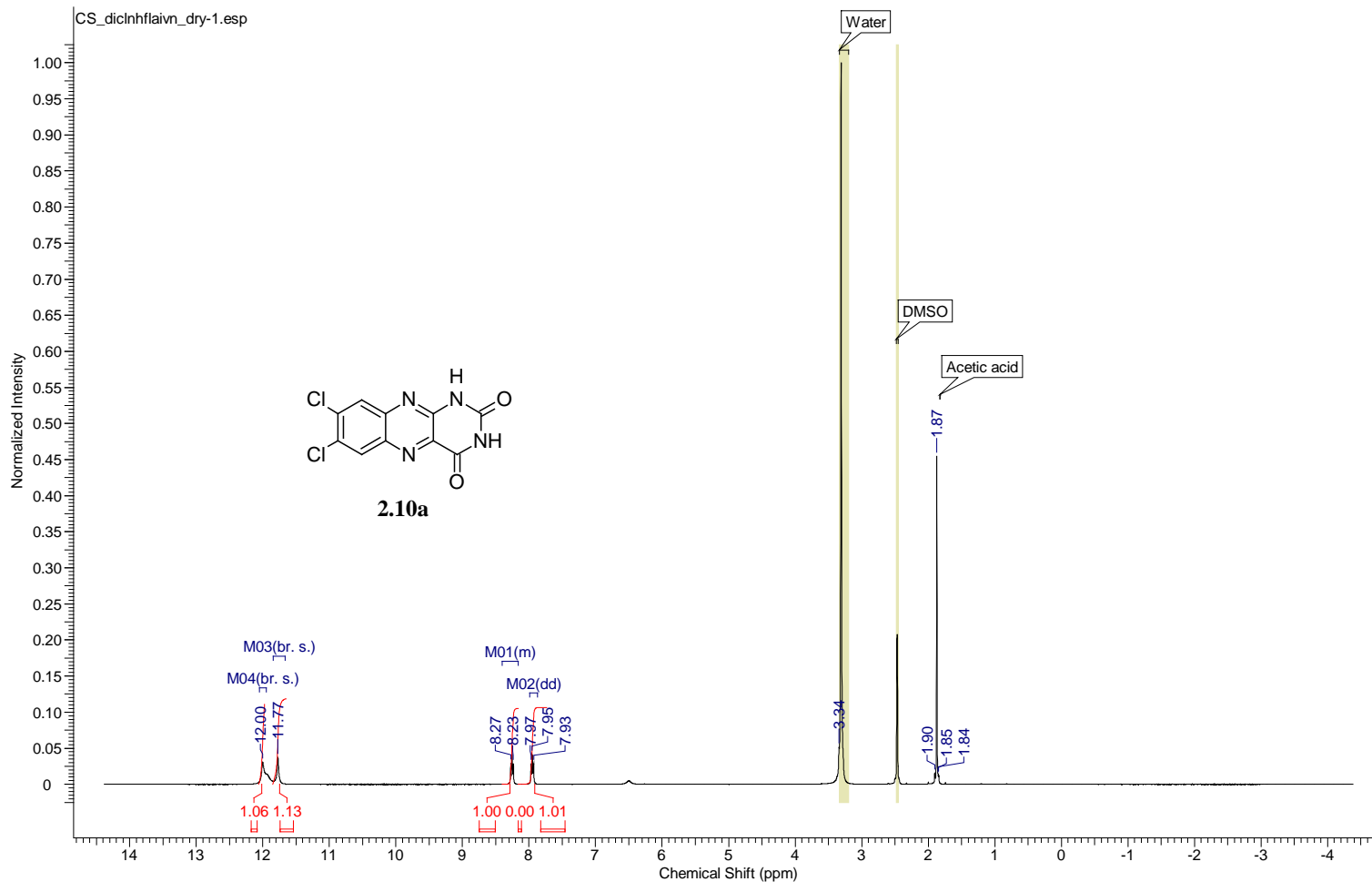
White solid. M.P.: 160 - 163 °C ^1H NMR (500 MHz, $[\text{D}_1]\text{CHCl}_3$, 25 °C) δ = 8.20 (d, $^3J(\text{H,H})$ = 8.0 Hz, 2 H; CH), 8.11 (d, $^3J(\text{H,H})$ = 8.6 Hz, 1 H; CH), 7.93 (d, $^3J(\text{H,H})$ = 8.0 Hz, 1 H; CH), 7.75 (d, $^3J(\text{H,H})$ = 8.0 Hz, 2 H; CH), 7.53 (t, $^3J(\text{H,H})$ = 7.4 Hz, 1 H; CH), 7.48 - 7.37 (m, 1 H; CH); ^{13}C NMR (125 MHz, $[\text{D}_1]\text{CHCl}_3$, 25 °C) δ = 166.2, 154.1, 136.9, 135.3, 132.4, 127.9, 126.8, 126.13, 126.10, 125.9, 123.7, 121.9; ^{19}F NMR(283MHz, $[\text{D}_1]\text{CHCl}_3$, 25 °C) δ = -62.7

4.74 tert-butyl (benzo[d]thiazol-2-ylmethyl)(methyl)carbamate

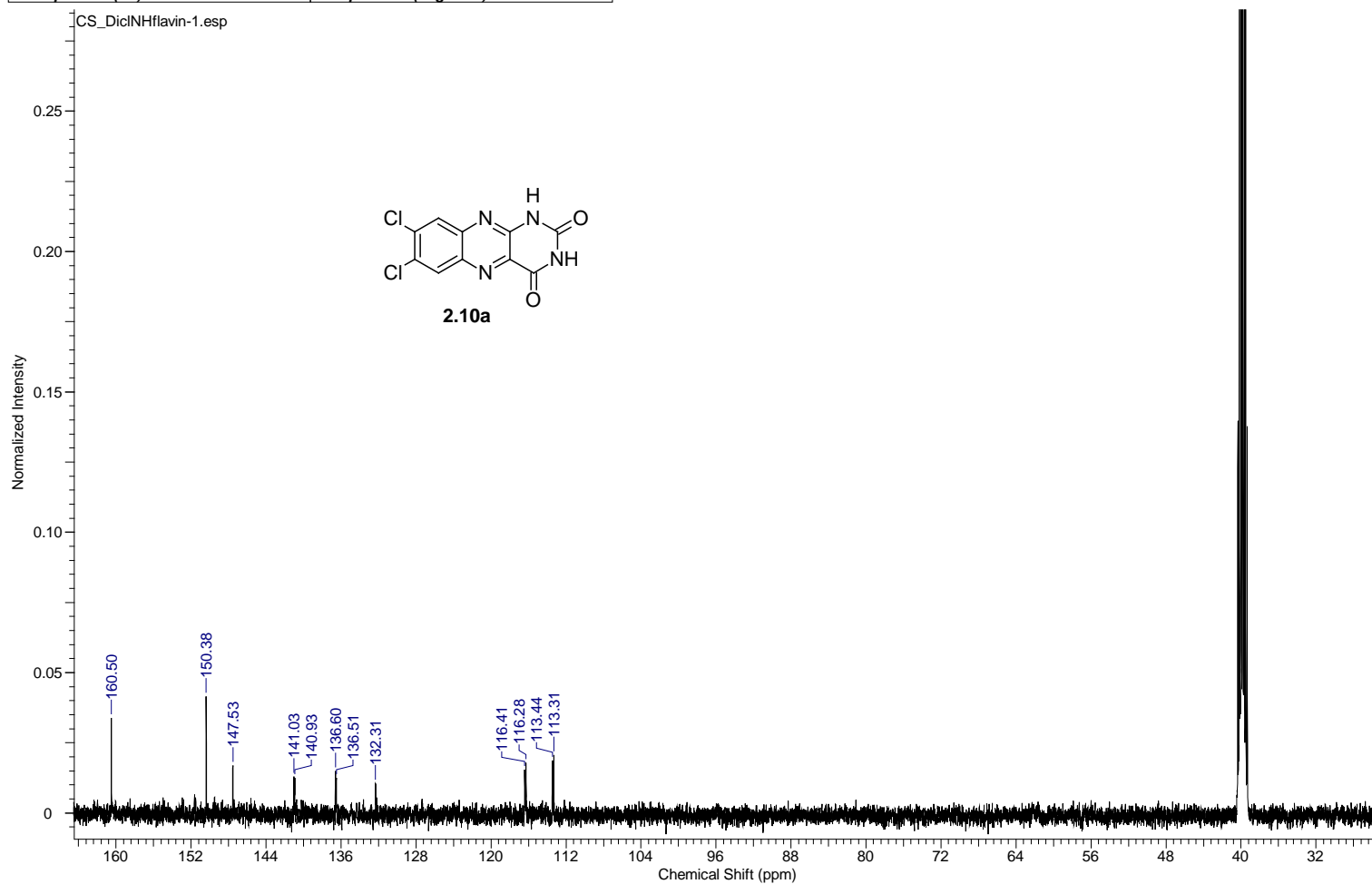
Colorless oil; ^1H NMR (500 MHz, $[\text{D}_1]\text{CHCl}_3$, 25 °C) δ = 7.98 (d, J = 7.6 Hz, 1 H), 7.87 (br.s., 1 H), 7.47 (br. s., 1 H), 7.38 (br. s., 1 H), 4.89 - 4.70 (m, 2 H), 3.10 - 2.91 (m, 3 H), 1.50 (m, 9 H); ^{13}C NMR (125 MHz, $[\text{D}_1]\text{CHCl}_3$, 25 °C) δ =169.87, 169.69, 155.92, 155.04, 153.12, 135.64, 135.29, 126.20, 125.26, 123.01, 121.86, 80.88, 80.62, 51.69, 50.95, 34.92, 34.82, 28.47; HRMS: $\text{C}_{14}\text{H}_{18}\text{N}_2\text{O}_2\text{S}+\text{Na}$, Calculated = 301.0981 m/z , Found = 301.0976

Appendix C
NMR Spectra of Compounds

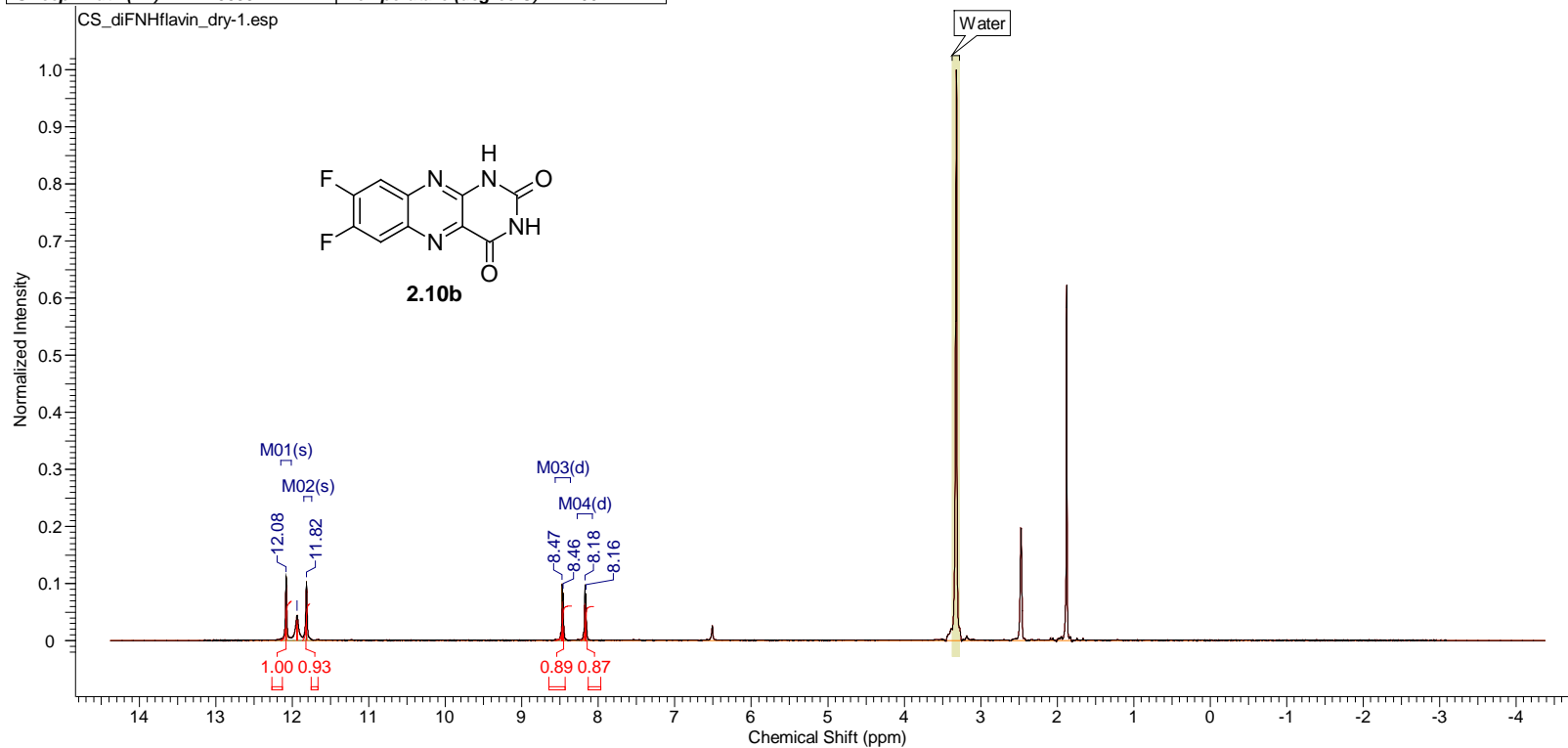
Acquisition Time (sec)	1.7459	Comment	single_pulse	Date	05 Nov 2011 08:04:28
Date Stamp	06 Nov 2011 00:15:06	File Name	C:\Users\chen\Desktop\DakinNMR\CS_diclnhflaivn_dry-1.jdf		
Frequency (MHz)	500.16	Nucleus	1H	Number of Transients	16
Original Points Count	16384	Owner	delta	Points Count	16384
Receiver Gain	44.00	Solvent	DMSO-d6	Pulse Sequence	single_pulse.ex2
Sweep Width (Hz)	9384.38	Temperature (degree C)	22.200	Spectrum Offset (Hz)	2500.7996
				Spectrum Type	STANDARD



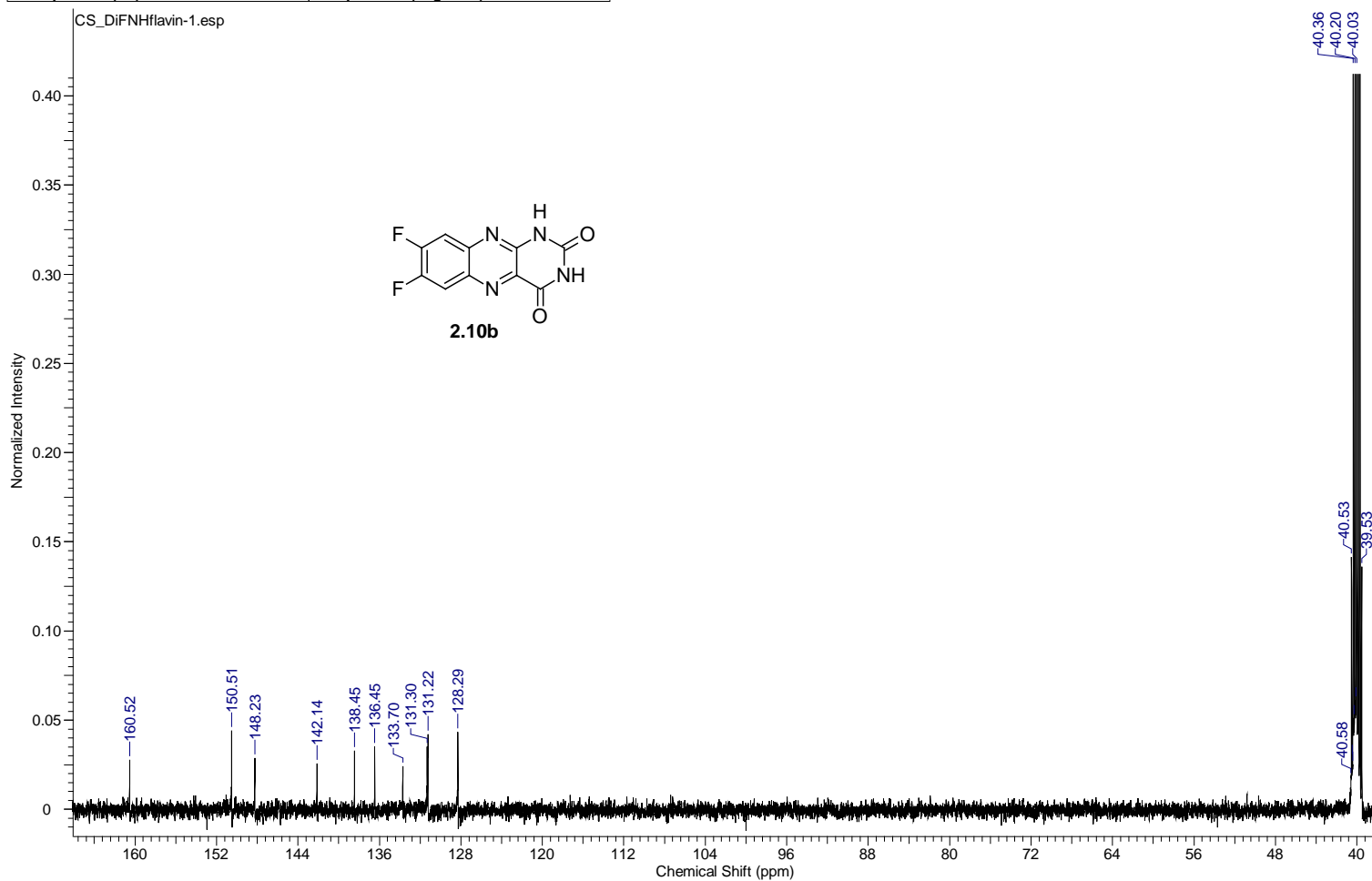
Acquisition Time (sec)	0.8336	Comment	single pulse decoupled gated NOE	Date	04 Nov 2011 11:47:25
Date Stamp	05 Nov 2011 03:58:02	File Name	C:\Users\chen\Desktop\DakinNMR\carbon\CS_DiclNHflavin-1.jdf	Number of Transients	260
Frequency (MHz)	125.77	Nucleus	13C	Origin	ECA 500
Original Points Count	32768	Owner	delta	Points Count	32768
Receiver Gain	50.00	Solvent	DMSO-d6	Spectrum Offset (Hz)	12553.6279
Sweep Width (Hz)	39308.18	Temperature (degree C)	22.500	Spectrum Type	STANDARD



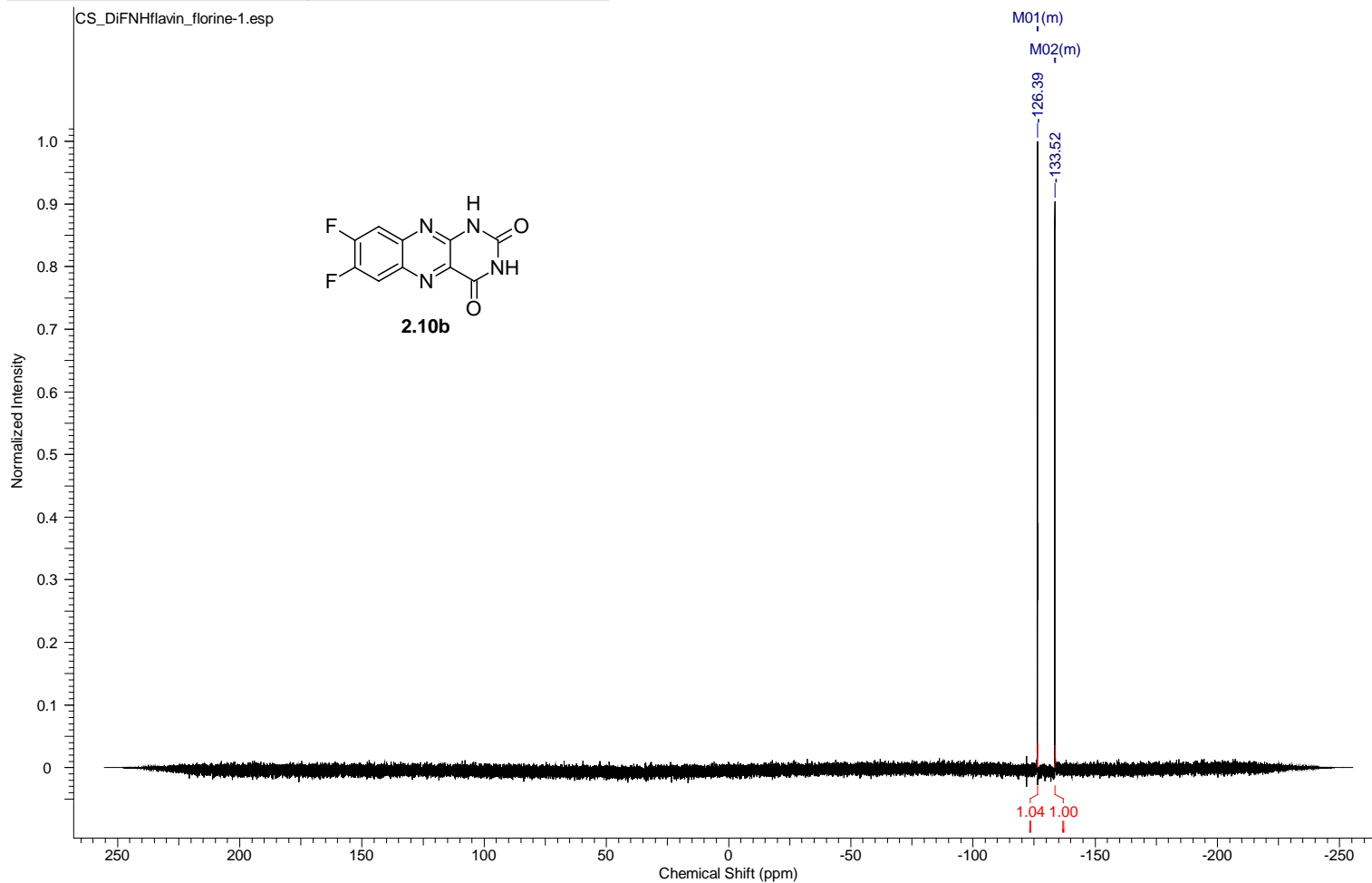
Acquisition Time (sec)	2.9072	Comment	single_pulse	Date	05 Nov 2011 08:44:44
Date Stamp	05 Nov 2011 07:31:45	File Name	C:\Users\chen\Desktop\DakinNMR\CS_diFNHflavin_dry-1.jdf		
Frequency (MHz)	300.53	Nucleus	1H	Number of Transients	4
Original Points Count	16384	Owner	delta	Points Count	16384
Receiver Gain	50.00	Solvent	DMSO-d6	Spectrum Offset (Hz)	1502.6483
Sweep Width (Hz)	5635.71	Temperature (degree C)	22.100	Spectrum Type	STANDARD



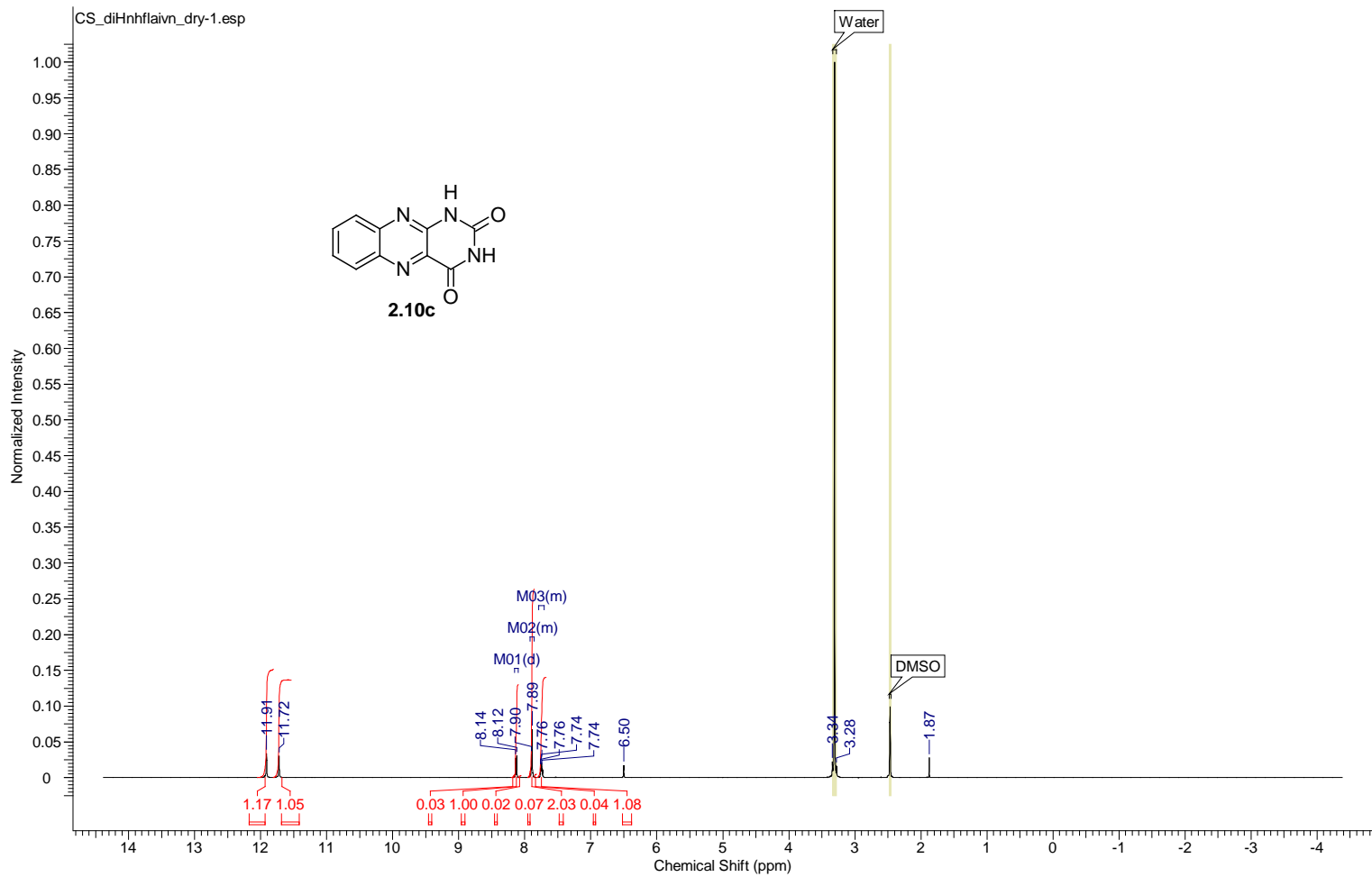
Acquisition Time (sec)	0.8336	Comment	single pulse decoupled gated NOE	Date	04 Nov 2011 11:29:23
Date Stamp	05 Nov 2011 03:40:00	File Name	C:\Users\chen\Desktop\DakinNMR\carbon\CS_DiFNHflavin-1.jdf		
Frequency (MHz)	125.77	Nucleus	13C	Origin	ECA 500
Original Points Count	32768	Owner	delta	Points Count	32768
Receiver Gain	50.00	Solvent	DMSO-d6	Spectrum Offset (Hz)	12576.5293
Sweep Width (Hz)	39308.18	Temperature (degree C)	22.500	Spectrum Type	STANDARD



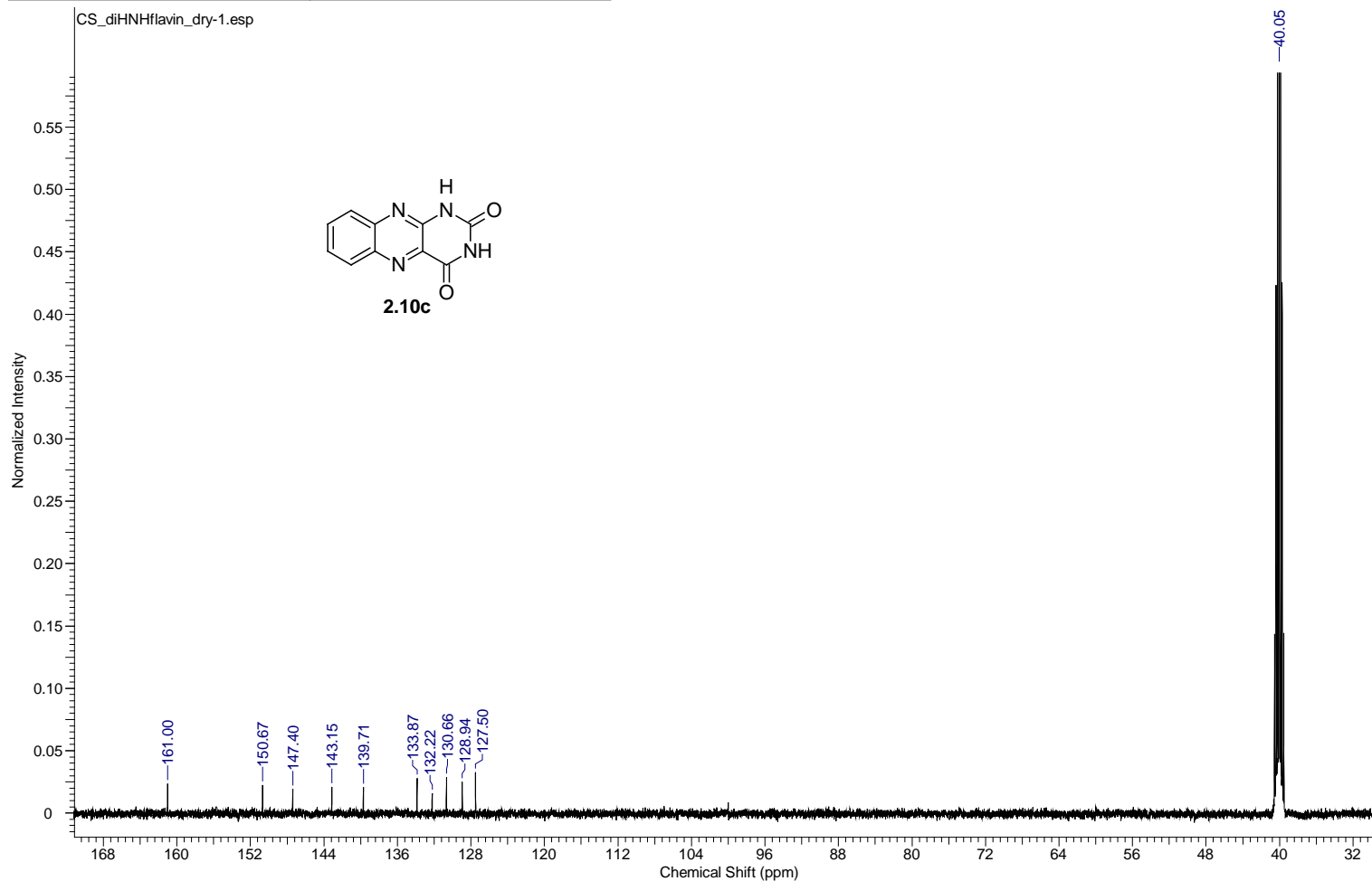
Acquisition Time (sec)	0.2726	Comment	single_pulse	Date	30 Dec 2011 08:31:14
Date Stamp	31 Dec 2011 01:29:18	File Name	C:\Users\chen\Desktop\DakinNMR\NMR PDF\DiF\Florine\CS_DiFNHflavin_florine-1.jdf		
Frequency (MHz)	470.62	Nucleus	19F	Number of Transients	15
Original Points Count	65536	Owner	delta	Points Count	65536
Receiver Gain	54.00	Solvent	DMSO-d6	Pulse Sequence	single_pulse.ex2
Sweep Width (Hz)	240384.63	Temperature (degree C)	21.700	Spectrum Offset (Hz)	0.0000
				Spectrum Type	STANDARD



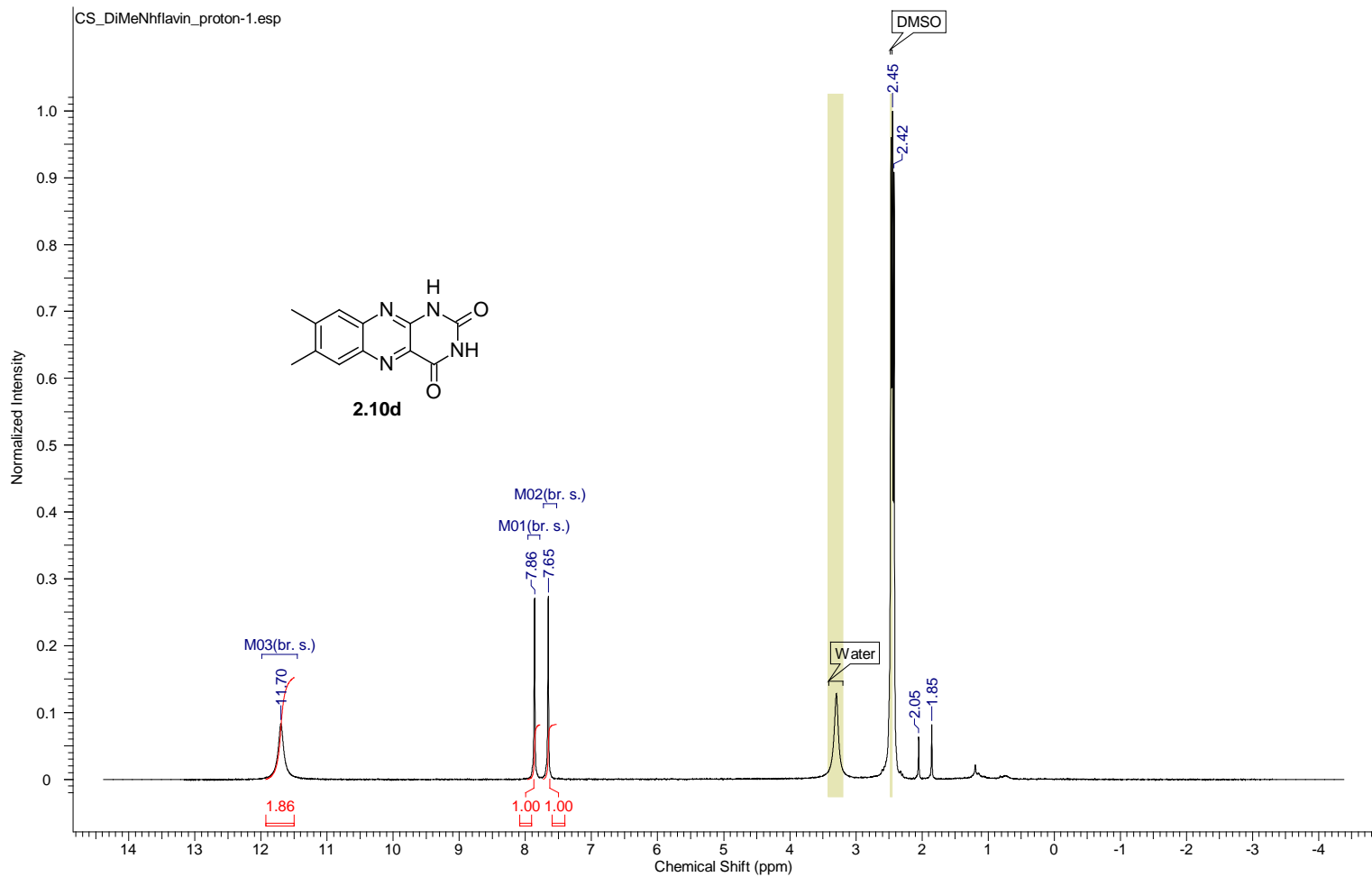
Acquisition Time (sec)	1.7459	Comment	single_pulse	Date	05 Nov 2011 08:48:07
Date Stamp	06 Nov 2011 00:58:45	File Name	C:\Users\chen\Desktop\DakinNMR\CS_diHnhflaivn_dry-1.jdf		
Frequency (MHz)	500.16	Nucleus	1H	Number of Transients	16
Original Points Count	16384	Owner	delta	Points Count	16384
Receiver Gain	44.00	Solvent	DMSO-d6	Pulse Sequence	single_pulse.ex2
Sweep Width (Hz)	9384.38	Temperature (degree C)	22.100	Spectrum Offset (Hz)	2500.7996
				Spectrum Type	STANDARD



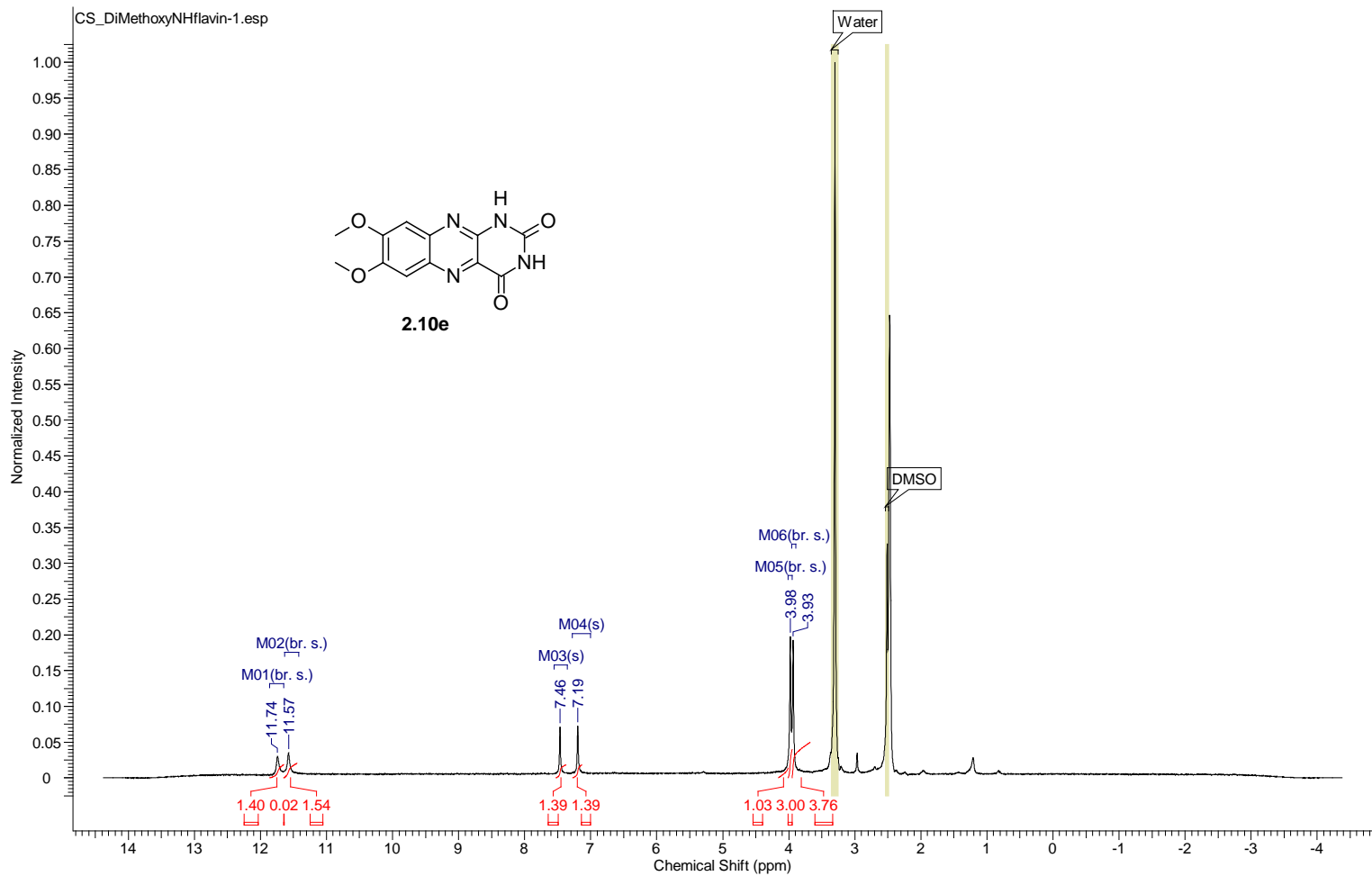
Acquisition Time (sec)	0.8336	Comment	single pulse decoupled gated NOE	Date	05 Nov 2011 08:59:41
Date Stamp	06 Nov 2011 01:10:19	File Name	C:\Users\chen\Desktop\DakinNMR\CS_diHNHflavin_dry-1.jdf	Number of Transients	260
Frequency (MHz)	125.77	Nucleus	13C	Origin	ECA 500
Original Points Count	32768	Owner	delta	Points Count	32768
Receiver Gain	50.00	Solvent	DMSO-d6	Spectrum Offset (Hz)	12576.5293
Sweep Width (Hz)	39308.18	Temperature (degree C)	22.700	Spectrum Type	STANDARD



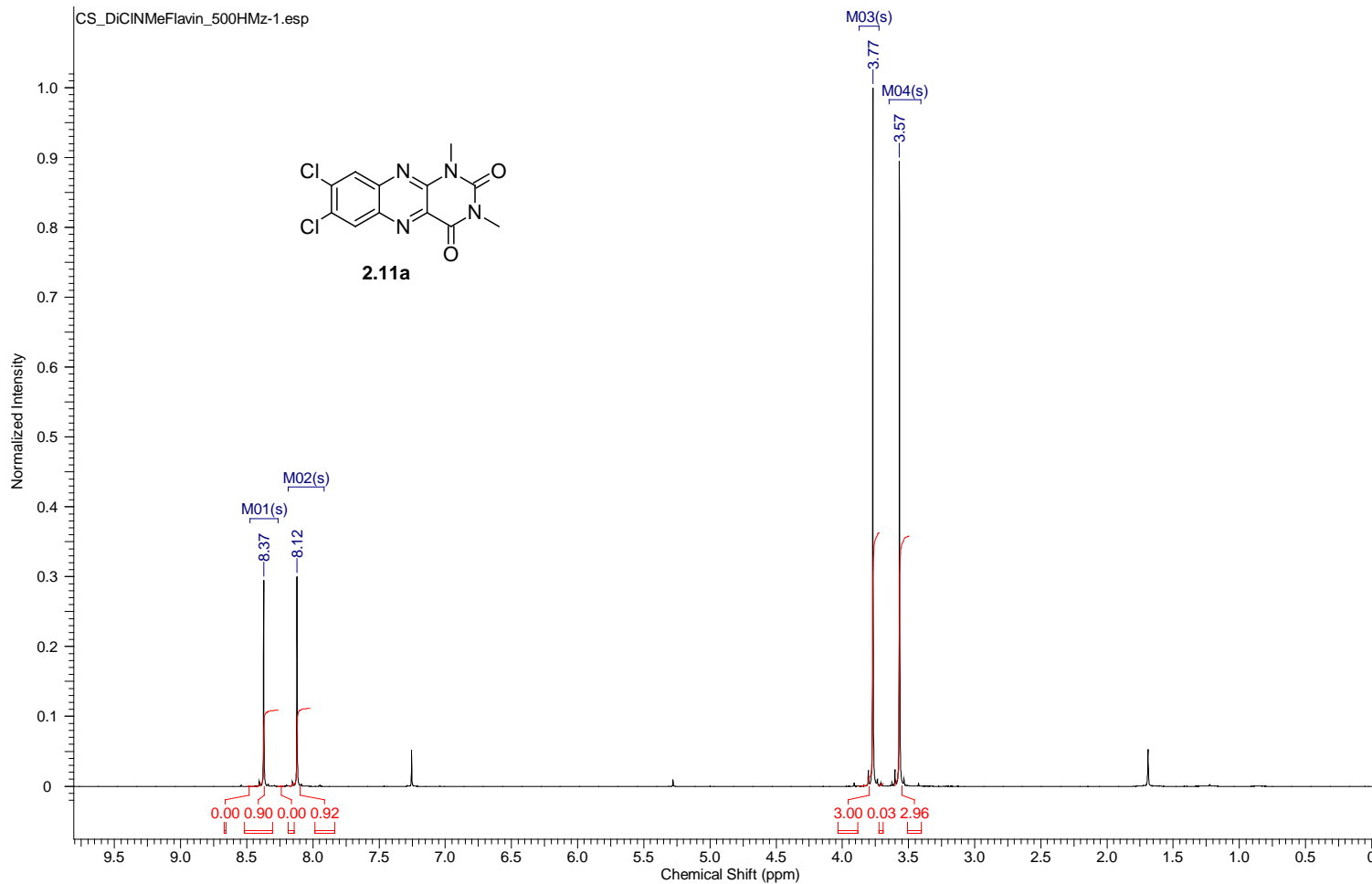
Acquisition Time (sec)	1.7459	Comment	single_pulse	Date	01 Dec 2011 13:28:21
Date Stamp	02 Dec 2011 06:24:38	File Name	F:\Dakin NMR\CS_DiMeNhfIavin_proton-1.jdf		
Frequency (MHz)	500.16	Nucleus	1H	Number of Transients	6
Original Points Count	16384	Owner	delta	Points Count	16384
Receiver Gain	48.00	Solvent	DMSO-d6	Pulse Sequence	single_pulse.ex2
Sweep Width (Hz)	9384.38	Temperature (degree C)	22.100	Spectrum Offset (Hz)	2500.7996
				Spectrum Type	STANDARD



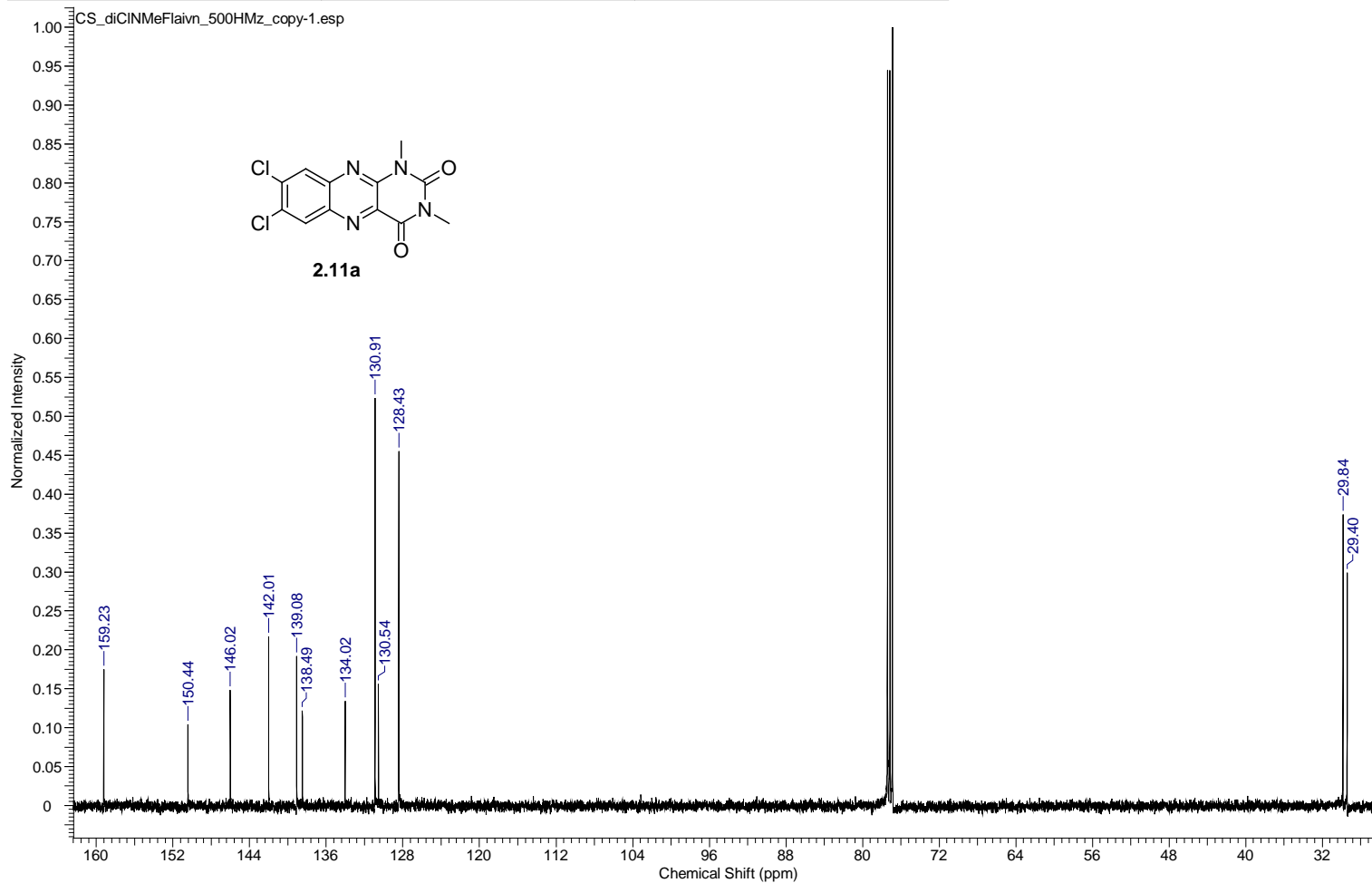
Acquisition Time (sec)	2.9072	Comment	single_pulse	Date	17 Nov 2011 16:44:17
Date Stamp	17 Nov 2011 16:16:38	File Name	C:\Users\chen\Desktop\DakinNMR\NMR PDF\DiMeO\CS_DiMethoxyNHflavin-1.jdf		
Frequency (MHz)	300.53	Nucleus	1H	Number of Transients	15
Original Points Count	16384	Owner	delta	Points Count	16384
Receiver Gain	46.00	Solvent	DMSO-d6	Spectrum Offset (Hz)	1502.6483
Sweep Width (Hz)	5635.71	Temperature (degree C)	22.000	Spectrum Type	STANDARD



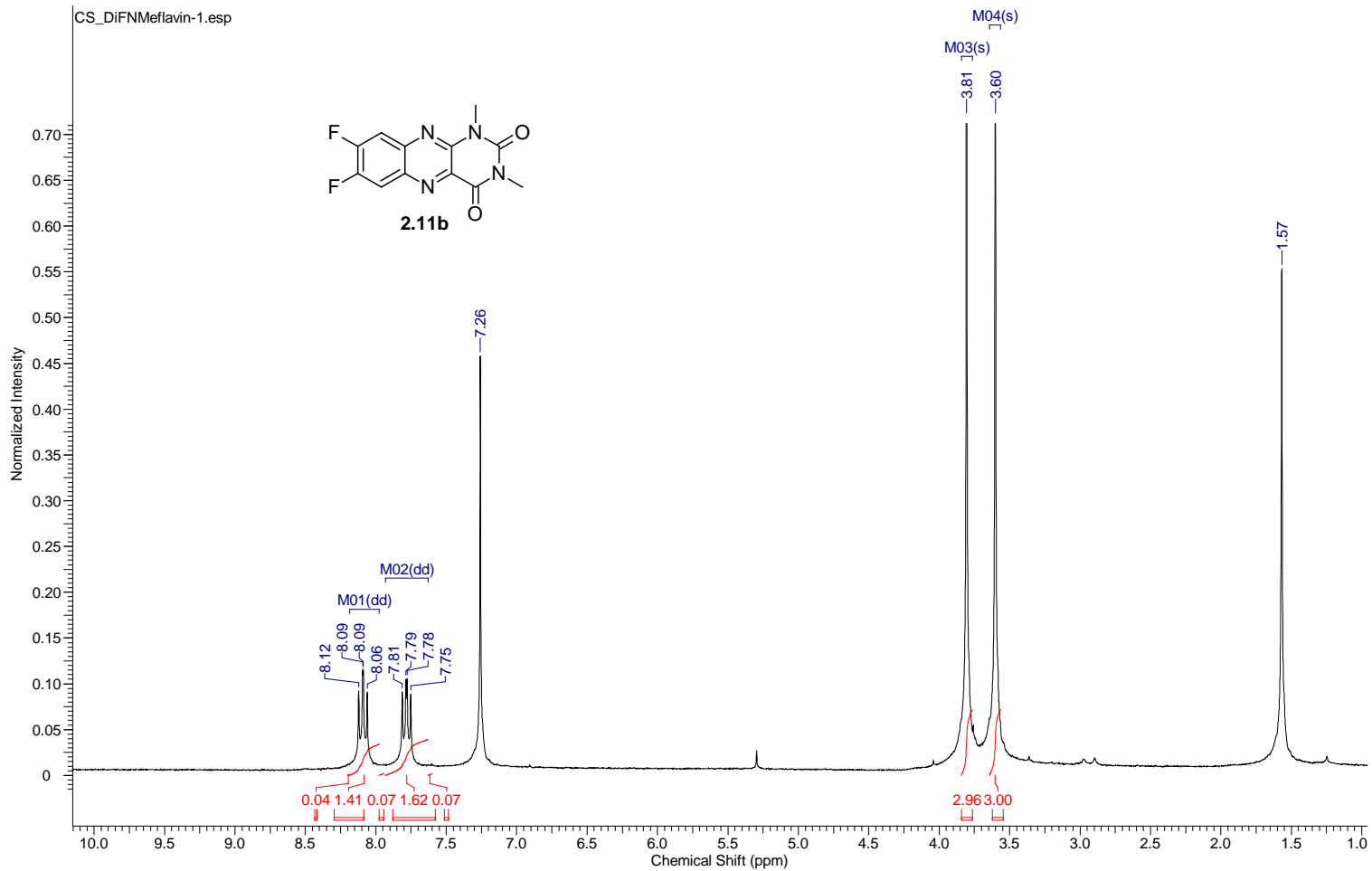
Acquisition Time (sec)	1.7459	Comment	single_pulse	Date	06 Nov 2011 08:18:49
Date Stamp	07 Nov 2011 01:14:57	File Name	C:\Users\chen\Desktop\DakinNMR\CS_DiCINMeFlavin_500HMz-1.jdf		
Frequency (MHz)	500.16	Nucleus	1H	Number of Transients	4
Original Points Count	16384	Owner	delta	Points Count	16384
Receiver Gain	42.00	Solvent	CHLOROFORM-d	Pulse Sequence	single_pulse.ex2
Spectrum Type	STANDARD	Sweep Width (Hz)	9384.38	Temperature (degree C)	22.200
				Spectrum Offset (Hz)	2500.7996



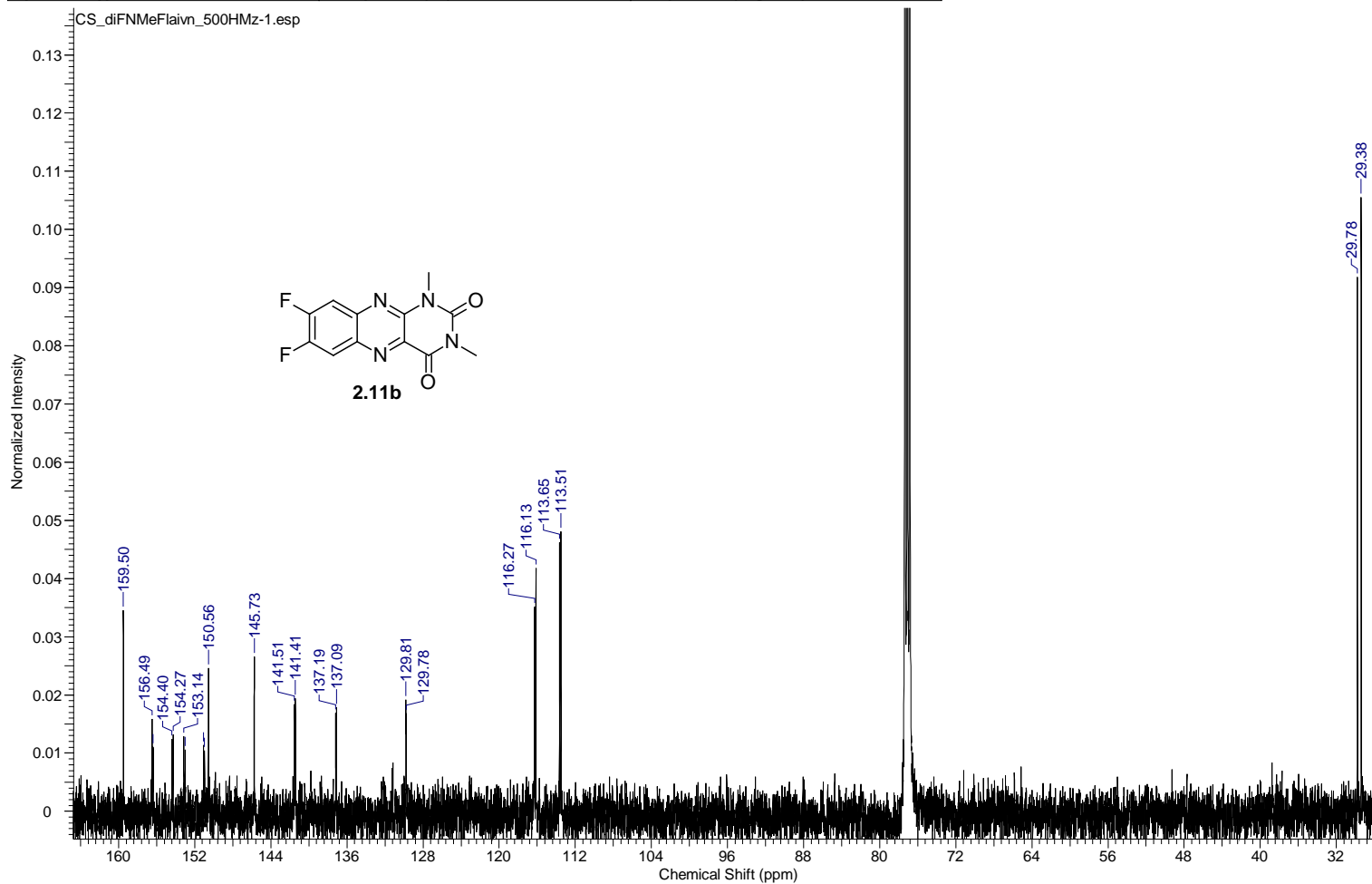
Acquisition Time (sec)	0.8336	Comment	single pulse decoupled gated NOE	Date	06 Nov 2011 08:25:30
Date Stamp	07 Nov 2011 01:21:38	File Name	C:\Users\ichen\Desktop\DakinNMR\carbon\CS_diCINMeFlainv_500HMz_copy-1.jdf	Number of Transients	180
Frequency (MHz)	125.77	Nucleus	13C	Origin	ECA 500
Original Points Count	32768	Owner	delta	Points Count	32768
Receiver Gain	50.00	Solvent	CHLOROFORM-d	Pulse Sequence	single_pulse_dec
Spectrum Type	STANDARD	Sweep Width (Hz)	39308.18	Temperature (degree C)	22.600
				Spectrum Offset (Hz)	12576.5293

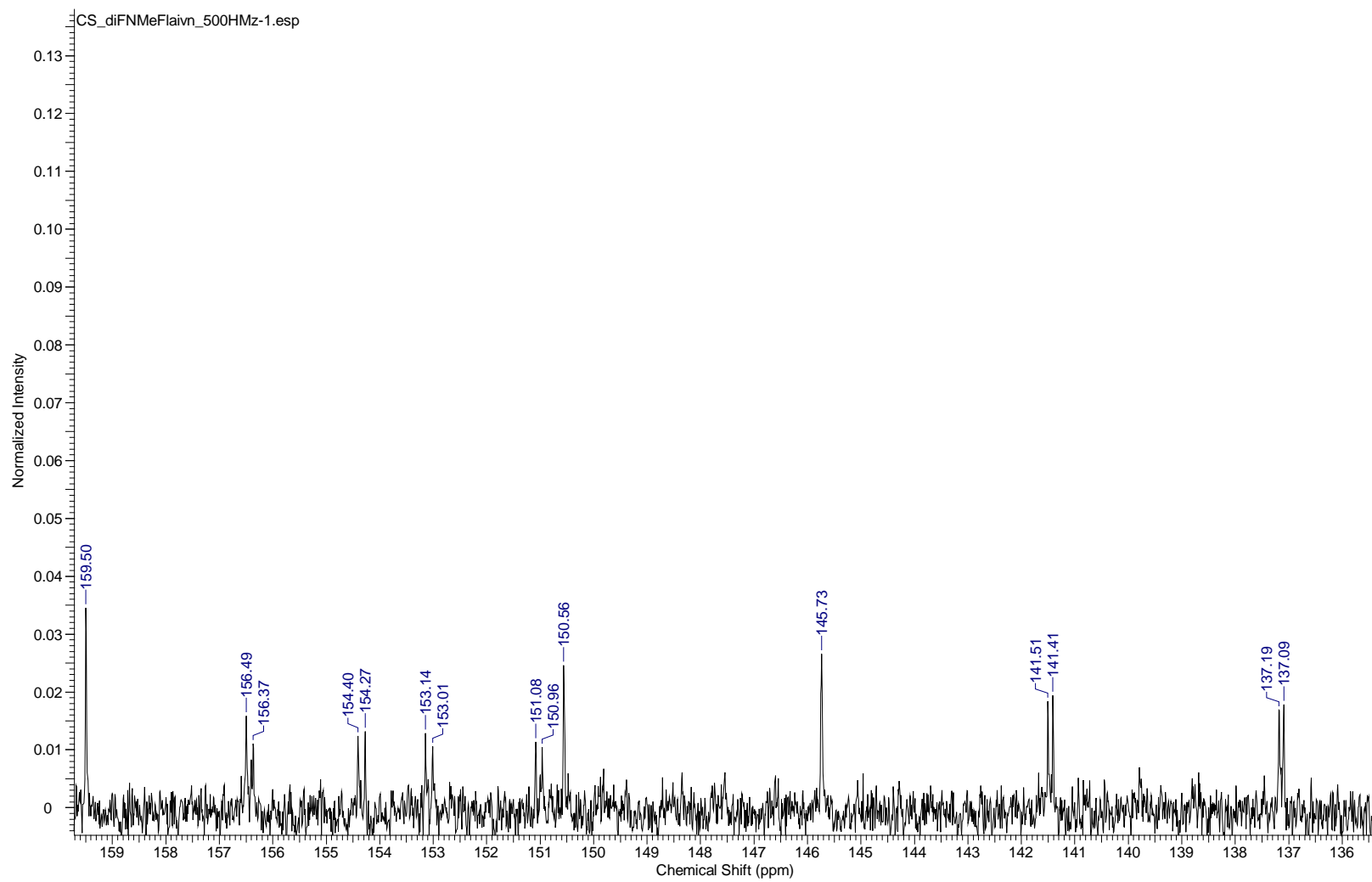


Acquisition Time (sec)	2.9072	Comment	single_pulse	Date	05 Nov 2011 12:30:59
Date Stamp	05 Nov 2011 11:17:59	File Name	C:\Users\chen\Desktop\DakinNMR\CS_DiFNMeflavin-1.jdf		
Frequency (MHz)	300.53	Nucleus	1H	Origin	ECX 300
Original Points Count	16384	Owner	delta	Points Count	16384
Receiver Gain	46.00	Solvent	CHLOROFORM-d	Pulse Sequence	single_pulse.ex2
Spectrum Type	STANDARD	Sweep Width (Hz)	5635.71	Temperature (degree C)	22.600

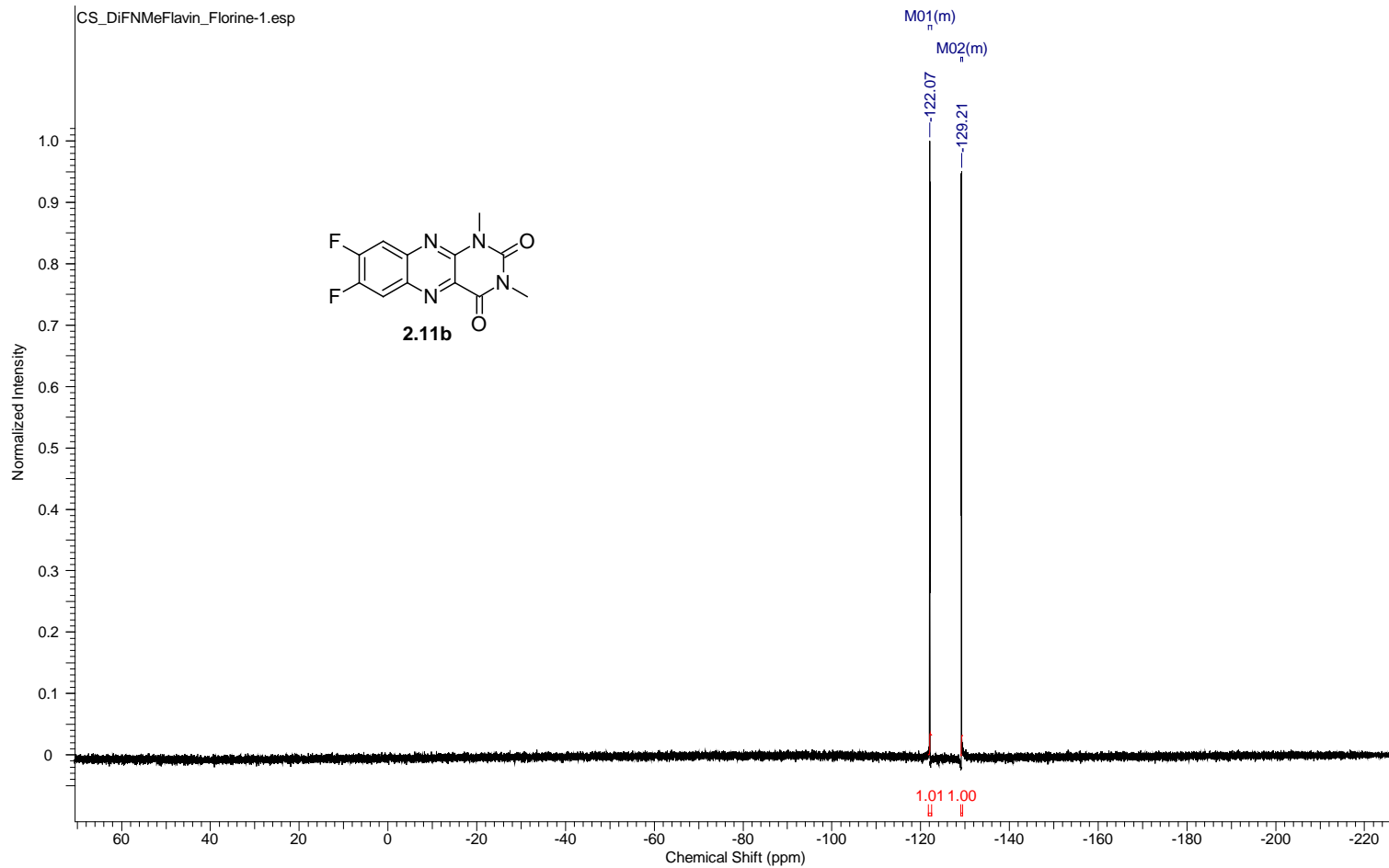


Acquisition Time (sec)	0.8336	Comment	single pulse decoupled gated NOE	Date	06 Nov 2011 08:04:19
Date Stamp	07 Nov 2011 01:00:27	File Name	C:\Users\chen\Desktop\DakinNMR\carbon\CS_diFNMeFlaivn_500HMz-1.jdf	Number of Transients	1000
Frequency (MHz)	125.77	Nucleus	13C	Origin	ECA 500
Original Points Count	32768	Owner	delta	Points Count	32768
Receiver Gain	50.00	Solvent	CHLOROFORM-d	Pulse Sequence	single_pulse_dec
Spectrum Type	STANDARD	Sweep Width (Hz)	39308.18	Temperature (degree C)	22.800
				Spectrum Offset (Hz)	12576.5293

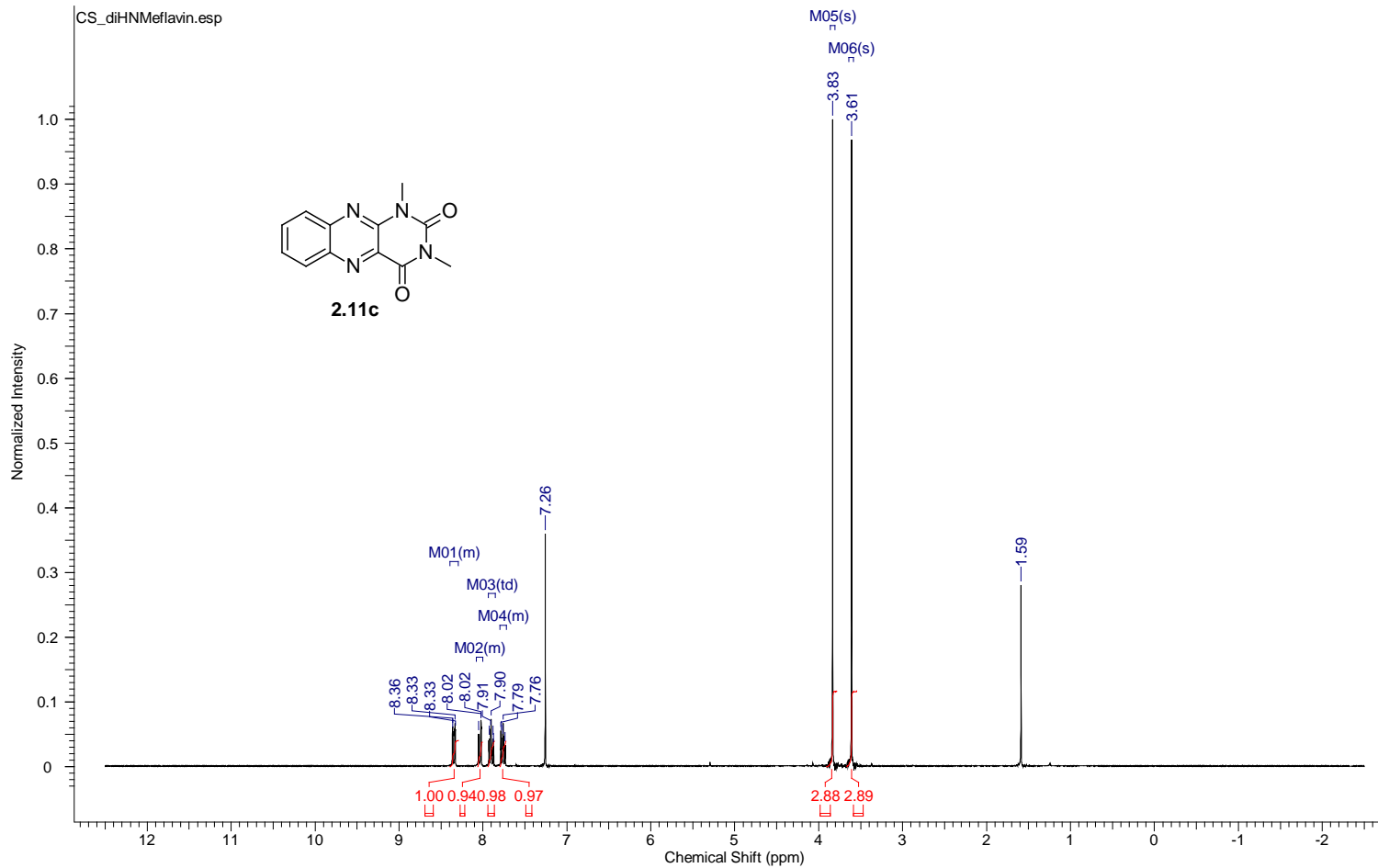




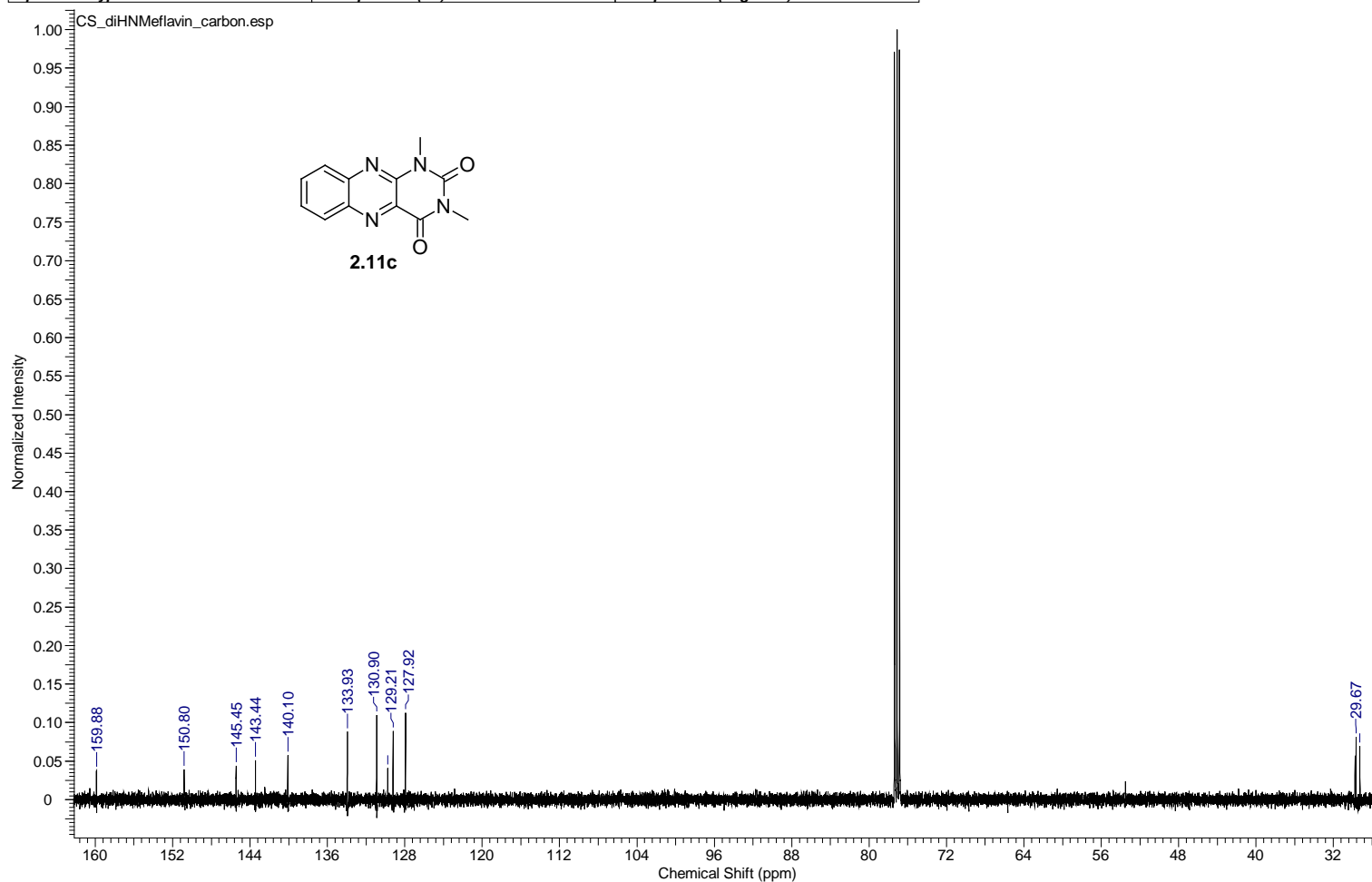
Acquisition Time (sec)	0.2726	Comment	single_pulse	Date	30 Dec 2011 08:26:09
Date Stamp	31 Dec 2011 01:24:13				
File Name	C:\Users\chen\Desktop\DakinNMR\NMR PDF\DiF\Florine\CS_DiFNMeFlavin_Florine-1.jdf			Frequency (MHz)	470.62
Nucleus	19F	Number of Transients	36	Origin	ECA 500
Owner	delta	Points Count	65536	Pulse Sequence	single_pulse.ex2
Solvent	CHLOROFORM-d	Spectrum Offset (Hz)	0.0000	Receiver Gain	56.00
Sweep Width (Hz)	240384.63	Temperature (degree C)	21.800	Spectrum Type	STANDARD



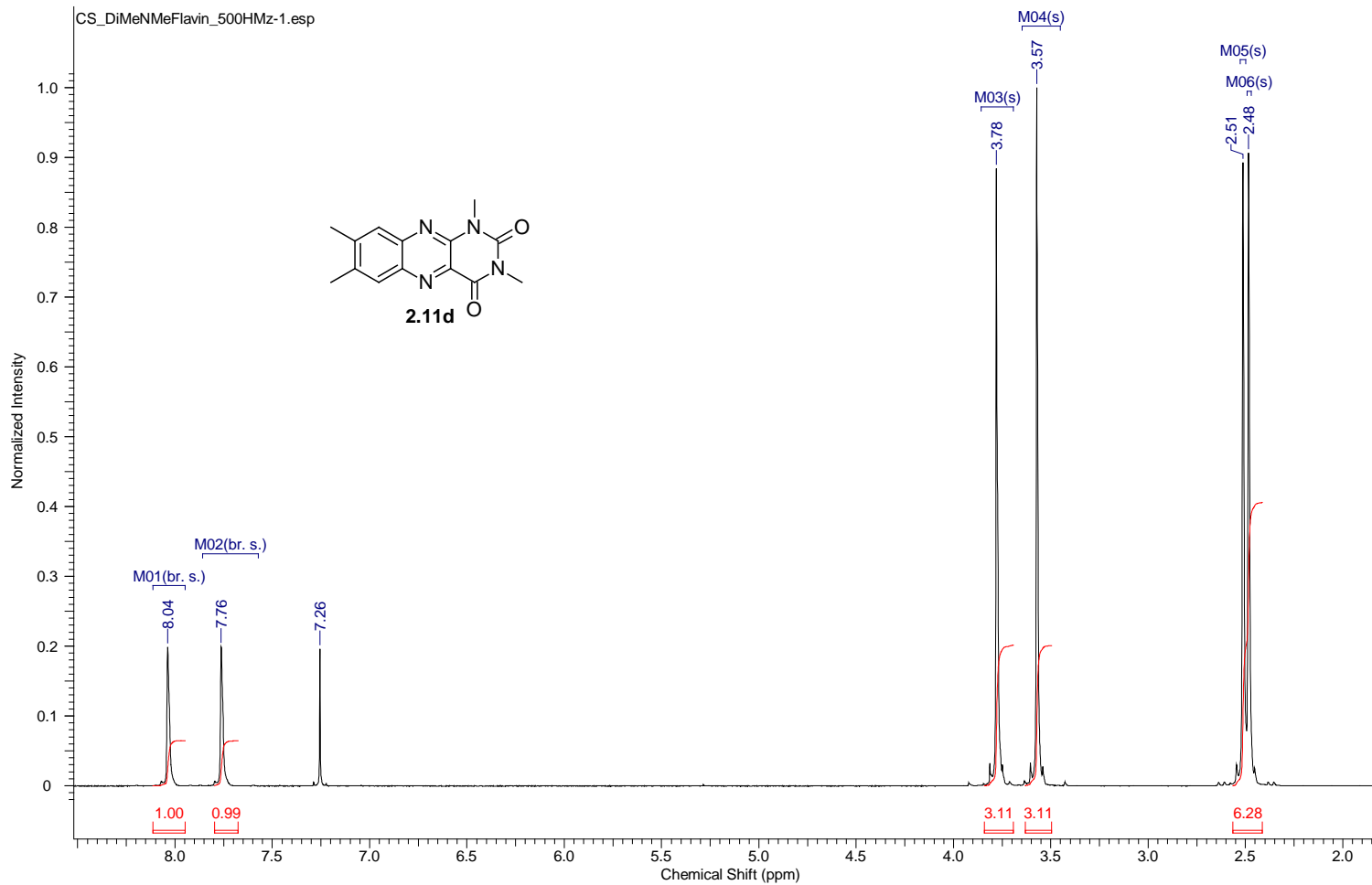
Acquisition Time (sec)	2.9074	Comment	single_pulse	Date	24 Apr 2010 07:54:17
Date Stamp	24 Apr 2010 07:38:58				
File Name	C:\Users\chen\Desktop\study\Foss\Shuai's Data\NMR DATA\NMR300M 072010\300MHZ\proton\CS_1043_SM-6.jdf				
Frequency (MHz)	300.53	Nucleus	1H	Number of Transients	11
Original Points Count	13107	Owner	delta	Points Count	13107
Receiver Gain	48.00	Solvent	CHLOROFORM-d	Spectrum Offset (Hz)	1502.6483
Sweep Width (Hz)	4508.15	Temperature (degree C)	21.000	Spectrum Type	STANDARD



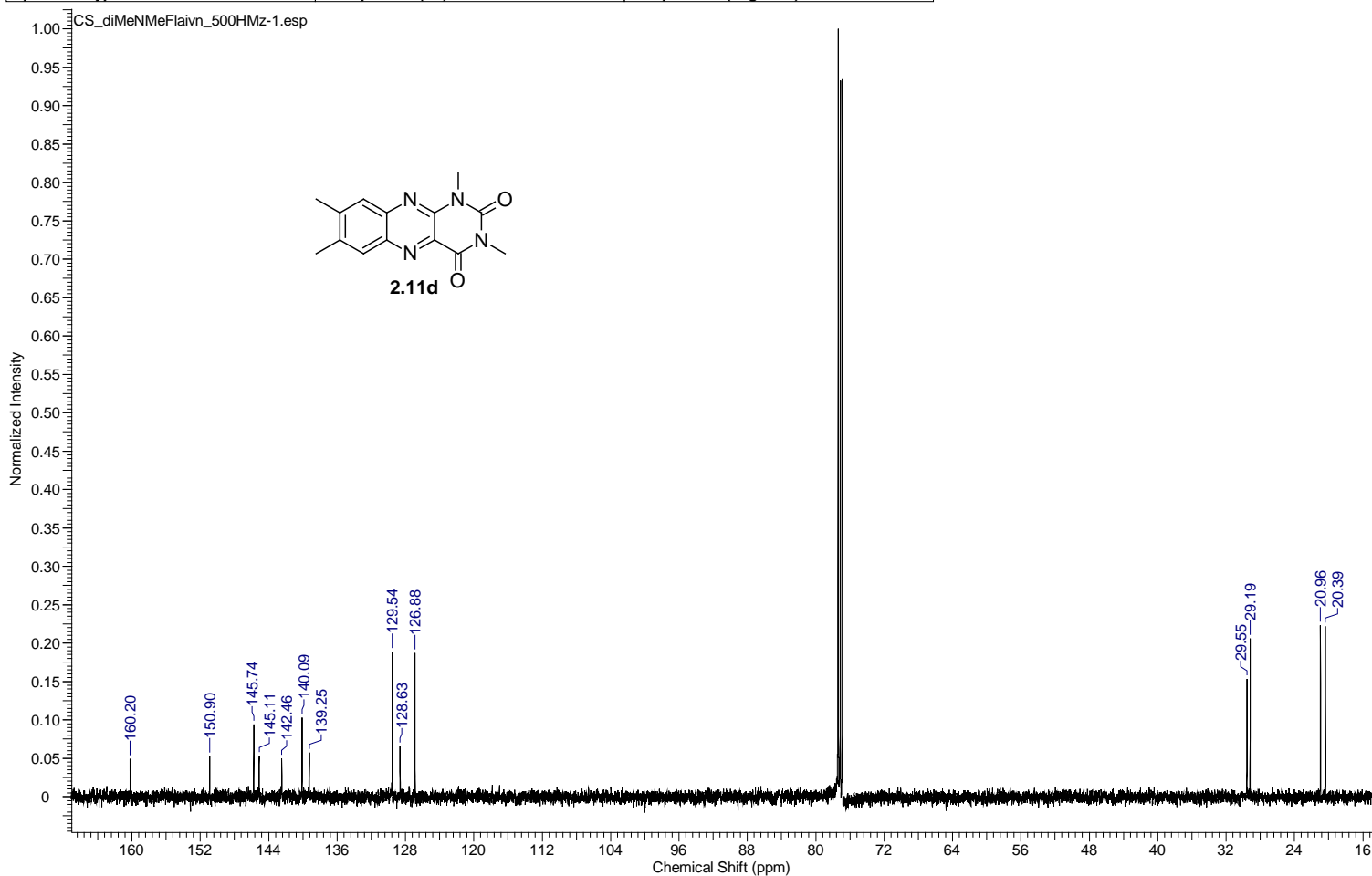
Acquisition Time (sec)	2.0840	Comment	single pulse decoupled gated NOE	Date	28 Sep 2009 17:27:29
Date Stamp	29 Sep 2009 10:36:52	File Name	C:\Users\chen\Desktop\DakinNMR\CS_1043_copy-2.jdf		
Frequency (MHz)	125.76	Nucleus	13C	Number of Transients	340
Original Points Count	65536	Owner	delta	Points Count	65536
Receiver Gain	28.00	Solvent	CHLOROFORM-d	Pulse Sequence	single_pulse_dec
Spectrum Type	STANDARD	Sweep Width (Hz)	31446.54	Temperature (degree C)	28.200



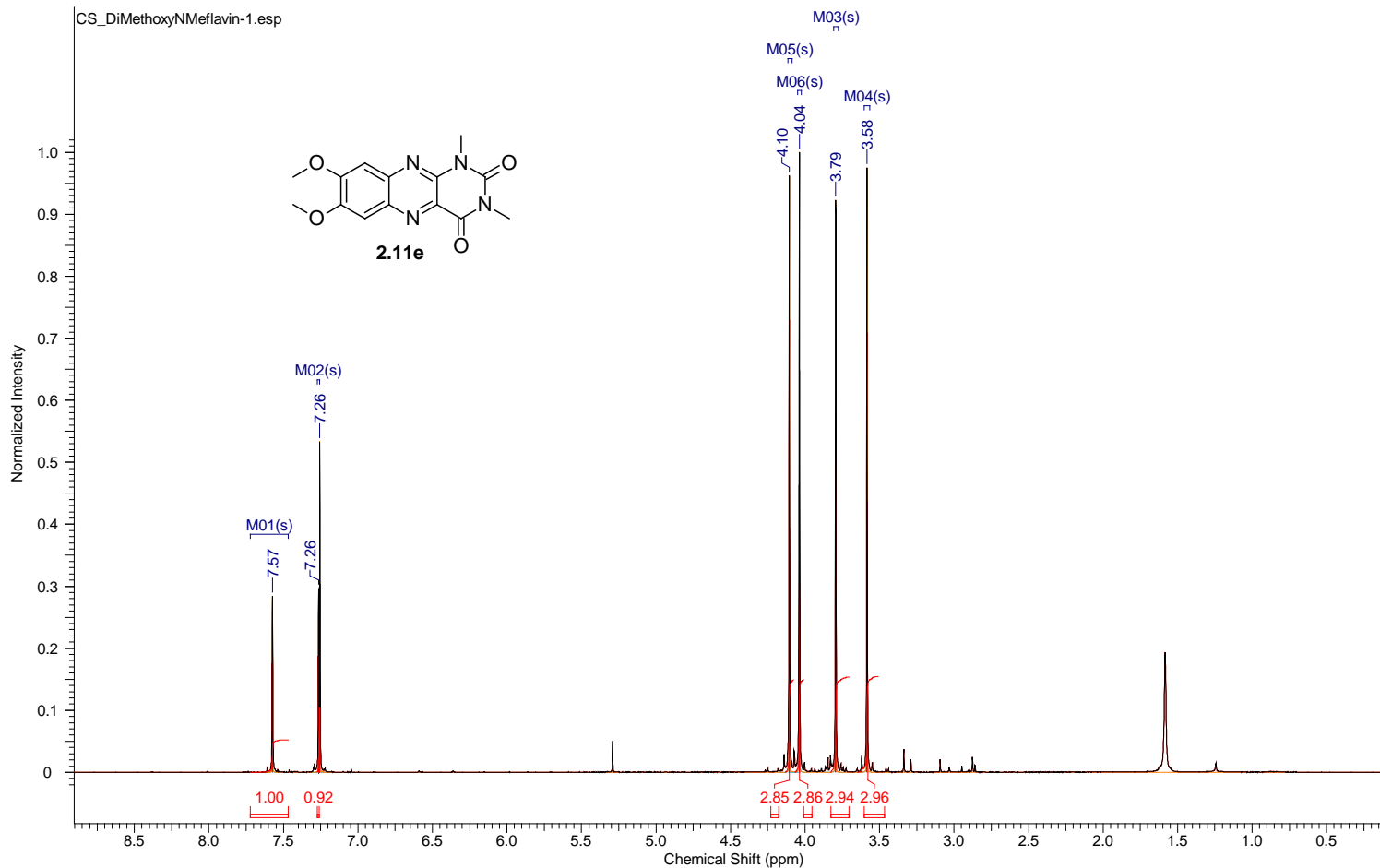
Acquisition Time (sec)	1.7459	Comment	single_pulse	Date	06 Nov 2011 08:09:59
Date Stamp	07 Nov 2011 01:06:07	File Name	C:\Users\chen\Desktop\DakinNMR\CS_DiMeNMeFlavin_500HMz-1.jdf		
Frequency (MHz)	500.16	Nucleus	1H	Number of Transients	4
Original Points Count	16384	Owner	delta	Points Count	16384
Receiver Gain	42.00	Solvent	CHLOROFORM-d	Pulse Sequence	single_pulse.ex2
Spectrum Type	STANDARD	Sweep Width (Hz)	9384.38	Temperature (degree C)	22.300



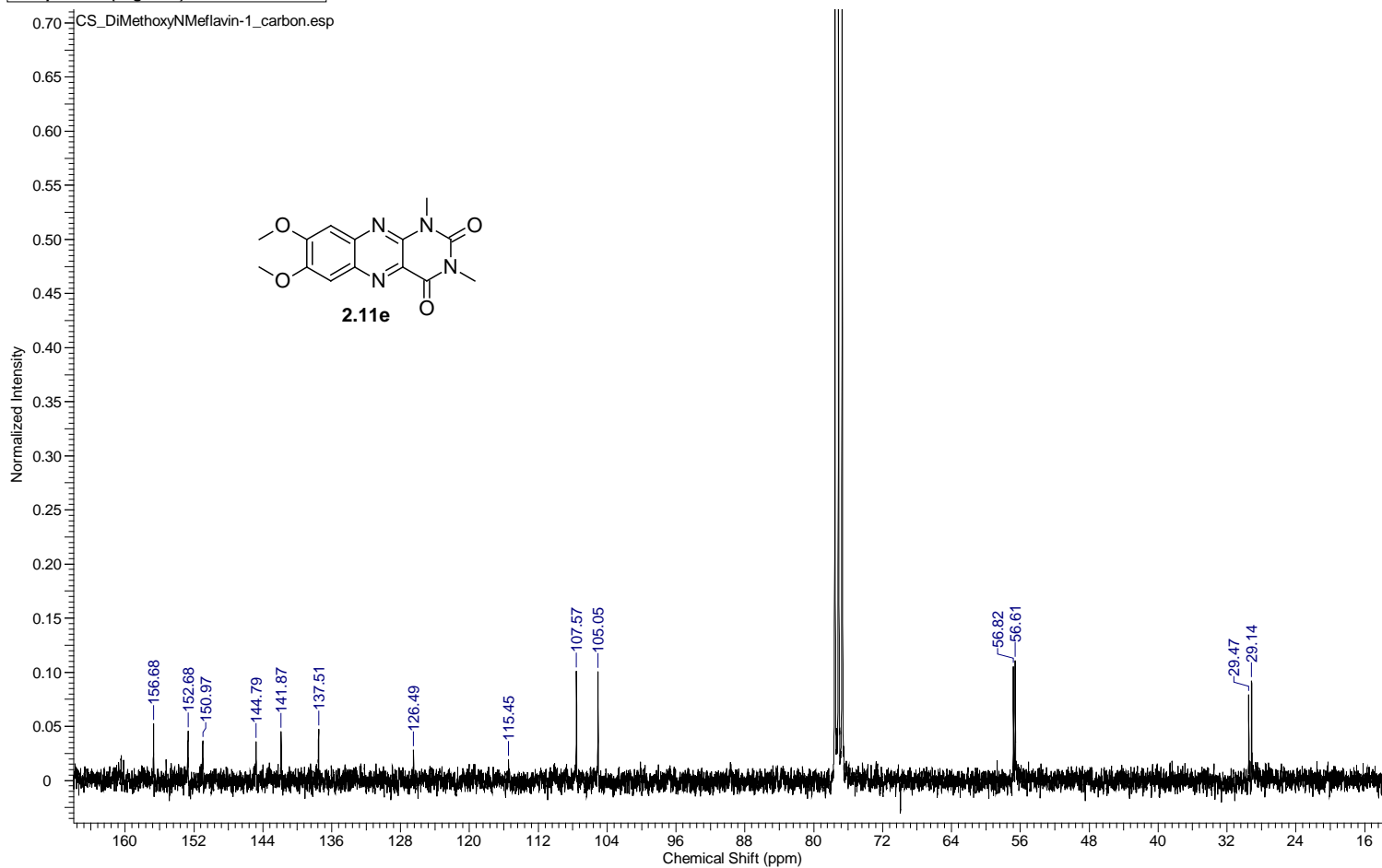
Acquisition Time (sec)	0.8336	Comment	single pulse decoupled gated NOE	Date	06 Nov 2011 08:14:54
Date Stamp	07 Nov 2011 01:11:03	File Name	C:\Users\chen\Desktop\DakinNMR\carbon\CS_diMeNMeFlaivn_500HMz-1.jdf		
Frequency (MHz)	125.77	Nucleus	¹³ C	Number of Transients	130
Original Points Count	32768	Owner	delta	Points Count	32768
Receiver Gain	50.00	Solvent	CHLOROFORM-d	Pulse Sequence	single_pulse_dec
Spectrum Type	STANDARD	Sweep Width (Hz)	39308.18	Temperature (degree C)	22.700



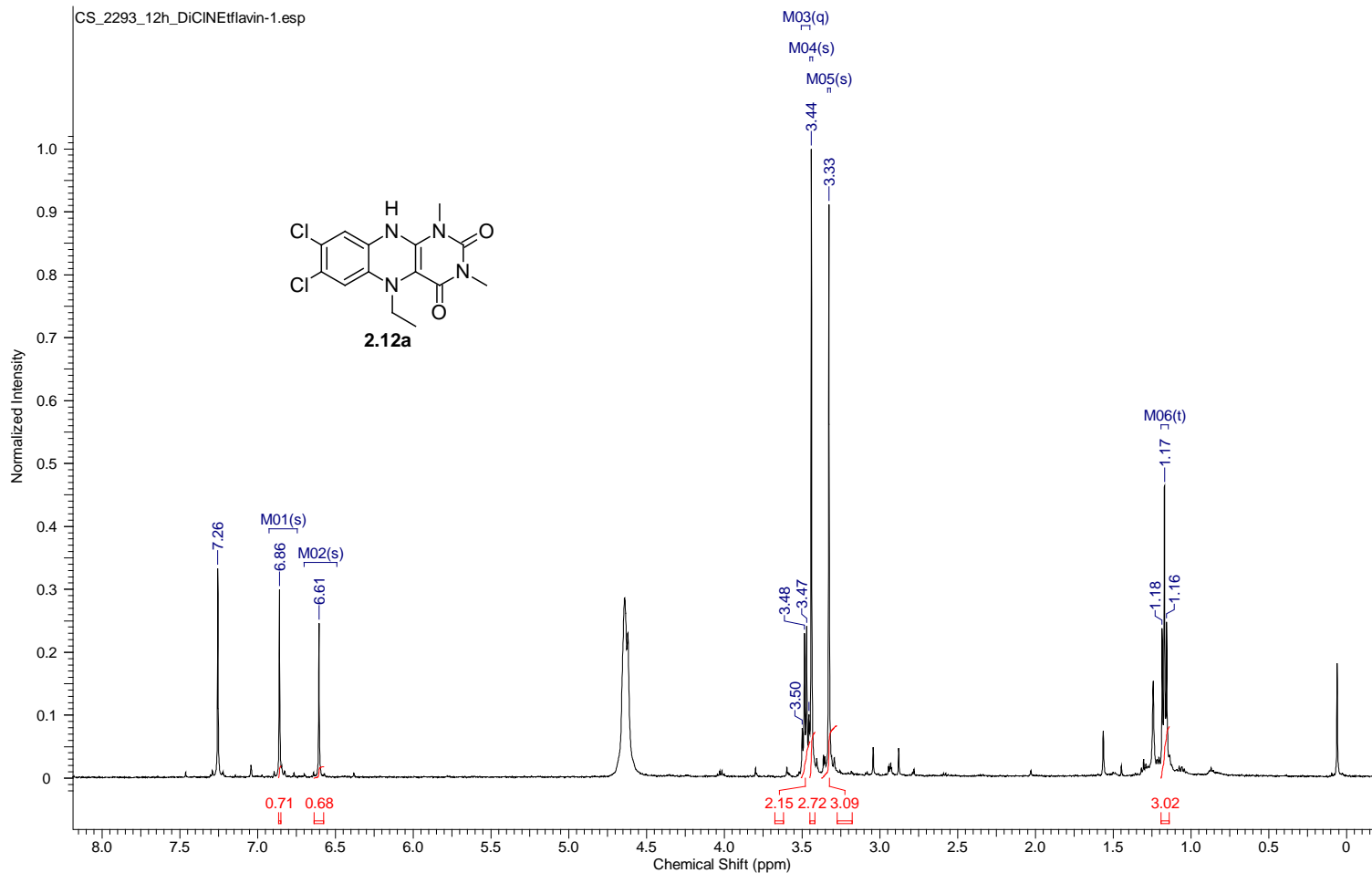
Acquisition Time (sec)	1.7459	Comment	single_pulse	Date	16 Nov 2011 14:09:18
Date Stamp	17 Nov 2011 07:05:29				
File Name	C:\Users\chen\Desktop\study\Foss\Shuai's Data\NMR DATA\500MHz\112511\aaaron\proton\CS_DimethoxyNMeFlavin-1.jdf				
Frequency (MHz)	500.16	Nucleus	1H	Number of Transients	11
Original Points Count	16384	Owner	delta	Points Count	16384
Receiver Gain	48.00	Solvent	CHLOROFORM-d	Spectrum Offset (Hz)	2500.7996
Sweep Width (Hz)	9384.38	Temperature (degree C)	22.300	Spectrum Type	STANDARD



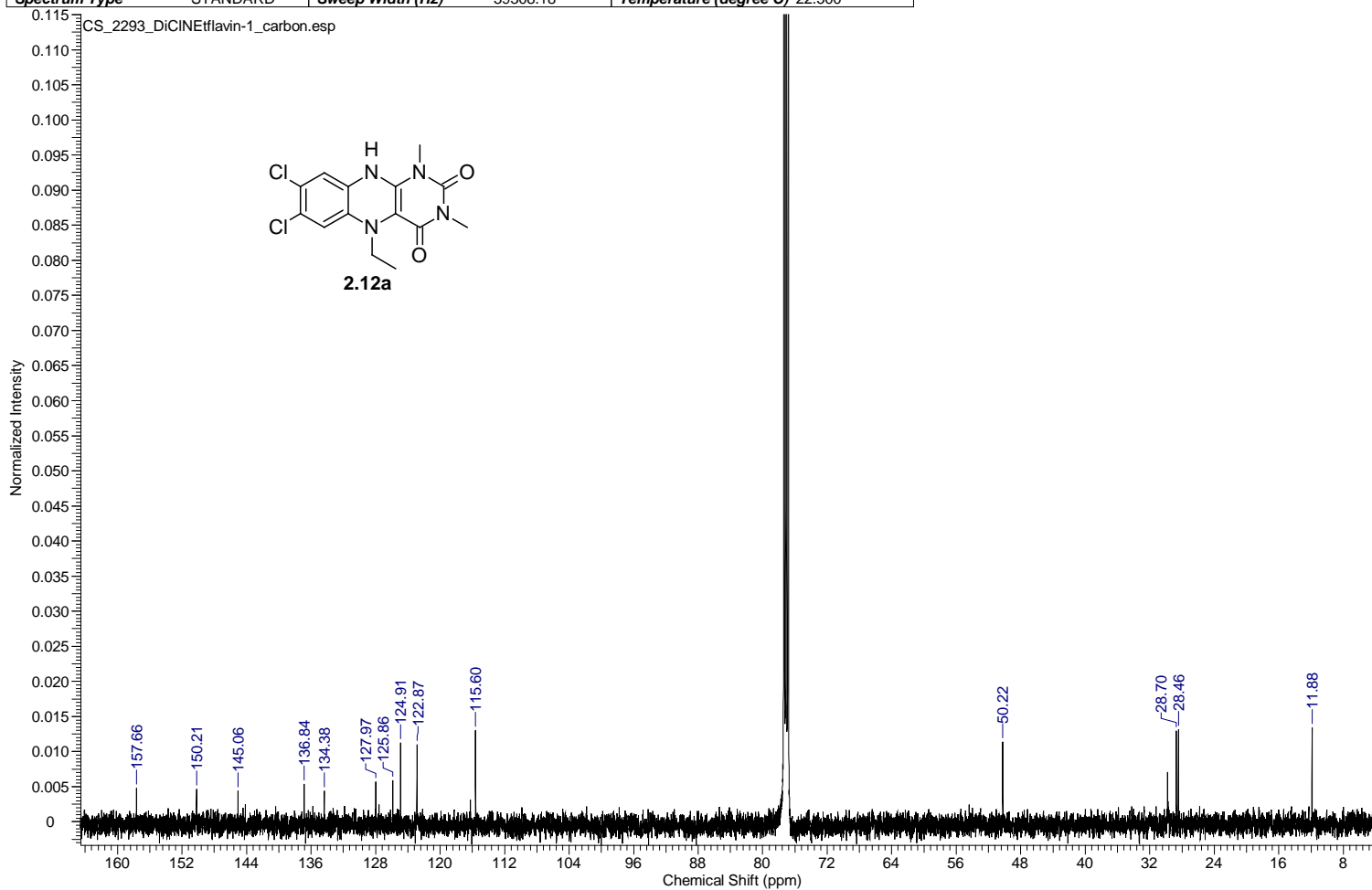
Acquisition Time (sec)	1.3841	Comment	single pulse decoupled gated NOE		Date	17 Nov 2011 16:31:49	
Date Stamp	17 Nov 2011 16:04:10						
File Name	C:\Users\chen\Desktop\DakinNMR\NMR PDF\DiMeOCS_DiMethoxyNMeFlavin-1_carbon.jdf			Frequency (MHz)	75.57		
Nucleus	13C	Number of Transients	1000	Origin	ECX 300	Original Points Count	32768
Owner	delta	Points Count	32768	Pulse Sequence	single_pulse_dec	Receiver Gain	50.00
Solvent	CHLOROFORM-d	Spectrum Offset (Hz)	7556.8232	Spectrum Type	STANDARD	Sweep Width (Hz)	23674.24
Temperature (degree C)	22.300						



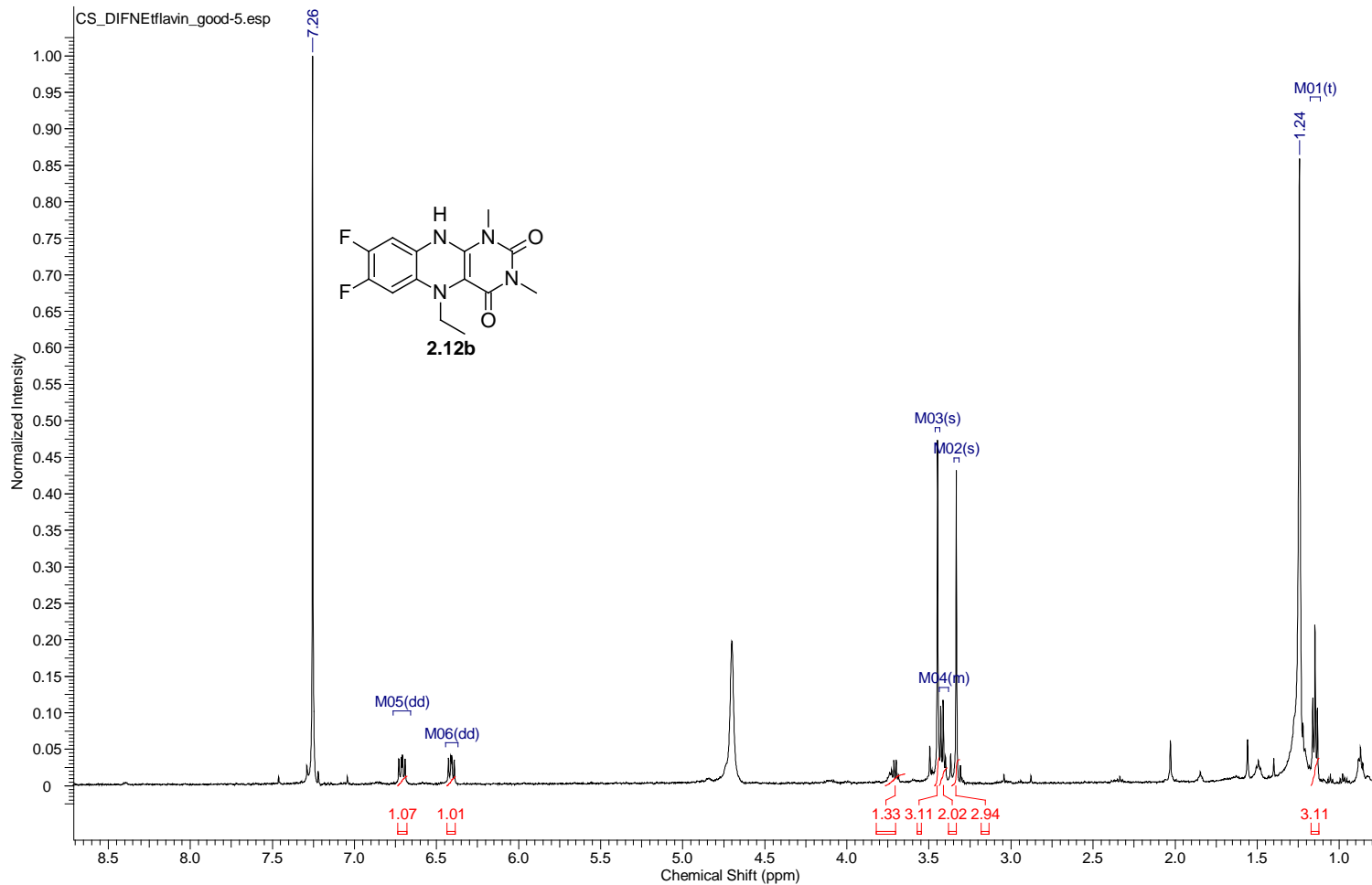
Acquisition Time (sec)	1.7459	Comment	single_pulse	Date	27 Dec 2011 08:48:32
Date Stamp	28 Dec 2011 01:46:35	File Name	C:\Users\lchen\Desktop\DakinNMR\NMR PDF\DiCl\CS_2293_12h_DiCINeTflavin-1.jdf		
Frequency (MHz)	500.16	Nucleus	1H	Number of Transients	16
Original Points Count	16384	Owner	delta	Points Count	16384
Receiver Gain	56.00	Solvent	CHLOROFORM-d	Pulse Sequence	single_pulse.ex2
Spectrum Type	STANDARD	Sweep Width (Hz)	9384.38	Temperature (degree C)	21.700



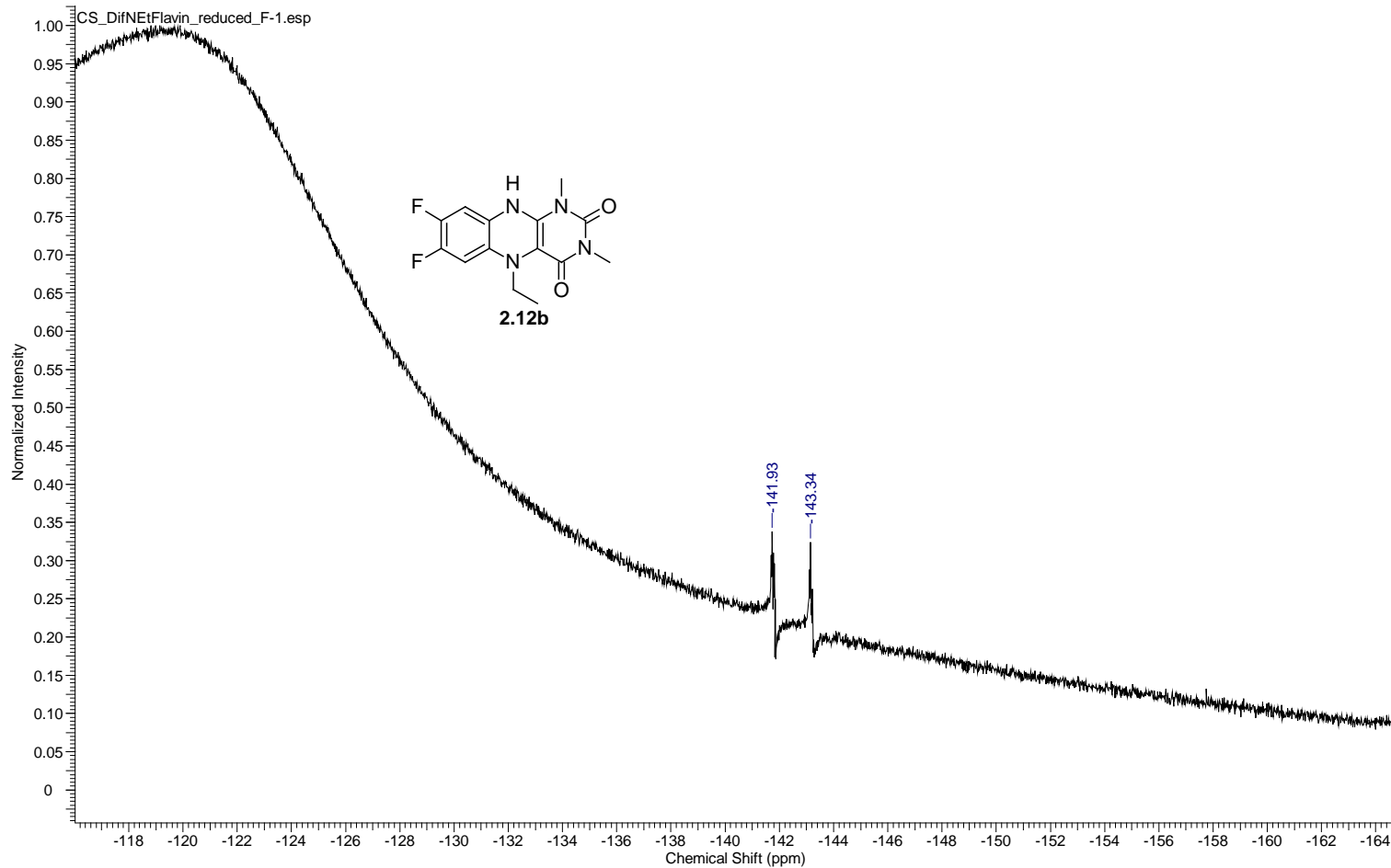
Acquisition Time (sec)	0.8336	Comment	single pulse decoupled gated NOE	Date	28 Dec 2011 03:08:52
Date Stamp	28 Dec 2011 14:19:10	File Name	G:\Dakin NMR\carbon\CS_2293_DiCINEflavin-1.jdf	Number of Transients	10000
Frequency (MHz)	125.77	Nucleus	13C	Origin	ECA 500
Original Points Count	32768	Owner	delta	Points Count	32768
Receiver Gain	50.00	Solvent	CHLOROFORM-d	Pulse Sequence	single_pulse_dec
Spectrum Type	STANDARD	Sweep Width (Hz)	39308.18	Temperature (degree C)	22.500



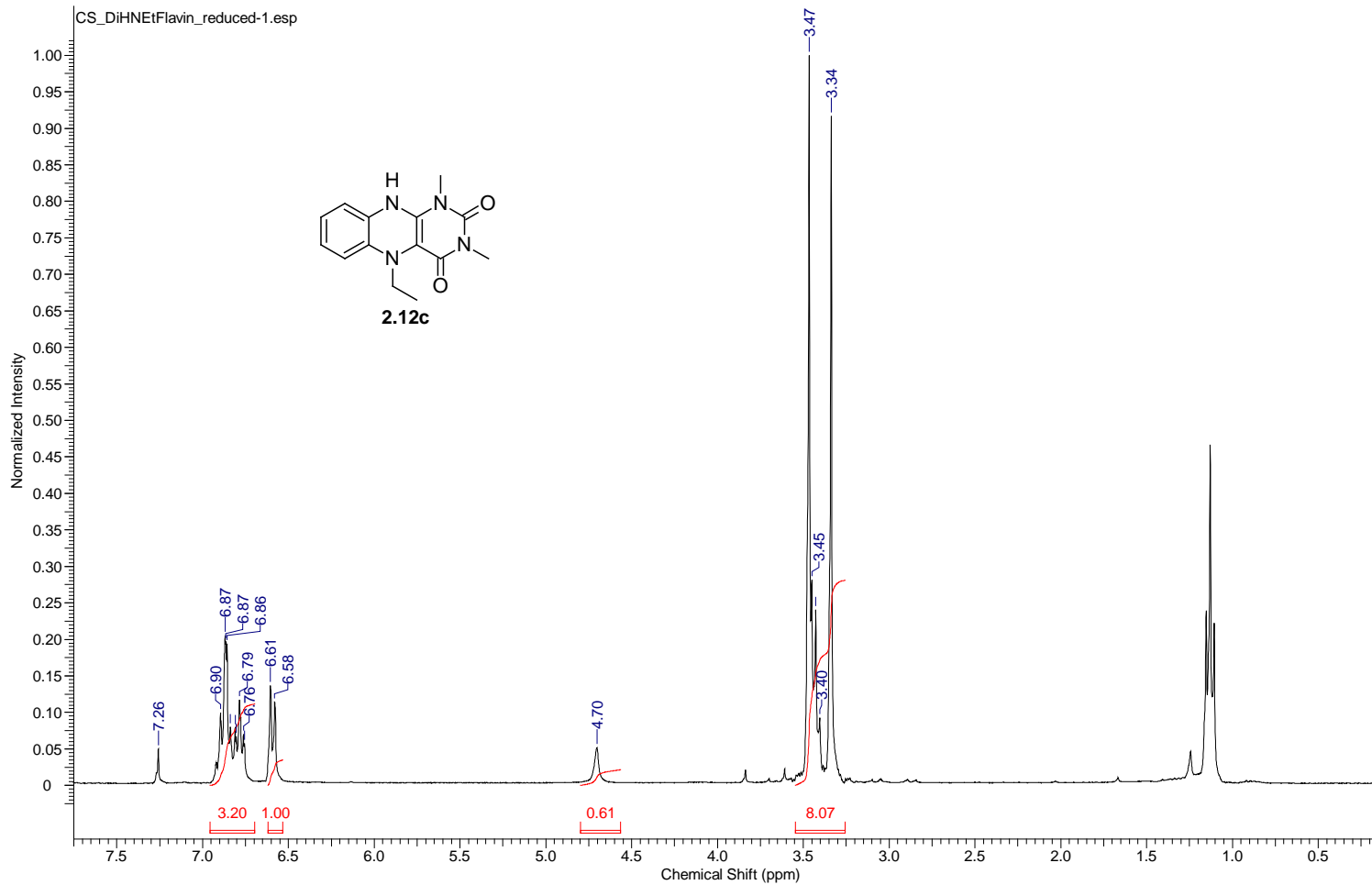
Acquisition Time (sec)	1.7459	Comment	single_pulse	Date	22 Nov 2011 09:21:58
Date Stamp	23 Nov 2011 02:18:12	File Name	C:\Users\chen\Desktop\DakinNMR\NMR PDF\DF\CS_DIFNEflavin_good-5.jdf		
Frequency (MHz)	500.16	Nucleus	1H	Number of Transients	16
Original Points Count	16384	Owner	delta	Points Count	16384
Receiver Gain	56.00	Solvent	CHLOROFORM-d	Pulse Sequence	single_pulse.ex2
Spectrum Type	STANDARD	Sweep Width (Hz)	9384.38	Temperature (degree C)	22.000



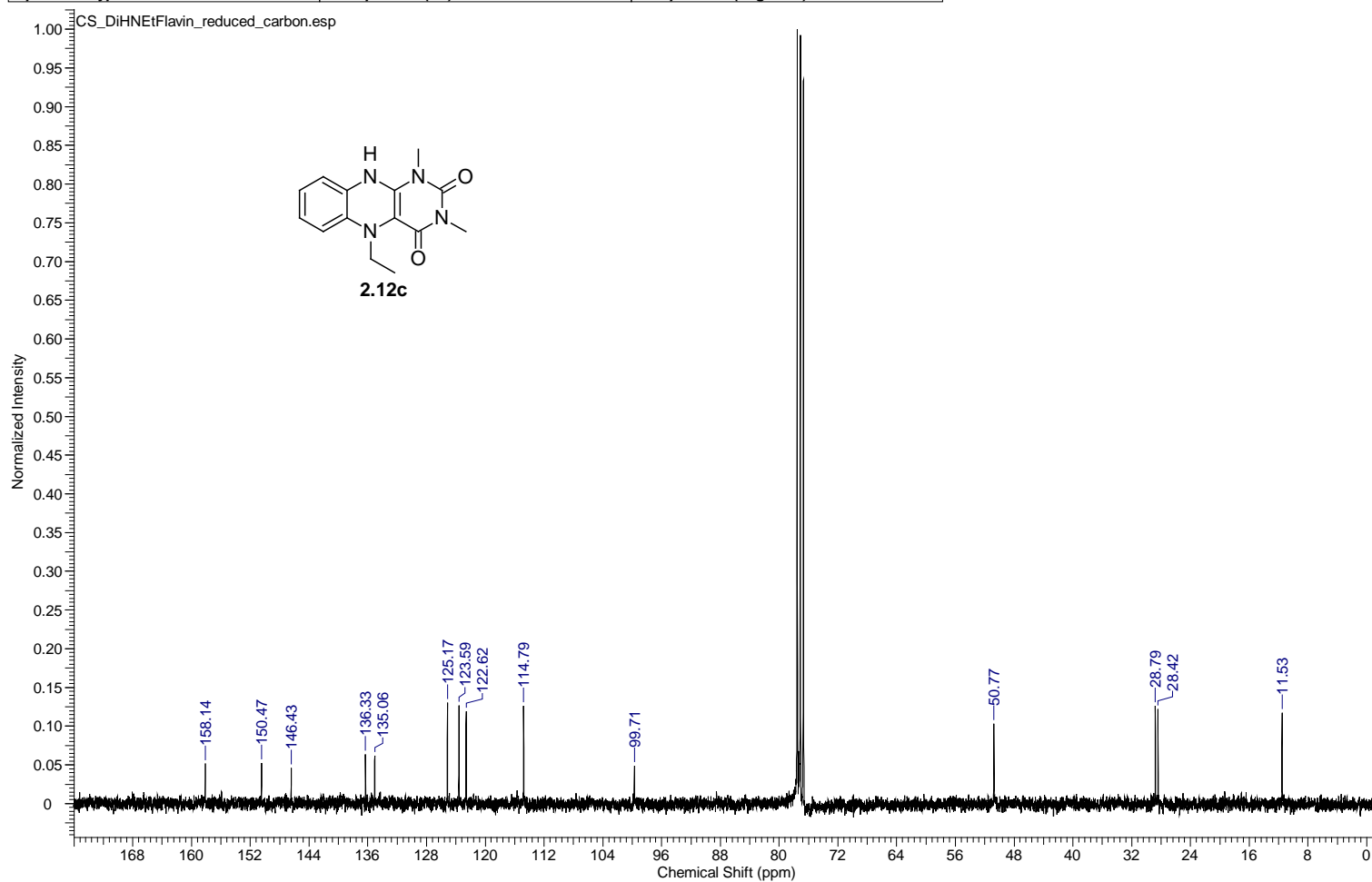
Acquisition Time (sec)	0.2307	Comment	single_pulse	Date	07 Dec 2011 11:35:52
Date Stamp	07 Dec 2011 11:07:56				
File Name	C:\Users\chen\Desktop\DakinNMR\NMR PDF\DiF\Florine\CS_DifNEtFlavin_reduced_F-1.jdf			Frequency (MHz)	282.78
Nucleus	19F	Number of Transients	196	Origin	ECX 300
Owner	delta	Points Count	32768	Pulse Sequence	single_pulse.ex2
Solvent	CHLOROFORM-d			Spectrum Offset (Hz)	0.0000
Sweep Width (Hz)	142045.45	Temperature (degree C)	26.000	Spectrum Type	STANDARD



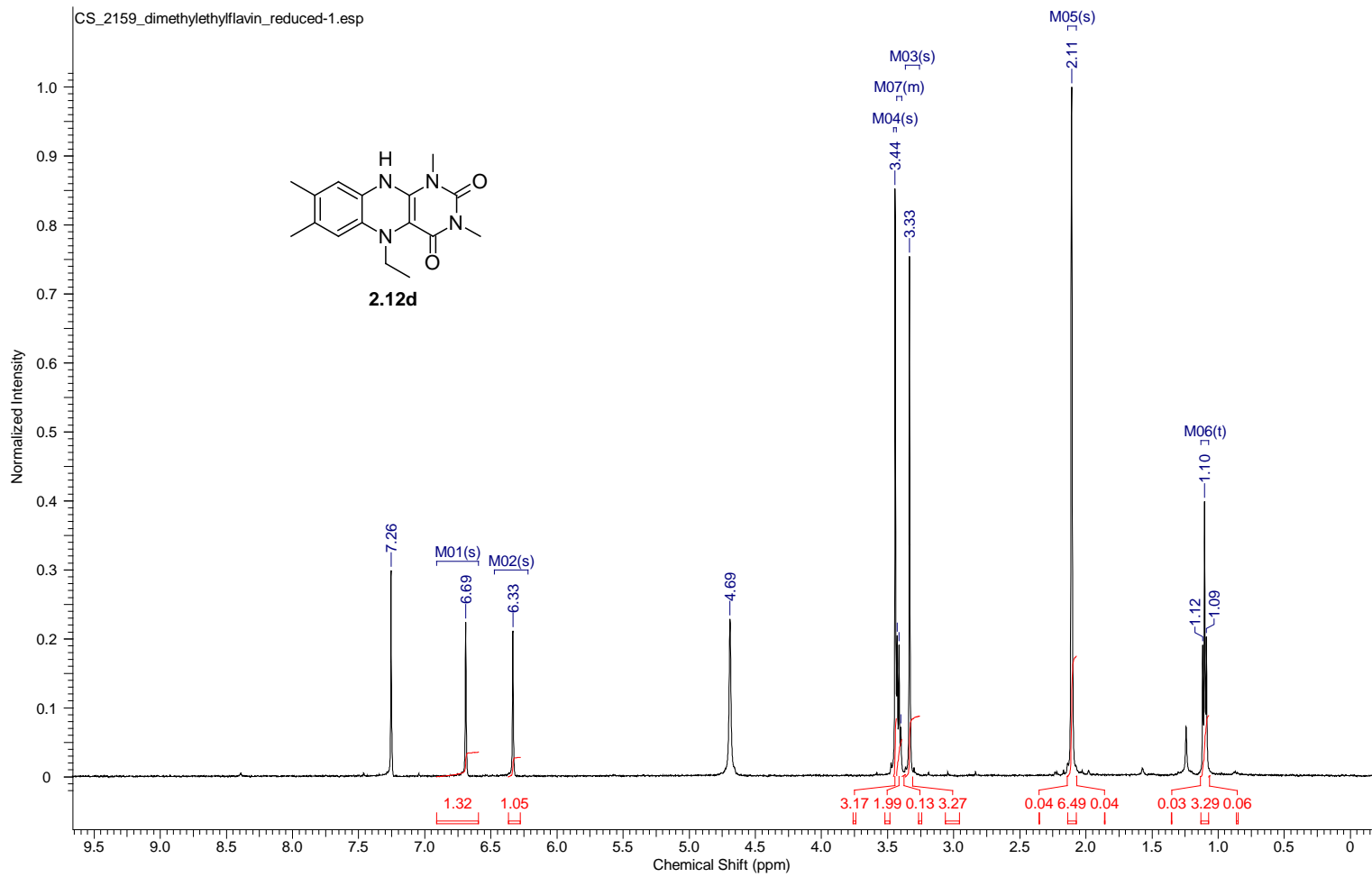
Acquisition Time (sec)	2.9072	Comment	single_pulse	Date	05 Nov 2011 12:38:42
Date Stamp	05 Nov 2011 11:25:43	File Name	C:\Users\shen\Desktop\DakinNMR\CS_DiHNEtFlavin_reduced-1.jdf		
Frequency (MHz)	300.53	Nucleus	1H	Number of Transients	24
Original Points Count	16384	Owner	delta	Points Count	16384
Receiver Gain	46.00	Solvent	CHLOROFORM-d	Pulse Sequence	single_pulse.ex2
Spectrum Type	STANDARD	Sweep Width (Hz)	5635.71	Temperature (degree C)	22.400



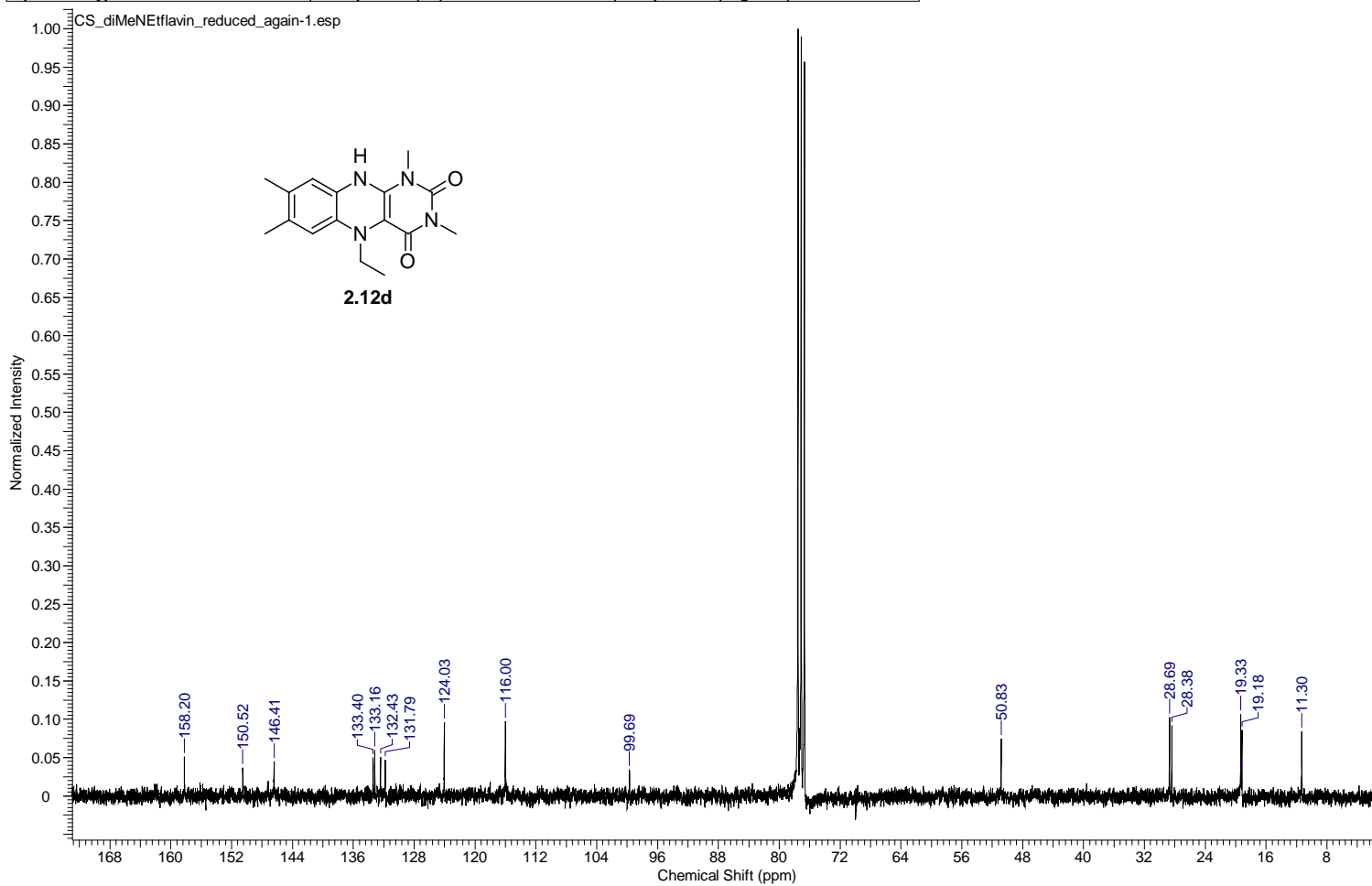
Acquisition Time (sec)	1.3841	Comment	single pulse decoupled gated NOE	Date	05 Nov 2011 14:47:18
Date Stamp	05 Nov 2011 13:34:18	File Name	C:\Users\chen\Desktop\DakinNMR\carbon\CS	DiHNEtFlavin_reduced_carbon.jdf	
Frequency (MHz)	75.57	Nucleus	13C	Number of Transients	3000
Original Points Count	32768	Owner	delta	Points Count	32768
Receiver Gain	50.00	Solvent	CHLOROFORM-d	Pulse Sequence	single_pulse_dec
Spectrum Type	STANDARD	Sweep Width (Hz)	23674.24	Temperature (degree C)	22.500



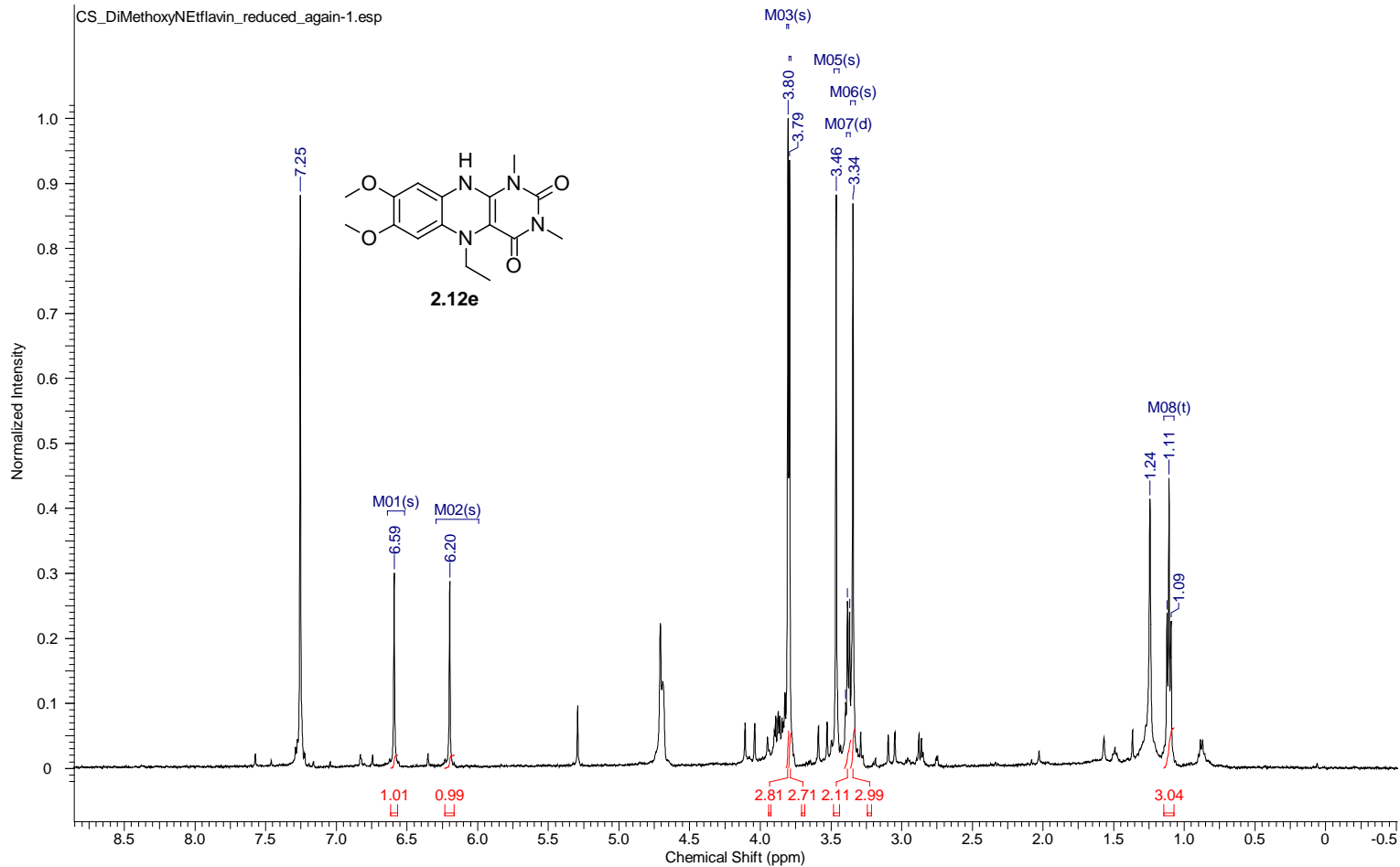
Acquisition Time (sec)	1.7459	Comment	single_pulse	Date	17 Sep 2011 12:27:59
Date Stamp	18 Sep 2011 04:40:32	File Name	C:\Users\ichen\Desktop\DakinNMR\CS_2159_dimethylethylflavin_reduced-1.jdf		
Frequency (MHz)	500.16	Nucleus	1H	Origin	ECA 500
Original Points Count	16384	Owner	delta	Points Count	16384
Receiver Gain	54.00	Solvent	CHLOROFORM-d	Pulse Sequence	single_pulse.ex2
Spectrum Type	STANDARD	Sweep Width (Hz)	9384.38	Spectrum Offset (Hz)	2500.7996
		Temperature (degree C)	22.000		



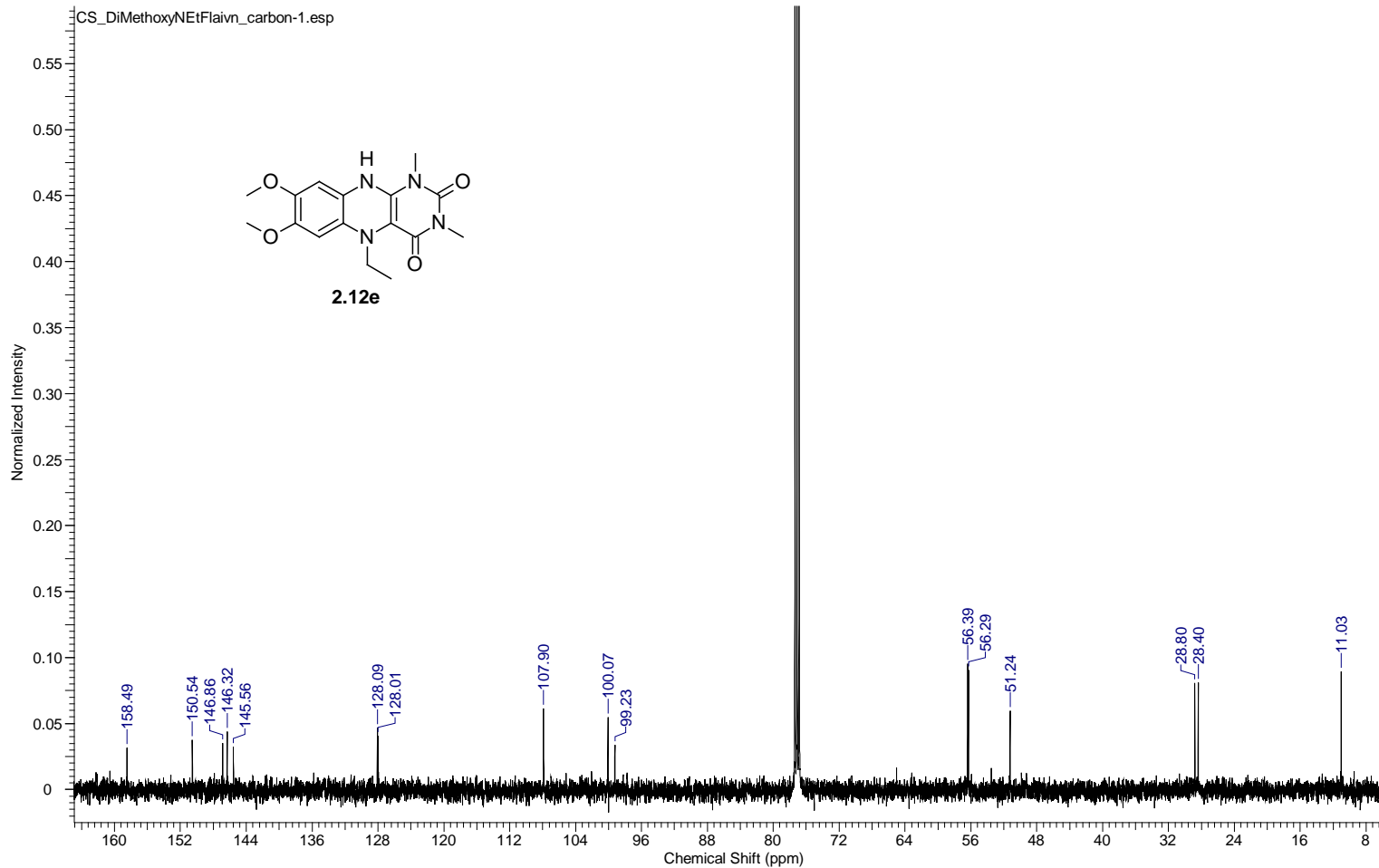
Acquisition Time (sec)	1.3841	Comment	single pulse decoupled gated NOE	Date	06 Nov 2011 10:36:31
Date Stamp	06 Nov 2011 10:09:01	File Name	F:\Dakin NMR\carbon\CS_diMeNEtflavin_reduced_again-1.jdf	Number of Transients	3000
Frequency (MHz)	75.57	Nucleus	13C	Origin	ECX 300
Original Points Count	32768	Owner	delta	Points Count	32768
Receiver Gain	50.00	Solvent	CHLOROFORM-d	Pulse Sequence	single_pulse_dec
Spectrum Type	STANDARD	Sweep Width (Hz)	23674.24	Spectrum Offset (Hz)	7556.8232
		Temperature (degree C)	22.100		



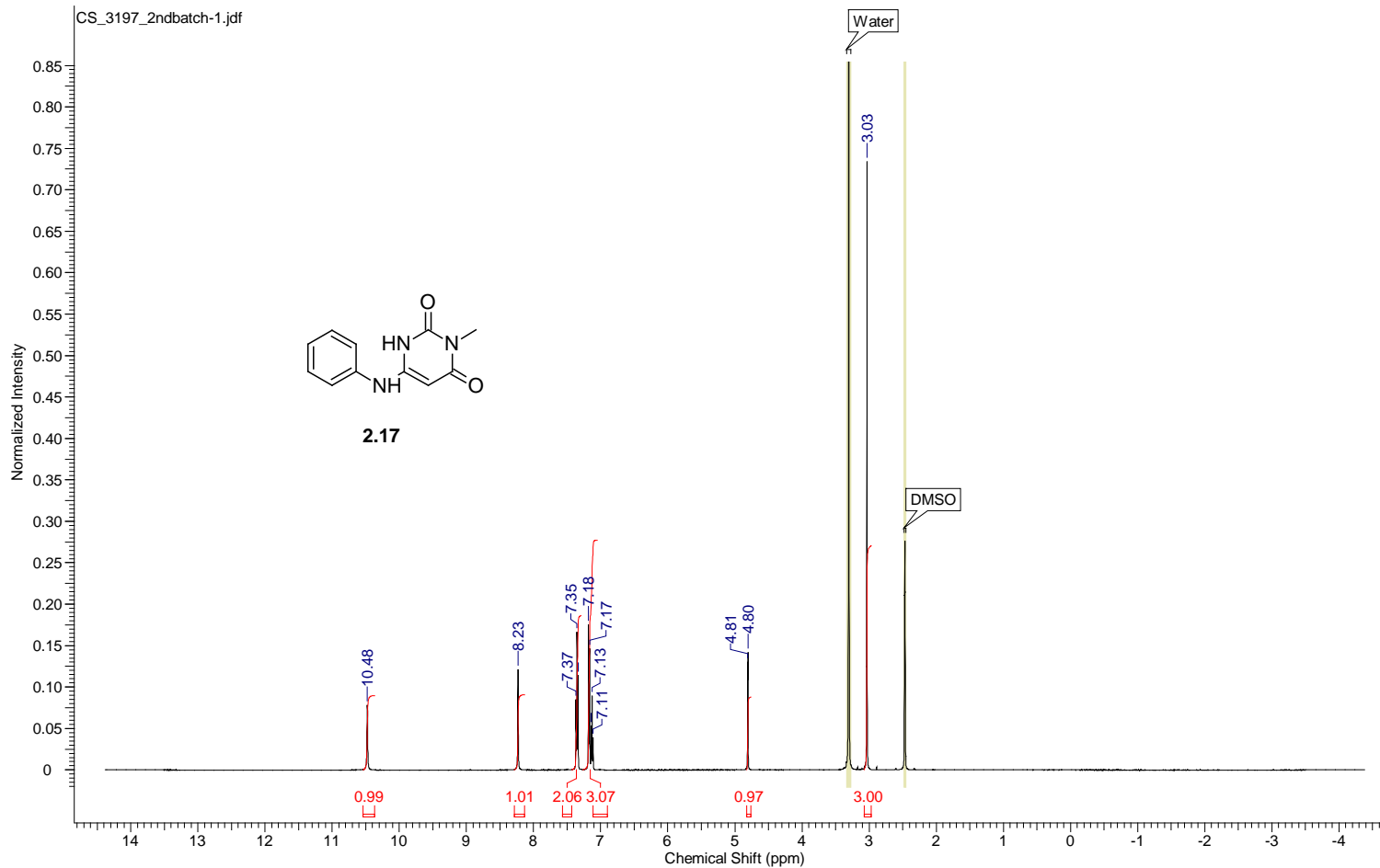
Acquisition Time (sec)	1.7459	Comment	single_pulse	Date	01 Dec 2011 12:32:08
Date Stamp	02 Dec 2011 05:28:25				
File Name	C:\Users\chen\Desktop\DakinNMR\NMR PDF\DiMeO\CS_DiMethoxyNEtflavin_reduced_again-1.jdf			Frequency (MHz)	500.16
Nucleus	1H	Number of Transients	9	Origin	ECA 500
Owner	delta	Points Count	16384	Pulse Sequence	single_pulse.ex2
Solvent	CHLOROFORM-d	Spectrum Offset (Hz)	2500.7996	Receiver Gain	56.00
Sweep Width (Hz)	9384.38	Temperature (degree C)	21.900	Spectrum Type	STANDARD



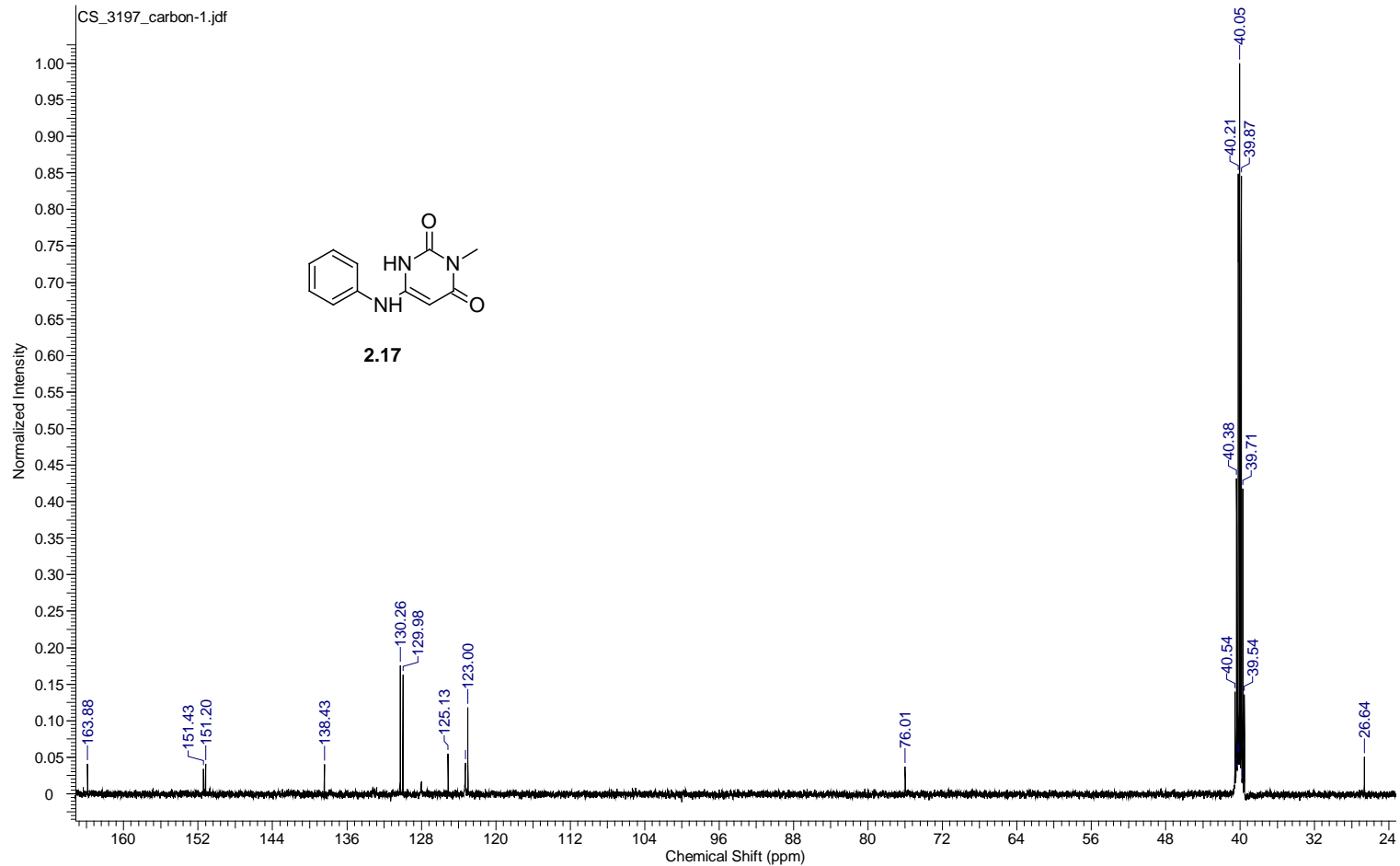
Acquisition Time (sec)	0.8336	Comment	single pulse decoupled gated NOE	Date	28 Nov 2011 16:55:19
Date Stamp	29 Nov 2011 09:51:35				
File Name	C:\Users\chen\Desktop\DakinNMR\NMR PDF\DiMeO\CS_DiMethoxyNEtFlaivn_carbon-1.jdf			Frequency (MHz)	125.77
Nucleus	13C	Number of Transients	390	Origin	ECA 500
Owner	delta	Points Count	32768	Pulse Sequence	single_pulse_dec
Solvent	CHLOROFORM-d	Spectrum Offset (Hz)	12576.5293	Spectrum Type	STANDARD
Temperature (degree C)	22.200			Receiver Gain	50.00
				Sweep Width (Hz)	39308.18



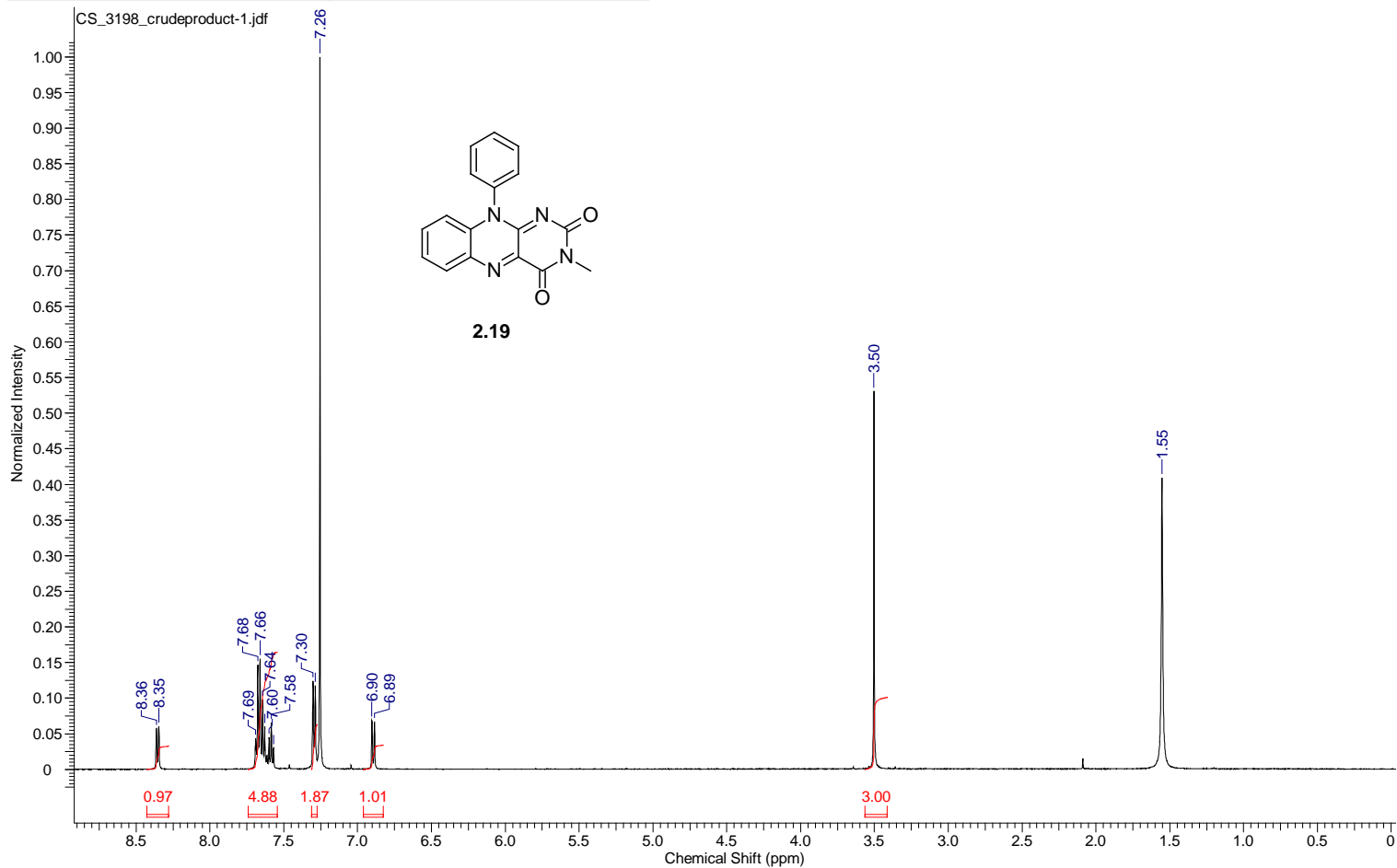
Acquisition Time (sec)	1.7459	Comment	single_pulse	Date	15 May 2012 08:49:43
Date Stamp	16 May 2012 01:06:18				
File Name	C:\Users\chen\Desktop\study\Foss\Shuai's Data\NMR DATA\500MHz\051012\aaaron\proton\CS_3197_2ndbatch-1.jdf				
Frequency (MHz)	500.16	Nucleus	1H	Number of Transients	16
Original Points Count	16384	Owner	delta	Points Count	16384
Receiver Gain	46.00	Solvent	DMSO-d6	Spectrum Offset (Hz)	2500.7996
Sweep Width (Hz)	9384.38	Temperature (degree C)	22.000	Spectrum Type	STANDARD



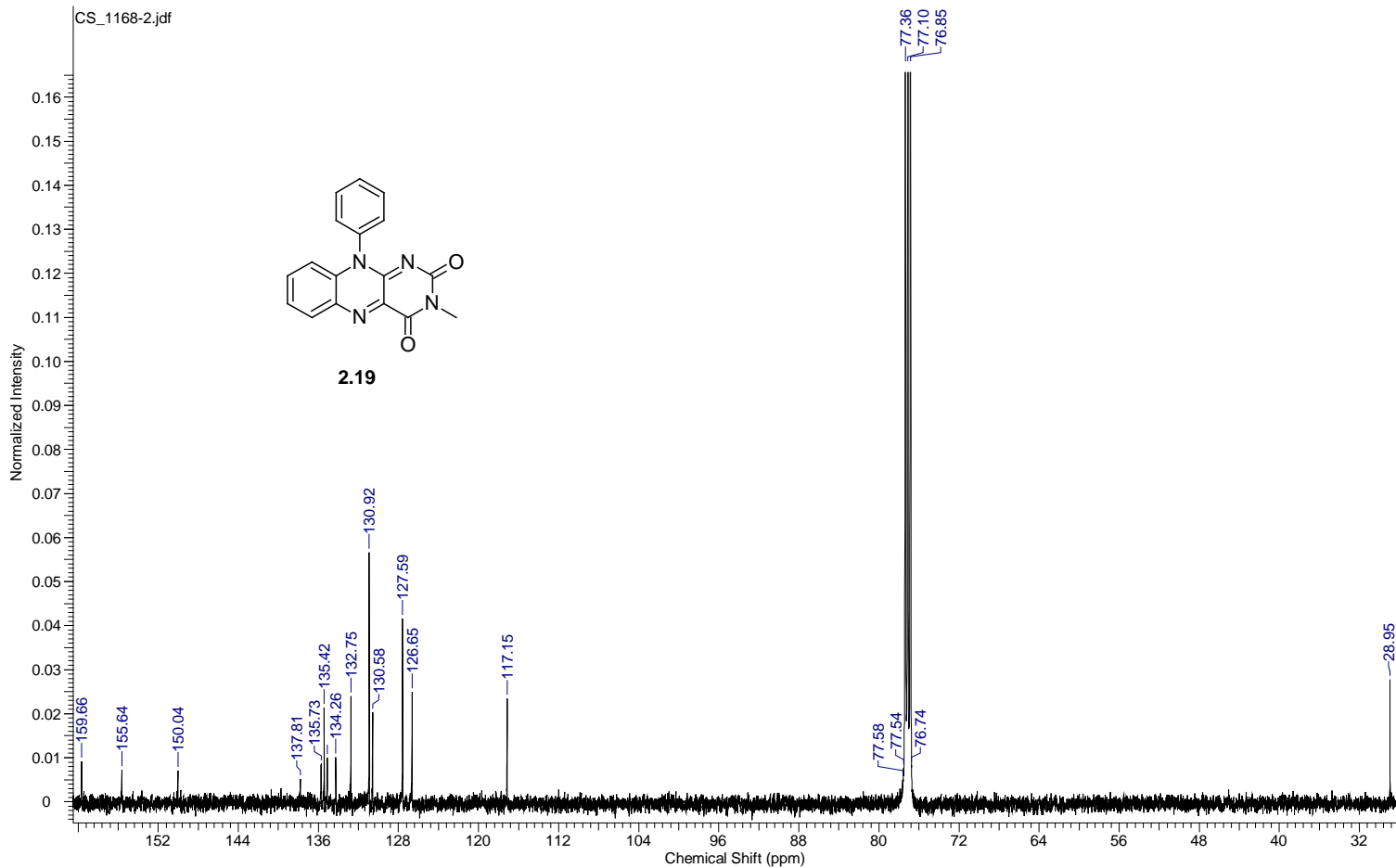
Acquisition Time (sec)	0.8336	Comment	single pulse decoupled gated NOE		Date	14 May 2012 09:01:18	
Date Stamp	15 May 2012 01:17:52						
File Name	C:\Users\chen\Desktop\study\Foss\Shuai's Data\NMR DATA\500MHz051012\aaon\carbon\CS_3197_carbon-1.jdf			Frequency (MHz)	125.77		
Nucleus	¹³ C	Number of Transients	120	Origin	ECA 500	Original Points Count	32768
Owner	delta	Points Count	32768	Pulse Sequence	single_pulse_dec	Receiver Gain	50.00
Solvent	DMSO-d6	Spectrum Offset (Hz)	12576.5293	Spectrum Type	STANDARD	Sweep Width (Hz)	39308.18
Temperature (degree C)	22.600						



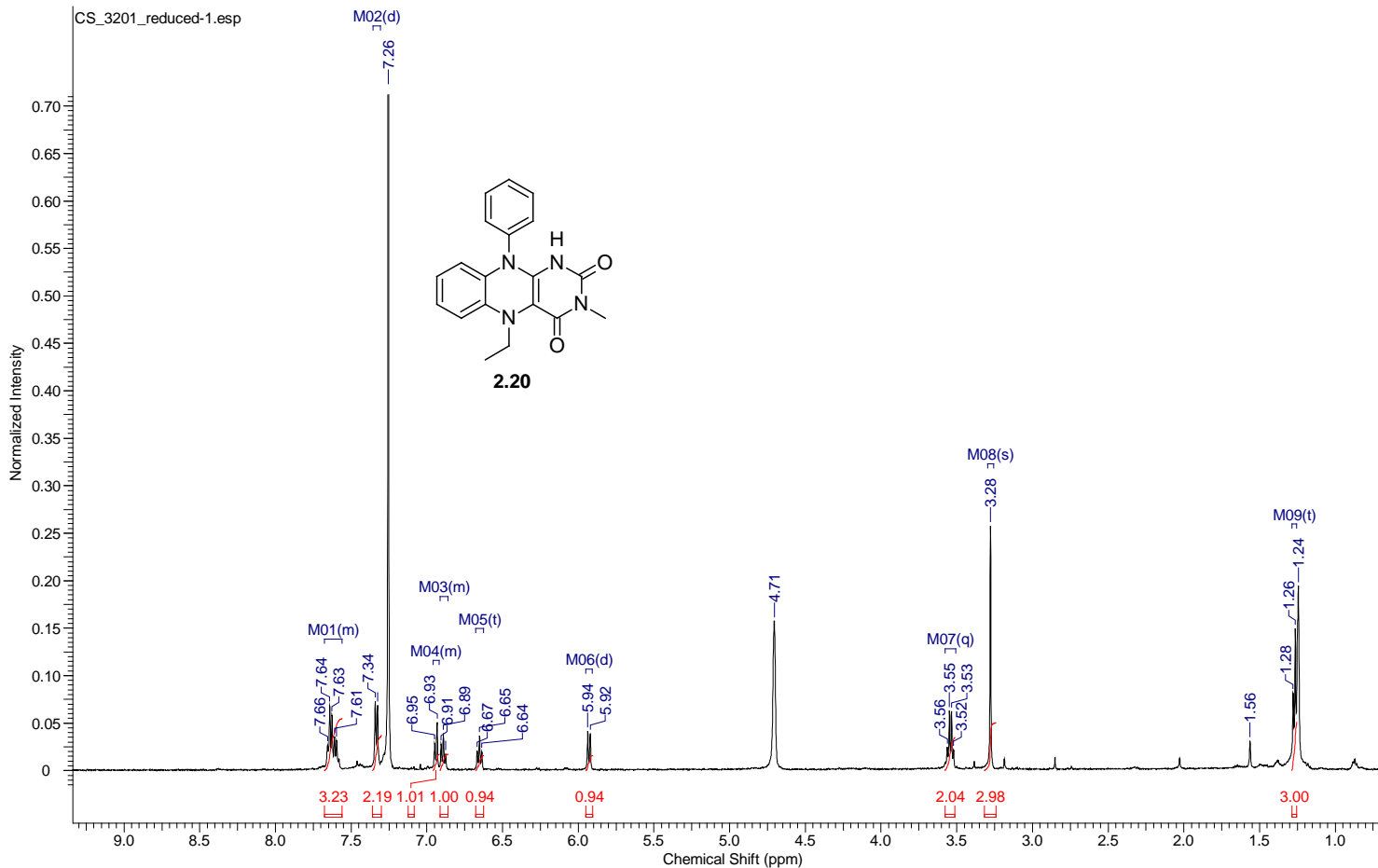
Acquisition Time (sec)	1.7459	Comment	single_pulse	Date	15 May 2012 12:06:10
Date Stamp	16 May 2012 04:22:45				
File Name	C:\Users\chen\Desktop\study\Foss\Shuai's Data\NMR DATA\500MHz\051012\aaaron\proton\CS_3198_crudeproduct-1.jdf				
Frequency (MHz)	500.16	Nucleus	¹ H	Number of Transients	13
Original Points Count	16384	Owner	delta	Points Count	16384
Receiver Gain	54.00	Solvent	CHLOROFORM-d	Spectrum Offset (Hz)	2500.7996
Sweep Width (Hz)	9384.38	Temperature (degree C)	22.200	Spectrum Type	STANDARD



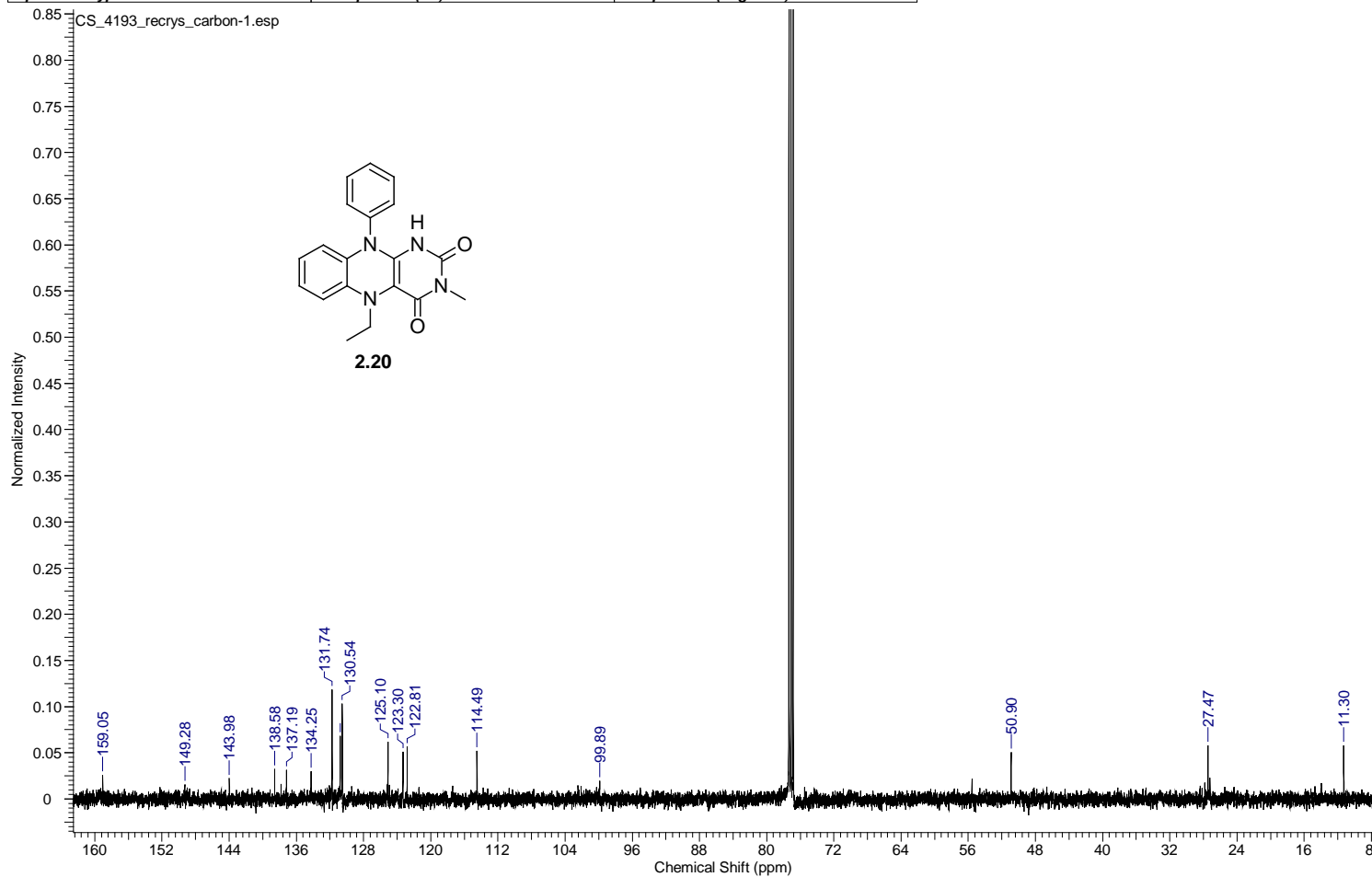
Acquisition Time (sec)	0.8336	Comment	single pulse decoupled gated NOE	Date	05 Nov 2010 01:17:07
Date Stamp	05 Nov 2010 11:51:28				
File Name	C:\Users\chen\Desktop\study\Foss\Shuai's Data\NMR DATA\NMR 12 28 2010\500mhz110810\aaaron\carbon\CS_1168-2.jdf				
Frequency (MHz)	125.77	Nucleus	¹³ C	Number of Transients	5000
Original Points Count	32768	Owner	delta	Points Count	32768
Receiver Gain	50.00	Solvent	CHLOROFORM-d	Spectrum Offset (Hz)	12576.5293
Sweep Width (Hz)	39308.18	Temperature (degree C)	22.400	Spectrum Type	STANDARD



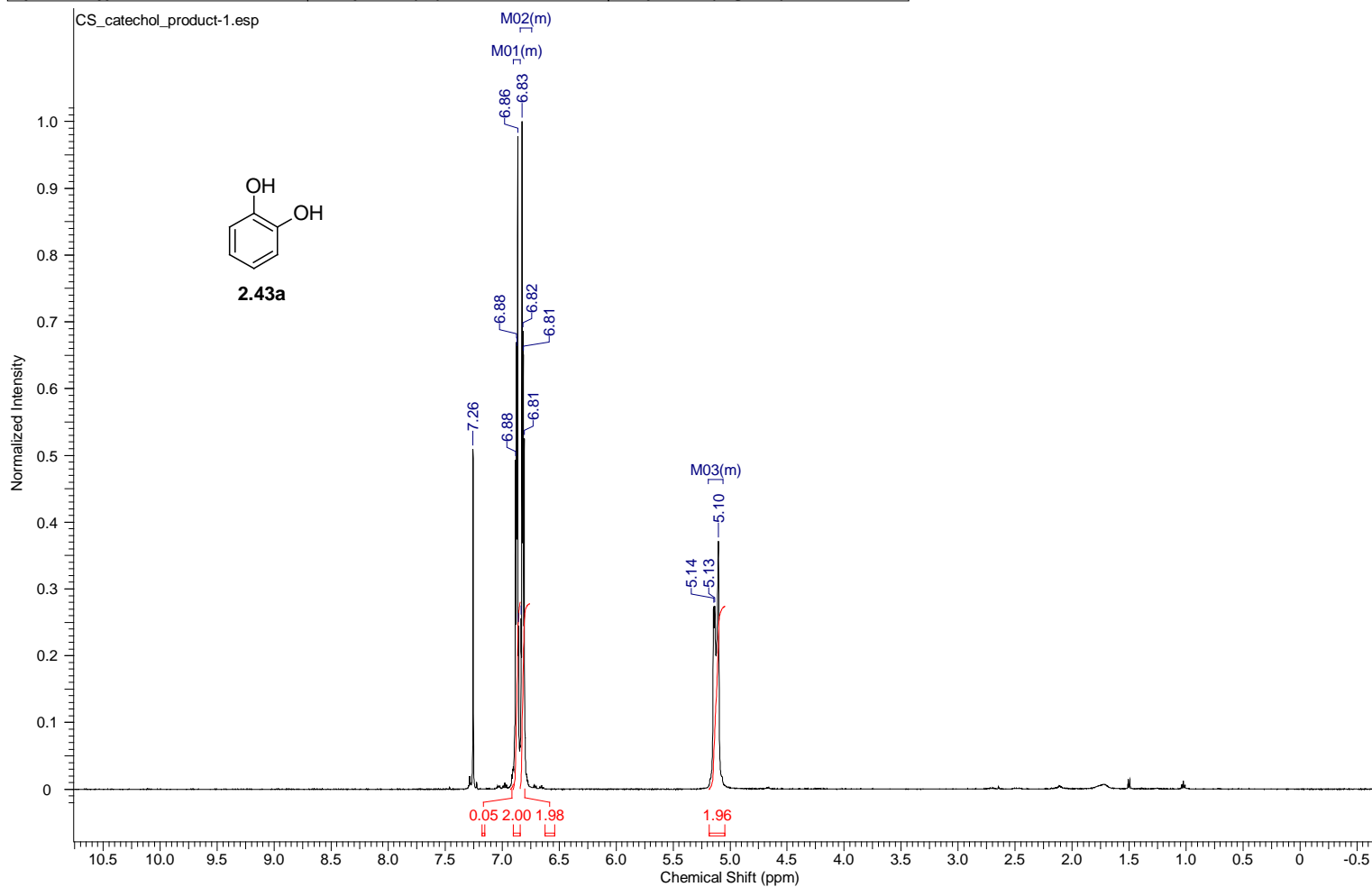
Acquisition Time (sec)	1.7459	Comment	single_pulse	Date	19 May 2012 11:54:31
Date Stamp	20 May 2012 04:11:08				
File Name	C:\Users\chen\Desktop\study\Foss\Shuai's Data\NMR DATA\500MHz\051012\aaaron\proton\CS_3201_reduced-1.jdf				
Frequency (MHz)	500.16	Nucleus	¹ H	Number of Transients	10
Original Points Count	16384	Owner	delta	Points Count	16384
Receiver Gain	56.00	Solvent	CHLOROFORM-d	Spectrum Offset (Hz)	2500.7996
Sweep Width (Hz)	9384.38	Temperature (degree C)	22.000	Spectrum Type	STANDARD



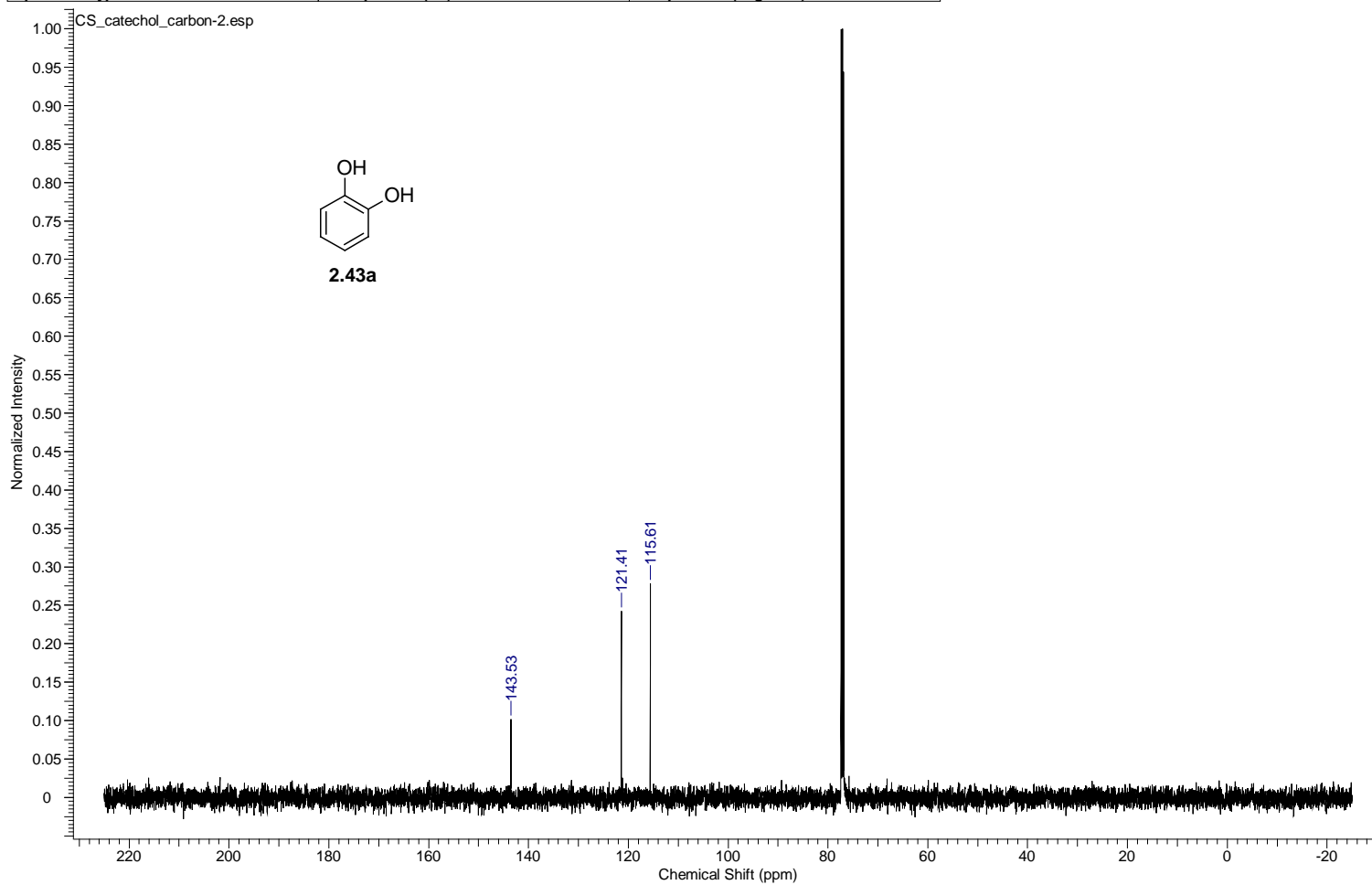
Acquisition Time (sec)	0.8336	Comment	single pulse decoupled gated NOE	Date	23 Oct 2012 07:58:01
Date Stamp	23 Oct 2012 18:11:24	File Name	G:\500MHz101512\laaron\carbon\CS_4193_recrys_carbon-1.jdf	Number of Transients	500
Frequency (MHz)	125.77	Nucleus	13C	Origin	ECA 500
Original Points Count	32768	Owner	delta	Points Count	32768
Receiver Gain	50.00	Solvent	CHLOROFORM-d	Pulse Sequence	single_pulse_dec
Spectrum Type	STANDARD	Sweep Width (Hz)	39308.18	Temperature (degree C)	23.000



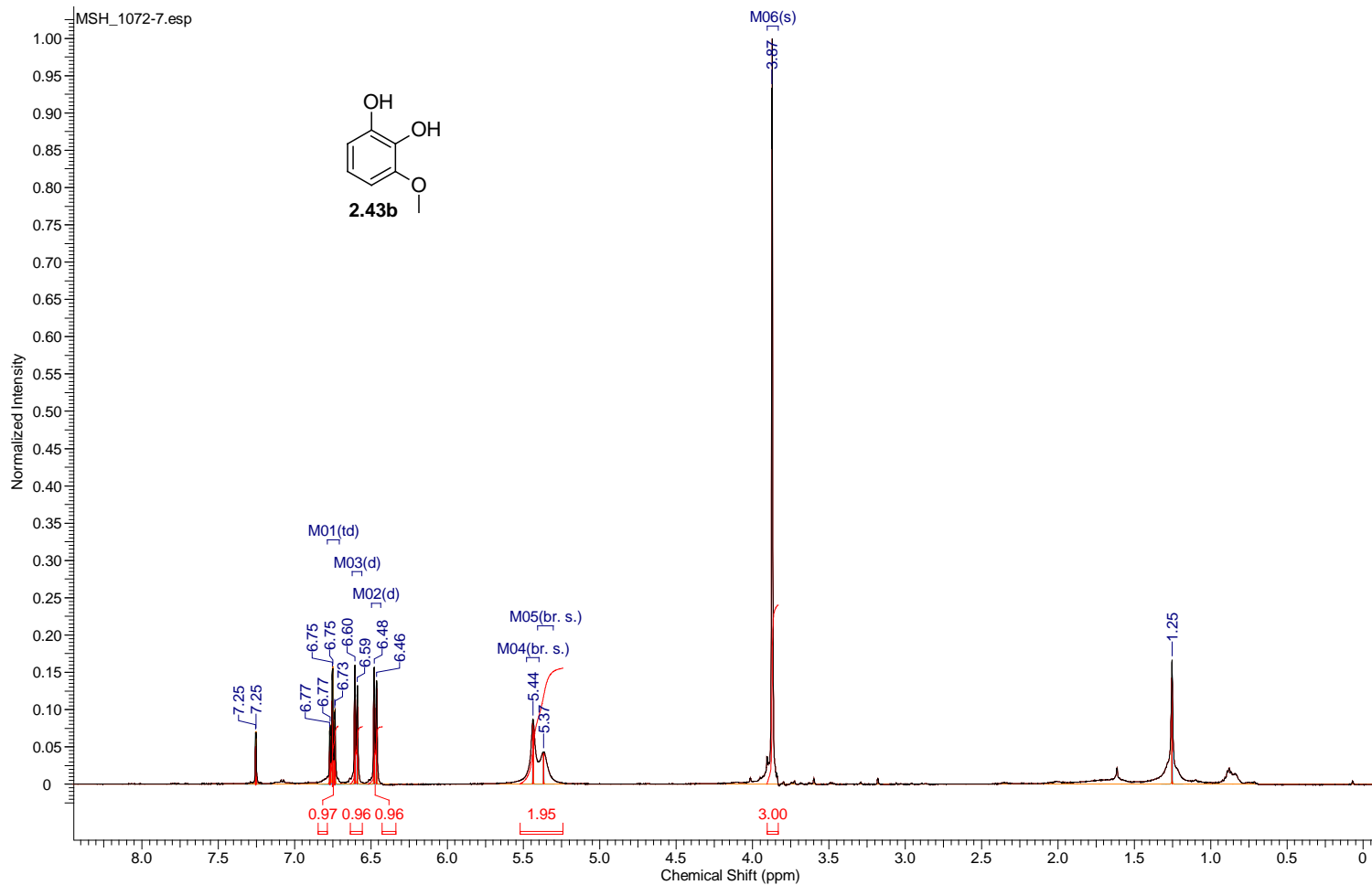
Acquisition Time (sec)	1.7459	Comment	single_pulse	Date	01 Dec 2011 09:01:22
Date Stamp	02 Dec 2011 01:57:39	File Name	C:\Users\chen\Desktop\DakinNMR\substrate study\CS_catechol_product-1.jdf		
Frequency (MHz)	500.16	Nucleus	1H	Number of Transients	4
Original Points Count	16384	Owner	delta	Points Count	16384
Receiver Gain	48.00	Solvent	CHLOROFORM-d	Pulse Sequence	single_pulse.ex2
Spectrum Type	STANDARD	Sweep Width (Hz)	9384.38	Temperature (degree C)	22.000



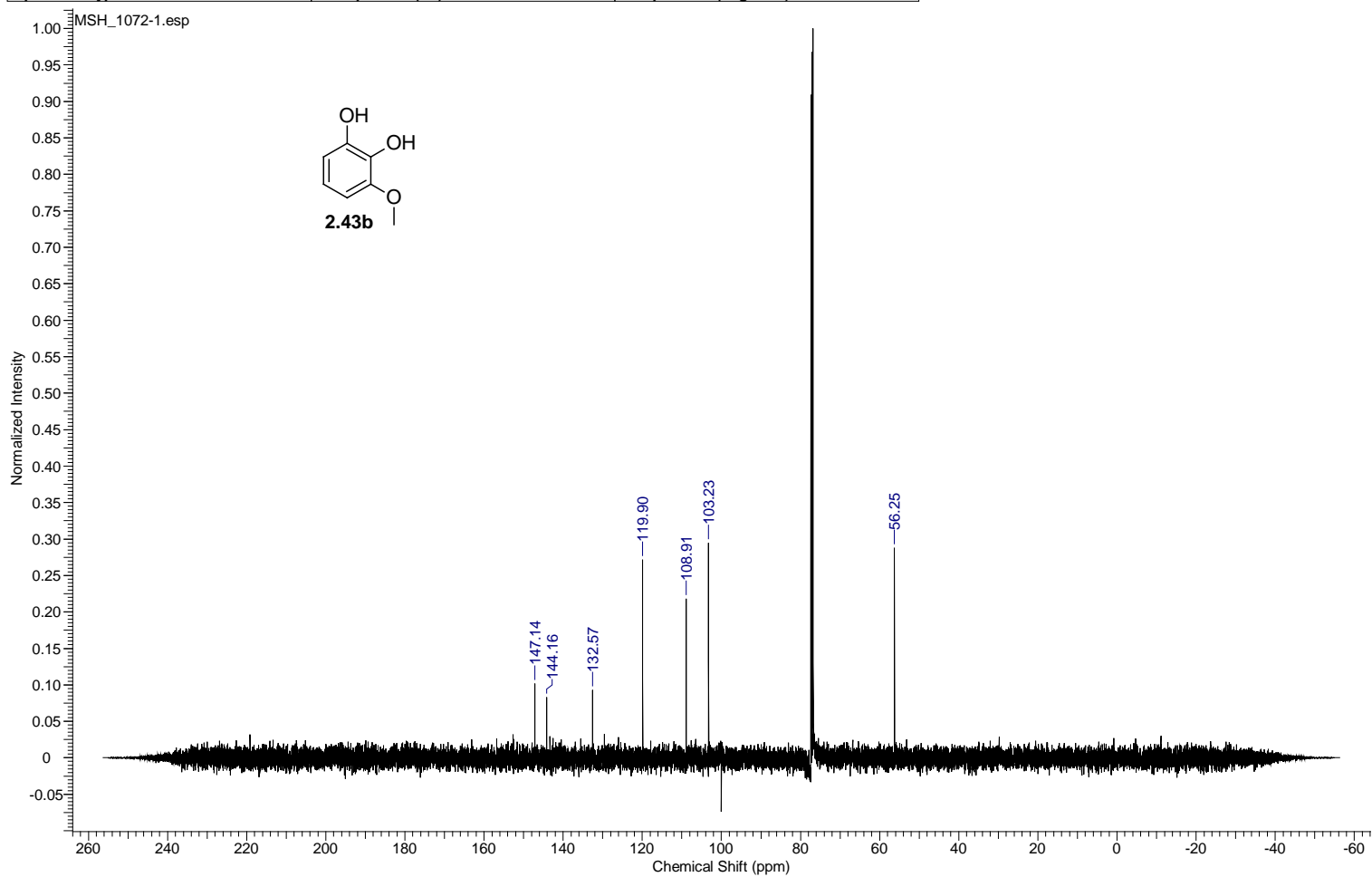
Acquisition Time (sec)	0.8336	Comment	single pulse decoupled gated NOE	Date	01 Dec 2011 09:02:41
Date Stamp	02 Dec 2011 01:58:57	File Name	C:\Users\chen\Desktop\DakinNMR\substrate study\CS_catechol_carbon-2.jdf		
Frequency (MHz)	125.77	Nucleus	13C	Number of Transients	30
Original Points Count	26214	Owner	delta	Points Count	26214
Receiver Gain	50.00	Solvent	CHLOROFORM-d	Pulse Sequence	single_pulse_dec
Spectrum Type	STANDARD	Sweep Width (Hz)	31444.86	Temperature (degree C)	22.300



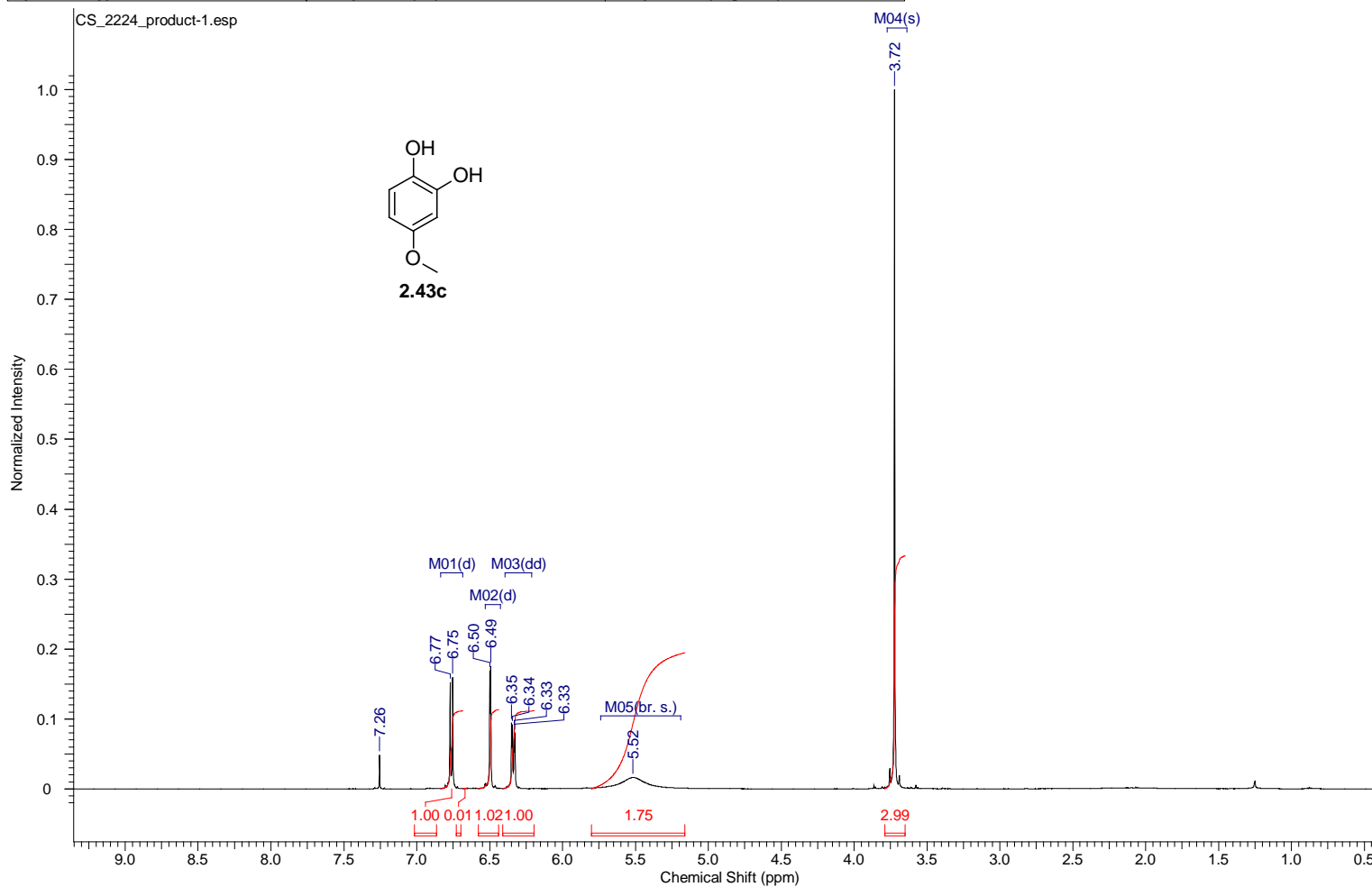
Acquisition Time (sec)	1.7460	Comment	single_pulse	Date	28 Oct 2011 11:19:01
Date Stamp	29 Oct 2011 03:28:44	File Name	C:\Users\chen\Desktop\DakinNMR\substrate study\MSH_1072-7.jdf		
Frequency (MHz)	500.16	Nucleus	1H	Number of Transients	4
Original Points Count	13107	Owner	delta	Points Count	13107
Receiver Gain	40.00	Solvent	CHLOROFORM-d	Pulse Sequence	single_pulse.ex2
Spectrum Type	STANDARD	Sweep Width (Hz)	7506.82	Temperature (degree C)	22.200



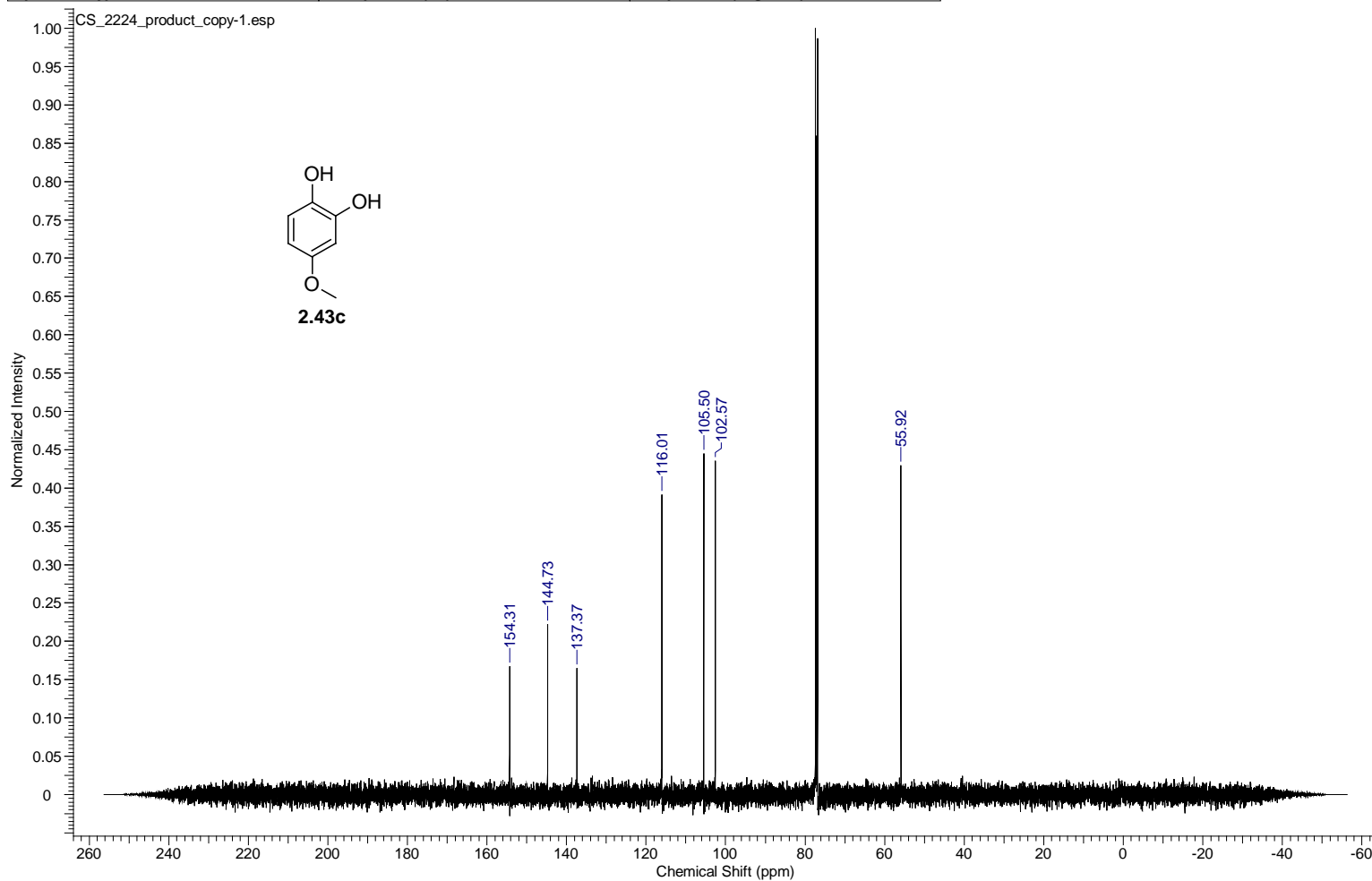
Acquisition Time (sec)	0.8336	Comment	single pulse decoupled gated NOE	Date	28 Oct 2011 11:19:55
Date Stamp	29 Oct 2011 03:30:29	File Name	C:\Users\chen\Desktop\DakinNMR\substrate study\MSH_1072-1.jdf		
Frequency (MHz)	125.77	Nucleus	13C	Number of Transients	40
Original Points Count	32768	Owner	delta	Points Count	32768
Receiver Gain	50.00	Solvent	CHLOROFORM-d	Pulse Sequence	single_pulse_dec
Spectrum Type	STANDARD	Sweep Width (Hz)	39308.18	Temperature (degree C)	22.500



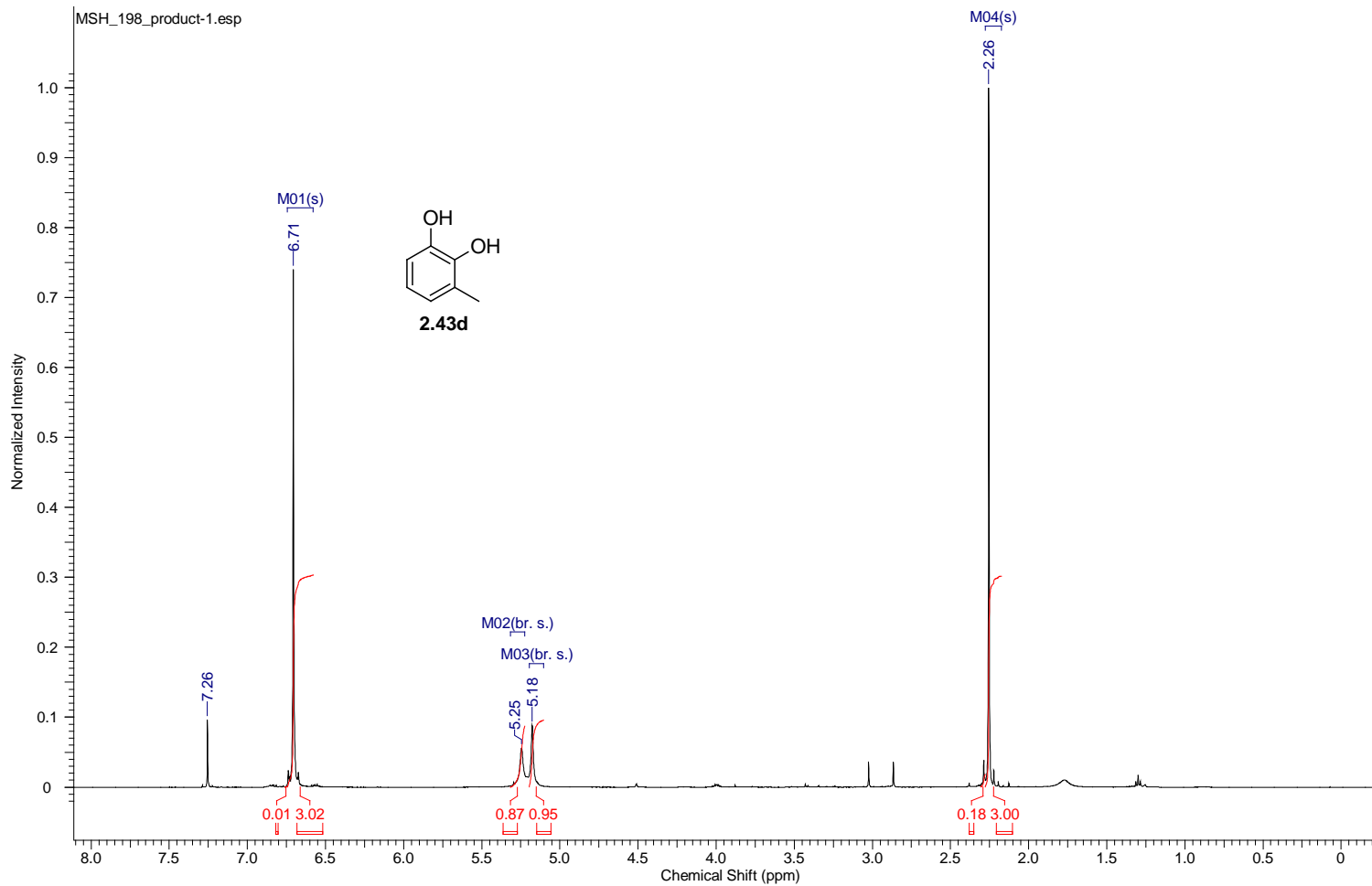
Acquisition Time (sec)	1.7459	Comment	single_pulse	Date	19 Nov 2011 12:01:09
Date Stamp	20 Nov 2011 04:57:22	File Name	C:\Users\chen\Desktop\DakinNMR\substrate study\CS_2224_product-1.jdf		
Frequency (MHz)	500.16	Nucleus	1H	Origin	ECA 500
Original Points Count	16384	Owner	delta	Points Count	16384
Receiver Gain	40.00	Solvent	CHLOROFORM-d	Pulse Sequence	single_pulse.ex2
Spectrum Type	STANDARD	Sweep Width (Hz)	9384.38	Temperature (degree C)	22.000



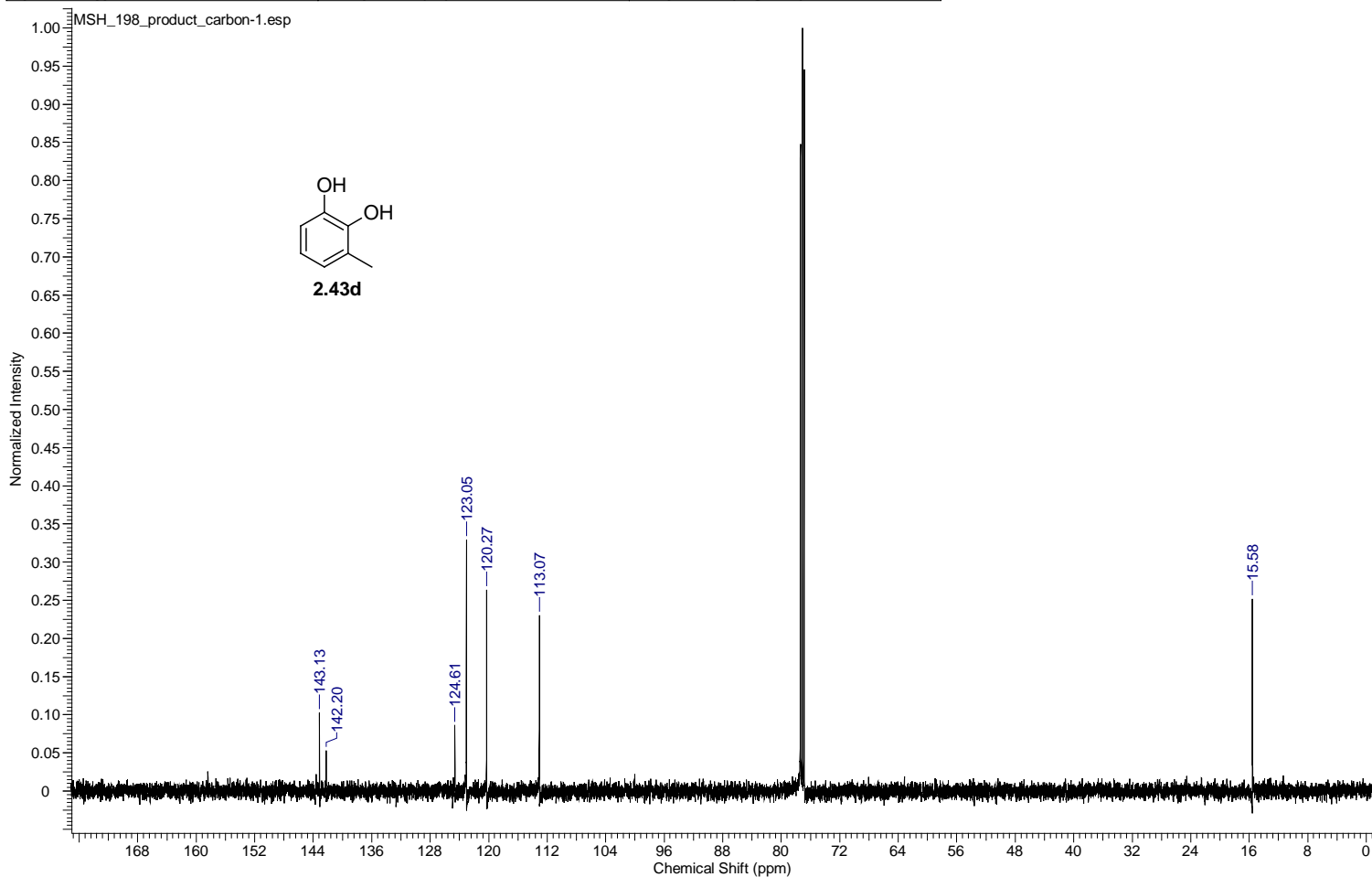
Acquisition Time (sec)	0.8336	Comment	single pulse decoupled gated NOE	Date	19 Nov 2011 12:03:24
Date Stamp	20 Nov 2011 04:59:37	File Name	C:\Users\chen\Desktop\DakinNMR\substrate study\CS_2224_product_copy-1.jdf		
Frequency (MHz)	125.77	Nucleus	13C	Number of Transients	50
Original Points Count	32768	Owner	delta	Points Count	32768
Receiver Gain	50.00	Solvent	CHLOROFORM-d	Pulse Sequence	single_pulse_dec
Spectrum Type	STANDARD	Sweep Width (Hz)	39308.18	Temperature (degree C)	22.400
				Spectrum Offset (Hz)	12576.5293



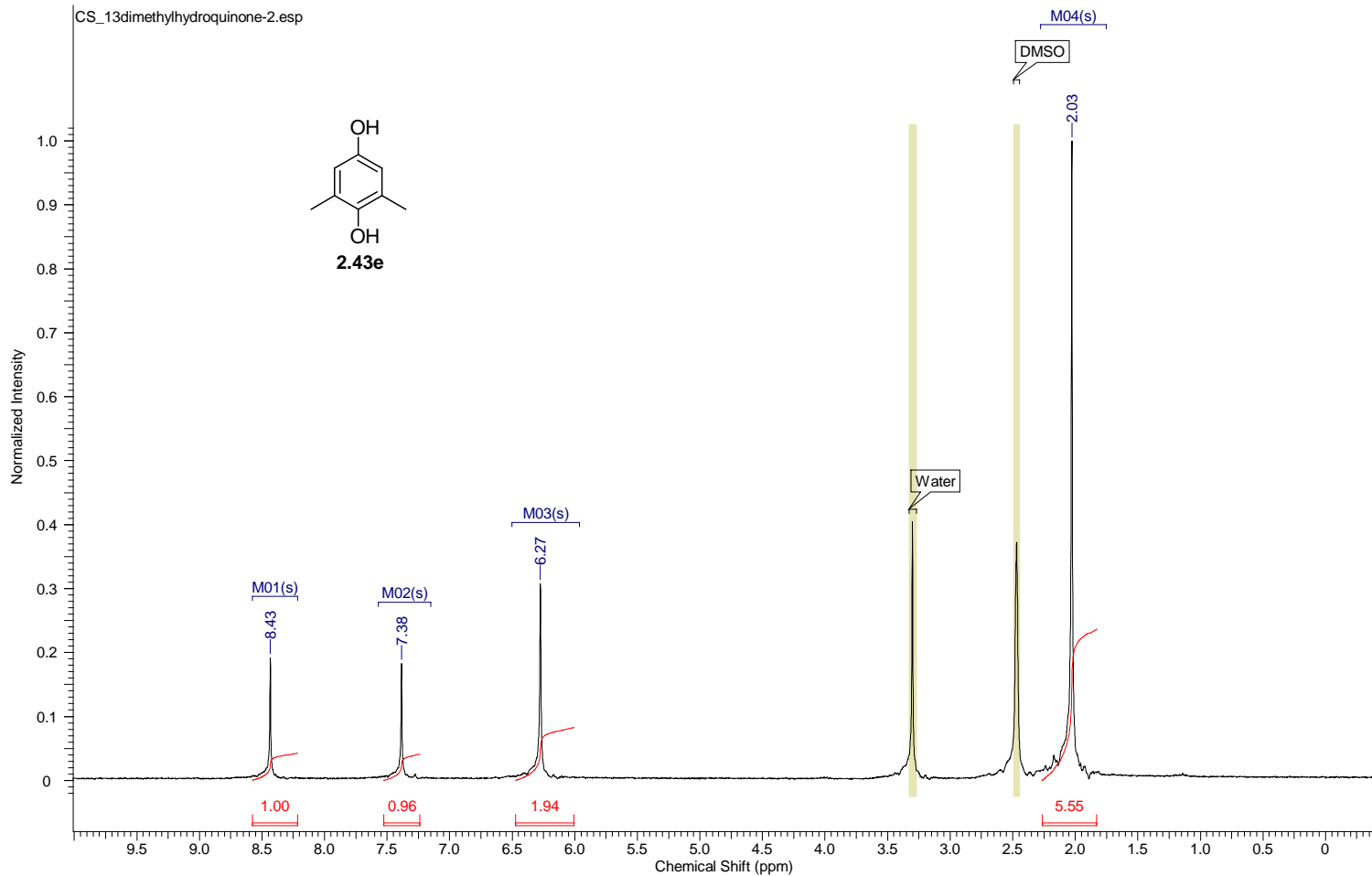
Acquisition Time (sec)	1.7459	Comment	single_pulse	Date	15 Dec 2011 11:11:23
Date Stamp	16 Dec 2011 04:09:21	File Name	C:\Users\chen\Desktop\DakinNMR\substrate study\MSH_198_product-1.jdf		
Frequency (MHz)	500.16	Nucleus	1H	Number of Transients	13
Original Points Count	16384	Owner	delta	Points Count	16384
Receiver Gain	44.00	Solvent	CHLOROFORM-d	Pulse Sequence	single_pulse.ex2
Spectrum Type	STANDARD	Sweep Width (Hz)	9384.38	Temperature (degree C)	22.300



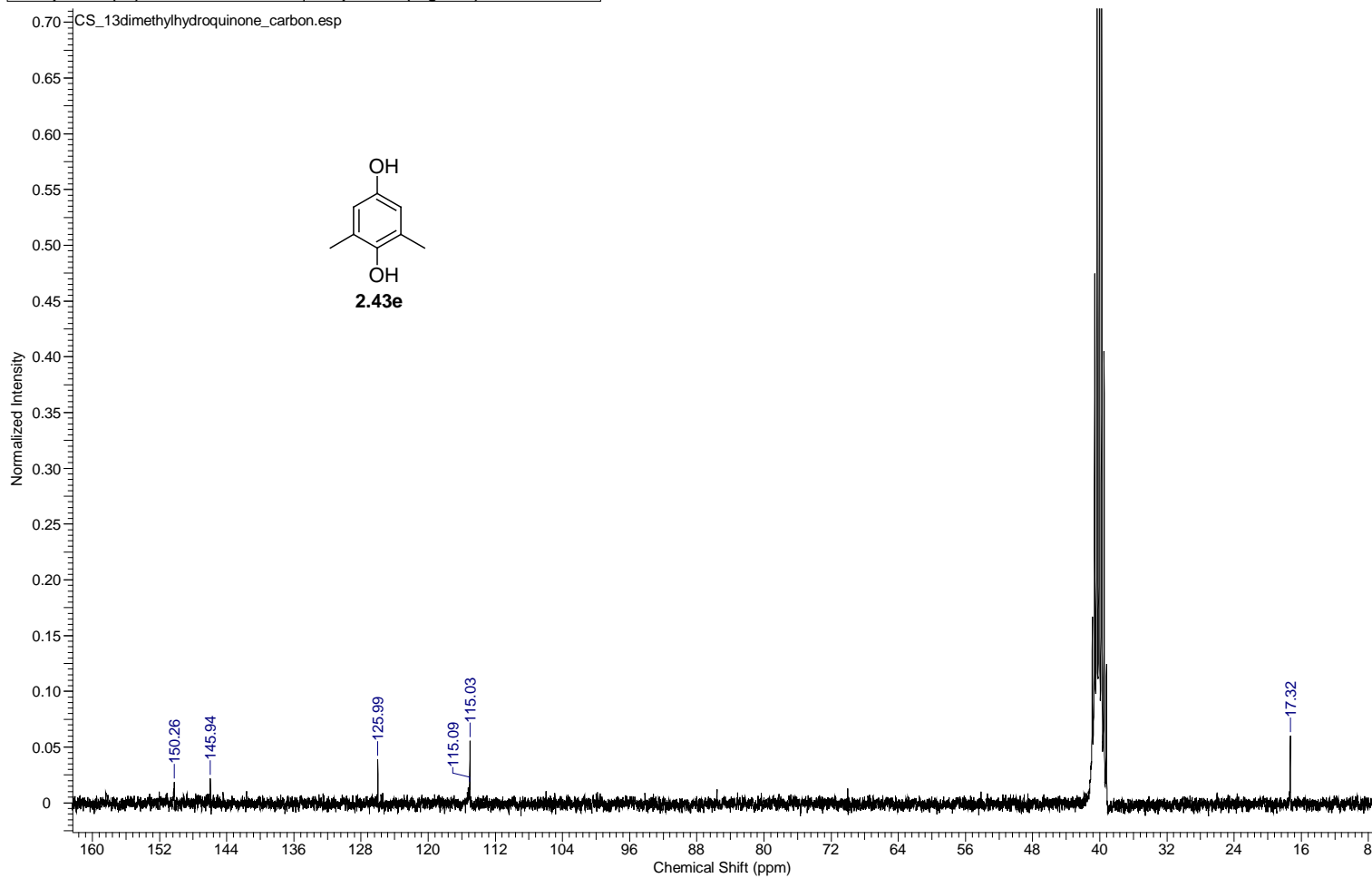
Acquisition Time (sec)	0.8336	Comment	single pulse decoupled gated NOE	Date	15 Dec 2011 11:09:28
Date Stamp	16 Dec 2011 04:07:26	File Name	C:\Users\chen\Desktop\DakinNMR\substrate study\MSH_198_product_carbon-1.jdf		
Frequency (MHz)	125.77	Nucleus	13C	Number of Transients	70
Original Points Count	32768	Owner	delta	Points Count	32768
Receiver Gain	50.00	Solvent	CHLOROFORM-d	Pulse Sequence	single_pulse_dec
Spectrum Type	STANDARD	Sweep Width (Hz)	39308.18	Temperature (degree C)	22.600



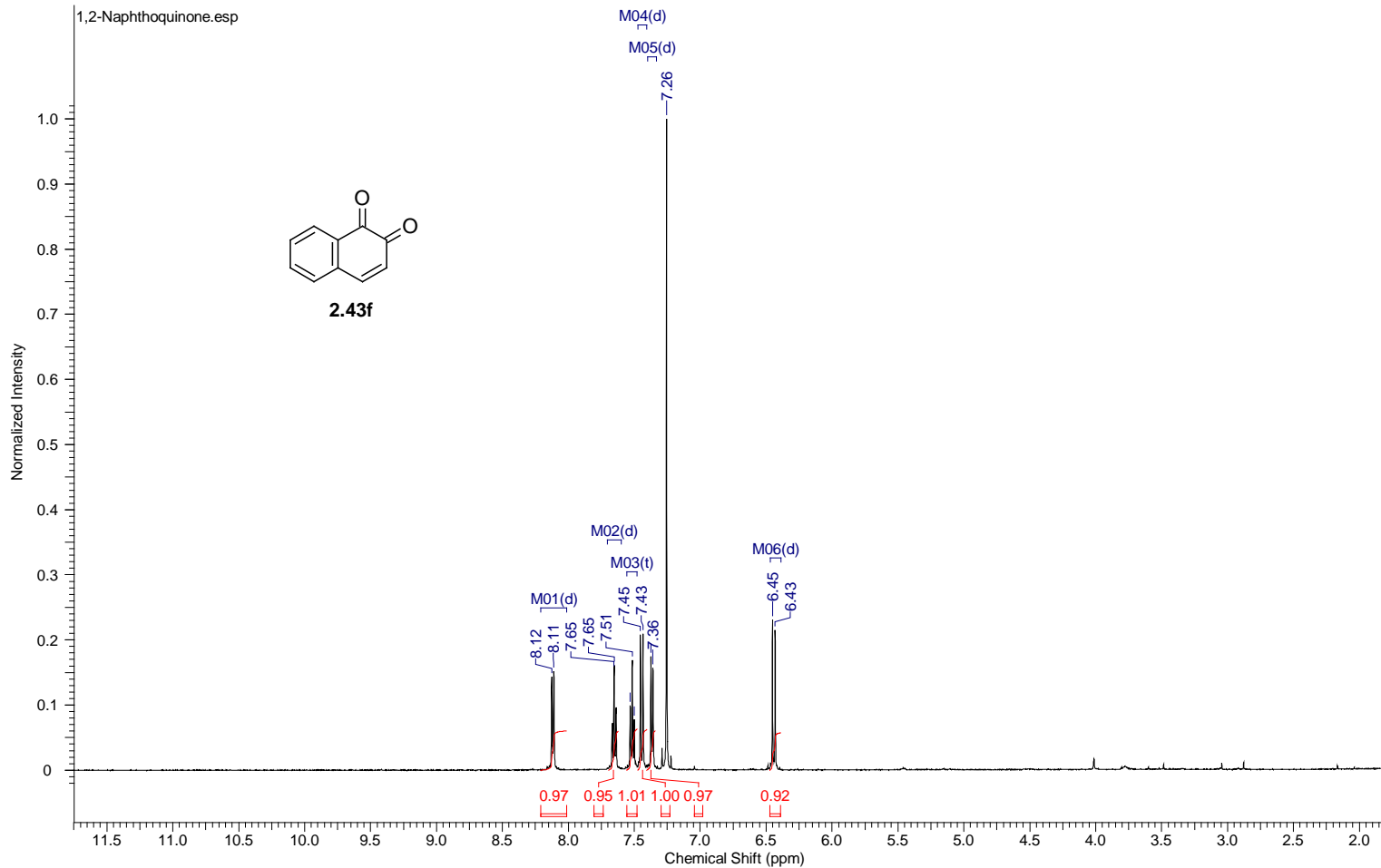
Acquisition Time (sec)	2.9072	Comment	single_pulse	Date	13 Dec 2011 16:46:58
Date Stamp	13 Dec 2011 16:18:57	File Name	F:\Dakin NMR\substract\CS_13dimethylhydroquinone-2.jdf		
Frequency (MHz)	300.53	Nucleus	1H	Number of Transients	4
Original Points Count	16384	Owner	delta	Origin	ECX 300
Receiver Gain	46.00	Solvent	DMSO-d6	Points Count	16384
Sweep Width (Hz)	5635.71	Temperature (degree C)	22.000	Pulse Sequence	single_pulse.ex2
				Spectrum Offset (Hz)	1502.6483
				Spectrum Type	STANDARD



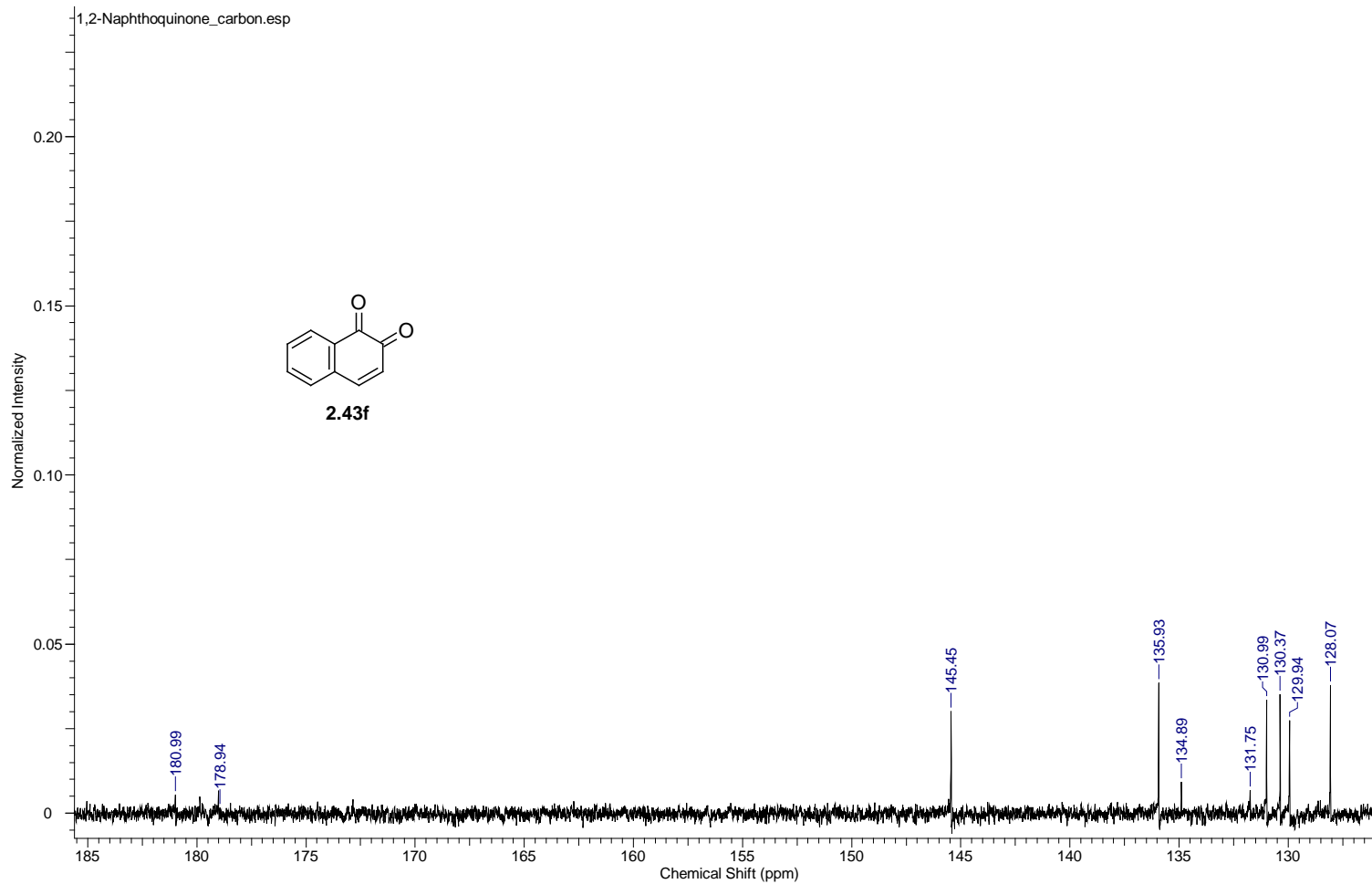
Acquisition Time (sec)	1.3841	Comment	single pulse decoupled gated NOE	Date	13 Dec 2011 17:30:08
Date Stamp	13 Dec 2011 17:02:07	File Name	F:\Dakin NMR\subtract\CS_13dimethylhydroquinone-1.jdf	Number of Transients	1000
Frequency (MHz)	75.57	Nucleus	13C	Origin	ECX 300
Original Points Count	32768	Owner	delta	Points Count	32768
Receiver Gain	50.00	Solvent	DMSO-d6	Pulse Sequence	single_pulse_dec
Sweep Width (Hz)	23674.24	Temperature (degree C)	22.000	Spectrum Offset (Hz)	7556.8232
				Spectrum Type	STANDARD



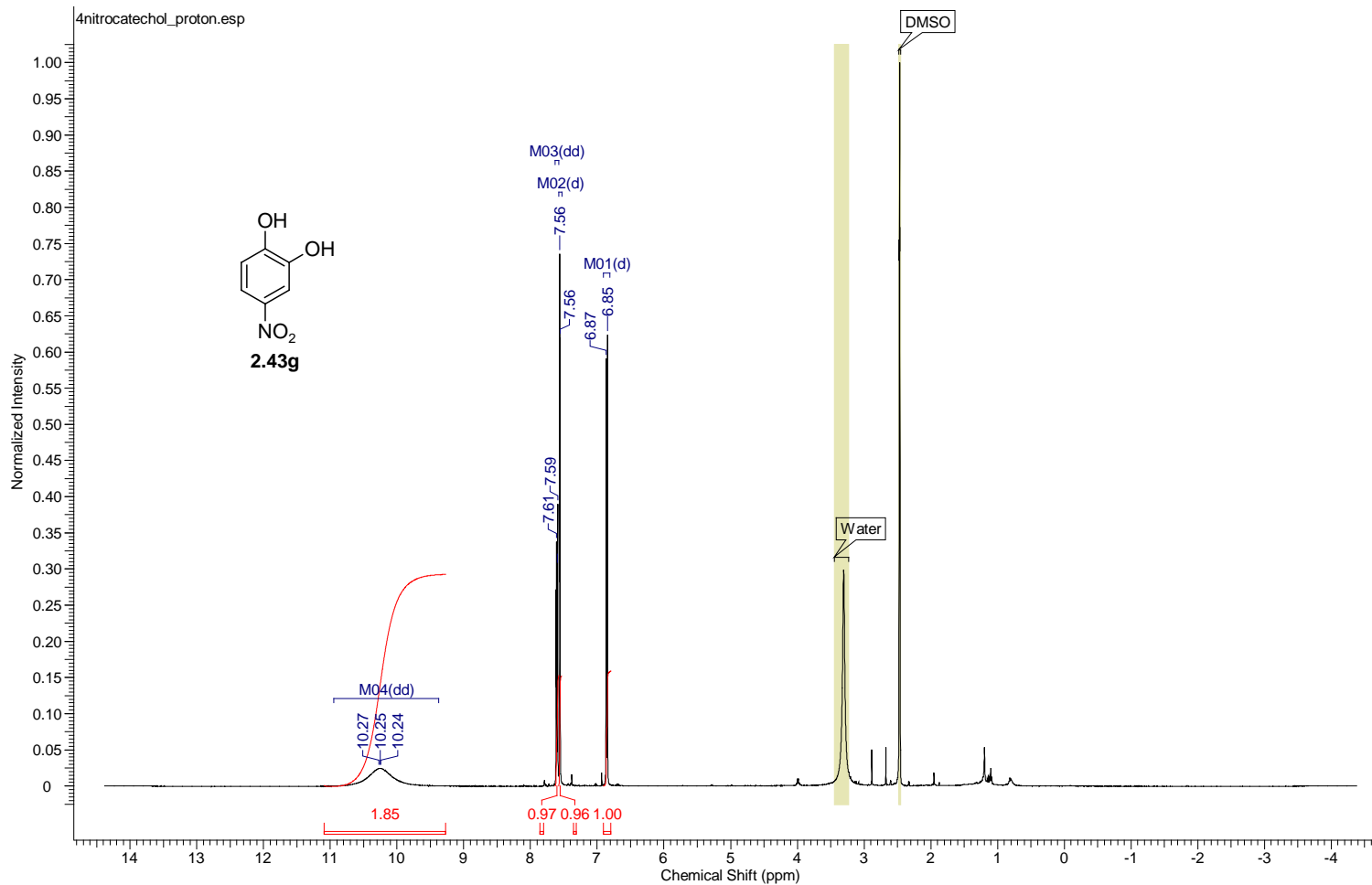
Acquisition Time (sec)	1.7459	Comment	single_pulse	Date	13 Dec 2011 12:48:03
Date Stamp	14 Dec 2011 05:46:00				
File Name	C:\Users\chen\Desktop\DakinNMR\substrate study\SubstrateNMR\PDFICS_naphthylcatechol-1.jdf			Frequency (MHz)	500.16
Nucleus	1H	Number of Transients	7	Origin	ECA 500
Owner	delta	Points Count	16384	Pulse Sequence	single_pulse.ex2
Solvent	CHLOROFORM-d	Spectrum Offset (Hz)	2500.7996	Receiver Gain	54.00
Sweep Width (Hz)	9384.38	Temperature (degree C)	21.900	Spectrum Type	STANDARD



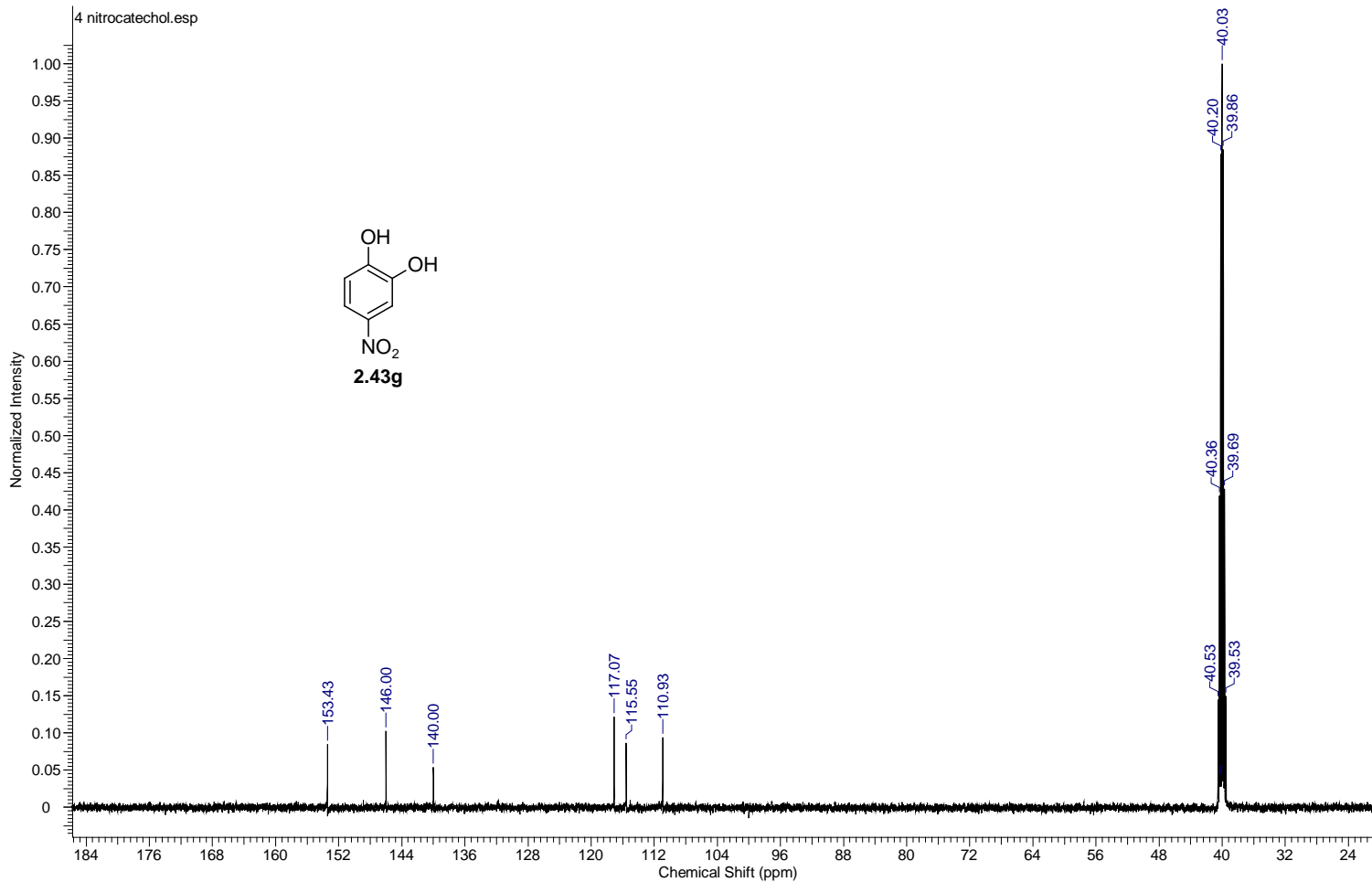
Acquisition Time (sec)	0.8336	Comment	single pulse decoupled gated NOE	Date	27 Dec 2011 10:05:12
Date Stamp	28 Dec 2011 03:03:15	File Name	C:\Users\chen\Desktop\DakinNMR\substrate study\naphthaquinone_again-1.jdf	Origin	ECA 500
Frequency (MHz)	125.77	Nucleus	¹³ C	Number of Transients	2000
Original Points Count	32768	Owner	delta	Points Count	32768
Receiver Gain	50.00	Solvent	CHLOROFORM-d	Pulse Sequence	single_pulse_dec
Spectrum Type	STANDARD	Sweep Width (Hz)	39308.18	Spectrum Offset (Hz)	12576.5293
		Temperature (degree C)	22.400		



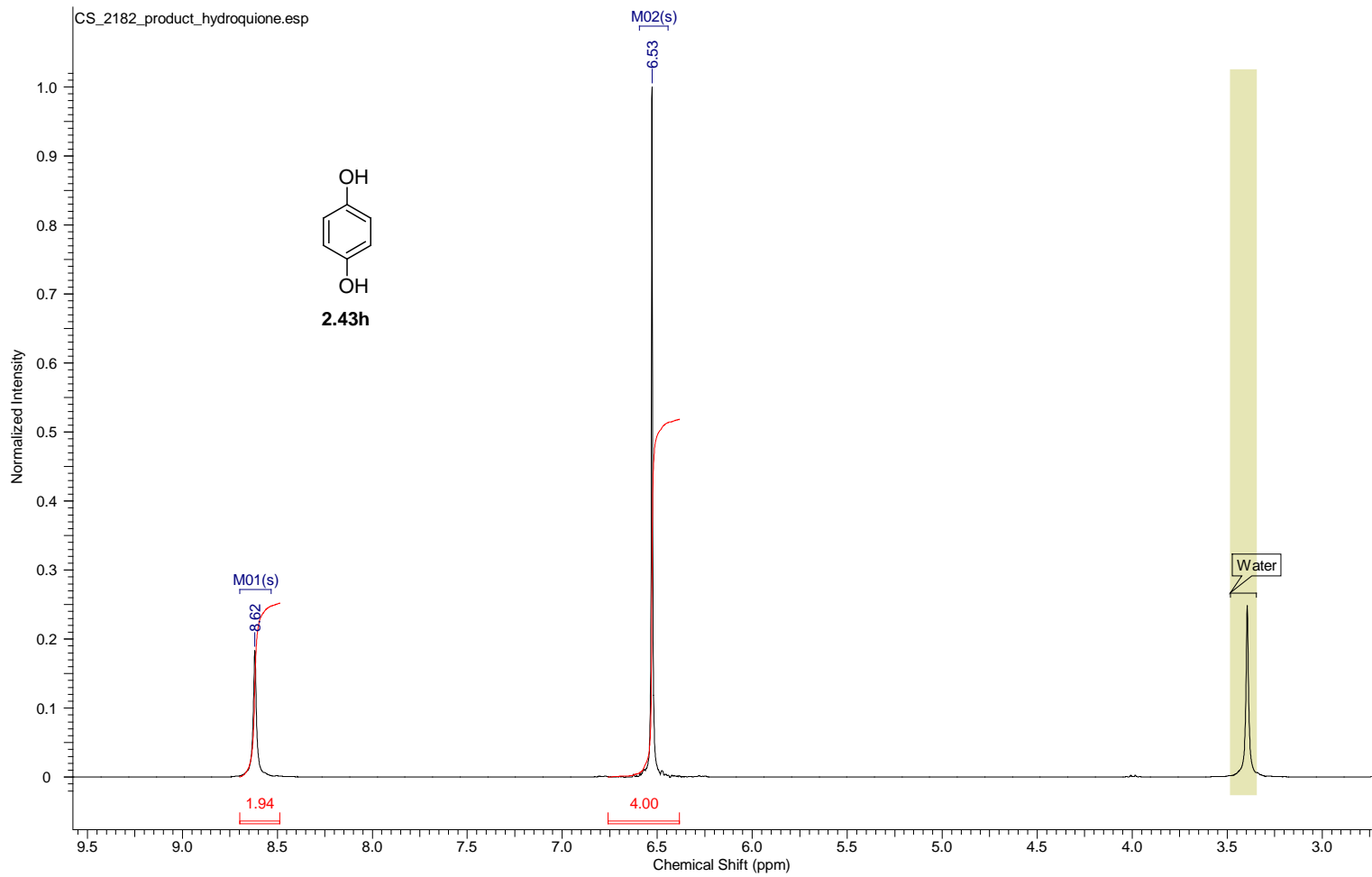
Acquisition Time (sec)	1.7459	Comment	single_pulse	Date	28 Jan 2012 11:35:55
Date Stamp	29 Jan 2012 04:35:18	File Name	G:\500MHz012512\aaaron\proton\CS_3052_product_proton-1.jdf		
Frequency (MHz)	500.16	Nucleus	1H	Number of Transients	16
Original Points Count	16384	Owner	delta	Points Count	16384
Receiver Gain	46.00	Solvent	DMSO-d6	Pulse Sequence	single_pulse.ex2
Sweep Width (Hz)	9384.38	Temperature (degree C)	21.900	Spectrum Offset (Hz)	2500.7996
				Spectrum Type	STANDARD



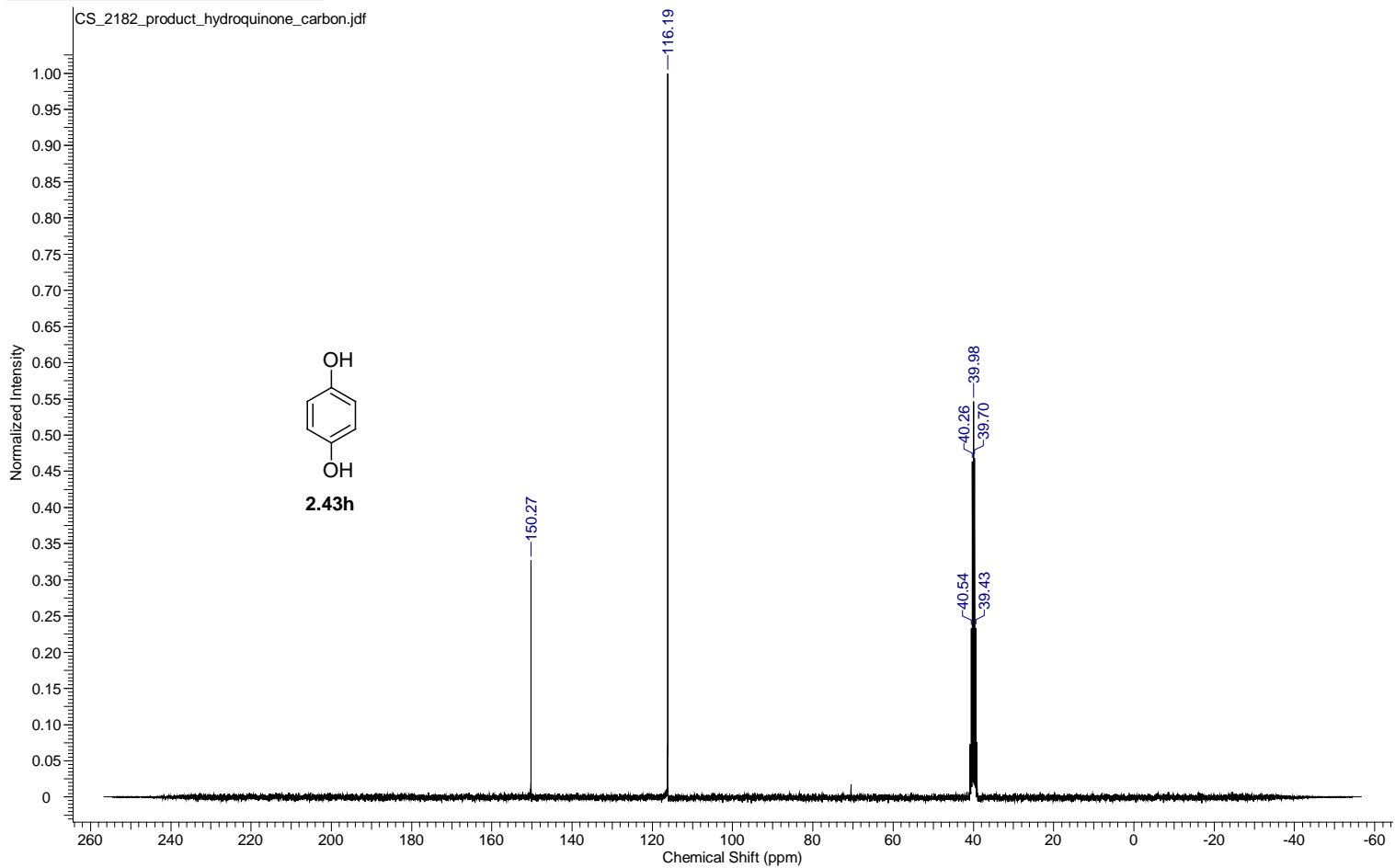
Acquisition Time (sec)	0.8336	Comment	single pulse decoupled gated NOE	Date	25 Jan 2012 13:06:55
Date Stamp	26 Jan 2012 06:06:17	File Name	G:\500MHz\012512\aaaron\carbon\CS_3049_carbon-1.jdf	Origin	ECA 500
Frequency (MHz)	125.77	Nucleus	13C	Number of Transients	80
Original Points Count	32768	Owner	delta	Points Count	32768
Receiver Gain	50.00	Solvent	DMSO-d6	Spectrum Offset (Hz)	12576.5293
Sweep Width (Hz)	39308.18	Temperature (degree C)	22.200	Spectrum Type	STANDARD



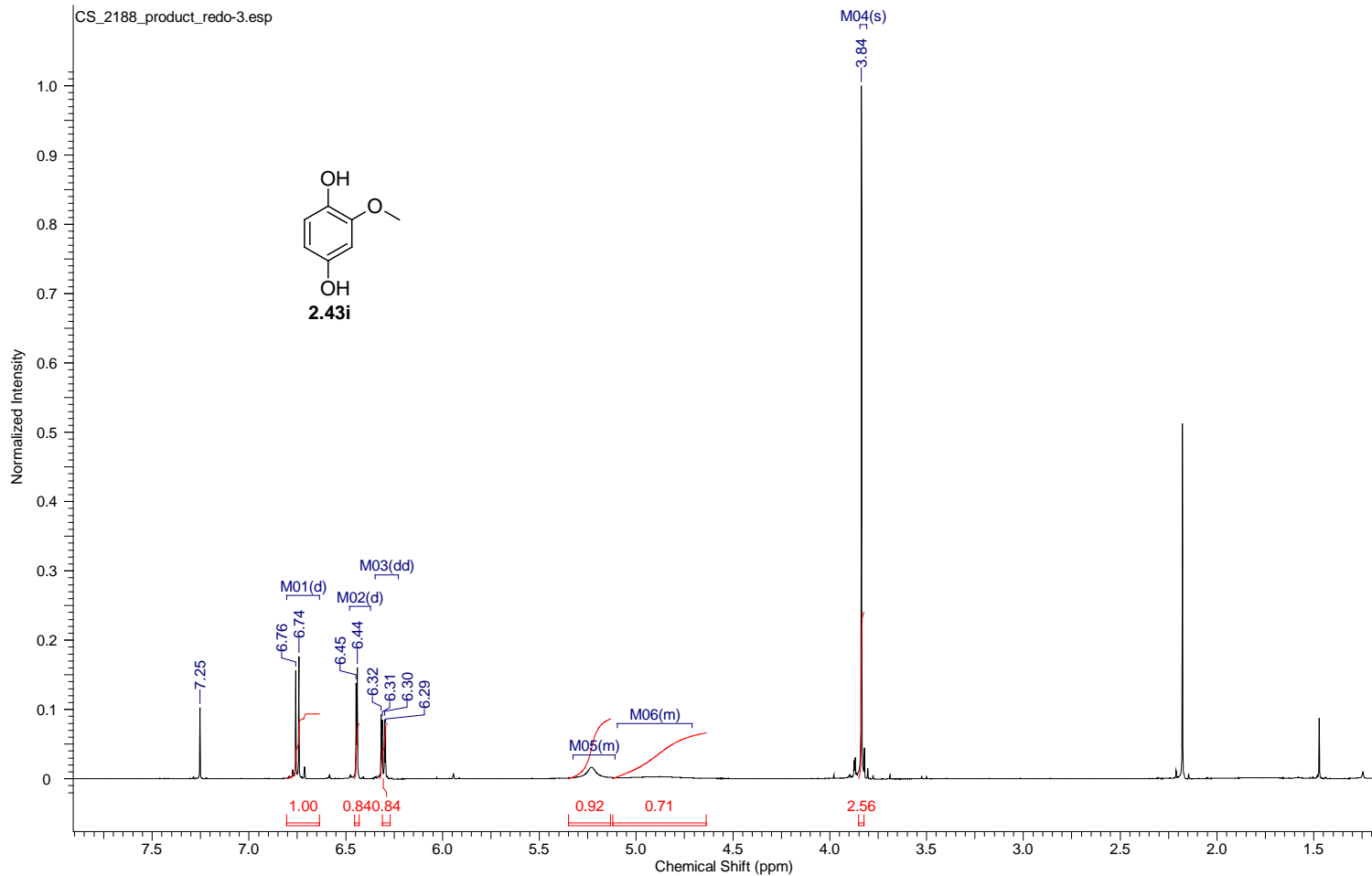
Acquisition Time (sec)	2.9072	Comment	single_pulse	Date	01 Dec 2010 08:55:33
Date Stamp	01 Dec 2010 08:40:57	File Name	C:\Users\chen\Desktop\DakinNMR\substrate study\CC_1018_product_DMSO-1.jdf		
Frequency (MHz)	300.53	Nucleus	1H	Origin	ECX 300
Original Points Count	16384	Owner	delta	Points Count	16384
Receiver Gain	38.00	Solvent	DMSO-d6	Spectrum Offset (Hz)	1502.6483
Sweep Width (Hz)	5635.71	Temperature (degree C)	20.800	Spectrum Type	STANDARD



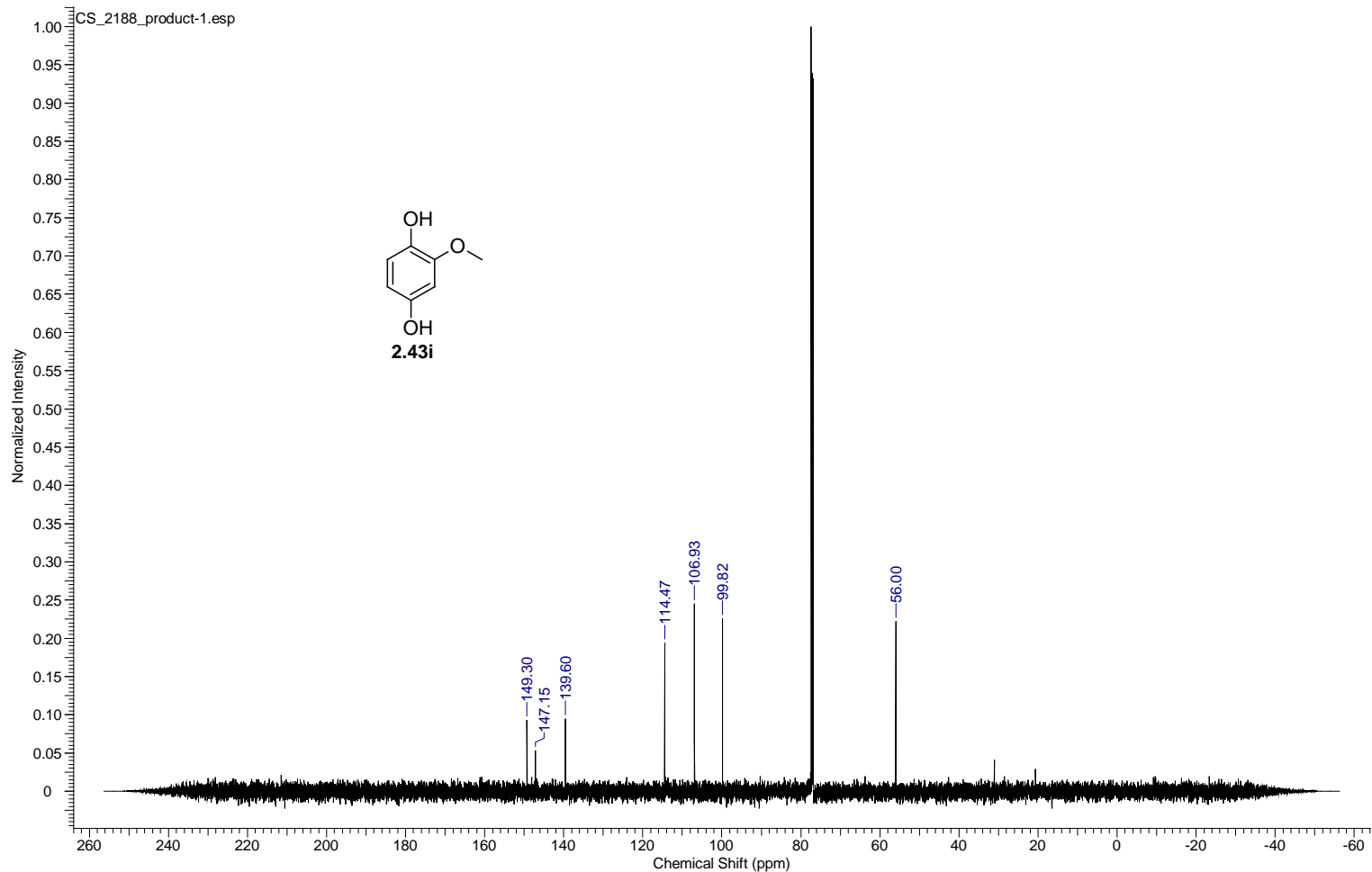
Acquisition Time (sec)	1.3841	Comment	single pulse decoupled gated NOE	Date	01 Dec 2010 09:10:38
Date Stamp	01 Dec 2010 08:56:02				
File Name	C:\Users\chen\Desktop\DakinNMR\substrate study\CS_2182_product_hydroquinone_carbon.jdf			Frequency (MHz)	75.57
Nucleus	13C	Number of Transients	330	Origin	ECX 300
Owner	delta	Points Count	32768	Pulse Sequence	single_pulse_dec
Solvent	DMSO-d6	Spectrum Offset (Hz)	7556.8232	Spectrum Type	STANDARD
Temperature (degree C)	21.200			Receiver Gain	50.00
				Sweep Width (Hz)	23674.24



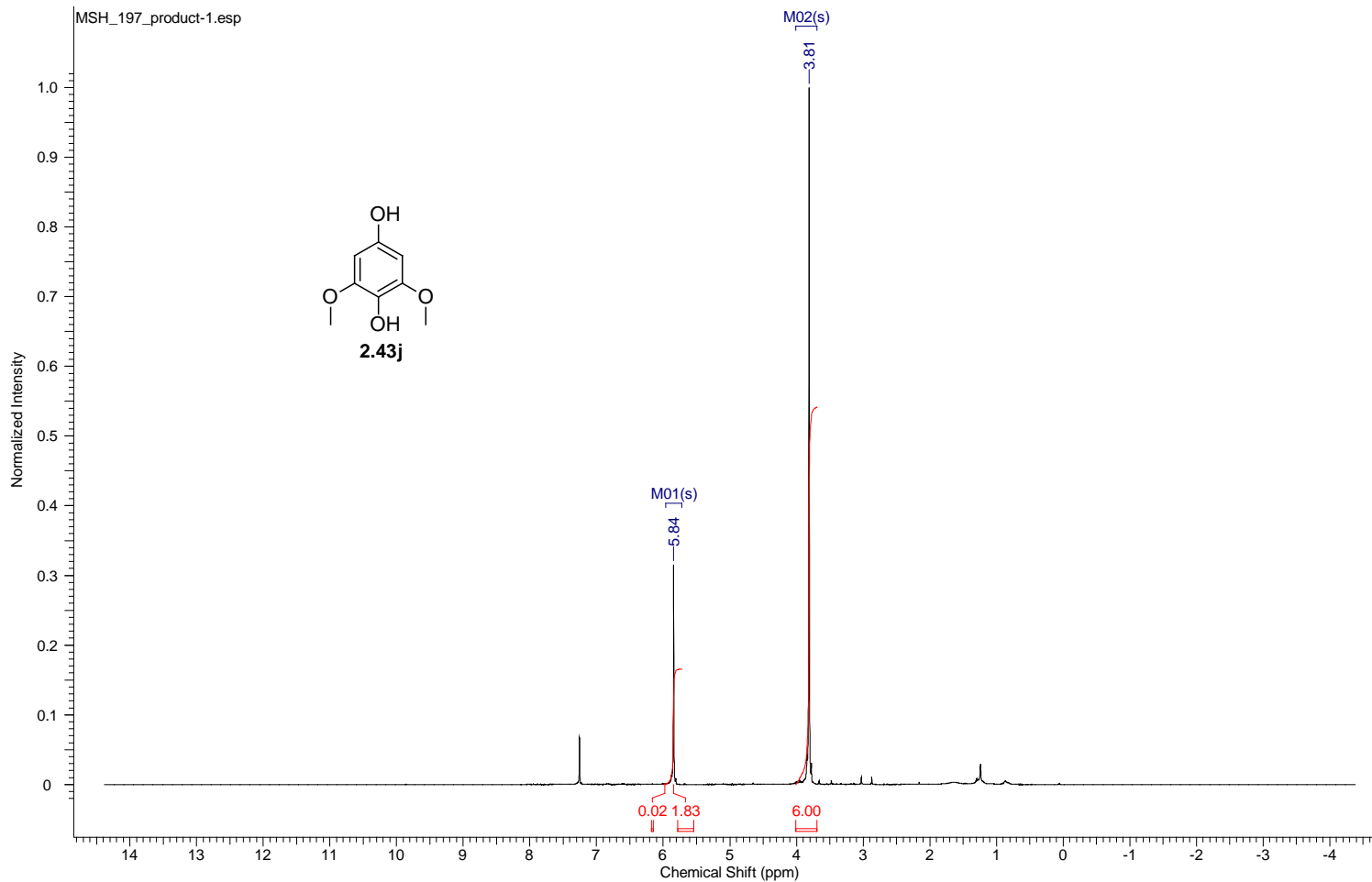
Acquisition Time (sec)	1.7460	Comment	single_pulse	Date	18 Nov 2011 11:40:20
Date Stamp	19 Nov 2011 04:35:36	File Name	C:\Users\chen\Desktop\DakinNMR\substrate study\CS_2188_product_redo-3.jdf		
Frequency (MHz)	500.16	Nucleus	1H	Origin	ECA 500
Original Points Count	13107	Owner	delta	Points Count	13107
Receiver Gain	44.00	Solvent	CHLOROFORM-d	Pulse Sequence	single_pulse.ex2
Spectrum Type	STANDARD	Sweep Width (Hz)	7506.82	Temperature (degree C)	22.200



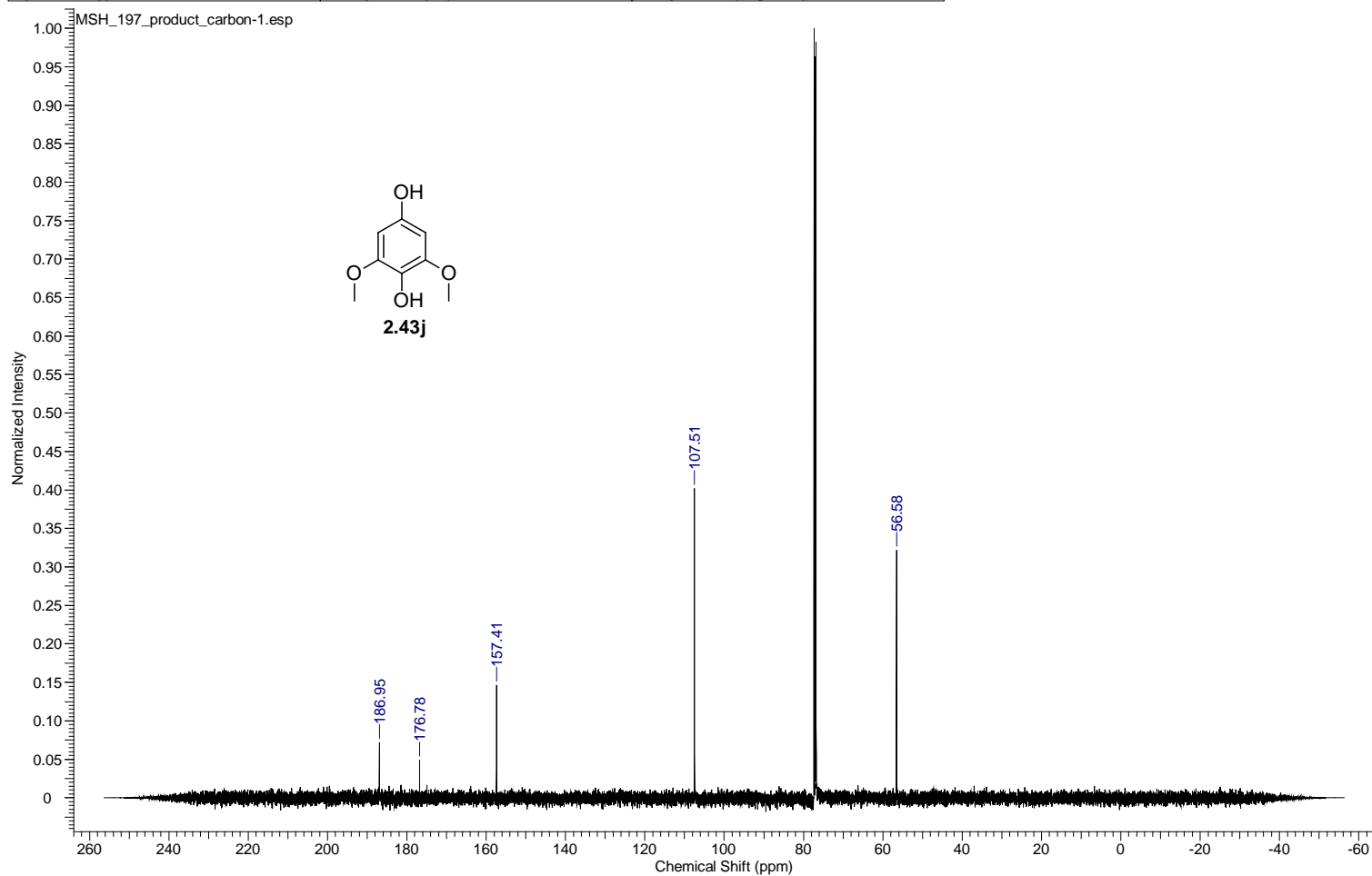
Acquisition Time (sec)	0.8336	Comment	single pulse decoupled gated NOE	Date	18 Nov 2011 11:41:42
Date Stamp	19 Nov 2011 04:37:54	File Name	C:\Users\chen\Desktop\DakinNMR\substrate study\CS_2188_product-1.jdf		
Frequency (MHz)	125.77	Nucleus	13C	Number of Transients	50
Original Points Count	32768	Owner	delta	Points Count	32768
Receiver Gain	50.00	Solvent	CHLOROFORM-d	Pulse Sequence	single_pulse_dec
Spectrum Type	STANDARD	Sweep Width (Hz)	39308.18	Temperature (degree C)	22.500



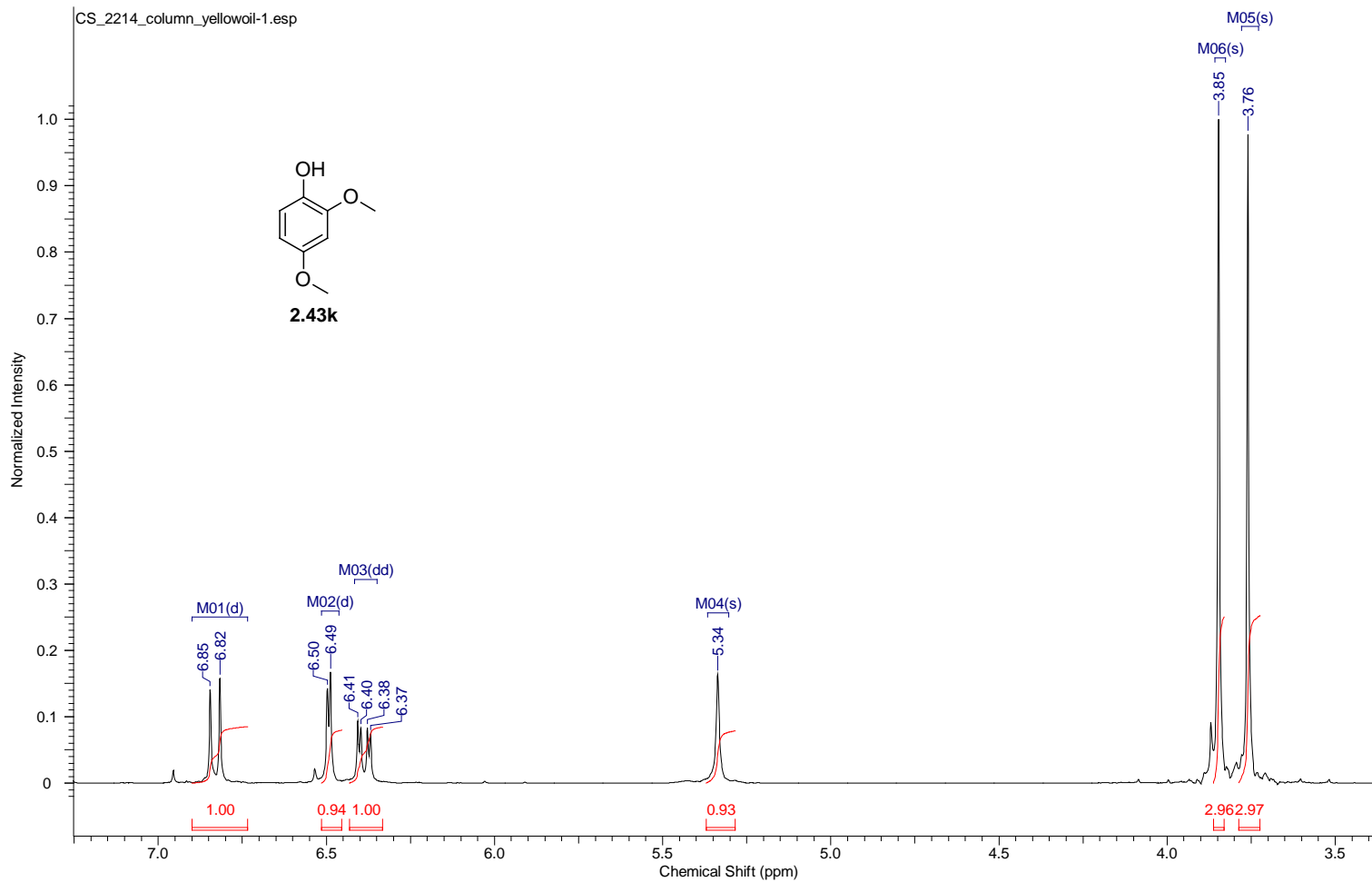
Acquisition Time (sec)	1.7459	Comment	single_pulse	Date	15 Dec 2011 10:58:11
Date Stamp	16 Dec 2011 03:56:09	File Name	C:\Users\chen\Desktop\DakinNMR\substrate study\MSH_197_product-1.jdf		
Frequency (MHz)	500.16	Nucleus	1H	Number of Transients	4
Original Points Count	16384	Owner	delta	Points Count	16384
Receiver Gain	44.00	Solvent	CHLOROFORM-d	Pulse Sequence	single_pulse.ex2
Spectrum Type	STANDARD	Sweep Width (Hz)	9384.38	Temperature (degree C)	22.200



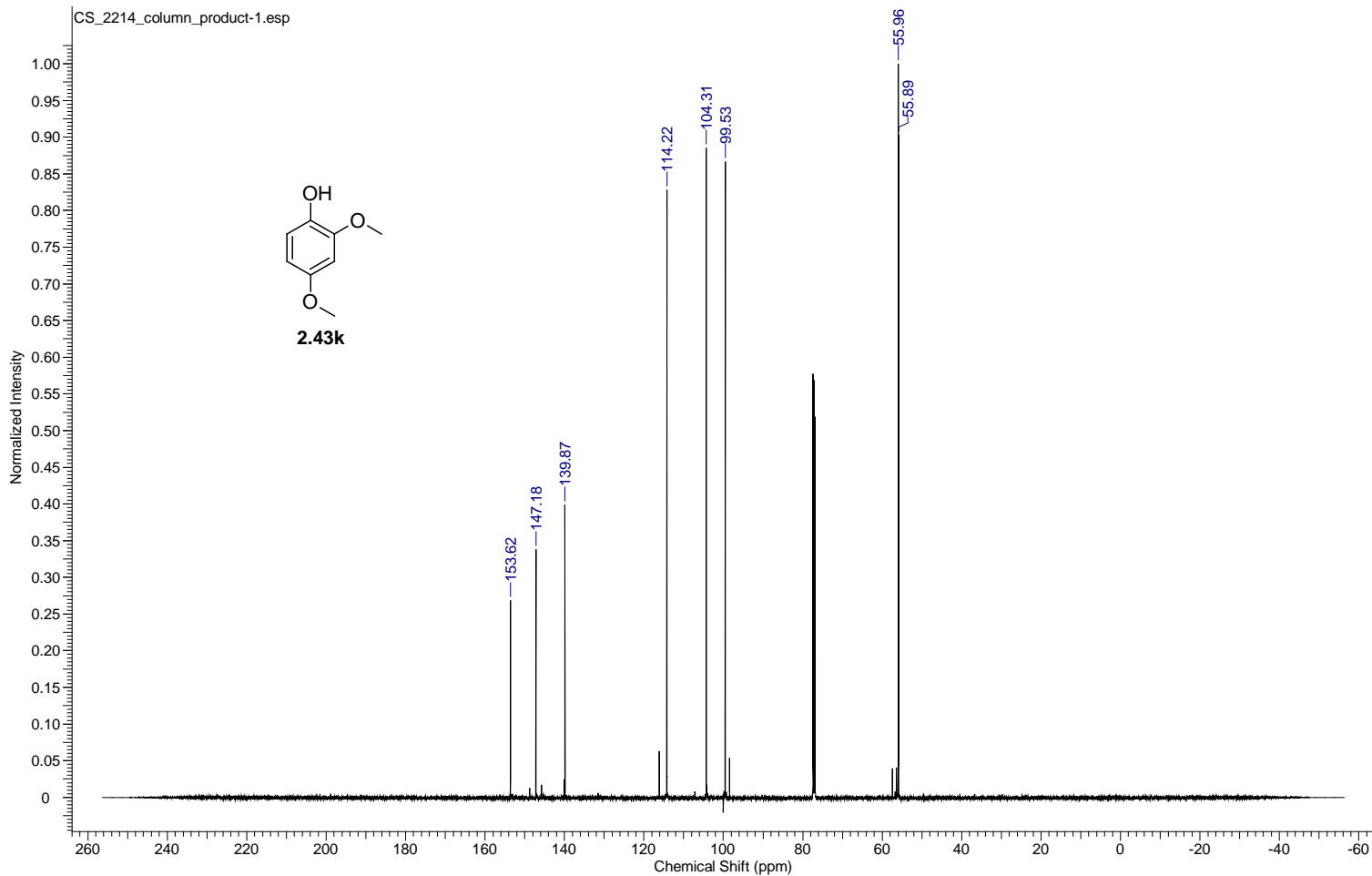
Acquisition Time (sec)	0.8336	Comment	single pulse decoupled gated NOE	Date	15 Dec 2011 11:04:09
Date Stamp	16 Dec 2011 04:02:07	File Name	C:\Users\chen\Desktop\DakinNMR\substrate study\MSH_197_product_carbon-1.jdf		
Frequency (MHz)	125.77	Nucleus	13C	Number of Transients	160
Original Points Count	32768	Owner	delta	Points Count	32768
Receiver Gain	50.00	Solvent	CHLOROFORM-d	Pulse Sequence	single_pulse_dec
Spectrum Type	STANDARD	Sweep Width (Hz)	39308.18	Temperature (degree C)	22.700



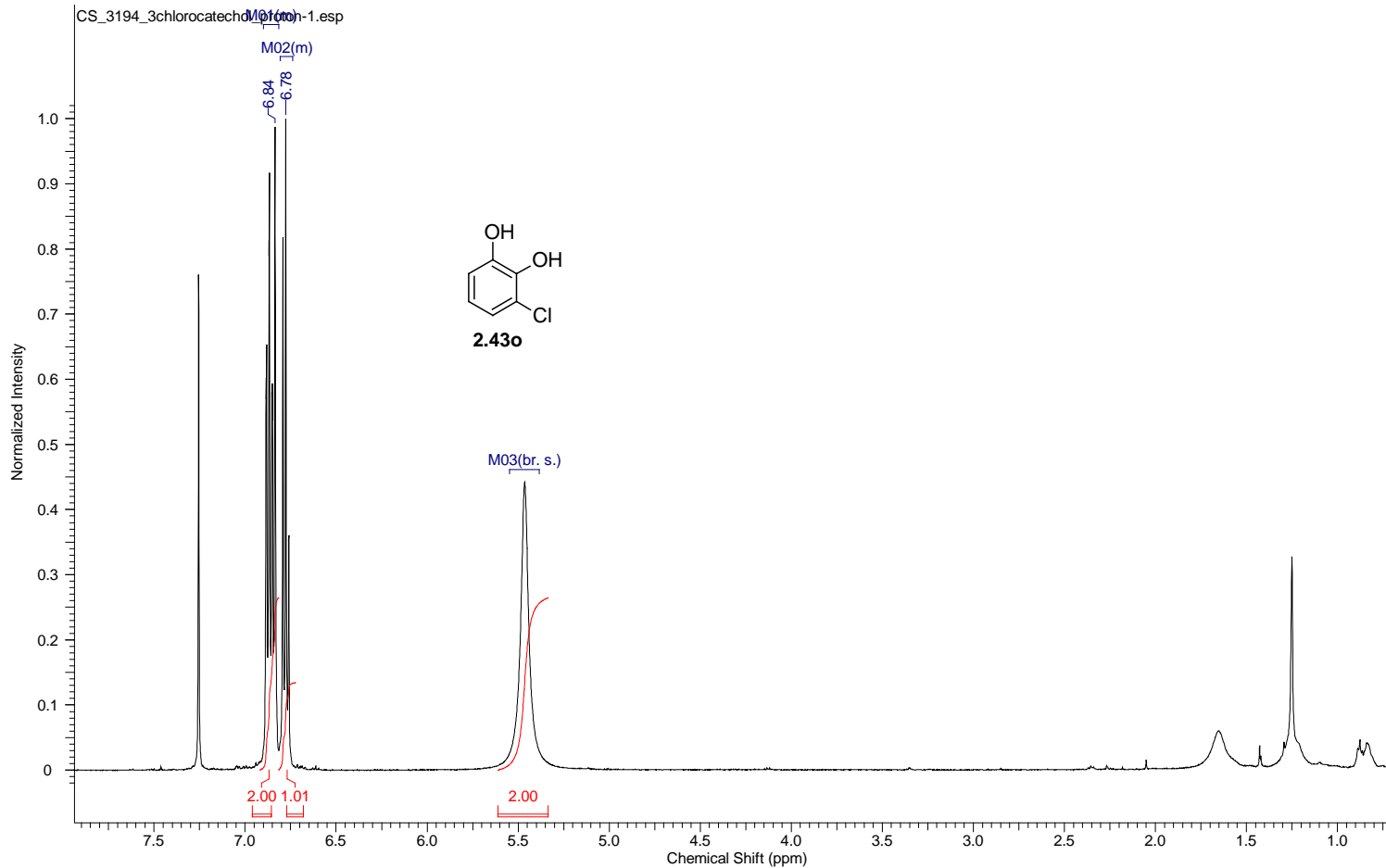
Acquisition Time (sec)	2.9072	Comment	single_pulse	Date	01 Dec 2010 12:10:57
Date Stamp	01 Dec 2010 11:56:21	File Name	C:\Users\chen\Desktop\DakinNMR\substrate study\CS_2214_column_yellowoil-1.jdf		
Frequency (MHz)	300.53	Nucleus	1H	Origin	ECX 300
Original Points Count	16384	Owner	delta	Points Count	16384
Receiver Gain	30.00	Solvent	CHLOROFORM-d	Pulse Sequence	single_pulse.ex2
Spectrum Type	STANDARD	Sweep Width (Hz)	5635.71	Temperature (degree C)	21.100



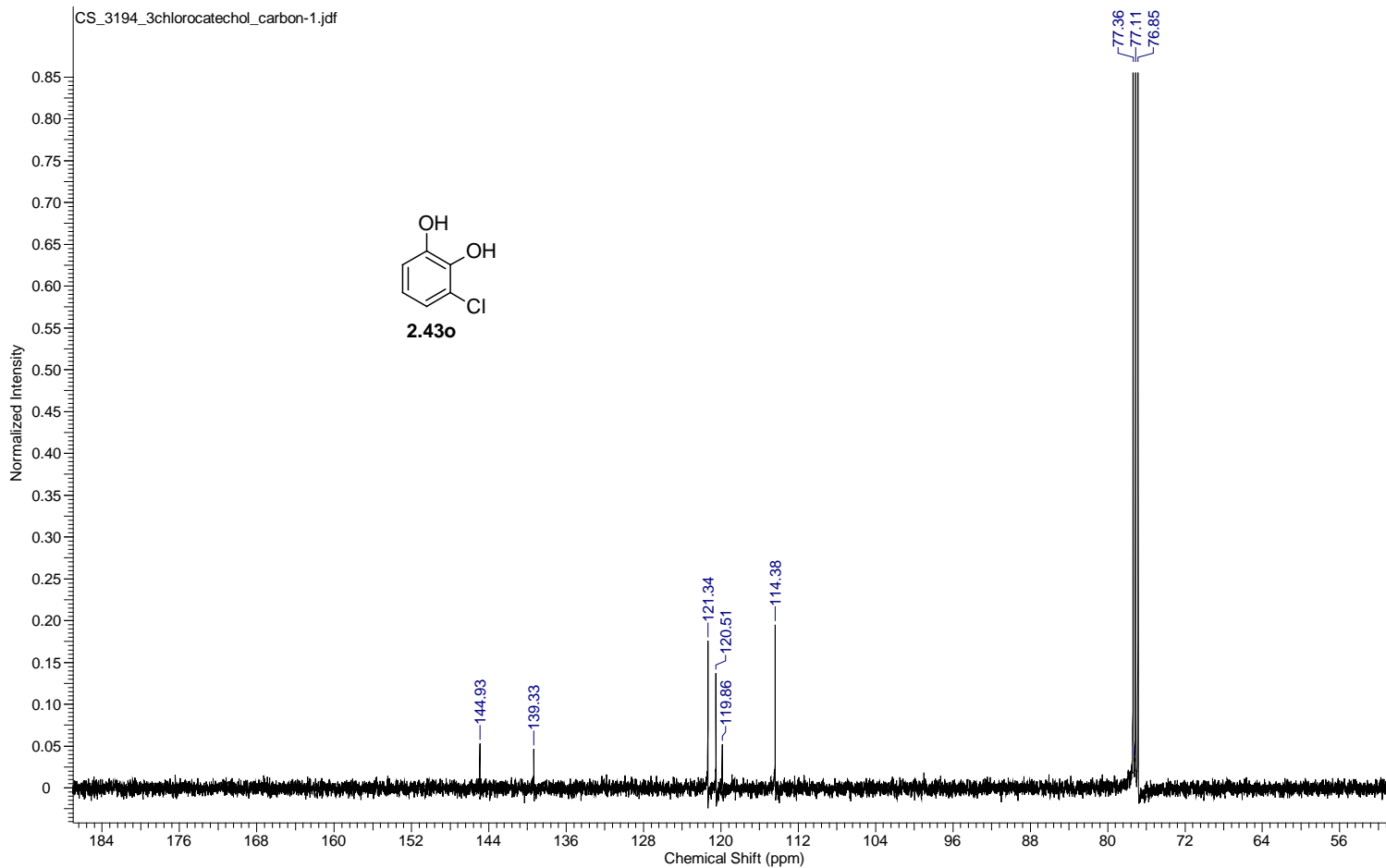
Acquisition Time (sec)	0.8336	Comment	single pulse decoupled gated NOE	Date	01 Dec 2010 13:00:48
Date Stamp	02 Dec 2010 06:08:34	File Name	C:\Users\lchen\Desktop\DakinNMR\substrate study\CS_2214_column_product-1.jdf	Number of Transients	1000
Frequency (MHz)	125.77	Nucleus	13C	Origin	ECA 500
Original Points Count	32768	Owner	delta	Points Count	32768
Receiver Gain	50.00	Solvent	CHLOROFORM-d	Pulse Sequence	single_pulse_dec
Spectrum Type	STANDARD	Sweep Width (Hz)	39308.18	Temperature (degree C)	21.800



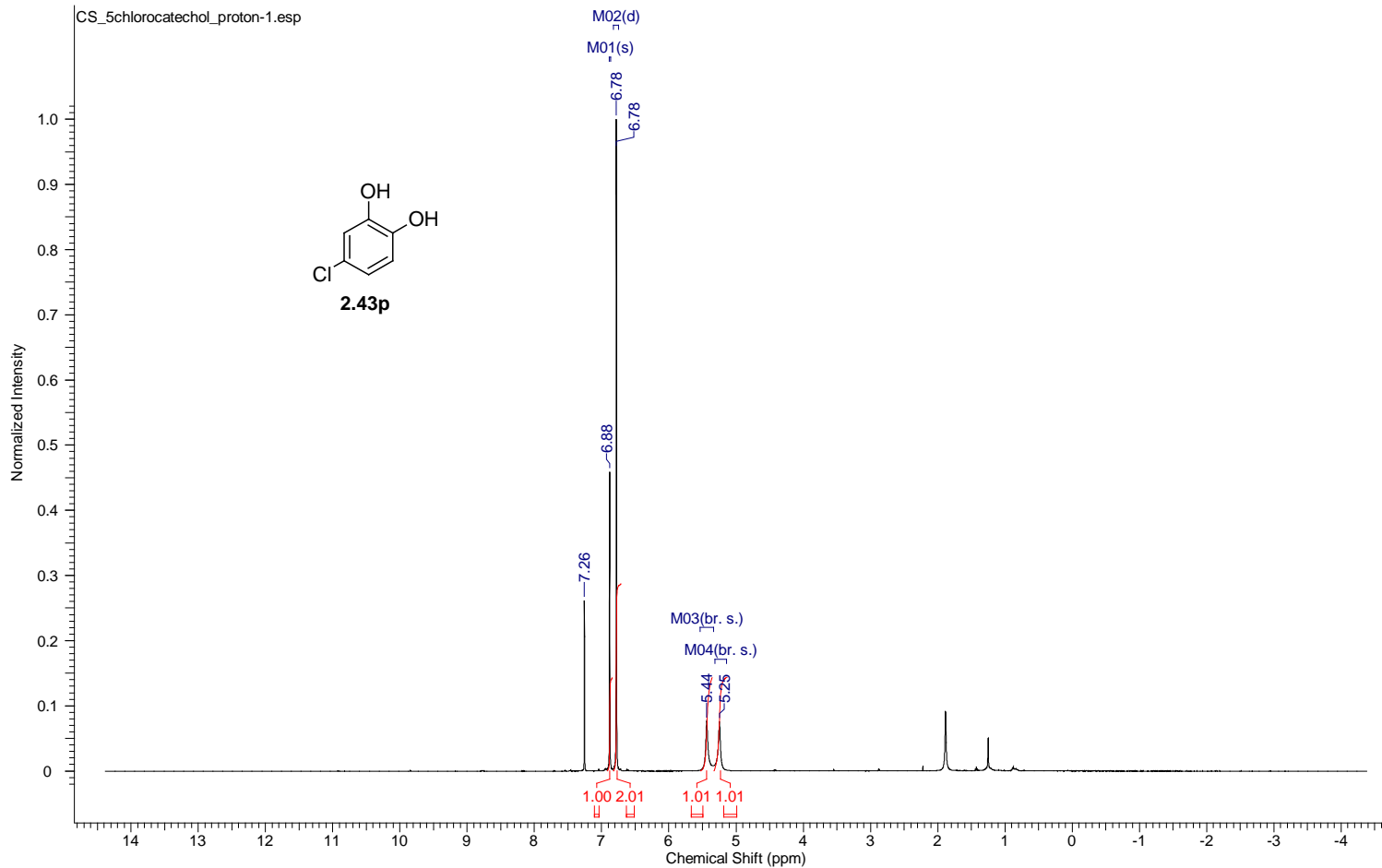
Acquisition Time (sec)	1.7459	Comment	single_pulse	Date	09 May 2012 13:20:51
Date Stamp	10 May 2012 05:37:24				
File Name	C:\Users\chen\Desktop\DakinNMR\Aerobic Dakin Oxidation\Substrate NMR\RAW_data\CS_3194_3chlorocatechol_proton-1.jdf				
Frequency (MHz)	500.16	Nucleus	¹ H	Number of Transients	4
Original Points Count	16384	Owner	delta	Points Count	16384
Receiver Gain	46.00	Solvent	CHLOROFORM-d	Spectrum Offset (Hz)	2500.7996
Sweep Width (Hz)	9384.38	Temperature (degree C)	22.400	Spectrum Type	STANDARD



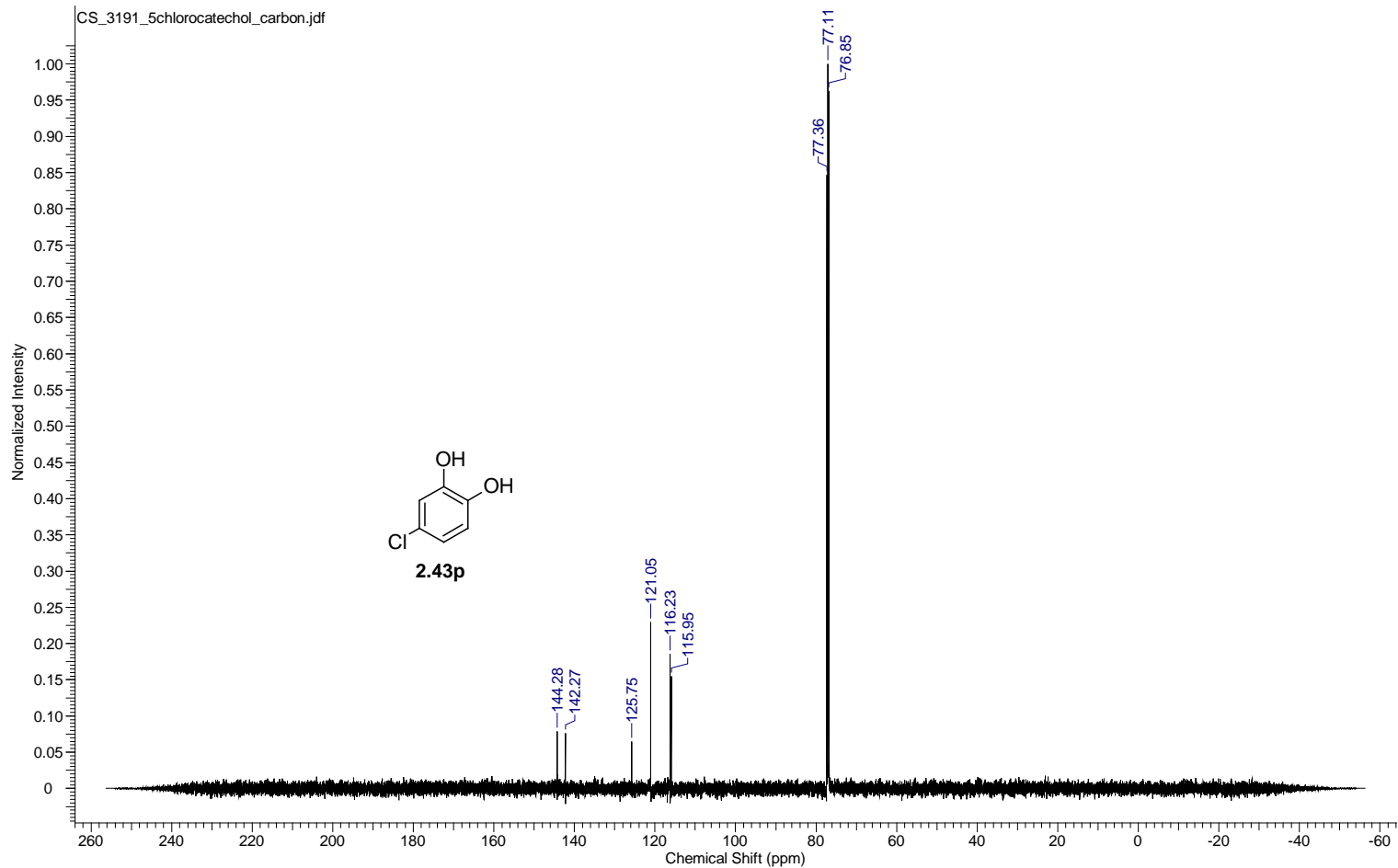
Acquisition Time (sec)	0.8336	Comment	single pulse decoupled gated NOE		Date	09 May 2012 13:24:50	
Date Stamp	10 May 2012 05:41:23						
File Name	C:\Users\chen\Desktop\DakinNMR\Aerobic Dakin Oxidation\Substrate NMR\RAW data\CS_3194_3chlorocatechol_carbon-1.jdf						
Frequency (MHz)	125.77	Nucleus	¹³ C	Number of Transients	100	Origin	ECA 500
Original Points Count	32768	Owner	delta	Points Count	32768	Pulse Sequence	single_pulse_dec
Receiver Gain	50.00	Solvent	CHLOROFORM-d	Spectrum Offset (Hz)	12576.5293	Spectrum Type	STANDARD
Sweep Width (Hz)	39308.18	Temperature (degree C)	22.900				



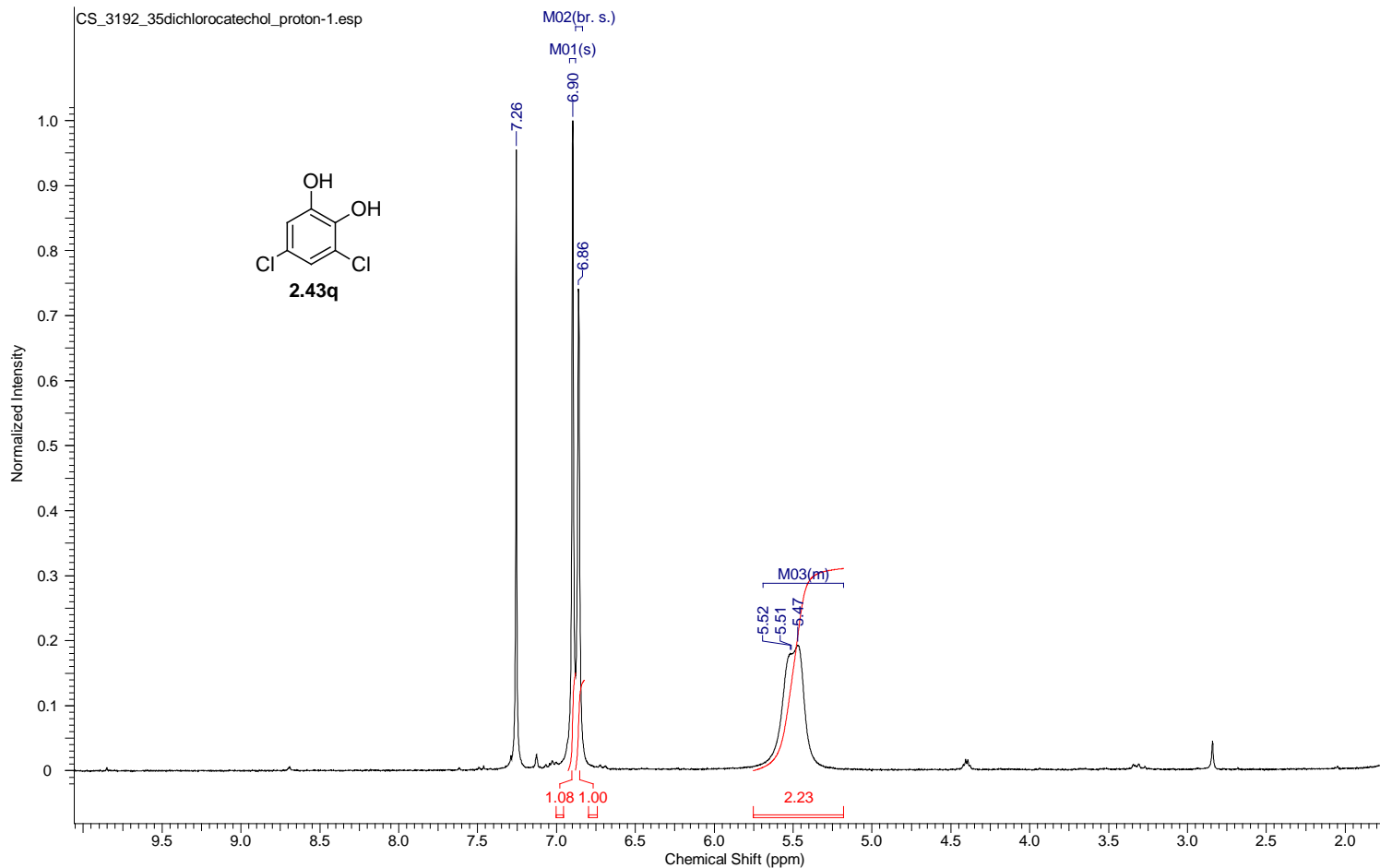
Acquisition Time (sec)	1.7459	Comment	single_pulse	Date	08 May 2012 08:06:03
Date Stamp	09 May 2012 00:22:34				
File Name	C:\Users\chen\Desktop\DakinNMR\Aerobic Dakin Oxidation\Substrate NMR\RAW_data\CS_3191_5chlorocatechol_proton.jdf				
Frequency (MHz)	500.16	Nucleus	1H	Number of Transients	16
Original Points Count	16384	Owner	delta	Points Count	16384
Receiver Gain	46.00	Solvent	CHLOROFORM-d	Spectrum Offset (Hz)	2500.7996
Sweep Width (Hz)	9384.38	Temperature (degree C)	22.600	Spectrum Type	STANDARD



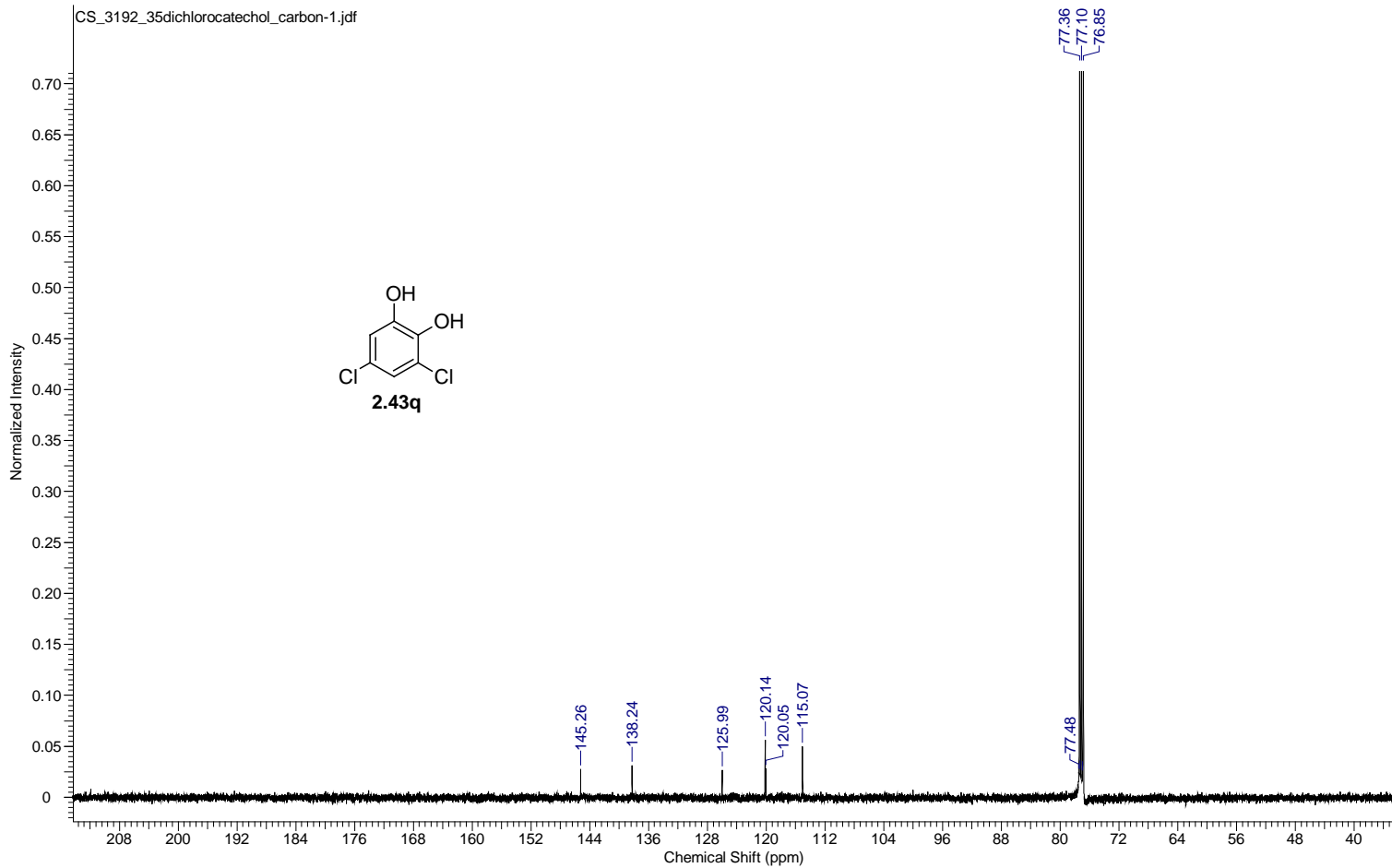
Acquisition Time (sec)	0.8336	Comment	single pulse decoupled gated NOE	Date	08 May 2012 08:09:53
Date Stamp	09 May 2012 00:26:25				
File Name	C:\Users\chen\Desktop\DakinNMR\Aerobic Dakin Oxidation\Substrate NMR\RAW data\CS_3191_5chlorocatechol_carbon.jdf				
Frequency (MHz)	125.77	Nucleus	¹³ C	Number of Transients	100
Original Points Count	32768	Owner	delta	Points Count	32768
Receiver Gain	50.00	Solvent	CHLOROFORM-d	Spectrum Offset (Hz)	12576.5293
Sweep Width (Hz)	39308.18	Temperature (degree C)	23.100	Spectrum Type	STANDARD



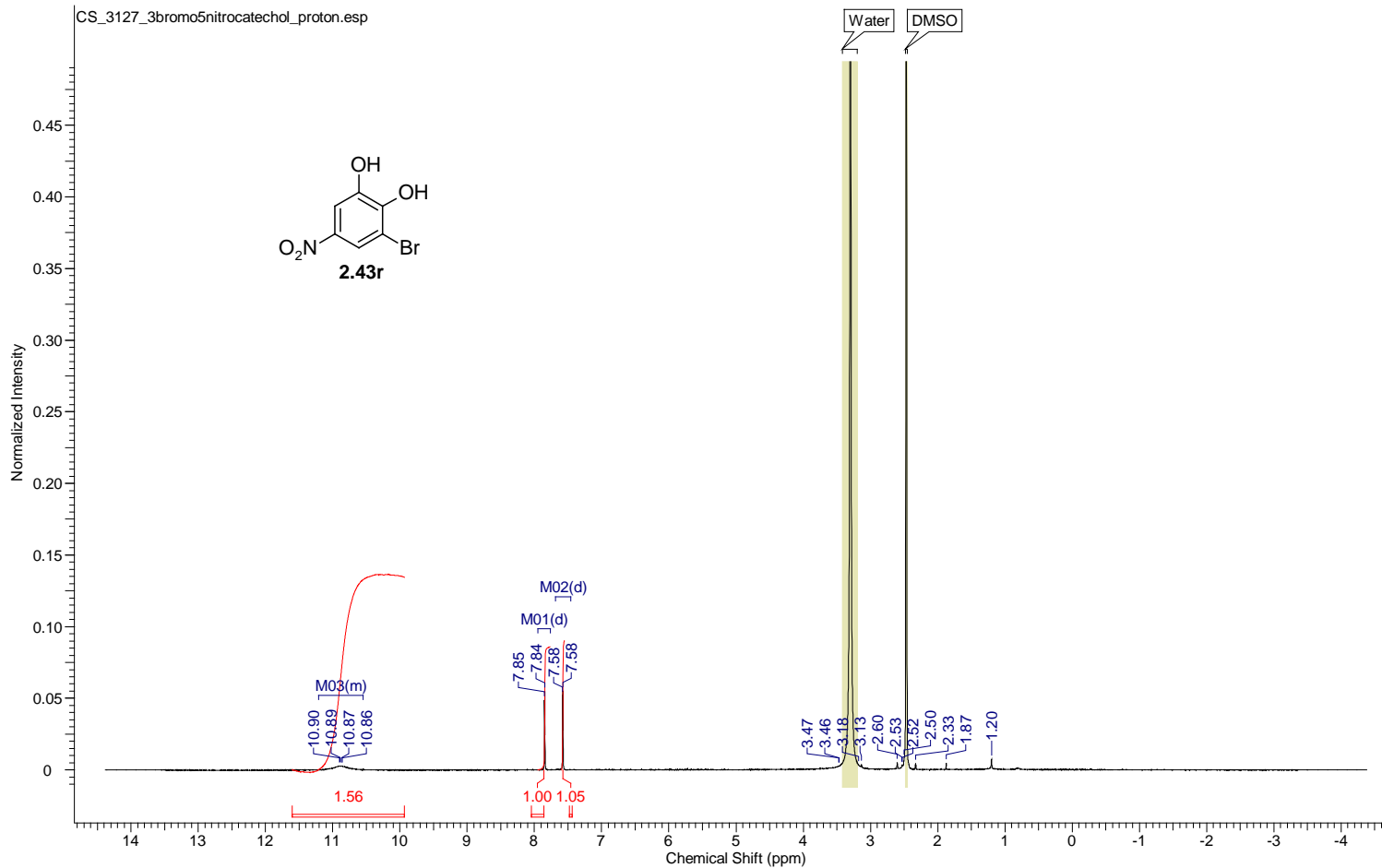
Acquisition Time (sec)	1.7459	Comment	single_pulse	Date	09 May 2012 12:36:30
Date Stamp	10 May 2012 04:53:02				
File Name	C:\Users\chen\Desktop\DakinNMR\Aerobic Dakin Oxidation\Substrate NMR\RAW_data\CS_3192_35dichlorocatechol_proton-1.jdf				
Frequency (MHz)	500.16	Nucleus	1H	Number of Transients	7
Original Points Count	16384	Owner	delta	Points Count	16384
Receiver Gain	50.00	Solvent	CHLOROFORM-d	Spectrum Offset (Hz)	2500.7996
Sweep Width (Hz)	9384.38	Temperature (degree C)	22.300	Spectrum Type	STANDARD



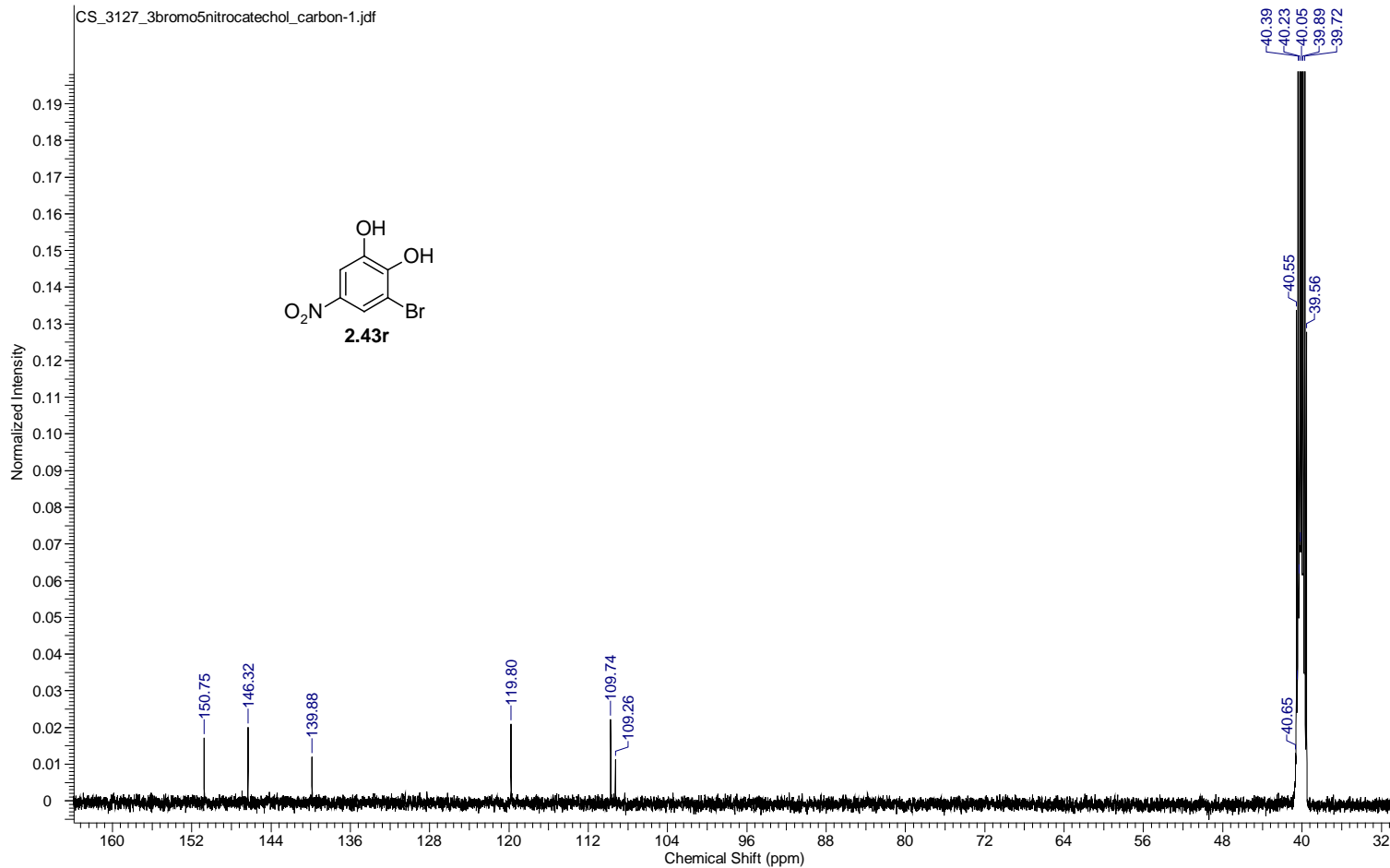
Acquisition Time (sec)	0.8336	Comment	single pulse decoupled gated NOE	Date	09 May 2012 13:12:38
Date Stamp	10 May 2012 05:29:10				
File Name	C:\Users\chen\Desktop\DakinNMR\Aerobic Dakin Oxidation\Substrate NMR\RAW data\CS_3192_35dichlorocatechol_carbon-1.jdf				
Frequency (MHz)	125.77	Nucleus	¹³ C	Number of Transients	1000
Original Points Count	32768	Owner	delta	Points Count	32768
Receiver Gain	50.00	Solvent	CHLOROFORM-d	Spectrum Offset (Hz)	12576.5293
Sweep Width (Hz)	39308.18	Temperature (degree C)	23.000	Spectrum Type	STANDARD



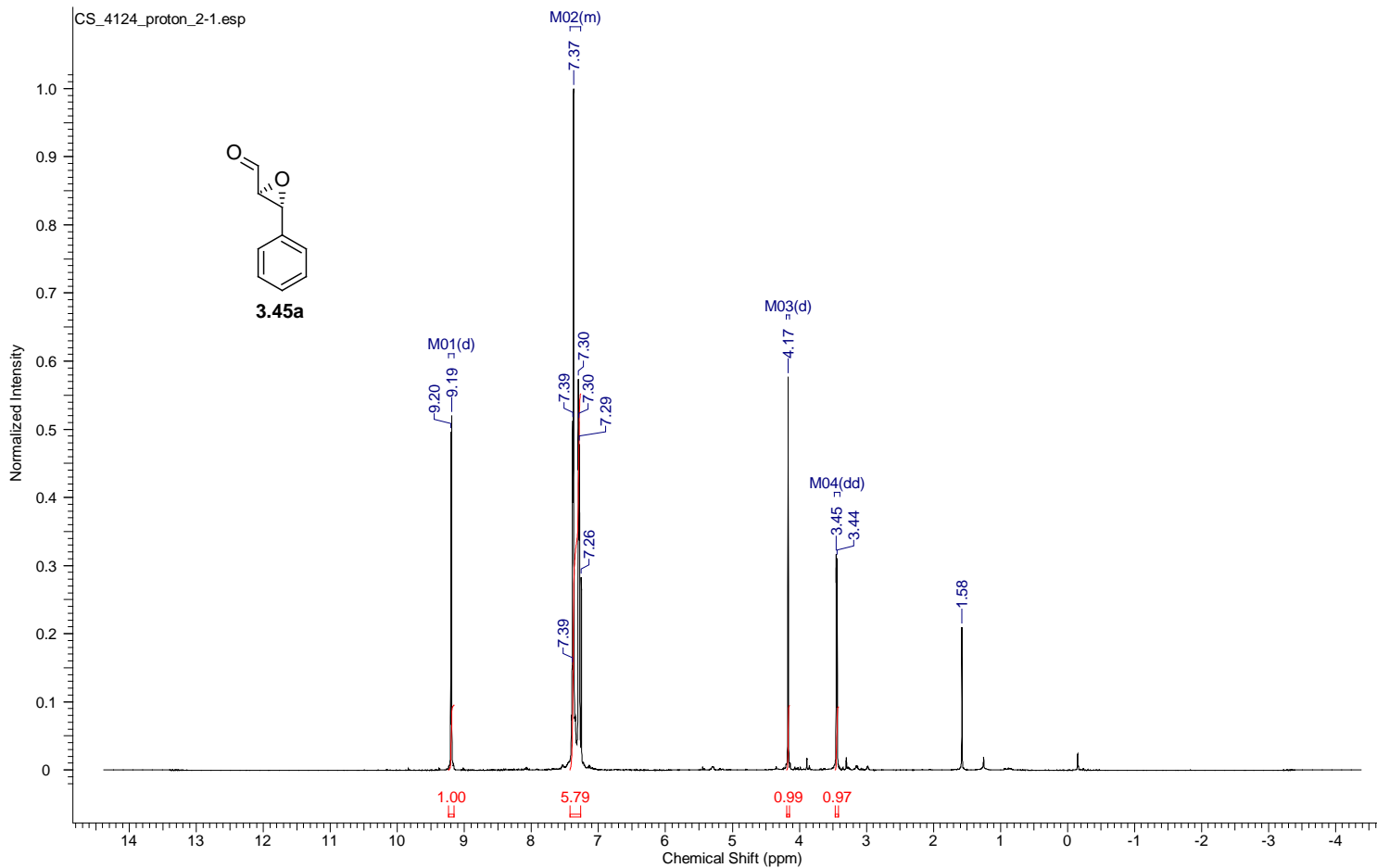
Acquisition Time (sec)	1.7459	Comment	single_pulse	Date	01 May 2012 10:04:51
Date Stamp	02 May 2012 02:21:20				
File Name	C:\Users\chen\Desktop\DakinNMR\Aerobic Dakin Oxidation\Substrate NMR\RAW_data\CS_3127_3bromo5nitrocatechol_proton.jdf				
Frequency (MHz)	500.16	Nucleus	1H	Number of Transients	11
Original Points Count	16384	Owner	delta	Points Count	16384
Receiver Gain	50.00	Solvent	DMSO-d6	Spectrum Offset (Hz)	2500.7996
Sweep Width (Hz)	9384.38	Temperature (degree C)	22.000	Spectrum Type	STANDARD



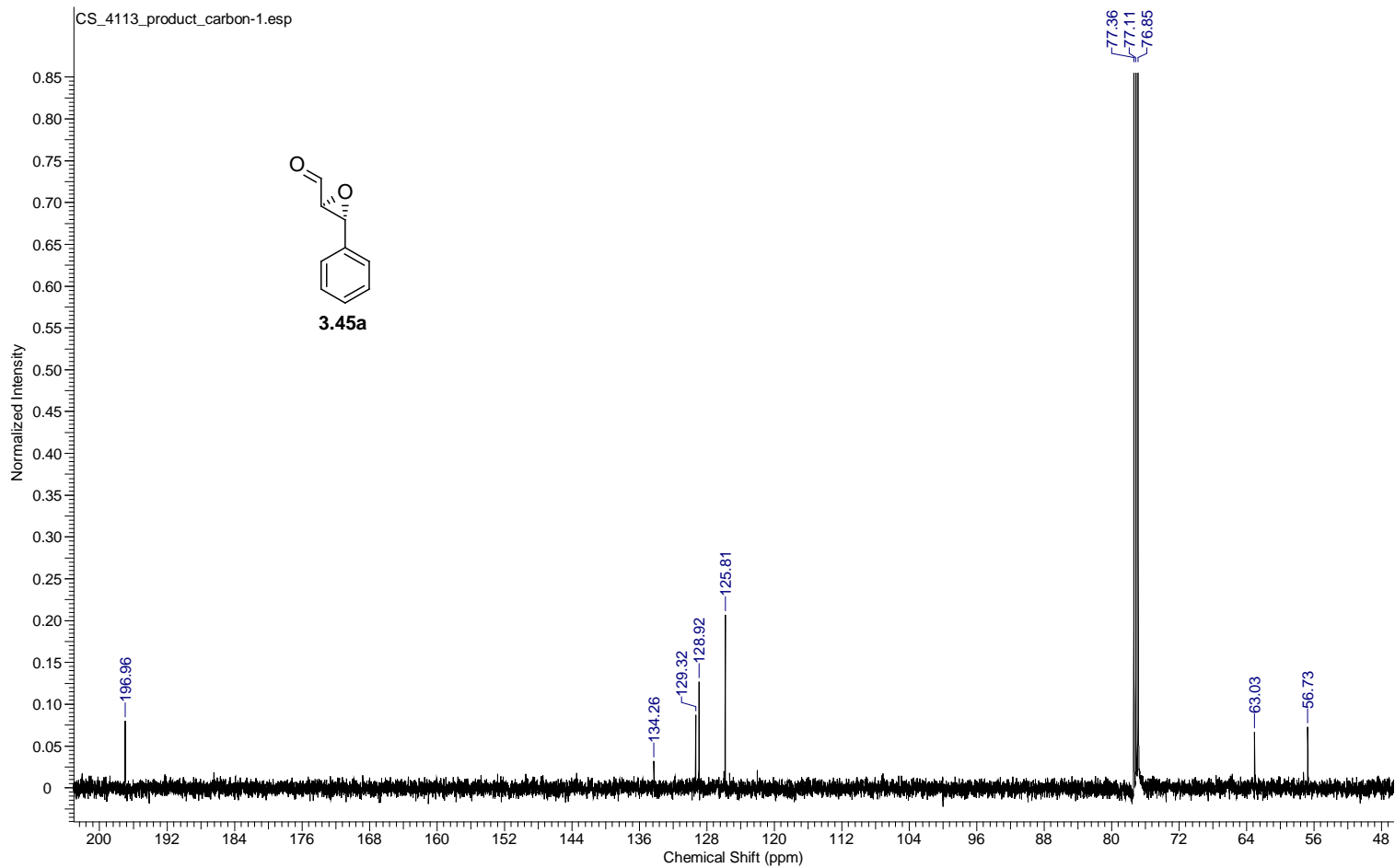
Acquisition Time (sec)	0.8336	Comment	single pulse decoupled gated NOE		Date	31 Mar 2012 11:28:37	
Date Stamp	01 Apr 2012 03:43:44						
File Name	C:\Users\chen\Desktop\DakinNMR\Aerobic Dakin Oxidation\Substrate NMR\RAW data\CS_3127_3bromo5nitrocatechol_carbon-1.jdf						
Frequency (MHz)	125.77	Nucleus	¹³ C	Number of Transients	1000	Origin	ECA 500
Original Points Count	32768	Owner	delta	Points Count	32768	Pulse Sequence	single_pulse_dec
Receiver Gain	50.00	Solvent	DMSO-d6	Spectrum Offset (Hz)	12576.5293	Spectrum Type	STANDARD
Sweep Width (Hz)	39308.18	Temperature (degree C)	23.300				



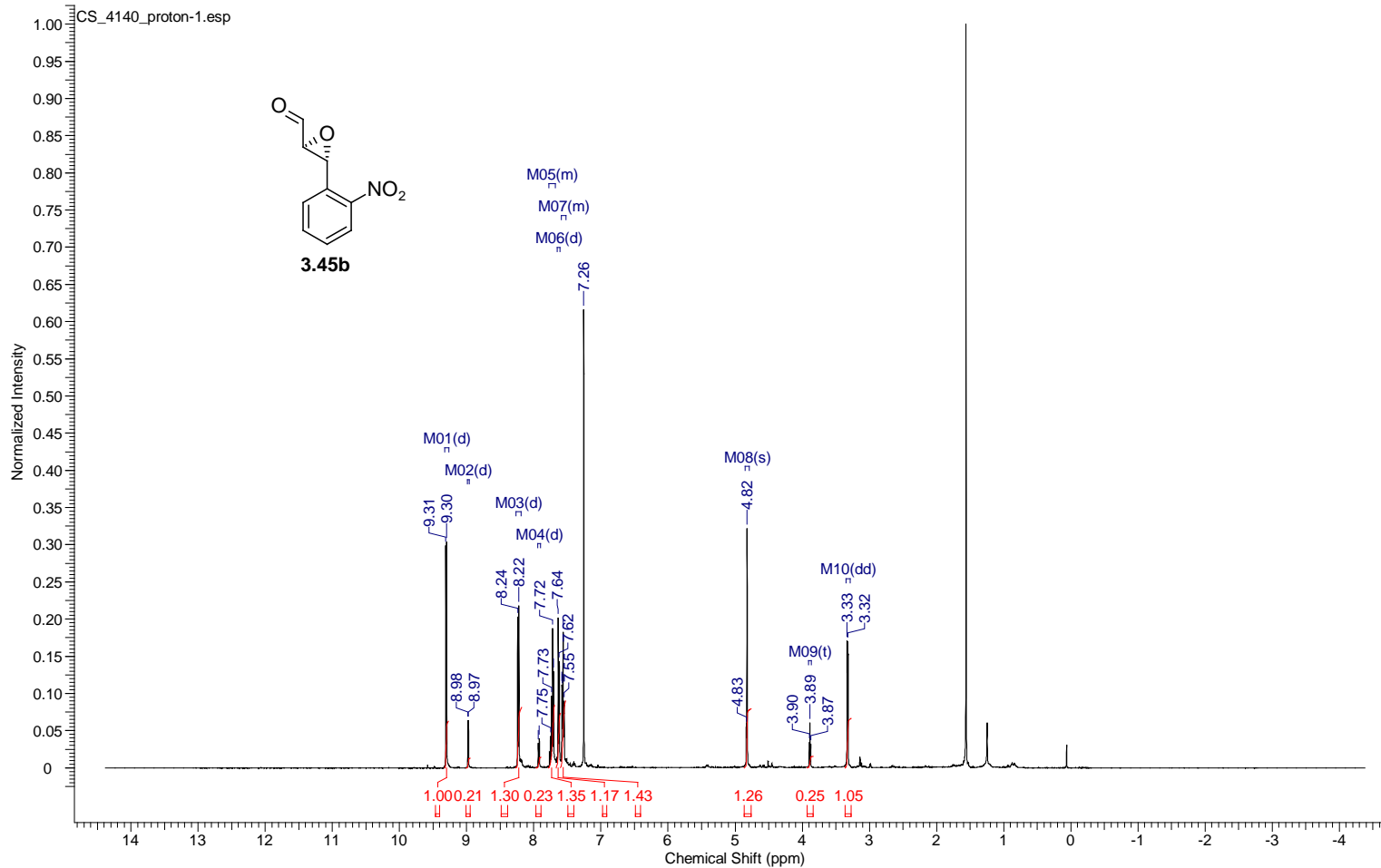
Acquisition Time (sec)	1.7459	Comment	single_pulse	Date	22 Aug 2012 08:27:31
Date Stamp	23 Aug 2012 00:46:14				
File Name	C:\Users\chen\Desktop\study\Foss\Shuai's Data\NMR DATA\500MHz\2\aaaron\proton\CS_4124_proton_2-1.jdf				
Frequency (MHz)	500.16	Nucleus	1H	Number of Transients	6
Original Points Count	16384	Owner	delta	Points Count	16384
Receiver Gain	42.00	Solvent	CHLOROFORM-d	Spectrum Offset (Hz)	2500.7996
Spectrum Type	STANDARD	Sweep Width (Hz)	9384.38	Temperature (degree C)	22.100



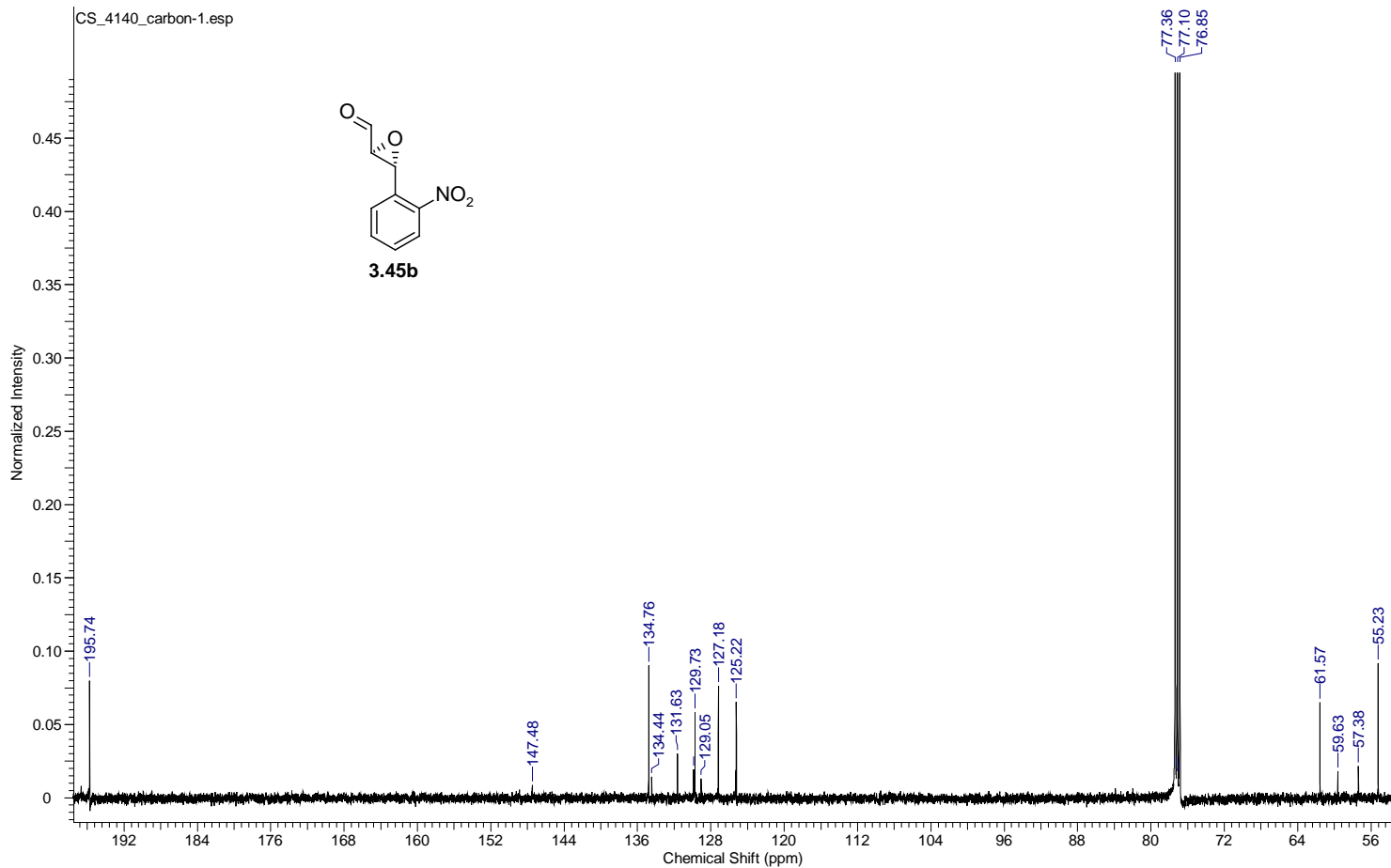
Acquisition Time (sec)	0.8336	Comment	single pulse decoupled gated NOE	Date	10 Aug 2012 12:52:59
Date Stamp	11 Aug 2012 05:11:37				
File Name	C:\Users\chen\Desktop\study\Foss\Shuai's Data\NMR DATA\500MHz083012\aaaron\carbon\CS_4113_product_carbon-1.jdf				
Frequency (MHz)	125.77	Nucleus	¹³ C	Number of Transients	70
Original Points Count	32768	Owner	delta	Points Count	32768
Receiver Gain	50.00	Solvent	CHLOROFORM-d	Spectrum Offset (Hz)	12576.5293
Sweep Width (Hz)	39308.18	Temperature (degree C)	22.400	Spectrum Type	STANDARD



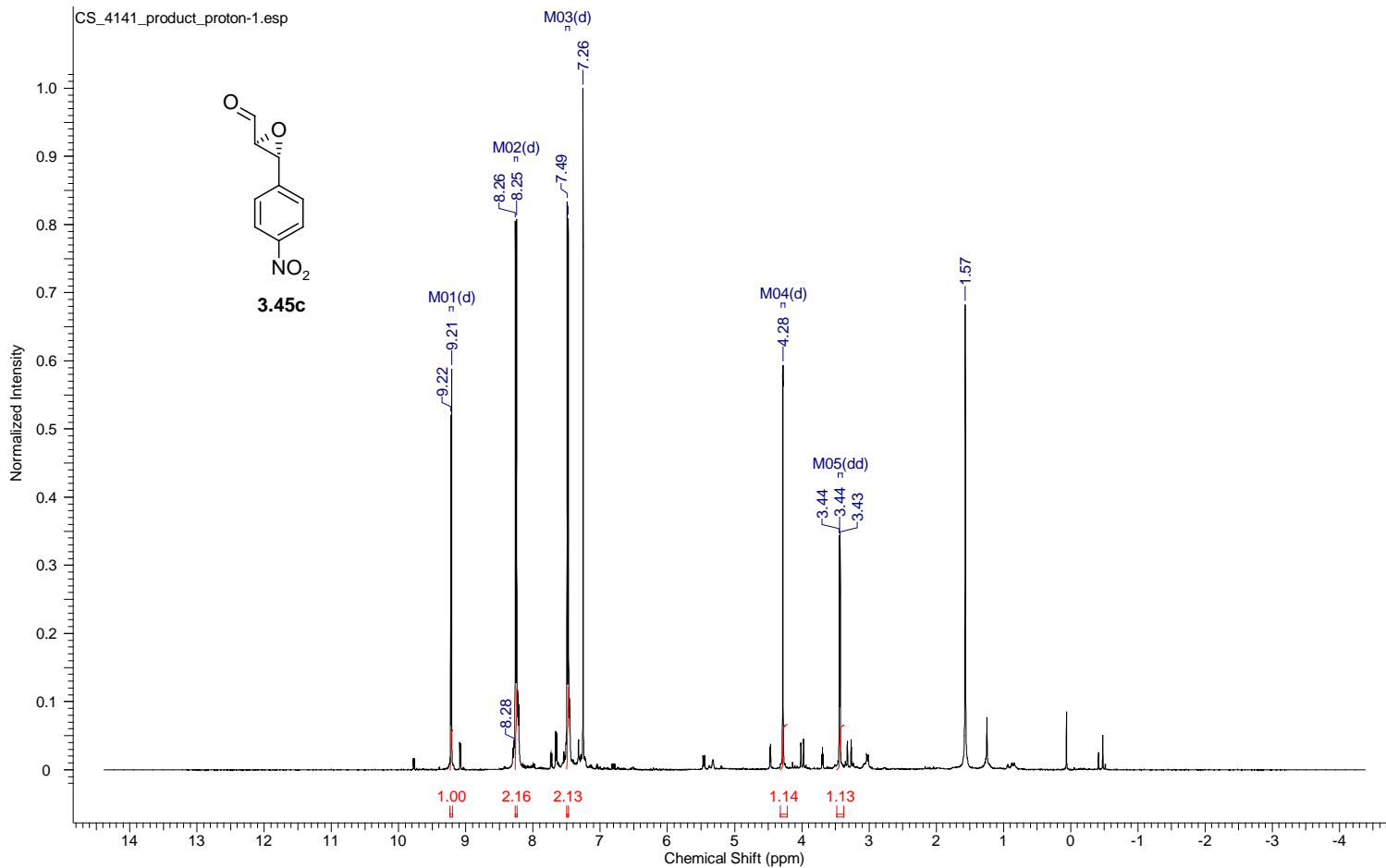
Acquisition Time (sec)	1.7459	Comment	single_pulse	Date	03 Sep 2012 09:31:51
Date Stamp	04 Sep 2012 01:50:39				
File Name	C:\Users\chen\Desktop\study\Foss\Shuai's Data\NMR DATA\500MHz083012\aaaron\proton\CS_4140_proton-1.jdf			Frequency (MHz)	500.16
Nucleus	1H	Number of Transients	8	Origin	ECA 500
Owner	delta	Points Count	16384	Pulse Sequence	single_pulse.ex2
Solvent	CHLOROFORM-d			Spectrum Offset (Hz)	2500.7996
Sweep Width (Hz)	9384.38	Temperature (degree C)	22.000	Spectrum Type	STANDARD



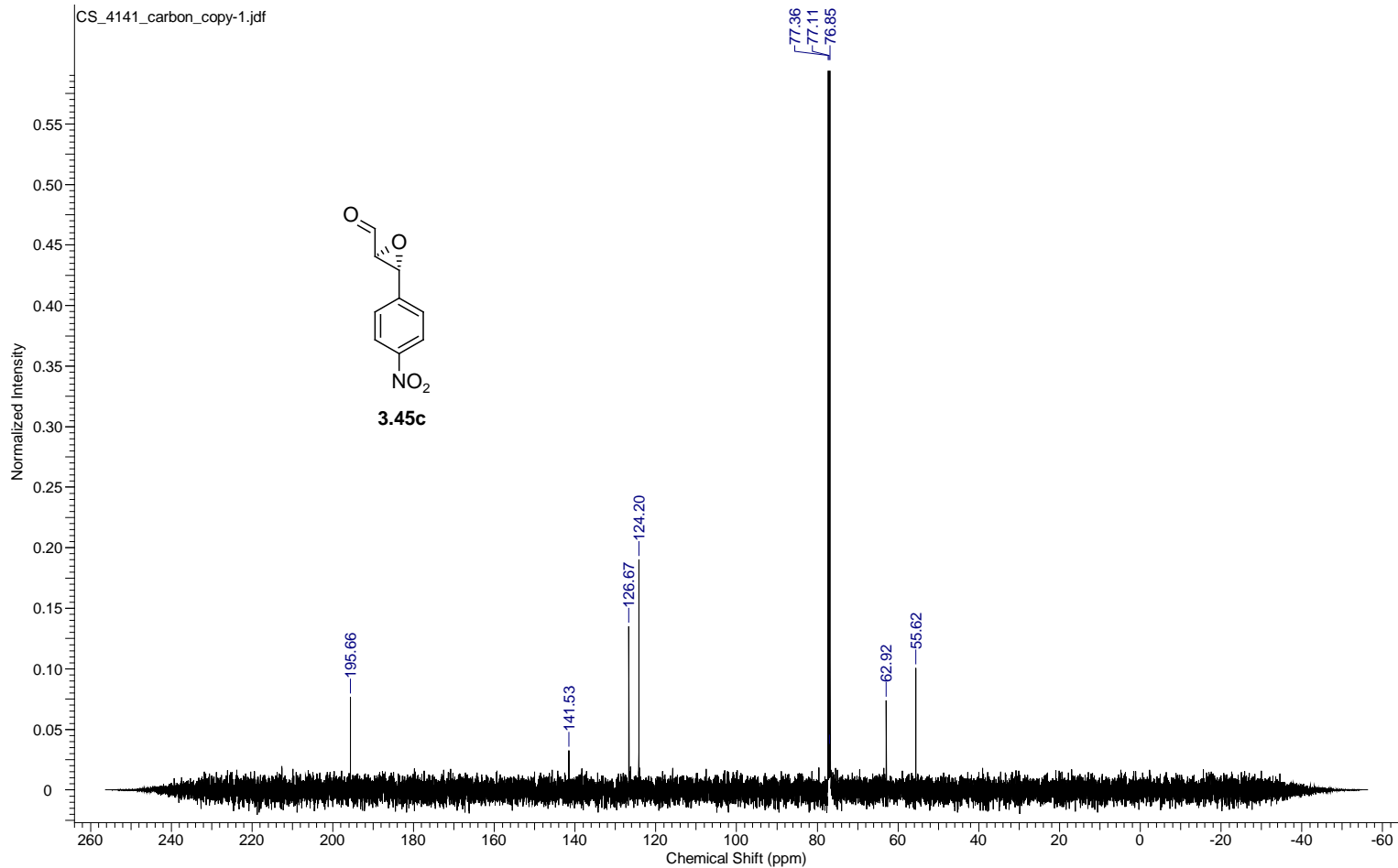
Acquisition Time (sec)	0.8336	Comment	single pulse decoupled gated NOE		Date	03 Sep 2012 10:08:01	
Date Stamp	04 Sep 2012 02:26:49						
File Name	C:\Users\chen\Desktop\study\Foss\Shuai's Data\NMR DATA\500MHz083012\aaaron\carbon\CS_4140_carbon-1.jdf			Frequency (MHz)	125.77		
Nucleus	¹³ C	Number of Transients	1000	Origin	ECA 500		
Owner	delta	Points Count	32768	Pulse Sequence	single_pulse_dec	Receiver Gain	50.00
Solvent	CHLOROFORM-d	Spectrum Offset (Hz)	12576.5293	Spectrum Type	STANDARD		
Temperature (degree C)	22.700						



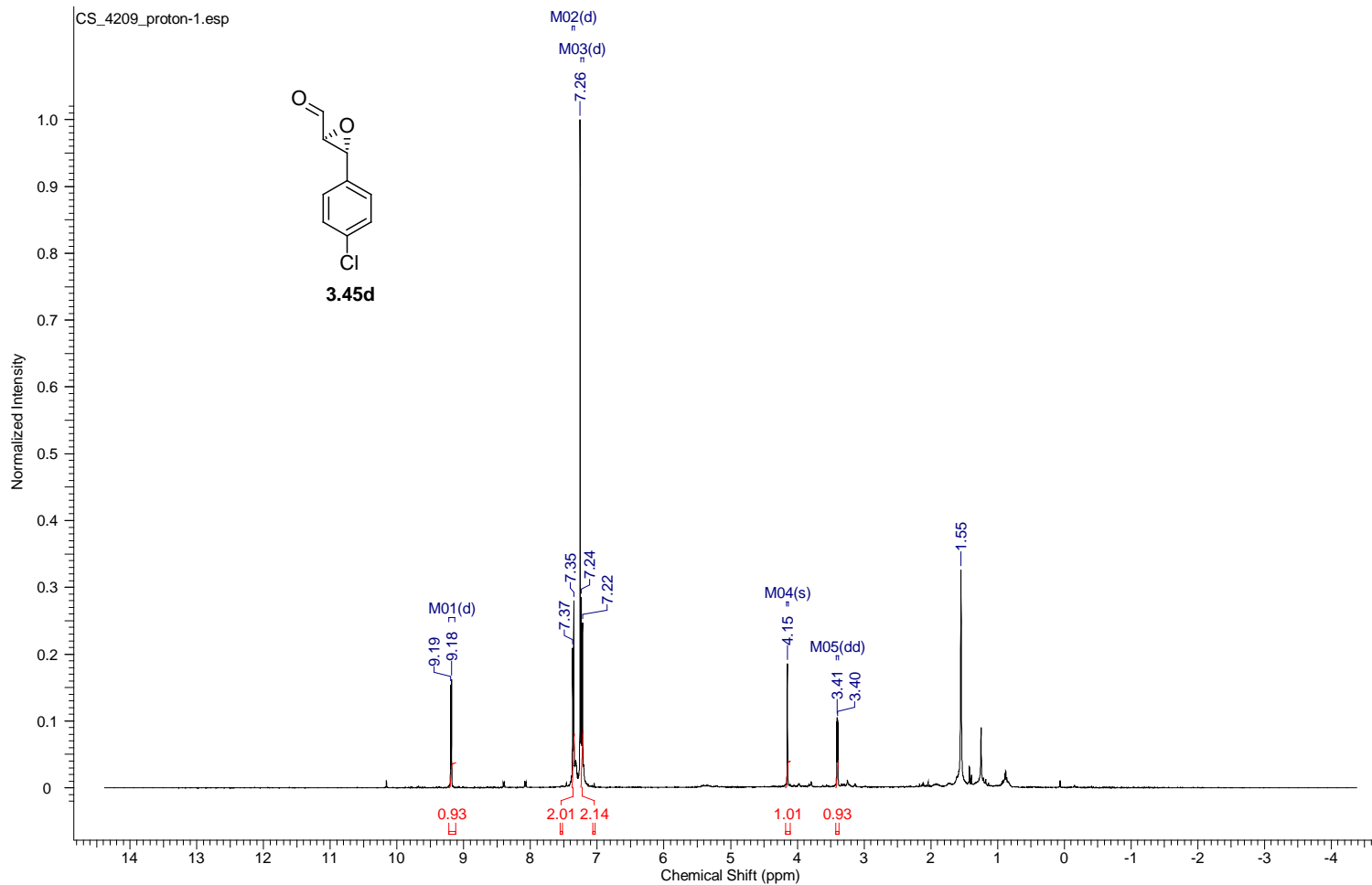
Acquisition Time (sec)	1.7459	Comment	single_pulse	Date	31 Aug 2012 11:21:37
Date Stamp	01 Sep 2012 03:40:23				
File Name	C:\Users\chen\Desktop\study\Foss\Shuai's Data\NMR DATA\500MHz\083012\aaaron\proton\CS_4141_product_proton-1.jdf				
Frequency (MHz)	500.16	Nucleus	1H	Number of Transients	7
Original Points Count	16384	Owner	delta	Points Count	16384
Receiver Gain	48.00	Solvent	CHLOROFORM-d	Spectrum Offset (Hz)	2500.7996
Sweep Width (Hz)	9384.38	Temperature (degree C)	22.200	Spectrum Type	STANDARD



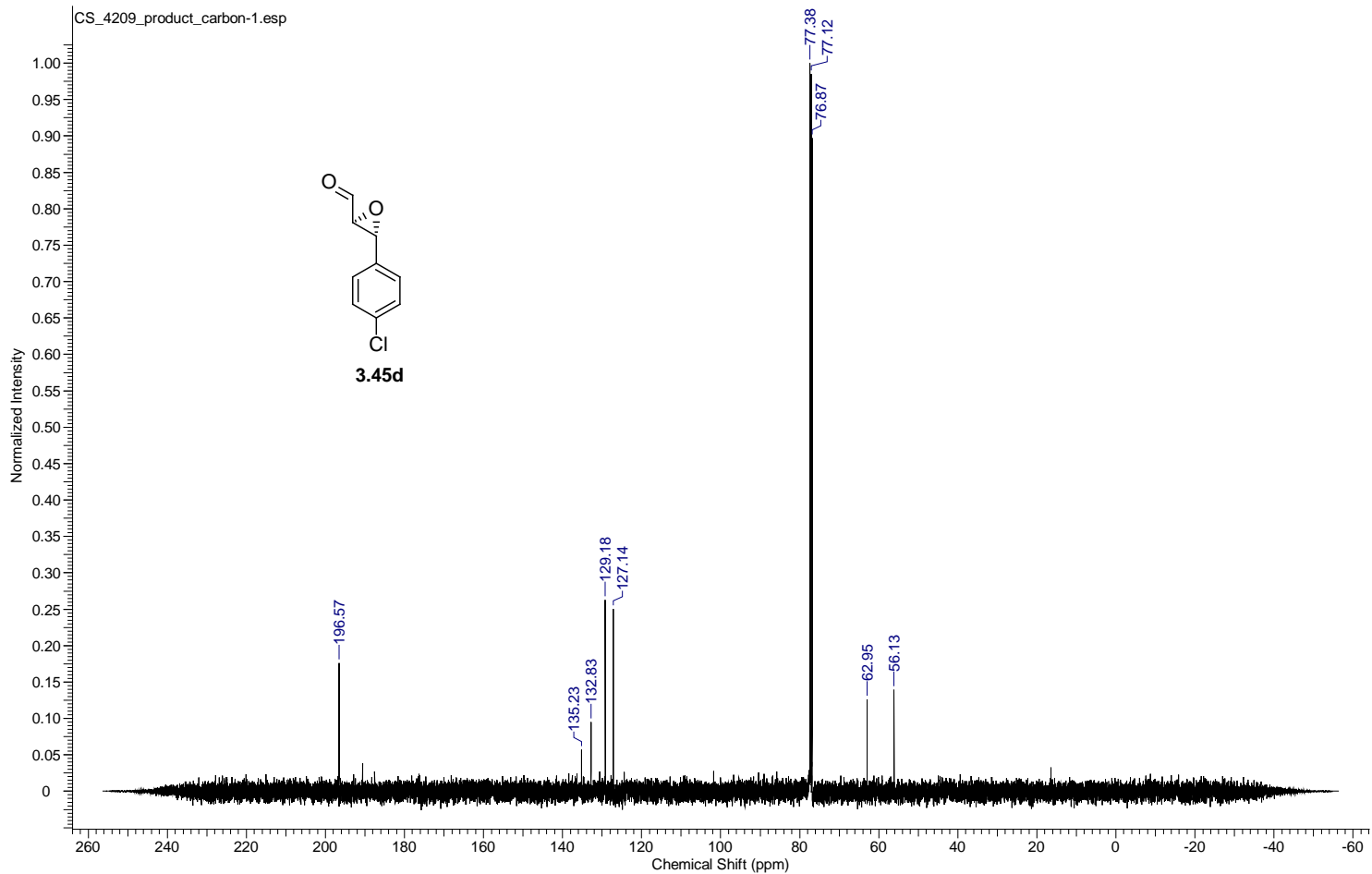
Acquisition Time (sec)	0.8336	Comment	single pulse decoupled gated NOE	Date	31 Aug 2012 11:24:05
Date Stamp	01 Sep 2012 03:42:51				
File Name	C:\Users\chen\Desktop\study\Foss\Shuai's Data\NMR DATA\500MHz083012\aaaron\carbon\CS_4141_carbon_copy-1.jdf			Frequency (MHz)	125.77
Nucleus	13C	Number of Transients	60	Origin	ECA 500
Owner	delta	Points Count	32768	Pulse Sequence	single_pulse_dec
Solvent	CHLOROFORM-d	Spectrum Offset (Hz)	12576.5293	Spectrum Type	STANDARD
Temperature (degree C)	22.600			Receiver Gain	50.00
				Sweep Width (Hz)	39308.18



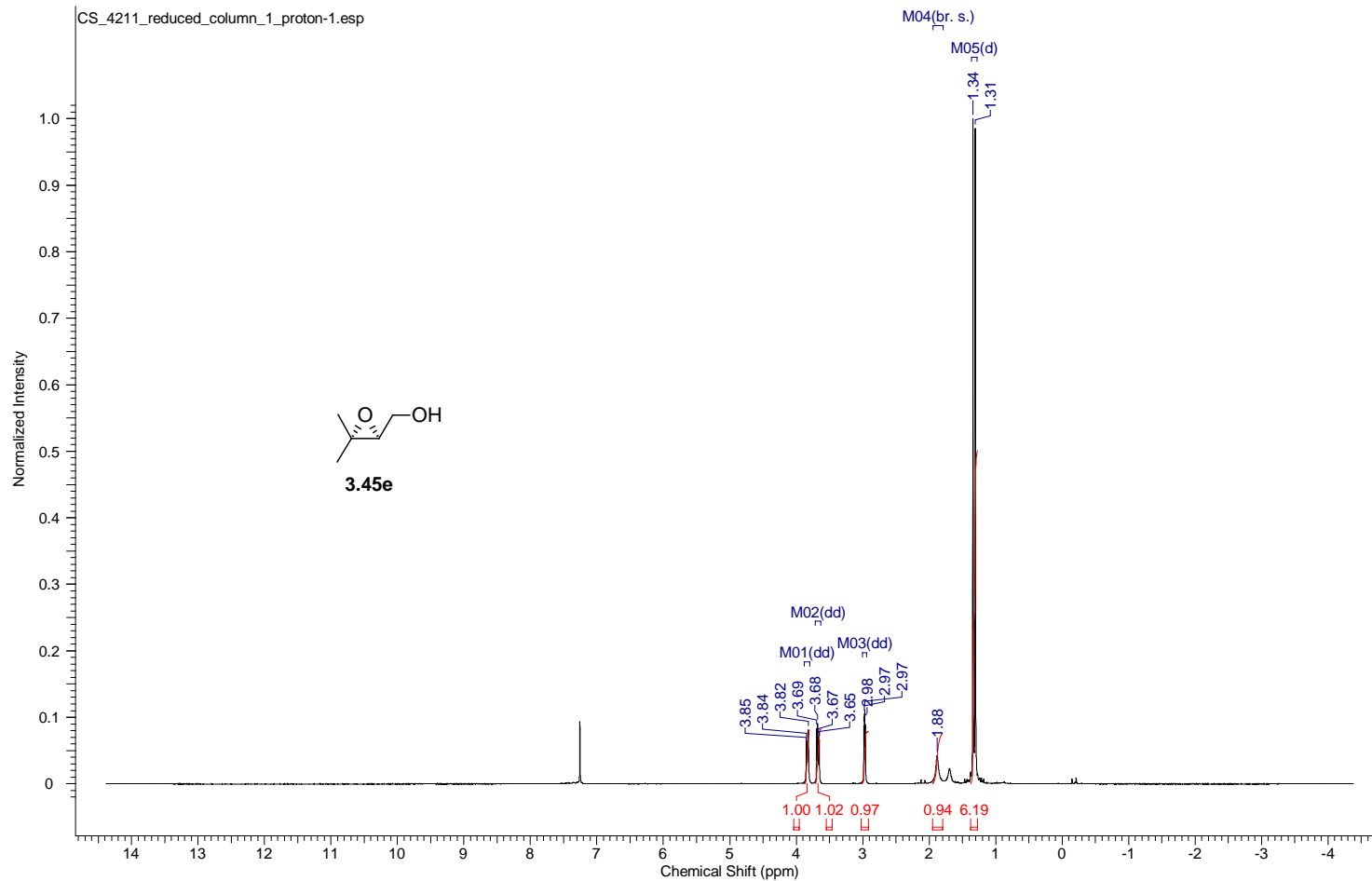
Acquisition Time (sec)	1.7459	Comment	single_pulse	Date	15 Nov 2012 08:13:37
Date Stamp	16 Nov 2012 01:00:25	File Name	G:\500MHz\111612\aaaron\proton\CS_4209_proton-1.jdf		
Frequency (MHz)	500.16	Nucleus	1H	Number of Transients	16
Original Points Count	16384	Owner	delta	Points Count	16384
Receiver Gain	50.00	Solvent	CHLOROFORM-d	Pulse Sequence	single_pulse.ex2
Spectrum Type	STANDARD	Sweep Width (Hz)	9384.38	Temperature (degree C)	20.800



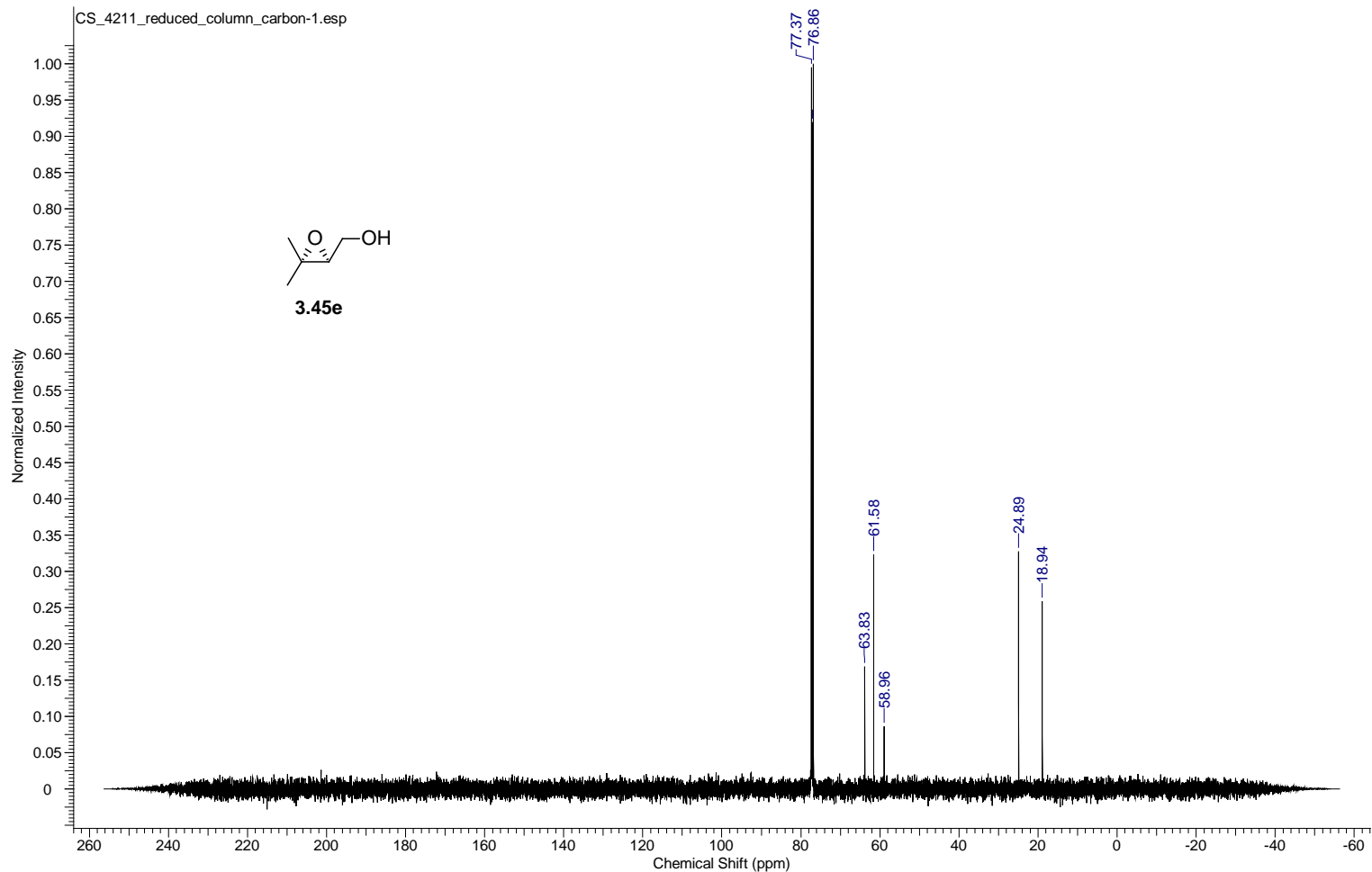
Acquisition Time (sec)	0.8336	Comment	single pulse decoupled gated NOE	Date	14 Nov 2012 07:23:43
Date Stamp	15 Nov 2012 00:10:30	File Name	G:\500MHz111612\laaron\carbon\CS_4209_product_carbon-1.jdf	Frequency (MHz)	125.77
Frequency (MHz)	125.77	Nucleus	¹³ C	Number of Transients	20
Original Points Count	32768	Owner	delta	Points Count	32768
Receiver Gain	50.00	Solvent	CHLOROFORM-d	Pulse Sequence	single_pulse_dec
Spectrum Type	STANDARD	Sweep Width (Hz)	39308.18	Temperature (degree C)	21.200
				Spectrum Offset (Hz)	12576.5293



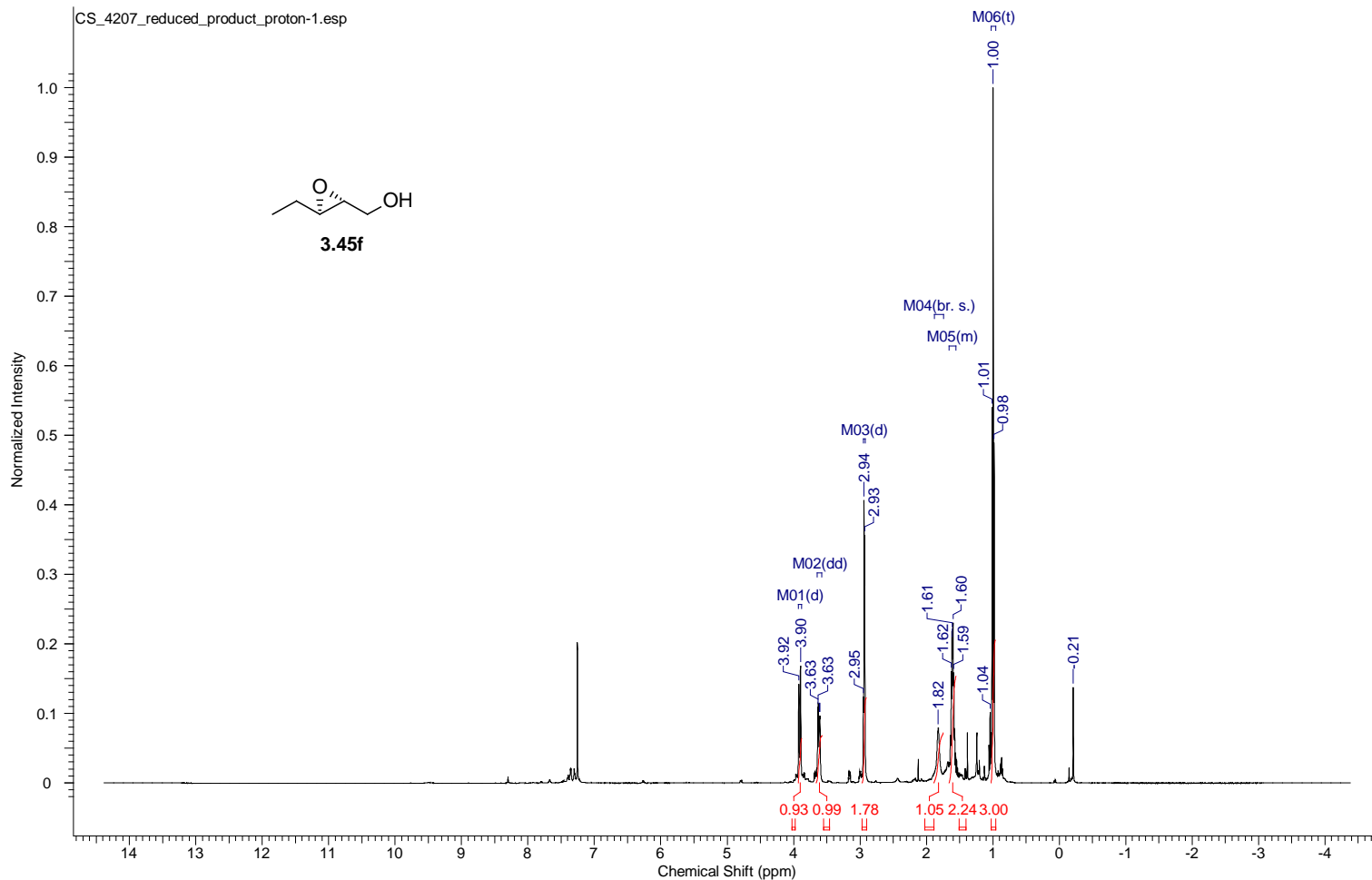
Acquisition Time (sec)	1.7459	Comment	single_pulse	Date	21 Nov 2012 07:14:11		
Date Stamp	22 Nov 2012 00:01:53	File Name	G:\500MHz\111612\aaaron\proton\CS_4211_reduced_column_1_proton-1.jdf				
Frequency (MHz)	500.16	Nucleus	1H	Number of Transients	10	Origin	ECA 500
Original Points Count	16384	Owner	delta	Points Count	16384	Pulse Sequence	single_pulse.ex2
Receiver Gain	42.00	Solvent	CHLOROFORM-d	Spectrum Offset (Hz)	2500.7996		
Spectrum Type	STANDARD	Sweep Width (Hz)	9384.38	Temperature (degree C)	21.000		



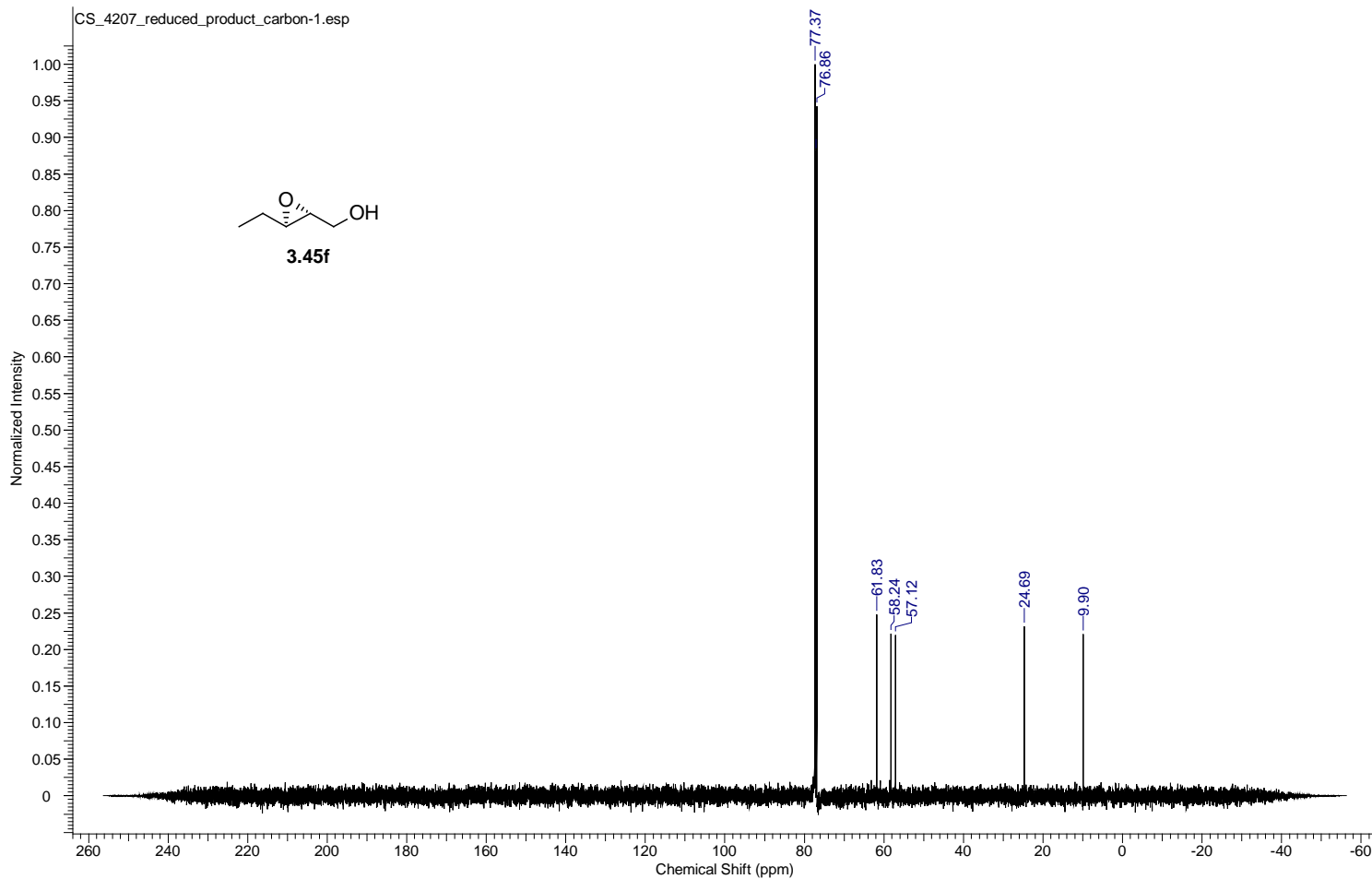
Acquisition Time (sec)	0.8336	Comment	single pulse decoupled gated NOE	Date	21 Nov 2012 07:16:31
Date Stamp	22 Nov 2012 00:04:13	File Name	G:\500MHz111612\laaron\carbon\CS_4211_reduced_column_carbon-1.jdf		
Frequency (MHz)	125.77	Nucleus	13C	Number of Transients	50
Original Points Count	32768	Owner	delta	Points Count	32768
Receiver Gain	50.00	Solvent	CHLOROFORM-d	Pulse Sequence	single_pulse_dec
Spectrum Type	STANDARD	Sweep Width (Hz)	39308.18	Temperature (degree C)	21.400



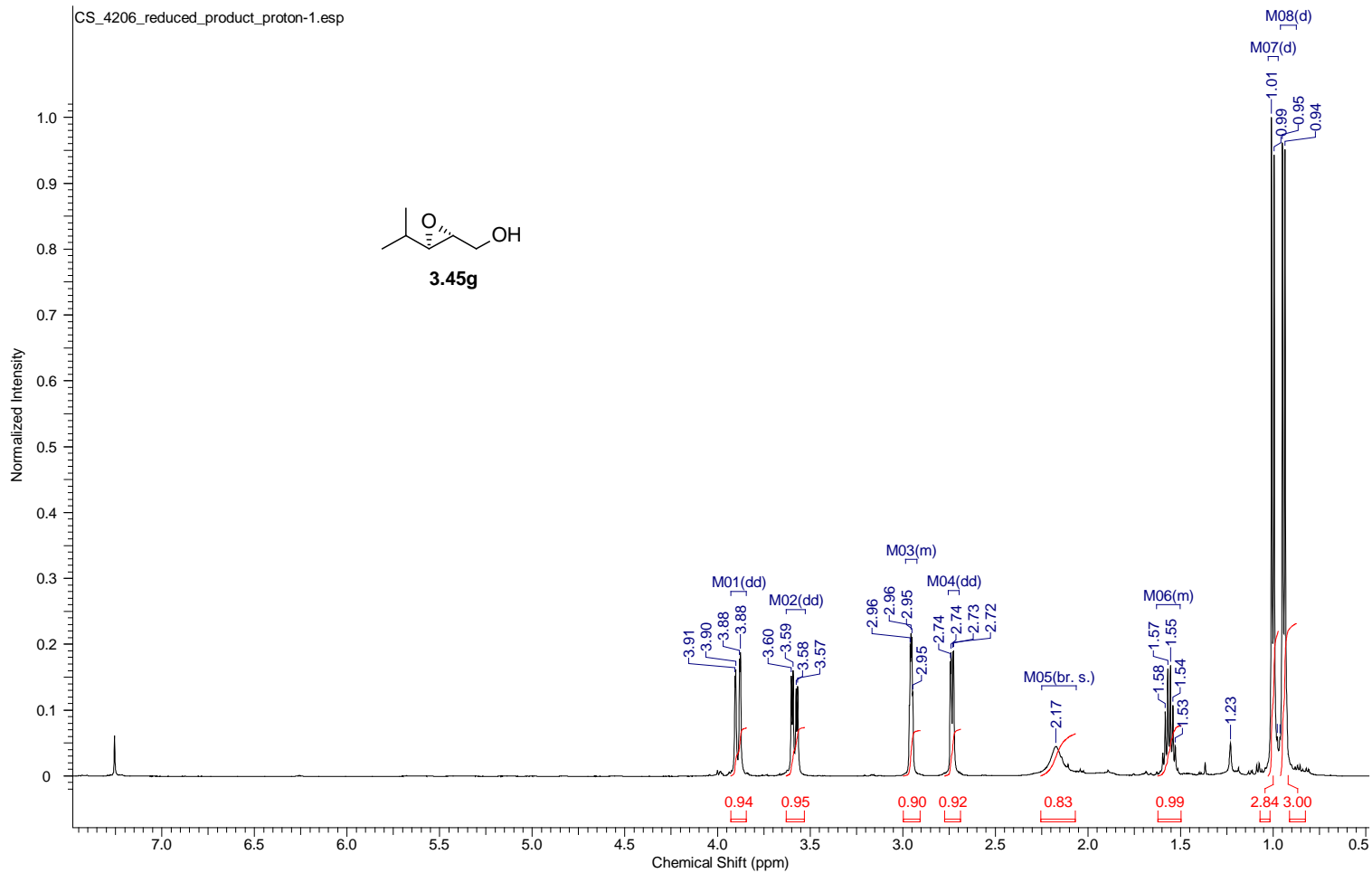
Acquisition Time (sec)	1.7459	Comment	single_pulse	Date	12 Nov 2012 10:15:14
Date Stamp	13 Nov 2012 03:02:00	File Name	G:\500MHz\111612\aaaron\proton\CS_4207_reduced_product_proton-1.jdf		
Frequency (MHz)	500.16	Nucleus	1H	Number of Transients	10
Original Points Count	16384	Owner	delta	Points Count	16384
Receiver Gain	40.00	Solvent	CHLOROFORM-d	Pulse Sequence	single_pulse.ex2
Spectrum Type	STANDARD	Sweep Width (Hz)	9384.38	Spectrum Offset (Hz)	2500.7996
		Temperature (degree C)	21.100		



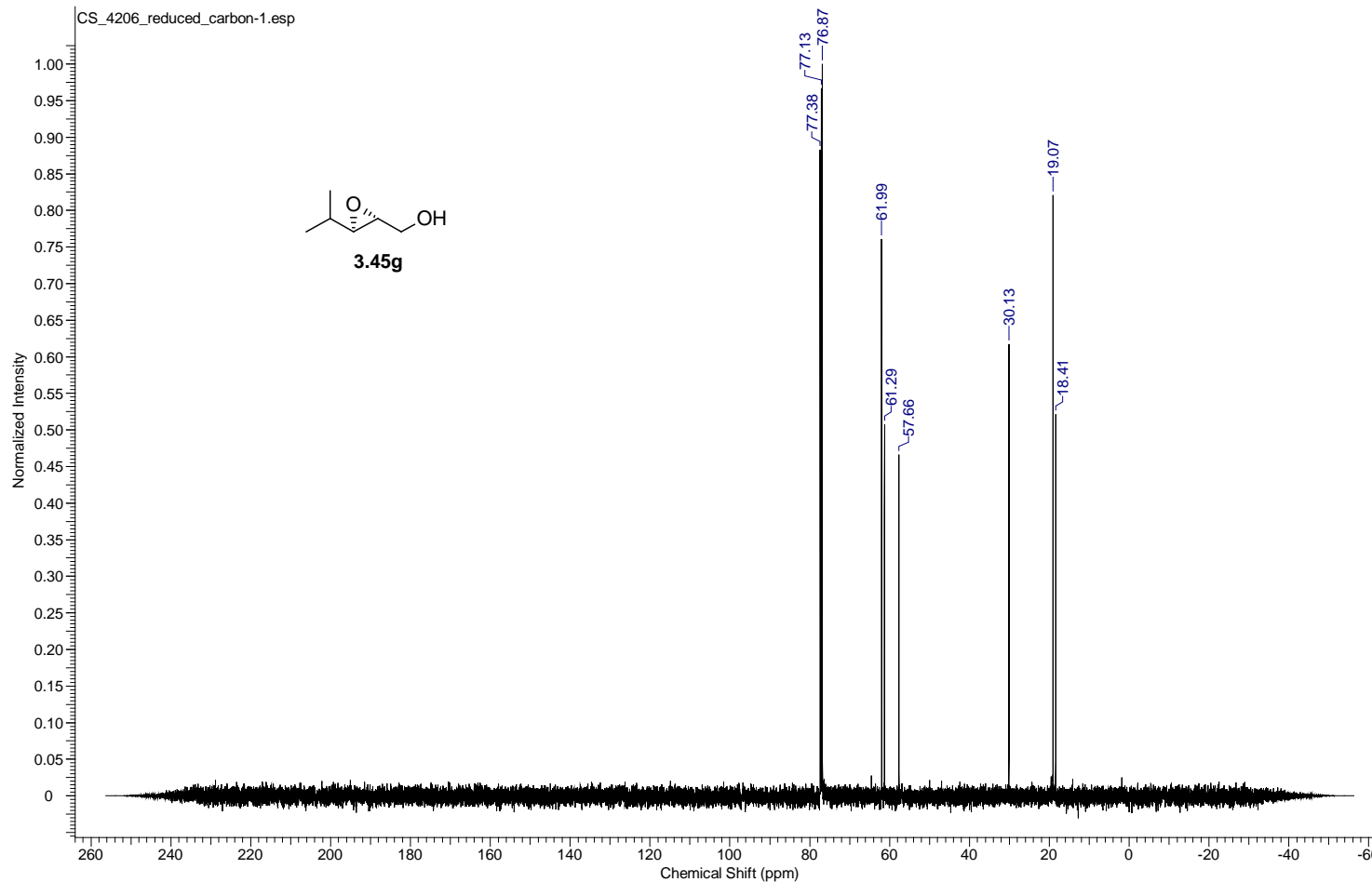
Acquisition Time (sec)	0.8336	Comment	single pulse decoupled gated NOE	Date	12 Nov 2012 10:17:33
Date Stamp	13 Nov 2012 03:04:20	File Name	G:\500MHz\111612\aaaron\carbon\CS_4207_reduced_product_carbon-1.jdf		
Frequency (MHz)	125.77	Nucleus	13C	Number of Transients	60
Original Points Count	32768	Owner	delta	Points Count	32768
Receiver Gain	50.00	Solvent	CHLOROFORM-d	Pulse Sequence	single_pulse_dec
Spectrum Type	STANDARD	Sweep Width (Hz)	39308.18	Temperature (degree C)	21.500



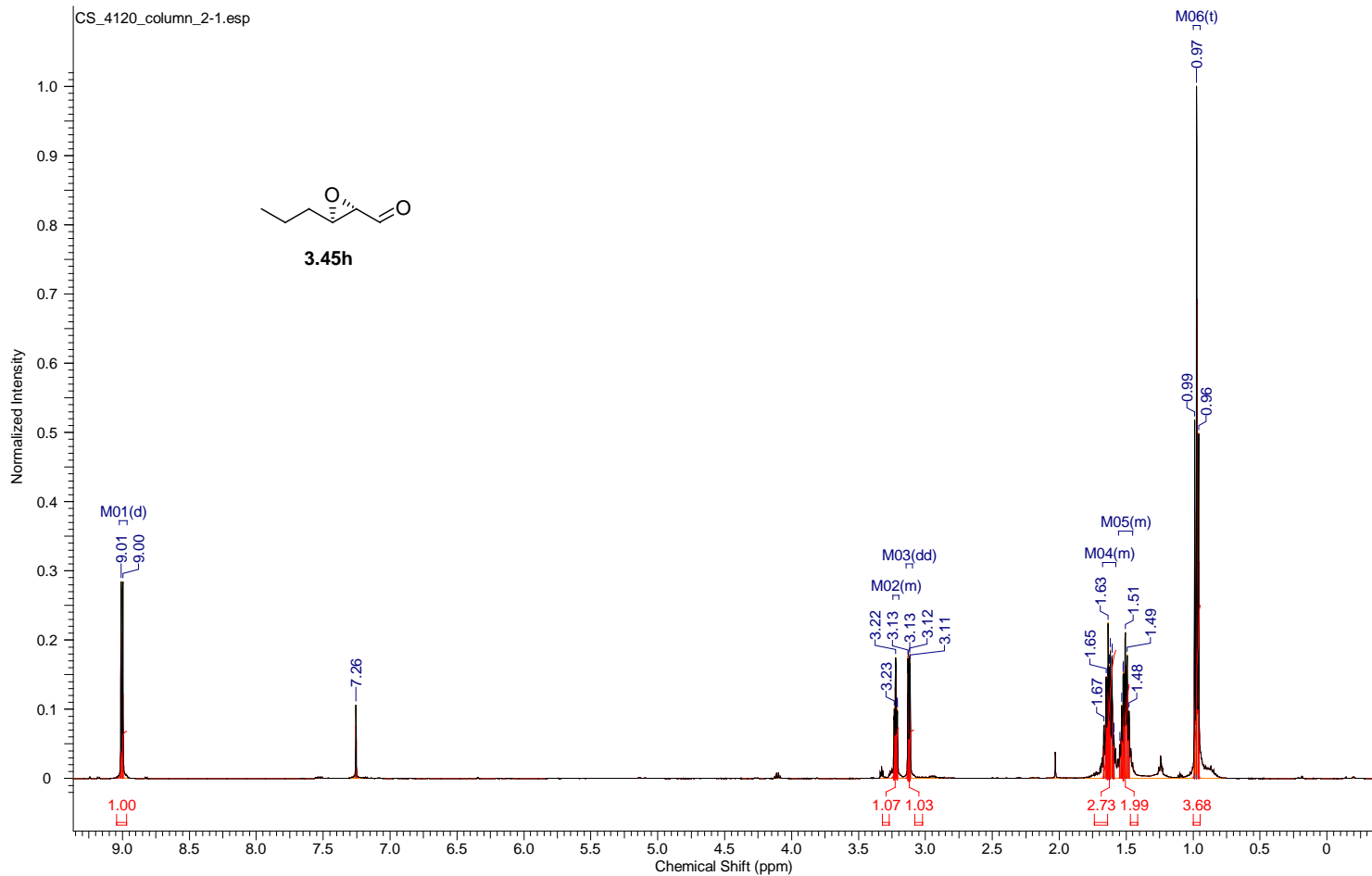
Acquisition Time (sec)	1.7459	Comment	single_pulse	Date	10 Nov 2012 12:34:08
Date Stamp	11 Nov 2012 05:20:54	File Name	G:\500MHz\111612\laaron\proton\CS_4206_reduced_product_proton-1.jdf		
Frequency (MHz)	500.16	Nucleus	1H	Origin	ECA 500
Original Points Count	16384	Owner	delta	Points Count	16384
Receiver Gain	30.00	Solvent	CHLOROFORM-d	Pulse Sequence	single_pulse.ex2
Spectrum Type	STANDARD	Sweep Width (Hz)	9384.38	Spectrum Offset (Hz)	2500.7996
		Temperature (degree C)	21.100		



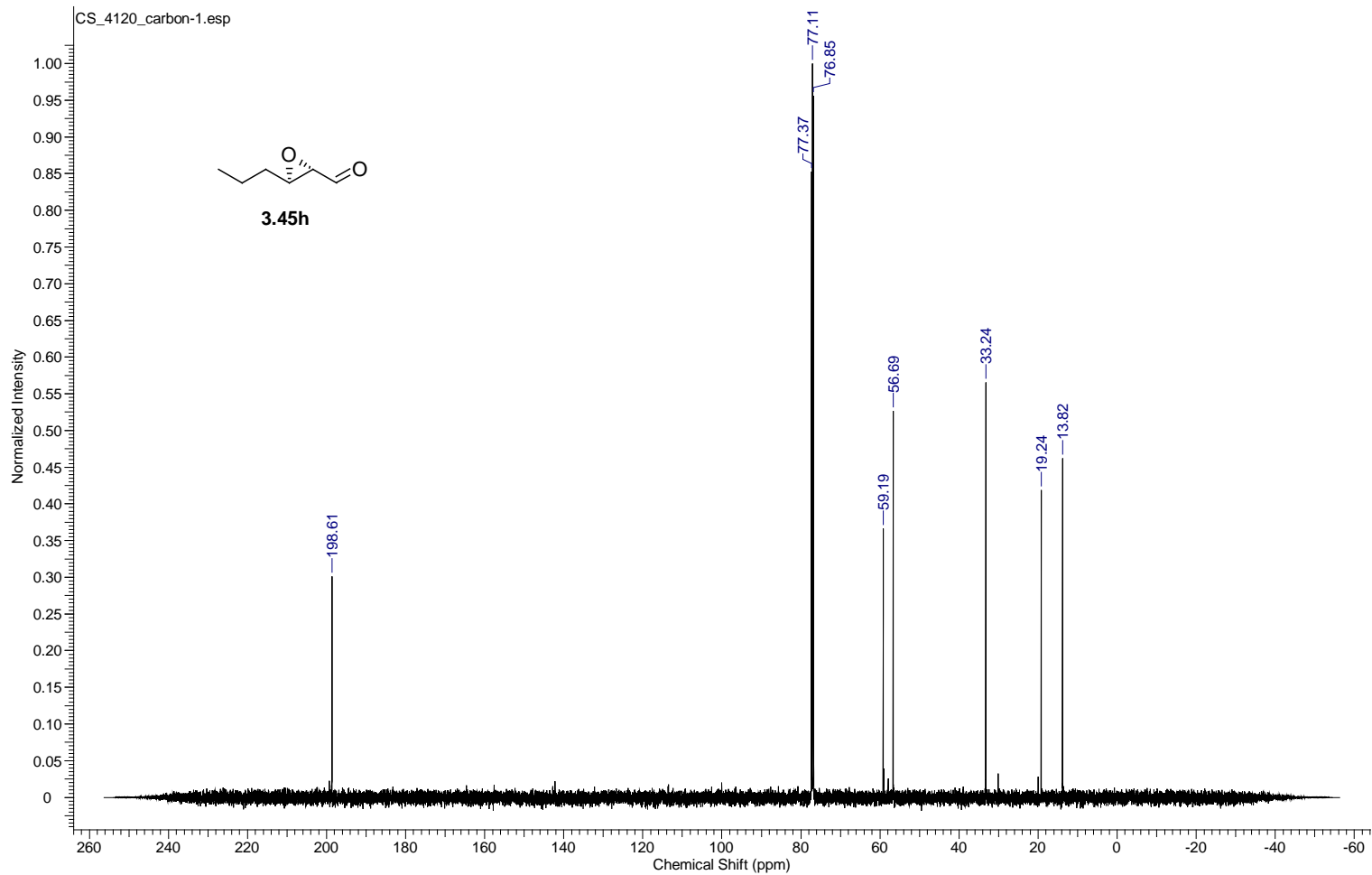
Acquisition Time (sec)	0.8336	Comment	single pulse decoupled gated NOE	Date	10 Nov 2012 12:36:08
Date Stamp	11 Nov 2012 05:22:53	File Name	G:\500MHz111612\laaron\carbon\CS_4206_reduced_carbon-1.jdf	Frequency (MHz)	125.77
Frequency (MHz)	125.77	Nucleus	13C	Number of Transients	50
Original Points Count	32768	Owner	delta	Points Count	32768
Receiver Gain	50.00	Solvent	CHLOROFORM-d	Pulse Sequence	single_pulse_dec
Spectrum Type	STANDARD	Sweep Width (Hz)	39308.18	Temperature (degree C)	21.500
				Spectrum Offset (Hz)	12576.5293



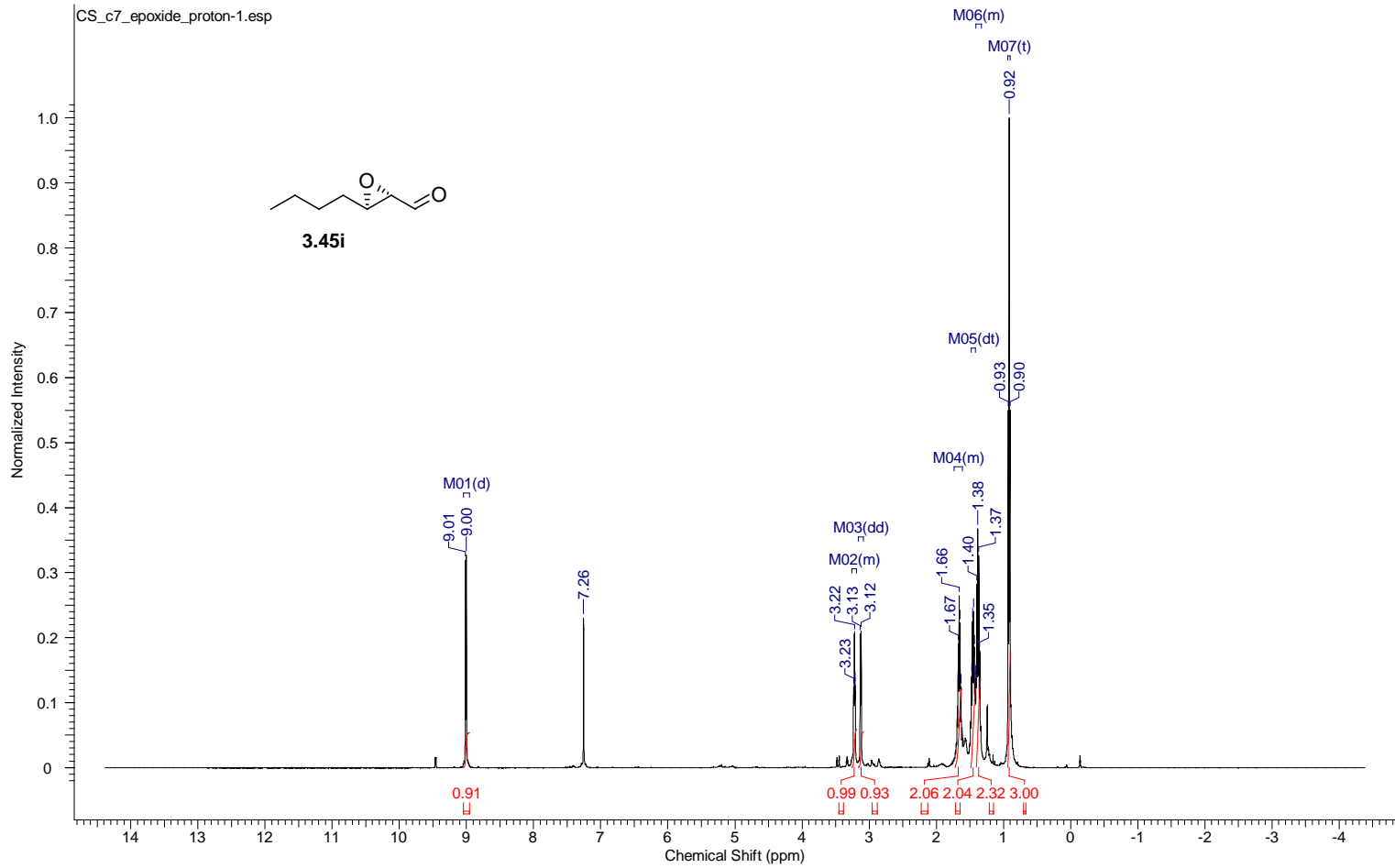
Acquisition Time (sec)	1.7459	Comment	single_pulse	Date	20 Aug 2012 12:13:47
Date Stamp	21 Aug 2012 04:32:29	File Name	G:\500MHz\083012\aaaron\proton\CS_4120_column_2-1.jdf		
Frequency (MHz)	500.16	Nucleus	1H	Number of Transients	9
Original Points Count	16384	Owner	delta	Points Count	16384
Receiver Gain	36.00	Solvent	CHLOROFORM-d	Pulse Sequence	single_pulse.ex2
Spectrum Type	STANDARD	Sweep Width (Hz)	9384.38	Temperature (degree C)	22.100
				Spectrum Offset (Hz)	2500.7996



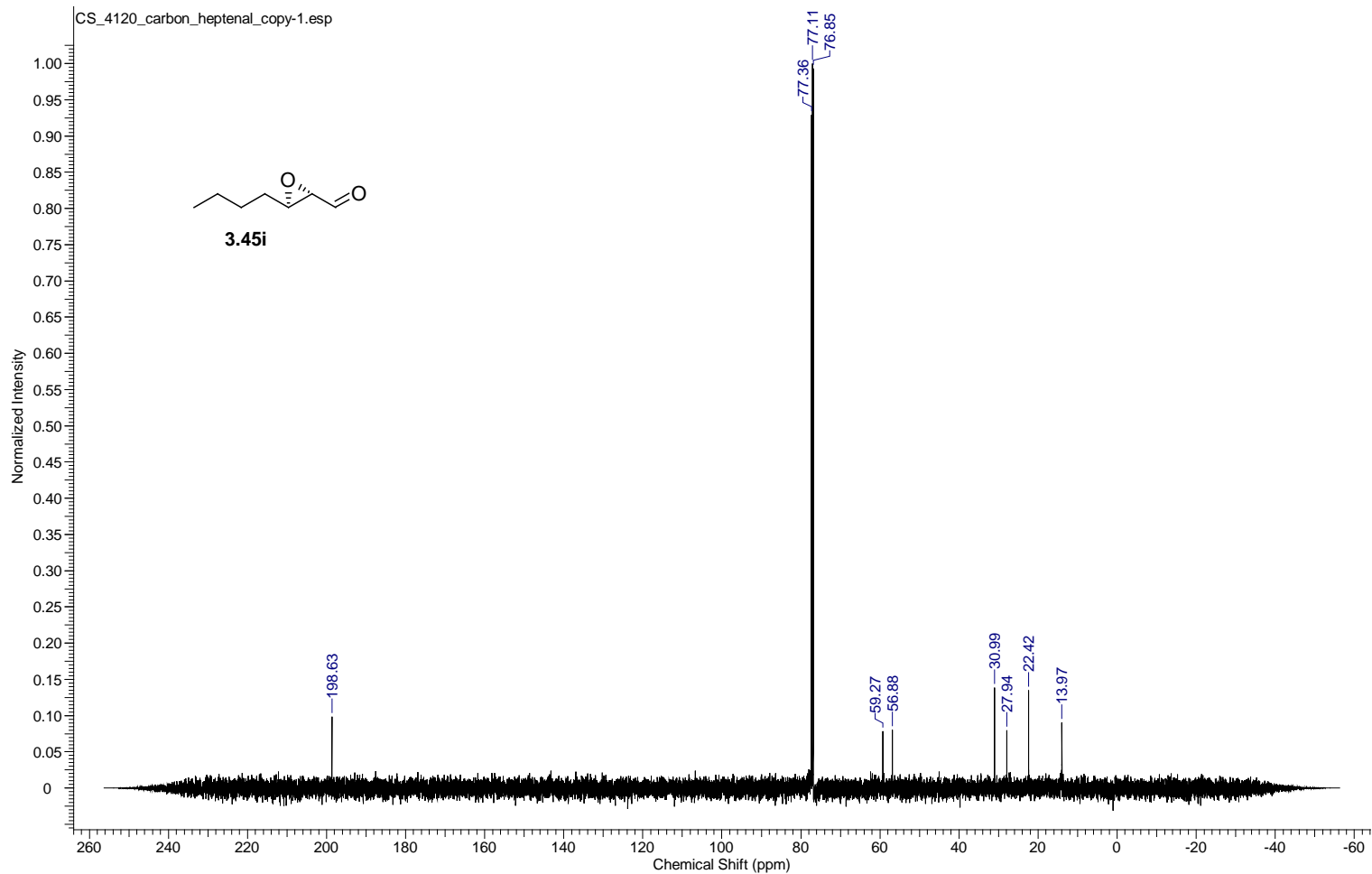
Acquisition Time (sec)	0.8336	Comment	single pulse decoupled gated NOE	Date	20 Aug 2012 12:18:53
Date Stamp	21 Aug 2012 04:37:34	File Name	G:\500MHz082412\laaron\carbon\CS_4120_carbon-1.jdf	Number of Transients	130
Frequency (MHz)	125.77	Nucleus	¹³ C	Origin	ECA 500
Original Points Count	32768	Owner	delta	Points Count	32768
Receiver Gain	50.00	Solvent	CHLOROFORM-d	Pulse Sequence	single_pulse_dec
Spectrum Type	STANDARD	Sweep Width (Hz)	39308.18	Temperature (degree C)	22.700
				Spectrum Offset (Hz)	12576.5293



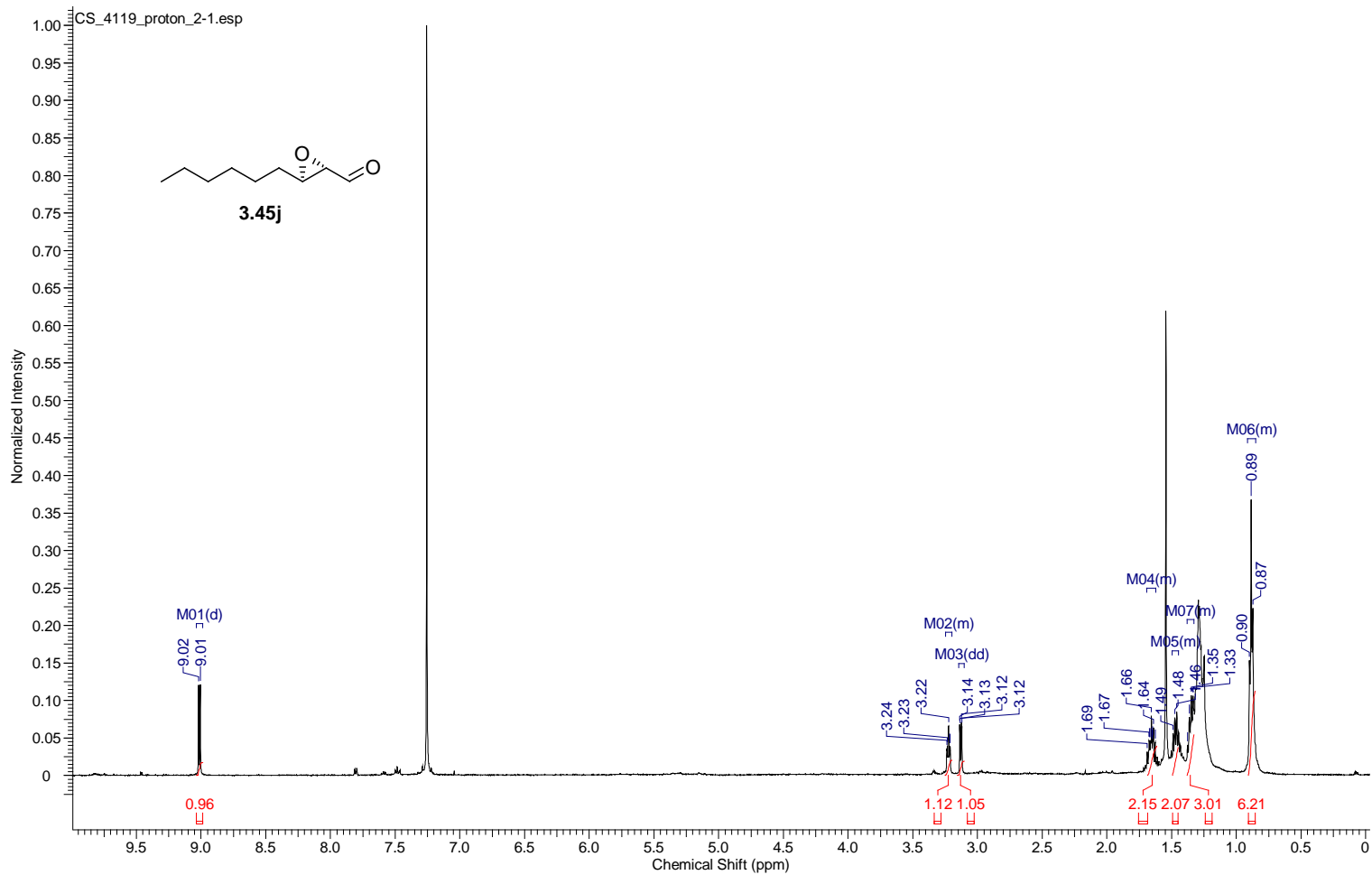
Acquisition Time (sec)	1.7459	Comment	single_pulse	Date	21 Feb 2013 12:57:16
Date Stamp	22 Feb 2013 05:40:26				
File Name	C:\Users\chen\Desktop\study\Foss\Shuai's Data\NMR DATA\500MHz\022213\aaaron\proton\CS_c7_epoxide_proton-1.jdf				
Frequency (MHz)	500.16	Nucleus	¹ H	Number of Transients	5
Original Points Count	16384	Owner	delta	Points Count	16384
Receiver Gain	42.00	Solvent	CHLOROFORM-d	Spectrum Offset (Hz)	2500.7996
Sweep Width (Hz)	9384.38	Temperature (degree C)	20.700	Spectrum Type	STANDARD



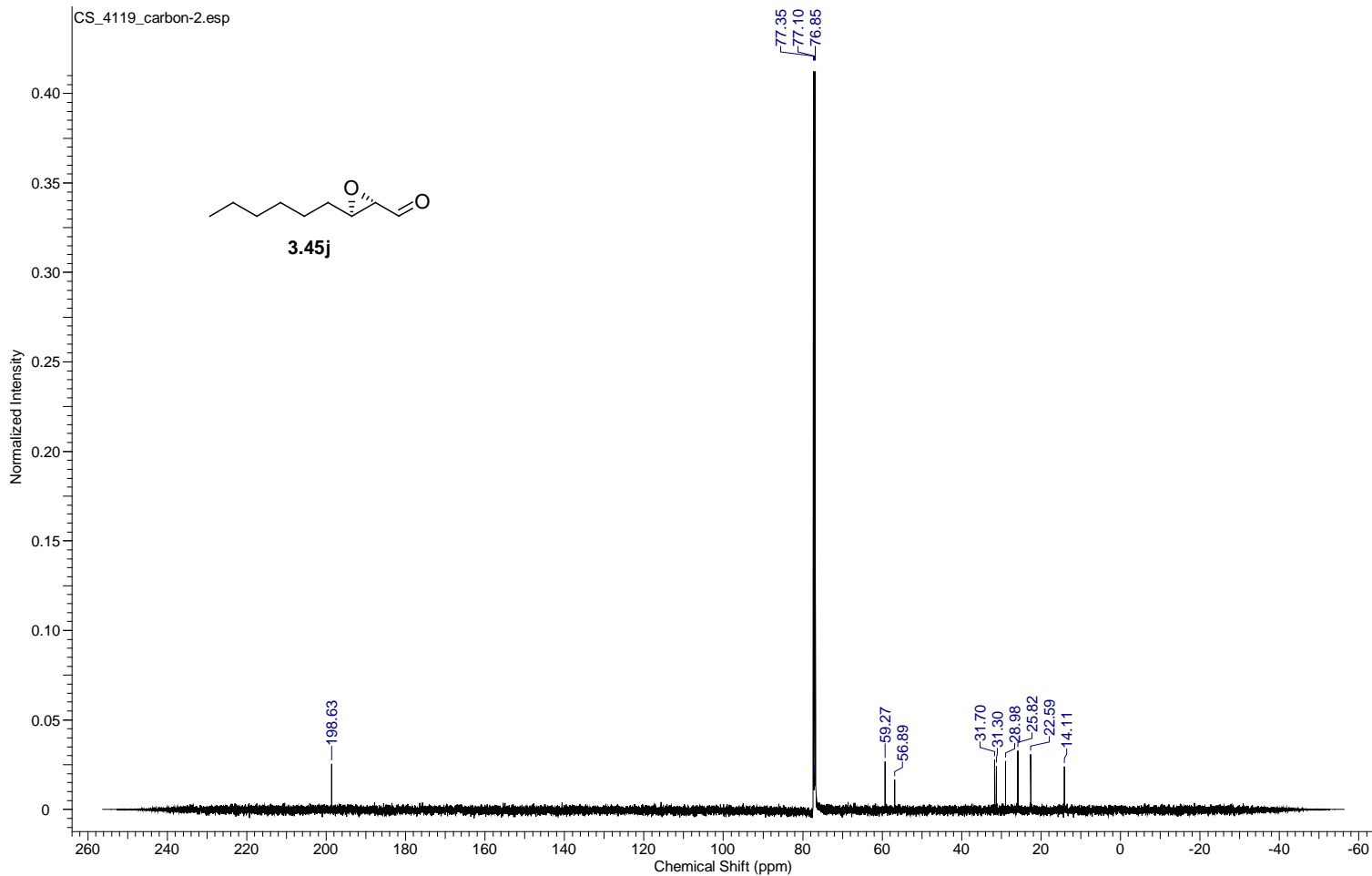
Acquisition Time (sec)	0.8336	Comment	single pulse decoupled gated NOE	Date	20 Aug 2012 13:23:06
Date Stamp	21 Aug 2012 05:41:47	File Name	G:\500MHz082412\laaron\carbon\CS_4120_carbon_heptenal_copy-1.jdf	Origin	ECA 500
Frequency (MHz)	125.77	Nucleus	13C	Number of Transients	40
Original Points Count	32768	Owner	delta	Points Count	32768
Receiver Gain	50.00	Solvent	CHLOROFORM-d	Pulse Sequence	single_pulse_dec
Spectrum Type	STANDARD	Sweep Width (Hz)	39308.18	Temperature (degree C)	22.500
				Spectrum Offset (Hz)	12576.5293



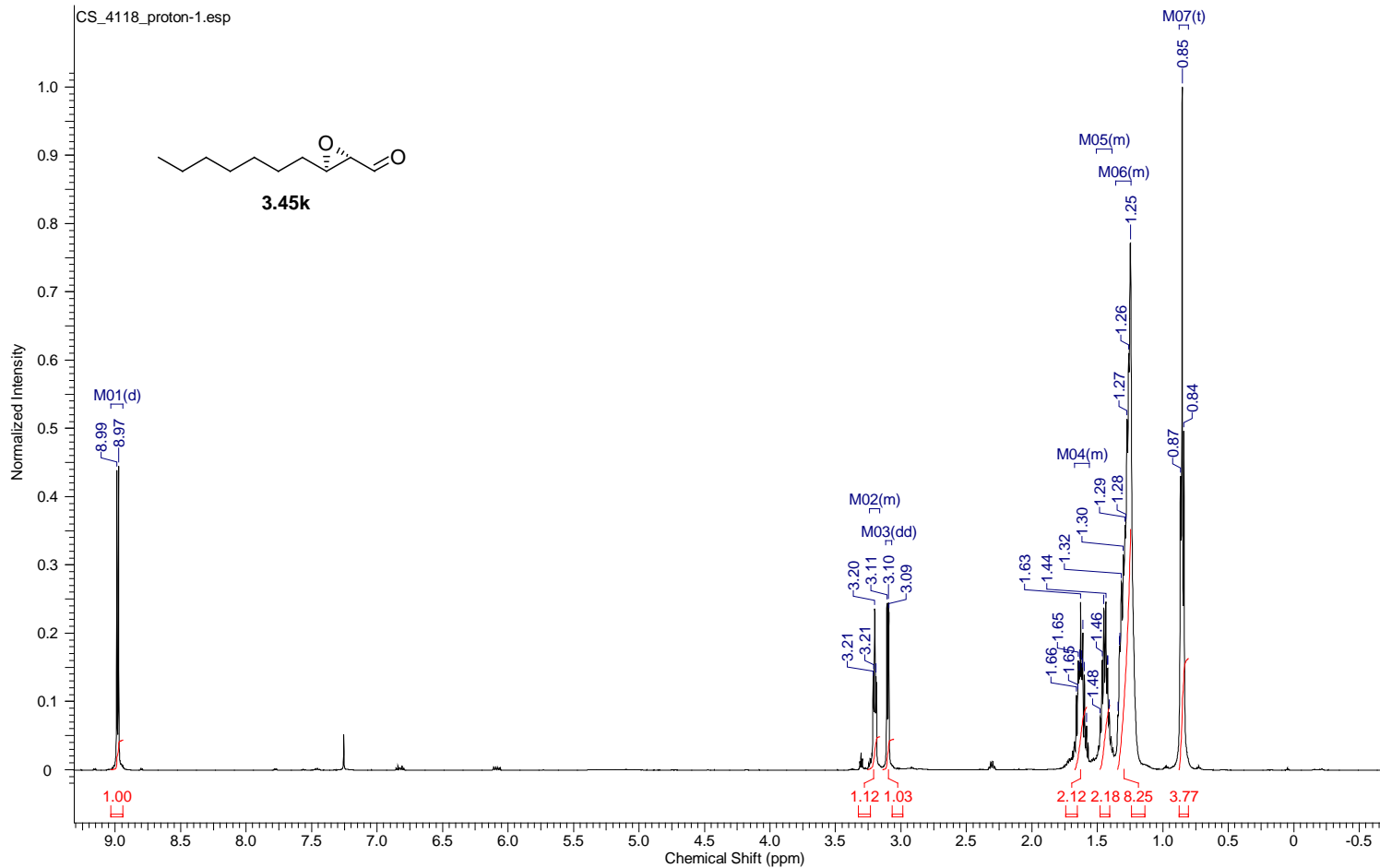
Acquisition Time (sec)	1.7459	Comment	single_pulse	Date	22 Aug 2012 10:42:01
Date Stamp	23 Aug 2012 03:00:43	File Name	G:\500MHz\2082412\laaron\proton\CS_4119_proton_2-1.jdf		
Frequency (MHz)	500.16	Nucleus	1H	Number of Transients	6
Original Points Count	16384	Owner	delta	Points Count	16384
Receiver Gain	50.00	Solvent	CHLOROFORM-d	Pulse Sequence	single_pulse.ex2
Spectrum Type	STANDARD	Sweep Width (Hz)	9384.38	Temperature (degree C)	22.200



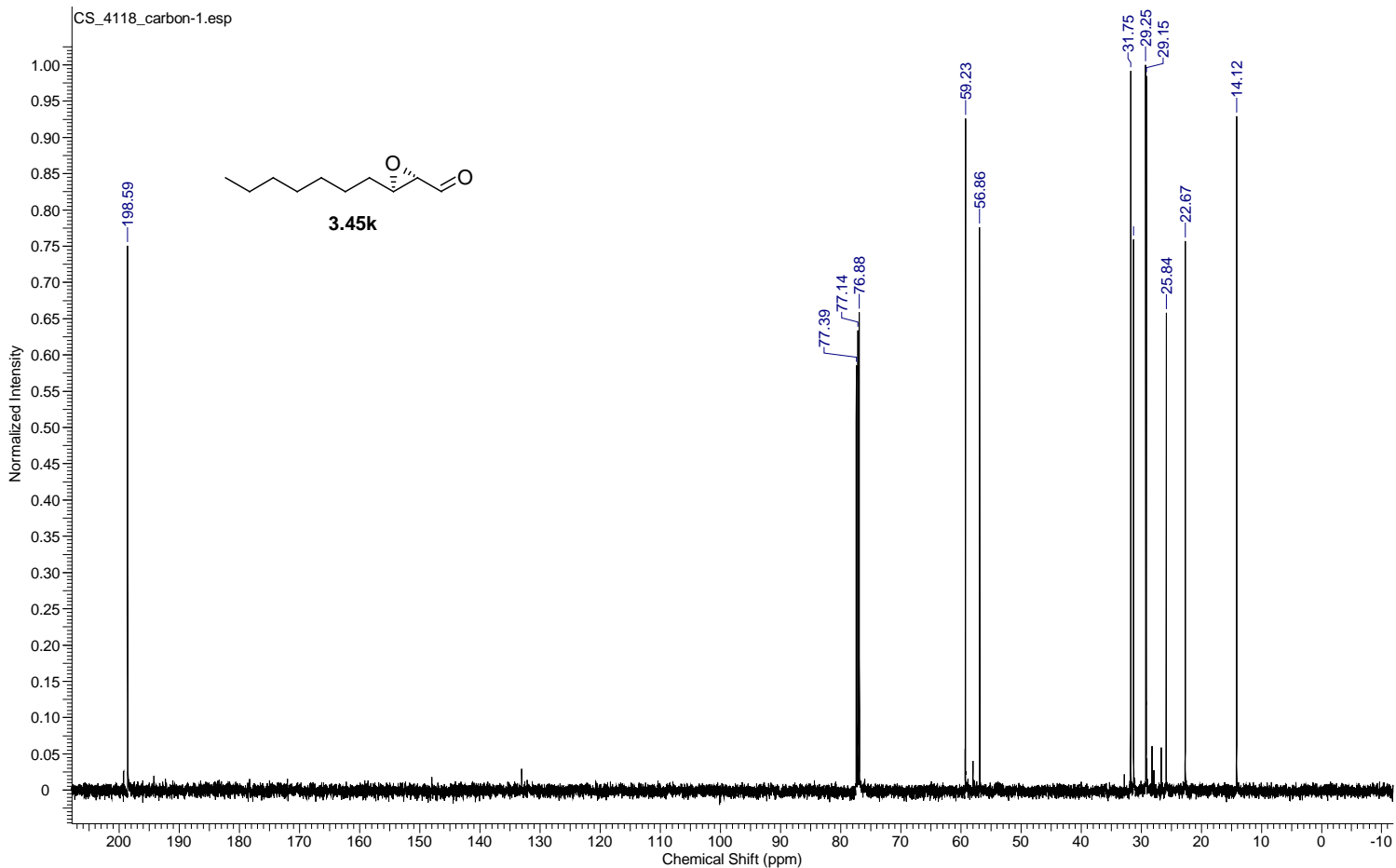
Acquisition Time (sec)	0.8336	Comment	single pulse decoupled gated NOE	Date	22 Aug 2012 14:46:59
Date Stamp	23 Aug 2012 07:05:42	File Name	G:\500MHz082412\laaron\carbon\CS_4119_carbon-2.jdf		
Frequency (MHz)	125.77	Nucleus	13C	Number of Transients	2000
Original Points Count	32768	Owner	delta	Points Count	32768
Receiver Gain	50.00	Solvent	CHLOROFORM-d	Pulse Sequence	single_pulse_dec
Spectrum Type	STANDARD	Sweep Width (Hz)	39308.18	Temperature (degree C)	22.600
				Spectrum Offset (Hz)	12576.5293



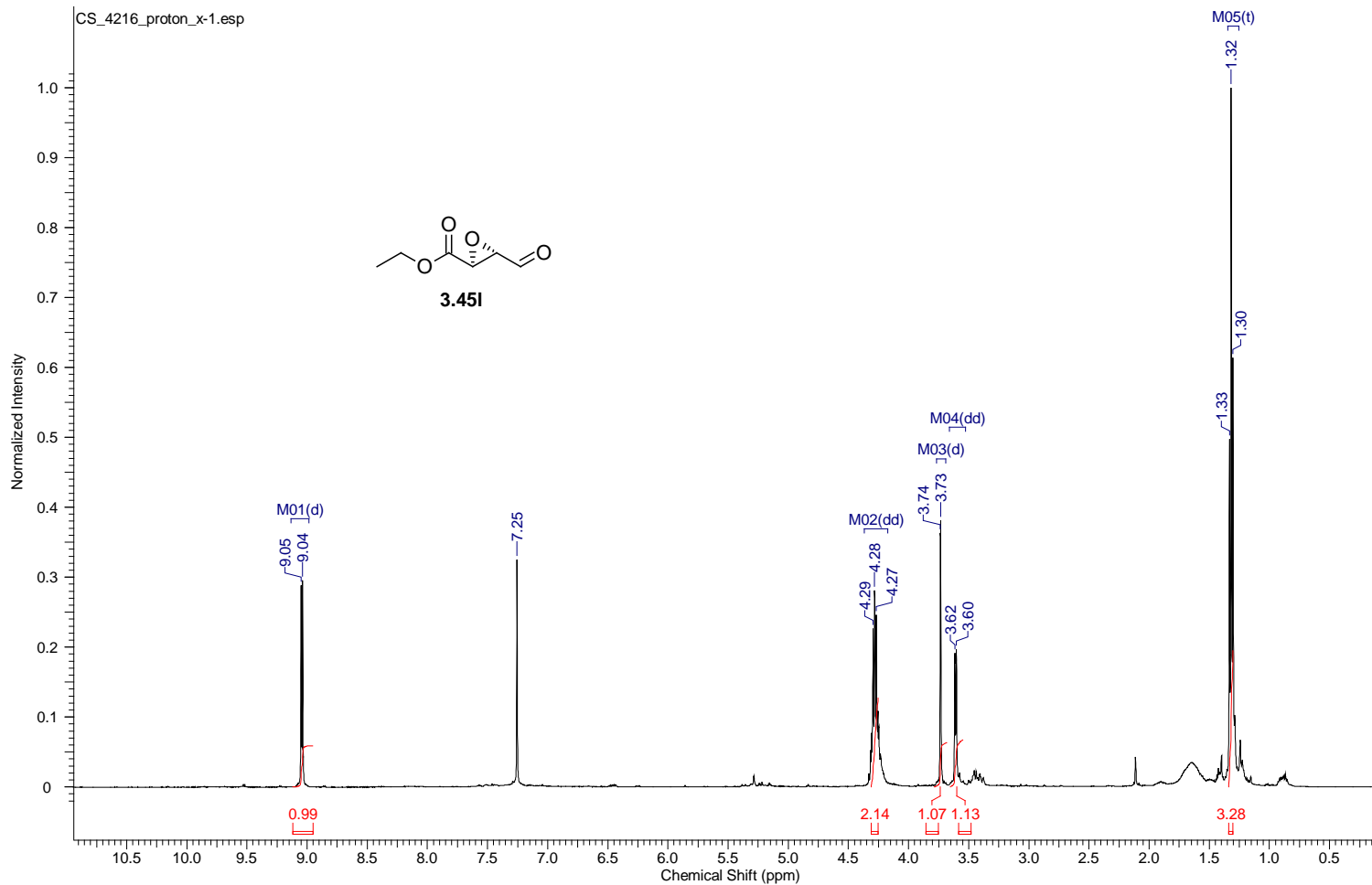
Acquisition Time (sec)	1.7459	Comment	single_pulse	Date	21 Aug 2012 12:32:15
Date Stamp	22 Aug 2012 04:50:57				
File Name	C:\Users\chen\Desktop\study\Foss\Shuai's Data\NMR DATA\500MHz083012\aaaron\proton\CS_4118_proton-1.jdf			Frequency (MHz)	500.16
Nucleus	1H	Number of Transients	7	Origin	ECA 500
Owner	delta	Points Count	16384	Pulse Sequence	single_pulse.ex2
Solvent	CHLOROFORM-d			Receiver Gain	24.00
Sweep Width (Hz)	9384.38	Temperature (degree C)	21.800	Spectrum Offset (Hz)	2500.7996
				Spectrum Type	STANDARD



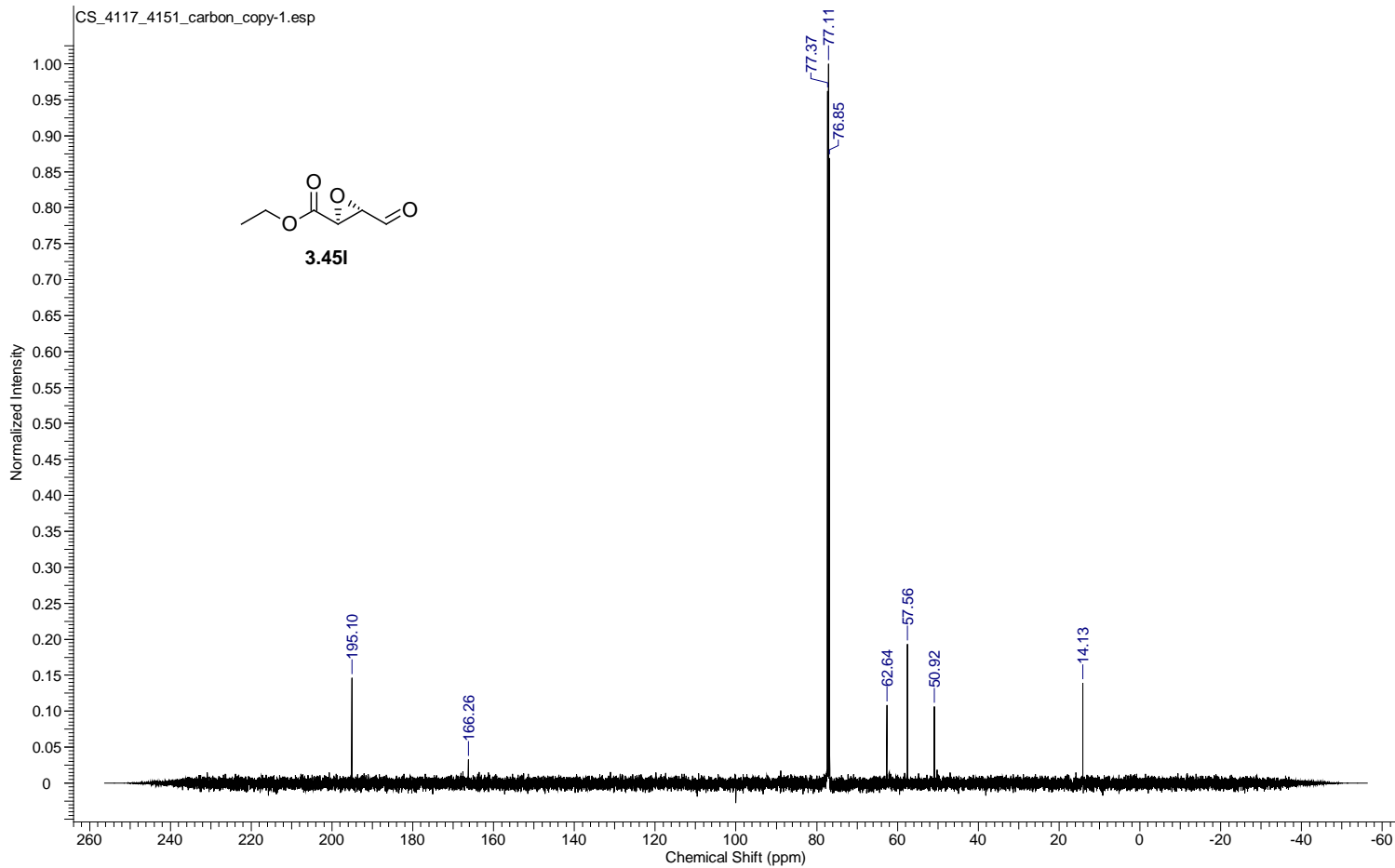
Acquisition Time (sec)	0.8336	Comment	single pulse decoupled gated NOE	Date	21 Aug 2012 12:34:04
Date Stamp	22 Aug 2012 04:52:46				
File Name	C:\Users\chen\Desktop\study\Foss\Shuai's Data\NMR DATA\500MHz082412\aaaron\carbon\CS_4118_carbon-1.jdf			Frequency (MHz)	125.77
Nucleus	13C	Number of Transients	40	Origin	ECA 500
Owner	delta	Points Count	32768	Pulse Sequence	single_pulse_dec
Solvent	CHLOROFORM-d	Spectrum Offset (Hz)	12576.5293	Spectrum Type	STANDARD
Temperature (degree C)	22.200			Sweep Width (Hz)	39308.18



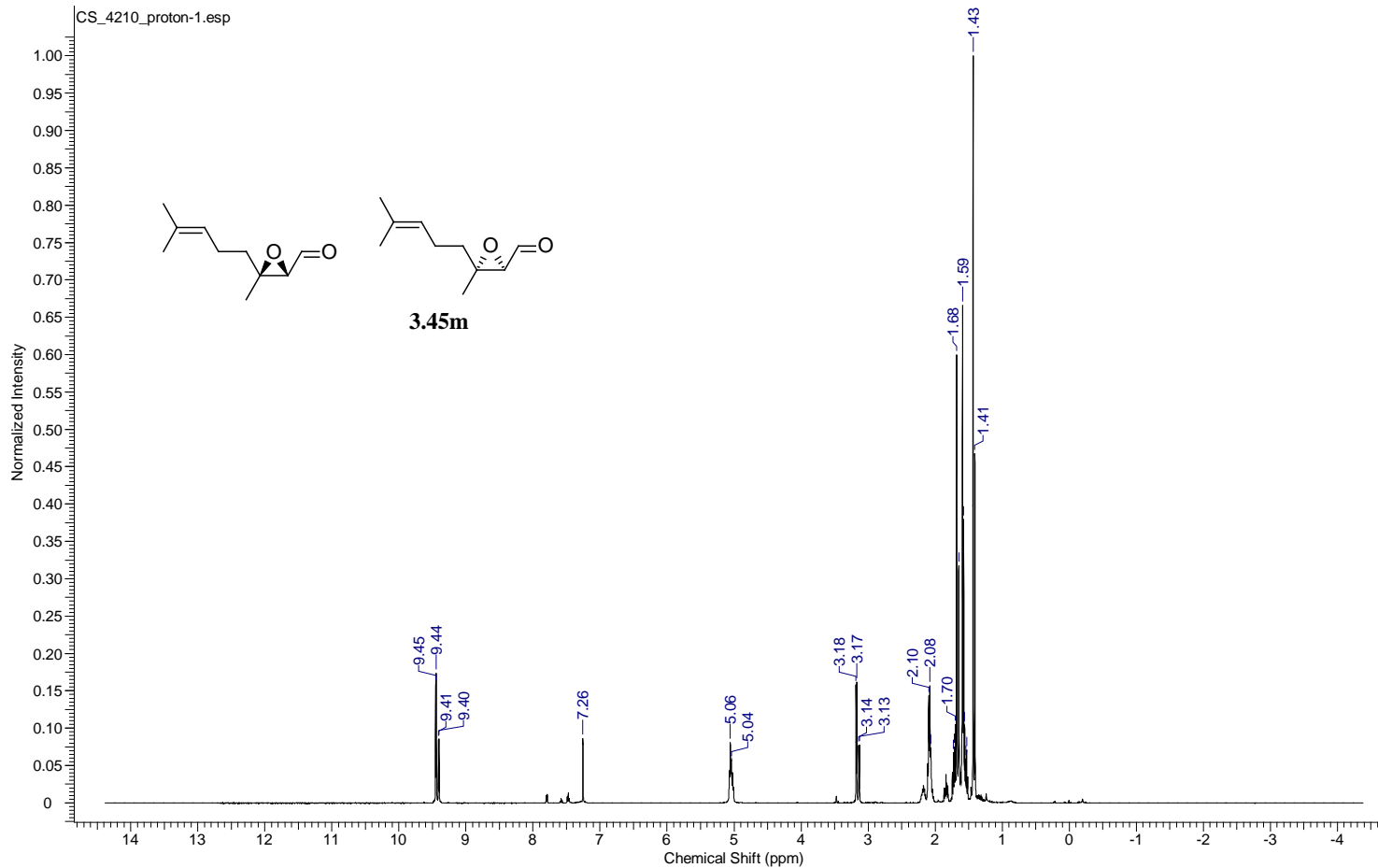
Acquisition Time (sec)	1.7459	Comment	single_pulse	Date	05 Dec 2012 10:07:12
Date Stamp	06 Dec 2012 02:55:00	File Name	G:\500Mhz120912\aaaron\proton\CS_4216_proton_x-1.jdf		
Frequency (MHz)	500.16	Nucleus	1H	Origin	ECA 500
Original Points Count	16384	Owner	delta	Points Count	16384
Receiver Gain	44.00	Solvent	CHLOROFORM-d	Pulse Sequence	single_pulse.ex2
Spectrum Type	STANDARD	Sweep Width (Hz)	9384.38	Temperature (degree C)	21.100



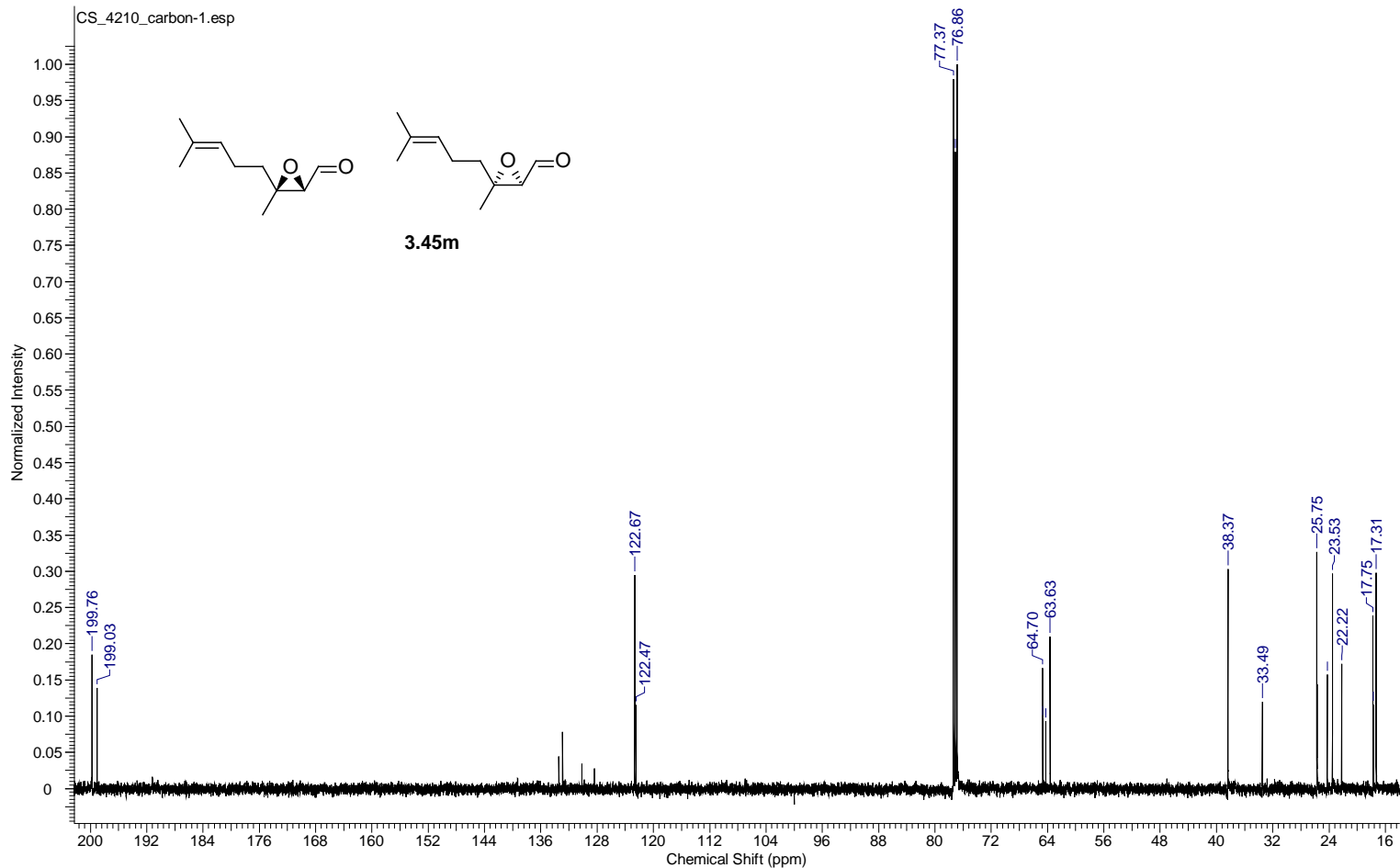
Acquisition Time (sec)	0.8336	Comment	single pulse decoupled gated NOE		Date	08 Sep 2012 13:08:09	
Date Stamp	09 Sep 2012 05:26:58						
File Name	C:\Users\chen\Desktop\study\Foss\Shuai's Data\NMR DATA\500MHz092012\aaaron\carbon\CS_4117_4151_carbon_copy-1.jdf						
Frequency (MHz)	125.77	Nucleus	¹³ C	Number of Transients	120	Origin	ECA 500
Original Points Count	32768	Owner	delta	Points Count	32768	Pulse Sequence	single_pulse_dec
Receiver Gain	50.00	Solvent	CHLOROFORM-d	Spectrum Offset (Hz)	12576.5293	Spectrum Type	STANDARD
Sweep Width (Hz)	39308.18	Temperature (degree C)	22.600				



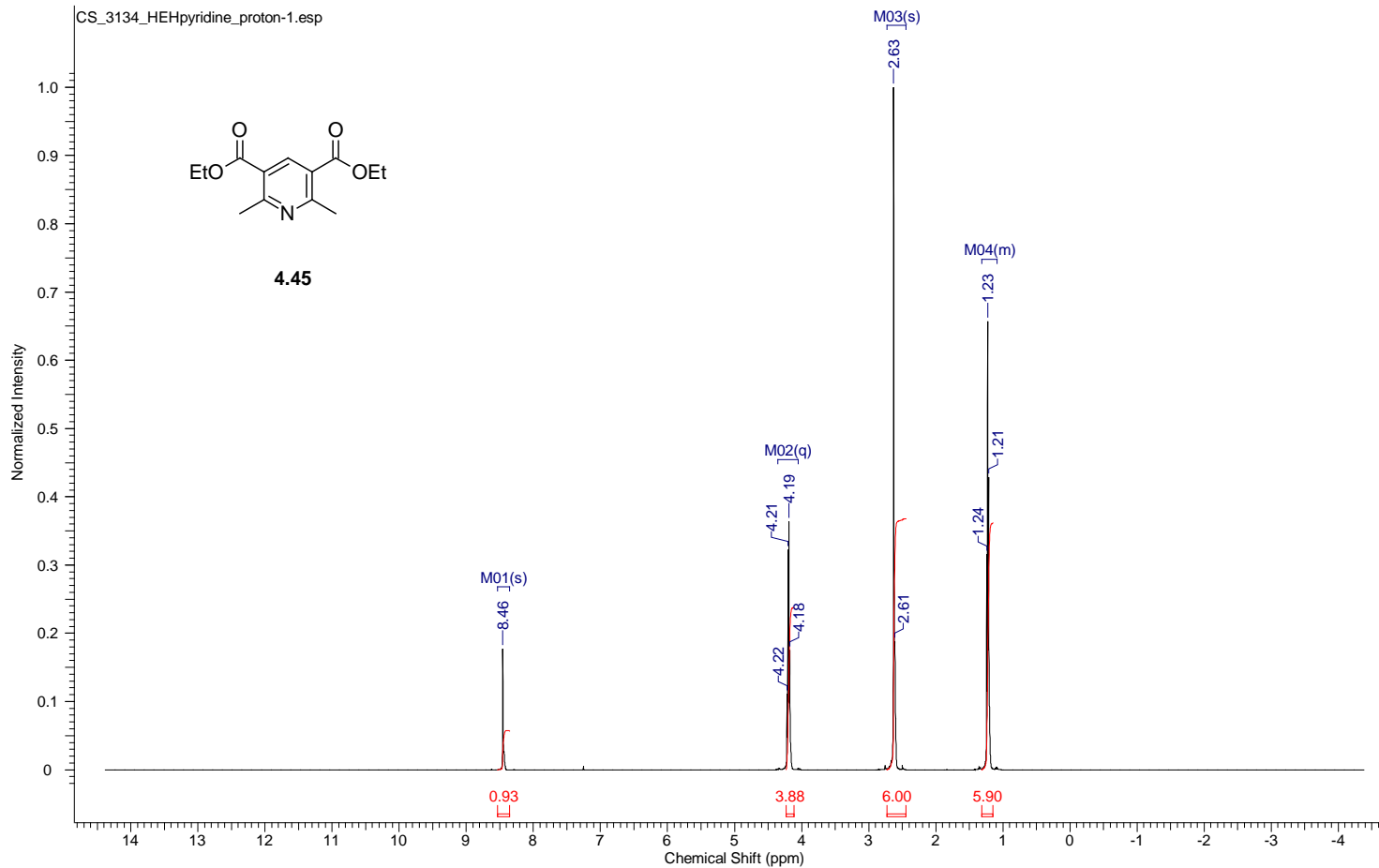
Acquisition Time (sec)	1.7459	Comment	single_pulse	Date	15 Nov 2012 08:20:41
Date Stamp	16 Nov 2012 01:07:29				
File Name	C:\Users\chen\Desktop\study\Foss\Shuai's Data\NMR DATA\500MHz\11612\laaron\proton\CS_4210_proton-1.jdf			Frequency (MHz)	500.16
Nucleus	1H	Number of Transients	7	Origin	ECA 500
Owner	delta	Points Count	16384	Pulse Sequence	single_pulse.ex2
Solvent	CHLOROFORM-d	Spectrum Offset (Hz)	2500.7996	Receiver Gain	34.00
Sweep Width (Hz)	9384.38	Temperature (degree C)	20.800	Spectrum Type	STANDARD



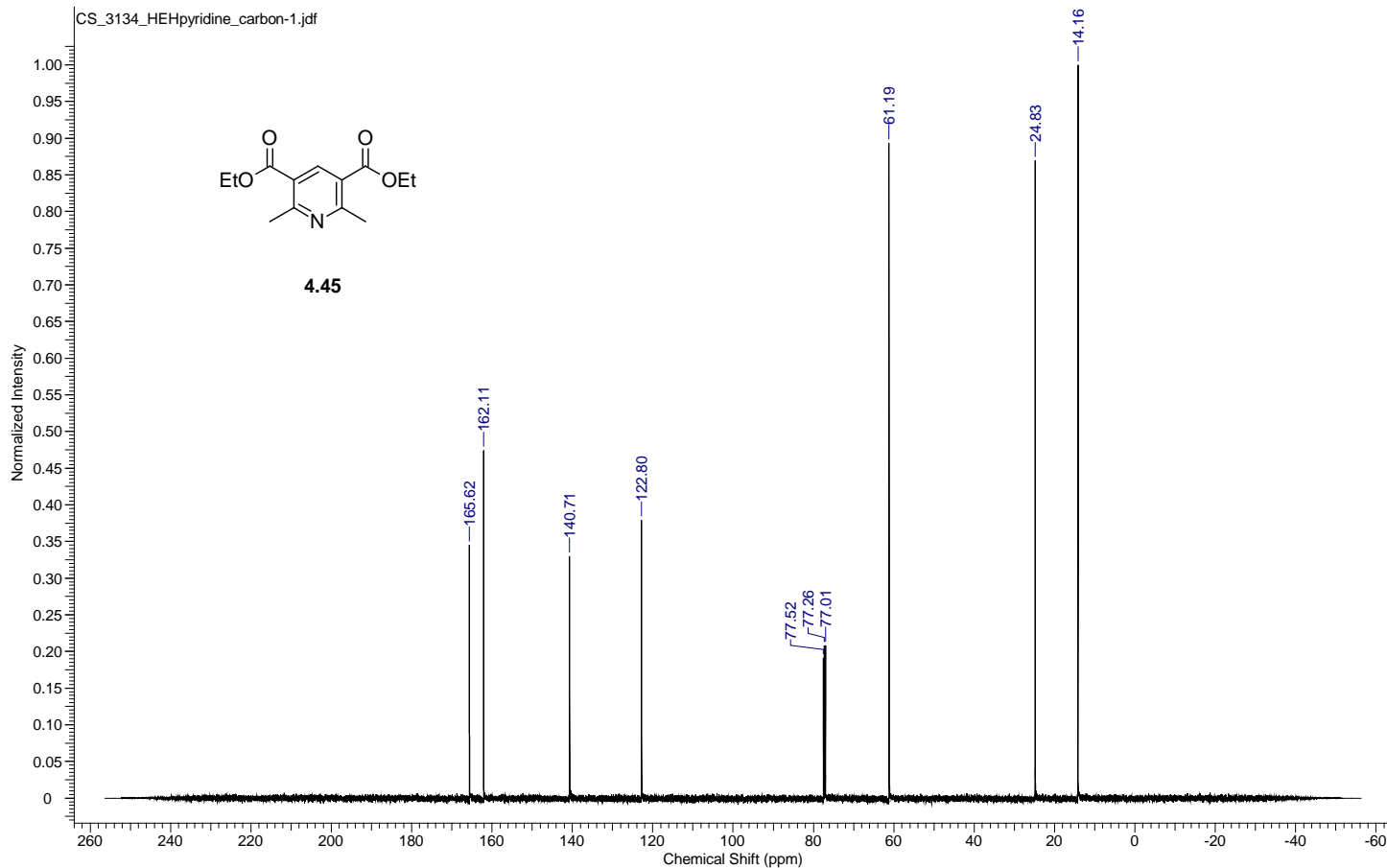
Acquisition Time (sec)	0.8336	Comment	single pulse decoupled gated NOE	Date	15 Nov 2012 08:25:55
Date Stamp	16 Nov 2012 01:12:43				
File Name	C:\Users\chen\Desktop\study\Foss\Shuai's Data\NMR DATA\500MHz\11612\aaaron\carbon\CS_4210_carbon-1.jdf			Frequency (MHz)	125.77
Nucleus	¹³ C	Number of Transients	140	Origin	ECA 500
Owner	delta	Points Count	32768	Pulse Sequence	single_pulse_dec
Solvent	CHLOROFORM-d	Spectrum Offset (Hz)	12576.5293	Spectrum Type	STANDARD
Temperature (degree C)	21.400			Sweep Width (Hz)	39308.18



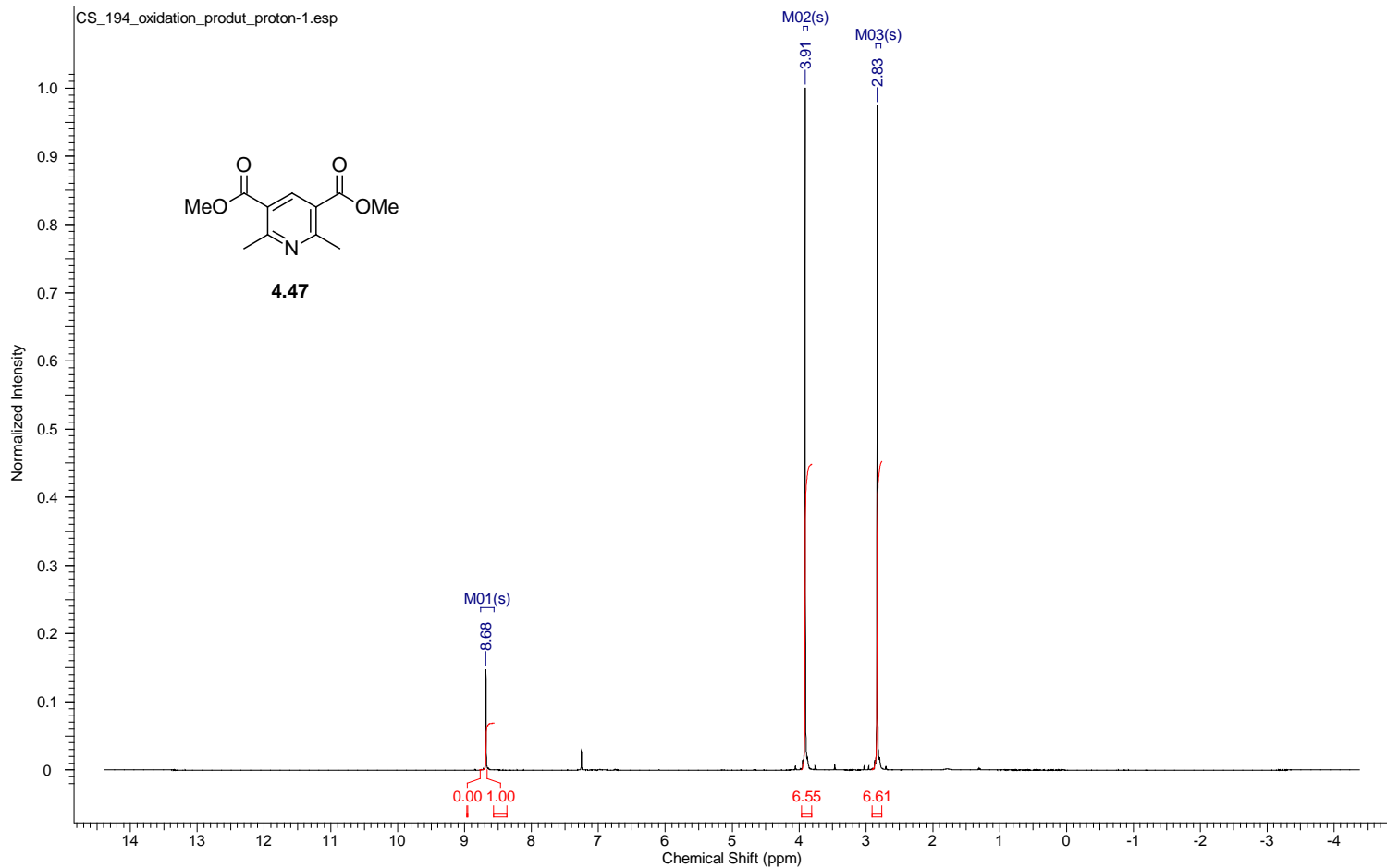
Acquisition Time (sec)	1.7459	Comment	single_pulse	Date	10 May 2012 12:49:29
Date Stamp	11 May 2012 05:06:02				
File Name	C:\Users\chen\Desktop\DakinNMR\Aerobic Dakin Oxidation\Substrate NMR\RAW_data\CS_3134_HEHpyridine_proton-1.jdf				
Frequency (MHz)	500.16	Nucleus	¹ H	Number of Transients	3
Original Points Count	16384	Owner	delta	Points Count	16384
Receiver Gain	16.00	Solvent	CHLOROFORM-d	Spectrum Offset (Hz)	2500.7996
Sweep Width (Hz)	9384.38	Temperature (degree C)	22.300	Spectrum Type	STANDARD



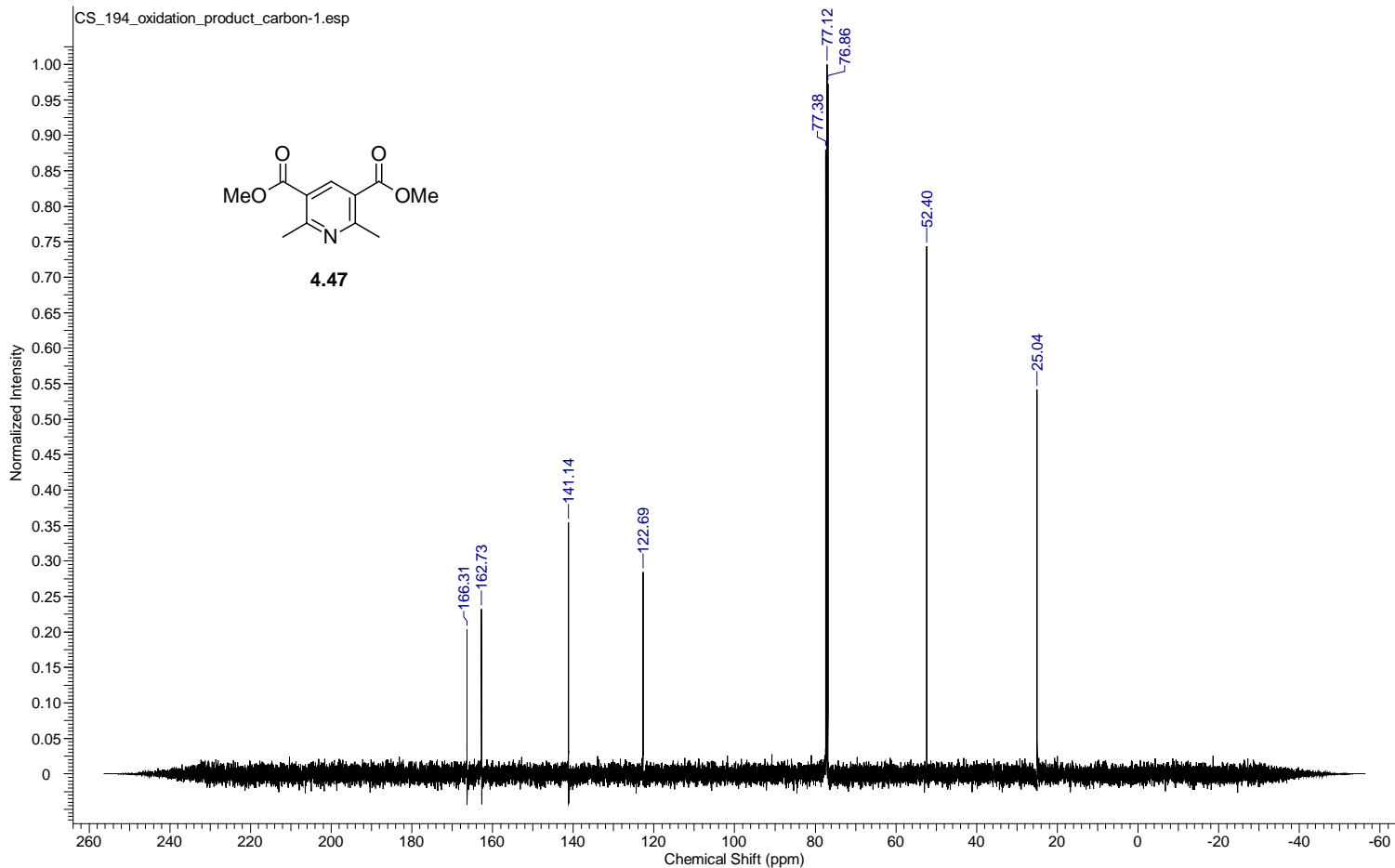
Acquisition Time (sec)	0.8336	Comment	single pulse decoupled gated NOE	Date	10 May 2012 12:50:27
Date Stamp	11 May 2012 05:07:00				
File Name	C:\Users\chen\Desktop\DakinNMR\Aerobic Dakin Oxidation\Substrate NMR\RAW_data\CS_3134_HEHpyridine_carbon-1.jdf				
Frequency (MHz)	125.77	Nucleus	13C	Number of Transients	20
Original Points Count	32768	Owner	delta	Points Count	32768
Receiver Gain	50.00	Solvent	CHLOROFORM-d	Spectrum Offset (Hz)	12576.5293
Sweep Width (Hz)	39308.18	Temperature (degree C)	22.500	Spectrum Type	STANDARD



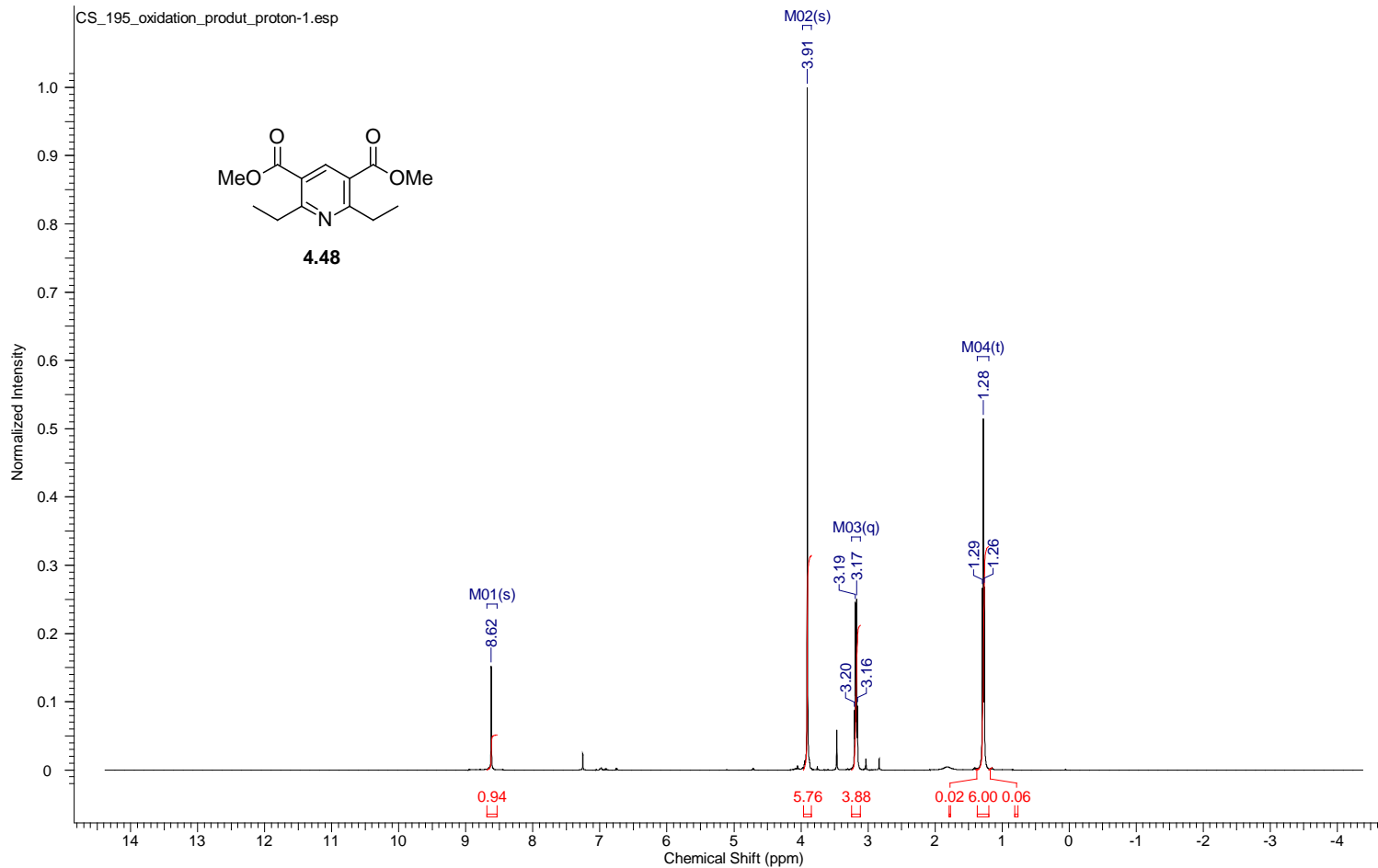
Acquisition Time (sec)	1.7459	Comment	single_pulse	Date	22 Sep 2012 09:10:41
Date Stamp	23 Sep 2012 01:29:37				
File Name	C:\Users\chen\Desktop\study\Foss\Shuai's Data\NMR DATA\500MHz\092012\laaron\proton\CS_194_oxidation_product_proton-1.jdf				
Frequency (MHz)	500.16	Nucleus	1H	Number of Transients	3
Original Points Count	16384	Owner	delta	Points Count	16384
Receiver Gain	36.00	Solvent	CHLOROFORM-d	Spectrum Offset (Hz)	2500.7996
Sweep Width (Hz)	9384.38	Temperature (degree C)	22.000	Spectrum Type	STANDARD



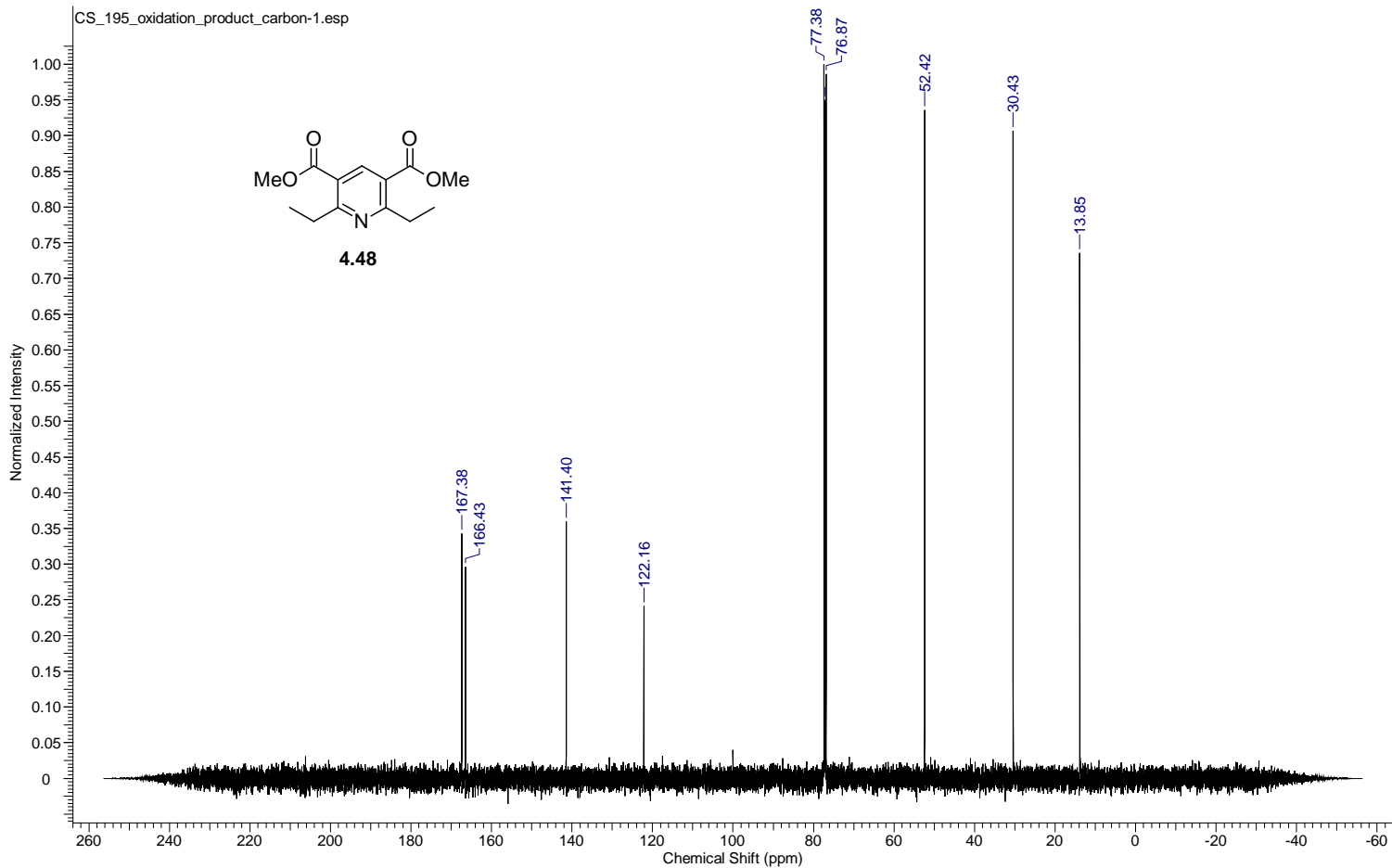
Acquisition Time (sec)	0.8336	Comment	single pulse decoupled gated NOE		Date	22 Sep 2012 09:12:02	
Date Stamp	23 Sep 2012 01:30:58						
File Name	C:\Users\chen\Desktop\study\Foss\Shuai's Data\NMR DATA\500MHz092012\aaaron\carbon\CS_194_oxidation_product_carbon-1.jdf						
Frequency (MHz)	125.77	Nucleus	¹³ C	Number of Transients	30	Origin	ECA 500
Original Points Count	32768	Owner	delta	Points Count	32768	Pulse Sequence	single_pulse_dec
Receiver Gain	50.00	Solvent	CHLOROFORM-d	Spectrum Offset (Hz)	12576.5293	Spectrum Type	STANDARD
Sweep Width (Hz)	39308.18	Temperature (degree C)	22.200				



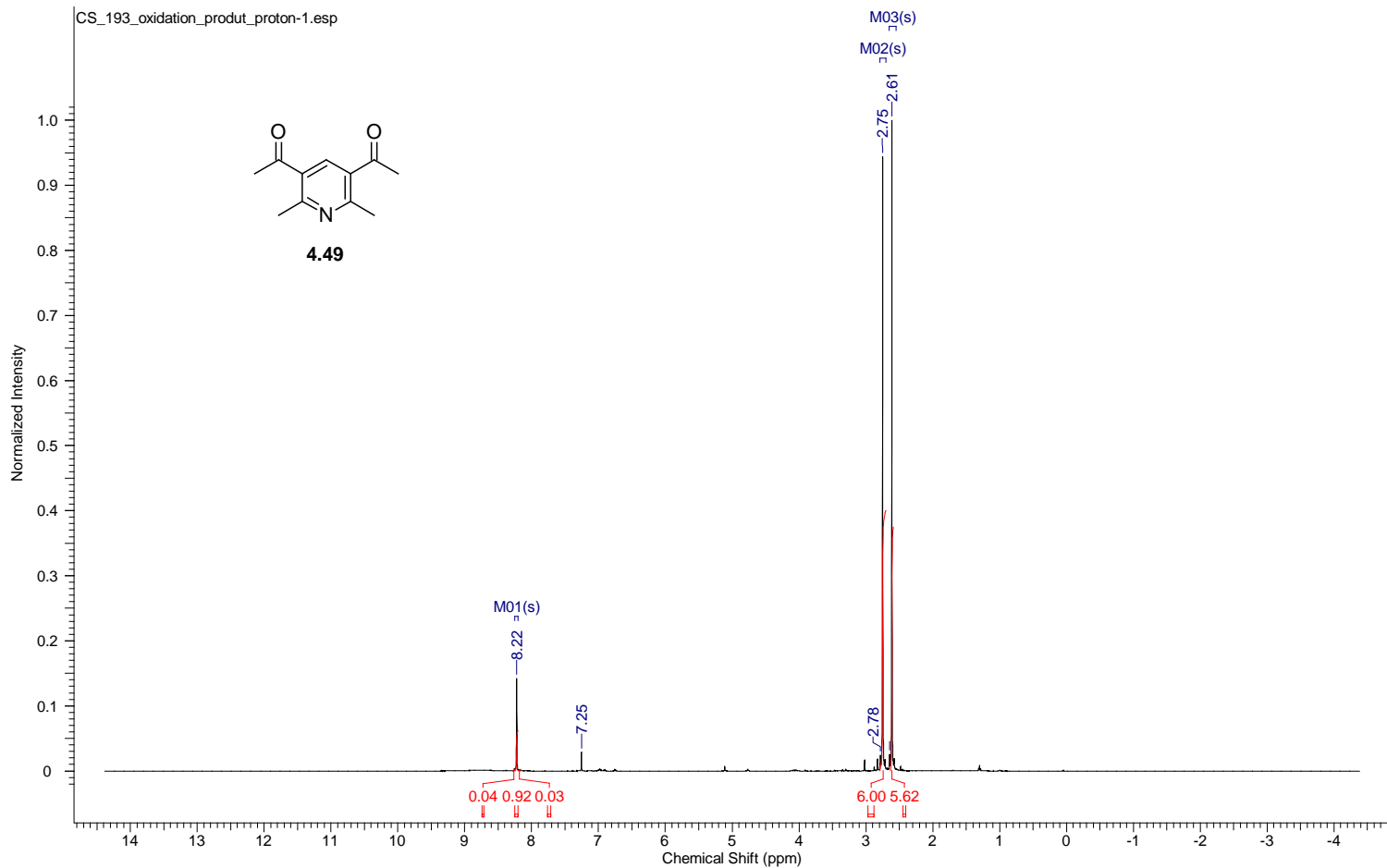
Acquisition Time (sec)	1.7459	Comment	single_pulse	Date	22 Sep 2012 09:16:22
Date Stamp	23 Sep 2012 01:35:18				
File Name	C:\Users\chen\Desktop\study\Foss\Shuai's Data\NMR DATA\500MHz092012\aaaron\proton\CS_195_oxidation_product_proton-1.jdf				
Frequency (MHz)	500.16	Nucleus	¹ H	Number of Transients	4
Original Points Count	16384	Owner	delta	Points Count	16384
Receiver Gain	32.00	Solvent	CHLOROFORM-d	Spectrum Offset (Hz)	2500.7996
Sweep Width (Hz)	9384.38	Temperature (degree C)	22.000	Spectrum Type	STANDARD



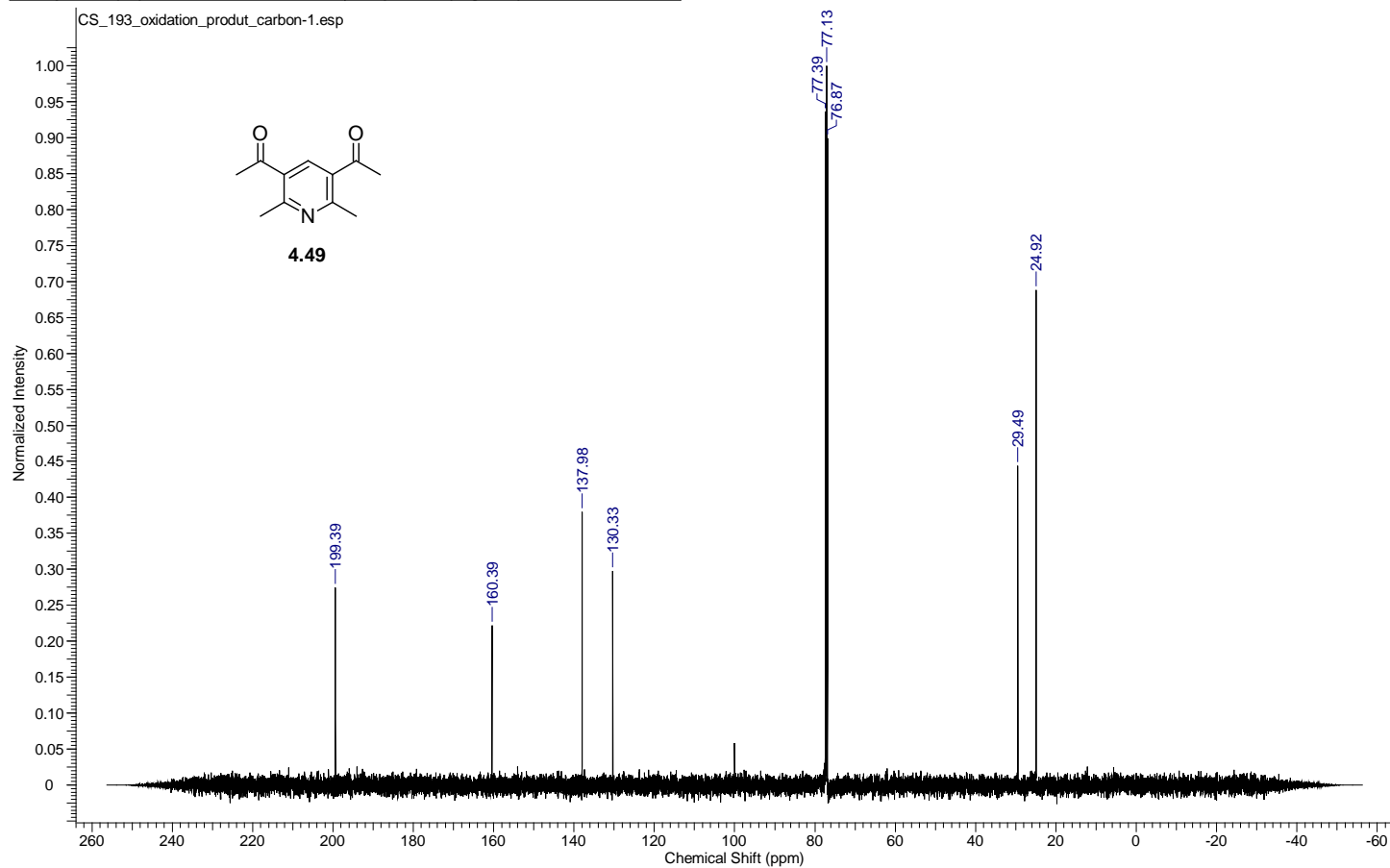
Acquisition Time (sec)	0.8336	Comment	single pulse decoupled gated NOE	Date	22 Sep 2012 09:17:45
Date Stamp	23 Sep 2012 01:36:40				
File Name	C:\Users\chen\Desktop\study\Foss\Shuai's Data\NMR DATA\500MHz092012\aaaron\carbon\CS_195_oxidation_product_carbon-1.jdf				
Frequency (MHz)	125.77	Nucleus	¹³ C	Number of Transients	30
Original Points Count	32768	Owner	delta	Points Count	32768
Receiver Gain	50.00	Solvent	CHLOROFORM-d	Spectrum Offset (Hz)	12576.5293
Sweep Width (Hz)	39308.18	Temperature (degree C)	22.300	Spectrum Type	STANDARD



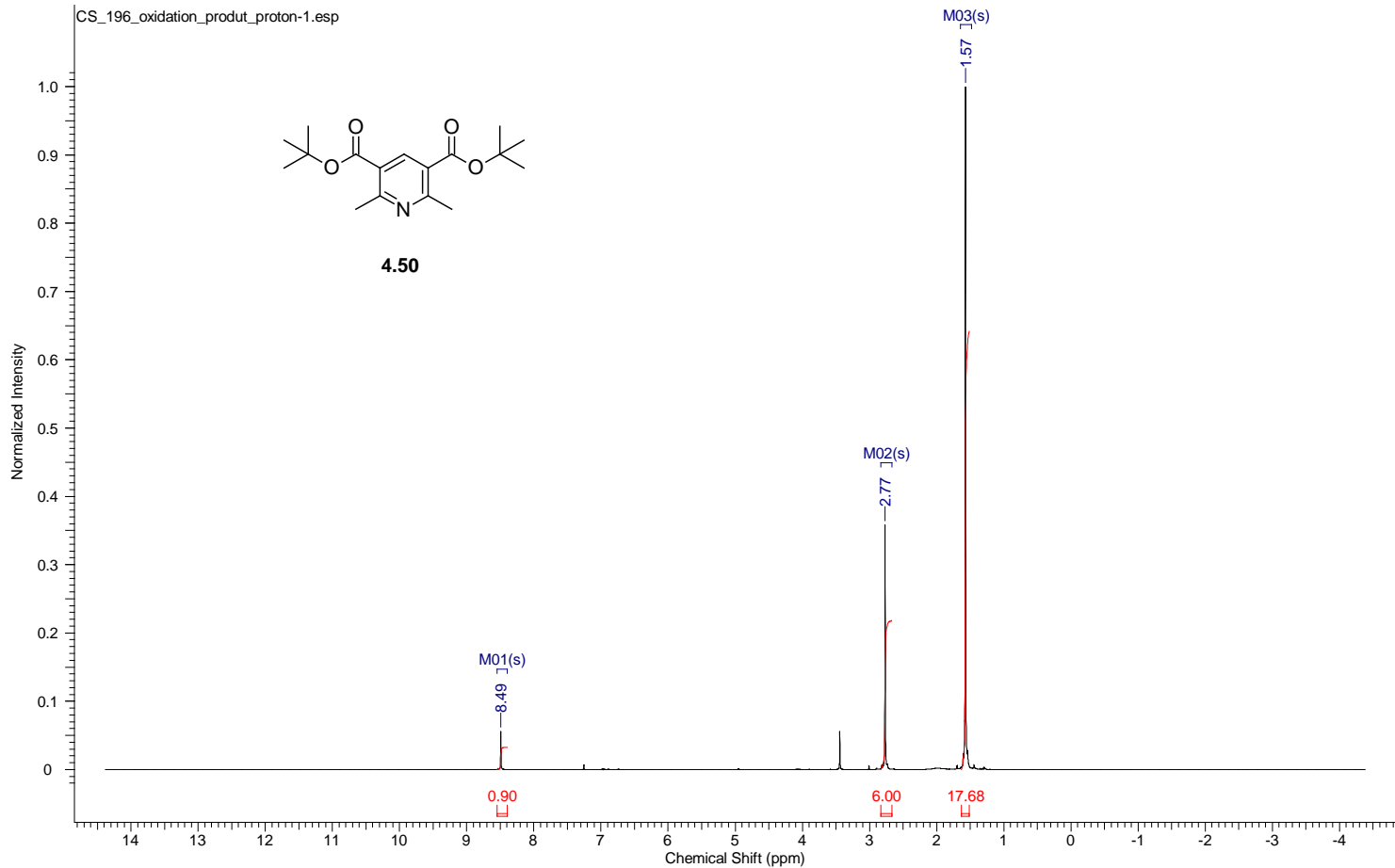
Acquisition Time (sec)	1.7459	Comment	single_pulse	Date	22 Sep 2012 09:04:52
Date Stamp	23 Sep 2012 01:23:48				
File Name	C:\Users\chen\Desktop\study\Foss\Shuai's Data\NMR DATA\500MHz\092012\laaron\proton\CS_193_oxidation_product_proton-1.jdf				
Frequency (MHz)	500.16	Nucleus	1H	Number of Transients	3
Original Points Count	16384	Owner	delta	Points Count	16384
Receiver Gain	36.00	Solvent	CHLOROFORM-d	Spectrum Offset (Hz)	2500.7996
Sweep Width (Hz)	9384.38	Temperature (degree C)	22.000	Spectrum Type	STANDARD



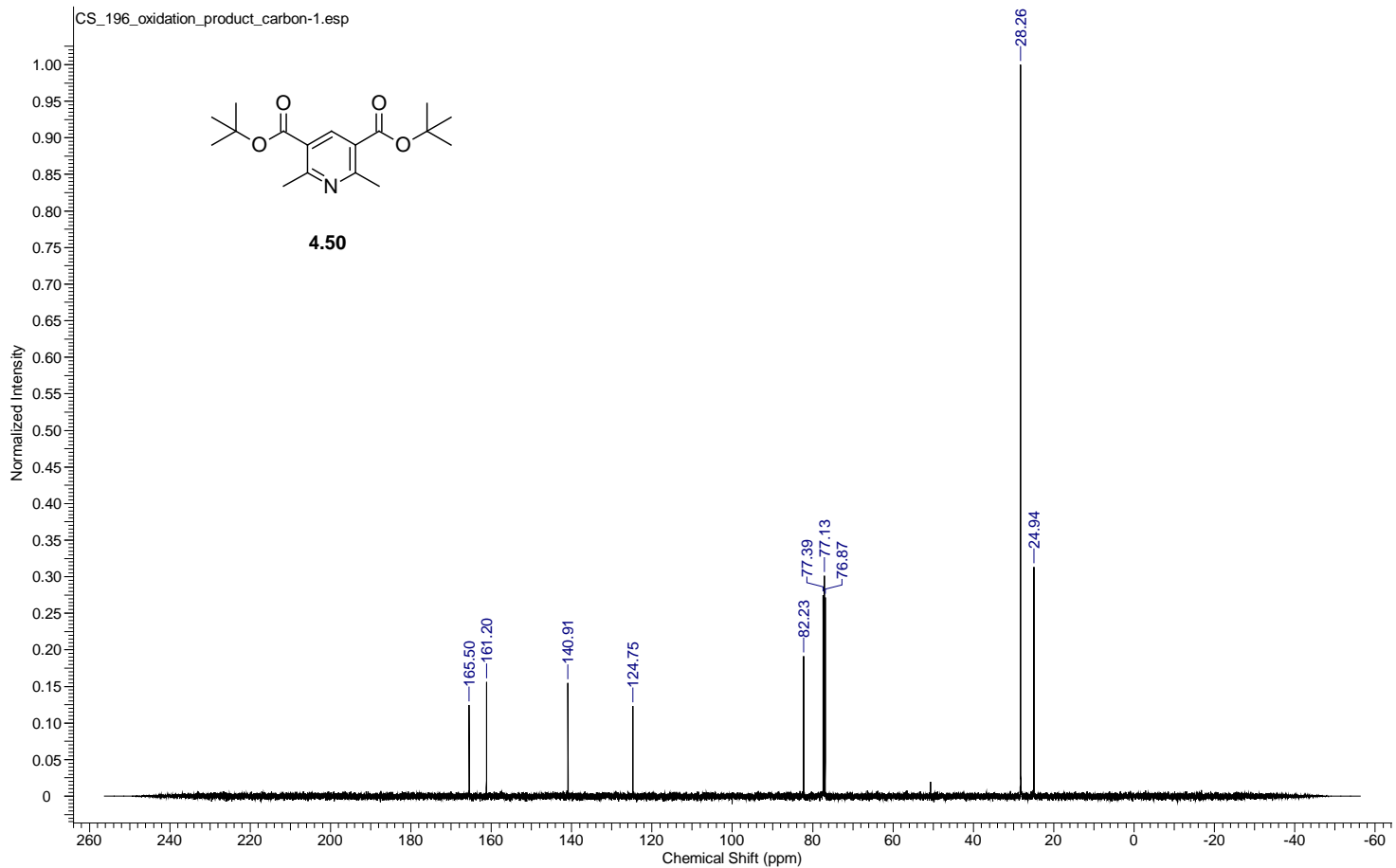
Acquisition Time (sec)	0.8336	Comment	single pulse decoupled gated NOE	Date	22 Sep 2012 09:06:31
Date Stamp	23 Sep 2012 01:25:27				
File Name	C:\Users\chen\Desktop\study\Foss\Shuai's Data\NMR DATA\500MHz092012\aaaron\carbon\CS_193_oxidation_product_carbon-1.jdf				
Frequency (MHz)	125.77	Nucleus	¹³ C	Number of Transients	40
Original Points Count	32768	Owner	delta	Points Count	32768
Receiver Gain	50.00	Solvent	CHLOROFORM-d	Spectrum Offset (Hz)	12576.5293
Sweep Width (Hz)	39308.18	Temperature (degree C)	22.300	Spectrum Type	STANDARD



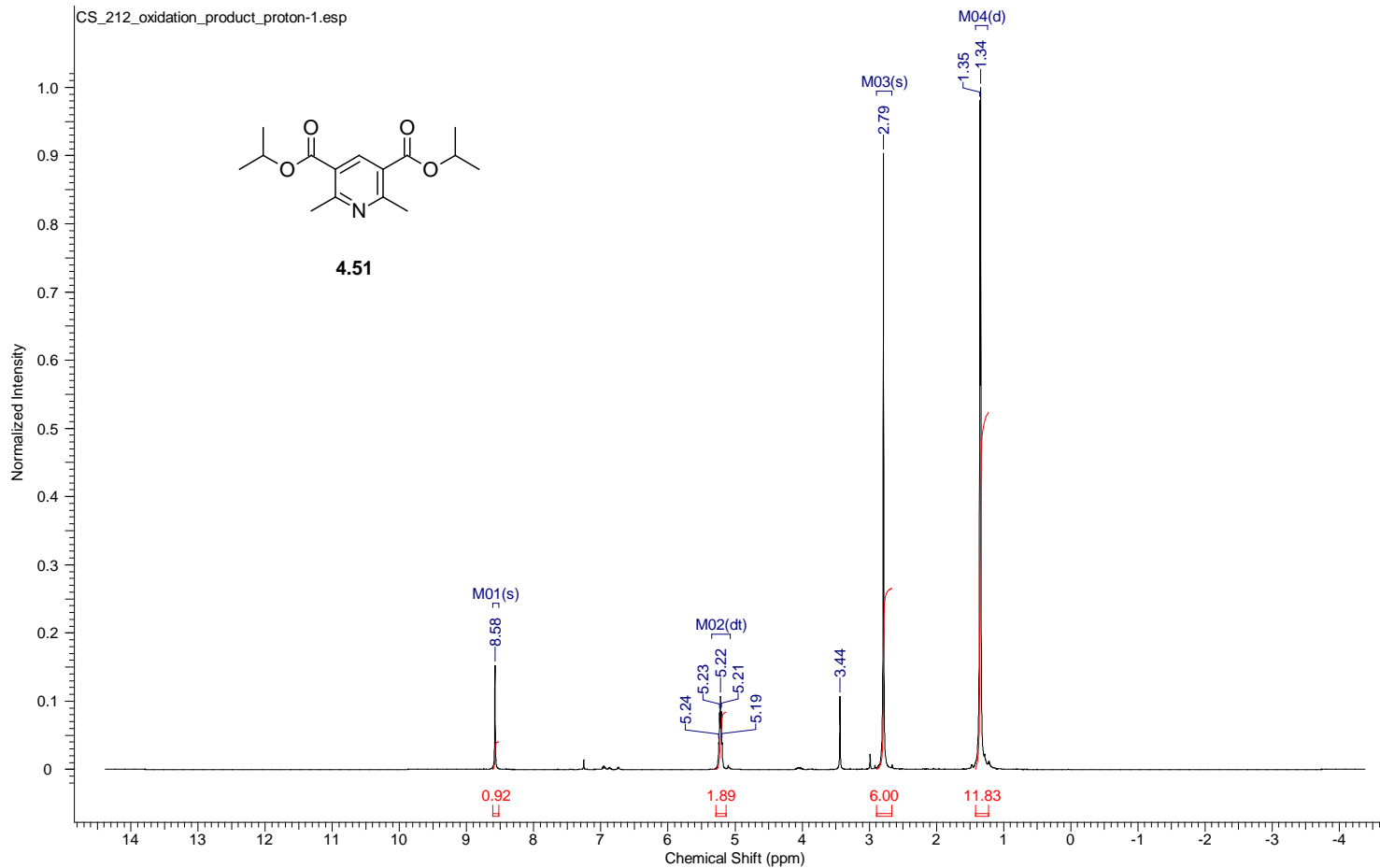
Acquisition Time (sec)	1.7459	Comment	single_pulse	Date	22 Sep 2012 09:22:07
Date Stamp	23 Sep 2012 01:41:03				
File Name	C:\Users\chen\Desktop\study\Foss\Shuai's Data\NMR DATA\500MHz092012\aaaron\proton\CS_196_oxidation_produ proton-1.jdf				
Frequency (MHz)	500.16	Nucleus	1H	Number of Transients	5
Original Points Count	16384	Owner	delta	Points Count	16384
Receiver Gain	26.00	Solvent	CHLOROFORM-d	Spectrum Offset (Hz)	2500.7996
Sweep Width (Hz)	9384.38	Temperature (degree C)	22.100	Spectrum Type	STANDARD



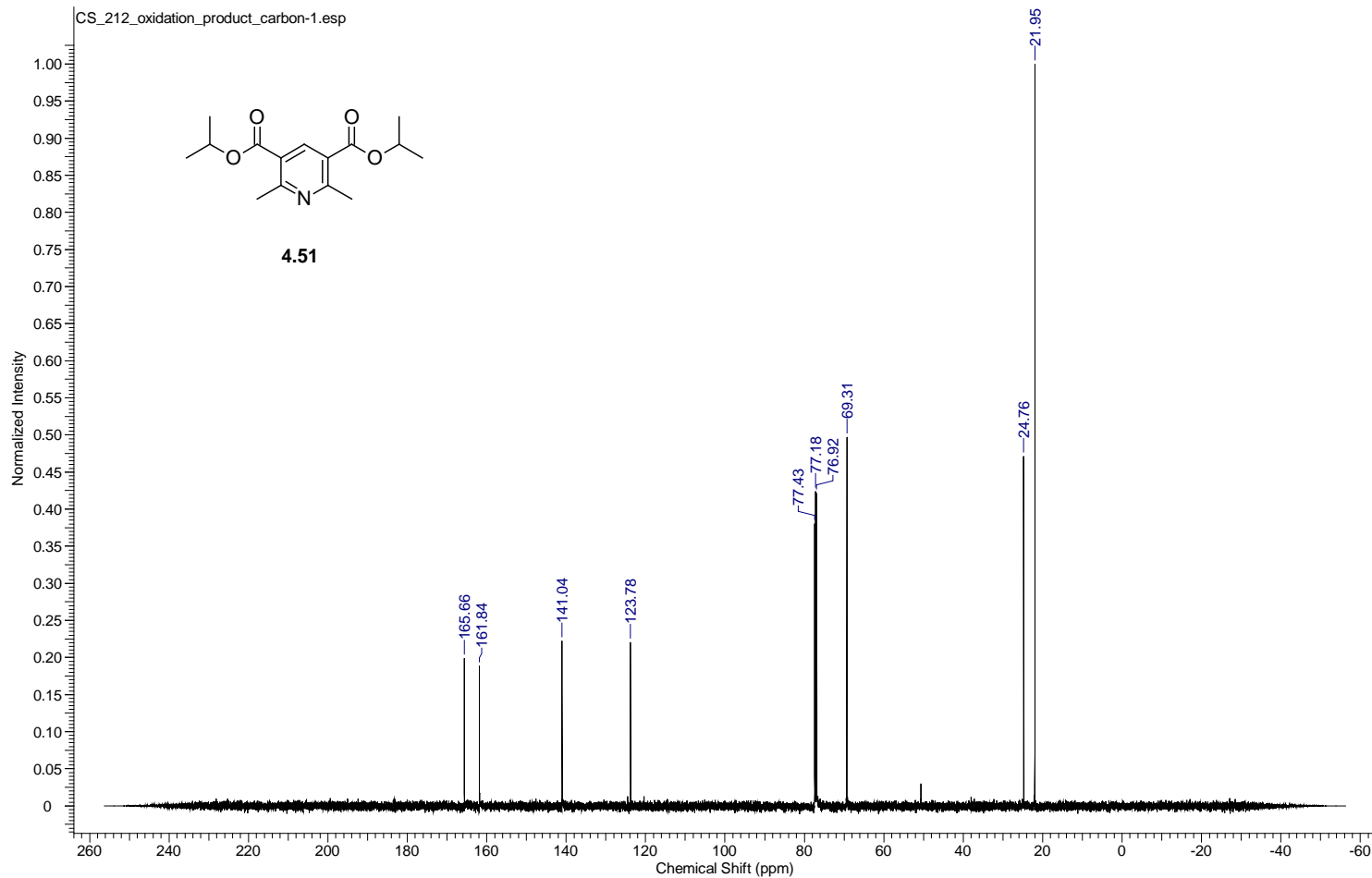
Acquisition Time (sec)	0.8336	Comment	single pulse decoupled gated NOE	Date	22 Sep 2012 09:23:24
Date Stamp	23 Sep 2012 01:42:19				
File Name	C:\Users\chen\Desktop\study\Foss\Shuai's Data\NMR DATA\500MHz092012\aaaron\carbon\CS_196_oxidation_product_carbon-1.jdf				
Frequency (MHz)	125.77	Nucleus	¹³ C	Number of Transients	30
Original Points Count	32768	Owner	delta	Points Count	32768
Receiver Gain	50.00	Solvent	CHLOROFORM-d	Spectrum Offset (Hz)	12576.5293
Sweep Width (Hz)	39308.18	Temperature (degree C)	22.400	Spectrum Type	STANDARD



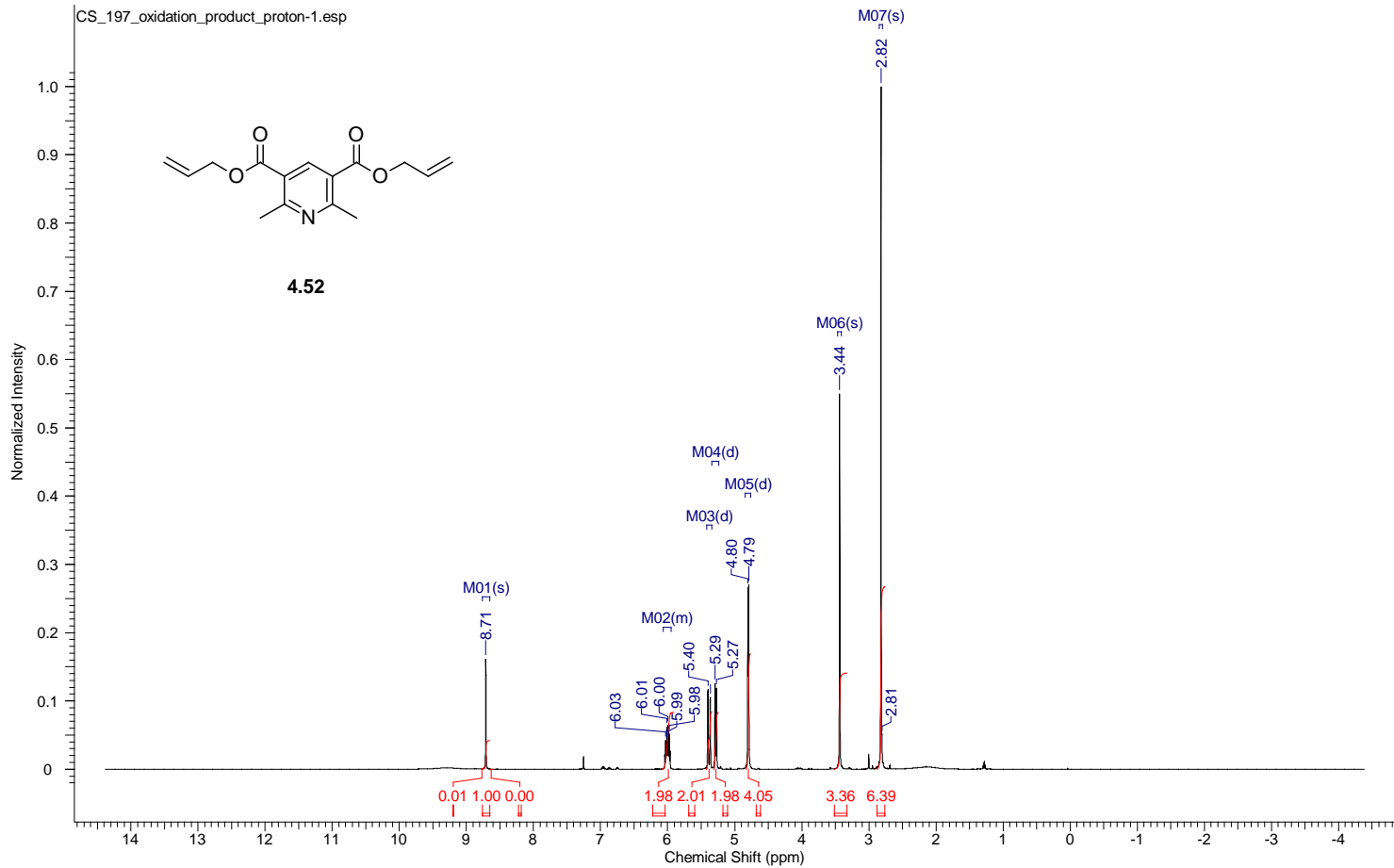
Acquisition Time (sec)	1.7459	Comment	single_pulse	Date	24 Sep 2012 13:17:16
Date Stamp	25 Sep 2012 05:36:12				
File Name	C:\Users\chen\Desktop\study\Foss\Shuai's Data\NMR DATA\500MHz\092012\aaaron\proton\CS_212_oxidation_product_proton-1.jdf				
Frequency (MHz)	500.16	Nucleus	¹ H	Number of Transients	3
Original Points Count	16384	Owner	delta	Points Count	16384
Receiver Gain	26.00	Solvent	CHLOROFORM-d	Spectrum Offset (Hz)	2500.7996
Sweep Width (Hz)	9384.38	Temperature (degree C)	22.200	Spectrum Type	STANDARD



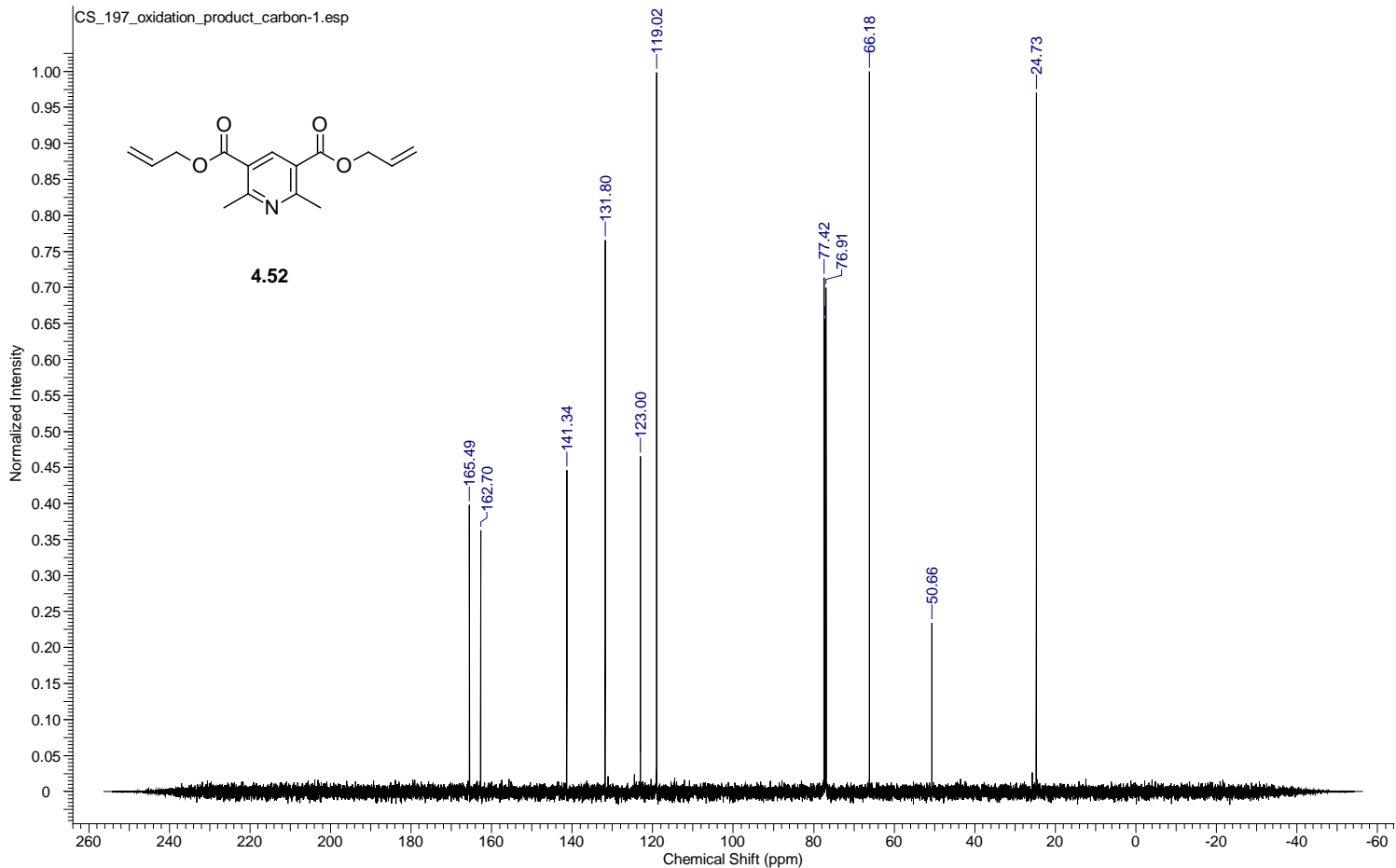
Acquisition Time (sec)	0.8336	Comment	single pulse decoupled gated NOE	Date	24 Sep 2012 13:18:32
Date Stamp	25 Sep 2012 05:37:29	File Name	G:\500MHz092012\aaaron\carbon\CS_212_oxidation_product_carbon-1.jdf		
Frequency (MHz)	125.77	Nucleus	13C	Number of Transients	30
Original Points Count	32768	Owner	delta	Points Count	32768
Receiver Gain	50.00	Solvent	CHLOROFORM-d	Pulse Sequence	single_pulse_dec
Spectrum Type	STANDARD	Sweep Width (Hz)	39308.18	Temperature (degree C)	22.400
				Spectrum Offset (Hz)	12576.5293



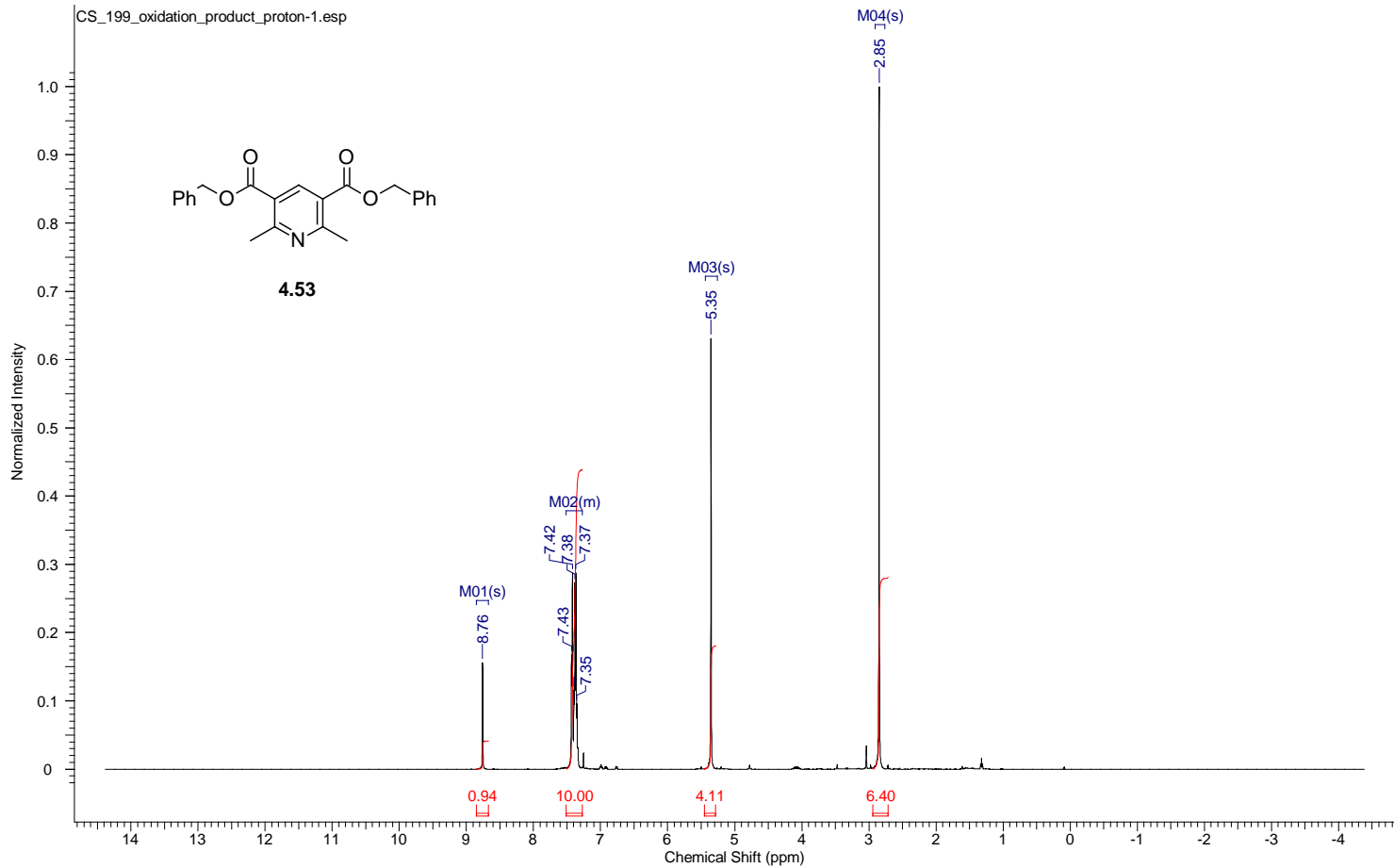
Acquisition Time (sec)	1.7459	Comment	single_pulse	Date	24 Sep 2012 13:04:46
Date Stamp	25 Sep 2012 05:23:43				
File Name	C:\Users\chen\Desktop\study\Foss\Shuai's Data\NMR DATA\500MHz\092012\aaaron\proton\CS_197_oxidation_product_proton-1.jdf				
Frequency (MHz)	500.16	Nucleus	¹ H	Number of Transients	10
Original Points Count	16384	Owner	delta	Points Count	16384
Receiver Gain	30.00	Solvent	CHLOROFORM-d	Spectrum Offset (Hz)	2500.7996
Sweep Width (Hz)	9384.38	Temperature (degree C)	22.100	Spectrum Type	STANDARD



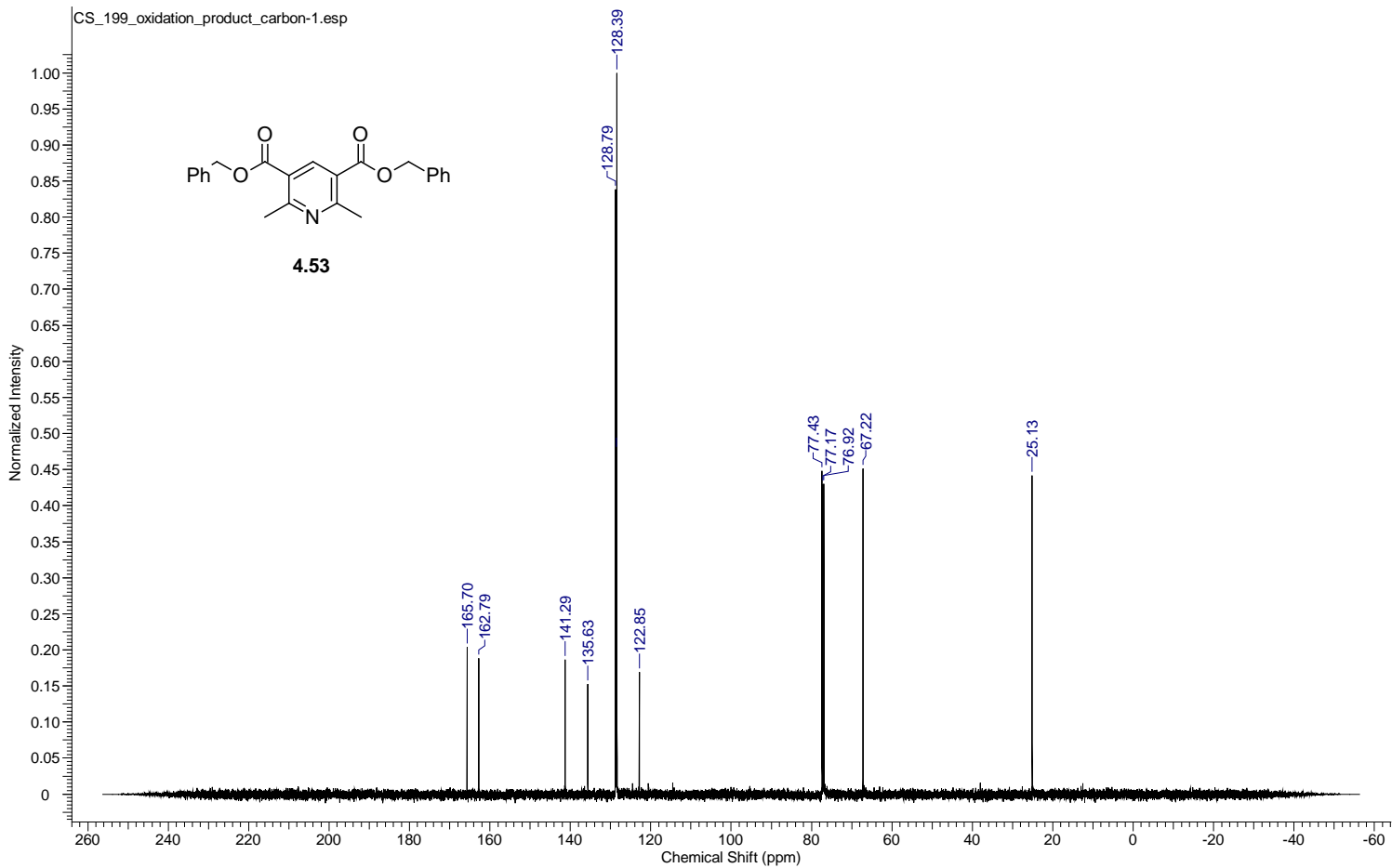
Acquisition Time (sec)	0.8336	Comment	single pulse decoupled gated NOE		Date	24 Sep 2012 13:06:39	
Date Stamp	25 Sep 2012 05:25:35						
File Name	C:\Users\chen\Desktop\study\Foss\Shuai's Data\NMR DATA\500MHz092012\aaaron\carbon\CS_197_oxidation_product_carbon-1.jdf						
Frequency (MHz)	125.77	Nucleus	¹³ C	Number of Transients	30	Origin	ECA 500
Original Points Count	32768	Owner	delta	Points Count	32768	Pulse Sequence	single_pulse_dec
Receiver Gain	50.00	Solvent	CHLOROFORM-d	Spectrum Offset (Hz)	12576.5293	Spectrum Type	STANDARD
Sweep Width (Hz)	39308.18	Temperature (degree C)	22.400				



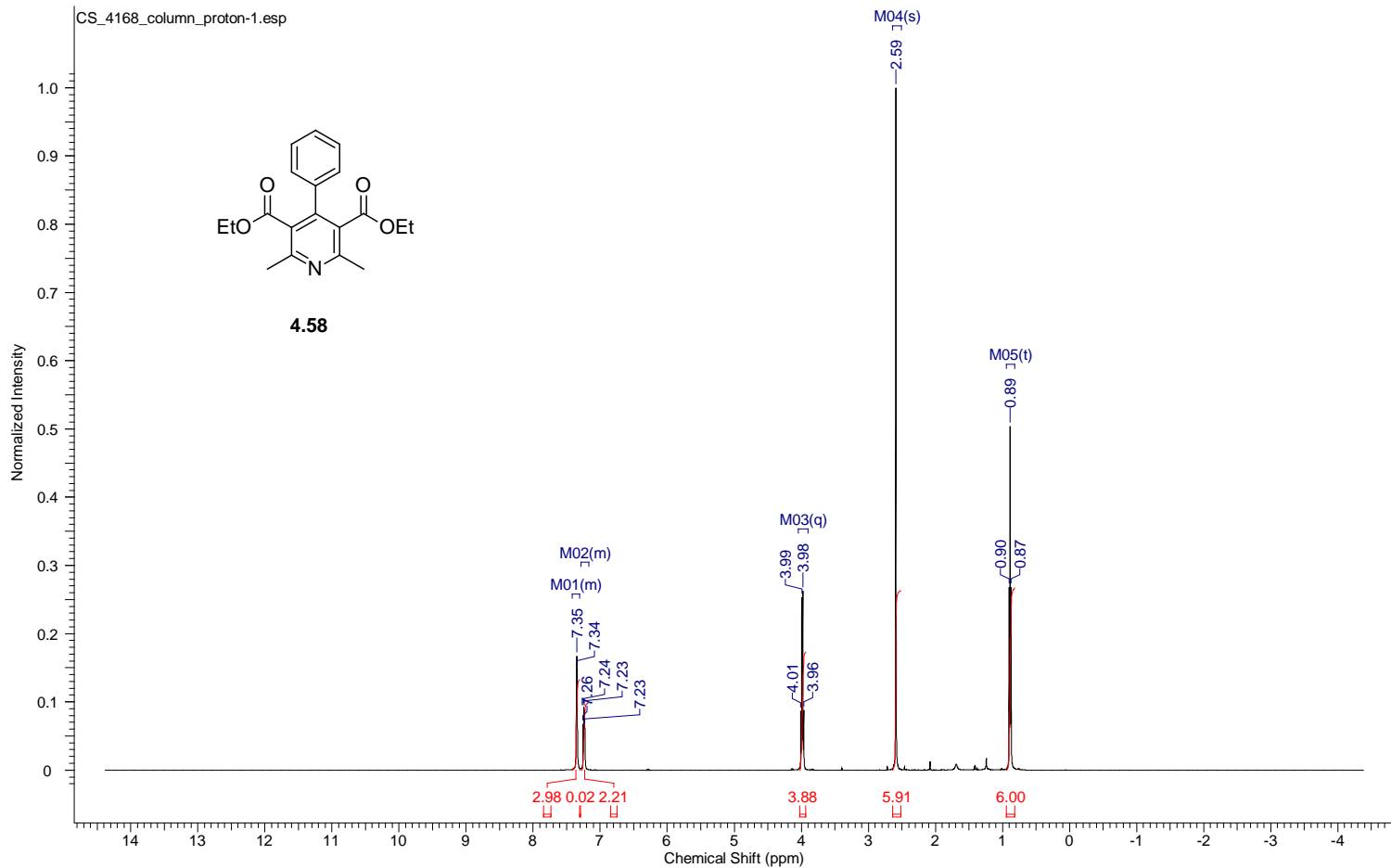
Acquisition Time (sec)	1.7459	Comment	single_pulse	Date	24 Sep 2012 13:11:15
Date Stamp	25 Sep 2012 05:30:11				
File Name	C:\Users\chen\Desktop\study\Foss\Shuai's Data\NMR DATA\500MHz092012\aaaron\proton\CS_199_oxidation_product_proton-1.jdf				
Frequency (MHz)	500.16	Nucleus	1H	Number of Transients	5
Original Points Count	16384	Owner	delta	Points Count	16384
Receiver Gain	30.00	Solvent	CHLOROFORM-d	Spectrum Offset (Hz)	2500.7996
Sweep Width (Hz)	9384.38	Temperature (degree C)	22.200	Spectrum Type	STANDARD



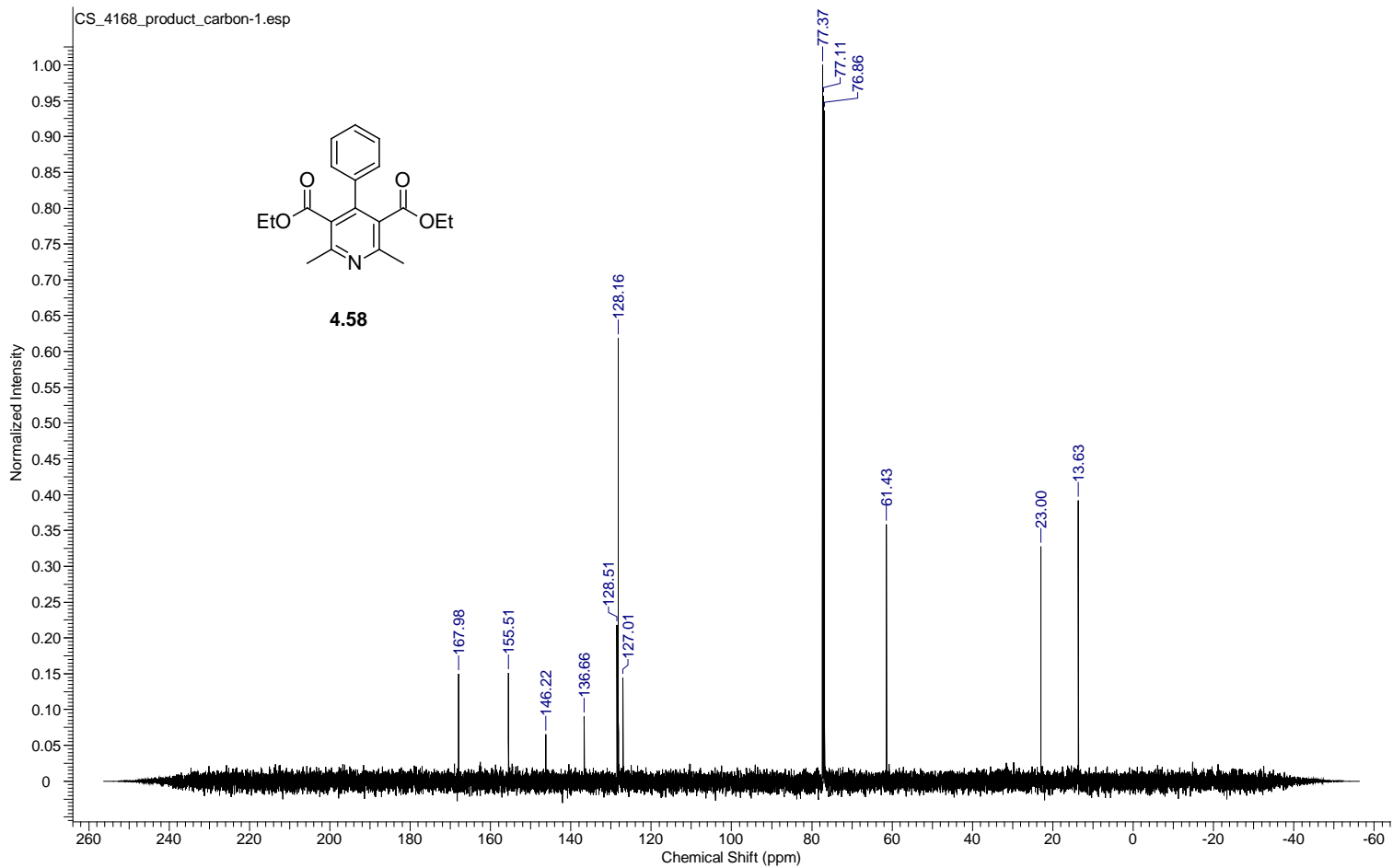
Acquisition Time (sec)	0.8336	Comment	single pulse decoupled gated NOE	Date	24 Sep 2012 13:12:53
Date Stamp	25 Sep 2012 05:31:50				
File Name	C:\Users\chen\Desktop\study\Foss\Shuai's Data\NMR DATA\500MHz092012\aaaron\carbon\CS_199_oxidation_product_carbon-1.jdf				
Frequency (MHz)	125.77	Nucleus	¹³ C	Number of Transients	40
Original Points Count	32768	Owner	delta	Points Count	32768
Receiver Gain	50.00	Solvent	CHLOROFORM-d	Spectrum Offset (Hz)	12576.5293
Sweep Width (Hz)	39308.18	Temperature (degree C)	22.500	Spectrum Type	STANDARD



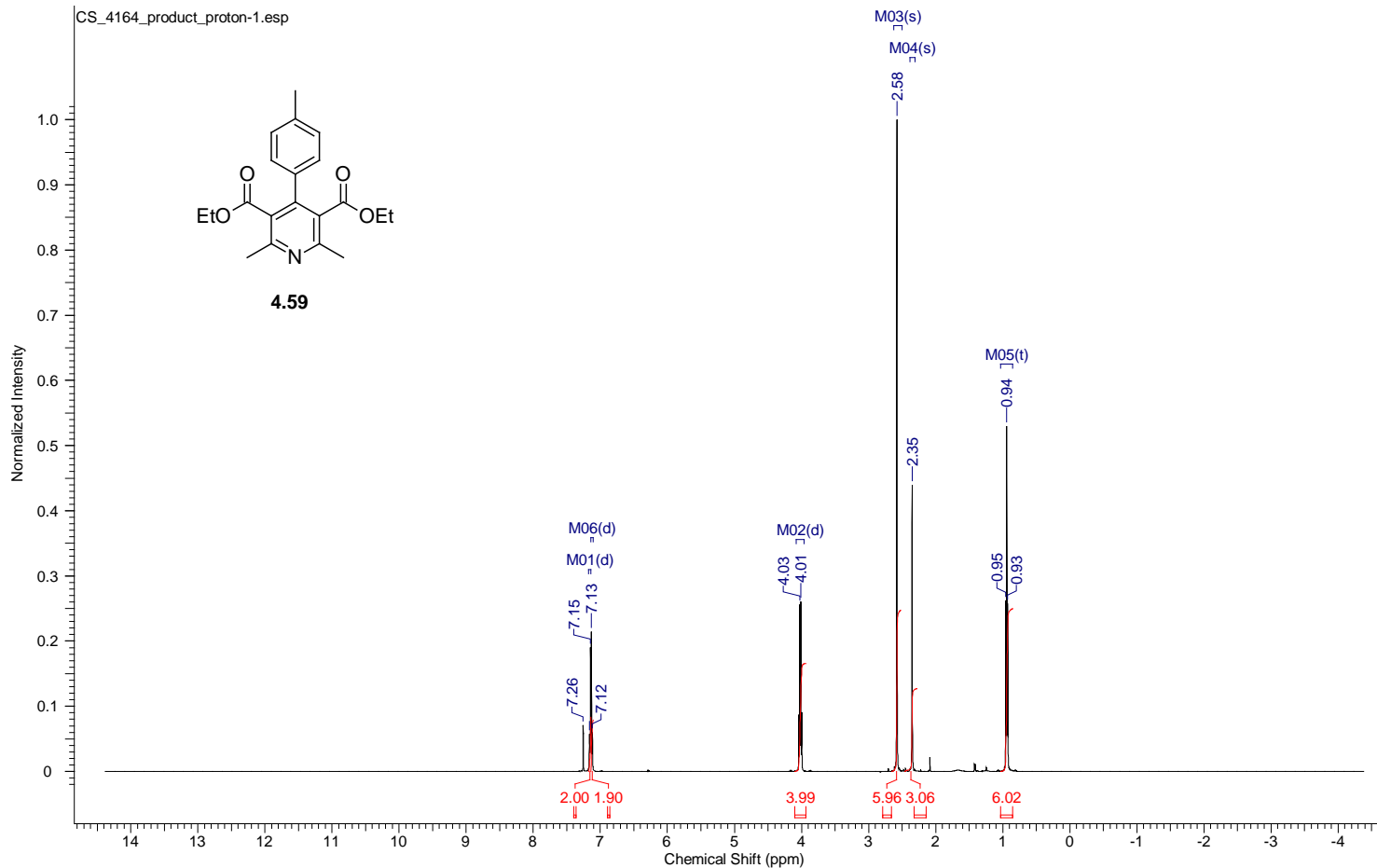
Acquisition Time (sec)	1.7459	Comment	single_pulse	Date	26 Sep 2012 13:23:22
Date Stamp	27 Sep 2012 05:42:19				
File Name	C:\Users\chen\Desktop\study\Foss\Shuai's Data\NMR DATA\500MHz\092012\laaron\proton\CS_4168_column_proton-1_jdf				
Frequency (MHz)	500.16	Nucleus	1H	Number of Transients	5
Original Points Count	16384	Owner	delta	Points Count	16384
Receiver Gain	40.00	Solvent	CHLOROFORM-d	Spectrum Offset (Hz)	2500.7996
Sweep Width (Hz)	9384.38	Temperature (degree C)	22.000	Spectrum Type	STANDARD



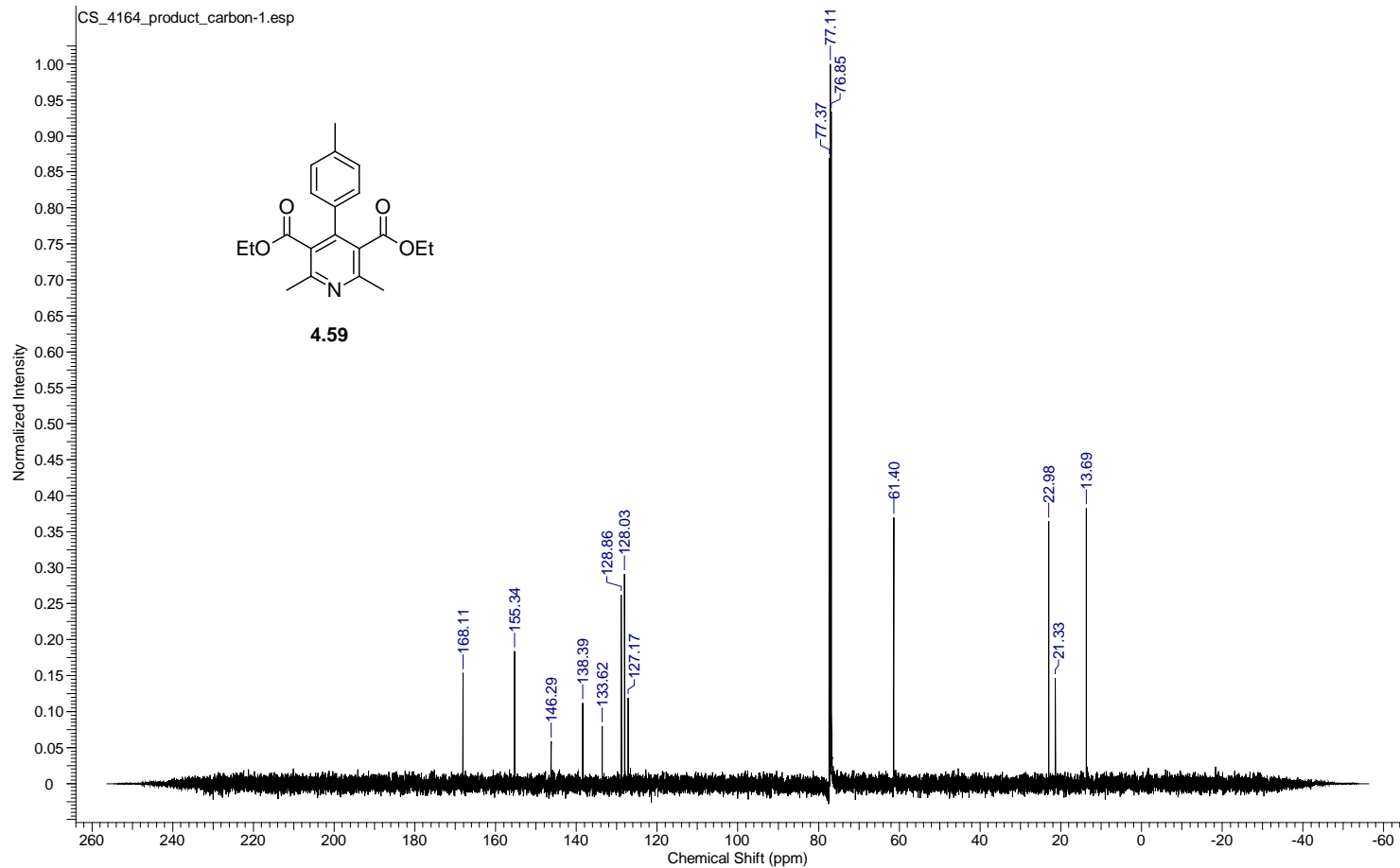
Acquisition Time (sec)	0.8336	Comment	single pulse decoupled gated NOE		Date	26 Sep 2012 13:25:53	
Date Stamp	27 Sep 2012 05:44:50						
File Name	C:\Users\chen\Desktop\study\Foss\Shuai's Data\NMR DATA\500MHz092012\aaaron\carbon\CS_4168_product_carbon-1.jdf						
Frequency (MHz)	125.77	Nucleus	¹³ C	Number of Transients	40	Origin	ECA 500
Original Points Count	32768	Owner	delta	Points Count	32768	Pulse Sequence	single_pulse_dec
Receiver Gain	50.00	Solvent	CHLOROFORM-d	Spectrum Offset (Hz)	12576.5293	Spectrum Type	STANDARD
Sweep Width (Hz)	39308.18	Temperature (degree C)	22.300				



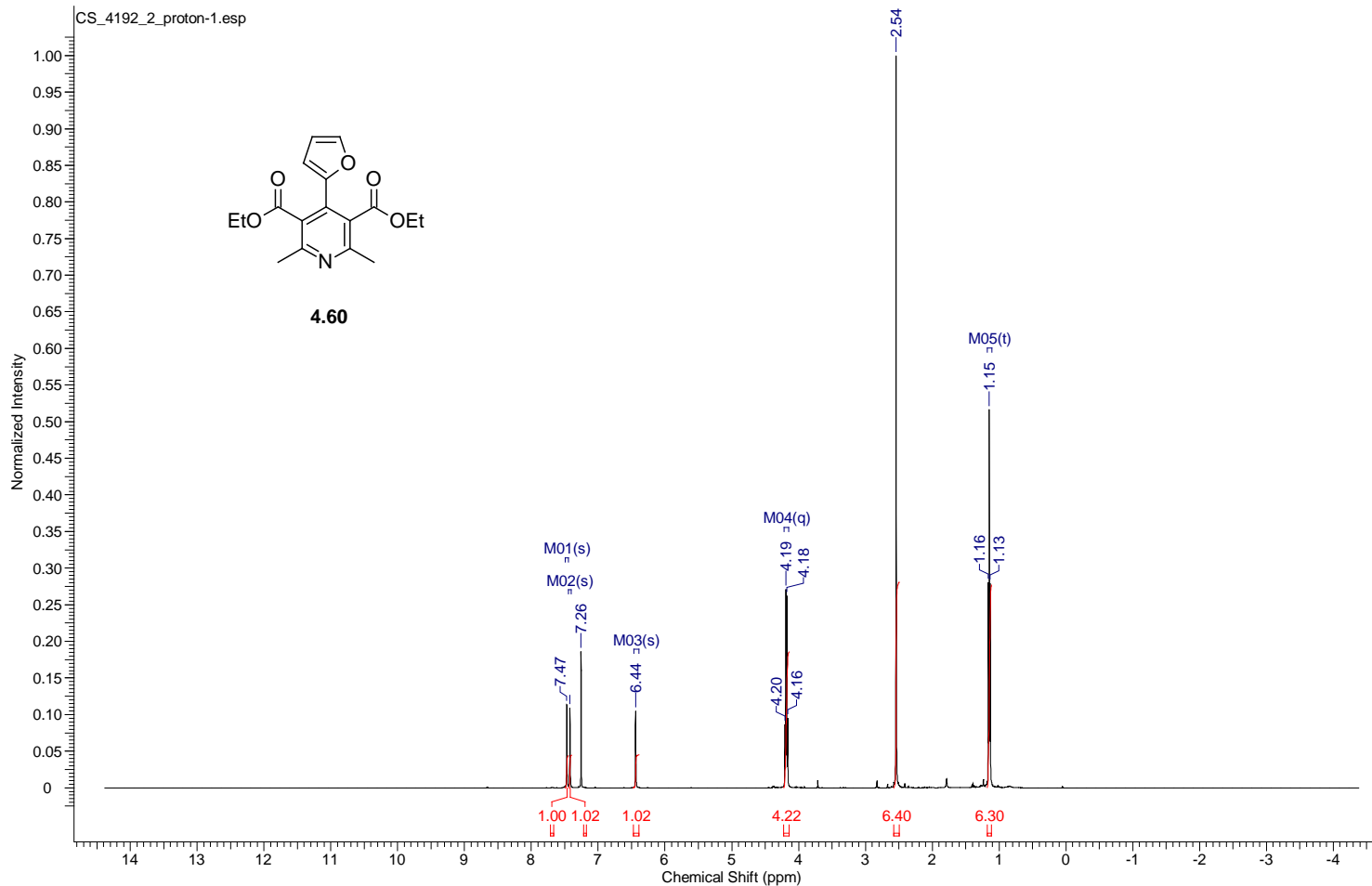
Acquisition Time (sec)	1.7459	Comment	single_pulse	Date	27 Sep 2012 08:47:58
Date Stamp	28 Sep 2012 01:06:56				
File Name	C:\Users\chen\Desktop\study\Foss\Shuai's Data\NMR DATA\500MHz\092012\aaaron\proton\CS_4164_product_proton-1.jdf				
Frequency (MHz)	500.16	Nucleus	1H	Number of Transients	4
Original Points Count	16384	Owner	delta	Points Count	16384
Receiver Gain	40.00	Solvent	CHLOROFORM-d	Spectrum Offset (Hz)	2500.7996
Sweep Width (Hz)	9384.38	Temperature (degree C)	22.200	Spectrum Type	STANDARD



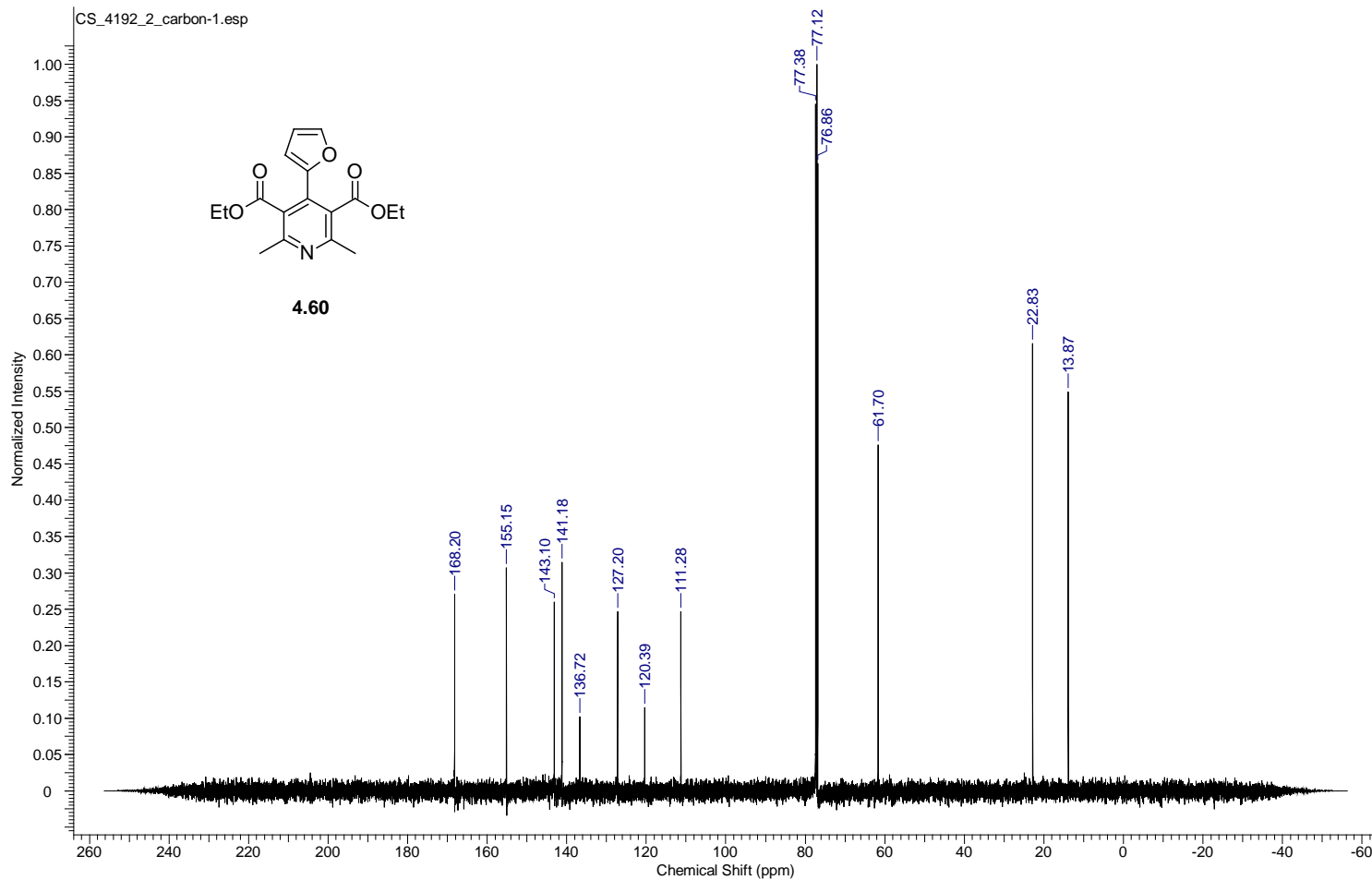
Acquisition Time (sec)	0.8336	Comment	single pulse decoupled gated NOE	Date	27 Sep 2012 08:47:07
Date Stamp	28 Sep 2012 01:06:05				
File Name	C:\Users\chen\Desktop\study\Foss\Shuai's Data\NMR DATA\500MHz\092012\aaaron\carbon\CS_4164_product_carbon-1.jdf				
Frequency (MHz)	125.77	Nucleus	¹³ C	Number of Transients	50
Original Points Count	32768	Owner	delta	Points Count	32768
Receiver Gain	50.00	Solvent	CHLOROFORM-d	Spectrum Offset (Hz)	12576.5293
Sweep Width (Hz)	39308.18	Temperature (degree C)	22.400	Spectrum Type	STANDARD



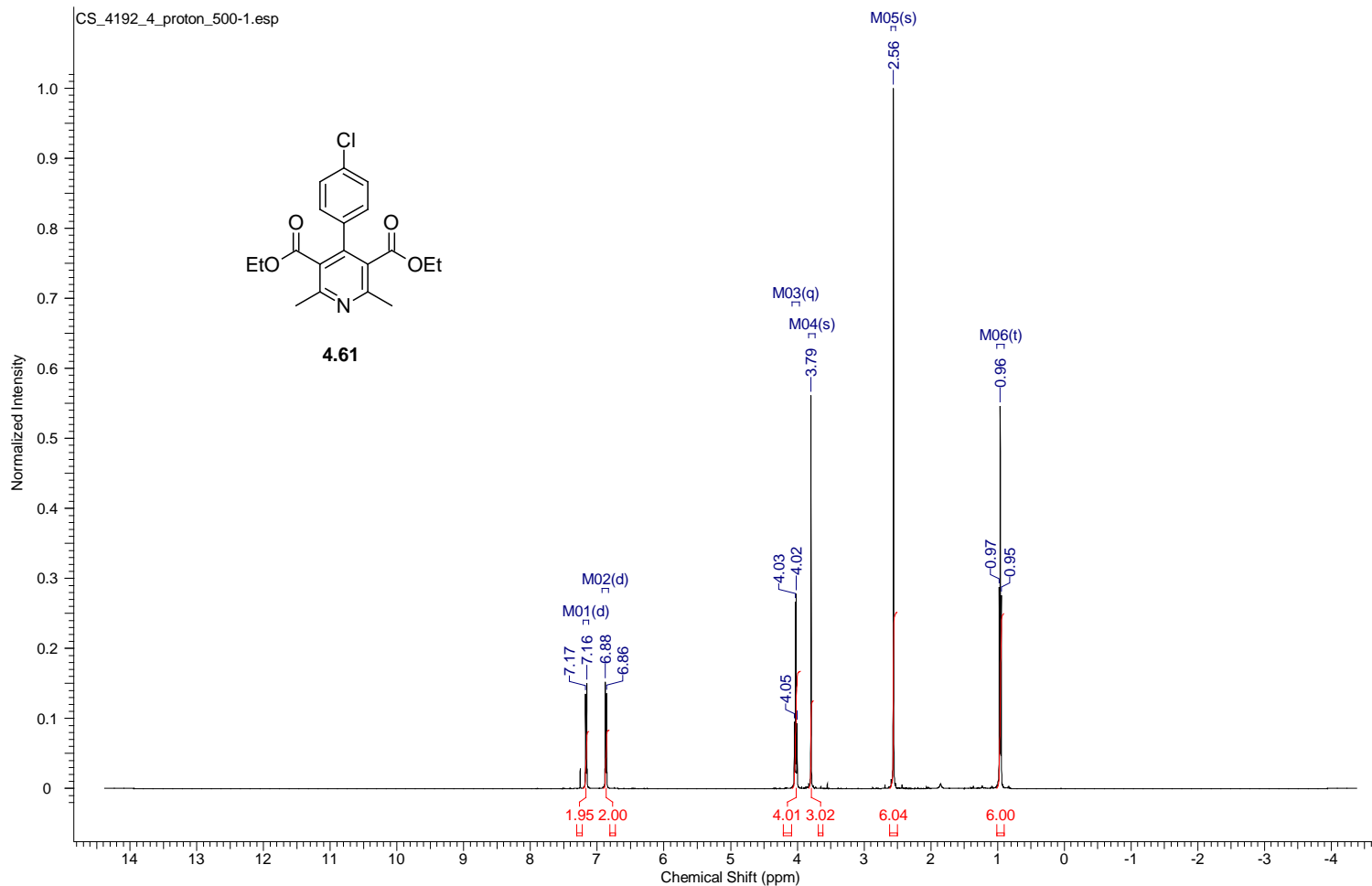
Acquisition Time (sec)	1.7459	Comment	single_pulse	Date	23 Oct 2012 11:35:34
Date Stamp	24 Oct 2012 03:36:42	File Name	G:\500MHz101512\aaaron\proton\CS_4192_2_proton-1.jdf		
Frequency (MHz)	500.16	Nucleus	1H	Number of Transients	4
Original Points Count	16384	Owner	delta	Points Count	16384
Receiver Gain	34.00	Solvent	CHLOROFORM-d	Pulse Sequence	single_pulse.ex2
Spectrum Type	STANDARD	Sweep Width (Hz)	9384.38	Temperature (degree C)	22.900



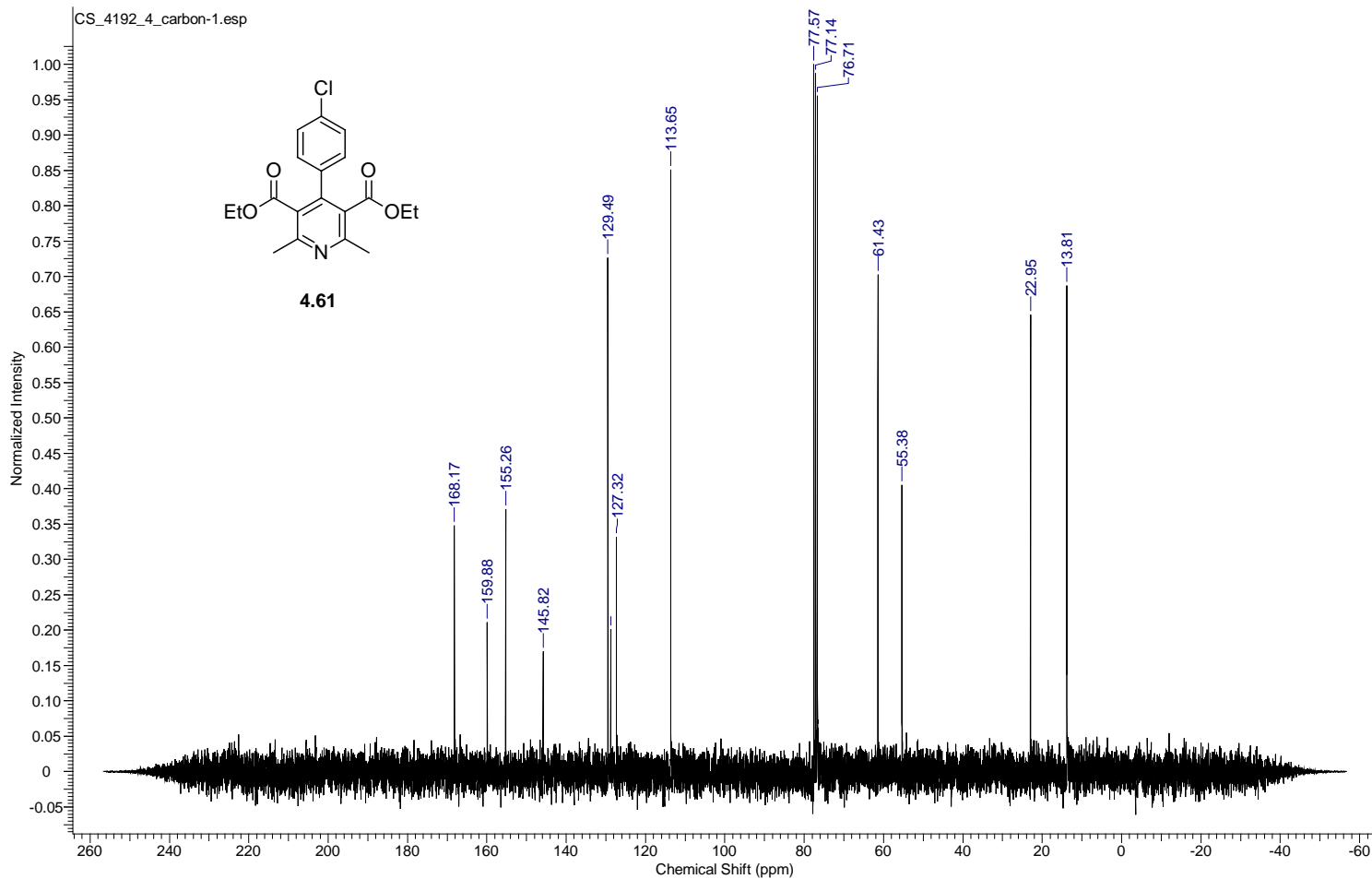
Acquisition Time (sec)	0.8336	Comment	single pulse decoupled gated NOE	Date	23 Oct 2012 11:36:52
Date Stamp	24 Oct 2012 03:38:01	File Name	G:\500MHz101512\laron\carbon\CS_4192_2_carbon-1.jdf	Frequency (MHz)	125.77
Original Points Count	32768	Owner	delta	Number of Transients	30
Receiver Gain	50.00	Solvent	CHLOROFORM-d	Points Count	32768
Spectrum Type	STANDARD	Sweep Width (Hz)	39308.18	Temperature (degree C)	23.100
				Origin	ECA 500
				Pulse Sequence	single_pulse_dec
				Spectrum Offset (Hz)	12576.5293



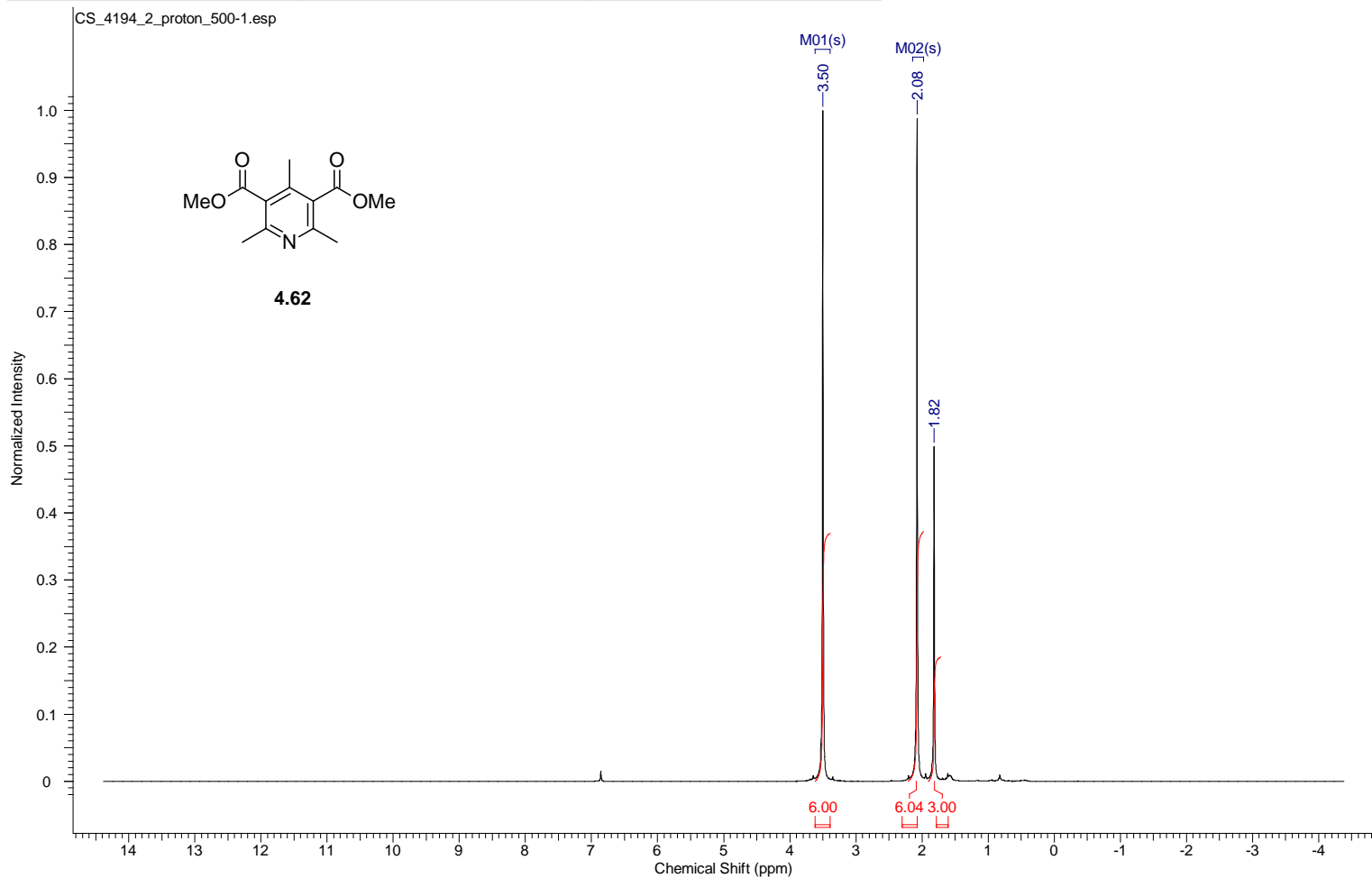
Acquisition Time (sec)	1.7459	Comment	single_pulse	Date	19 Oct 2012 10:26:01
Date Stamp	20 Oct 2012 02:27:08	File Name	G:\500MHz101512\aaaron\proton\CS_4192_4_proton_500-1.jdf		
Frequency (MHz)	500.16	Nucleus	1H	Number of Transients	10
Original Points Count	16384	Owner	delta	Points Count	16384
Receiver Gain	30.00	Solvent	CHLOROFORM-d	Pulse Sequence	single_pulse.ex2
Spectrum Type	STANDARD	Sweep Width (Hz)	9384.38	Temperature (degree C)	21.000



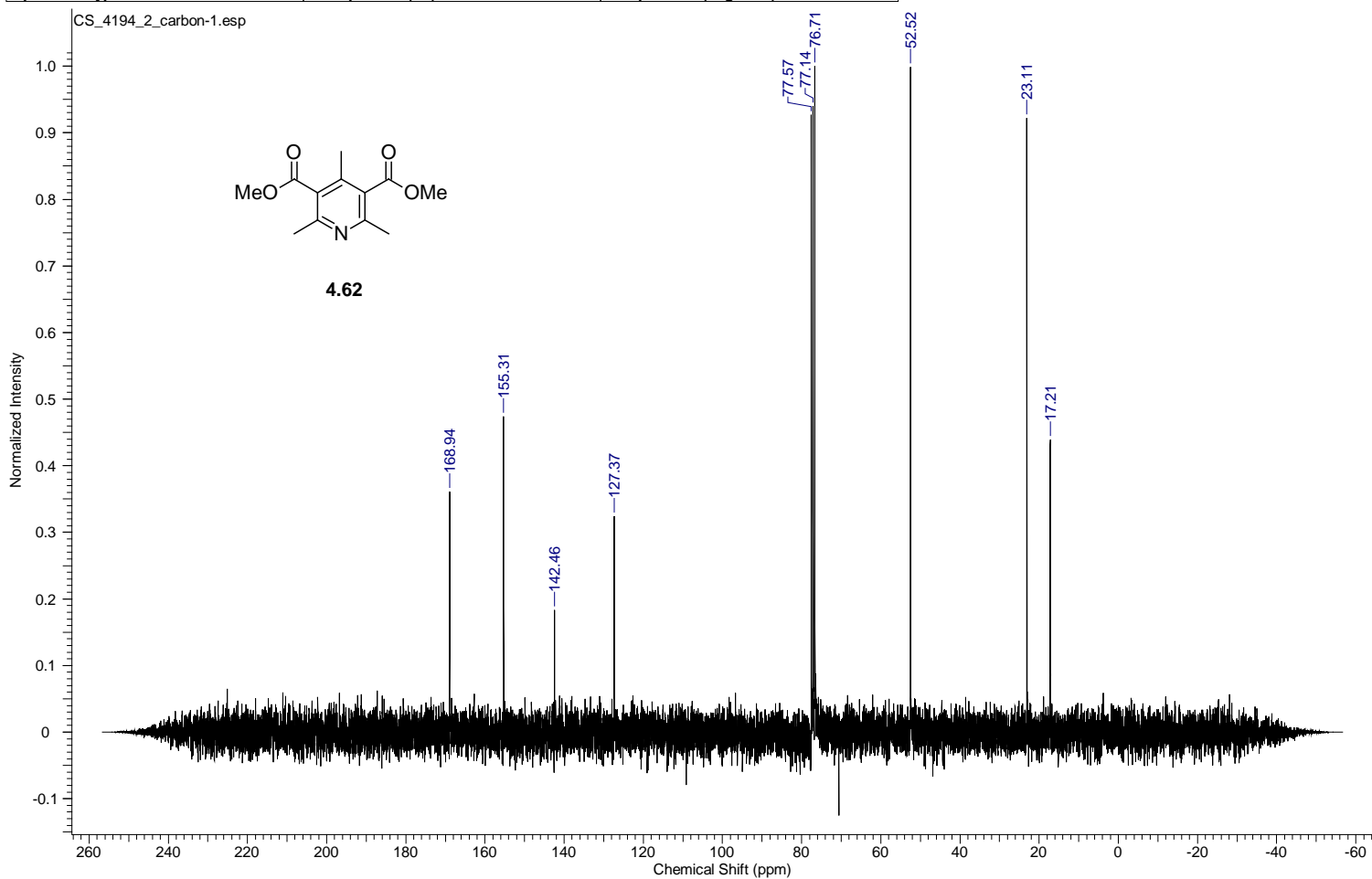
Acquisition Time (sec)	1.3841	Comment	single pulse decoupled gated NOE	Date	16 Oct 2012 11:37:13
Date Stamp	16 Oct 2012 11:22:45	File Name	G:\500MHz101512\carbon\CS_4192_4_carbon-1.jdf	Frequency (MHz)	75.57
Original Points Count	32768	Nucleus	13C	Number of Transients	70
Receiver Gain	50.00	Owner	delta	Points Count	32768
Spectrum Type	STANDARD	Solvent	CHLOROFORM-d	Pulse Sequence	single_pulse_dec
		Sweep Width (Hz)	23674.24	Temperature (degree C)	22.100
				Spectrum Offset (Hz)	7556.8232



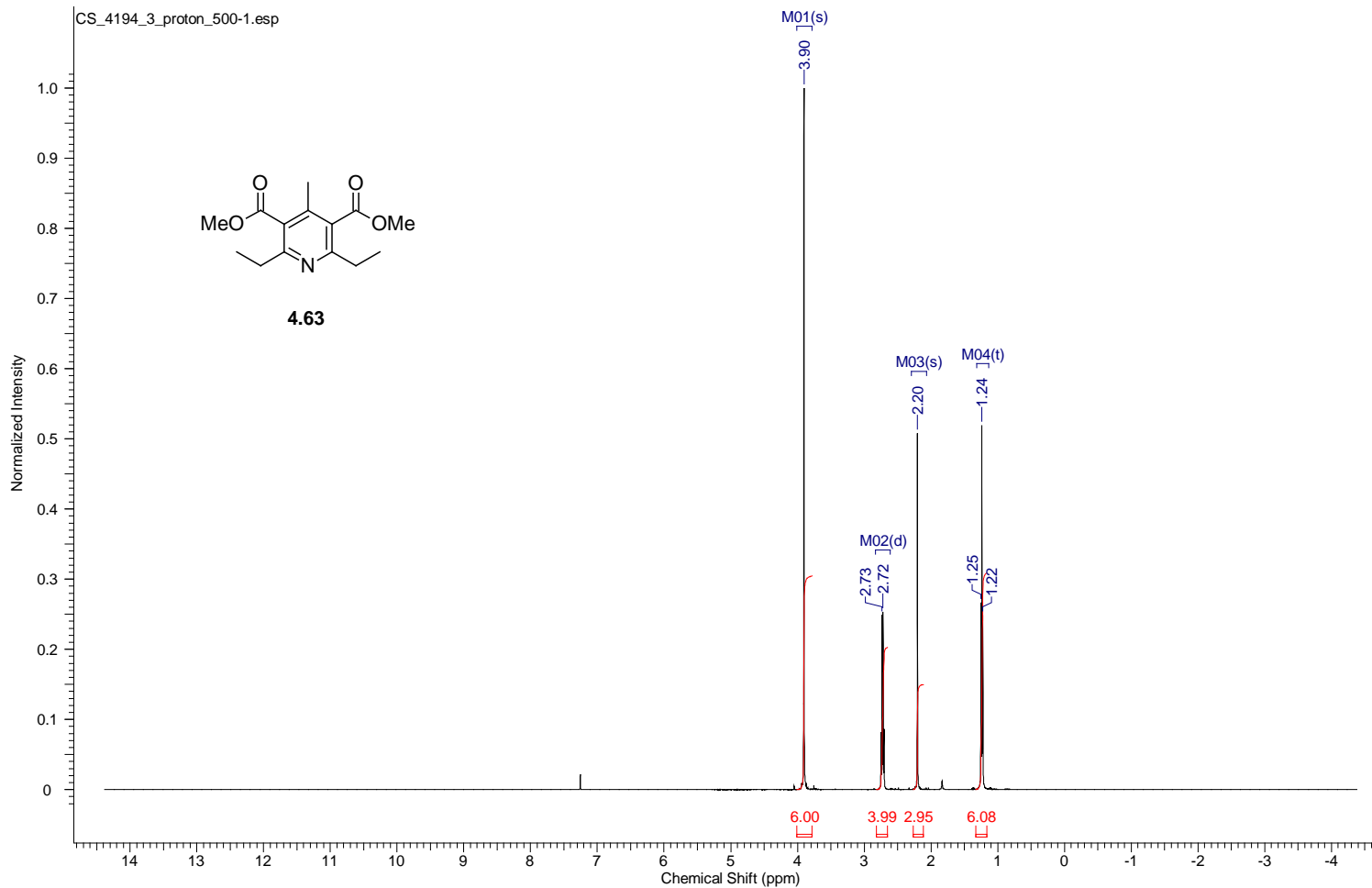
Acquisition Time (sec)	1.7459	Comment	single_pulse	Date	19 Oct 2012 10:35:24
Date Stamp	20 Oct 2012 02:36:31	File Name	G:\500MHz\101512\aaaron\proton\CS_4194_2_proton_500-1.jdf		
Frequency (MHz)	500.16	Nucleus	1H	Number of Transients	4
Original Points Count	16384	Owner	delta	Points Count	16384
Receiver Gain	30.00	Solvent	CHLOROFORM-d	Pulse Sequence	single_pulse.ex2
Spectrum Type	STANDARD	Sweep Width (Hz)	9384.38	Temperature (degree C)	21.100



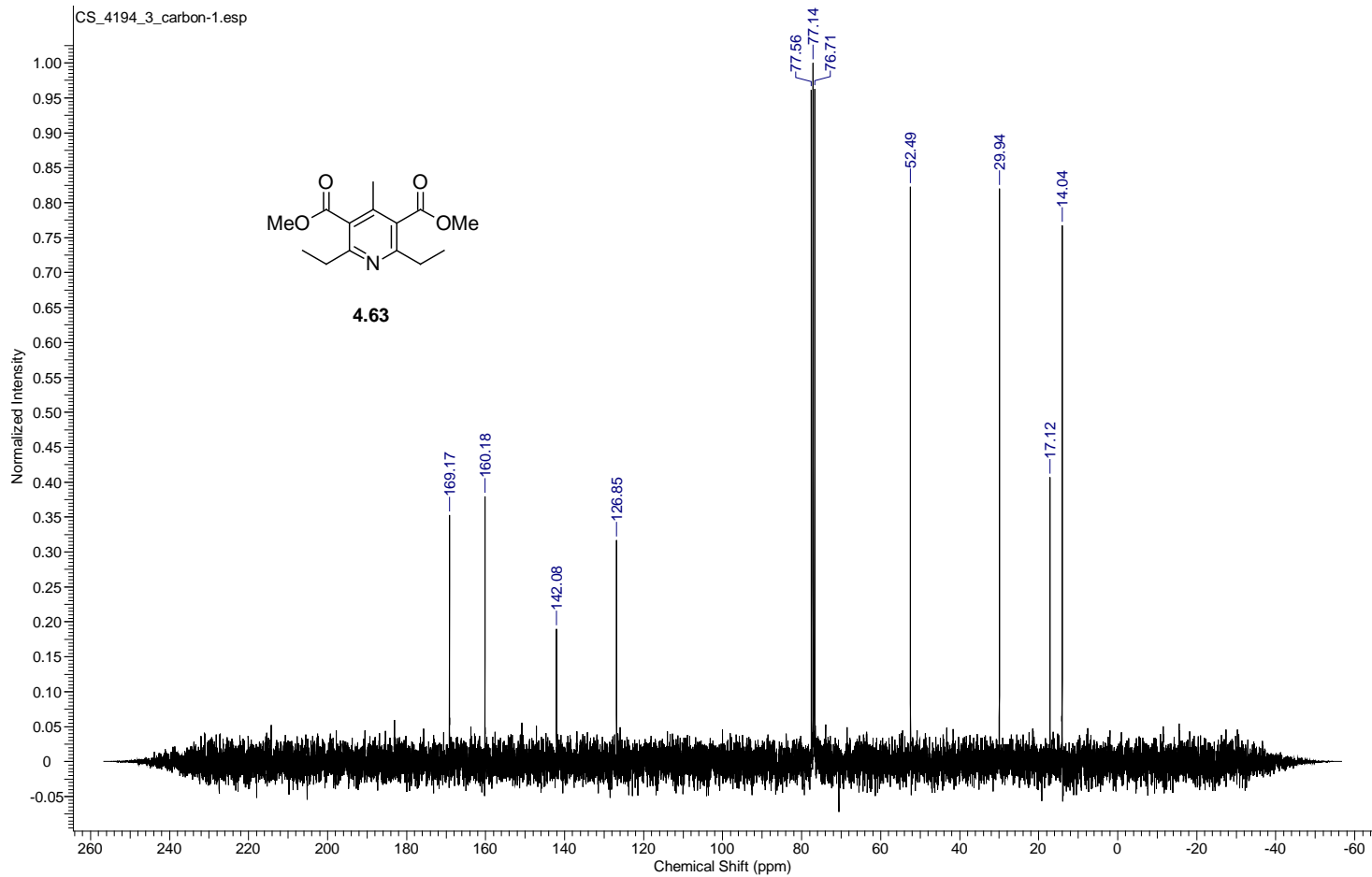
Acquisition Time (sec)	1.3841	Comment	single pulse decoupled gated NOE	Date	16 Oct 2012 11:20:55
Date Stamp	16 Oct 2012 11:06:27	File Name	G:\500MHz101512\carbon\CS_4194_2_carbon-1.jdf	Origin	ECX 300
Frequency (MHz)	75.57	Nucleus	13C	Number of Transients	60
Original Points Count	32768	Owner	delta	Points Count	32768
Receiver Gain	50.00	Solvent	CHLOROFORM-d	Pulse Sequence	single_pulse_dec
Spectrum Type	STANDARD	Sweep Width (Hz)	23674.24	Temperature (degree C)	22.700



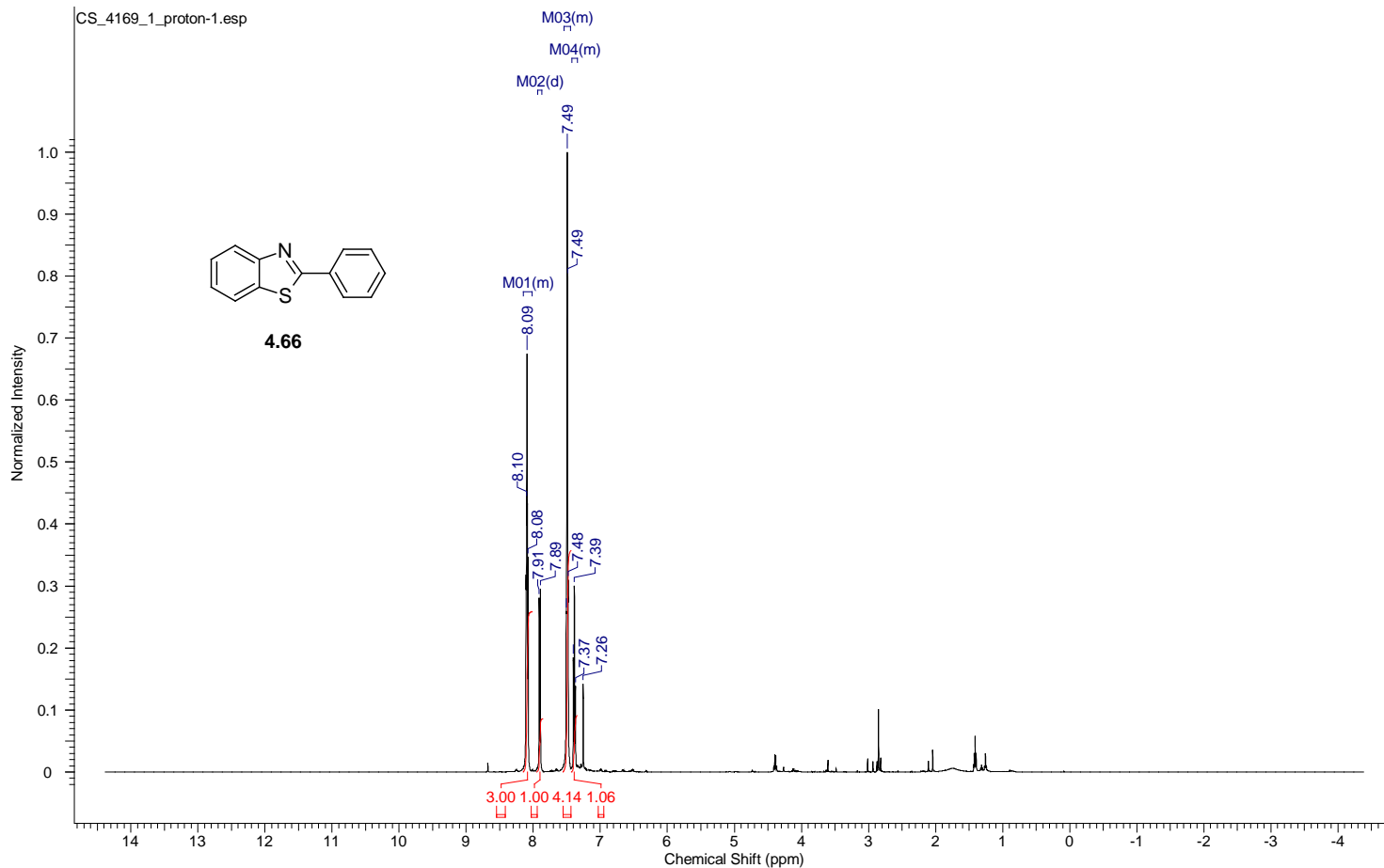
Acquisition Time (sec)	1.7459	Comment	single_pulse	Date	19 Oct 2012 10:39:20
Date Stamp	20 Oct 2012 02:40:26	File Name	G:\500MHz101512\aaaron\proton\CS_4194_3_proton_500-1.jdf		
Frequency (MHz)	500.16	Nucleus	1H	Number of Transients	2
Original Points Count	16384	Owner	delta	Points Count	16384
Receiver Gain	30.00	Solvent	CHLOROFORM-d	Pulse Sequence	single_pulse.ex2
Spectrum Type	STANDARD	Sweep Width (Hz)	9384.38	Temperature (degree C)	21.100



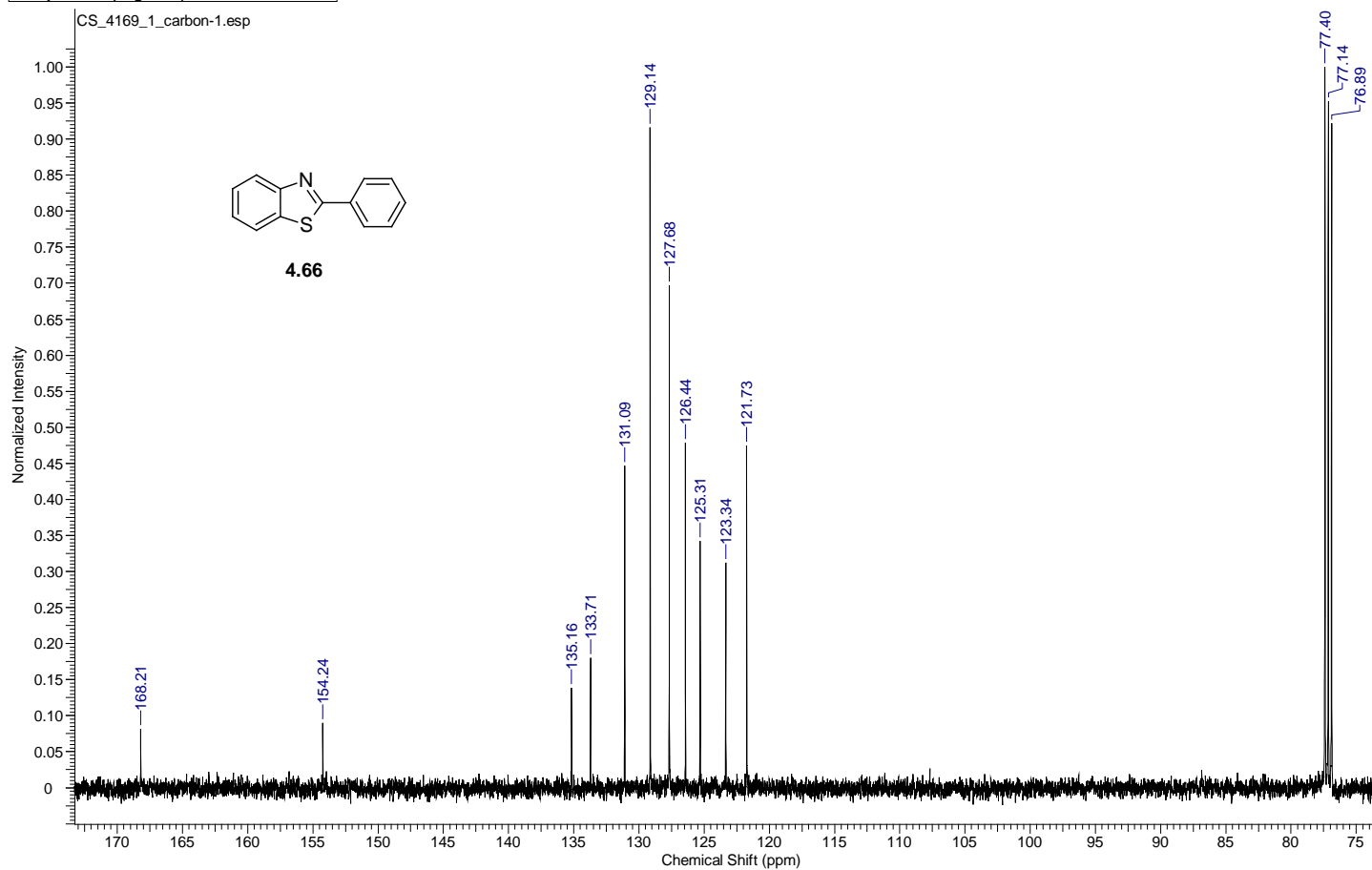
Acquisition Time (sec)	1.3841	Comment	single pulse decoupled gated NOE	Date	16 Oct 2012 11:27:15
Date Stamp	16 Oct 2012 11:12:46	File Name	G:\500MHz101512\carbon\CS_4194_3_carbon-1.jdf		
Frequency (MHz)	75.57	Nucleus	13C	Number of Transients	50
Original Points Count	32768	Owner	delta	Points Count	32768
Receiver Gain	50.00	Solvent	CHLOROFORM-d	Pulse Sequence	single_pulse_dec
Spectrum Type	STANDARD	Sweep Width (Hz)	23674.24	Temperature (degree C)	22.500
				Spectrum Offset (Hz)	7556.8232



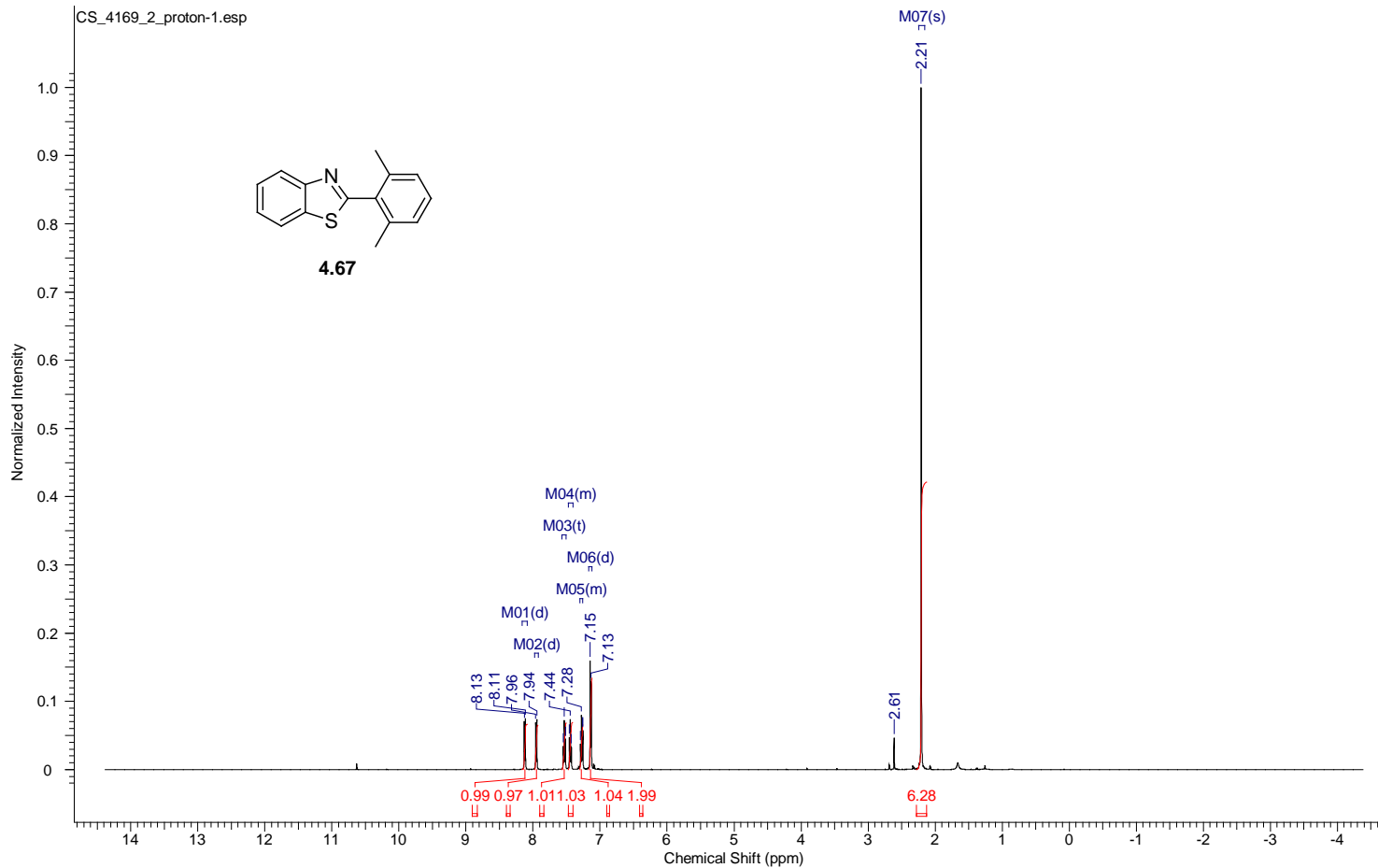
Acquisition Time (sec)	1.7459	Comment	single_pulse	Date	28 Sep 2012 09:26:58
Date Stamp	29 Sep 2012 01:45:56				
File Name	C:\Users\chen\Desktop\study\Foss\Shuai's Data\NMR DATA\500MHz092012\aaaron\proton\CS_4169_1_proton-1.jdf				
Frequency (MHz)	500.16	Nucleus	1H	Number of Transients	5
Original Points Count	16384	Owner	delta	Points Count	16384
Receiver Gain	40.00	Solvent	CHLOROFORM-d	Pulse Sequence	single_pulse.ex2
Spectrum Type	STANDARD	Sweep Width (Hz)	9384.38	Temperature (degree C)	22.000



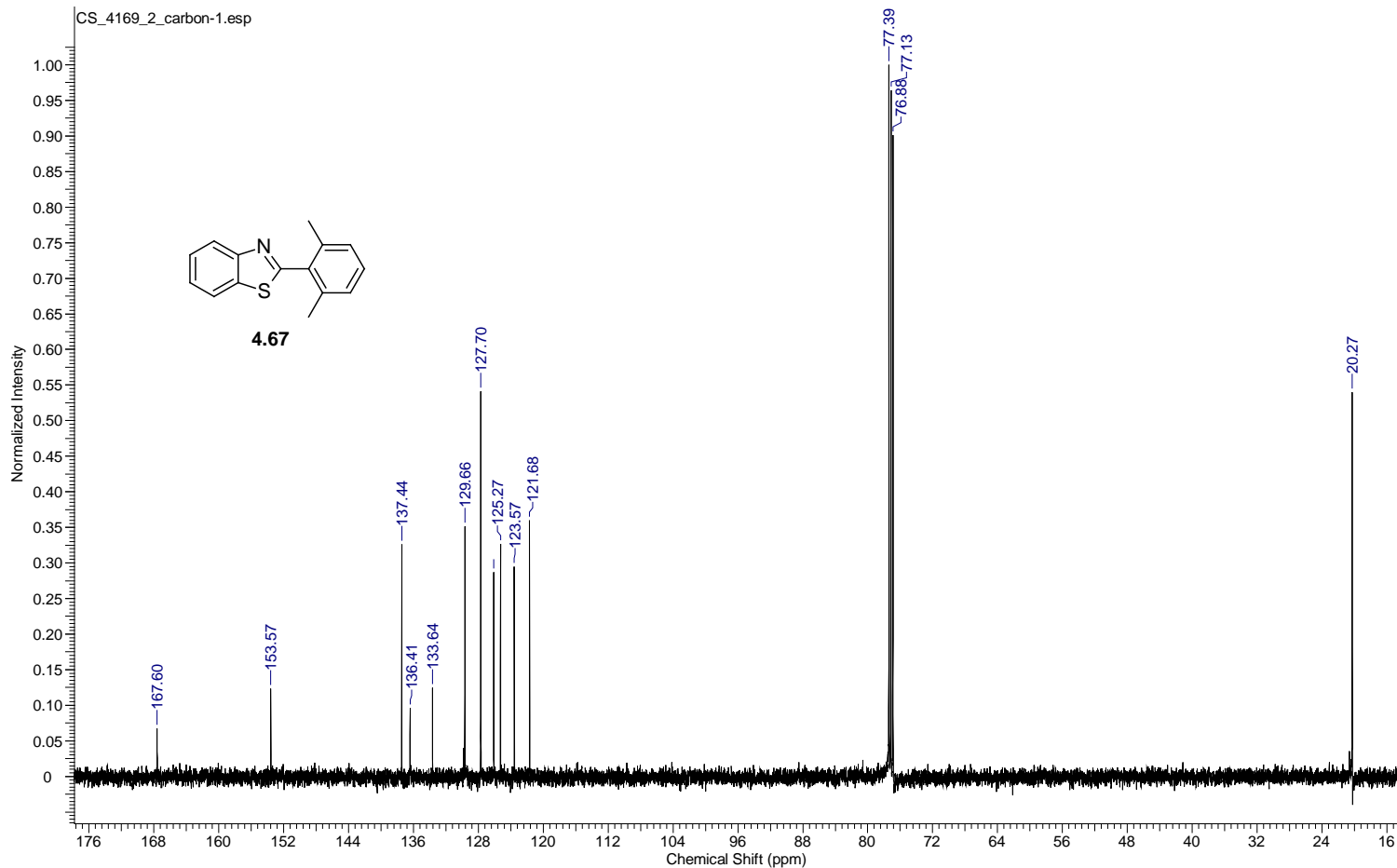
Acquisition Time (sec)	0.8336	Comment	single pulse decoupled gated NOE	Date	28 Sep 2012 09:28:37
Date Stamp	29 Sep 2012 01:47:35				
File Name	C:\Users\chen\Desktop\study\Foss\Shuai's Data\NMR DATA\500MHz092012\aaon\carbon\CS_4169_1_carbon-1.jdf			Frequency (MHz)	125.77
Nucleus	13C	Number of Transients	40	Origin	ECA 500
Owner	delta	Points Count	32768	Pulse Sequence	single_pulse_dec
Solvent	CHLOROFORM-d	Spectrum Offset (Hz)	12576.5293	Spectrum Type	STANDARD
Temperature (degree C)	22.300				



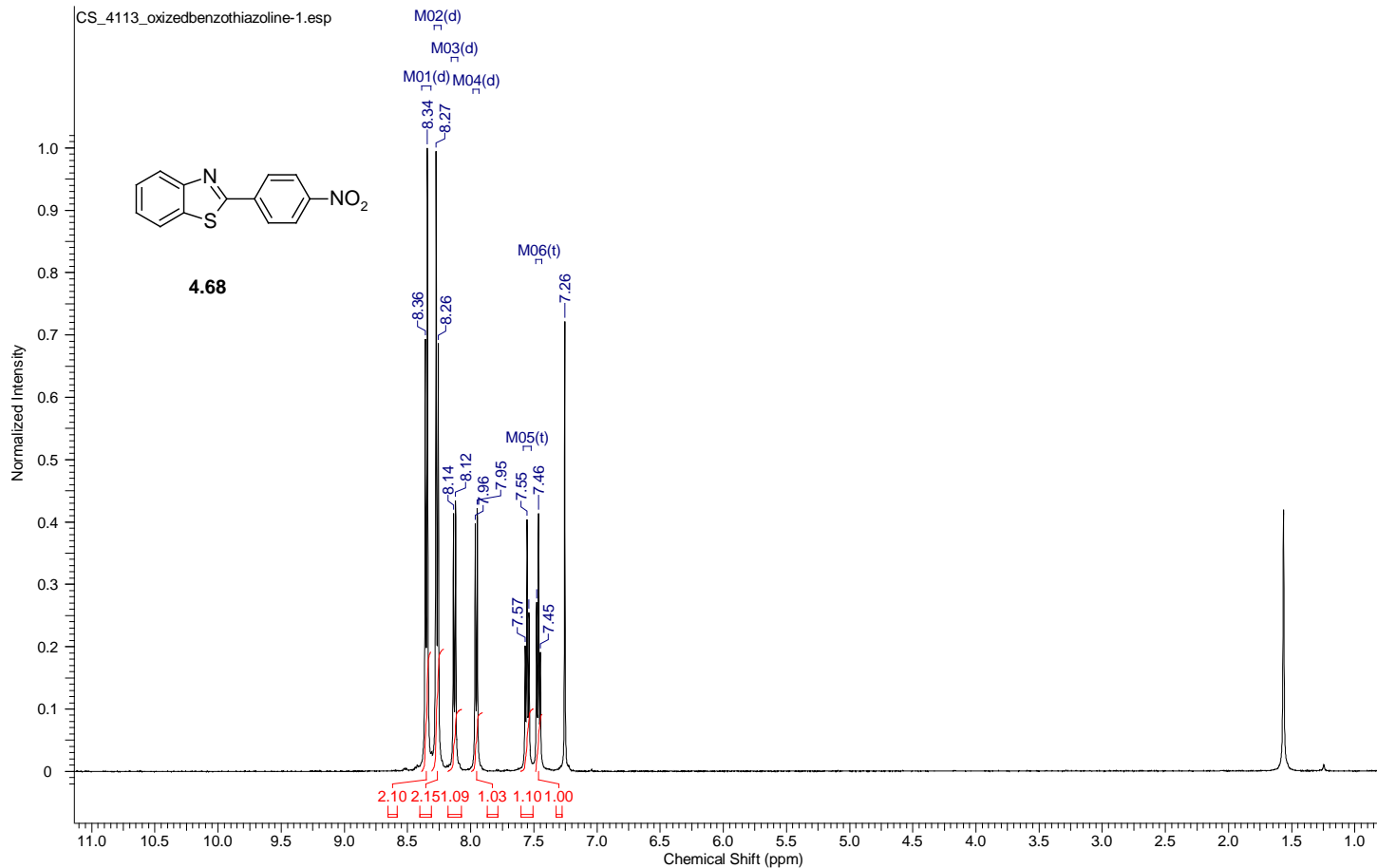
Acquisition Time (sec)	1.7459	Comment	single_pulse	Date	28 Sep 2012 09:34:20
Date Stamp	29 Sep 2012 01:53:18				
File Name	C:\Users\chen\Desktop\study\Foss\Shuai's Data\NMR DATA\500MHz\092012\laaron\proton\CS_4169_2_proton-1.jdf				
Frequency (MHz)	500.16	Nucleus	1H	Number of Transients	4
Original Points Count	16384	Owner	delta	Points Count	16384
Receiver Gain	40.00	Solvent	CHLOROFORM-d	Spectrum Offset (Hz)	2500.7996
Spectrum Type	STANDARD	Sweep Width (Hz)	9384.38	Temperature (degree C)	22.000



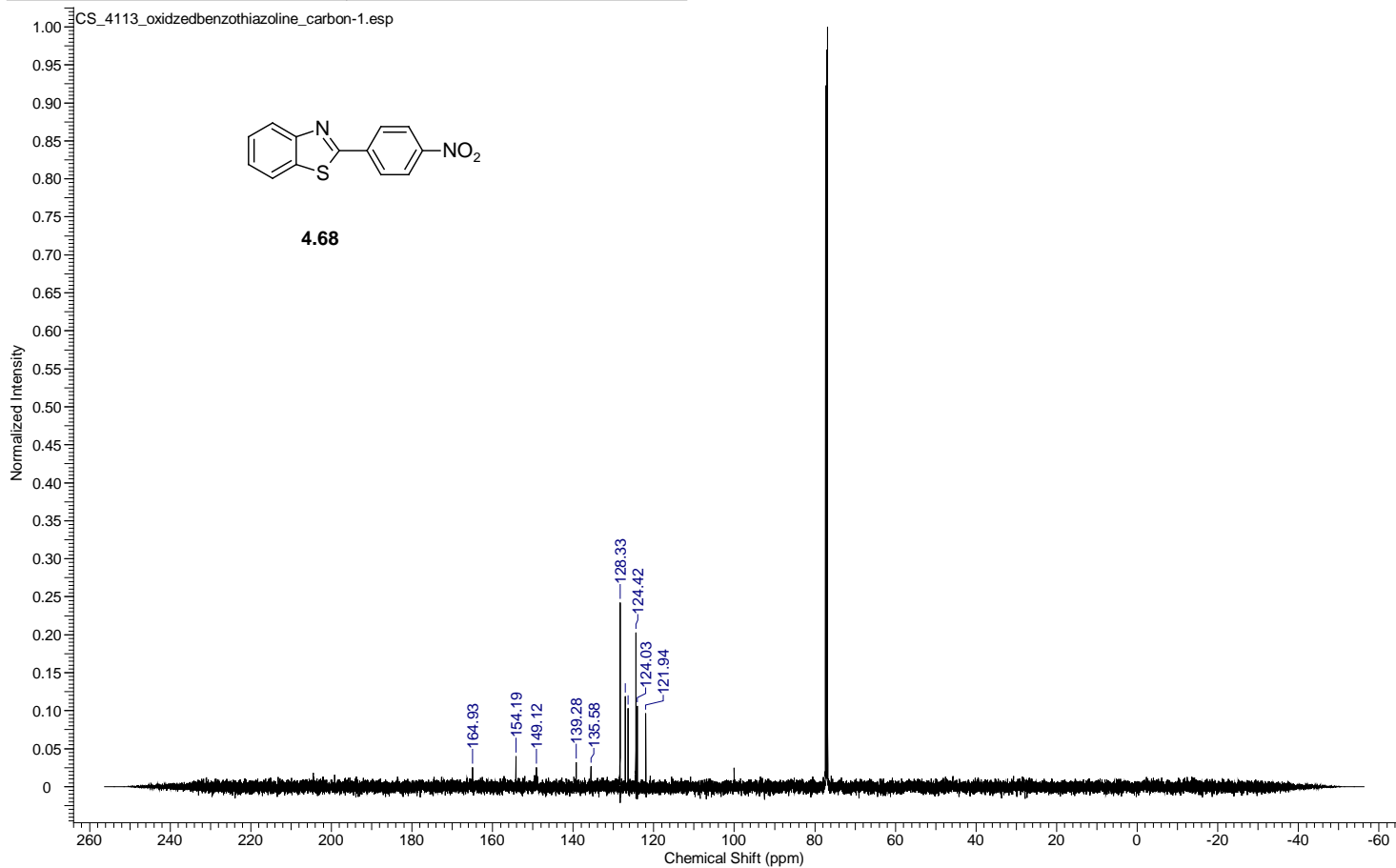
Acquisition Time (sec)	0.8336	Comment	single pulse decoupled gated NOE	Date	28 Sep 2012 09:36:19
Date Stamp	29 Sep 2012 01:55:17				
File Name	C:\Users\chen\Desktop\study\Foss\Shuai's Data\NMR DATA\500MHz\092012\aaaron\carbon\CS_4169_2_carbon-1.jdf			Frequency (MHz)	125.77
Nucleus	¹³ C	Number of Transients	50	Origin	ECA 500
Owner	delta	Points Count	32768	Pulse Sequence	single_pulse_dec
Solvent	CHLOROFORM-d	Spectrum Offset (Hz)	12576.5293	Spectrum Type	STANDARD
Temperature (degree C)	22.400			Sweep Width (Hz)	39308.18



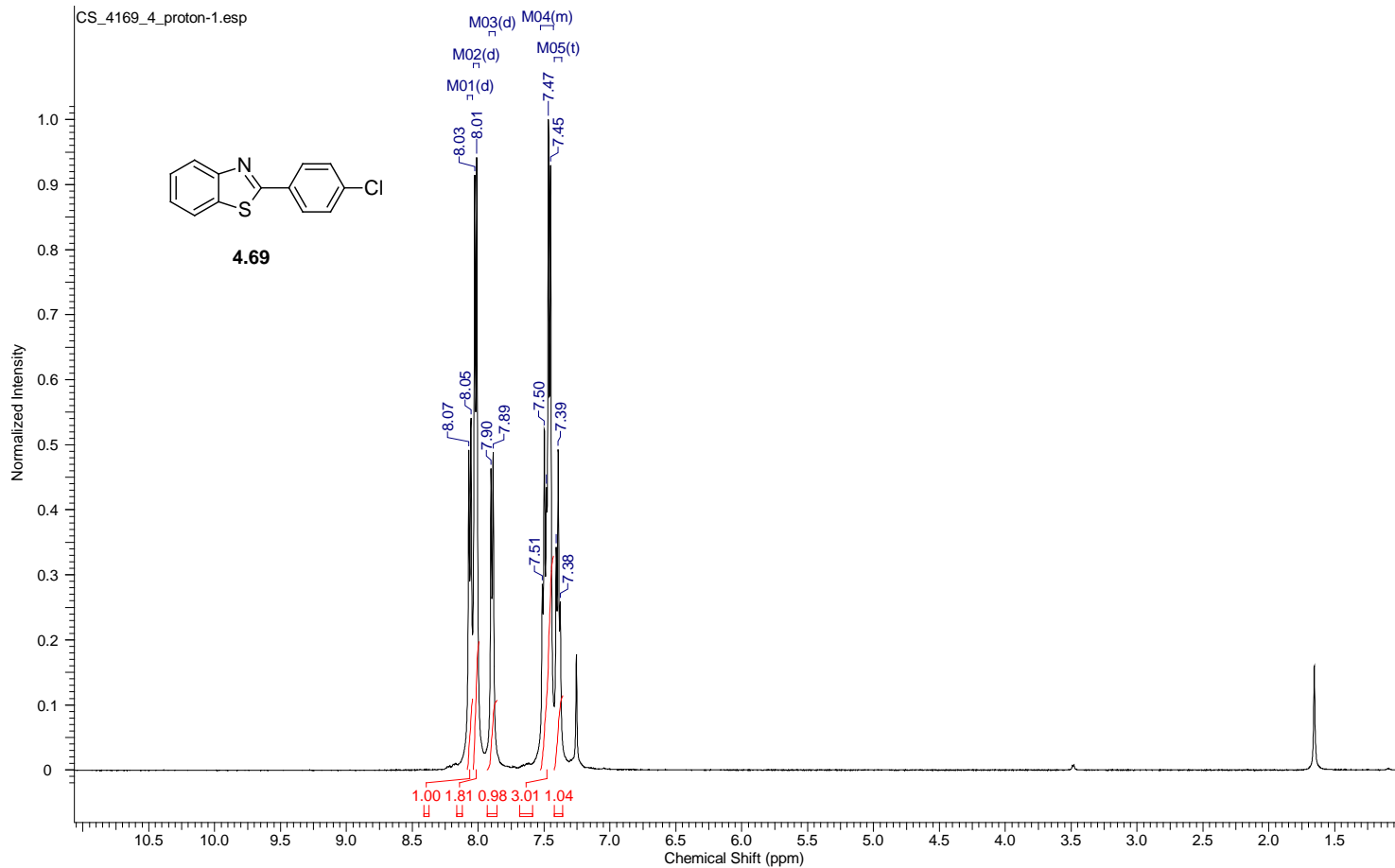
Acquisition Time (sec)	1.7459	Comment	single_pulse	Date	10 Aug 2012 11:51:50
Date Stamp	11 Aug 2012 04:10:28				
File Name	C:\Users\chen\Desktop\study\Foss\Shuai's Data\NMR DATA\500MHz\083012\laaron\proton\CS_4113_oxizedbenzothiazoline-1.jdf				
Frequency (MHz)	500.16	Nucleus	1H	Number of Transients	6
Original Points Count	16384	Owner	delta	Points Count	16384
Receiver Gain	48.00	Solvent	CHLOROFORM-d	Spectrum Offset (Hz)	2500.7996
Sweep Width (Hz)	9384.38	Temperature (degree C)	22.100	Spectrum Type	STANDARD



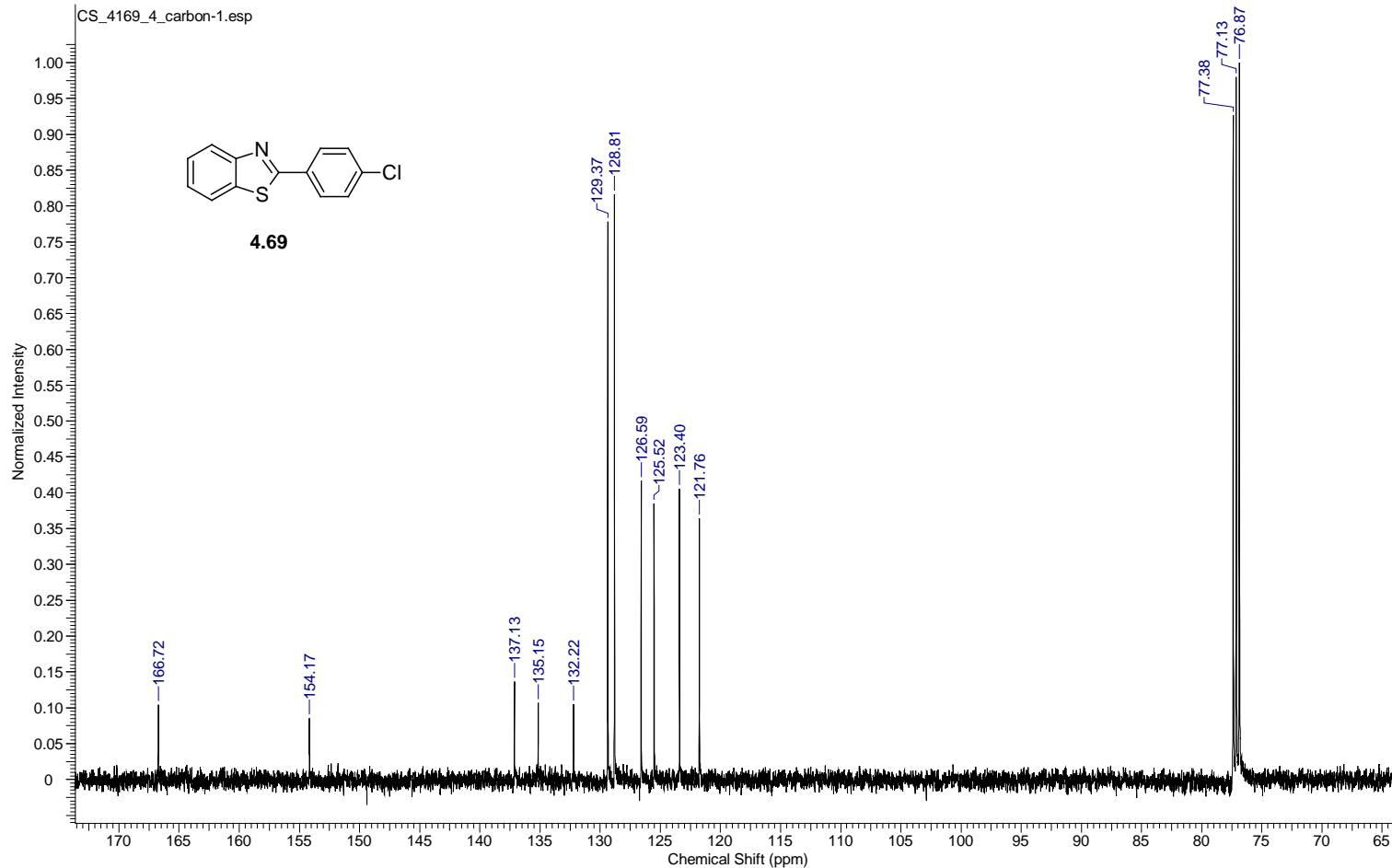
Acquisition Time (sec)	0.8336	Comment	single pulse decoupled gated NOE	Date	10 Aug 2012 11:57:23
Date Stamp	11 Aug 2012 04:16:01				
File Name	C:\Users\ichen\Desktop\study\Foss\Shuai's Data\NMR DATA\500HMz081312\aaaron\carbon\CS_4113_oxidzedbenzothiazoline_carbon-1.jdf				
Frequency (MHz)	125.77	Nucleus	13C	Number of Transients	140
Original Points Count	32768	Owner	delta	Points Count	32768
Receiver Gain	50.00	Solvent	CHLOROFORM-d	Spectrum Offset (Hz)	12576.5293
Sweep Width (Hz)	39308.18	Temperature (degree C)	22.600	Spectrum Type	STANDARD



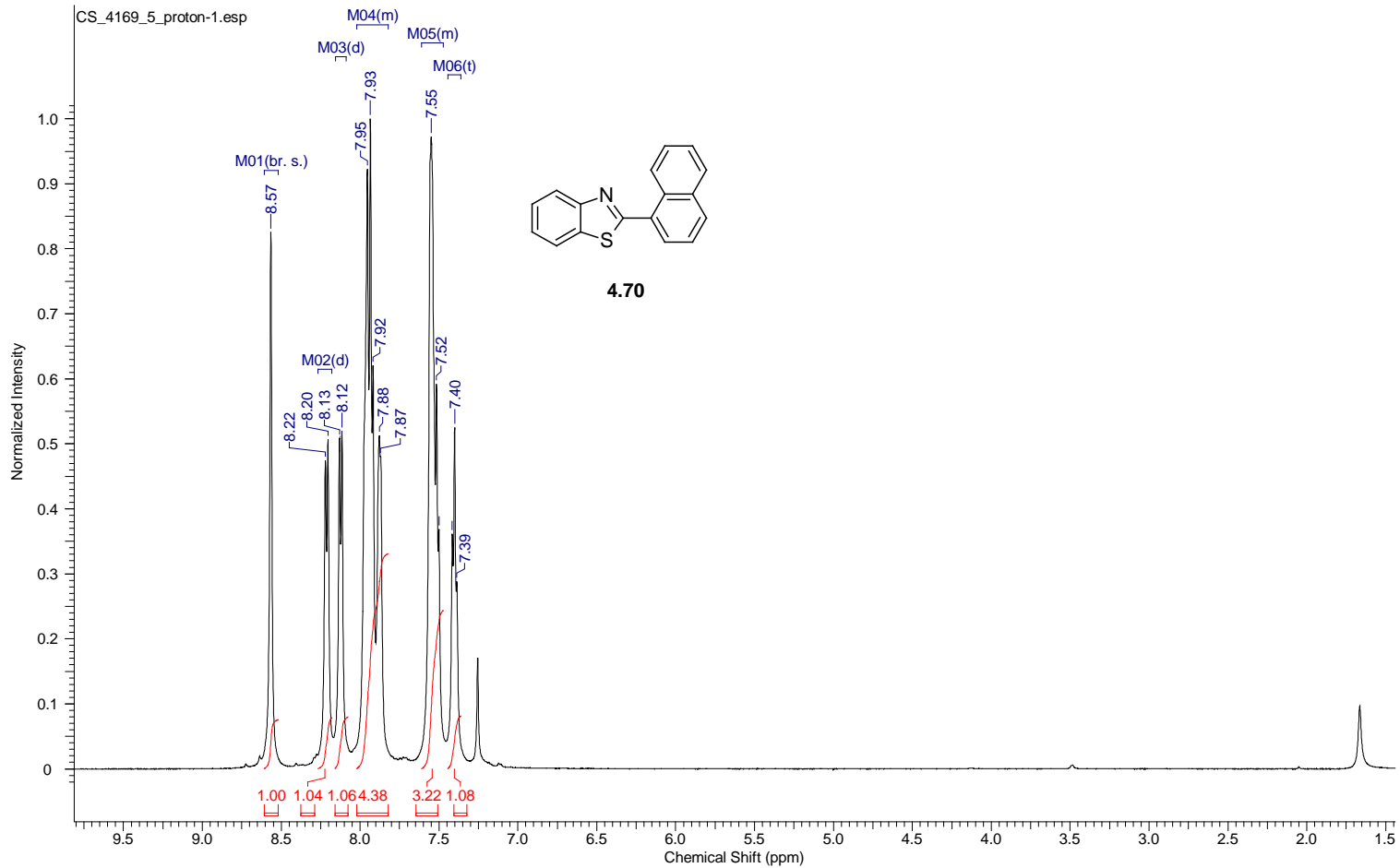
Acquisition Time (sec)	1.7459	Comment	single_pulse	Date	28 Sep 2012 09:40:33
Date Stamp	29 Sep 2012 01:59:31				
File Name	C:\Users\chen\Desktop\study\Foss\Shuai's Data\NMR DATA\500MHz\092012\laaron\proton\CS_4169_4_proton-1.jdf				
Frequency (MHz)	500.16	Nucleus	1H	Number of Transients	3
Original Points Count	16384	Owner	delta	Points Count	16384
Receiver Gain	44.00	Solvent	CHLOROFORM-d	Pulse Sequence	single_pulse.ex2
Spectrum Type	STANDARD	Sweep Width (Hz)	9384.38	Temperature (degree C)	22.000



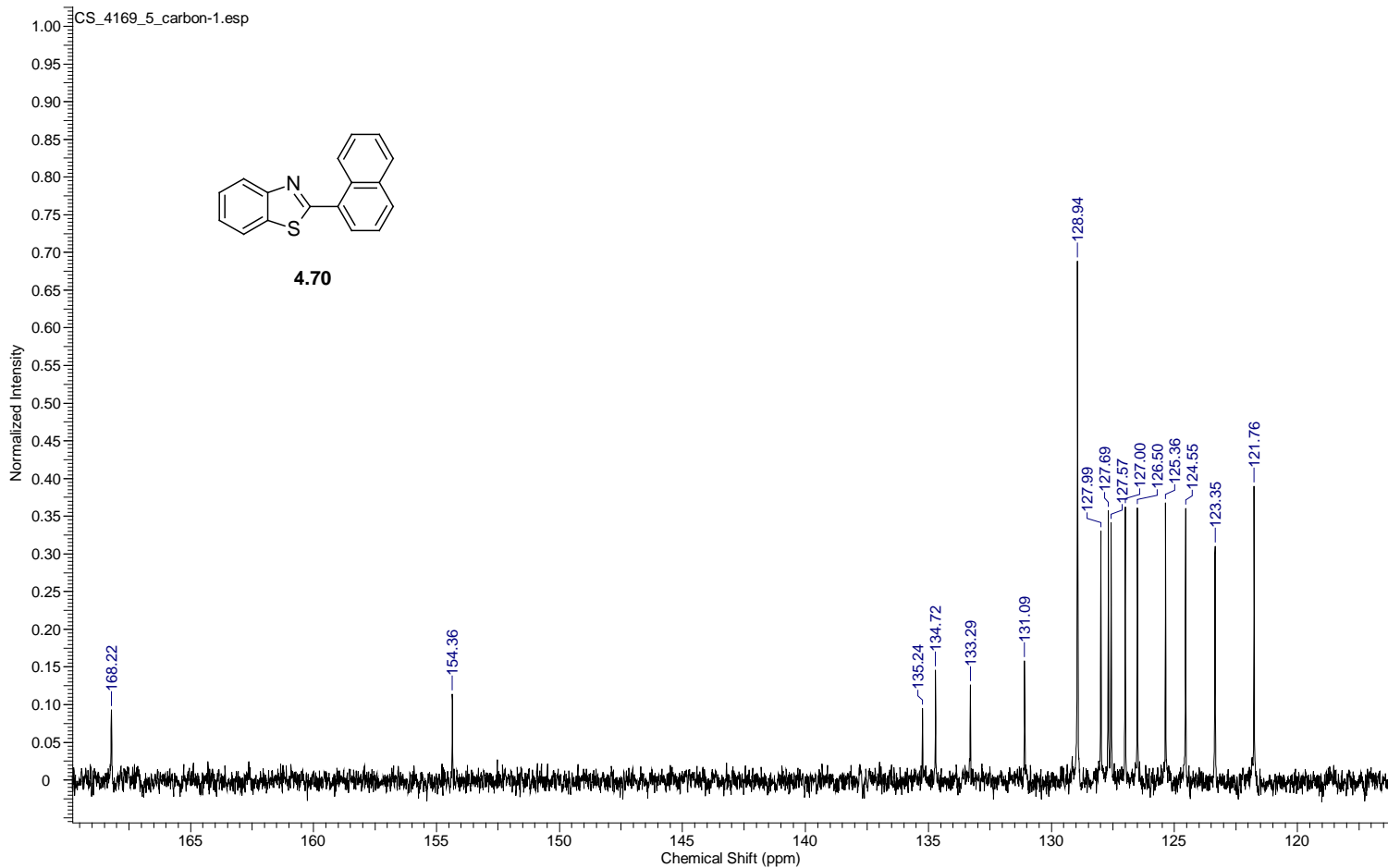
Acquisition Time (sec)	0.8336	Comment	single pulse decoupled gated NOE	Date	28 Sep 2012 09:43:16
Date Stamp	29 Sep 2012 02:02:14				
File Name	C:\Users\chen\Desktop\study\Foss\Shuai's Data\NMR DATA\500MHz092012\aaaron\carbon\CS_4169_4_carbon-1.jdf			Frequency (MHz)	125.77
Nucleus	13C	Number of Transients	70	Origin	ECA 500
Owner	delta	Points Count	32768	Pulse Sequence	single_pulse_dec
Solvent	CHLOROFORM-d	Spectrum Offset (Hz)	12576.5293	Spectrum Type	STANDARD
Temperature (degree C)	22.500			Sweep Width (Hz)	39308.18



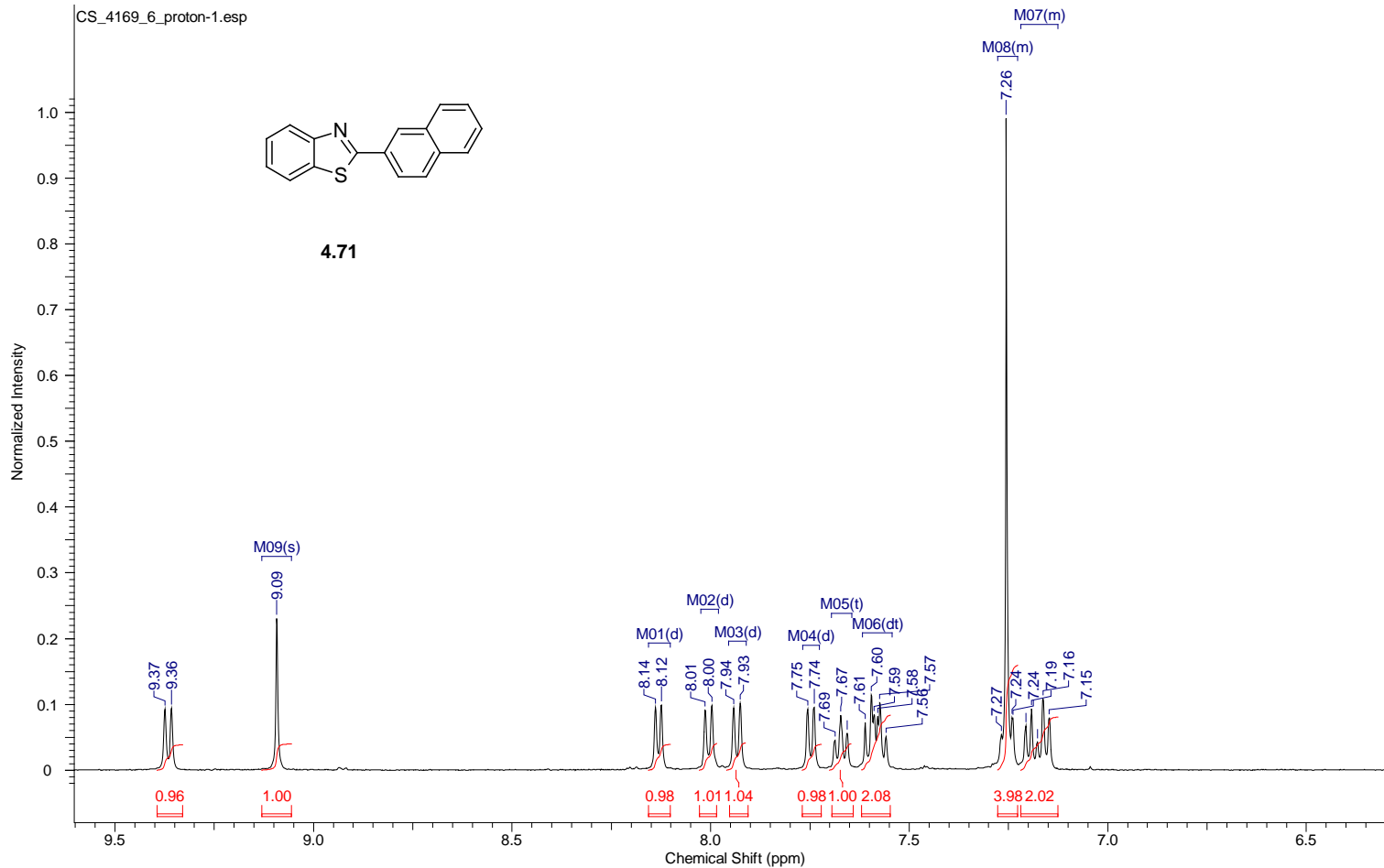
Acquisition Time (sec)	1.7459	Comment	single_pulse	Date	28 Sep 2012 09:47:47
Date Stamp	29 Sep 2012 02:06:45				
File Name	C:\Users\chen\Desktop\study\Foss\Shuai's Data\NMR DATA\500MHz092012\aaaron\proton\CS_4169_5_proton-1.jdf				
Frequency (MHz)	500.16	Nucleus	1H	Number of Transients	5
Original Points Count	16384	Owner	delta	Points Count	16384
Receiver Gain	40.00	Solvent	CHLOROFORM-d	Pulse Sequence	single_pulse.ex2
Spectrum Type	STANDARD	Sweep Width (Hz)	9384.38	Temperature (degree C)	22.100



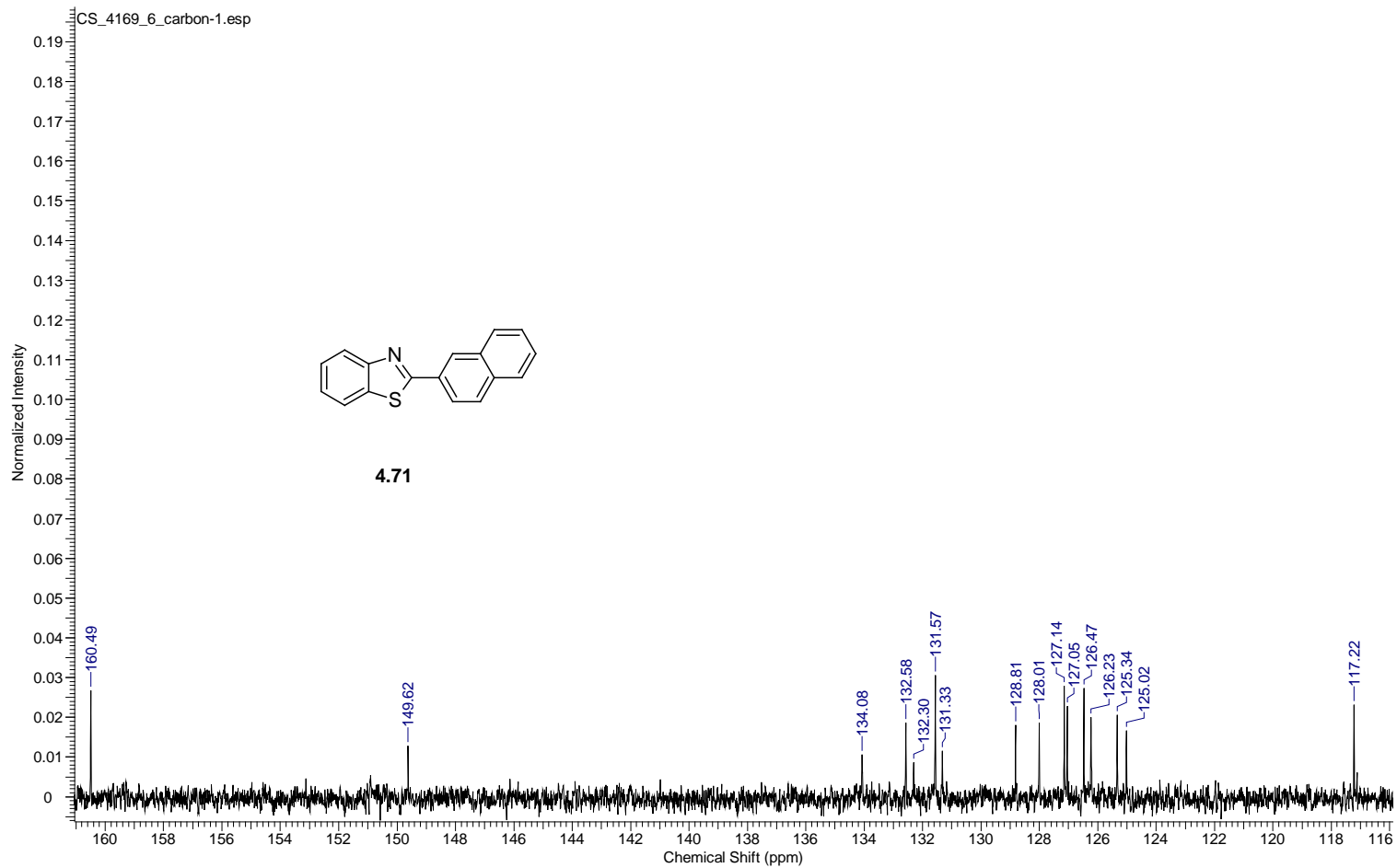
Acquisition Time (sec)	0.8336	Comment	single pulse decoupled gated NOE	Date	28 Sep 2012 09:49:47
Date Stamp	29 Sep 2012 02:08:45				
File Name	C:\Users\chen\Desktop\study\Foss\Shuai's Data\NMR DATA\500MHz092012\aaaron\carbon\CS_4169_5_carbon-1.jdf			Frequency (MHz)	125.77
Nucleus	13C	Number of Transients	50	Origin	ECA 500
Owner	delta	Points Count	32768	Pulse Sequence	single_pulse_dec
Solvent	CHLOROFORM-d	Spectrum Offset (Hz)	12576.5293	Spectrum Type	STANDARD
Temperature (degree C)	22.400			Sweep Width (Hz)	39308.18



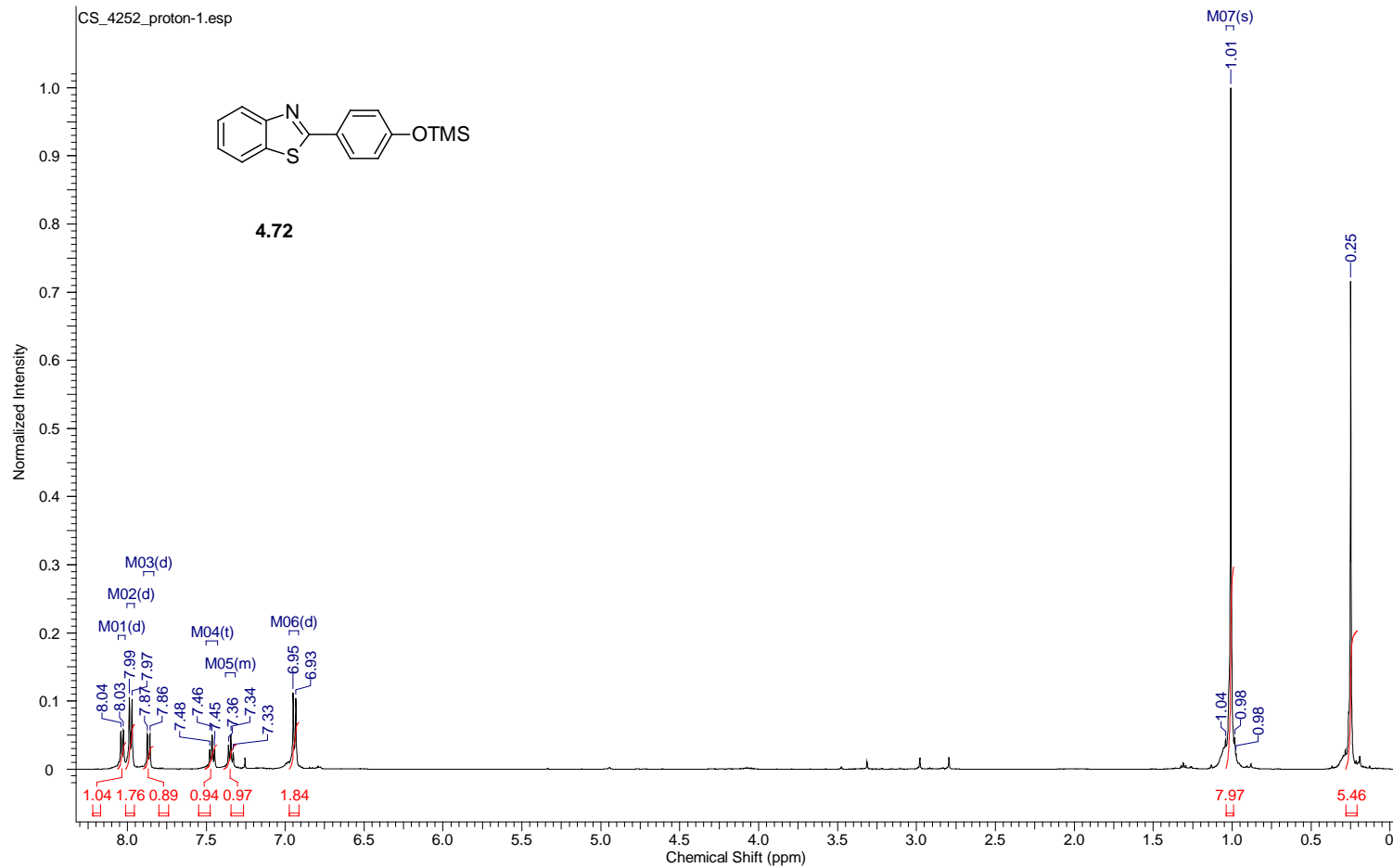
Acquisition Time (sec)	1.7459	Comment	single_pulse	Date	28 Sep 2012 09:54:00
Date Stamp	29 Sep 2012 02:12:58				
File Name	C:\Users\chen\Desktop\study\Foss\Shuai's Data\NMR DATA\500MHz092012\laaron\proton\CS_4169_6_proton-1.jdf				
Frequency (MHz)	500.16	Nucleus	¹ H	Number of Transients	5
Original Points Count	16384	Owner	delta	Points Count	16384
Receiver Gain	54.00	Solvent	CHLOROFORM-d	Pulse Sequence	single_pulse.ex2
Spectrum Type	STANDARD	Sweep Width (Hz)	9384.38	Temperature (degree C)	22.100



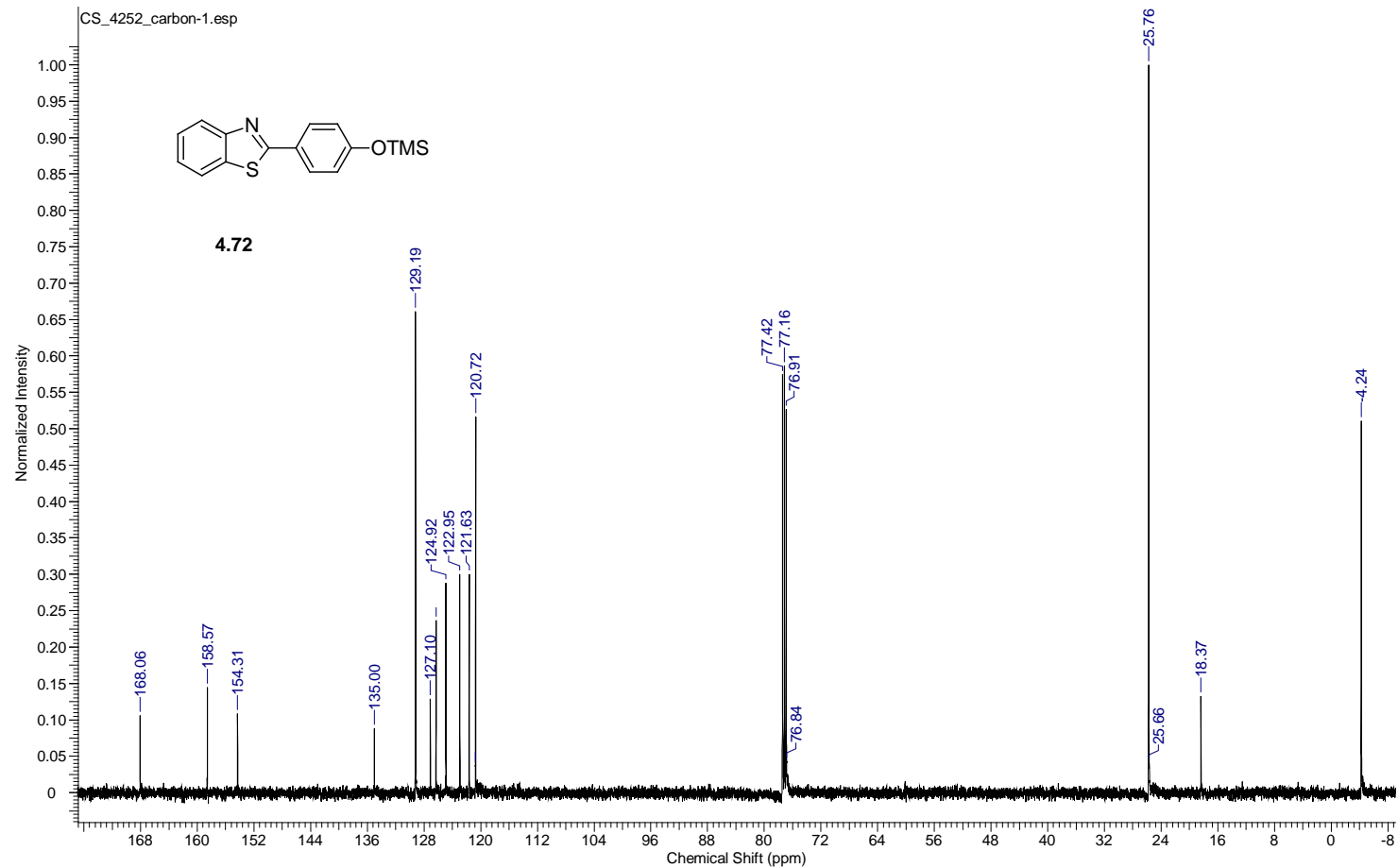
Acquisition Time (sec)	0.8336	Comment	single pulse decoupled gated NOE	Date	28 Sep 2012 10:37:27
Date Stamp	29 Sep 2012 02:56:25				
File Name	C:\Users\chen\Desktop\study\Foss\Shuai's Data\NMR DATA\500MHz092012\aaaron\carbon\CS_4169_6_carbon-1.jdf			Frequency (MHz)	125.77
Nucleus	¹³ C	Number of Transients	1200	Origin	ECA 500
Owner	delta	Points Count	32768	Pulse Sequence	single_pulse_dec
Solvent	CHLOROFORM-d	Spectrum Offset (Hz)	12576.5293	Spectrum Type	STANDARD
Temperature (degree C)	22.700			Sweep Width (Hz)	39308.18



Acquisition Time (sec)	1.7459	Comment	single_pulse	Date	23 Jan 2013 10:51:12
Date Stamp	24 Jan 2013 03:34:09				
File Name	C:\Users\chen\Desktop\study\Foss\Shuai's Data\NMR DATA\500MHz\012913\laaron\proton\CS_4252_proton-1.jdf			Frequency (MHz)	500.16
Nucleus	1H	Number of Transients	5	Origin	ECA 500
Owner	delta	Points Count	16384	Pulse Sequence	single_pulse.ex2
Solvent	CHLOROFORM-d			Receiver Gain	30.00
Sweep Width (Hz)	9384.38	Temperature (degree C)	21.000	Spectrum Offset (Hz)	2500.7996
				Spectrum Type	STANDARD

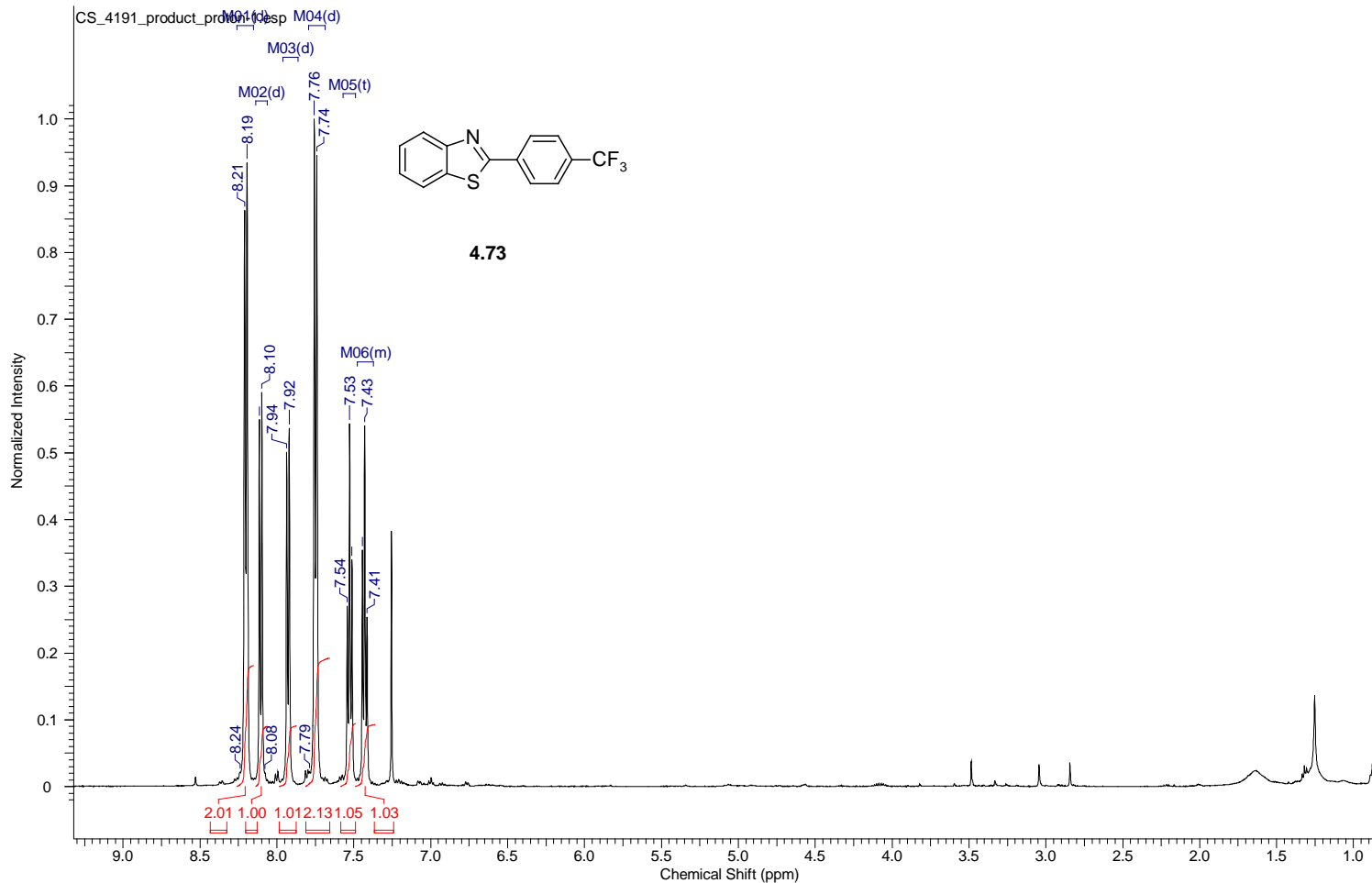


Acquisition Time (sec)	0.8336	Comment	single pulse decoupled gated NOE	Date	23 Jan 2013 10:53:43
Date Stamp	24 Jan 2013 03:36:40				
File Name	C:\Users\chen\Desktop\study\Foss\Shuai's Data\NMR DATA\500MHz012913\aaaron\carbon\CS_4252_carbon-1.jdf			Frequency (MHz)	125.77
Nucleus	¹³ C	Number of Transients	60	Origin	ECA 500
Owner	delta	Points Count	32768	Pulse Sequence	single_pulse_dec
Solvent	CHLOROFORM-d	Spectrum Offset (Hz)	12576.5293	Spectrum Type	STANDARD
Temperature (degree C)	21.400	Receiver Gain	50.00	Sweep Width (Hz)	39308.18

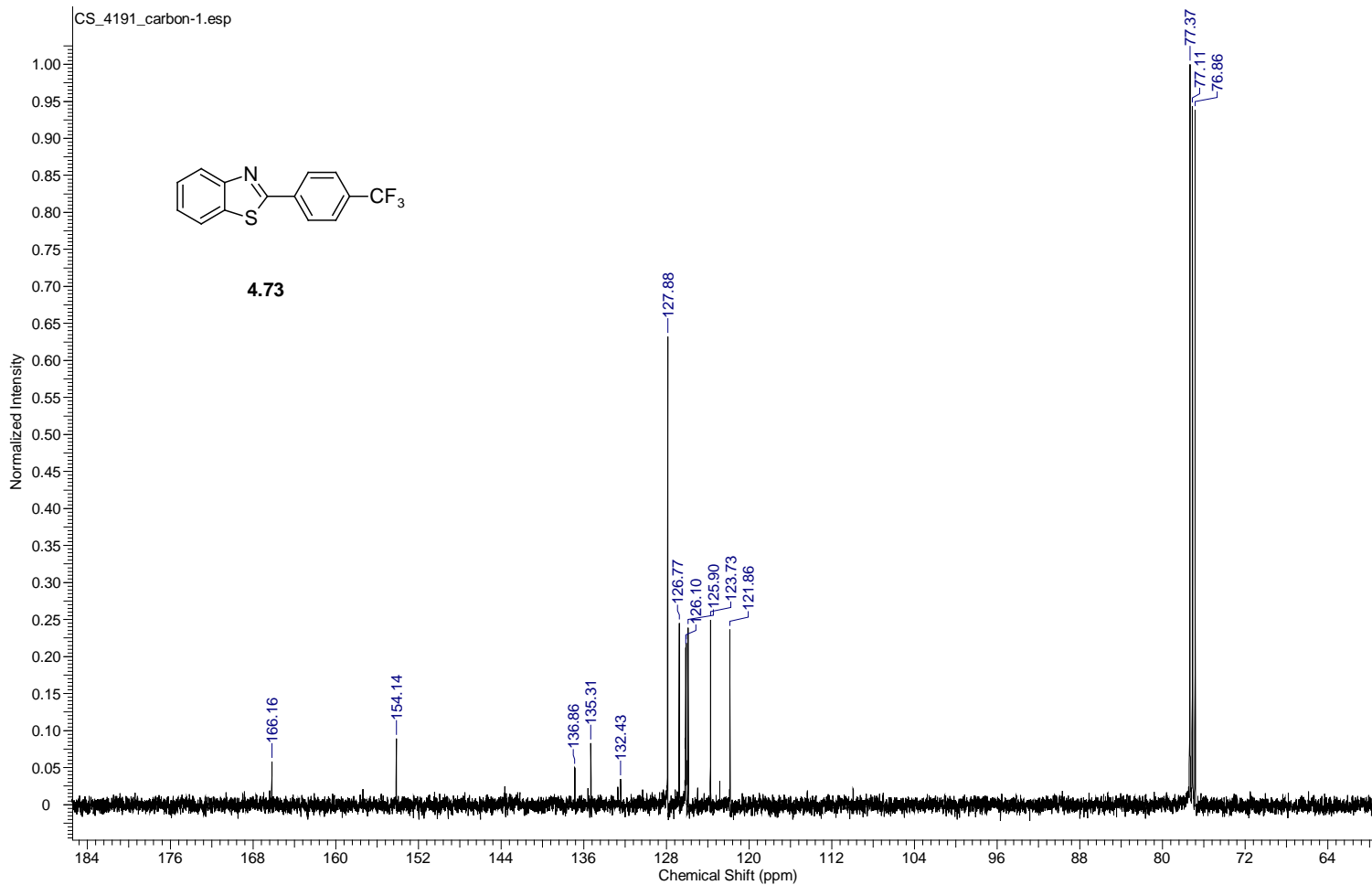


Acquisition Time (sec)	1.7459	Comment	single_pulse	Date	13 Oct 2012 13:08:04
Date Stamp	14 Oct 2012 05:27:09	File Name	G:\500MHz101512\aaaron\proton\CS_4191_product_proton-1.jdf		
Frequency (MHz)	500.16	Nucleus	1H	Number of Transients	5
Original Points Count	16384	Owner	delta	Points Count	16384
Receiver Gain	44.00	Solvent	CHLOROFORM-d	Pulse Sequence	single_pulse.ex2
Spectrum Type	STANDARD	Sweep Width (Hz)	9384.38	Temperature (degree C)	22.000

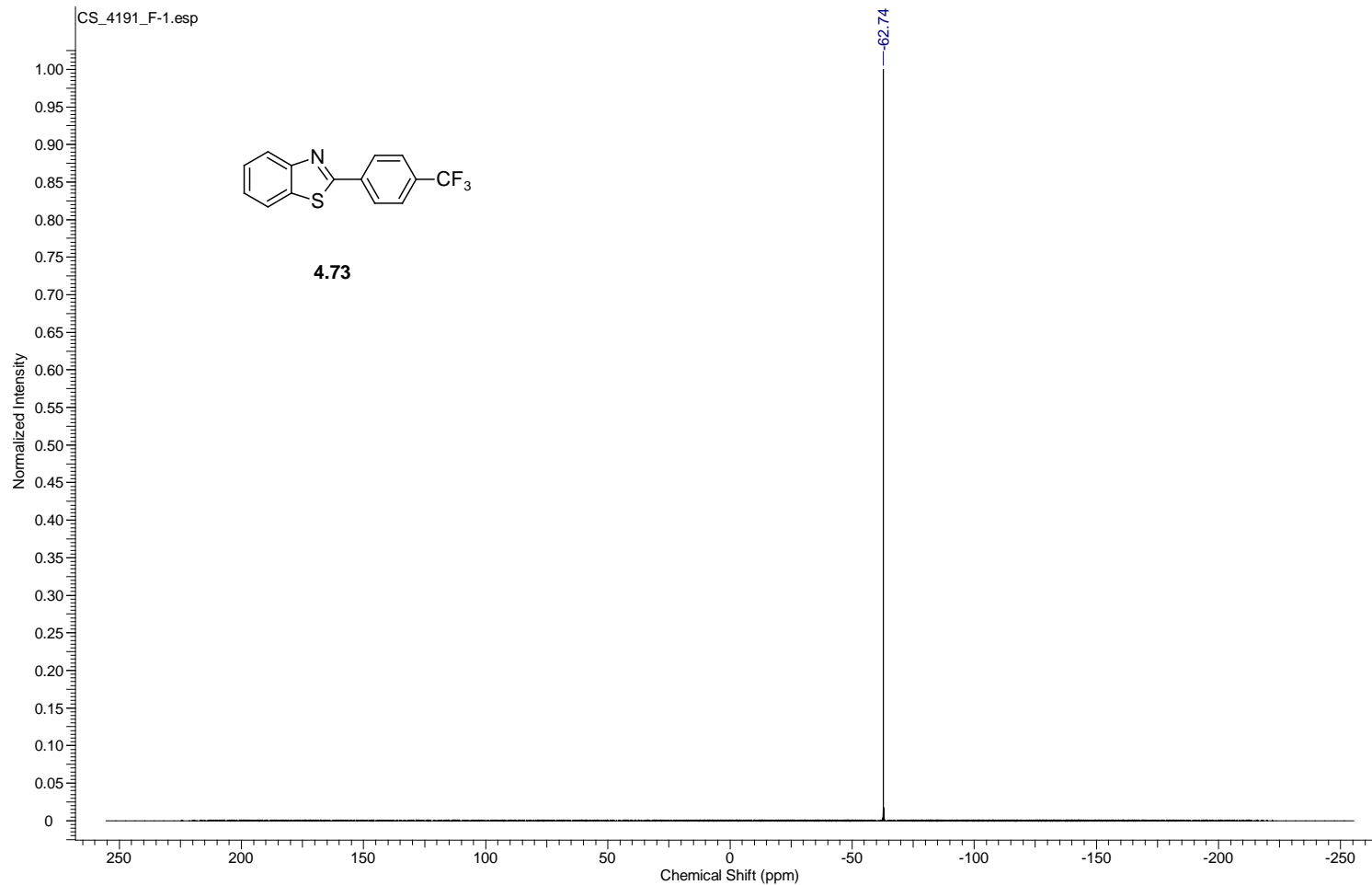
270



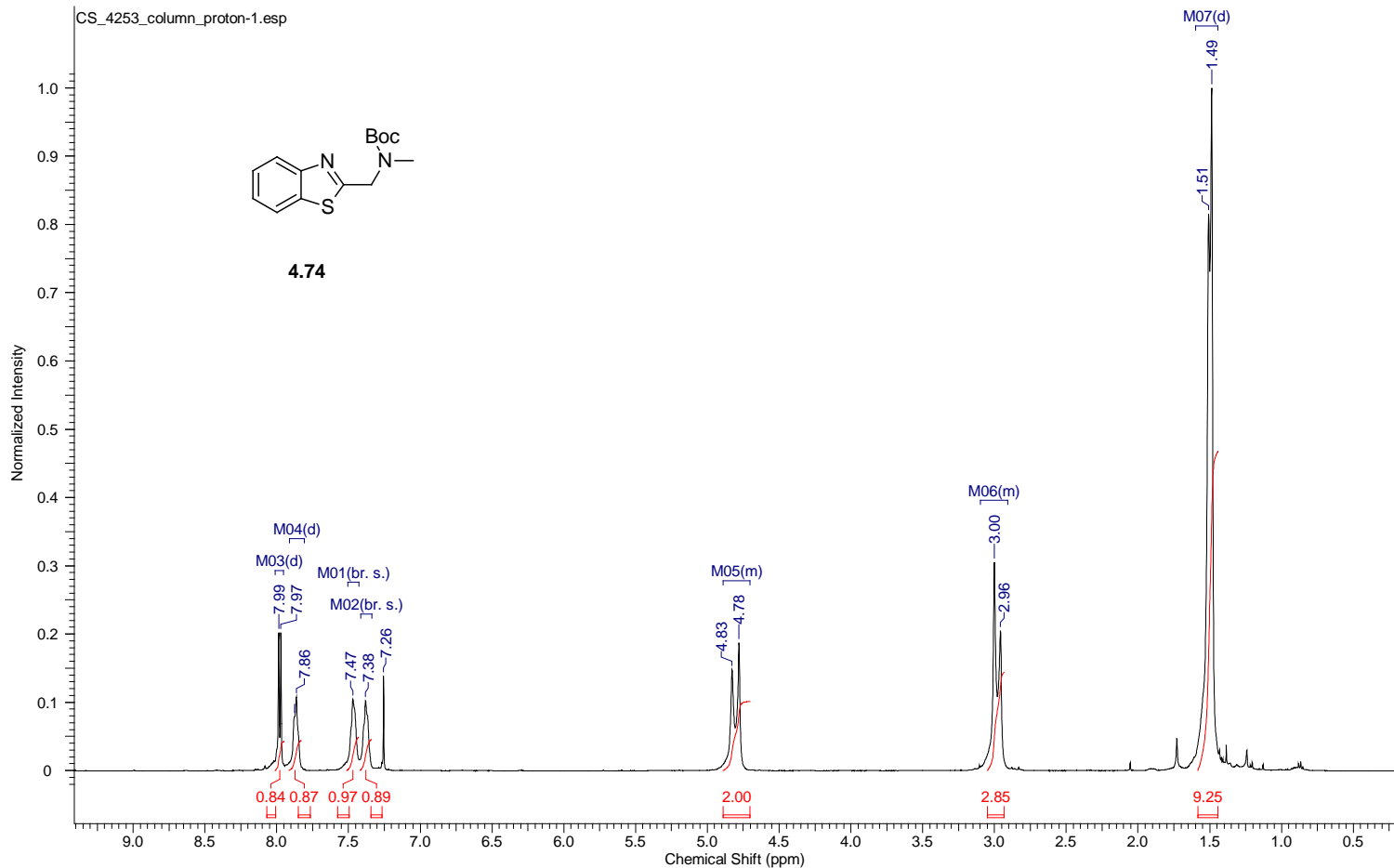
Acquisition Time (sec)	0.8336	Comment	single pulse decoupled gated NOE	Date	13 Oct 2012 13:10:34
Date Stamp	14 Oct 2012 05:29:38	File Name	G:\500MHz101512\laaron\carbon\CS_4191_carbon-1.jdf	Number of Transients	60
Frequency (MHz)	125.77	Nucleus	¹³ C	Origin	ECA 500
Original Points Count	32768	Owner	delta	Points Count	32768
Receiver Gain	50.00	Solvent	CHLOROFORM-d	Pulse Sequence	single_pulse_dec
Spectrum Type	STANDARD	Sweep Width (Hz)	39308.18	Spectrum Offset (Hz)	12576.5293
		Temperature (degree C)	22.400		



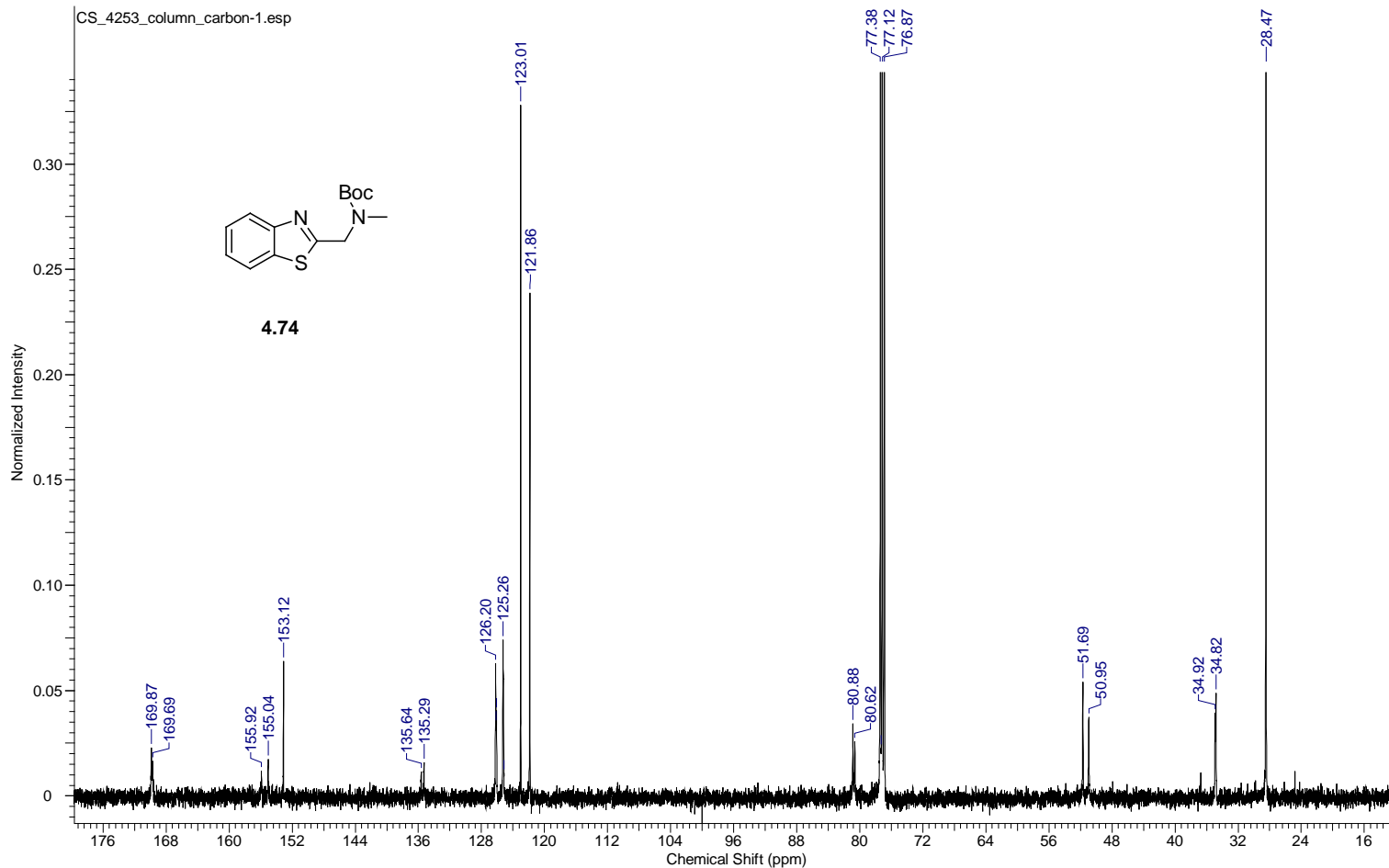
Acquisition Time (sec)	0.2726	Comment	single_pulse	Date	13 Oct 2012 13:11:39
Date Stamp	14 Oct 2012 05:30:44	File Name	G:\500MHz101512\aaaron\proton\CS_4191_F-1.jdf		
Frequency (MHz)	470.62	Nucleus	19F	Number of Transients	3
Original Points Count	65536	Owner	delta	Points Count	65536
Receiver Gain	52.00	Solvent	CHLOROFORM-d	Pulse Sequence	single_pulse.ex2
Spectrum Type	STANDARD	Sweep Width (Hz)	240384.63	Temperature (degree C)	22.200
				Spectrum Offset (Hz)	0.0000



Acquisition Time (sec)	1.3081	Comment	single_pulse	Date	26 Jan 2013 08:14:12
Date Stamp	27 Jan 2013 00:57:10				
File Name	C:\Users\chen\Desktop\study\Foss\Shuai's Data\NMR DATA\500MHz\012913\laaron\proton\CS_4253_column_proton-1.jdf				
Frequency (MHz)	500.16	Nucleus	1H	Number of Transients	14
Original Points Count	16384	Owner	delta	Points Count	16384
Receiver Gain	36.00	Solvent	CHLOROFORM-d	Spectrum Offset (Hz)	2500.7996
Sweep Width (Hz)	12525.05	Temperature (degree C)	20.900	Spectrum Type	STANDARD



Acquisition Time (sec)	0.8336	Comment	single pulse decoupled gated NOE		Date	26 Jan 2013 08:50:12	
Date Stamp	27 Jan 2013 01:33:10						
File Name	C:\Users\chen\Desktop\study\Foss\Shuai's Data\NMR DATA\500MHz012913\aaaron\carbon\CS_4253_column_carbon-1.jdf						
Frequency (MHz)	125.77	Nucleus	13C	Number of Transients	1000	Origin	ECA 500
Original Points Count	32768	Owner	delta	Points Count	32768	Pulse Sequence	single_pulse_dec
Receiver Gain	50.00	Solvent	CHLOROFORM-d	Spectrum Offset (Hz)	12576.5293	Spectrum Type	STANDARD
Sweep Width (Hz)	39308.18	Temperature (degree C)	21.400				



References

1. Massey, V. *Biochem. Soc. Trans.* 2000, *28*, 283-296.
2. Kuhn, R.; Reinemund, K.; Weygand, F. *Ber.* 1934, *67*, 1460-1463
3. Karrer, P.; Schöpp, K.; Benz, F. *Helv. Chim. Acta.* 1935, *18*, 426-429
4. Theorell, H. *Biochem. Z.* 1935, *275*, 344-346
5. Bruice, T. B. *Acc. Chem. Res.* 1980, *13*, 256-262
6. Gelalcha F. G. *Chem. Rev.* 2007, *107*, 3338-3361
7. Sono, M.; Roach, M. P.; Coulter, E. D.; Dawson, J. H. *Chem. Rev.* 1996, *96*, 2841-2887
8. Donoghue, N. A.; Norris, D. B.; Trudgill, P. W. *Eur. J. Biochem.* 1976, *63*, 175-192
9. Malito, E.; Alfieri, A.; Fraaije, M. W.; Mattevi, A. *Proc. Natl. Acad. Sci. USA* 2004, *101*, 13157-13162
10. Torres Pazmino D. E.; Baas, J. B.; Janssen, D. B.; Fraaije, M. W. *Biochemistry*, 2008, *47*, 4082-4093
11. List, B. *Chem. Rev.* 2007, *107*, 5414-5415
12. Murahashi, S.-I.; Oda, T.; Masui, Y. *J. Am. Chem. Soc.* 1989, *111*, 5002-5003
13. Imada, Y.; Iida, H.; Ono, S.; Murahashi, S.-I. *J. Am. Chem. Soc.* 2003, *125*, 2868-2869
14. Lindén, A. A.; Krüger, L.; Bäckvall, J.-E. *J. Org. Chem.* 2003, *68*, 5890-5896
15. Lindén, A. A.; Johansson, M.; Hermans, N.; Bäckvall, J.-E. *J. Org. Chem.* 2006, *71*, 3849-3853
16. Baxová, L.; Cibulka, R.; Hampl, F. *J. Mol. Catal. A: Chem.* 2007, *277*, 53-60
17. Marsh, B. J.; Carbery, D. R. *Tetrahedron Lett.* 2010, *51*, 2362-2365
18. Zurek, J.; Cibulka, R.; Dvoráková, H.; Svoboda, J. *Tetrahedron Lett.* 2010, *51*, 1083-1086

19. Shinkai, S.; Yamaguchi, T.; Manabe, O.; Toda, F. *J. Chem. Soc. Chem Commun.* 1988, 21, 1399-1401.
20. Jurok, R.; Cibulka, R.; Dvoráková, H.; Hampl, F.; Hodačová, J. *Eur. J. Org. Chem.* 2010, 27, 5217–5224
21. Mojr, V.; Herzig, V.; Budesinsky, M.; Cibulka, R.; Kraus, T. *Chem. Commun.* 2010, 46, 7599–7601
22. Iida, H.; Iwahana, S.; Mizoguchi, T.; Yashima, E. *J. Am. Chem. Soc.* 2012, 134, 15103-15113
23. Bergstad, K.; Bäckvall, J.-E. *J. Org. Chem.* 1998, 63, 6650-6655
24. Ménová, P.; Cibulka, R. *J. Mol. Catal. A: Chem.* 2012, 363, 362-370
25. Mazzini, C.; Lebreton, J.; Furstoss, R. *J. Org. Chem.* 1996, 61, 8-9
26. Murahashi, S.-I.; Ono, S.; Imada, Y. *Angew. Chem.* 2002, 114, 2472-2474
27. Imada, Y.; Iida, H.; Murahashi, S.-I.; Naota, T. *Angew. Chem. Int. Ed.* 2005, 44, 1704-1706
28. Jayapaul, J.; Hodenius, M.; Arns, S.; Lederle, W.; Lammer, T.; Comba, P.; Kiessling, F.; Gaetjens, J. *Biomaterials.* 2011, 32, 5863-5871
29. Nöll, G.; Trawöger, S.; Sanden-Flohe, M. V.; Dick, B.; Grininger, M. *ChemBioChem* 2009, 10, 834 –837.
30. Baeyer, A.; Villiger, V. *Ber. Dtsch. Chem. Ges.* 1899, 32, 3625-3631
31. Brink, G.-J. T.; Arends, I. W. C. E.; Sheldon, R. A. *Chem. Rev.* 2004, 104, 4105-4123
32. Strukul, G. *Angew. Chem. Int. Ed.* 1998, 37, 1198-1209
33. Schrader, S.; Dehmlow, E. V. *Org. Prep. Proc. Int.* 2000, 32, 125-134
34. Kaneda, K.; Ueno, S.; Imanaka, T.; Shimotsuma, E.; Nishiyama, Y.; Ishii, Y. *J. Org. Chem.* 1994, 59, 2915-2919
35. Fukuda, O.; Sakaguchi, S.; Ishii, Y. *Tetrahedron Lett.* 2001, 42, 3479-3482
36. Carlqvist, P.; Eklund, R.; Brinck, T. *J. Org. Chem.* 2001, 66, 1193-1199

37. Yoneda, F.; Sakuma, Y.; Ichiba, M.; Shinomura, K. *J. Am. Chem. Soc.* 1976, *98*, 830-835
38. Xu, S.; Wang, Z.; Li, Y.; Zhang, X.; Wang, H.; Ding, K. *Chem. Eur. J.* 2010, *16*, 3021-3035
39. Yamazaki, S. *Chem. Lett.* 1997, *12*, 127-128
40. Bernini, R.; Coratti, A.; Provenzano, G.; Fabrizi, G.; Tofanic, D. *Tetrahedron*, 2005, *61*, 1821-1825
41. Silva, E. T. D.; Caamara, C. A.; Antunes, O. A. C.; Barreiro, E. J.; Fraga, C. A. M. *Synth. Commun.* 2008, *38*, 784-788
42. Kaballm, G. W.; Reddy, N. K.; Narayana, C. *Tetrahedron Lett.*, 1992, *33*, 865-866.
43. Roy, A.; Reddy, K. R.; Mohanta, P. K.; Ila, H.; Junjappat, H. *Synth. Commun.* 1999, *29*, 3781-3791
44. Varma, R. S.; Naicker, K. P. *Org. Lett.* 1999, *1*, 189-191
45. Murray, A. T.; Matton, P.; Fairhurst, N. W. G.; John, M. P.; Carbery, D. R. *Org. Lett.* 2012, *14*, 3656-3659
46. Kuran, W.; Mazanek, E. *J. Organomet. Chem.* 1990, *384*, 13-17
47. Lavilla, R. *J. Chem. Soc., Perkin Trans. 1* VL - 2002, 1141-1156.
48. Zheng, C.; You, S.-L. *Chem. Soc. Rev.* 2012, *41*, 2498-2518
49. Rueping, M.; Dufour, J.; Schoepke, F. R. *Green Chem.* 2011, *13*, 1084-1105
50. Kaneda, K.; Haruna, S.; Imanaka, T.; Hamamoto, M.; Nishiyama, Y.; Ishii, Y. *Tetrahedron Lett.* 1992, *33*, 6827-6830
51. Bolm, C.; Schlingloff, G.; Weickhardt, K. *Tetrahedron Lett.* 1993, *34*, 3405-3408
52. Kaneda, K.; Ueno, S.; Imanaka, T.; Shimotsuma, E.; Nishiyama, Y.; Ishii, Y. *J. Org. Chem.* 1994, *59*, 2915-2917
53. Murthy, Y. V. S. N.; Massey, V. *J. Biol. Chem.* 1998, *273*, 8975-8982
54. Minidis, A. B.; Bäckvall, J. E. *Chem-Eur J.* 2001, *7*, 297-302
55. Li, X.-L.; Fu, Y. *J. Mol. Struct.-THEOCHEM* 2008, *856*, 112-118

56. Jacobsen, E. N.; Taylor, M. S. *Angew. Chem. Int. Ed.* 2006, **45**, 1521–1539
57. Doyle, A. G.; Jacobsen, E. N. *Chem. Rev.* 2007, **107**, 5713–5743
58. Melchiorre, P. *Angew. Chem. Int. Ed.* 2012, **51**, 9748-9770
59. Lelais, G.; MacMillan, D. W. C. *Aldrichimica Acta.* 2006, **39**, 79-87
60. Weitz, E.; Scheffer, A. *Chem. Ber.* 1921, **54**, 2327
61. Katsuki, T.; Sharpless, K. B. *J. Am. Chem. Soc.* 1980, **102**, 5974-5978
62. Zhang, W.; Loebach, J. L.; Wilson, S. R.; Jacobsen, E. N. *J. Am. Chem. Soc.* 1990, **112**, 2801–2803
63. Wang, Z.-X.; Tu, Y.; Frohn, M.; Zhang, J.-R.; Shi, Y. *J. Am. Chem. Soc.* 1997, **119**, 11224-11235
64. Bunton, C. A.; Minkoff, G. J. *J. Chem. Soc.* 1949, 665-670
65. Pluim, H.; Wynberg, H. *J. Org. Chem.* 1980, **45**, 2498-2504
66. Lygo, B.; Wainwright, P. G. *Tetrahedron* 1999, **55**, 6289-6295
67. Corey, E. J.; Zhang, F.-Y. *Org. Lett.* 1999, **1**, 1287-1291
68. Arai, S.; Tsuge, H.; Shioiri, T. *Tetrahedron Lett.* 1998, **39**, 7563-7565
69. Juliá, S.; Masana, J.; Vega, J. C. *Angew. Chem., Int. Ed.* 1980, **19**, 929-933
70. Colonna, S.; Molinari, H.; Banfi, S.; Juliá, S.; Masana, J.; Alvarez, A. *Tetrahedron* 1983, **39**, 1635-1641
71. Elston, C. L.; Jackson, R. F. W.; MacDonald, S. J. F.; Murray, P. J. *Angew. Chem. Int. Ed.* 1997, **36**, 410-414
72. Jacques, O.; Richards, S. J.; Jackson, R. F. W. *Chem. Commun.* 2001, 2712-2716
73. Marigo, M.; Franzén, J.; Poulsen, T. B.; Zhuang, W.; Jørgensen, K. A. *J. Am. Chem. Soc.* 2005, **127**, 6964-6968
74. Lee, S.; MacMillan, D. W. C. *Tetrahedron* 2006, **62**, 11413-11420
75. Punniyamurthy, T.; Velusamy, S.; Iqbal, J. *Chem. Rev.* 2012, **105**, 2329–2364

76. Budnik, R. A.; Kochi, J. K. *J. Org. Chem.* 1976, *41*, 1384-1391
77. Punniyamurthy, T.; Bhatia, B.; Reddy, M. M.; Maikap, G. C.; Iqbal, J. *Tetrahedron* 1997, *53*, 7649-7656
78. Nam, W.; Baek, S. J.; Lee, K. A.; Ahn, B. T.; Muller, J. G.; Burrows, C. J.; Valentine, J. S. *Inorg. Chem.* 1996, *35*, 6632-6638
79. Imagawa, K.; Nagata, T.; Yamada, T.; Mukaiyama, T. *Chem. Lett.* 1994, 527-532
80. Yamada, T.; Imagawa, K.; Nagata, T.; Mukaiyama, T. *Bull. Chem. Soc. Jpn.* 1994, *67*, 2248-2253
81. Yamada, T.; Imagawa, K.; Nagata, T.; Mukaiyama, T. *Chem. Lett.* 1992, 2231-2236
82. Bhattacharjee, S.; Anderson, J. A. *Chem. Commun.* 2004, 554-558
83. Rhodes, B.; Rowling, S.; Tidswell, P.; Woodward, S.; Brown, S. M. *J. Mol. Catal. A: Chem.* 1997, *116*, 375-379
84. Ito, Y. N.; Katsuki, T. *Bull. Chem. Soc. Jpn.* 1999, *72*, 603-607
85. Katsuki, T. *J. Synth. Org. Chem. Jpn.* 1995, *53*, 940-944
86. Jacobsen, E. N. *Catalytic Asymmetric Synthesis*; Ojima, I., Ed.; VCH: Weinheim, Germany, 1993
87. Bryliakov, K. P.; Kholdeeva, O. A.; Vanina, M. P.; Talsi, E. P. *J. Mol. Catal. A: Chem.* 2002, *178*, 47-52
88. Kawai, H.; Okusu, S.; Yuan, Z.; Tokunaga, E.; Yamano, A.; Shiro, M.; Shibata, N. *Angew. Chem. Int. Ed.* 2013, *52*, 2221-2225
89. Cui, L.; Furuhashi, S.; Tachikawa, Y.; Tada, N.; Miura, T.; Itoh, A. *Tetrahedron Lett.* 2013, *54*, 162-165
90. Minami, A.; Shimaya, M.; Suzuki, G.; Migita, A.; Shinde, S. S.; Sato, K.; Watanabe, K.; Tamura, T.; Oguri, H.; Oikawa, H. *J. Am. Chem. Soc.* 2012, *134*, 7246-7249
91. Katsuyama, Y.; Harmrolfs, K.; Pistorius, D.; Li, Y.; Müller, R. *Angew. Chem. Int. Ed.* 2012, *51*, 9437-9440
92. Mueller, N. J.; Stueckler, C.; Hall, M.; Macheroux, P.; Faber, K. *Org. Biomol. Chem.* 2009, *7*, 1115-1119

93. Zhao, G.-L.; Ibrahem, I.; Sundén, H.; Córdova, A. *Adv. Synth. Catal.* 2007, **349**, 1210-1224
94. Yang, J.; Hechavarria Fonseca, M.; List, B. *Angew. Chem. Int. Ed.* 2004, **43**, 6660-6662.
95. Zhu, C.; Falck, J. R. *Chemcatchem* 2011, **3**, 1850-1851
96. Zheng, C.; You, S.-L. *Chem. Soc. Rev.* 2012, **41**, 2498-2518
97. Aziz, F.; Mirza, G. A. *Talanta* 1964, **11**, 889-892
98. Massey, V. *J. Biol. Chem.* 1994, **269**, 22459-22462.
99. Hantzsch, A. *Justus Liebigs Ann. Chem.* 1882, **215**, 1-82
100. Kumar, A.; Maurya, R. A.; Sharm, S. *Bioorg. Med. Chem. Lett.* 2009, **19**, 4432-4436
101. Love, B.; Goodman, M.; Snader, K.; Tedeschi, R.; Macko, E. *J. Med. Chem.* 1974, **17**, 956-965
102. Bossert, F.; Meyer, H.; Wehinger, E. *Angew. Chem. Int. Ed. Engl.* 1981, **20**, 762-769
103. Guengerich, F. P.; Brian, W. R.; Iwasaki, M.; Sari, M. A.; Baarnhielm, C.; Berntsson, P. *J. Med. Chem.* 1991, **34**, 1838-1844
104. Bischhoff, H.; Angerbauer, R.; Bender, E.; Bischoff, J. A.; Petzinna, D.; Pfitzner, J.; Porter, M. C.; Schmidt, D.; Thomas, G. *Atherosclerosis* 1997, **135**, 119
105. Mashraqui, S. H.; Kamik, M. A. *Tetrahedron Lett.* 1998, **39**, 4895-4898
106. Heravi, M. M.; Derikvand, F.; Hassan-Pour, S.; Bakhtiari, K.; Bamoharram, F. F.; Oskooie H. A. *Bioorg. Med. Chem. Lett.* 2007, **17**, 3305-3309
107. Chai, L.; Zhao, Y.; Sheng, Q.; Liu, Z-Q. *Tetrahedron Lett.* 2006, **47**, 9283-9285
108. Nakamichi, N.; Kawashita, Y.; Hayashi, M. *Org. Lett.* 2002, **4**, 3955-3957
109. Eynde, J.-J. V.; D'Oraxio, R.; Haverbeke, Y. V. *Tetrahedron* 1994, **50**, 2419-2484

110. Wang, D.; Liu, Q; Chen, B.; Zhang, L.; Tung, C.; Wu, L. *Chinese Sci. Bull.* 2010, *55*, 2855–2858
111. Le Bozec, L.; Moody, C. J. *Aust. J. Chem.* 2009, *62*, 639–647
112. Zhu, C; Falck, J. R. *ChemCatChem* 2011, *3*, 1850-1851
113. Zhu, C.; Akiyama, T. *Org. Lett.* 2009, *11*, 4180-4183
114. Sakamoto, T.; Mori, K.; Akiyama, T. *Org. Lett.* 2012, *14*, 3312-3315
115. Yadav, G. S.; Senthilkumar, G. P. *Int. J. Pharm. Drug Dev. Res.* 2011, *3*, 1-7
116. Bochatay, V. N.; Boissarie, P. J.; Murphy, J. A.; Suckling, C. J.; Lang, S. *J. Org. Chem.*, 2013, *78*, 1471-1477
117. Zhao, J.; Huang, H.; Wu, W.; Chen, H.; Jiang, H. *Org. Lett.* 2013, *15*, 2604-2607
118. Sun, Y.; Jiang, H.; Wu, W.; Zeng, W.; Wu, X. *Org. Lett.*, 2013, *15*, 1598-1601
119. Liao, Y.; Qi, H.; Chen, S.; Jiang, P.; Zhou, W.; Deng, G.-J. *Org. Lett.* 2012, *14*, 6004–6007
120. Kemal, C.; Bruce, T. C. *Proc. Nat. Acad. Sci. USA* 1976, *73*, 995-999
121. Imada, Y.; Iida, H.; Ono, S.; Masui, Y.; Murahashi, S.-I. *Chem. Asian J.* 2006, *1*, 136–147
122. Lynn, M. A.; Carlson, L. J.; Hwangbo, H.; Tanski, J. M.; Tyler, L. *A. J. Mol. Struct.* 2012, *1011*, 81–93

Biographical Information

Shuai Chen received his BS in Polymer Material and Engineering from Donghua University, Shanghai, China. In 2008, he joined Professor Frank Foss's group at University of Texas at Arlington to study organic chemistry. His research focused on using biomimetic organocatalyst to achieve environmental friendly synthesis of valuable small molecules. He is going to study medicinal chemistry as a postdoctoral fellow under the supervision of Professor Jeffery Winkler at University of Pennsylvania after obtaining his PhD.